INTERNATIONAL COUNCIL FOR BUILDING RESEARCH STUDIES AND DOCUMENTATION

WORKING COMMISSION W18A - TIMBER STRUCTURES

CIB - W18 A

VOLUME I

MEETING TWENTY - TWO

BERLIN

GERMAN DEMOCRATIC REPUBLIC

SEPTEMBER 1989

CONTENTS

1. LIST OF PARTICIPANTS

1.1 CIB-W-18A-members

CANADA

J D	Barrett	University of British Columbia, Vancouver
E	Karacabeyli	Forintek Canada, Vancouver
B	Madsen	University of British Columbia, Vancouver
V	Mathur	Forest Canada, Ottawa
C K A	Stieda	Forintek Canada, Vancouver

DENMARK

H J	Larsen	Danish Building Research Institute, Horsholm
T F	Nielsen	Danish Building Research Institute, Horsholm
H	Riberholt	Technical University of Denmark, Lyngby

FEDERAL REPUBLIC OF GERMANY

H	Brüninghoff	University of Wuppertal
O	Eberhart	University of Karlsruhe
J	Ehlbeck	University of Karlsruhe
M	Gerold	University of Karlsruhe
P	Glos	University of München
H	Werner	University of Karlsruhe

FINLAND

I	Absek	Helsinki University of Technology
J	Kangas	Technical Research Centre of Finland
T	Toratti	Helsinki University of Technology

FRANCE

P	Racher	CUST - University
F	Rouger	CTBA Department

GERMAN DEMOCRATIC REPUBLIK

W	Rug	Academy of Building Berlin

ITALY

G	Bignotti	Holzbau AG, Brixen
A	Ceccotti	University of Florence
A	Vignoli	University of Florence

JAPAN

T	Nakai	Forestry and Forest Products Research Institute
M	Yasumura	Building Research Institute Tsukuba

NETHERLANDS

A J M	Leijten	Technical University, Delft

NORWAY

E	Aasheim	Norwegian Institute of Wood Technology, Oslo

SWEDEN

B	Edlund	Chalmers University of Technology, Goteborg
U	Girhammar	Byggmetodik AB
B	Hedlund	Swedish National Testing Institute
B	Källsner	Swedish Institute for Wood Technology Research, Stockholm
J	König	Swedish Institute for Wood Technology Research, Stockholm
S	Mohager	Swedish National Testing Institute

UNITED KINGDOM

A R	Abbott	TRADA, High Wycombe
H T	Burgess	TRADA, High Wycombe
A R	Fewell	Building Research Establishment, Watford
C J	Mettem	TRADA, High Wycombe
R F	Marsh	Ove Arup + Partners
J G	Sunley	Self employed

UNITED STATES OF AMERICA

B	Douglas	National Forest Products Association
E	Elias	American Plywood Association, Tacoma
D W	Green	USDA Forest Products Laboratory, Madison
R C	Mitzner	American Plywood Association, Tacoma

1.2 CMEA members

CZECHOSLOWAKAI

P	Dutko	Technical University of Bratislava
B	Kozelough	Research Institute for Timber Engineering, Bratislava
V	Mahuliak	Research Institute for Timber Engineering, Bratislava
A	Pozgai	Technical College Zvolen
J	Sedlar	Research Institute for Timber Engineering, Bratislava

GERMAN DEMOCRATIC REPUBLIC

R	Apitz	VEB BMK Industrie and Hafenbau
M	Badstube	Academy of Building, Berlin
E	Delock	Academy of Building, Berlin
K	Erler	Technical College, Wismar
	Fischer	VEB Structural Components and Fibrebuilding Materials
K	Geier	VEB Structural Components and Fibrebuilding Materials
	Grimm	VEB Structural Components and Fibrebuilding Materials
T	Hanack	Academy of Building, Berlin
B	Hertel	VEB Structural Components and Fibrebuilding Materials
	Hoeher	Staatliche Bauaufsicht
P	Kaiser	Technical College, Wismar
M	Kiesel	Technical College, Wismar
E	Koitzsch	VEB Structural Components and Fibrebuilding Materials
E	Kothe	Technical University, Dresden
L	Krahmer	Ministerium für Bauwesen
W	Kreissig	Academy of Building, Berlin

U	Laduch	Technical College, Wismar
K	Lissner	Academy of Building, Berlin
S	Patzig	Academy of Building, Berlin
R	Plessow	Academy of Building, Berlin
K	Schulze	Academy of Building, Berlin
A	Seemann	Academy of Building, Berlin
R	Siemoneit	Academy of Building, Berlin
W	Vogt	HAB, Weimar
K H	Zimmer	Technical University Dresden

HUNGARY

A	Josza	University for Forest Science and Timber Industry, Sopron
F	Ronai	University for Forest Science and Timber Industry, Sopron

POLAND

B	Bany	Institute of Industrial Building, Warsaw
R	Ganowicz	Agricultural University of Poznan
J	Kerste	Technical College, Rzeszow
Z	Mielczarek	Technical College, Poznan
W	Nozynsky	Institute of Industrial Building, Warsaw

USSR

	Baltrusatis	Polytechnikum, Kaunas
A S	Freidin	Timber Structure Department of TS NIISK, Moscow
L	Kowaltschuk	Timber Structure Department of TS NIISK, Moscow
T	Lomakin	Timber Structure Department of TS NIISK, Moscow
Y	Slavik	Timber Structure Department of TS NIISK, Moscow
S B	Turkowski	Timber Structure Department of TS NIISK, Moscow

2. CHAIRMAN'S INTRODUCTION

DR STIEDA opened the meeting and welcomed the participants, in particular those from the CMEA countries, who would be joining the meeting on 26 and 27 September. Special thanks were extended to DR RUG for his efforts in preparing for this conference and for making the local necessary travel and accommodation arrangements.

3. COOPERATION WITH OTHER ORGANISATIONS

ISO/TC 165: MR LARSEN said that no meeting of this group had been held since the last CIB-W18A meeting in Parksville, as the current phase of work has come to an end. Future activity will be focussed on producing European Standards.

RILEM: DR CECCOTTI gave a brief outline of the objectives and recent activities of the four timber-related groups:

- 'Behaviour of Timber Structures under Seismic Actions', under the chairmanship of PROFESSOR NIELSEN of the Danish Building Research Institute held its first meeting in Florence earlier this year. A state-of-the-art report is currently being drafted. The next meeting will be held to coincide with the CIB-W18A meeting in Lisbon in September 1990.

- 'Application of Fracture Mechanics to Timber Structures', is chaired by PROFESSOR RANTA-MAUNUS and held its first meeting in Finland. A state-of-the-art report is currently being drafted and the group is planning to complete its work by August 1990.

- 'Behaviour of Timber and Concrete Composite Load-bearing Structures', is chaired by DR CECCOTTI. The next meeting will be held in Spring 1990, in Hildesheim, followed by a meeting later in the year, to coincide with the CIB-W18A meeting in Lisbon.

- 'Creep in Timber Constructions', under the chairmanship of PROFESSOR MORLIER, held its first meeting in Paris in May. The next meeting is scheduled for London in February 1990.

DR CECCOTTI added that several members of the RILEM Technical Committees are also CIB-W18A members. This will ensure future close collaboration between RILEM and CIB.

EUROCODE 5: MR LARSEN said that the comment period for Eurocode 5 ended in March 1989 and that comments have been received from most European and EFTA countries. These comments are now being reviewed, from which a revised draft will be prepared, which should be ready for publication in about one and a half years. The EFTA countries will participate in this process. A draft of EC5 Part 2 covering components, including diaphragm structures and bridges has also been drafted. It is anticipated that the draft will soon be sent to the Commission, when it will be requesting its incorporation into EC5 as one document.

CEN/TC 124: MR LARSEN explained that work has reached the stage where the first group of draft Standards, approximately 14 in number, will be discussed in October, then sent out for comment. These cover glulam (all except strength classes), testing (structures, panel products, determination of properties of glulam, embedding strength of dowel-type fasteners) and timber (prepared sizes, strength classes, test standards, interpretation of test results to produce characteristic values, grading requirements and machine stress grading).

PROFESSOR EHLBECK added that there are European groups other than TC 124 working on subjects related to timber engineering, including adhesives, panel products and preservatives. In reply to PROFESSOR EHLBECK, MR SUNLEY said that there are five CEN Committees concerned with wood, which collectively have a current programme for producing 120 Standards. These are:-

- TC 38 'Wood Preservation', comprising 10 Working Groups, one of which is looking at hazard classification;
- TC 103 'Wood Adhesives', will produce seven Standards relating to solid timber for load-bearing structures, adhesives for plywood, test methods for assessing strength properties for adhesives;
- TC 112 - this committee currently has four Working Groups, but this will soon be extended to six, to cover particleboard, plywood, fibreboard, test methods (coordinated for all board materials), formaldehyde and wood-based cement boards;
- TC 124 'Solid Timber', already described above by MR LARSEN;
- TC 175 'Round and Sawn Timber for Non-structural Use' - this Group has only met once, but includes some items of relevance to CIB-W18A, for example, references, measurement methods, symbols.

There are other CEN/TCs in which timber also has representation, including TC 125 'Fire' (independent of material). Timber needs to keep a close watching brief on the work of this group.

In answer to a question from PROFESSOR GLOS, asking whether EC5 will be published as a CEN Standard, or a CEC document, MR LARSEN replied that most probably the work will be transferred to CEN during re-drafting and will be published as a CEN Standard. DR STIEDA asked if there is a formal procedure for resolving disputes arising from voting. MR LARSEN replied that no such procedure is yet in place, but the situation is constantly evolving.

MR RIBERHOLT asked what was meant by symbols and what did they cover? MR SUNLEY said that it meant notation for general wood use. DR STIEDA asked if the CEN Technical Committees communicate with each other to coordinate their work. MR SUNLEY replied that this does happen, as many people sit on more than one CEN Committee. DR CECCOTTI asked if there were any timber representatives on the Fire Committee. MR SUNLEY replied that the chairman of TC 127 is from the UK but that he and the other UK representatives have no timber experience. In view of this, a lobby group has been proposed in the UK, to ensure that the timber interests do not suffer.

CEI-BOIS/FEMIB: In his report, PROFESSOR BRUNINGHOFF said that the sub-Committee is currently concentrating its efforts on promotion activities and that no technical work is in progress. A European glulam award is to be presented for the first time in November, in Paris.

IABSE: PROFESSOR EDLUND said that IABSE is a world-wide association, concentrating mainly on structural engineering and is dominated by people with predominantly steel and concrete interests. There were no timber representatives at the meeting held at Helsinki earlier this year. It is intended to coordinate the timing of the next IABSE meeting with the planned International Timber Engineering Conference being organised by TRADA, which will be held in London in September 1991 (see below). The LISBON meeting earlier this year on durability of structures had 700 participants and was dominated by concrete. Only one paper relating to timber was presented. A symposium on mixed structures/composites will be held in Brussels in September 1990. There has already been a very large interest in this meeting and many offers have been received for papers for presentation, although few are related to timber. A symposium on bridges is to be held in Leningrad in 1991, with the call for papers due out in early 1990. The Working Commission on Composite Structures met earlier this year in Zurich, to consider serviceability limit states for buildings. The discussion should be of interest to CIB-W18A members.

IUFRO S5.02: In the absence of PROFESSOR HOFFMEYER, who is chairman of this Group, a summary of activities was given by PROFESSOR GLOS, who said it was recently agreed by IUFRO that S5.02 would have two Vice-Chairmen, himself and DR GREEN. The next meeting is to be held in Fredericton, New Brunswick from 30 July to 2 August 1990, when discussions will centre on wood quality and user needs in conjunction with IUFRO Wood Quality Group S5.01. Other topics covered will be stress grading, joint behaviour, duration of load, dynamic behaviour, applied fracture mechanics and reliability. DR GREEN added that the meeting will follow the format decided at the last meeting in Finland. The XIX IUFRO World Congress will take place in Montreal from 5-11 August 1990. Within the total programme, different sessions will be allocated to S5.02, including quality of wood structural materials, improving engineered timber use and timber for tomorrow's structures.

1990 Timber Engineering Conference in Japan: DR NAKAI said that this Conference will be held from 23-25 October 1990 in Shinjuku, Japan. The deadline for papers has been extended to 30 September 1989 and full papers will be required by the Secretariat by 30 June 1990. At present, approximately 80 papers have been received, primarily from Japan, Canada and the USA. It is planned during the Conference to hold special programmes on full-scale house tests and seismic and wind loading. The registration fee is expected to be around $200.

LNEC, Portugal: as no-one from LNEC was present, DR STIEDA said that an invitation has been received from the Structural Engineering Laboratory of LNEC to hold the 1990 meeting of CIB-W18A. This has already been accepted. The meeting will commence on Tuesday 11 September and will finish at 12 noon on Friday 14 September.

1991 Timber Engineering Conference: MR ABBOTT gave a brief summary of the arrangements for the 1991 International Timber Engineering Conference, which will be held in London, England on 2-5 September. The suggestion for this Conference was initiated by the UK Timber Engineering Group and organisation is being undertaken by TRADA. The Conference will last for four full days and will have three broad themes covering research, design and manufacture, and construction. A first announcement for this Conference was sent out with the advance papers for this meeting and the first call for papers will be sent out during October. The venue for the Conference is Church House in Westminster.

CIB-W18B: PROFESSOR MADSEN said that a brief meeting of W18B was held in New Zealand last month at the International Timber Engineering Conference. The Chairman of the Group, DR LEICESTER, is planning to hold a Conference in 1992 in Malaysia, on timber engineering centred on hardwood.

4. TRUSSED RAFTER SUB-GROUP

The participants were: MR COUZENS, MR SMITH, DR KALLSNER, MR KARACABEYLI, DR AASHEIM, PROFESSOR BRUNINGHOFF, DR BIGNOTTI and MR RIBERHOLT.

The object of the meeting was to discuss realistic and practical design methods for timber trussed rafters. As Chairman of the sub-group, MR RIBERHOLT said that he has prepared a paper giving a simplified trussed rafter design method for EC5 and that this has been circulated to all members and will be presented later in the meeting. It was agreed that a meeting of the sub-group would be held on Tuesday afternoon and that a plenary discussion would be held at the end of the CIB meeting, on Thursday morning.

5. ADDITIONAL ITEM

PROFESSOR GLOS said that plans are in hand to hold a meeting on reliability-based design concepts for timber engineering in Autumn 1990. The plans are still tentative at this stage, but anyone interested should contact PROFESSOR GLOS or MR LARSEN during this meeting or later for more details and to give their suggestions for the format of the meeting and the topics to be included. MR LARSEN added that the meeting is being organised by PROFESSOR BODIG as a NATO scientific seminar and therefore participation will be by invitation only.

6. LOAD SHARING

Paper 22-8-1 'Reliability analysis of visco-elastic floors' by Rouger, Barrett and Foschi was presented by DR ROUGER, who said that the work was based around a visco-elastic adaptation of the floor analysis program originally developed by PROFESSOR FOSCHI. DR STIEDA commented that the finite element model described was obviously a very powerful tool and asked how it could be used by code writers to simplify the design process. DR ROUGER replied that he believed it could be used to derive more accurate creep factors for certain structures. DR STIEDA asked which elements of a composite structure contribute most to the overall performance and hence would repay further study. DR ROUGER commented that strain redistributions within structures are not fully understood and that study into these areas could yield benefits.

MR LARSEN said that one of the conclusions of the paper is that the probability of failure is not affected and this might suggest that no further work is necessary. He then asked if deflections can be detected sufficiently accurately on real structures to enable the work to be used for practical design. DR ROUGER replied that for complex stress situations such as a floor supported on all four edges, the deflection amplification factors would be larger than can be calculated by consideration of the joists alone. DR STIEDA added that traditional design methods have evolved around traditional materials, for which certain materials assumptions have been made. However, there is limited knowledge and experience of new materials and simulations using this program could greatly assist in the evaluation of components made using them. MR FEWELL asked why a log-normal distribution had been used for all variables - was this because it was appropriate to the data set, or was it to simplify calculations? DR ROUGER responded that it is because the data available was log normal. However, the model works equally well with other distributions.

7. STRESS GRADING

Paper 22-5-1 'Fundamental vibration frequency as a parameter for grading sawn lumber' by Nakai, Tanaka and Nagau was presented by DR NAKAI, who concluded that fundamental vibration frequency may be used as a parameter for grading sawn timber. DR STIEDA asked if the use of frequency measurement is seen as a practical grading tool in Japan. DR NAKAI said that increasing use of such techniques is expected and once the principles have been established, it is hoped that it will be taken up by industrial companies. In response to a question from DR CECCOTTI, DR NAKAI said that the mean value of moisture content of the timbers referred to in the paper was 19%. DR STIEDA asked if other species were going to be tested. DR NAKAI said that investigations were already under way into other domestic Japanese species. PROFESSOR GLOS pointed out that if calculations were made from frequency measurement, it was necessary to know the density of timber, and asked how this was measured. DR NAKAI said that this was achieved by weighing the individual pieces.

8. MECHANICAL JOINTS AND FASTENERS

Paper 22-7-1 'End-grain connections with laterally loaded steel bolts' by Ehlbeck and Gerold was presented by PROFESSOR EHLBECK. Referring to the paper, MR RIBERHOLT asked why the stresses shown in Figure 5 were at an angle to the bolt and do not extend to the edge of the timber. PROFESSOR EHLBECK said that the stresses compare with the finite element predictions shown in Figure 7. MR GEROLD added that for equilibrium, the streses must include friction as well as lateral stresses, which have different distributions. Within this work, attempts were made to identify a plane where the stresses are nearly homogeneous. This is at 45%, as shown in Figure 7. Also, the length of the line in Figure 7 does not imply the magnitude of the stress, but merely its direction. MR RIBERHOLT asked how the wood properties are modelled. PROFESSOR EHLBECK said that for embedding strength, an elastic-plastic relationship was assumed, as shown in Figure 6. MR LARSEN expressed concern that frictional forces along the bolt had not been included, as these could be significant.

Paper 22-7-2 'Determination of perpendicular-to-grain tensile stresses in joints with dowel-type fasteners - a draft proposal for design rules' by Ehlbeck, Gorlacher and Werner, was presented by PROFESSOR EHLBECK, who suggested that the simplified design method in the CIB Code which has provisionally been accepted for the draft EC5 can lead to uncertainties in joint strength. MR KARACABEYLI asked if it was possible to calculate the failure in the connectors using the same approach as in the previous papers, ie are the tension perpendicular to grain stresses critical in design? PROFESSOR EHLBECK said that this was possible, but only if the edge distances are small. MR KARACABEYLI further asked what diameter fasteners were used in the work. PROFESSOR EHLBECK replied between 10 and 30 mm, but that only a small number of tests were done with the larger diameters. MR GEROLD added that if the ratio ac/h is greater than 0.7, tension failures will result. This is in accord with Figure 3 in the previous paper.

Paper 22-7-3 'Design of double-shear joints with non-metallic dowels; a proposal for a supplement of the design concept' by Ehlbeck and Eberhardt was presented by PROFESSOR EHLBECK. Referring to Figure 3, MR LARSEN pointed out that there would be no plastic hinge in the dowel until the point of failure and therefore it is not possible to have the proposed mode 3a in the analysis when the connector is still carrying a moment. Responding to a question from MR RIBERHOLT about the practical use of this work with non-metallic dowels, PROFESSOR EHLBECK said that there are many reasons why steel is not desirable, for example, for fire resistance design, and in these situations, non-metallic connectors are highly desirable.

DR LEIJTEN presented his paper 22-7-4 'The effect of load on strength of timber joints at high working load level'. MR KARACABEYLI commented that in reality, wood becomes harder with time. DR LEIJTEN agreed and said that the results confirm this phenomenon. MR BURGESS added that the author had said that damage relates to a loss of strength: however, it is possible to have a duration of load effect without strength loss. Consequently, it is not possible to predict duration of load effects by measuring strength after a long period of time. The results in the paper do not show loss of strength, but a loss in the capacity to deform. DR STIEDA asked MR BURGESS if he was suggesting that the load deformation curve will be different from that obtained from original material. MR BURGESS replied that it would.

Paper 22-7-5 'Plasticity requirements for portal frame corners' by Gunnewijk and Leijten was presented by DR LEIJTEN. There was no discussion.

Paper 22-7-6 'Background information on design of glulam rivet connections in CS/CAN3-086.1-M89' by Karacabeyli and Janssens was presented by MR KARACABEYLI. In answer to a question from DR CECCOTTI on the ductility of the joints, MR KARACABEYLI said that some cyclic loading tests have been made and that the results are available. PROFESSOR MADSEN added that in seismic situations the ductility would have to be ensured by correct sizing and design of steel plates.

DR YASUMURA presented Paper 22-7-7 'Mechanical properties of joints in glued-laminated beams under reversed cyclic loading'. Answering a question from DR CECCOTTI regarding viscous damping, DR YASUMURA showed graphs of equivalent viscous damping versus deflection for bolted joints. MR KARACABEYLI asked about load sharing and how this affects the capacity of such joints under reversed cyclic loading. DR YASUMURA replied that this subject has not yet been fully studied and so it is not possible at present to predict long-term performance. DR STIEDA asked if there is a standard procedure in Japan for cyclic testing, or was it necessary to develop methods for this research? DR YASUMURA replied that there are methods for cyclic testing of materials and wall panels, but not for joints and therefore methods had to be developed.

Paper 22-7-8 'Strength of glued lap timber joints' by Glos and Horstmann was presented by PROFESSOR GLOS, who commented that there is increasing interest in the use of glued joints for trusses. In response to a question from DR CECCOTTI about the effects of moisture content and how this should be catered for in design, PROFESSOR GLOS said that this was not part of the study and therefore it was only possible at this time to recommend glued joints for buildings with constant climatic conditions. Further research work is needed for other exposure conditions. MR RIBERHOLT commented that the paper discusses absolute values for length and width of joints and asked if there is some relation between joint strength and member thickness and if so, can it be quantified? PROFESSOR GLOS replied that thickness does have an effect and that there is an optimum member thickness of around 40mm. Below this value, a lower strength will result due to differences in elasticity of jointed members, and at higher thicknesses, a lower strength will result due to increasing joint eccentricity. DR LEIJTEN said that with mechanically fastened joints there is advance warning of failure due to short-term overload, but this is not so with glued joints, which typically fail in a brittle manner. He then questioned whether this necessitated a higher factor of safety. In ensuing discussion, it was generally agreed that this is the responsibility of code writers. MR RIBERHOLT added that attitudes should change towards glued joints, as they can now be designed to be both robust and durable. Answering DR BIGNOTTI, PROFESSOR GLOS said that there is now sufficient information to carry out efficient design of glued trusses.

9. DISCUSSION ON FUTURE RESEARCH REQUIREMENTS FOR JOINTS

DR STIEDA opened the discussion by suggesting that extensive research has been carried out on individual connectors and their performance in full-size structures and that now there is a need for research to investigate the interaction between connectors in a joint. MR RIBERHOLT added that efforts should be concentrated on evaluating moment stiff connections which lead to wood failures behind the connector, where the strength of the joint is governed by the perpendicular to grain strength of the timber. PROFESSOR EHLBECK commented that improved information is needed on slip moduli for serviceability design, with more precise information for a wider range of connectors. There is also a lack of internationally agreed calculation methods for mechanically composite elements. In summary, DR STIEDA said that three topics had emerged where further research was needed:-

1. Slip in mechanically connected joints
2. Tensile stresses perpendicular to grain
3. Size/configuration/number of connectors and their influence on joint performance.

PROFESSOR EHLBECK said that design information is needed on joints with different fasteners in a single joint, all of which will have different slip characteristics and strengths. PROFESSOR GLOS suggested that research is needed to develop new types of joint, which can transfer higher loads. New methods of connecting timber are also needed. MR RIBERHOLT reinforced this view, by stating that in the past emphasis has largely been on dowel-type connectors, which are intrinsically a very bad way to transfer forces between members.

MR ELIAS said that problems are still being experienced in North America with material quality for fasteners and that there is a need to improve material specification. PROFESSOR MADSEN agreed with this. PROFESSOR GLOS suggested that more effort should be concentrated on the aesthetic quality of joints and also their fire resistance properties.

PROFESSOR EHLBECK suggested that the damping effect of joint types for seismic design would be worthy of further investigation. DR CECCOTTI agreed with this and suggested that the new RILEM Technical Committee will, in the near future, suggest research needs in this area. DR STIEDA added that yield capacity, as well as damping factor, is important for seismic design.

PROFESSOR EDLUND commented that durability and long-term behaviour of glued joints is important and research is needed in this area, particularly to look at chemical breakdown of adhesives. DR STIEDA added that timber can be treated with fire-retardant chemicals and said that research is needed to define the long-term behaviour of joints in such treated timber. MR RIBERHOLT commented that several connectors had been put forward in recent years for use in end-grain. In the Eurocode, low values have been put forward for the load-bearing capacities of such connectors and further research could be beneficial in this area.

With regard to glued joints, PROFESSOR GLOS said that a test method is urgently needed to predict the long-term behaviour of new types of adhesives. PROFESSOR MADSEN added that strict quality control is required for glued joints, particularly if they are to be used in the field.

10. MECHANICAL JOINTS AND FASTENERS (continued)

Paper 22-7-9 'Toothed rings type "Bistyp 0 75" at the joints of firwood' by DR KERSTE was presented by the author. In response to a question from MR METTEM, DR KERSTE said that the density of fir and pine tested was between 420 and 500 kg/m^3.

Paper 22-7-10 'Calculation of joints and fastenings as compared with the international state' by Zimmer and Lissner was presented by PROFESSOR ZIMMER, who gave a comparison of design methods for joints in various national codes. In response to a question on the differences between the recommendations for nailed joints in the Danish code and the Eurocode, MR LARSEN said that the Danish code was based on fewer species and that originally it was written for square section nails which are common in Denmark.

Papers 22-7-11 'Joints on glued-in steel bars present relatively new and progressive solution in terms of timber structure design' and 22-7-12 'The development of design codes for timber structures made of composite bars with plate joints based on cylindrical nails' were not presented.

Paper 22-7-13 'Designing of glued wood structures joints on glued-in bars' by DR TURKOVSKY was presented by the author, who showed slides of typical timber construction in the USSR. MR RIBERHOLT asked if there are any design procedures for such joints for tension perpendicular to grain which enable the bolts and the wood to work together, or is it assumed that the bolts take the whole load? DR TURKOVSKY replied that the length of the bars are varied according to design. Commenting on the use of steel bars as diagonal reinforcement in the ends of beams, DR STIEDA asked how this is carried out in practice. DR TURKOVSKY replied that the bars are glued in at 45° and that they reduce the shear stresses in the timber member by 30% and eliminate tension perpendicular to grain stresses. Answering a question from DR STIEDA, DR TURKOVSKY said that epoxies and phenol formaldehyde glues have been used in these types of joints.

11. STRUCTURAL STABILITY

MR BURGESS introduced his paper 22-15-1 'Suggested changes in Code bracing recommendations for beams and columns', in which it was concluded that the bracing force at each restraint need be 2.5% of the end force in braced members. This was the classic case of a simple problem requiring a complicated solution, resulting in simple recommendations. PROFESSOR BRUNINGHOFF commented that a similar rule exists in the German Code and that this is acceptable for the design of the member, but that a method of designing the bracing structure is needed. PROFESSOR GANOWICZ asked if optimisation was considered in the study, ie where should bracing of a given stiffness be applied, to achieve maximum critical loads? MR BURGESS replied that this had not been considered and could form a useful extension of the work.

Paper 22-15-2 'Research and development of timber frame structures for agriculture in Poland' by Kus and Kerste was presented by DR KERSTE. There was no discussion.

DR YASUMURA presented Paper 22-15-5 'Seismic behaviour of arched frames in timber construction'. Regarding modification factors for ductility in the nodes of structures, DR CECCOTTI suggested that not all structures should be treated uniformly. PROFESSOR MADSEN said that work has been undertaken in Canada to investigate the response of plywood frame wall constructions under seismic loading. The conclusions of this work highlight that the nailed connections are vital to the performance, with the material properties of the sheathing being far less critical. PROFESSOR MADSEN added that it was interesting to see a failure taking place in the centre of an arch and asked how this failure developed. How did the structure behave as cycling increased? DR YASUMURA replied that the frames failed in a brittle manner, with cracks initiated in the centre. Responding to a question from DR FREIDIN, DR YASUMURA commented that in his experiments, the rate of loading was such that it took 15-20 minutes to complete one cycle. DR CECCOTTI added that it is difficult to simulate actual seismic conditions and slow test rates are on the safe side.

Paper 22-15-6 'The robustness of timber structures' by Mettem and Marcroft was presented by MR METTEM, who explained that the work behind this paper was initiated in response to the need to demonstrate the ability of timber structures to withstand accidental damage to satisfy UK authorities. MR LARSEN questioned the wisdom of highlighting such potential problem areas and reasoned that it would be better to place greater emphasis on making good quality, well-built structures. MR SUNLEY re-emphasised the UK view on accidental damage and the insistence that this is covered in structural codes. MR METTEM said that as far as the authors are aware, there have been no conclusive discussions as to what values are to be inserted in EC9 for accidental actions. MR LARSEN replied that it is understood by the EC5 drafters to be a specified characteristic value and that it should be specified by national bodies dealing with accidental actions in the loading codes.

Paper 22-15-7 'The influence of geometrical and structural imperfections on the load-bearing capacity of timber columns' by DR DUTKO was presented by the author. Responding to a question from MR BURGESS regarding the mathematical solutions employed, DR DUTKO said that a two-part equation was used for the analysis for slenderness ratios greater than 0.75 and a quadratic parabolic curve for slenderness ratios less than 0.75.

12. LAMINATED MEMBERS

Paper 22-12-1 'The dependence of the bending strength on the glued laminated timber girder depth' by Badstube and Schoene was presented by PROFESSOR BADSTUBE. Responding to a question from MR RIBERHOLT, PROFESSOR BADSTUBE said that the experimental work was carried out on GDR quality Grade 2 timber, which has a density of 480 kg/m^3. Responding to a question from MR KARACABEYLI about some of the beams which were not evaluated, PROFESSOR BADSTUBE said that those beams which failed due to manufacturing errors were not considered in the study.

DR HEDLUND introduced his paper, 22-12-2 'Acid deterioration of glulam beams in buildings from the early half of the 1960s' and said that the problem related to cold setting phenol resins. Responding to a question from DR STIEDA, DR HEDLUND said that the effect of deterioration was not thought to be markedly influenced by poor quality control of glulam fabrication.

Paper 22-12-3 'Experimental investigation of normal stress distribution in glued laminated wooden arches' by Mielczarek and Chanaj was presented by PROFESSOR MIELCZAREK. Answering a question from PROFESSOR EHLBECK, PROFESSOR MIELCZAREK said that the stresses discussed in the paper were calculated from strain measurements using simple elastic theory.

PROFESSOR GANOWICZ introduced his paper 22-12-4 'Ultimate strength of wooden beams with tension reinforcement as a function of random material properties'. Answering various questions, PROFESSOR GANOWICZ said that the species tested was pine and that bending strengths of the reinforced beams of between 70 and 80 MPa were achieved. The work only dealt with short-term strengths and the creep properties are being investigated in another set of experiments. MR KARACABEYLI asked if plans were in hand to test under different environmental conditions. PROFESSOR GANOWICZ replied not at present, as he had been unsuccessful in attracting sponsorship for this research.

13. GLUED JOINTS

Introducing his paper 22-18-1 'Perspective adhesives and protective coatings for wood structures', DR FREIDIN presented the results of studies investigating the durability of adhesives against moisture and time effects. Answering a question from DR HEDLUND, DR FREIDIN clarified that the adhesive types assessed were cold setting phenol resorcinol adhesives at temperatures up to 40°C.

14. ENVIRONMENTAL CONDITIONS

Paper 22-11-1, 'Corrosion and adaptation factors for chemically aggressive media with timber structures' was introduced by DR ERLER, who concluded that, in general, timber is more resistant to the majority of common aggressive chemical agents than steel and concrete.

15. STRUCTURAL CODES

Paper 22-102-1 'New GDR timber design code, state and development' by Rug, Badstube and Kofent was presented by DR RUG, who pointed out that the code is based on limit state design and closely follows EC5. Answering a question from PROFESSOR GLOS, DR RUG said that the strength values are based predominantly on timber from Germany, but also on timber from USSR.

Paper 22-102-2 'Timber strength parameters for the new USSR design code and its comparison with international code' by Slavik, Denesh and Ryumina was introduced by DR SLAVIK. Commenting on the small difference between the safety factors for visual and machine graded timber, PROFESSOR GLOS enquired as to which type of grading machines these factors were derived for. DR SLAVIK replied that two machines were used - the Computermatic and the Finnograder, the latter of which gave the better results. With reference to glulam, MR METTEM asked if the aim is to classify glulam as an element, or to grade the laminations from which glulam members are made? DR SLAVIK replied that the data refers to solid sawn timber with cross-sections 30-50 x 150mm. No glued elements have yet been tested. MR FEWELL pointed out that the Finnograder operates by measuring a number of characteristics and relates these to strength by multiple regression. He asked if the author used the equation supplied with the machine, or were experiments undertaken to develop equations specific to Russian timber? DR SLAVIK replied that he had collaborated with Finland and had sent parcels of Russian timber for testing and that a model was developed specific to this material. Answering a question from MR ELIAS, DR SLAVIK said that spruce, pine and fir were tested and that there were regional as well as species differences. Also, density of timber was included in the strength analyses.

Paper 22-102-3 'Norwegian timber design code - extract from a new version' by Aasheim and Solli was presented by DR AASHEIM, who highlighted the main differences between this version and the original limit state design code, which was introduced in 1973. This new version also includes revised visual grading rules. MR SUNLEY gave a brief summary of the strength class system developed for EC5. MR METTEM pointed out that the EC5 draft has recommendations for limiting deflections and asked how this is being catered for in the Norwegian code. DR AASHEIM replied that simplified rules for deflections, as well as for floor vibrations, which were originally in the loading code, have now been reintroduced into the timber code.

16. CIB TIMBER CODE

Paper 22-100-2 'Proposal for including size effects in CIB-W18A timber design code' was introduced by PROFESSOR MADSEN and was followed by Paper 22-6-1 'Size effects and property relationships for Canadian 2-inch dimension lumber', which was presented by DR BARRETT. These papers were discussed simultaneously. DR GREEN added to the presentation by giving a brief summary of the ASTM recommendations for size effects, which was followed by discussion on the comparison between European and North American size factors from DR GREEN, PROFESSOR GLOS, DR BARRETT and PROFESSOR MADSEN.

MR SUNLEY said that efforts should be directed at simplifying code clauses and asked whether the suggestion was to initially increase characteristic values to accommodate such wide variations in size effects? MR FEWELL commented that different grading methods have been found to introduce considerable variations in the size effects and that grading methods will have to be considered in any future European code and standard development. PROFESSOR GLOS commented that efforts should be directed at implementing research into standards, which cannot be done without considering loading effects. To some extent, these balance out the size effects. DR FREIDIN added that shear strains, concentrations under point loads and other loading configurations are all important and can mask size effects, particularly in bending, unless they are properly taken into account.

Papers 22-10-3 'Thin-walled wood-based flanges in composite beams' and 22-100-3 'CIB structural timber design code - proposed changes of section on thin-flanged beams' were both presented by DR KONIG. There was no discussion.

Paper 22-100-1 'Proposal for including an updated design method for bearing stresses in CIB structural timber design code' was presented by PROFESSOR MADSEN. MR BURGESS sought clarification for the introduction of the new method which does not appear to cover all the aspects of the old method, particularly with regard to the situation of tension in the top fibres near the shoulders, which varies as a function of bearing length. PROFESSOR MADSEN replied that the reason for the proposed changes is to cover situations where loads are applied at the ends of members.

Paper 22-100-4 'Modification factor for aggressive media - a proposal for a supplement to the CIB model code' by Erler and Rug was introduced by DR ERLER. MR LARSEN commented on the value of such work and suggested that it would be easier, instead of modification factors, to describe the layer of wood that would be destroyed as a function of time. DR KONIG suggested that it would be preferable to formulate the problem in a similar manner to fire design, ie to specify a corrosion rate analogous to the charring rate and to design the member size accordingly. DR ERLER replied that it would be possible to use a reduction of the cross-section as suggested, but added that the aim within the Polish code is to move towards modification factors.

Paper 22-100-5 'Timber design code in Czechoslovakia and comparison with CIB model code' by Dutko and Kozelouh was introduced by PROFESSOR KOZELOUH. PROFESSOR GLOS asked what is the magnitude of the factor of safety. PROFESSOR KOZELOUH replied a value is not yet specified, as there is insufficient data to determine it. Answering a further question, PROFESSOR KOZELOUH confirmed that the code is a hybrid between a permissible stress and a limit state design code.

17. STATISTICS AND DATA ANALYSIS

Paper 22-17-1 'Comment on the strength classes in Eurocode 5 by analysis of a stochastic model for grading' was presented by DR KIESEL. PROFESSOR GLOS commented that the findings in this paper deserve considerable discussion, but that this was not the correct forum in which to undertake it. The paper presented a theoretical study of what can happen if certain grading rules and distributions are used and care is required in interpreting these results when they are used in practice.
t

18. LIMIT STATE DESIGN

Paper 22-1-1 'Reliability-theoretical investigation into timber components' by Badstube, Rug and Plessow was presented by PROFESSOR BADSTUBE. DR STIEDA said that calculation of the safety index beta had been done in other countries and asked if any comparisons had been made with this work. PROFESSOR BADSTUBE replied that the basis of the calculations was similar to EC5 - however, further work is required to assess the effects of load combinations. DR STIEDA added that the ratio of dead to live load factors will affect the value of the safety index.

19. DURATION OF LOAD

Paper 22-9-1 'Long-term tests with glued laminated timber girders' by Badstube, Rug and Schone was presented by PROFESSOR BADSTUBE. MR METTEM commented on the interesting nature of the research and added that similar work is being undertaken in the UK. MR KARACABEYLI asked if any control group specimens were tested in short-term loading. PROFESSOR BADSTUBE replied that short-term test data is available for all experiments, including glulam strength and finger joint strength. DR LEIJTEN said that similar work had been initiated in The Netherlands in 1962 and he agreed to make a copy of the report available to PROFESSOR BADSTUBE.

Paper 22-9-2 'Strength of one-layer solid and lengthways glued elements of wood structures and its alteration from sustained load' by Kovaltschuk and Boitemirova was presented by DR KOVALTSCHUK. Answering a question from MR KARACABEYLI, DR KOVALTSCHUK said that strength during different durations and intensities of load was calculated as a ratio of the short-term strength.

20. TIMBER BEAMS

Paper 22-10-1 'Design of end-notched beams' by Larsen and Gustafsson was presented by MR LARSEN, who proposed a fracture mechanics approach to the design of end-notched beams. DR STIEDA asked if work on specimen development is being undertaken by RILEM. MR LARSEN replied that this was the case, as MR GUSTAFSSON, the joint author of the paper, is a RILEM member. Answering a question from DR KOVALTSCHUK about testing speed, MR LARSEN replied that this was in accordance with CIB recommendations, such that failure occurs in a few minutes.

Paper 22-10-2 'Dimensions of wooden flexural members under constant loads' was presented by DR POZGAI. PROFESSOR MADSEN asked how this work would be applied in practice, in view of the smallness of the test specimens. DR POZGAI commented that it would only be applicable to clear defect-free members. PROFESSOR GANOWICZ added that the extrapolation to structural size timbers is also a function of temperature and moisture content.

Paper 22-10-4 'Calculation of wooden bars with flexible joints in accordance with the Polish standard code and strict theoretical methods' was presented by PROFESSOR MIELCZAREK. PROFESSOR EHLBECK asked if it is proposed to change the Polish codes for such components subjected to concentrated loading. PROFESSOR MIELCZAREK replied that it is not necessary to change, but that users should be made aware that differences may exist. MR LARSEN asked what were the estimated slip moduli and how were they obtained? PROFESSOR MIELCZAREK said that these were indicated in the Polish standard.

21. PLYWOOD

Paper 22-4-2 'Estimation of characteristic values for wood-based panel products' was introduced by MR ELIAS. Commenting on the 10% rule, MR RIBERHOLT suggested that the same concept could be investigated for glulam and other structural products. MR LARSEN asked why the RILEM test method gave higher values than the full-size panel tests. Making reference to work at TRADA, MR ELIAS replied that with wider specimens, there is increased probability for locating the weakest area in the panel. MR ABBOTT gave details of the work in progress at TRADA, in which the proposed CEN testing methods are being assessed on a variety of panel products, including plywood, oriented strand board, chipboard and cement bonded particleboard.

22. STRESSES FOR SOLID TIMBER

Paper 22-6-2 'Moisture content adjustment for in-grade data' was presented by DR BARRETT, with additional comments provided by DR GREEN. PROFESSOR EHLBECK asked what is the consequence of this work and is there a need to change existing codes with regard to modification factors for moisture classes. DR BARRETT replied that the CEN draft seems to allow for any adjustment that can be demonstrated to be satisfactory, ie that can be substantiated by test. The information provided in this paper gives an approach when test data is not available. PROFESSOR GLOS commented on the large differences in bending strength and queried whether this was a function of the sampling strategy used. DR BARRETT agreed that this could be one explanation. DR NAKAI said that it is difficult to measure the true moisture content of members and that often, in Japan for example, a sample with an acceptable moisture content measured at the surface can have a moisture content above fibre saturation point at the centre. DR GREEN agreed that this was a valid point and said that all the work described related to 2-inch lumber. It has been agreed that it can be applied up to 4 inches, but not to any larger sizes.

Paper 22-6-3 'A discussion of lumber property relationships in Eurocode 5' by Green and Kretschmann, was presented by DR GREEN. Referring to the comparisons contained in the paper, MR LARSEN pointed out that testing was not undertaken in accordance with the CEN standard, in that pieces were not selected for testing which contained grade determining defects in the middle third of the span. DR GREEN said that specimens with random placement of defects were used, but that very little difference was found when comparing the results with those obtained from specimens with defects in the middle third.

Paper 22-6-4 'Effect of wood preservatives on the strength properties of wood' was presented by DR RONAI. Seeking clarification on the work, MR RIBERHOLT asked if tests were conducted on full-size or small clear specimens and whether the treated specimens were tested after or before drying to the same moisture content as the control. DR RONAI said that the specimens were small-size and that they were dried under vacuum to between 12 and 13% before testing. DR RONAI also confirmed that the material was pre-dried before preservative treatment.

23. TIMBER COLUMNS

Paper 22-2-2 'Proposals for the design of compressed timber members by adopting the second-order stress theory' by Laduch and Kaiser, was presented by DR KAISER. PROFESSOR BRUNINGHOFF asked what was the permanent load assumed for creep purposes. DR KAISER said approximately 30% of ultimate short-term load. PROFESSOR EHLBECK said that a paper had recently been published by DR BLASS on the effect of creep on the strength of columns and suggested that this might be helpful. MR LARSEN said that creep influences on columns should be included in codes. However, this was not done because the design philosphy cannot cope. Creep is taken account of in the safety factors.

24. TRUSSED RAFTERS

MR RIBERHOLT gave a brief introduction to his paper 22-14-1, 'Guidelines for design of timber trussed rafters', which was discussed during the meeting of the Trussed Rafter sub-group earlier in the week. The paper had been generally accepted at this meeting and it was agreed that comments should be sent to MR RIBERHOLT within two weeks, following which the paper will be revised and circulated to all members of the sub-group. The aim is to reach agreement by the end of the year and then to present a final version at the 1990 CIB-W18A meeting.

25. OTHER BUSINESS

The Chairman expressed the thanks of members to DR RUG and his staff for his efficient organisation of this meeting. He also expressed appreciation to MR ABBOTT for his work as Secretary in preparing the papers for the meeting.

DR STIEDA then closed the 22nd meeting of CIB-W18A and said he looked forward to seeing members in Lisbon, Portugal next year, for the 23rd meeting which will be held from 11-14 September.

26. List of CIB-W18A Papers
Berlin 1989

26. LIST OF CIB-W18A PAPERS
BERLIN, GERMAN DEMOCRATIC REPUBLIC 1989

(Note: Asterisk "*" denotes papers presented by CMEA participants)

22-1-1 *	Reliability-Theoretical Investigation into Timber Components A Proposal for a Supplement of the Design Concept - M Badstube, W Rug and R Plessow
22-2-1	Buckling and Reliability Checking of Timber Columns - S Huang, P M Yu and J Y Hong
22-2-2 *	Proposal for the Design of Compressed Timber Members by Adopting the Second-Order Stress Theory - P Kaiser
22-4-1 *	Scientific Research into Plywood and Plywood Building Constructions the Results and Findings of which are Incorporated into Construction Standard Specifications of the USSR - I M Guskov
22-4-2	Evaluation of Characteristic values for Wood-Based Sheet Materials - E G Elias
22-5-1	Fundamental Vibration Frequency as a Parameter for Grading Sawn Timber - T Nakai, T Tanaka and H Nagao
22-6-1	Size Effects and Property Relationships for Canadian 2-inch Dimension Lumber - J D Barrett and H Griffin
22-6-2	Moisture Content Adjustements for In-Grade Data - J D Barrett and W Lau
22-6-3	A Discussion of Lumber Property Relationships in Eurocode 5 - D W Green and D E Kretschmann
22-6-4 *	Effect of Wood Preservatives on the Strength Properties of Wood - F Ronai
22-7-1	End Grain Connections with Laterally Loaded Steel Bolts A draft proposal for design rules in the CIB Code - J Ehlbeck and M Gerold
22-7-2	Determination of Perpendicular-to-Grain Tensile Stresses in Joints with Dowel-Type Fasteners - A draft proposal for design rules - J Ehlbeck, R Görlacher and H Werner
22-7-3	Design of Double-Shear Joints with Non-Metallic Dowels A proposal for a supplement of the design concept - J Ehlbeck and O Eberhart
22-7-4	The Effect of Load on Strength of Timber Joints at high Working Load Level - A J M Leijten
22-7-5	Plasticity Requirements for Portal Frame Corners - R Gunnewijk and A J M Leijten
22-7-6	Background Information on Design of Glulam Rivet Connections in CSA/CAN3-086.1-M89 - A proposal for a supplement of the design concept - E Karacabeyli and D P Janssens

22-12-3 * Experimental Investigation of normal Stress Distribution in Glue Laminated Wooden Arches - Z Mielczarek and W Chanaj

22-12-4 * Ultimate Strength of Wooden Beams with Tension Reinforcement as a Function of Random Material Properties - R Candowicz and T Dziuba

22-14-1 Guidelines for Design of Timber Trussed Rafters - H Riberholt

22-15-1 Suggested Changes in Code Bracing Recommendations for Beams and Columns - H J Burgess

22-15-2 * Research and Development of Timber Frame Structures for Agriculture in Poland - S Kus and J Kerste

22-15-3 * Ensuring of Three-Dimensional Stiffness of Buildings with Wood Structures - A K Shenghelia

22-15-5 Seismic Behavior of Arched Frames in Timber Construction - M Yasumura

22-15-6 The Robustness of Timber Structures - C J Mettem and J P Marcroft

22-15-7 * Influence of Geometrical and Structural Imperfections on the Limit Load of Wood Columns - P Dutko

22-17-1 * Comment on the Strength Classes in Eurocode 5 by an Analysis of a Stochastic Model of Grading - A proposal for a supplement of the design concept - M Kiesel

22-18-1 * Perspective Adhesives and Protective Coatings for Wood Structures - A S Freidin

22-100-1 Proposal for Including an Updated Design Method for Bearing Stresses in CIB W18 - Structural Timber Design Code - B Madsen

22-100-2 Proposal for Including Size Effects in CIB W18A Timber Design Code - B Madsen

22-100-3 CIB Structural Timber Design Code - Proposed Changes of Section on Thin-Flanged Beams - J König

22-100-4* Modification Factor for "Aggressive Media" - a Proposal for a Supplement to the CIB Model Code - K Erler and W Rug

22-100-5* Timber Design Code in Czechoslovakia and Comparison with CIB Model Code - P Dutko and B Kozelouh

22-102-1* New GDR Timber Design Code, State and Development - W Rug, M Badstube and W Kofent

27. Current List of CIB-W18A Papers

27. CURRENT LIST OF CIB-W18A PAPERS

Technical papers presented to CIB-W18A are identified by a code CIB-W18A/a-b-c, where:

a denotes the meeting at which the paper was presented. Meetings are classified in chronological order:

1 Princes Risborough, England; March 1973
2 Copenhagen, Denmark; October 1973
3 Delft, Netherlands; June 1974
4 Paris, France; February 1975
5 Karlsruhe, Federal Republic of Germany; October 1975
6 Aalborg, Denmark; June 1976
7 Stockholm, Sweden; February/March 1977
8 Brussels, Belgium; October 1977
9 Perth, Scotland; June 1978
10 Vancouver, Canada; August 1978
11 Vienna, Austria; March 1979
12 Bordeaux, France; October 1979
13 Otaniemi, Finland; June 1980
14 Warsaw, Poland; May 1981
15 Karlsruhe, Federal Republic of Germany; June 1982
16 Lillehammer, Norway; May/June 1983
17 Rapperswil, Switzerland; May 1984
18 Beit Oren, Israel; June 1985
19 Florence, Italy; September 1986
20 Dublin, Ireland; September 1987
21 Parksville, Canada; September 1988
22 Berlin, German Democratic Republic; September 1989

b denotes the subject:

1 Limit State Design
2 Timber Columns
3 Symbols
4 Plywood
5 Stress Grading
6 Stresses for Solid Timber
7 Timber Joints and Fasteners
8 Load Sharing
9 Duration of Load
10 Timber Beams
11 Environmental Conditions
12 Laminated Members
13 Particle and Fibre Building Boards
14 Trussed Rafters
15 Structural Stability
16 Fire
17 Statistics and Data Analysis
18 Glued Joints
100 CIB Timber Code
101 Loading Codes
102 Structural Design Codes
103 International Standards Organisation
104 Joint Committee on Structural Safety
105 CIB Programme, Policy and Meetings
106 International Union of Forestry Research Organisations

c is simply a number given to the papers in the order in which they appear:

Example: CIB-W18/4-102-5 refers to paper 5 on subject 102 presented at the fourth meeting of W18.

Listed below, by subjects, are all papers that have to date been presented to W18. When appropriate some papers are listed under more than one subject heading.

LIMIT STATE DESIGN

TIMBER COLUMNS

6-100-1	Comments on Document 5-100-1, Design of Solid Timber Columns - H J Larsen and E Theilgaard
6-2-1	Lattice Columns - H J Larsen
6-2-2	A Mathematical Basis for Design Aids for Timber Columns - H J Burgess
6-2-3	Comparison of Larsen and Perry Formulas for Solid Timber Columns - H J Burgess
7-2-1	Lateral Bracing of Timber Struts - J A Simon
8-15-1	Laterally Loaded Timber Columns: Tests and Theory - H J Larsen
17-2-1	Model for Timber Strength under Axial Load and Moment - T Poutanen
18-2-1	Column Design Methods for Timber Engineering - A H Buchanan, K C Johns, B Madsen
19-2-1	Creep Buckling Strength of Timber Beams and Columns - R H Leicester
19-12-2	Strength Model for Glulam Columns - H J Blaß
20-2-1	Lateral Buckling Theory for Rectangular Section Deep Beam-Columns - H J Burgess
20-2-2	Design of Timber Columns - H J Blaß
21-2-1	Format for Buckling Strength - R H Leicester
21-2-2	Beam-Column Formulae for Design Codes - R H Leicester
21-15-1	Rectangular Section Deep Beam - Columns with Continuous Lateral Restraint - H J Burgess
21-15-2	Buckling Modes and Permissible Axial Loads for Continuously Braced Columns - H J Burgess
21-15-3	Simple Approaches for Column Bracing Calculations - H J Burgess
21-15-4	Calculations for Discrete Column Restraints - H J Burgess
22-2-1	Buckling and Reliability Checking of Timber Columns - S Huang, P M Yu and J Y Hong
22-2-2	Proposal for the Design of Compressed Timber Members by Adopting the Second-Order Stress Theory - P Kaiser

SYMBOLS

PLYWOOD

11-6-1 Evaluation of Lumber Properties in the United States - W L Galligan and J H Haskell

11-6-2 Stresses Perpendicular to Grain - K Möhler

11-6-3 Consideration of Combined Stresses for Lumber and Glued Laminated Timber (addition to Paper CIB-W18/9-6-4) - K Möhler

12-6-1 Strength Classifications for Timber Engineering Codes - R H Leicester and W G Keating

12-6-2 Strength Classes for British Standard BS 5268 - J R Tory

13-6-1 Strength Classes for the CIB Code - J R Tory

13-6-2 Consideration of Size Effects and Longitudinal Shear Strength for Uncracked Beams - R O Foschi and J D Barrett

13-6-3 Consideration of Shear Strength on End-Cracked Beams - J D Barrett and R O Foschi

15-6-1 Characteristic Strength Values for the ECE Standard for Timber - J G Sunley

16-6-1 Size Factors for Timber Bending and Tension Stresses - A R Fewell

16-6-2 Strength Classes for International Codes - A R Fewell and J G Sunley

17-6-1 The Determination of Grade Stresses from Characteristic Stresses for BS 5268: Part 2 - A R Fewell

17-6-2 The Determination of Softwood Strength Properties for Grades, Strength Classes and Laminated Timber for BS 5268: Part 2 - A R Fewell

18-6-1 Comment on Papers: 18-6-2 and 18-6-3 - R H Leicester

18-6-2 Configuration Factors for the Bending Strength of Timber - R H Leicester

18-6-3 Notes on Sampling Factors for Characteristic Values - R H Leicester

18-6-4 Size Effects in Timber Explained by a Modified Weakest Link Theory - B Madsen and A H Buchanan

18-6-5 Placement and Selection of Growth Defects in Test Specimens - H Riberholt

18-6-6 Partial Safety-Coefficients for the Load-Carrying Capacity of Timber Structures - B Norén and J-O Nylander

19-6-1 Effect of Age and/or Load on Timber Strength - J Kuipers

TIMBER JOINTS AND FASTENERS

13-7-3 International Acceptance of Manufacture, Marking and Control of Finger-jointed Structural Timber - B Norén

13-7-4 Design of Joints with Nail Plates - Calculation of Slip - B Norén

13-7-5 Design of Joints with Nail Plates - The Heel Joint - B Källsner

13-7-6 Nail Deflection Data for Design - H J Burgess

13-7-7 Test on Bolted Joints - P Vermeyden

13-7-8 Comments to paper CIB-W18/12-7-3 "Design of Joints with Nail Plates" - B Norén

13-7-9 Strength of Finger Joints - H J Larsen

13-100-4 CIB Structural Timber Design Code. Proposal for Section 6.1.5 Nail Plates - N I Bovim

14-7-1 Design of Joints with Nail Plates (second edition) - B Norén

14-7-2 Method of Testing Nails in Wood (second draft, August 1980) - B Norén

14-7-3 Load-Slip Relationship of Nailed Joints - J Ehlbeck and H J Larsen

14-7-4 Wood Failure in Joints with Nail Plates - B Norén

14-7-5 The Effect of Support Eccentricity on the Design of W- and WW-Trussed with Nail Plate Connectors - B Källsner

14-7-6 Derivation of the Allowable Load in Case of Nail Plate Joints Perpendicular to Grain - K Möhler

14-7-7 Comments on CIB-W18/14-7-1 - T A C M van der Put

15-7-1 Final Recommendation TT-1A: Testing Methods for Joints with Mechanical Fasteners in Load-Bearing Timber Structures. Annex A Punched Metal Plate Fasteners - Joint Committee RILEM/CIB-3TT

16-7-1 Load Carrying Capacity of Dowels - E Gehri

16-7-2 Bolted Timber Joints: a Literature Survey - N Harding

16-7-3 Bolted Timber Joints: Practical Aspects of Construction and Design; a Survey - N Harding

16-7-4 Bolted Timber Joints: Draft Experimental Work Plan - Building Research Association of New Zealand

17-7-1 Mechanical Properties of Nails and their Influence on Mechanical Properties of Nailed Timber Joints Subjected to Lateral Loads - I Smith, L R J Whale, C Anderson and L Held

17-7-2 Notes on the Effective Number of Dowels and Nails in Timber Joints - G Steck

18-7-1 Model Specification for Driven Fasteners for Assembly of Pallets and Related Structures - E G Stern and W B Wallin

18-7-2 The Influence of the Orientation of Mechanical Joints on their Mechanical Properties - I Smith and L R J Whale

18-7-3 Influence of Number of Rows of Fasteners or Connectors upon the Ultimate Capacity of Axially Loaded Timber Joints - I Smith and G Steck

18-7-4 A Detailed Testing Method for Nailplate Joints - J Kangas

18-7-5 Principles for Design Values of Nailplates in Finland - J Kangas

18-7-6 The Strength of Nailplates - N I Bovim and E Aasheim

19-7-1 Behaviour of Nailed and Bolted Joints under Short-Term Lateral Load - Conslusions from Some Recent Research - L R J Whale, I Smith B O Hilson

19-7-2 Glued Bolts in Glulam - H Riberholt

19-7-3 Effectiveness of Multiple Fastener Joints According to National Codes and Eurocode 5 (Draft) - G Steck

19-7-4 The Prediction of the Long-Term Load Carrying Capacity of Joints in Wood Structures - Y M Ivanov and Y Y Slavic

19-7-5 Slip in Joints under Long-Term Loading - T Feldborg and M Johansen

19-7-6 The Derivation of Design Clauses for Nailed and Bolted Joints in Eurocode 5 - L R J Whale and I Smith

19-7-7 Design of Joints with Nail Plates - Principles - B Norén

19-7-8 Shear Tests for Nail Plates - B Norén

19-7-9 Advances in Technology of Joints for Laminated Timber - Analyses of the Structural Behaviour - M Piazza and G Turrini

19-15-1 Connections Deformability in Timber Structures: a Theoretical Evaluation of its Influence on Seismic Effects - A Ceccotti and A Vignoli

20-7-1 Design of Nailed and Bolted Joints-Proposals for the Revision of Existing Formulae in Draft Eurocode 5 and the CIB Code - L R J Whale, I Smith and H J Larsen

22-7-10 Calculation of Joints and Fastenings as Compared with the International State - K Zimmer and K Lissner

22-7-11 Joints on Glued-in Steel Bars Present Relatively New and Progressive Solution in Terms of Timber Structure Design - G N Zubarev, F A Boitemirov and V M Golovina

22-7-12 The Development of Design Codes for Timber Structures made of Compositive Bars with Plate Joints based on Cyclindrical Nails - Y V Piskunov

22-7-13 Designing of Glued Wood Structures Joints on Glued-in Bars - S B Turkovsky

LOAD SHARING

3-8-1 Load Sharing - An Investigation on the State of Research and Development of Design Criteria - E Levin

4-8-1 A Review of Load-Sharing in Theory and Practice - E Levin

4-8-2 Load Sharing - B Norén

19-8-1 Predicting the Natural Frequencies of Light-Weight Wooden Floors - I Smith and Y H Chui

20-8-1 Proposed Code Requirements for Vibrational Serviceability of Timber Floors - Y H Chui and I Smith

21-8-1 An Addendum to Paper 20-8-1 - Proposed Code Requirements for Vibrational Serviceability of Timber Floors - Y H Chui and I Smith

21-8-2 Floor Vibrational Serviceability and the CIB Model Code - S Ohlsson

22-8-1 Reliability Analysis of Viscoelastic Floors - F Rouger, J D Barrett and R O Foschi

DURATION OF LOAD

3-9-1 Definitions of Long Term Loading for the Code of Practice - B Norén

4-9-1 Long Term Loading of Trussed Rafters with Different Connection Systems - T Feldborg and M Johansen

5-9-1 Strength of a Wood Column in Combined Compression and Bending with Respect to Creep - B Källsner and B Norén

6-9-1 Long Term Loading for the Code of Practice (Part 2) - B Norén

6-9-2 Long Term Loading - K Möhler

6-9-3 Deflection of Trussed Rafters under Alternating Loading during a Year - T Feldborg and M Johansen

TIMBER BEAMS

5-10-1 The Design of Timber Beams - H J Larsen

9-10-1 The Distribution of Shear Stresses in Timber Beams - F J Keenan

9-10-2 Beams Notched at the Ends - K Möhler

11-10-1 Tapered Timber Beams - H Riberholt

13-6-2 Consideration of Size Effects in Longitudinal Shear Strength for Uncracked Beams - R O Foschi and J D Barrett

13-6-3 Consideration of Shear Strength on End-Cracked Beams - J D Barrett and R O Foschi

18-10-1 Submission to the CIB-W18 Committee on the Design of Ply Web Beams by Consideration of the Type of Stress in the Flanges - J A Baird

18-10-2 Longitudinal Shear Design of Glued Laminated Beams - R O Foschi

19-10-1 Possible Code Approaches to Lateral Buckling in Beams - H J Burgess

19-2-1 Creep Buckling Strength of Timber Beams and Columns - R H Leicester

20-2-1 Lateral Buckling Theory for Rectangular Section Deep Beam-Columns - H J Burgess

20-10-1 Draft Clause for CIB Code for Beams with Initial Imperfections - H J Burgess

20-10-2 Space Joists in Irish Timber - W J Robinson

20-10-3 Composite Structure of Timber Joists and Concrete Slab - T Poutanen

21-10-1 A Study of Strength of Notched Beams - P J Gustafsson

22-10-1 Design of Endnotched Beams - H J Larsen and P J Gustafsson

22-10-2 Dimensions of Wooden Flexural Members under Constant Loads - A Pozgai

22-10-3 Thin-Walled Wood-Based Flanges in Composite Beams - J König

22-10-4 The Calculation of Wooden Bars with flexible Joints in Accordance with the Polish Standart Code and Strict Theoretical Methods - Z Mielczarek

ENVIRONMENTAL CONDITIONS

5-11-1 Climate Grading for the Code of Practice - B Norén

6-11-1 Climate Grading (2) - B Norén

9-11-1 Climate Classes for Timber Design - F J Keenan

19-11-1 Experimental Analysis on Ancient Downgraded Timber Structures - B Leggeri and L Paolini

19-6-5 Drying Stresses in Round Timber - A Ranta-Maunus

22-11-1 Corrosion and Adaptation Factors for Chemically Aggressive Media with Timber Structures - K Erler

LAMINATED MEMBERS

6-12-1 Directives for the Fabrication of Load-Bearing Structures of Glued Timber - A van der Velden and J Kuipers

8-12-1 Testing of Big Glulam Timber Beams - H Kolb and P Frech

8-12-2 Instruction for the Reinforcement of Apertures in Glulam Beams - H Kolb and P Frech

8-12-3 Glulam Standard Part 1: Glued Timber Structures; Requirements for Timber (Second Draft)

9-12-1 Experiments to Provide for Elevated Forces at the Supports of Wooden Beams with Particular Regard to Shearing Stresses and Long-Term Loadings - F Wassipaul and R Lackner

9-12-2 Two Laminated Timber Arch Railway Bridges Built in Perth in 1849 - L G Booth

9-6-4 Consideration of Combined Stresses for Lumber and Glued Laminated Timber - K Möhler

11-6-3 Consideration of Combined Stresses for Lumber and Glued Laminated Timber (addition to Paper CIB-W18/9-6-4) - K Möhler

12-12-1 Glulam Standard Part 2: Glued Timber Structures; Rating (3rd draft)

12-12-2 Glulam Standard Part 3: Glued Timber Structures; Performance (3 rd draft)

13-12-1 Glulam Standard Part 3: Glued Timber Structures; Performance (4th draft)

14-12-1 Proposals for CEI-Bois/CIB-W18 Glulam Standards - H J Larsen

14-12-2 Guidelines for the Manufacturing of Glued Load-Bearing Timber Structures - Stevin Laboratory

14-12-3 Double Tapered Curved Glulam Beams - H Riberholt

14-12-4 Comment on CIB-W18/14-12-3 - E Gehri

18-12-1 Report on European Glulam Control and Production Standard - H Riberholt

18-10-2 Longitudinal Shear Design of Glued Laminated Beams - R O Foschi

19-12-1 Strength of Glued Laminated Timber - J Ehlbeck and F Colling

19-12-2 Strength Model for Glulam Columns - H J Blaß

19-12-3 Influence of Volume and Stress Distribution on the Shear Strength and Tensile Strength Perpendicular to Grain - F Colling

19-12-4 Time-Dependent Behaviour of Glued-Laminated Beams - F Zaupa

21-12-1 Modulus of Rupture of Glulam Beam Composed of Arbitrary Laminae - K Komatsu and N Kawamoto

21-12-2 An Appraisal of the Young's Modulus Values Specified for Glulam in Eurocode 5 - L R J Whale, B O Hilson and P D Rodd

21-12-3 The Strength of Glued Laminated Timber (Glulam): Influence of Lamination Qualities and Strength of Finger Joints - J Ehlbeck and F Colling

21-12-4 Comparison of a Shear Strength Design Method in Eurocode 5 and a More Traditional One - H Riberholt

22-12-1 The Dependence of the Bending Strength on the Glued Laminated Timber Girder Depth - M Badstube, W Rug and W Schone

22-12-2 Acid Deterioration of Glulam Beams in Buildings from the Early Half of the 1960s - Prelimination summary of the research project; Overhead pictures - B A Hedlund

22-12-3 Experimental Investigation of normal Stress Distribution in Glue Laminated Wooden Arches - Z Mielczarek and W Chanaj

22-12-4 Ultimate Strength of Wooden Beams with Tension Reinforcement as a Function of Random Material Properties - R Candowicz and T Dziuba

PARTICLE AND FIBRE BUILDING BOARDS

7-13-1 Fibre Building Boards for CIB Timber Code (First Draft) - O Brynildsen

9-13-1 Determination of the Bearing Strength and the Load-Deformation Characteristics of Particleboard - K Möhler, T Budianto and J Ehlbeck

TRUSSED RAFTERS

13-14-3 Comparison of 3 Truss Models Designed by Different Assumptions for Slip and E-Modulus - K Möhler

14-14-1 Wood Trussed Rafter Design - T Feldborg and M Johansen

14-14-2 Truss-Plate Modelling in the Analysis of Trusses - R O Foschi

14-14-3 Cantilevered Timber Trusses - A R Egerup

14-7-5 The Effect of Support Eccentricity on the Design of W- and WW-Trusses with Nail Plate Connectors - B Källsner

15-14-1 Guidelines for Static Models of Trussed Rafters - H Riberholt

15-14-2 The Influence of Various Factors on the Accuracy of the Structural Analysis of Timber Roof Trusses - F R P Pienaar

15-14-3 Bracing Calculations for Trussed Rafter Roofs - H J Burgess

15-14-4 The Design of Continuous Members in Timber Trussed Rafters with Punched Metal Connector Plates - P O Reece

15-14-5 A Rafter Design Method Matching U.K. Test Results for Trussed Rafters - H J Burgess

16-14-1 Full-Scale Tests on Timber Fink Trusses Made from Irish Grown Sitka Spruce - V Picardo

17-14-1 Data from Full Scale Tests on Prefabricated Trussed Rafters - V Picardo

17-14-2 Simplified Static Analysis and Dimensioning of Trussed Rafters - H Riberholt

17-14-3 Simplified Calculation Method for W-Trusses - B Källsner

18-14-1 Simplified Calculation Method for W-Trusses (Part 2) - B Källsner

18-14-2 Model for Trussed Rafter Design - T Poutanen

19-14-1 Annex on Simplified Design of W-Trusses - H J Larsen

19-14-2 Simplified Static Analysis and Dimensioning of Trussed Rafters - Part 2 - H Riberholt

19-14-3 Joint Eccentricity in Trussed Rafters - T Poutanen

20-14-1 Some Notes about Testing Nail Plates Subjected to Moment Load - T Poutanen

20-14-2 Moment Distribution in Trussed Rafters - T Poutanen

20-14-3 Practical Design Methods for Trussed Rafters - A R Egerup

19-17-1 Load Factors for Proof and Prototype Testing - R H Leicester

19-6-2 Confidence in Estimates of Characteristic Values - R H Leicester

21-6-1 Draft Australian Standard: Methods for Evaluation of Strength and Stiffness of Graded Timber - R H Leicester

21-6-2 The Determination of Characteristic Strength Values for Stress Grades of Structural Timber. Part 1 - A R Fewell and P Glos

22-17-1 Comment on the Strength Classes in Eurocode 5 by an Analysis of a Stochastic Model of Grading - A proposal for a supplement of the design concept - M Kiesel

GLUED JOINTS

20-18-1 Wood Materials under Combined Mechanical and Hygral Loading - A Martensson and S Thelandersson

20-18-2 Analysis of Generalized Volkersen - Joints in Terms of Non-Linear Fracture Mechanics - P J Gustafsson

20-18-3 The Complete Stress-Slip Curve of Wood-Adhesives in Pure Shear - H Wernersson and P J Gustafsson

22-18-1 Perspective Adhesives and Protective Coatings for Wood Structures - A S Freidin

CIB TIMBER CODE

2-100-1 A Framework for the Production of an International Code of Practice for the Structural Use of Timber - W T Curry

5-100-1 Design of Solid Timber Columns (First Draft) - H J Larsen

5-100-2 A Draft Outline of a Code for Timber Structures - L G Booth

6-100-1 Comments on Document 5-100-1; Design of Solid Timber Columns - H J Larsen and E Theilgaard

6-100-2 CIB Timber Code: CIB Timber Standards - H J Larsen and E Theilgaard

7-100-1 CIB Timber Code Chapter 5.3 Mechanical Fasteners; CIB Timber Standard 06 and 07 - H J Larsen

8-100-1 CIB Timber Code - List of Contents (Second Draft) - H J Larsen

9-100-1 The CIB Timber Code (Second Draft)

11-100-1 CIB Structural Timber Design Code (Third Draft)

11-100-2 Comments Received on the CIB Code

a U Saarelainen
b Y M Ivanov
c R H Leicester
d W Nozynski
e W R A Meyer
f P Beckmann; R Marsh
g W R A Meyer
h W R A Meyer

11-100-3 CIB Structural Timber Design Code; Chapter 3 - H J Larsen

12-100-1 Comment on the CIB Code - Sous-Commission Glulam

12-100-2 Comment on the CIB Code - R H Leicester

12-100-3 CIB Structural Timber Design Code (Fourth Draft)

13-100-1 Agreed Changes to CIB Structural Timber Design Code

13-100-2 CIB Structural Timber Design Code. Chapter 9: Performance in Fire

13-100-3a Comments on CIB Structural Timber Design Code

13-100-3b Comments on CIB Structural Timber Design Code - W R A Meyer

13-100-3c Comments on CIB Structural Timber Design Code - British Standards Institution

13-100-4 CIB Structural Timber Design Code. Proposal for Section 6.1.5 Nail Plates - N I Bovim

14-103-2 Comments on the CIB Structural Timber Design Code - R H Leicester

15-103-1 Resolutions of TC 165-meeting in Athens 1981-10-12/13

21-100-1 CIB Structural Timber Design Code. Proposed Changes of Sections on Lateral Instability, Columns and Nails - H J Larsen

22-100-1 Proposal for Including an Updated Design Method for Bearing Stresses in CIB W18 - Structural Timber Design Code - B Madsen

22-100-2 Proposal for Including Size Effects in CIB W18A Timber Design Code - B Madsen

22-100-3 CIB Structural Timber Design Code - Proposed Changes of Section on Thin-Flanged Beams - J König

22-100-4 Modification Factor for "Aggressive Media" - a Proposal for a Supplement to the CIB Model Code - K Erler and W Rug

22-100-5 Timber Design Code in Czechoslovakia and Comparison with CIB Model Code - P Dutko and B Kozelouh

LOADING CODES

4-101-1 Loading Regulations - Nordic Committee for Building Regulations

4-101-2 Comments on the Loading Regulations - Nordic Committee for Building Regulations

STRUCTURAL DESIGN CODES

1-102-1 Survey of Status of Building Codes, Specifications etc., in USA - E G Stern

1-102-2 Australian Codes for Use of Timber in Structures - R H Leicester

1-102-3 Contemporary Concepts for Structural Timber Codes - R H Leicester

1-102-4 Revision of CP 112 - First Draft, July 1972 - British Standards Institution

4-102-1 Comparsion of Codes and Safety Requirements for Timber Structures in EEC Countries - Timber Research and Development Association

4-102-2 Nordic Proposals for Safety Code for Structures and Loading Code for Design of Structures - O A Brynildsen

4-102-3 Proposal for Safety Codes for Load-Carrying Structures - Nordic Committee for Building Regulations

4-102-4 Comments to Proposal for Safety Codes for Load-Carrying Structures - Nordic Committee for Building Regulations

4-102-5 Extract from Norwegian Standard NS 3470 "Timber Structures"

4-102-6 Draft for Revision of CP 112 "The Structural Use of Timber" - W T Curry

8-102-1 Polish Standard PN-73/B-03150: Timber Structures; Statistical Calculations and Designing

8-102-2 The Russian Timber Code: Summary of Contents

9-102-1 Svensk Byggnorm 1975 (2nd Edition); Chapter 27: Timber Construction

11-102-1 Eurocodes - H J Larsen

13-102-1 Program of Standardisation Work Involving Timber Structures and Wood-Based Products in Poland

17-102-1 Safety Principles - H J Larsen and H Riberholt

17-102-2 Partial Coefficients Limit States Design Codes for Structural Timberwork - I Smith

18-102-1 Antiseismic Rules for Timber Structures: an Italian Proposal - G Augusti and A Ceccotti

18-1-2 Eurocode 5, Timber Structures - H J Larsen

19-102-1 Eurocode 5 - Requirements to Timber - Drafting Panel Eurocode 5

19-102-2 Eurocode 5 and CIB Structural Timber Design Code - H J Larsen

19-102-3 Comments on the Format of Eurocode 5 - A R Fewell

19-102-4 New Developments of Limit States Design for the New GDR Timber Design Code - W Rug and M Badstube

19-7-3 Effectiveness of Multiple Fastener Joints According to National Codes and Eurocode 5 (Draft) - G Steck

19-7-6 The Derivation of Design Clauses for Nailed and Bolted Joints in Eurocode 5 - L R J Whale and I Smith

19-14-1 Annex on Simplified Design of W-Trusses - H J Larsen

20-102-1 Development of a GDR Limit States Design Code for Timber Structures - W Rug and M Badstube

21-102-1 Research Activities Towards a New GDR Timber Design Code Based on Limit States Design - W Rug and M Badstube

22-102-1 New GDR Timber Design Code, State and Development - W Rug, M Badstube and W Kofent

22-102-2 Timber Strength Parameters for the New USSR Design Code and its Comparison with International Code - Y Y Slavik, N D Denesh and E B Ryumina

22-102-3 Norwegian Timber Design Code - Extract from a New Version - E Aasheim and K H Solli

INTERNATIONAL STANDARDS ORGANISATION

3-103-1 Method for the Preparation of Standards Concerning the Safety of Structures (ISO/DIS 3250) - International Standards Organisation ISO/TC98

4-103-1 A Proposal for Undertaking the Preparation of an International Standard on Timber Structures - International Standards Organisation

5-103-1 Comments on the Report of the Consultion with Member Bodies Concerning ISO/TC/P129 - Timber Structures - Dansk Ingeniorforening

7-103-1 ISO Technical Committees and Membership of ISO/TC 165

8-103-1 Draft Resolutions of ISO/TC 165

12-103-1 ISO/TC 165 Ottawa, September 1979

13-103-1 Report from ISO/TC 165 - A Sorensen

14-103-1 Comments on ISO/TC 165 N52 "Timber Structures; Solid Timber in Structural Sizes; Determination of Some Physical and Mechanical Properties"

14-103-2 Comments on the CIB Structural Timber Design Code - R H Leicester

21-103-1 Concept of a Complete Set of Standards - R H Leicester

JOINT COMMITTEE ON STRUCTURAL SAFETY

3-104-1 International System on Unified Standard Codes of Practice for Structures - Comité Européen du Béton (CEB)

7-104-1 Volume 1: Common Unified Rules for Different Types of Construction and Material - CEB

CIB PROGRAMME, POLICY AND MEETINGS

1-105-1 A Note on International Organisations Active in the Field of Utilisation of Timber - P Sonnemans

5-105-1 The Work and Objectives of CIB-W18-Timber Structures - J G Sunley

10-105-1 The Work of CIB-W18 Timber Structures - J G Sunley

15-105-1 Terms of Reference for Timber - Framed Housing Sub-Group of CIB-W18

19-105-1 Tropical and Hardwood Timbers Structures - R H Leicester

21-105-1 First Conference of CIB-W18B, Tropical and Hardwood Timber Structures Singapore, 26 - 28 October 1987 - R H Leicester

INTERNATIONAL UNION OF FORESTRY RESEARCH ORGANISATIONS

7-106-1 Time and Moisture Effects - CIB W18/IUFRO 55.02-03 Working Party

CIB -W18A / 22-1-1

INTERNATIONAL COUNCIL FOR BUILDING RESEARCH STUDIES AND DOCUMENTATION

WORKING COMMISSION W18A - TIMBER STRUCTURES

RELIABILITY-THEORETICAL INVESTIGATION INTO TIMBER COMPONENTS

A proposal for a supplement of the design concept

by

M Badstube, W Rug and R Plessow
Academy of Building of the GDR
Institute for Industrial Buildings
German Democratic Republic

MEETING TWENTY - TWO

BERLIN

GERMAN DEMOCRATIC REPUBLIC

SEPTEMBER 1989

1. Introduction

Structural components made of timber are being designed by adopting the hitherto prevailing admissible stress method /9/ and the limit states method.
The design according to the limit states method has been accomplished in compliance with the draft of the new GDR Code (TGL 33 135/04 E 89; see /1/) which was largely approximated to the Eurocode 5, E. 10/87 (see /2/).
The components designed by adopting the above-mentioned methods have been subjected to a reliability-theoretical analysis. The calculation (design) covered the safety index β.

2. Dimensioning of the components

The studies and investigations are being carried out by using three components made of quality grade (GK) II sawn coniferous timber (NSH) with the strength grade C 5 according to /2/ which are being exposed to different types of stressing (loading); they are being designed by applying the admissible stress method and the limit states method (see Figure 2).
The calculation is being performed according to /9/ and /1/ for two girders subjected to bending and one eccentrically loaded compression member. The applied characteristic actions (dead load g_k, use load p_k, snow load s_k, wind load w_k), load factors γ and combination factors Ψ can be seen in Figure 3.
The characteristic actions are being applied with both the admissible stress method and the limit states method.
When designing the components by means of the limit states method, the factors being selected are $\gamma_M = 1.4$ as the material factor and $K_{mod,1} = 0.9$ as the modification factor concerning the "period of action". The characteristic values of the strength (characteristic indices are 5%-fractiles from test data obtained with the application of the 3-parametric Weibull distribution) and of the modulus of elasticity can be drawn from Figure 1 for quality grade II sawn coniferous timber (NSH GK II).

Figure 4 includes the check requirements (conditions) and the percentages of utilization of the admissible stresses and of the design values of the strengths for the two design methods. One can see the small consumption of timber when applying the limit states method in the case of the individual examples A and B (girders subjected to bending !). With the example C (flexural compression member !), no economic advantage resulting from the application of the limit states method can be determined.

3. Result of the reliability-theoretical investigations

The components indicated in Figure 2 are being subjected to a reliability-theoretical investigation which is being accomplished according to the first-order reliability theory.

The investigation into the influence of the random scatterings of loads and strengths on the safety and reliability of a load-bearing system is the content of the reliability theory.

In this connection, the prevailing safety level is characterized by the safety index β or an equivalent operative failure probability P_f (see Figure 5). In the reliability theory, loads and strengths are being represented as random (accidental) quantities X_i +). Subject to the accident, a random quantity can adopt various values.
Figure 5 shows distribution densities f (X_i) and the limit state equation for two transformed random quantities X_i.
Up to 7 random quantities are being applied in the calculation and design of the components.
Thus, a 7-dimensional space is available in which each random quantity X_i with its distribution function and distribution density are distributed at random.

The first-order reliability theory is characterized by the fact that in the design point $\hat{P}^*$(see Figure 5) the distribution

+) In the authors' instance, the random quantities X_i are as follows: g, p_1, p_2, s, q, c, f (see Figure 7).

functions of the random quantities are being approximated by normal distributions.
The calculation procedure is the content of the "Beta 10" computer program (see Figure 6).
By means of said program, approximate values of β and P_f are being computed for an arbitrary limit state with stochastically independent random quantities which (i.e. the limit state) is to be entered as a special subprogram. Various distribution functions (normal distribution NV, Weibull distribution WV, logarithmic normal distribution LNV and others) can be taken into consideration.
The program is computing the failure probability according to the normal tail approximation.
The distribution densities of the loads are being drawn from /5/ taking into account /6/ (see Figure 7).
The distribution densities of the strengths are being determined according to /7/ (see Figure 7).
The conversion of the loads into stresses is being accomplished by means of the cross-sectional values which are resulting from the dimensioning (design) for σ_k = zul σ (admissible stress method) and for $\sigma_d = f_d$ +) (limit states method).
The limit state equation (see Figure 5) $\hat{g} = \hat{f} - \hat{\sigma}$ will be prepared for each component and includes up to 7 random quantities (see Figure 8)

The reliability-theoretical design (calculation) produced the following results:

(a) The amount of the safety index β is in the case of the design cross section for σ_k = zul σ :
β = 2.5 up to 4.7 (see Figure 9)
and for $\sigma_d = f_d$:
β = 2.5 up to 3.5 (see Figure 9).

+) σ_k is the stress from the characteristic values of the loads
σ_d is the stress from the design values of the loads
f_d is the design value of the strength

One can see, that the safety index required for all construction methods $_{erf}\beta \geqq 3.5$ of the reliability grade III according to /8/ is lower with part of the investigated timber components.

The safety level for the design (dimensioning) of $\sigma_d = f_d$ (limit states method) is below that of the design of $\sigma_k = {}_{zul}\sigma$ (admissible stress method).

Within the range of $\beta \leqq 3.5$, the shortfall amounts to 0 up to 19 % and is thus still justifiable.

(b) The amount of the failure probability P_f is in the case of the design cross section for $\sigma_k = {}_{zul}\sigma$:

$P_f = 0.001 \cdot 10^{-3}$ up to $6.3 \cdot 10^{-3}$ (see Figure 9)

and for $\sigma_d = f_d$:

$P_f = 0.3 \cdot 10^{-3}$ up to $6.1 \cdot 10^{-3}$ (see Figure 9).

One can see that the failure probability required for all construction methods $_{erf}P_f = 0.23 \cdot 10^{-3}$ of the reliability grade III according to /8/ is being exceeded with nearly all investigated timber components.

(c) The design cross section for $\sigma_d = f_d$ in compliance with the limit states method is based upon the material factor of $\gamma_M = 1.4$.

The results as shown in Figure 9 are largely dependent on the distribution densities of the loads. They are being revised at present. Thus, the results described hereinbefore are only initial orientation data.

4. Summary

The following three timber components are being investigated in terms of the reliability theory:

A) purlin of an industrial building
B) intermediate floor beam of an office building
C) wall frame post of an office building.

In this connection, the design cross sections from the check requirements (conditions) of $\sigma_k = {}_{zul}\sigma$ and $\sigma_d = f_d$ are being assumed.
The safety level prevailing with $\sigma_d = f_d$ (limit states method) is still justifiably below that prevailing with $\sigma_k = {}_{zul}\sigma$ (admissible stress method). The safety level for the admissible stress method is in the case of the investigated timber components in part lower than that of other construction methods. The results and findings cannot be generalized since only a few application examples are available.
With the distribution densities of the loads exercising a considerable influence on the results and findings, the same shall be regarded only for information and orientation purposes.

5. References

/1/ Industrial GDR Code Specification No. TGL 33 135/04 E 89
"Holzbau, Tragwerke, Berechnung, Bauliche Durchbildung"
(Timber construction; Loadbearing systems; Calculation; Structural design)
Draft, September 1989

/2/ Eurocode 5
"Holzbauwerke" - Deutsche Entwurfsfassung
(Timber structures - German draft wording)
October 1987

/3/ Forschungsbericht G 3 "Grenzzustände Holzbau"
(Research report G 3 "Limit states in timber construction")
Academy of Building of the GDR, Institute for Industrial Buildings - Berlin, November 1987

/4/ Kiesel, :
"Beitrag zur Ermittlung der Verteilungsfunktion der Festigkeitseigenschaften des Bauholzes unter besonderer Berücksichtigung des Festigkeitsverhaltens bei der Druckbeanspruchung für eine Bemessung nach der Methode der Grenzzustände"
(Paper on the determination of the distribution function of the strength properties of structural timber with particular consideration of the strength behaviour under compressive stress for a design by adopting the limit states method)
Wismar College of Technology; Research report G 4; Wismar, October 1987

/5/ Spaethe, G.:
"Die Sicherheit tragender Baukonstruktionen"
(The safety of loadbearing building constructions)
Published by: Verlag für Bauwesen - Berlin, 1987

(- 5. References / continued -)

/6/ Steck, G.:
"Die Zuverlässigkeit des Vollholzbalkens unter reiner Biegung"
(The reliability of the solid timber beam subjected to pure bending)
Karlsruhe University; Dissertation (thesis), 1982

/7/ Freingruber, H.-Chr.:
"Anwendung des neuen Sicherheitskonzepts im Bereich des Holzbaues - Vorteile und Vergleich mit der bisherigen Bemessungspraxis Besonderheiten des Holzbaues"
(Application of the new safety concept in the field of timber construction - Advantages and comparison with the hitherto prevailing design practice as to particularities of timber construction)
Published in: ÖJAZ, 132th y., No. 9/1987; Vienna, 1987

/8/ Spaethe, G.:
"Zuverlässigkeitskonzeption für tragende Baukonstruktionen"
(Reliability conception for loadbearing building constructions)
Academy of Building of the GDR; Berlin, September 1986

/9/ Industrial GDR Code Specification No. TGL 33 135/01:
"Holzbau, Tragwerke, Berechnung, Bauliche Durchbildung"
(Timber construction; Loadbearing systems; Calculation; Structural design) - January 1984

/10/ Rug, W.; Badstube, M.; Kofent, W.:
New GDR Timber Design Code - State and Development
CIB W 18 Meeting Twenty-Two, Berlin/GDR

Stressing		Source	Coniferous timber					
			sawn structural timber			glued laminated timber		
			quality grade I	II	III	grade 1	2	3
			Strength grade acc. to Eurocode 5 /2/ C 6	C5	C3	C6	C5	C4
bending	$f_{m,k}$	test 1)	29,6	26,4	23,9	27,9	28,1	27,0
		Euroc. 2)	28,5	24	19	28,5	24	21,5
		specif.	28,5	24	19	28,8	24	21,5 5)
tension	$f_{t,o,k}$	test	22,7	13,1	7,1	---	---	---
		Euroc.	17	14,5	11,5	---	---	---
		specif.	17	14,5	7,1	---	---	---
tension on key-dove-tailed timber	$f_{t,o,k}$	test	---	14,4	---	---	---	---
		Euroc.	---	---	---	---	---	---
		specif.	---	14,4	---	14,4	4,8	14,4
compres-sion	$f_{c,o,k}$	test	22,3	20,4	18,5	---	---	---
		Euroc.	26	21,5	17,5	---	---	---
		specif.	24	21,5	17,5	24	22,3	24
bending	$E_{o,k}$	test	8600	7600	7200	10100	9700	9500
		Euroc.	8550	7440	6650	8550	7440	7095
		specif.	8500	7500	6500	8500	7500	8500
bending	$E_{o,mean}$	test	12300	11300	10500	11500	10800	11000
		Euroc.	12000	11000	9000	12000	11000	10000
		specif.	12000	11000	9000	12000	11000	10000

Figure 1: Characteritic values and mean values of the strength and of the modulus of elasticity, in N/mm^2

Footnotes to Fig. 1:

1) Values from test acc. to /3/ and /4/

2) Values from the Eurocode 5 acc. to /2/

3) Values from the TGL Gdr Code Specification acc. to /1/

4) Grades of glued laminated timber:

Grade 1: All layers consist of sawn coniferous timber (NSH) of the quality grade (GK) II.
The staggering between the Key-dovetail connections (KZV) is always = 250 mm

Grade 2: External layers within the range of 1/6 of the girder depth consist of NSH GK II, internal layers of NSH GK III.
KZV = 250 mm is found only in the external layers.

Grade 3: All layerssconsist of NSH GK II with KZV = 0.

5) $f_{m,c,k} = 24 \frac{N}{mm^2}$

Example	Component	System
A	purlin of an industrial building	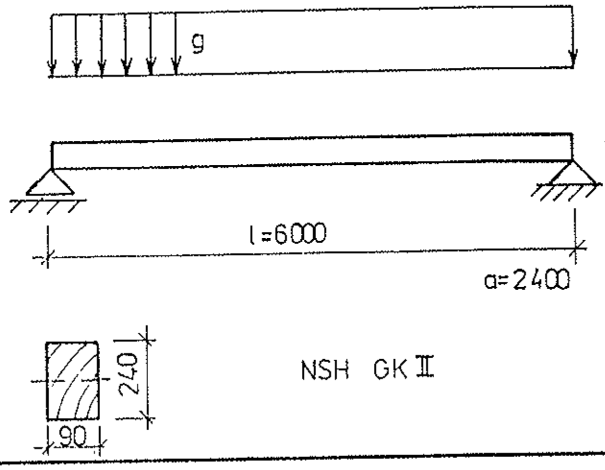
B	intermediate floor beam of an office building	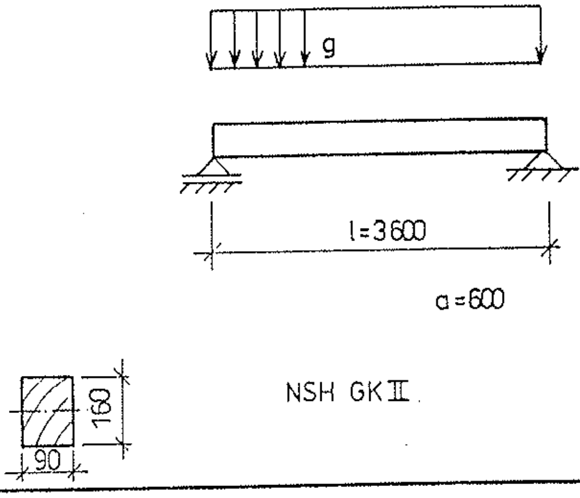
C	wall frame post of an office building	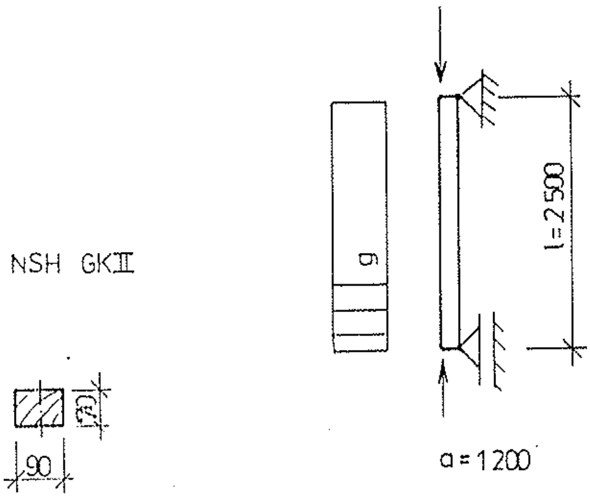

Figure 2: Application examples

Loading	Application example A	B	C
dead load	$g_K = 0{,}27 \ \frac{KN}{m^2}$ $\gamma = 1{,}1$	$g_K = 0{,}95 \ \frac{KN}{m^2}$ $\gamma = 1{,}1$	$g_K = 2{,}3 \ \frac{KN}{m^2}$ $\gamma = 1{,}1$
use load		$p_K = 2{,}75 \ \frac{KN}{m^2}$ $\gamma = 1{,}4$	$p_K = 2{,}75 \ \frac{KN}{m^2}$ $\gamma = 1{,}4$ $\psi = 0{,}9$
snow load	$s_K = K_S \cdot C \cdot s_{0,K}$ $= 1 \cdot 1 \cdot 0{,}5$ $= 0{,}5 \ \frac{KN}{m^2}$ $\gamma = 1{,}4$		$s_K = K_S \cdot C \cdot s_{0,K}$ $= 1{,}01 \cdot 0{,}63 \cdot 0{,}7$ $= 0{,}445 \ \frac{KN}{m^2}$ $\gamma = 1{,}4$ $\psi = 0{,}9$
wind Load			$w_K = C \cdot q_{0,K}$ $= 1 \cdot 0{,}55$ $= 0{,}55 \ \frac{KN}{m^2}$ $\gamma = 1{,}2$ $\psi = 0{,}9$

Combination of the actions in general :

$$S_d = \gamma_G \cdot G_K + \sum \psi_i \cdot \gamma_{Q,i} \cdot Q_{K,i}$$

with $G_K = g$ (here as related to the ground area)

$$Q_{K,i} = p_K \, , s_K \, , w_K$$

Figure 3 : Characteristic actions

Load and combination factors

Example	Admissible stress method acc. to /9/ — check requirement	utilization of admissible σ	Limit states method acc. to /1/ & /2/ — check requirement	utilization of admissible σ
A	$\sigma \leq$ admissible σ_m $9{,}6 < 10 \ \frac{N}{mm^2}$	96%	$\sigma_d \leq f_{m,d}$ $12{,}5 < 15{,}4 \ \frac{N}{mm^2}$	81%
B	$\sigma \leq$ admissible σ_m $9{,}4 < 10 \ \frac{N}{mm^2}$	94%	$\sigma_d \leq f_{m,d}$ $12{,}4 < 15{,}4 \ \frac{N}{mm^2}$	80,5%
C	$\omega \cdot \sigma_c + \frac{\text{admissible } \sigma_{c,o}}{\text{admissible } \sigma_m} \cdot \sigma_m$ $\leq$ admissible $\sigma_{c,o}$ $5{,}6 + 4{,}3 = 9{,}9$ $< 10 \ \frac{N}{mm^2}$	99%	$\frac{1}{K_c} \cdot \sigma_{c,d} + \frac{1}{K_m} \cdot \frac{f_{c,o,d}}{f_{m,d}} \cdot$ $\cdot \sigma_{m,d} \leq f_{c,o,d}$ $7{,}9 + 5{,}8 = 13{,}7$ $< 13{,}8 \ \frac{N}{mm^2}$	99%

Figure 4: Check requirements

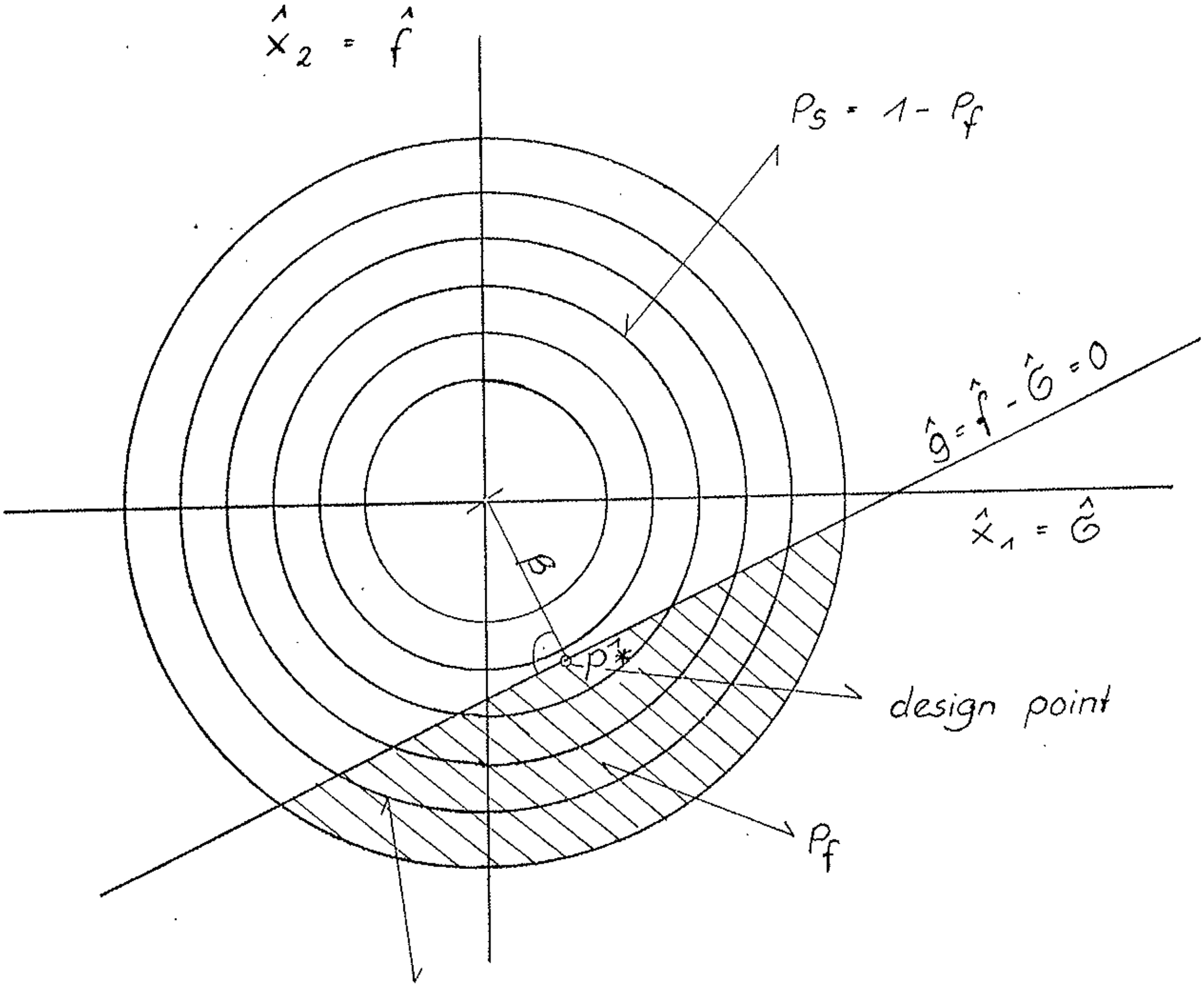

Meanings:

P_S probability of survival

$\hat{\sigma}$ transformed random quantity of the stress

$$\hat{\sigma} = \frac{\sigma - \sigma_{mean}}{s_\sigma} \; ; \quad s_\sigma \text{ standard deviation}$$

s_{mean} mean value

$\hat{f}$ transformed random quantity of the strength

$$\hat{f} = \frac{f - f_{mean}}{s_f} \; ; \quad s_f \text{ standard deviation}$$

f_{mean} mean value

β safety index $\quad \beta = \dfrac{f_{mean} - \sigma_{mean}}{\sqrt{s_f^2 + s_\sigma^2}}$

Figure 5: Representation of the safety index β and of the failure probability P_f for 2 random quantities.

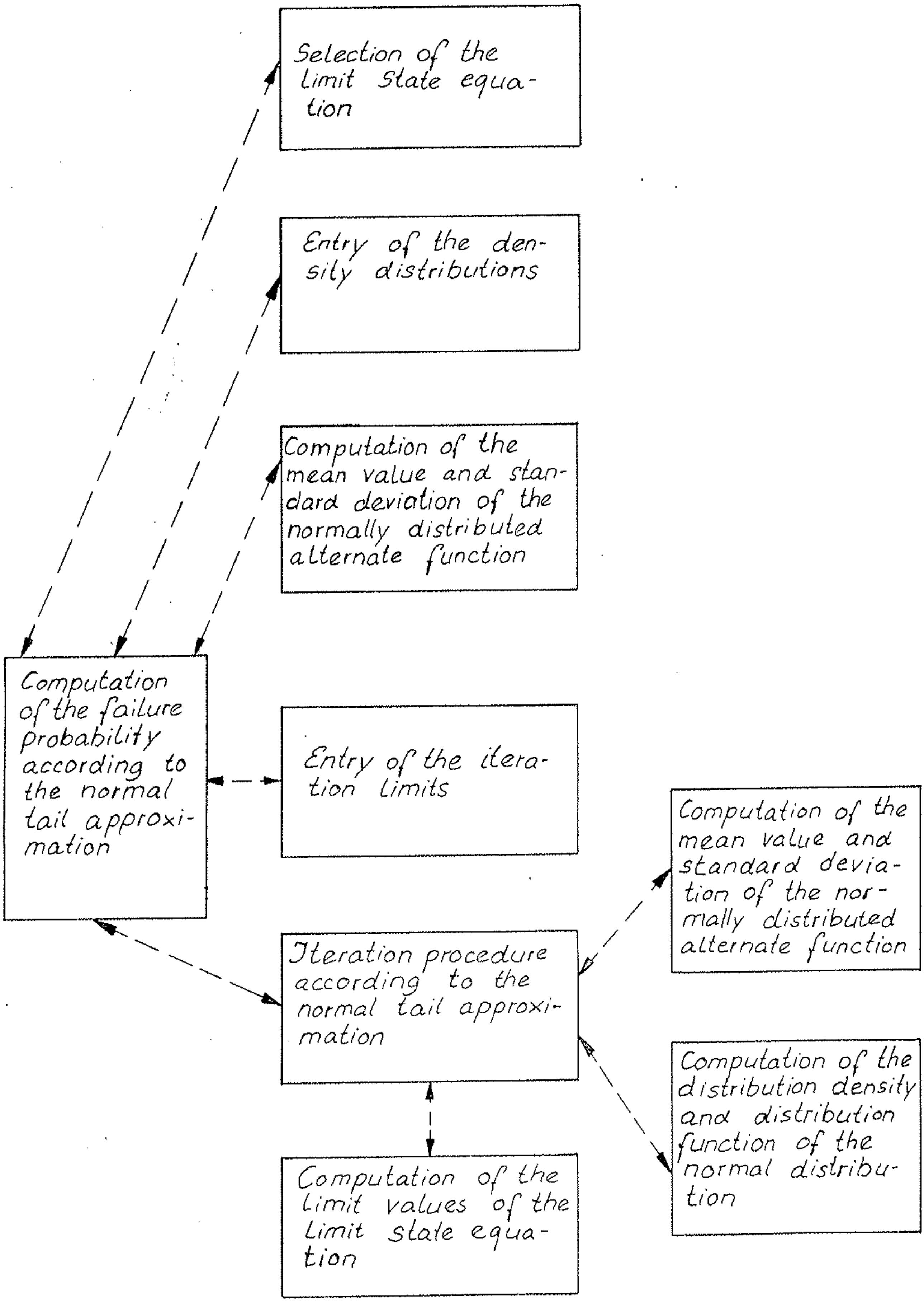

Figure 6: "Beta 10" computer program

Program structure

Random quantity	Application example A	B	C
dead load	$g_{mean} = 0{,}27 \frac{KN}{m^2}$ $v_g = 0{,}1$	$g_{mean} = 1{,}7 \frac{KN}{m^2}$ $v_g = 0{,}1$	$g_{mean} = 2{,}17 \frac{KN}{m^2}$ $v_g = 0{,}1$
long - time use load		$p_{1,mean} = 0{,}75 \frac{KN}{m^2}$ $v_{p_1} = 0{,}47$	$p_{1,mean} = 0{,}75 \frac{KN}{m^2}$ $v_{p_1} = 0{,}47$
short - time use load		$p_{2,mean} = 1{,}24 \frac{KN}{m^2}$ $v_{p_2} = 0{,}9$	$p_{2,mean} = 1{,}24 \frac{KN}{m^2}$ $v_{p_2} = 0{,}9$
snow load	$s_{mean} = 0{,}5 \frac{KN}{m^2}$ $v_s = 0{,}2$		$s_{mean} = 0{,}5 \frac{KN}{m^2}$ $v_s = 0{,}2$
dynamic pressure			$q_{mean} = 0{,}738 \frac{KN}{m^2}$ $v_q = 0{,}21$
aerodynamic coefficient			$c_{mean} = 1$ $v_c = 0{,}1$
strength	$f_{m,mean} = 37 \frac{N}{mm^2}$ $v_f = 0{,}27$ $K_{mod,1} = 0{,}9$	$f_{m,mean} = 37 \frac{N}{mm^2}$ $v_f = 0{,}27$ $K_{mod,1} = 0{,}9$	$f_{c,0,mean} = 32 \frac{N}{mm^2}$ $v_f = 0{,}18$ $K_{mod,1} = 0{,}9$

Meanings:

x_{mean} = mean value , v_x = variation coefficient

Figure 7: Distribution densities of the loads and strengths

Example	Limit state equation
A	$g = f_m \cdot k_{mod,1} - (\sigma_{m,g} + \sigma_{m,s})$
B	$g = f_m \cdot k_{mod,1} - (\sigma_{m,g} + \sigma_{m,p1} + \sigma_{m,p2})$
C	$g = f_{c,0} \cdot k_{mod,1} - (\sigma_{c,0,g} + \sigma_{c,0,p1} + \sigma_{c,0,p2} + \sigma_{c,0,s} + \sigma_{m,w} \cdot c)$

Meanings:

f = Distribution density of the strength. The distribution density is characterized by the mean value and variation coeffizient (see Figure 7).

σ = Distribution density of the stress due to the loads g, p_1, p_2, s, w (see Figure 7).

c = Distribution density of the aerodynamic coeffizient.

Figure 8: Limit state equations

Example	Number of the random quantities	Design cross section for σ_K = admissible σ:		Design cross section for $\sigma_d = f_d$:	
		β (-)	p_f (-)	β (-)	p_f (-)
A	3	4,7	$0{,}001 \cdot 10^{-3}$	3,45	$0{,}28 \cdot 10^{-3}$
B	4	3,15	$0{,}829 \cdot 10^{-3}$	2,64	$4{,}19 \cdot 10^{-3}$
C	7	2,5	$6{,}26 \cdot 10^{-3}$	2,51	$6{,}06 \cdot 10^{-3}$

Figure 9: Calculated values of the safety index β and of the failure probability p_f.

CIB -W18A / 22-2-1

INTERNATIONAL COUNCIL FOR BUILDING RESEARCH STUDIES AND DOCUMENTATION

WORKING COMMISSION W18A - TIMBER STRUCTURES

BUCKLING AND RELIABILITY CHECKING OF TIMBER COLUMNS

by

S Huang, P M Yu and J Y Hong
Chongqing Institute of Architecture and Engineering
Dept. of Civil Engineering
China

MEETING TWENTY - TWO

BERLIN

GERMAN DEMOCRATIC REPUBLIC

SEPTEMBER 1989

BUCKLING AND RELIABILITY CHECKING OF TIMBER COLUMNS

S.Y. Huang, P.M. Yu, J.Y. Hong

Chongqing Institute of Architecture and Engineering
Dept of Civil Engineering, Shapinba, Chongqing, CHINA

ABSTRACT

Based on the results of tests of timber columns in axial compression in China over years, this paper advances two different curves A and B of buckling coefficients related to domestic wood species. The reliability of timber columns for four species are calibrated. These results and conclutions have been contributed to modifying China Code for Timber Structure Design (GBJ 5-73).

INTRODUCTION

In previous Cina Code for timber structure design, the buckling coefficient of the axial compressed columns is determined by using the tangent-modulus theory or Engesser-Karman's reduced-modulus theory, based on the stress-strain relationship of clear wood. That buckling coefficient is a single curve used for various species. That is not completely available for recent situation of China. Because, in China, although the products of timber are not plentiful however there is a lot of species. and all the timber utilized in practice are knotty or other defective. In addition it is found recently that for some species the reliabilities of axially loaded timber columns designed by previous code are less than requirements calculated according to the theory of reliability in building structure. Therefore the suitable value of buckling coefficients should be reasonablely determined.

As early as in 1968, the tests of timber columns made of Yunnan Pine(Pinus yunnanensis Franch.) with knots in contrast with free knots were carried out. Both specimens with knots and without knots were cut from a same log and were nearby reciprocally. However only a few observations was obtained due to the complication of the problem. In 1973, the tests on axially loaded columns of structural timber made of Sichuan Fir (Abies fargesii Franch.) were carried out.

Then a curve of buckling coefficients was proposed preliminarily on the bases of those two tests. However for the columns with the medium slenderness ratio, It seems that the values calculated from proposed curve are remarkable lower than ones from previous code. Thus no convincing observations could be approved at the conference on modifying code in 1973.

The theory of reliability in building structure having been advanced in recent years, failure probability of members can be measured by the value of reliability indices β . In order to use the theory better on timber columns, the tests on axially loaded columns made of Sichuan Fir (structural timber, grade 3.) were carried out again in 1984. Its real aim was to verify futher the curve of buckling coefficients and to research the variability of load-carrying capacity of timber columns in axial compression.

Meanwhere, in the period of 1975-1984, similar tests on some species such as Mumahuang (Casuarina equisetifolia), Longyuanan (Eucalyptus exserta) and Popar (Populus bolleana) were carried out in Guangdong, Xinjiang and other provinces of China, with the unified plan and arrangements from the Working Group Modifying Code for Timber Structure Design. As a result of these tests on a large amount of specimens, not only it has been verified that the curve of buckling coefficients proposed in 1973, is correct, but also it has been found that the curves are related to wood species tested.

According to the theory of reliability in building structure, it is reasonable that the values of reliabilities indices should be substantially equal to each other for various species. Considering the situation of supply and utilization of species in China, then two curves A and B of buckling coefficients of axially loaded timber columns, which are correlative to different species, have been proposed and approved at the meeting in 1985.

BUCKLING COEFFICIENTS

It has been shown in tests that the failure load N_K of axially loaded column is related to three factos. The first one is the geometric characteristics S of the column, such as area A, moment of inertia I of section and length l of the column. The second and third are elastic modulus E and strength f_u of materials. That can be expressed as

$$N_K = \Phi(S, f_u, E)$$

It has also been shown that the column with smaller slenderness ratio fails in breaking off and the stress at failure is mainly related to strength of material otherwise the column with longer slenderness ratio fails in losing stability and the stress at failure is mainly related to elastic modulus of material.

Considering that, a typical analysis is made on the data of tests of short and long columns respectively. A relationship between failure stress σ_K and strength f_u or elastic modulus E of material is obtained respectively:

For short column

$$\sigma_K = \frac{N_K}{A} = k f_u \qquad (1)$$

For long column

$$\sigma_K = \frac{N_K}{A} = t \frac{\pi^2 E}{\lambda^2} \qquad (2)$$

Where the coefficients k and t are respectively equivalent to the reducing coefficients of the strength f_u and elastic modulus E of material of column due to its uneven character of timber. Both can be determined by tests. i.e.

$$k = \frac{\sigma_K}{f_u} \qquad t = \frac{\sigma_K \lambda^2}{E \pi^2}$$

Contrasting Eq.(2) with Eular's formula, we find that tE in Eq.(2) is equivalent to a reduced modulus E_k :

$$E_K = t E = \frac{\sigma_K \lambda^2}{\pi^2}$$

The reduced modulus E_K is only a nominal quantity, involving effect of elasticity as

The curves of buckling coefficients by tests — Table 1

species (local)	quality grade	buckling coefficients: for long column	buckling coefficients: for short and middle-length column	test date	tested by
Yunnan Pine	II	$\frac{3000}{\lambda^2}$	$\frac{1}{1+(\lambda/76.72)^2}$	1968	Sichuan Institute of Building Science Research(SIBSR) and CIAE
Yunnan Pine	I	$\frac{2980}{\lambda^2}$	$\frac{1}{1+(\lambda/76.5)^2}$	1968	Chongqing Institute of Architecture and Engineering(CIAE), SIBSR
Sichuan Fir	II	$\frac{3100}{\lambda^2}$	$\frac{1}{1+(\lambda/67.58)^2}$	1971	SIBSR CIAE
Sichuan Fir	II	$\frac{2994}{\lambda^2}$	$\frac{1}{1+(\lambda/66.29)^2}$	1984	Southwest Institute of Building Design, SIBSR, CIAE
Xinjiang Poplar	II	$\frac{2921}{\lambda^2}$	$\frac{1}{1+(\lambda/62.15)^2}$	1983	Xinjiang Institute of Building Science Research
Guangdong Longyuanan	II	$\frac{2935}{\lambda^2}$	$\frac{1}{1+(\lambda/68.27)^2}$	1984	Guangdong Institute of Building Science Research(GIBSR)
Guangdong Mumahuang	II	$\frac{3410}{\lambda^2}$	$\frac{1}{1+(\lambda/86.59)^2}$	1977	Huanan Institute of Industry GIBSR

well as unevennes of material. It may be called equivalent elastic modulus of the column.

For middle-length columns between long and short columns with various slenderness, the relationship between coefficients k and t can be found by interaction analysis. A coordinate system can be set up with $t=E_K/E$ as vertical ordinate, indicating "long column effect" and with $k=\sigma_K/f_u$ as horizontal axes, indicating "short column effect". Thus, we can obtain a test formula of buckling coefficient of axially loaded timber columns, using the relationship between coefficients k and t from statistics of test data.

Each point shown in Figure 1, is a mean value of group of tested specimens. The t-k relation obtained from tests of axially loaded columns can be represented in a simple form of straight line. As shown in Figure 1.

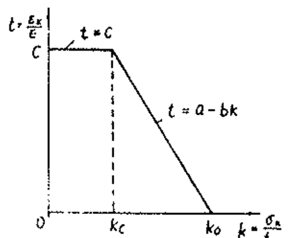

Figure 1.

When $k \le k_c$ $\quad t = c$ (3)

When $k > k_c$ $\quad t = a - bk$ (4)

The intersecting point $k_0=a/b$ of the slant straight line and horizontal axes in Fig.1, indicates the extent of influence of reduction in compression strength parallel to the grain due to material unevenness. The intersecting point t=c of the horizontal straight line and vertical ordinate, indicates the extent of influence of weakness in compression elasticity due to material unevenness. Both k_0 and c are coefficients less than 1.0.

Substituting E_K in Eq.(3) or (4) into Eulor's formula, we have:
For long column

$$\sigma_k = \frac{\pi^2}{\lambda^2}\cdot cE_{15} \qquad (5)$$

For middle-length column

$$\sigma_k = \frac{a\pi^2 E_{15}/\lambda^2}{1+b\pi^2 E_{15}/\lambda^2 f_{15}} \qquad (6)$$

Where E_{15} and f_{15} are compression elasticity modulus and strength parallel to the grain of clear small standard pieces (wood free of defect) with moisture content of 15 percent, respectively.

Then buckling coefficients of axially loaded timber columns are defined as:

$$\varphi = \frac{\sigma_k}{k_0 f_{15}} \qquad (7)$$

From Eqs.(5),(6) and (7), we may get:
For long column

$$\varphi = \frac{c}{k_0}\cdot\frac{\pi^2 E_{15}}{\lambda^2 f_{15}} = \frac{\pi^2 (c/k_0)(E_{15}/f_{15})}{\lambda^2} \qquad (8)$$

For short or middle-length column

$$\varphi = \frac{a\pi^2 E_{15}/\lambda^2 f_{15}}{k_0(1+b\pi^2 E_{15}/\lambda^2 f_{15})} = \frac{1}{1+(\lambda/\pi\sqrt{bE_{15}/f_{15}})^2} \qquad (9)$$

Analysising all the test data of axially loaded timber columns obtained from tests in China,in accordance with the method above mentioned, that is, substituting the c, b and k_0 of that test into Eqs.(8) and (9), we can obtain the buckling coefficients of axially loaded timber columns listed in Table 1.

ESSENTIAL STATISTIC PARAMETERS

The statistic parameters of loads in this paper are taken from the Code, Common Unified Design Standard of Building Structure (GBJ 68-84). Those of resistances are based on reference documents. Others are determined by analysis of related test information.

The influence coefficients K_t, K_0 and K_A take into account respectively the effect of duration of loading, the effect of natural defects of timber and the uncertainty of area of section.

The influence coefficients K_{f15} and K_{E15} take into account respectively the uncertainties of compression strength and elasticity modulus parallel to the grain of clear small standard pieces with moisture content of 15%.

Their average values and the coefficients of variation can be consulted from background.

The reliabilities indices β as final results for four species

Table 2

Slenderness ratio			20	40	60	75	80	91	100
S_k / G_k	0.2	Fir	3.0288	3.1542	3.2130		3.2068	3.0922	3.0922
		Pine	3.7454	3.8907	3.9878	3.7130	3.7130	3.7130	3.7130
		Spruce	3.2676	3.3834	3.4516		3.1555	3.1555	3.1555
		Larch	3.4505	3.4239	3.3296	3.2594	3.2594	3.2594	3.2594
	0.3	Fir	3.0346	3.1571	3.2146		3.2089	3.0993	3.0993
		Pine	3.7401	3.8605	3.9744	3.7116	3.7116	3.7116	3.7116
		Spruce	3.2703	3.3827	3.4490		3.1618	3.1618	3.1618
		Larch	3.4502	3.4225	3.3291	3.2643	3.2643	3.2643	3.2643
	0.5	Fir	3.0036	3.1157	3.1689		3.1652	3.0743	3.0743
		Pine	3.6750	3.8001	3.8841	3.6609	3.6609	3.6609	3.6609
		Spruce	3.2291	3.3306	3.3907		3.1344	3.1344	3.1344
		Larch	3.4004	3.3667	3.2775	3.2329	3.2329	3.2329	3.2329
L_k/G_k	1.5	Fir	3.6542	3.7416	3.7830		3.7811	3.7138	3.7138
		Pine	4.1937	4.2879	4.3516	4.1931	4.1931	4.1931	4.1931
		Spruce	3.8355	3.9133	3.9590		3.7630	3.7630	3.7630
		Larch	3.9729	3.9435	3.8691	3.8435	3.8435	3.8435	3.8435

In addition, consider that the uncertainty of slenderness ratio of columns may be relatively small and it can be neglected.

In order to find the accuracy of calculation of resistance capacity of columns, the tests on axially loaded timber columns made of Sichuan Fir were carried out in 1984. The specimens of columns wre with section of 100x100 mm, and slenderness ratios from 25 to 125. All the specimens were kept indoor, dried in natural climate without air-conditioner, and were in equilibrium moisture content when testing.

The coefficient K_p taking into account the accuracy of calculation of resistance capacity of columns shall be treated as a ratio of failure stress tested to its stress calculated from Eq.(5) or (6).

Based on those tests, so we obtain:

average value of K_p	0.9911
standard deviation of K_p	0.1402
coefficient of variation of K_p	0.1415

It is necessary to point out that the value of coefficient of variation (0.1415) involves the influence of effect of natural defects, for each tested column existing actually defects within the limits of quality criterion of material in code GBJ 5-73. However, the influence of effect of natural defects has already been taken into account in calculation of material strength so that consideration should not be taken repeatedly here. Therefore the coefficient of variation of accuracy of calculation equation for axially loaded timber columns shall be simply taken as

$$\delta_{K_p} = \sqrt{0.1415^2 - \delta_{K_o}^2}$$

RESISTANCE CAPACITIES

Resistance capacity of axial compressed columns can be represented as

$$R = N = \varphi f A$$

Where φ is buckling coefficient which can be determined by Eq.(8) or (9).

Considering the factors influencing resistance capacity, we have respectively:

For long column

$$N = K_p\ \varphi\ (K_o K_t K_{f15} \mu_{f15})\ (K_A A_d)$$

$$= K_p \cdot \frac{c\ \pi^2 (K_t K_{E15} \mu_{E15})}{k_o \lambda^2 (K_t K_{f15} \mu_{f15})} (K_o K_t K_{f15} \mu_{f15})\ (K_A A_d)$$

$$= K_p \cdot \frac{c\ \pi^2}{k_o \lambda^2} (K_o K_t K_{E15} \mu_{E15})\ (K_A A_d)$$

For short or middle-length column

$$N = K_p \cdot \frac{K_o K_t K_{f15} \mu_{f15}}{1 + [\lambda^2 K_t K_{f15} \mu_{f15}] / [b \pi^2 K_t K_{E15} \mu_{E15}]} (K_A A_d)$$

Where K_p, K_o, K_t, K_{f15}, K_{E15} and K_A are treated as random variables independent reciprocally; A_d is design value of section area of column; μ_{f15} and μ_{E15} are mean values of compression strength and elasticity modulus parallel to the grain with moisture content of 15 percent respectively.

Mean value of resistance capacities is:

For long column

$$\mu_N = \frac{c\ \pi^2}{k_o \lambda^2} A_d \mu_{E15} \cdot K_p K_o K_t K_A K_{E15} \Big|_{\mu}$$

For short or middle-length column

$$\mu_N = (K_p\ K_o K_t K_{f15} K_A) \Big|_{\mu} \frac{1}{1 + (\lambda / \lambda_c)^2} \mu_{f15} A_d$$

Where

$$\lambda_c = \pi \sqrt{b\ \frac{K_{E15} \mu_{E15}}{K_{f15} \mu_{f15}} \Big|_{\mu}}$$

Design value of resistance capacities can be calculated as follows

$$N_d = \varphi_d\ f_c\ A_d \tag{10}$$

that is:

for long column

$$N_d = \varphi_d\ f_c A_d = \frac{c_1}{\lambda^2} f_c\ A_d$$

for short or middle-length column

$$N_d = \varphi_d\ f_c\ A_d = \frac{1}{1 + (\lambda / c_2)^2} f_c\ A_d$$

Where φ_d is determined by one of buckling coefficient curves defined in code GBJ 5-88 according to wood species; f_c is design value of compression strength parallel to the grain.

For resistance capacities the ratio of mean value to design value may be notated as

$$K_R = \mu_N / N_d$$

and they may be represented as respectively:

for long column

$$K_R = (K_p K_o K_t K_A K_{E15}) \Big|_{\mu} \frac{c \pi^2 \mu_{E15}}{c_1 k_o f_c} \tag{11}$$

for short or middle-length column

The curves of buckling coefficients of timber columns in code GBJ 5-88 Table 3

wood species in Chinese	* in Latin	strength grade		buckling coefficients
Bomu, Dongbeiluoyesong*	*Larix gmelini	TC17	Curve A	$\lambda \leqslant 75$ $\varphi = \frac{1}{1+(\lambda/80)^2}$
Tieshan*, Yulinyunshan Xinanyunshan*	*Tsuga spp. *Picea purpurea	TC15		
Limu*, Qinggang	*Quercus spp.	TB20		$\lambda > 75$ $\varphi = 3000/\lambda^2$
Maweisong, Hongsong*, Zhanzisong Xinjiangluoyesong, Yunnansong*	*Pinus spp. *P. yunnanensis	TC13	Curve B	$\lambda \leqslant 91$ $\varphi = \frac{1}{1+(\lambda/65)^2}$
Xibeiyunshan*, Xinjiangyunshan* Shanmu, Lengshan*	*Picea asperata *Abies spp.	TC11		
Shuiqulíu*	*Fraxinus mandshurica	TB17		$\lambda > 91$ $\varphi = 2800/\lambda^2$
Huamu*	*Betula spp.	TB15		

$$K_R = (K_p K_o K_t K_A K_{f15})\big|_\mu \ (\mu_{f15}/f_c)\,[1+(\lambda/c_2)^2] \,/\, [1+(\lambda/\lambda_c)^2] \tag{12}$$

Since K_p, K_o, K_t, K_A, K_{E15} and K_{f15} in above equations are treated as random variables which are independent of each other, notated as X_i, then the coefficient of variation of resistance capacities can be calculated by following relations

$$\delta_R = \delta_N = \sqrt{\sum\left(\frac{X_i}{\mu_N}\cdot\frac{\partial N}{\partial X_i}\Big|_\mu\right)^2 \delta_{X_i}^2}$$

For long column,

$$\delta_R = \sqrt{\delta_{K_p}^2+\delta_{K_o}^2+\delta_{K_t}^2+\delta_{K_A}^2+\delta_{K_{E15}}^2} \tag{13}$$

and for short or middle-length column,

$$\delta_R = \left[\delta_{K_p}^2+\delta_{K_o}^2+\delta_{K_A}^2+\delta_{K_t}^2+\left[\frac{1}{1+(\lambda/\lambda_c)^2}\right]^2\delta_{K_{f15}}^2 + \left[\frac{1}{1+(\lambda_c/\lambda)^2}\right]^2\delta_{K_{E15}}^2\right]^{\frac{1}{2}} \tag{14}$$

Using Eqs.(11), (12), (13), and (14), we can calculate K_R and δ_R for various species, such as Fir, Pine, spruce and Larch in this paper.

CHECKING COMPUTATIONS FOR THE RELIABILITY

The reliability of axially loaded timber columns can be calculated with 'check point method' suggested in Common Unified Design Standard of Building Structure (GBJ 68-84). Three factors, which are permanent load, snow load (or living load on the floor of office building) and resistance capacities, are treated as random variables independent reciprocally.

Their probability distributions and statistic parameters are assumed as follows:

Permanent load, Normal distribution, $\mu_G/G_k = 1.06$, $\delta_G = 0.07$;

Snow load, Extreme value distribution of type 1, $\mu_S/S_K = 1.139$, $\delta_S = 0.225$;

Living load on the floor of office building, Extreme value distribution of type 1, $\mu_L/L_k = 0.70$, $\delta_L = 0.29$;

Resistance capacity, Logorithmic Normal distribution, $\mu_R/N_d = K_R$ and δ_R are obtained from Eqs.(11),(12),(13) and (14).

According to the design method of ultimate limit state based-probability, in the code for timber structure design, in ordinary cases the axially loaded columns should be satisfied the following condition:

$$1.2\, N_{G_k} + 1.4\, N_{Q_k} = N_d$$

Where :
N_{G_k} and N_{Q_k} are criterion values of the effects of actions due to permanent and living load respectively;

1.2 and 1.4 are partial coefficients for permanent and living load respctively;

N_d is design value of resistance capacity determined by Eq.(10).

Based on above information, μ_G, μ_S, μ_R, δ_G, δ_S and δ_R, the reliability index β, listed in Table 2, can be obtained by means of 'check point method' suggested in code (GBJ 68-84).

CONCLUSIONS

After computation of checking reliability of axially loaded timber columns, it has been shown in Table 2 that the reliabilities indices β of timber columns made of Sichuan Fir, Yunnan Pine, Spruce and Northeast Larch are substantially approximated to each other and specially, it is rather well for same species at various slenderness retios and finally, it is confirmed that the curves, A and B, of buckling coefficients of axial compressed timber columns in the new code, GBJ 5-88, listed in Table 3, are available for their corresponding wood species.

REFERENCES

[1] Working Group Modifying the Code for Timber Structure Design, "tests on the axial compressed columns with knots of Yunnan Pine and Sichuan Fir", YEJIN JIANZHU No.7, 1975.

[2] S.Y. Huang, "A report of experimental research on stability of timber members in axial compression", JOURNAL OF CHONGQING INSTITUTE OF ARCHITECTURE AND ENGINEERING No.3, No.4, 1986.

CIB -W18A / 22-2-2

INTERNATIONAL COUNCIL FOR BUILDING RESEARCH STUDIES AND DOCUMENTATION

WORKING COMMISSION W18A - TIMBER STRUCTURES

PROPOSAL FOR THE DESIGN OF COMPRESSED TIMBER MEMBERS BY ADOPTING THE SECOND-ORDER STRESS THEORY

by

P Kaiser
Wismar College of Technology
Section of Construction Engineering Technology
German Democratic Republic

MEETING TWENTY - TWO

BERLIN

GERMAN DEMOCRATIC REPUBLIC

SEPTEMBER 1989

0. Introduction

In the GDR, for several years work is being accomplished with a view to replacing the admissible stress method by the limit states design method. In terms of the limit state of the loadbearing capacity, the design (calculation) shall prevent the loss of the strength or of the stability of a structure.

At an international and national scale, there is a trend towards an application of the second-order stress theory in the design of compressed members where by means of a magnification factor the moment from the first-order theory is being increased to the moment according to the second-order theory. This approach has already been introduced into the specifications of steel construction and of concrete construction as well. The application of a magnification factor also in timber construction will result in providing the possibility of a uniform design code specification for the three main building materials.

A proposal is being made for the design of compressed members with the incorporation of the knowledge and findings concerning

- the limit states method,
- the second-order stress theory,
- the long-term behaviour of the timber (creep behaviour).

1. Proposal for the design of compressed members

The limit state of the loadbearing capacity is regarded as reached if at the compressed edge of the cross section the design value of the compression strength is achieved.

The equation to be used at the limit state of the loadbearing capacity is as follows:

$$\sigma_c * (1 + m * \eta_{cr} * k_\rho) = \sigma_c * (1 + m * \eta_{cr\rho}) \leq R_{c0}$$
$$\sigma_c * (1 + m_0 * \eta_{cr\rho}) + \sigma_m * \eta_{cr\rho} \leq R_{c0} \quad (1)$$

where

R_{c0}	is the design value of the compression strength;	$R_{c0} \mathrel{\hat{=}} f_{c0}$
σ_c	is the compressive stress;	$\sigma_c = N_c / A$
m	is the eccentricity dimension;	$m = m_0 + m_p$
m_0	is the random eccentricity dimension;	
m_p	is the eccentricity dimension due to additional flexural stressing;	$m_p = \sigma_m / \sigma_c$
σ_m	is the additional bending stress;	
η_{cr}	is the magnification factor depending on the ratio of R_E / σ_c;	
k_ρ	is the factor for considering the long-term behaviour depending on the ratio of $R_E / \sigma_{c,A}$;	
R_E	is the Euler's stress;	$R_E \mathrel{\hat{=}} \sigma_E$
$\sigma_{c,A}$	is the compressive stress due to permanent load.	

2. Explanations to the proposal

2.1. On the magnification factor η_{cr} or $\eta_{cr\rho}$, respectively

The magnification factor η_{cr} serves for the determination of the moment according to the second-order theory.

$$M^{II} = M^{I} * \eta_{cr}$$

η_{cr} is being determined by solving the differential equation of the bending line (elastic curve) as follows:

$$\eta_{cr} = \frac{R_E / \sigma_c + k_M}{R_E / \sigma_c - 1} \qquad (2)$$

When taking into consideration the ratio of the permanent load to the total load $k_c = \sigma_{c,A} / \sigma_c$, the following applies to the magnification factor depending on k_c:

$$\eta_{cr} = \eta_{cr}\left(\frac{R_E}{\sigma_c}\right) * k_\rho\left(\frac{R_E}{\sigma_{c,A}}\right) = \eta_{cr}\left(\frac{R_E}{\sigma_c}\right) * k_\rho\left(\frac{R_E}{k_c * \sigma_c}\right) \qquad (3)$$

With regard to the cases mentioned hereinafter, the following is applicable:

$$k_c = 0 \longrightarrow \eta_{cr\rho} = \eta_{cr}\left(\frac{R_E}{\sigma_c}\right) \quad ; \quad k_\rho = 1$$

$$k_c = 1 \longrightarrow \eta_{cr\rho} = \eta_{cr}\left(\frac{R_E}{\sigma_c}\right) * k_\rho\left(\frac{R_E}{\sigma_c}\right)$$

2.2. On the factor k_ρ

The factor k_ρ implies the increase of the member deflection due to flexural creep for a period of 50 years.

In the case of short-term loading, the elastic deflection f_{el} is to be determined from the magnitude of the pre-deformation f_0 and the magnitude of the ratio of R_E / σ_c.

$$f_{el} = f_0 * (\eta_{cr} - 1)$$

with $$\eta_{cr} = \frac{N * (f_0 + f_{el})}{N * f_0}$$

$$= 1 + \frac{f_{el}}{f_0}$$

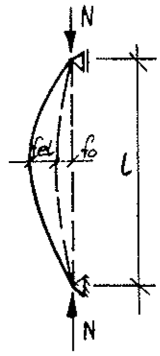

Figure 1

If loadings are acting for a longer period, additional deflections due to creep will occur.

$$f_k = \rho * f_{el}$$

where ρ is a coefficient of creep according to a function developed by Gressel for constant climatic conditions and a loading degree of 20 to 30 %.

$$\rho = 1.032 * (1 - \exp-(t/22013)^{0.54986})$$

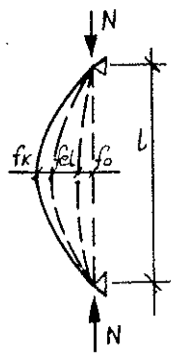

Figure 2

The increase of the deflection due to f_k results also in an increase of the elastic deflection f_{el}. The total elastic deflection is being determined with an application of the pre-deformation f_0 and the creep deformation f_k as follows:

$$f_{el} = (f_0 + f_k) * (\eta_{cr} - 1)$$

The increase of the elastic deflection Δf is again causing a creep deflection.

$$f_k = \rho * \Delta f$$

The creep deflection due to the first elastic deflection is further continuing.

The total period (duration) of the loading is being logarithmically subdivided into 10 time intervals. The increase of the deflections will be considered for each interval.

The magnification factor $\eta_{cr\rho}$ with a long-term loading is to be determined according to the following equation:

$$\eta_{cr\rho} = \frac{f_{tot}}{f_0} = \frac{f_0 + \rho_{10} * \Delta f_1 + \rho_9 * \Delta f_2 + \ldots + \rho_2 * \Delta f_9 + \rho_1 * \Delta f_{10}}{f_0} * \eta_{cr} \qquad (4)$$

Thus, the factor k is as follows:

$$k_\rho = \frac{\eta_{cr\rho}}{\eta_{cr}} = 1 + \frac{\rho_{10} * \Delta f_1 + \rho_9 * \Delta f_2 + \ldots + \rho_2 * \Delta f_9 + \rho_1 * \Delta f_{10}}{f_0} \qquad (5)$$

2.3. Assumption of a random eccentricity dimension m_0

Vicariously for geometrical and structural imperfections, the maximum random eccentricity m_0 with a sinusoidal pre-curvature (pre-deflection) of the member is being applied.

The eccentricity dimension m_0 is defined as the ratio of the maximum member curvature f_0 to the heart width k ($\hat{=}$ r) of the cross section.

As for m_0, the values determined by Möhler are being used.

$$m_0 = 0.1 + \lambda / k_0 \qquad (6)$$

Table 1: Values of k_0

Quality class (grade)	I	II	III
Square timber	230	140	70
Round timber	200	125	50
Glued laminated timber		250	

2.4. Inclusion of additional loadings due to bending moments

If additional bending moments are occurring with a compressed member, they are being attributed to an additional planned eccentricity e_p.

$$\sigma_m = \frac{M^I}{W} \quad ; \quad \sigma_c = \frac{N_c}{A}$$

$$e_p = \frac{M^I}{N_c} = \frac{\sigma_m * W}{\sigma_c * A} = \frac{\sigma_m}{\sigma_c} * k$$

$$m_p = \frac{e_p}{k} = \frac{\sigma_m}{\sigma_c} \qquad (7)$$

Subject to the shape of the moment diagram, the shape factor k_M is to be considered in the magnification factor η_{cr}. The value of k_M is identical with the Dischinger's value of δ.

$$cr = \frac{R_E / \sigma_c + k_M}{R_E / \sigma_c - 1} = \frac{M_{add} + N * f_0 + N * v}{M_{add} + N * f_0}$$

3. Comparison with the CIB Code or EUROCODE 5, respectively

With a view to enabling a comparison between the proposed equation (1) as mentioned hereinbefore and the equation (5.1.7. a) as included in the CIB Code, the following is being specified:

- The loadbearing capacity of the cross section is exhausted if R_{c0} is being reached at the compressed edge.
- The eccentricity dimension m_0 in equation (1) is identical with $\eta * \lambda$ in equation (5.1.7. a) of the CIB Code.
  With the factors as per EUROCODE 5, the following applies:
  for solid timber: $\eta = 0.006 \longrightarrow m_0 = \lambda/166.7$
  for glued laminated timber: $\eta = 0.004 \longrightarrow m_0 = \lambda/250$

- In the CIB Code, the long-term behaviour is being considered only by an assignment of the actions to a class of the load action period. A consideration of the increase of the deflection and thus of the moment due to material creep is not included in the CIB Code.
  This is the reason why the comparison is being accomplished without considering the creep deflection. The following applies: $k_\rho = 1$.
- Related (reference) values are being introduced as follows:
  $\varkappa_c = \sigma_c / R_{c0}$; $\varkappa_m = \sigma_m / R_{c0}$; $\varkappa_E = R_E / R_{c0}$

Thus, the equations read as follows:

$$\varkappa_{(1)} = \varkappa_c * \left(1 + m_0 * \frac{\varkappa_E}{\varkappa_E - \varkappa_c} \right) + m * \frac{\varkappa_E}{\varkappa_E - \varkappa_c} \leqq 1 \qquad (1^*)$$

$$\varkappa_{(CIB)} = \frac{\varkappa_c}{k_c} + \varkappa_m * \frac{1}{1 - k_c * \frac{\varkappa_c}{\varkappa_E}} \leqq 1 \qquad (5.1.7.a^*)$$

As for the maximum utilization of the cross section ($\varkappa = 1$), the following applies according to equation (1^*) and according to equation ($5.1.7.\ a^*$):

$$\max \varkappa_c = A - \sqrt{A^2 - \varkappa_E * (1 - \varkappa_m)}$$

with $\qquad A = 0.5 * (\varkappa_E * (1 + m_0) + 1 + k_M * \varkappa_m)$

For $k_M = 0$, it is $A = 0.5 * (\varkappa_E * (1 + m_0) + 1)$

The two equations are identical. This is also being illustrated by Figure 3 for an example which is based on the regulations included in Specification No. 174/88 of the State Building Supervision Authority of the GDR.

On the chance that the cross section is not being utilized up to a maximum degree ($\varkappa \neq 1$), the stress components for compressive and flexural stressing are being determined in a different way.

The magnification factors for the compressive stress

$$\frac{1}{k_c} \qquad \text{and} \qquad 1 + m * \frac{\varkappa_E}{\varkappa_E - \varkappa_c}$$

as well as for the bending stress

$$\frac{1}{1 - k_c * \frac{\varkappa_c}{\varkappa_E}} \qquad \text{and} \qquad \frac{\varkappa_E}{\varkappa_E - \varkappa_c}$$

are not identical.

The determination of the value of k_c in the CIB Code is based on the assumption that $\varkappa_{(CIB)}$ is equal to 1; thus the compressive stresses are being too much increased by k_c.

By means of the example for $\lambda = 100$, the difference is demonstrated in Figure 4.

4. Summary

As compared with the design formulae applied hitherto in timber construction, the proposed equation (1) is based on the limit states method with a direct application of the second-order theory by means of a magnification factor η_{cr}.

The determination of the stresses is being accomplished in a general form according to

$$\sigma = \sigma_c + \eta_{cr} * \sigma_m.$$

Thus, the stresses and strains are strictly divided into compressive stresses and bending stresses.

The bending stress component resulting from the random eccentricity m_0 ($\hat{=} \eta * \lambda$) is also being included in the bending stresses and not in the compressive stresses, such as - for instance - by means of a factor of $1/k_c$. Since k_c is being determined on the assumption of a full utilization of the cross section, the compressive stress component is always being too much increased.

Equation (1) is proposed to be applied as the design form with a view to thus indicating the stress components in a more actual or real way.

As to the determination of the random eccentricity m_0, a differentiation according to Table 1 included hereinbefore is regarded to be significant and useful.

An additional direct consideration of creep deformations due to loads acting for a long period has not transpired from the bibliography. Here the application of the factor k_ρ is being proposed.

Figure 5 covers a comparison of the present proposal with the CIB Code by means of the example of quality class II sawn coniferous timber.

Said comparison is based on the values included in the Specification No. 174/88 of the State Building Supervision Authority of the GDR for the present proposal and for the CIB Code.

A differentiation in terms of time classes is being accomplished. The following modification factors $\gamma_{d,1}$ concerning "Long-term behaviour at the limit state of the loadbearing capacity (GZT)" and the following components of $k_c = \sigma_{c,A} / \sigma_c$ are applicable:

Time class	$\gamma_{d,1}$	k_c
A	0.85	$1 \geqq k_c > 0.85$
B	1	$0.85 \geqq k_c > 0.15$
C	1.2	$0.15 \geqq k_c \geqq 0$

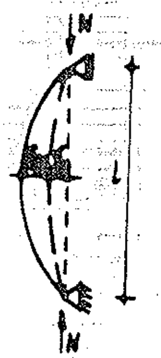

Figure 1

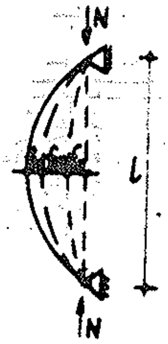

Figure 2

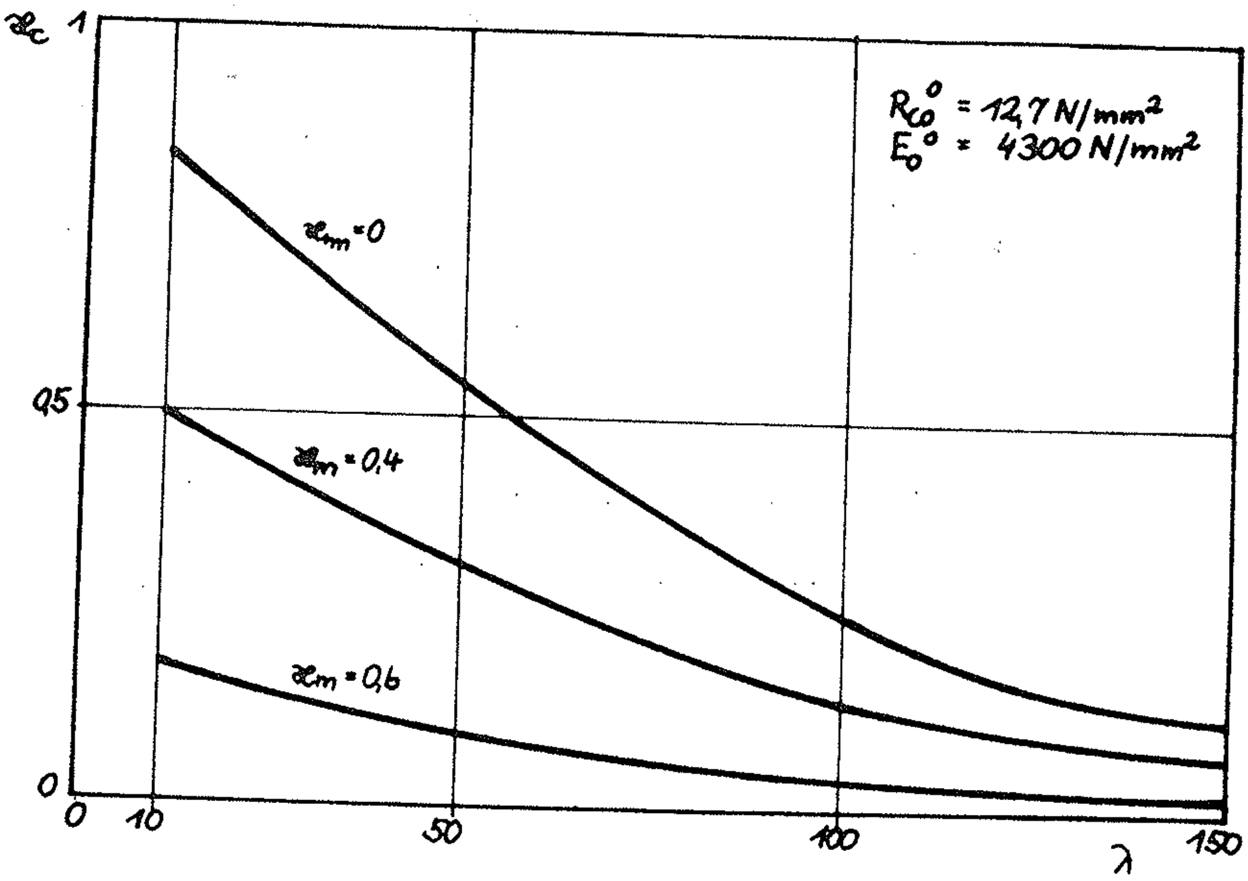

Figure 3: Dependence of $\varkappa_c$ on λ for different $\varkappa_m$ ($K_M = 0$)

(for quality class II sawn structural timber of the time class C)

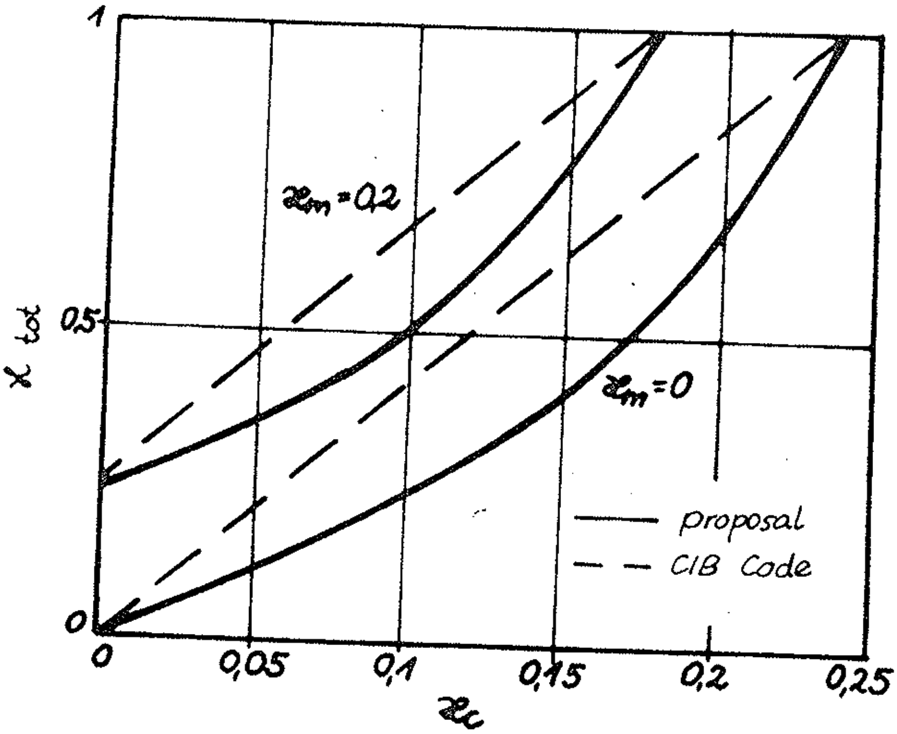

Figure 4: Comparison in terms of the components of $\varkappa_c$ and $\varkappa_m$ in $\varkappa_{tot}$ for $\lambda = 100$

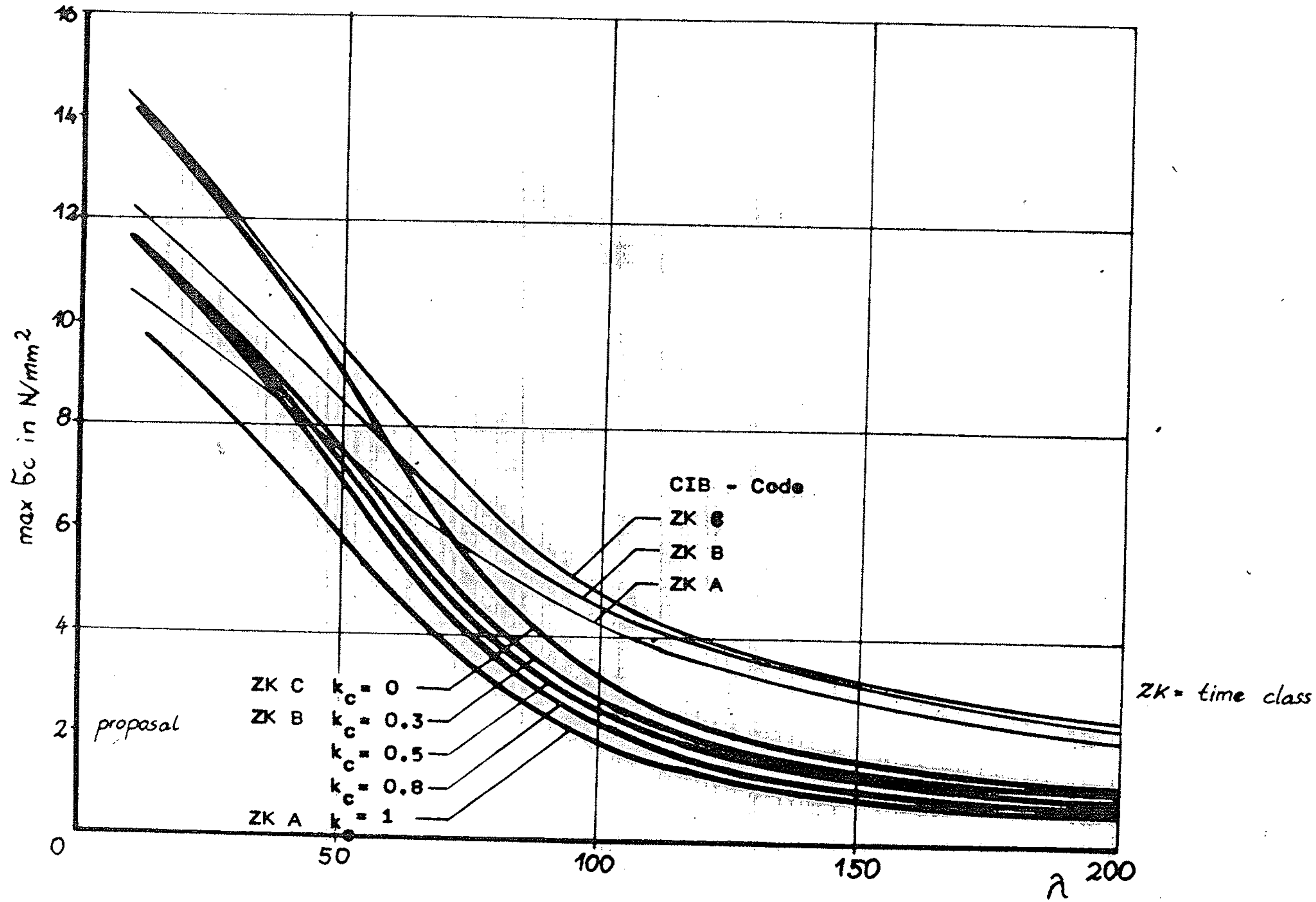

Figure 5: Dependence of max σ_c on λ acc. to the proposal and acc. to the CIB Code

CIB -W18A / 22-4-1

INTERNATIONAL COUNCIL FOR BUILDING RESEARCH STUDIES AND DOCUMENTATION

WORKING COMMISSION W18A - TIMBER STRUCTURES

SCIENTIFIC RESEARCH INTO PLYWOOD AND PLYWOOD BUILDING CONSTRUCTIONS THE RESULTS AND FINDINGS OF WHICH ARE INCORPORATED INTO CONSTRUCTION STANDARD SPECIFICATIONS OF THE USSR

by

I M Guskov
Moscow Civil Engineering Institute (MISI)
Faculty of Timber and Plastic Constructions
USSR

MEETING TWENTY - TWO

BERLIN

GERMAN DEMOCRATIC REPUBLIC

SEPTEMBER 1989

SCIENTIFIC RESEARCH INTO PLYWOOD AND PLYWOOD BUILDING CONSTRUCTIONS THE RESULTS AND FINDINGS OF WHICH ARE INCORPORATED INTO CONSTRUCTION STANDARD SPECIFICATIONS OF THE U.S.S.R.

By Dr. I. M. Guskov,
Moscow Civil Engineering Institute (MISI) "V. V. Kuibyshev",
Faculty of Timber and Plastic Constructions,
Moscow / USSR

The building industry of the USSR is widely using glued birch and larch plywood of the grade "FSF" and bakelite-impregnated plywood of the grade "FBS" being manufactured of birch veneer similar to the glued veneer with an increased pressure and being provided with a surface which is protected from moisture. In addition to plywood panels, plywood pipes, plywood section girders and other sections are being used as building materials.

The basic data and values included in the construction standard specification SNiP II-25-80 "Planning and Design Standards. Timber Constructions" for the calculation and design of glued plywood building constructions have been obtained as a result of comprehensive research works performed in the USSR.

For several years, at the MISI "V. V. Kuibyshev" institute investigations into the strength and deformation of glued birch plywood of the "FSF" grade are being performed with different types of the one-dimensional (linear) state of stress taking into consideration the load action period (duration) and the influence of moisture.

Tests and investigations carried out by G. P. Makarov applied to the strength and deformability of glued plywood having a thickness of 10 mm with transverse bending in the plane of the plywood panel and perpendicular to the plane but also with tension and compression in the plane. The values of the strength properties and elasticity characteristics of the plywood with the indicated types of short-term load action as well as considering the grain direction in the external layers of the plywood are shown in Table 1 hereinafter.

Table 1

Type of the state of stress	Strength and elasticity characteristics of the structural plywood	Grain direction of the external veneer plies to the longitudinal axes of the test specimens, α (degrees)				
		0	15	45	75	90
tension	ultimate strength, MPa	77,5	48,5	23,4	38,9	64,0
	modulus of elasticity, MPa	11560	8224	3596	6540	10800
	transverse deformation coefficient	0,174	0,43	0,505	0,449	0,058
compression	ultimate strength, MPa	50,5	43,6	31,0	36,4	46,0
	modulus of elast., MPa	11140	8230	3445	6570	10000
	transverse deform. coeff.	0,127	0,351	0,625	0,334	0,081
bending in the panel plane	ultimate strength, MPa	77,5	48,0	26,6	37,0	59,5
	modulus of elast., MPa	9480	4623	2391	3433	6538
bending perpendicular to the panel plane	ultimate strength, MPa	86,0	46.8	23.5	35.0	59.5
	modulus of elast., MPa	9953	470	1595	2781	4670

After the creep curves of the "FSF" grade glued birch plywood, the long-term (fatigue) strength of the plywood and the modification factors for the long-term strength were being determined which are indicated in Table 2 hereinafter.

Table 2

Type of the state of stress of the "FSF" grade glued birch plywood; grain direction in the external veneer plies to the longitudinal axis, α (degrees)	Long-term (fatigue) strength, MPa	Material factor, fatigue strength, K_{fs}
tension		
α = 0	44.6	0.58
α = 45	12.6	0.54
α = 90	35.8	0.56
compression		
α = 0	27.8	0.55
α = 90	25.3	0.55
bending in the panel plane		
α = 0	41.8	0.54
α = 90	33.1	0.53
bending perpendicular to the panel plane		
α = 0	47.3	0.55
α = 90	30.3	0.51

The analysis of the creep curves over a period of 100 days showed that with transverse bending perpendicular to the panel plane and in the panel plane as well as with tension and compression in the panel plane these curves are practically largely approximating to their asymptotes.

After the curves concerning the change of the long-term deformation moduli of "FSF" grade glued birch plywood, the limit values of the reduction coefficients for the magnitude of the moduli of elasticity of the plywood with transverse bending perpendicular to the panel plane and in the panel plane, with tension and compression in the panel plane depending on the grain direction in the external veneer layers were being determined which are indicated in the Table 3 hereinafter.

Table 3

Angle of inclination of the grains of the external veneer plies to the longitudinal axis of the test specimens, α (degrees)	Type of the state of stress			
	tension	compression	bending in the panel plane	bending perpendicular to the panel plane
0	0.59	0.59	0.74	0.67
45	0.55	0.55	0.63	0.585
90	0.57	0.56	0.71	0.65

The curves concerning the change of the long-term deformation moduli of "FSF" grade glued birch plywood over a period of 75 to 78 days are nearly completely approximating to their asymptotes.

Based on the results and findings of the tests and investigations, formulae for the calculation of the limit values of the strength and of the moduli of elasticity of "FSF" grade birch plywood with transverse bending for any inclination of the grains in the external veneer layers have been proposed.

J. A. Lobanov performed investigations into the strength and deformability of "FSF" grade birch plywood subjected to shear stressing. The shear strength tests were mainly performed with test specimens recommended by the "GOST 1143-41" code for the testing of five-ply plywood. In individual cases, test specimens as indicated in the "GOST 11496-65" code have been investigated.

Table 4 following hereinafter includes results and findings of the shear strength tests with plywood considering the thickness, the number of plies and the moisture of the plywood.

Table 4

Plywood moisture content, %	Shear strength (MPa) of seven-ply "FSF" grade glued birch plywood with a thickness (mm) of			
	7.7	8.5 - 8.7	9.5	10
4 - 5	-	4.00 - 4.72	-	2.60
6.5 - 7.5	-	4.17 - 4.44	3.55 - 3.96	-
9 - 10	5.50	4.44 - 4.70	3.56 - 3.74	2.61
17.5 - 18.5	5.55	4.50 - 4.60	2.98 - 3.00	2.04
20	5.25	4.30	-	-
30	3.50	2.80	1.79 - 2.33	1.28

The results and findings of the investigation of the influence of the angle between the direction of the shear force and the direction of the grains in the external veneer plies on the shear strength of the plywood are included in Table 5 hereinafter (see page 6).

The analysis of the test results and findings verified the view taken by American researchers saying that the shear strength of plywood at angles of $\alpha = 0^{\circ}$ and $\alpha = 90^{\circ}$ is equal to 3/8 and at an angle of $\alpha = 45^{\circ}$ is equal to 0.5 of the shear strength along the grain direction of that kind of timber which the plywood has been manufactured from.

The plywood shear strength tests with shearing-off have been performed using test specimens recommended by German standard specifications for testing the shear strength of structural timber along the grain direction. The test results are included in Table 6 hereinafter (see page 7).

Based on results and findings of tests of long duration performed on loading lever-type test stands using plywood test specimens, at the MISI "V. V. Kuibyshev" institute the strength limits (ultimate strengths) of "FSF" grade glued birch plywood and the material factors of the fatigue strength for the main types of the state of stress have been determined. The material

Table 5

Grade of glued birch plywood, thickness, number of plies	Test specimens according to the type of	Number of test specimens, pcs.	Plywood moisture content, %	Angle between the direction of the grains in the external plies and the force, α (deg.)	Mean value of the strength, MPa	Mean square deviation, MPa	Mean error of the arithmetical mean, MPa	Variation coefficient, %	Accuracy coefficient, %
FSF, $\frac{B}{BB}$,	GOST 11496-65	20	12	0	4.51	0.9	0.200	20	4.54
		20	12	45	5.57	1.02	0.222	18.4	3.98
		20	12	90	4.32	1.01	0.218	23.3	5.00
9.5 mm, 7 plies	GOST 1143-41	75	12	0	3.61	0.73	0.085	20.2	2.35

Table 6

Angle between the shear force direction and the grains in the external veneer layers of the plywood, α (degrees)	Plywood moisture content, %	Mean value of the shear strength of "FSF" grade glued birch plywood, MPa
0	4.0	12.4 - 14.3
	9.6	11.1
	12.0	12.0
	17.0	9.6
	30.0	6.3 - 7.0
90	4.0	14.8 - 15.7
	9.6	12.4
	12.0	14.0
	30.0	7.2 - 8.3
45	4.0	23.6 - 24.5
	9.6	21.8
	12.0	19.4
	17.0	18.0
	30.0	12.2 - 12.4

(continued from page 5)

factors for the long-term (fatigue) strength of glued birch plywood with a moisture content amounting up to 10 % are shown in Table 7 hereinafter (see page 8).

I. M. Guskov has accomplished theoretical and experimental investigations into the strength and deformability of glued birch plywood subjected to compression and compressive strain perpendicular to the panel plane.

As an initial characteristic of the compression strength and the resistance to compressive strain of the plywood with a load action perpendicular to the panel plane, a specific strength limit R_{sp} was assumed which has been determined by

Table 7

Direction of the force application	Type of the state of stress								
	Tension in the panel plane	Compression in the panel plane	Bending in the panel plane	Bending out of the panel plane — Angle between the grain direction in the external plies and the test specimen axis (degrees)			Shear with longitudinal shearing-off	Shear with transverse shearing-off	Compression and compressive strain
				0	90	45			
Along the grains of the external plywood layers	0.58	0.55	0.54	-	-	-	0.50	0.54	-
Across the grains of the external plywood layers	0.56	0.55	0.53	-	-	-	0.50	0.54	-
At an angle of 45° to the grains of the external plywood layers	0.54	0.54	0.52	-	-	-	0.50	0.54	-
Perpendicularly to the panel plane	-	-	-	0.55	0.52	0.51	-	-	0.67

(continued from page 7)

means of mechanical tests of the plywood specimens both with compression and compressive strain over the whole surface and with local compression and local compressive strain as well.

The tests were performed by analogy with tests and investigations carried out with a view to determining the specific strength limit with local compression and compressive strain acting on structural timber across the grain in compliance with the "GOST 16483.2-70" code.

The tests and investigations showed that the specific strength limit of the plywood with compression and compressive strain perpendicular to the panel plane depends on the plywood thickness b and not on the dimensions of the platen (press die) a and on the type of compression and compressive strain (over the whole surface or locally). The mean values of the specific strength limits of "FSF" grade glued birch plywood with compression and compressive strain perpendicular to the panel plane (at a moisture content of 7 to 10 %) are indicated in Table 8 hereinafter.

Table 8

Specific strength limits, R_{sp}, MPa	Plywood thickness, b, mm	Specific strength limits, R_{sp}, MPa	Plywood thickness, b, mm
6.83 - 7.33	30	8.39 - 8.60	12
7.00 - 7.30	24	8.20	10
7.83 - 8.53	18		

The transition from the specific strength limit of the plywood with compression and compressive strain perpendicular to the panel plane to the standard strength and subsequently to the calculated (specified) strength was accomplished by means of conventional methods being applied in the determination of the corresponding strength characteristics for structural timber.

As for plywood being 10 to 30 mm thick with a moisture content of 7 to 10 %, the specific strength limit R_{sp}, the standard strength R^{st} and the calculated strength R with compression and compressive strain acting perpendicularly to the plywood panel plane can be determined according to the following formulae:

$$R_{sp}\ (b) = (9.35 - 0.085\ b)\ \text{MPa};$$
$$R^{st}\ (b) = (7.50 - 0.075\ b)\ \text{MPa};$$
$$R\ (b) = (5.00 - 0.050\ b)\ \text{MPa}.$$

The author has performed at the MISI "V. V. Kuibyshev" institute theoretical and experimental investigations into the deformation of glued birch plywood with local compression and compressive strain acting perpendicularly to the plywood panel plane.

The following conditions and prerequisites were assumed as a basis for the theoretical solution of the problem concerning the action of local compression and compressive strain on plywood:

1. The plywood test specimen consists of a non-linearly elastic layer with a thickness of b which is being placed on a rigid base plate and being compressed by a square press die (platen) with a side dimension of a (see Figure 1).+)
2. There is a friction occurring between the non-linearly elastic layer and the rigid platen as well as between the non-linearly elastic layer and the base plate.
3. The vertical displacement of the platen w_m consists of the vertical displacement w_{cs} caused by the plywood surface compressive strain and the vertical displacement w_{in} due to the indentation of the platen into the plywood as follows:

$$w_m = (\sigma_m, a, b) = w_{cs}\ (\sigma_{cs}) + w_{in}\ (\sigma_m, a, b)$$

+) The figures mentioned in the present paper can be found at the end of the text!

where σ_m is the stress below the platen.

The problem of the dependence of the compressive strain deformation on the irregularity (unevenness or roughness) of the plywood surface has been solved in the following way. In compliance with the "GOST 7016-75" code, the characteristic feature for determining the class of irregularity of the plywood surface concerned is the value of

$$R_{z\ max} = \frac{1}{5} \sum_{i=1}^{5} H_{i\ max}$$

where $H_{i\ max}$ is the maximum value of the irregularities at five sections (i = 5) of the investigated plywood surface within the basic length l of the measuring instrument (see Figure 2).

Based on the assumption that the maximum heights of the irregularities of the profile H_i are random values being subject to the normal distribution law, the mean height of the irregularities of the plywood profile can be determined as follows:

$$H_m = \frac{R^m_{z\ max}}{2} .$$

The model of the profile of the irregular plywood surface can be assumed as a system of indents (teeth) having the shape of equal-leg triangles with an equal height H_m and a base of any width. With the application of such a model, one can assume that the maximum value of the compressive strain deformations on the two surfaces of the plywood panel shall amount to half the mean height of the irregularities of these surfaces, that is to say

$$w^t_{cs} = \frac{2H_m}{2} = \frac{R^m_{z\ max}}{2} .$$

It must be mentioned that the compressive strain deformations on both plywood surfaces will be approximately equal since with a local action of compression and compressive strain the ends of the plywood panel sections projecting over the platen are being lifted due to the stressing of the grains below the platen.

The theoretical conclusions as to the maximum value of the compressive strain deformations have been verified by experimental investigations. As a result of the experiments it has been clarified that the compressive strain deformations are depending on the stress σ_m and not on the thickness of the plywood panel and the dimensions of the platen.

Table 9 shows the values of the compressive strain deformations on both plywood panel surfaces with the class of surface irregularity $\nabla\partial 6$ subject to the stress σ_m.

T a b l e 9

Stress σ_m, MPa	Compressive strain deformation w_{cs}, mm	Stress σ_m, MPa	Compressive strain deformation w_{cs}, mm
1	0.012	6	0.051
2	0.022	7	0.056
3	0.031	8	0.056
4	0.036	9	0.056
5	0.042	10	0.056

From the data included in Table 9 hereinbefore it follows that the compressive strain deformations are virtually occurring at the beginning of the loading of the test specimen and are decaying at a stress amounting to about 6 MPa.

In the theoretical solution of the problem as to a local compression acting on the plywood - i.e. as to the indentation of the platen -, results and findings of the investigation into the deformation of a linearly elastic layer with a limited (finite) thickness being placed on a rigid base with the indentation of a rigid platen into the same have been applied accordingly. +)

+) See the footnote reference at the following page!

According to this investigation, the deformations of an elastic layer with an absence of displacements at the interface (boundary) of "elastic layer - base plate" in the direction of the main axes of the coordinates can be described by means of equations being composed of trigonometrical Fourier series as follows:

$$u = \sum_m \sum_n U_{mn}(z) \sin \alpha x \ \cos \beta y ;$$

$$v = \sum_m \sum_n V_{mn}(z) \cos \alpha x \ \sin \beta y ;$$

$$w_{in} = \sum_m \sum_n W_{mn}(z) \ \cos \alpha x \ \cos \beta y ;$$

where $\alpha = m\pi/L_x$; $\beta = n\pi/L_y$, with L_x and L_y being the dimensions of the elastic layer in the direction of the X and Y axes.

Taking into consideration the following limiting conditions:

with $z = 0$ $\quad u = 0, \ v = 0, \ w_{in} = 0,$

with $z = b$ $\quad \tau_{xz} = 0, \ \tau_{yz} = 0, \ W_{mn} = 10^{-3}\alpha_{mn}$,

the equation of the vertical displacement of the platen (press die) is being obtained as follows:

$$w_{in} = 10^{-3} \sum a_{mn} \cos \alpha_m x \ \sin \beta_n y$$

where $$a_{mn} = \frac{4}{L_x L_y} \int_{-\frac{L_y}{2}}^{\frac{L_y}{2}} \int_{-\frac{L_x}{2}}^{\frac{L_x}{2}} f(xy) \cos \frac{m\pi x}{L_x} \cos \frac{n\pi y}{L_y} \, dx \, dy.$$

The calculations were accomplished by adopting the finite element method with the employment of a computer. As a result

+) Reference applying to the investigation mentioned at the foregoing page:
Milovich, D. M.; Tournier, J. P.: Stresses and deformations in an elastic layer subjected to stressing by a rigid rectangular plate. - Published in: Der Bauingenieur, 1974, No. 2.

of the investigation and based on it, a formula for the calculation of the depth of indentation of the platen into a linearly elastic layer being placed on a rigid base was deduced as follows:

$$w_{in}\ (\sigma_m,\ a,\ b) \ = \ \frac{\sigma_m\ a}{E}\,\mathcal{J}_w.$$

For the determination of the dimensionless (pure) coefficient $\mathcal{J}_w$ depending on the transverse deformation index μ of the material and - in the case of a square platen - on the ratio of b/a (with b being the thickness of the linearly elastic layer and a being the side dimension of the platen), diagrams (curves) have been prepared for materials with coefficients μ amounting to 0.05, 0.15, 0.30 and 0.45 (see Figure 3).

Since - as becomes apparent from the investigations - the modulus of deformation of the plywood subjected to compression is a variable value depending with local compression on the stress below the platen σ_m, the proposed equation can be applied if one changes over to the term of the secant-line modulus of elasticity with compressive action $E_s\ (\sigma_m)$ which is well-known in structural mechanics. The new formula reads then as follows:

$$w_m\ (\sigma_m,\ a,\ b) \ = \ w_{cs}\ (\sigma_m) + \frac{\sigma_m\ a}{E_s(\sigma_m)}\,\mathcal{J}_w^{\mu=0.05}\ .$$

Thus, the total deformations of plywood due to local compression and compressive strain with a load action perpendicular to the plywood panel plane can be determined according to an equation for which a diagram (curve) of the coefficients $\mathcal{J}_w^{\mu=0.05}$ for materials with a transverse deformation index amounting to about $\mu = 0.05$ must be provided.

When carrying out the tests and investigations, three series of test specimens and platens with an equal ratio of b/a - e.g. b/a = 24/120 = 18/90 = 12/60 = 0.20 - have been selected;

this rendered it possible for each stress intensity to provide a system of three equations with the three unknowns $w_{cs}(\sigma_m)$, $E_s(\sigma_m)$ and $J_w^{\mu=0.05}$ into which the results of the experiments were introduced. As a result of the experimental-theoretical investigation, a diagram of the dimensionless coefficient $J_w^{\mu=0.05}$ (see Figure 3) was provided for materials with a transverse deformation index of $\mu = 0.05$ which plywood is being classed with.

In addition to this, the secant-line moduli of elasticity with compressive loading of plywood for the corresponding compression stresses and the values of the compressive-strain deformations of plywood on the two surfaces have been calculated.
It was clarified that the value of the secant-line modulus of elasticity of "FSF" grade structural plywood (birch) with compressive action is being described by the following expression (term):

$$E_s\,(\sigma_m) = \frac{9100}{0.9\,\sigma_m + 1}\ \text{MPa} \qquad (1)$$

Based on a comparison of the corresponding results and findings of the investigation of glued birch plywood subjected to local compression and local compressive strain as well as to compression and compressive strain on the whole surface with a load action perpendicular to the plywood panel plane, it was found out that the deformations due to compression and compressive strain of the plywood on the whole surface can be calculated by applying the following formula:

$$w_n\,(\sigma_n, a, b) = w_{cs}(\sigma_n) + \frac{\sigma_n\, a}{E_s(\sigma_n)} J_w^{\mu=0.05}(1 + 2J_w^{\mu=0.05})$$

where $w_{cs}\,(\sigma_n)$ are the deformations due to compressive strain on the two surfaces, to be determined according to Table 9 hereinbefore;

$E_s\,(\sigma_n)$ is the secant-line modulus of elasticity with compressive loading, to be determined according to formula (1) with a substitution of σ_n for σ_m.

The theory of the compression and compressive strain acting on plywood perpendicularly to the panel plane - taking into consideration the anisotropic properties of wood - can also be extended to structural timber as well since plywood is a material being manufactured on a timber basis.

Creep tests with glued birch plywood subjected to a load action perpendicular to the panel plane have been carried out using test specimens in the shape of a rectangular parallelepiped with side dimensions of 12 x 60 x 60 mm. The compression and compressive strain were applied only on the whole surface. The tests were accomplished on test stands with a load application by means of lever systems. The specimens were tested at five different load increments corresponding to 20, 40, 60, 80 and 100 % of the specific strength limit of the plywood obtained during mechanical tests with an amount of 10 MPa.

The instantaneous deformation W_{inst} of the test specimens was determined within 1 second after the load application. The specimens were tested for a period of 200 days under normal temperature and moisture conditions (with a moisture content of 7 to 8 %). After the creep curves, the maximum deformations due to compression and compressive strain W_{perm} have been determined (i.e. when the deformation of the test specimens was completed).

After the lapse of the indicated period of time, the moisture conditions for the testing of the specimens were modified: the moisture content of the test specimens being exposed to the loading was increased to 28 - 30 %; now an increase of the deformations over the time has been observed. The specimens with the increased moisture content were tested for a period of 400 days. The creep curves of the test specimens in the wet state were showing a tendency of decay. The maximum deformations of the test specimens with an increased moisture content - W^{im}_{perm} - have been determined accordingly.

The results of the creep tests of the plywood specimens subjected to compression and compressive strain acting perpendicularly to the panel plane are indicated in Table 10 hereinafter.

Table 10

Type of the deformation	Moisture content of the test specimens	Mean arithmetical values of the creep deformations of the "FSF" grade glued birch plywood test specimens sized 12 x 60 x 60 mm with compression load acting on the whole surface perpendicularly to the panel plane				
		with a stress σ, (MPa) amounting to:				
		2	4	6	8	10
Instantaneous deformation	7 - 8	0.076	0.098	0.116	0.194	0.349
Permanent deformation	7 - 8	0.229	0.287	0.435	1.008	2.105
Permanent deformation	28 - 30	0.400	0.624	1.295	2.879	4.178

After the completion of the creep tests of glued birch plywood test specimens with compression load acting perpendicularly to the plywood panel plane, the laterial surfaces of both the tested and non-tested specimens have been examined by means of a metallographical microscope "MIM-8" with a view to checking and detecting structural changes of the wood within the layers of the plywood veneer. The side faces of the test specimens were being abraded (ground) in advance. The individual sections of the veneer plies have been photographed through the microscope with a 500-fold magnification on technical high-contrast reproduction process plates with a sensitivity amounting to 5.5.

The microscopical analysis revealed that the plywood which has not been subjected to compression and compressive-strain tests with a load acting perpendicularly to the plywood panel plane is virtually retaining the macrostructure being typical of birch wood. However, there are sections in it where the libriform vessels, the water-carrying vessels and the medullary rays have been heavily deformed or destroyed already during the process of manufacturing the plywood in the presses (see Figure 4).

It has been clarified that with an increase of the compression force acting perpendicularly to the plywood panel plane the quantity of the deformed and destroyed structural elements of the wood per unit volume of the plywood is increasing. A particularly intensive destruction of the structural elements of the wood can be observed in the case of permanent compression stresses acting perpendicularly to the plywood panel plane and exceeding 4 MPa.

As a result of the compression and compressive-strain tests performed on "FSF" grade glued birch plywood with a load action perpendicular to the plane of the plywood panel, a 4 MPa design value of the resistance (strength) of this type of plywood to compression and compressive strain acting perpendicularly to the plane has been included in the "SNiP II-25-80" code specification.

G. P. Makarov was performing at the MISI "V. V. Kuibyshev" institute investigations into the plane state of stress of plywood in terms of biaxial tension and biaxial compression (on the condition of not permitting a loss of stability with a given value of deflection due to loss of stability).

For the tests and investigations, a special facility with a ratio of the lateral lever arms amounting to 1 : 2 has been manufactured (see Figure 5).

The tests were carried out using cruciform test specimens the four supporting ends of which have been reinforced by plywood butt straps being at least 5 mm thick. The wood grains in the external veneer layers of the plywood butt straps were directed at an angle of 90^{o} to the application direction of the tensile or compressive stress. Plywood test specimens of the following two types have been investigated:

1. specimens with a loading area of 100 x 100 mm, and
2. specimens with a loading area of 80 x 80 mm.

The grain direction in the external plywood layers of the loading area of the test specimens was either coinciding with the direction of the force application in one of the axes or was forming an angle of 45^{o} with the force application direction in both axes.

In the biaxial tension tests, the destruction (failure) of the test specimens occurred on a line located at an angle of 45^{o} to the direction of action of the applied forces, i.e. in the direction of action of the principal stresses, irrespective of the angle of inclination of the wood grains in the external plywood layers of the loading area of the test specimens to the force application direction.

The evaluation of the loadbearing behaviour of the plywood with a plane state of stress was accomplished by applying a generalized strength criterion for anisotropic materials which has been developed by I. I. Goldenblat, V. A. Kopylov et al. and which is applicable to materials the strength constants of which are complying with the compatibility condition as follows:

$$\frac{1}{\sigma_x^t} - \frac{1}{\sigma_y^t} = \frac{1}{\sigma_x^c} + \frac{1}{\sigma_y^c} = \frac{1}{\tau_{45}^t} - \frac{1}{\tau_{45}^c} \qquad (2)$$

where σ_x^c and σ_y^c are the limit values of the compression strength of plywood in the panel plane with an action of the compressive force along and/or across the grains in the external plywood layers;

σ_x^t and σ_y^t are the limit values of the tensile strength of plywood in the panel plane with an action of the tensile force along and/or across the grains in the external plywood layers;

τ_{45}^t and τ_{45}^c are the limit values of the shear strength of plywood with an action of the shear forces at an angle of 45^o to the direction of the grains in the external plywood layers.

The limit values of the shear strength of plywood - τ_{45}^t and τ_{45}^c - with an action of the shear forces at an angle of 45^o to the grain direction in the external plywood layers as included in the equation (2) hereinbefore have not been determined. However, since it is well-known that in the case of one-dimensional (uniaxial) tension or compression in the plywood panel plane the deformation of the plywood is following the Hooke's law until failure (destruction), the conditions of the shear strength of plywood will be defined as follows:

$$\tau_{45}^t = G_{45}^t \gamma_{45}^t ;$$

$$\tau_{45}^c = G_{45}^c \gamma_{45}^c ,$$

where G_{45}^t, G_{45}^c, γ_{45}^t, γ_{45}^c are the shear moduli of the plywood and the limit values of the deformations due to shear in planes being located at an angle of 45^o to the grain direction of the wood in the external plywood layers; they have been obtained as a result of diagonal tests of plywood specimens with an application of tensile or compressive forces, respectively, in the X-axis (see Figure 6).

The shear moduli of the plywood G_{45}^t and G_{45}^c can be calculated analytically according to the formulae of the strength of materials as follows:

$$G_{45}^{t} = \frac{E_x^t\, E_x^c}{E_y^t\,(1+\mu_{xy}^c) + E_x^c\,(1+\mu_{xy}^t)} \;;$$

$$G_{45}^{c} = \frac{E_x^t\, E_x^c}{E_x^t\,(1+\mu_{xy}^c) + E_y^c\,(1+\mu_{xy}^t)} \;,$$

where E_x^t, E_x^c, E_y^t, E_y^c, μ_{xy}^t, μ_{xy}^c are the corresponding moduli of elasticity and transverse deformation coefficients with uniaxial tension and compression.

The limit values of the shear deformations of the plywood with diagonal loading tests with an action of the tensile forces in the X-axis are being calculated theoretically according to the formula

$$\gamma_{45}^{t} = \left(1 + \frac{E_x^t \mu_{yx}^c + E_y^c}{E_y^c \mu_{xy}^t + E_x^c}\right) \varepsilon_y^c \,,$$

whereas with an action of the compressive forces in the X-axis they are being determined according to the formula

$$\gamma_{45}^{c} = \left(1 + \frac{E_x^c \mu_{yx}^t + E_y^t}{E_y^t \mu_{xy}^c + E_x^c}\right) \varepsilon_x^c \,,$$

where ε_x^c and ε_y^c are the corresponding critical limit values of the deformations due to compression, taking into consideration the direction of the action of the shear stresses, which for plywood are equal to

$$\varepsilon_x^c = \sigma_x^c / E_x^c \;;$$

$$\varepsilon_y^c = \sigma_y^c / E_y^c \,.$$

Thus, the dependencies (relationships) enabling to calculate the limit values of the shear strength of plywood with a shear force acting at an angle of 45° to the symmetry axes according to their elasticity and strength characteristics obtained from tension and compression tests are assuming the following form:

$$\tau^{t}_{45} = \sigma^{c}_{x}/(1 + \frac{E^{c}_{x}}{E^{t}_{x}}\mu^{t}_{xy}) ;$$

$$\tau^{c}_{45} = \sigma^{c}_{y}/(1 + \frac{E^{c}_{y}}{E^{t}_{y}}\mu^{t}_{yx}) ,$$

where σ^{c}_{x} and σ^{c}_{y} are the ultimate compressive strengths of the plywood with one-dimensional state of stress.

The values of the shear moduli and of the ultimate shear strengths of plywood with a shear force acting at an angle of 45° to the grain direction in the external plywood layers which have been determined by applying the formulae indicated hereinbefore are shown in Table 11 hereinafter.

Table 11

Type of the state of stress	Shear modulus G_{45} (MPa)	Shear strength τ_{45} (MPa)
tension	4945.0	44.0
compression	4837.4	42.6

Since the compatibility condition being applicable to plywood reads as follows:

$$\frac{1}{77.5} - \frac{1}{64.0} - \frac{1}{50.5} + \frac{1}{46.0} = \frac{1}{44.0} - \frac{1}{42.6} ;$$

$$- 0.0000081 \approx - 0.0000085,$$

the strength condition according to the generalized criterion (e.g. for the case of biaxial tension) is being expressed as follows:

- with a coincidence of the grain direction in the external plywood layers of the loading area of the test specimen with the direction of the acting forces in one of the axes by means of the formula

$$\frac{\sigma_x^c - \sigma_x^t}{2\sigma_x^t \sigma_x^c}\sigma_{11} - \frac{\sigma_y^c - \sigma_y^t}{2\sigma_y^t \sigma_y^c}\sigma_{22} + \frac{1}{2}\left\{\left(\frac{\sigma_x^t + \sigma_x^c}{\sigma_x^t \sigma_x^c}\right)^2 \sigma_{11}^2 + \right.$$

$$+\left(\frac{\sigma_y^t + \sigma_y^c}{\sigma_y^t \sigma_y^c}\right)\sigma_{22}^2 - \left[\left(\frac{\sigma_x^t + \sigma_x^c}{\sigma_x^t \sigma_x^c}\right)^2 + \left(\frac{\sigma_y^t + \sigma_y^c}{\sigma_y^t \sigma_y^c}\right)^2 - \right.$$

$$\left.\left. - \left(\frac{\tau_{45}^t + \tau_{45}^c}{\tau_{45}^t \tau_{45}^c}\right)^2\right]\sigma_{11}\,\sigma_{22}\right\}^{\frac{1}{2}} \leqq 1 \;;$$

- with a grain direction in the external plywood layers of the loading area being located at an angle of 45^o to the direction of the acting forces by means of the formula

$$\frac{\sigma_x^c - \sigma_x^t}{2\sigma_x^t \sigma_x^c}\sigma_{11} - \frac{\sigma_y^c - \sigma_y^t}{2\sigma_y^t \sigma_y^c}\sigma_{22} + \frac{1}{2}\left\{\left(\frac{\sigma_x^t + \sigma_x^o}{\sigma_x^t \sigma_x^c}\right)^2 \sigma_{11}^2 + \right.$$

$$+\left(\frac{\sigma_y^t + \sigma_y^c}{\sigma_y^t \sigma_y^c}\right)\sigma_{22}^2 + \left[\left(\frac{\sigma_x^t + \sigma_x^c}{\sigma_x^t \sigma_x^c}\right)^2 + \left(\frac{\sigma_y^t + \sigma_y^c}{\sigma_y^t \sigma_y^c}\right)^2 - \right.$$

$$\left.\left. - \left(\frac{\tau_{45}^t + \tau_{45}^c}{\tau_{45}^t \tau_{45}^c}\right)^2\right]\sigma_{11}\,\sigma_{22} + \frac{4\tau_{xy}^2}{\tau_o^2}\right\}^{\frac{1}{2}} \leqq 1 \,,$$

where σ_x^t, σ_y^t, σ_x^c, σ_y^c, τ_{45}^t, τ_{45}^c, τ_{xy}, τ_o

are the strength constants of the material;

σ_{11} and σ_{22} are the stresses acting in the material with a biaxial (plane) state of stress.

Based on an analysis of experimental results and data obtained by tests of glued birch plywood with a plane state of stress, the criterion of the fatigue strength of plywood components with a plane state of stress has been proposed by means of which it becomes possible to determine in advance the load-bearing behaviour of plywood with a biaxial action of forces. Such a prediction is necessary since - as a rule - in actual structures plywood is being found in a plane state of stress.

Experimental investigations into the strength of "FSF" grade glued birch plywood with a simultaneous action of normal and shear (tangential) stresses between the plywood layers have been carried out by V.V. Fedorov at the MISI "V. V. Kuibyshev" institute.

In some glued timber structures - for instance in glued plywood lozenge units of vaulted lamella roofs with no-hinged joints -, between the layers of the plywood panel normal stresses (tension and compression) and shear stresses can act simultaneously. As a result of tests performed using special test specimens it was found out that in the case of a simultaneous action of shear stresses τ_{xy} and normal stresses σ_y between the plywood layers the shear strength in the joint between the veneer plies is increasing with an increase of the stresses σ_y as follows:

$$\tau_{xy} = 4.6 + 0.35\ \sigma_y, \qquad \text{with } \sigma_y \leq 3.5 \text{ MPa.}$$

It has been determined that the modulus of elasticity of the plywood with tension acting perpendicularly to the plywood panel plane amounts to 1500 MPa whereas the ultimate tensile strength acting perpendicularly to the plane amounts to 2.6 MPa.

One of the first vaulted lamella roof structures consisting of composite glued plywood lozenge units has been developed in the USSR by G. G. Karlsen and B. A. Osvenski. The plywood webs of the lozenge units with a box section are being reinforced at the ends and in the central area by solid intermediate layers consisting of short panels which are vertically jointed with one another. The metal-free connection of the lozenge units is being accomplished by means of two timber inserts being placed into the openings of the open-worked lozenge units and being fixed on both sides in grooves at the ends of the touching lozenge units.

B. A. Osvenski proposed a vaulted lamella roof structure with a rigid (hingeless) connection of the glued plywood lozenge units in the joints. The touching (butted) glued plywood lozenge units with a box section are being centered in the joint in such a way that the normal compressive forces are being transferred immediately in the ends (faces); thus, the possibility of the formation of a bending moment out of the lozenge unit plane occurring in vaulted lamella roofs of conventional structures is being excluded.

With a view to leading through the ends of the bottom flange of the touching glued plywood lozenge units, openings of an adequate size are being cut out in the plywood webs in the middle area of the open-worked lozenge units concerned. At the ends of the lozenge units, staggered butt straps are being glued on to their lateral edges in the region of the top and bottom lozenge units which are intended to serve as a support of the X-shaped steel erection lozenge units.

With a hingeless solution of the joints of the vault, the bending moments in the joints are being sustained both by the touching and by the continuous lozenge units (as a result of the existence of X-shaped steel components). Due to the existence of the X-shaped steel members, a high tightness of the joint connection is ensured. On otherwise equal conditions, the transverse force in the lozenge units with a hingeless joint connection is by far smaller than the transverse force in lozenge units with a hinged solution of the joints. Thus, vaulted lamella roof structures with a hingeless joint design are lighter and more reliable in their loadbearing behaviour than vaulted lamella roofs with a hinged design of the joints.

V. V. Fedorov has elaborated at the MISI "V.V. Kuibyshev" institute a methodology for the calculation and designing of hingeless joints of vaulted lamella roofs consisting of glued plywood lozenge units according to the construction proposed by B. A. Osvenski.

A. L. Rabinovich carried out a theoretical investigation into the problem of the anisotropy of the elastic properties of orthotropic timber-based engineering materials which plywood is to be classed with.

Based on an analysis of the diagrams representing the variation of the moduli of elasticity of orthotropic materials, it has been determined that these diagrams of the surfaces can be expressed by equations of the fourth order whereas the coefficients of these equations are components of fourth-rank tensors.

N. G. Tchencov has studied the problem of the deformations of plywood as an elastic orthotropic panel. He determined that in those directions not coinciding with the principal axes of symmetry of the plywood test specimen having the shape of a rectangular parallelepiped the strains are depending both on the normal forces and on the shear forces whereas the translations (displacements) are depending not only on the shear forces but also on the normal forces as well.

Theoretical and experimental investigations into the anisotropy have been accomplished by E. K. Ashkenasi at the Leningrad "S. M. Kirov" Academy of Forestry and Timber Technology. Said studies and experiments were based on the hypothesis saying that plywood as a material is a continuous solid (compact) anisotropic medium with an orthogonal symmetry of the strength properties. A hypothesis was established as to the tensoriality of the strength characteristics of plywood which was understood to imply that a modification (change) of these characteristics depending on the orientation (direction) of the state of stress in the material concerned is occurring in compliance with laws which are being approximated by formulae of the transformation of tensor components with a rotation of the coordinate axes.

Based on the established hypothesis, it was suggested to introduce the term of "strength tensor" being constructed analogously to the tensor of elastic constants of the fourth order, and thus tensorial formulae have been obtained determining the strength characteristics of plywood in terms of tension, compression and pure shear with any orientation of these modifications (changes) as to the three axes of symmetry of the orthotropic material concerned.

Of recent years, at a number of research institutes and colleges of the USSR - including the Moscow MISI "V.V. Kuibyshev" institute - theoretical and experimental studies and investigations have been carried out concerning different types of constructions to be manufactured using plywood, such as:

- glued plywood beams,
- glued plywood panels,
- trusses made of plywood sections (profiles),
- trusses with reinforcing sheets made of plywood,
- plywood arches and frames,
- arches and frames made of plywood pipes, spatial constructions made of prefabricated glued plywood components, etc.

Moreover, work is being performed with a view to developing new types of plywood to be used for structural purposes.

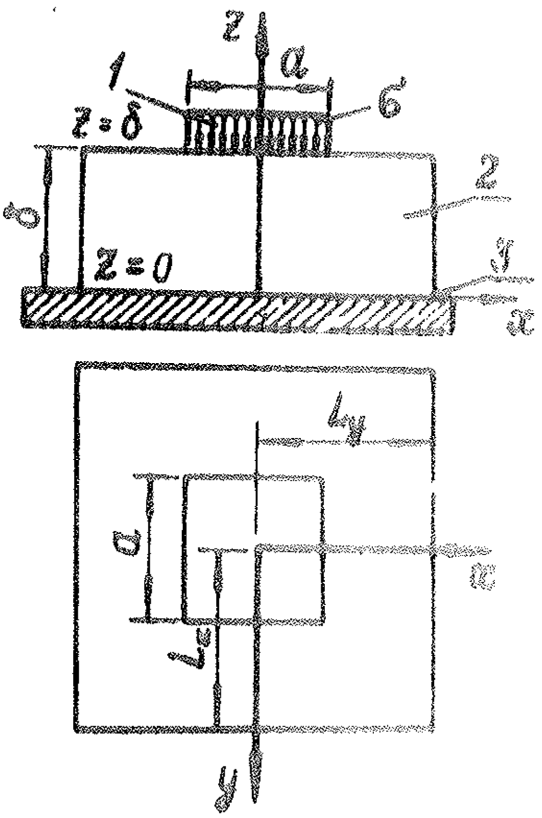

Figure 1. Schematic representation of the behaviour of plywood with local compression and compressive strain perpendicular to the panel plane: 1 - rigid platen (press die); 2 - non-linearly elastic layer (of plywood), 3 - rigid base plate

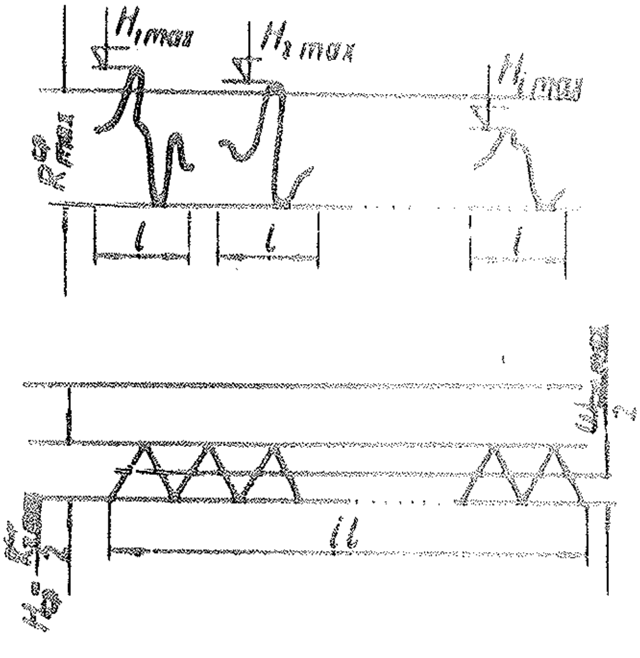

Figure 2. Irregularity of the plywood surface: a) actual profiles of the irregular surface of the plywood test specimen on i investigated sections with a basic length l; b) model of the profile of the investigated irregular plywood surface

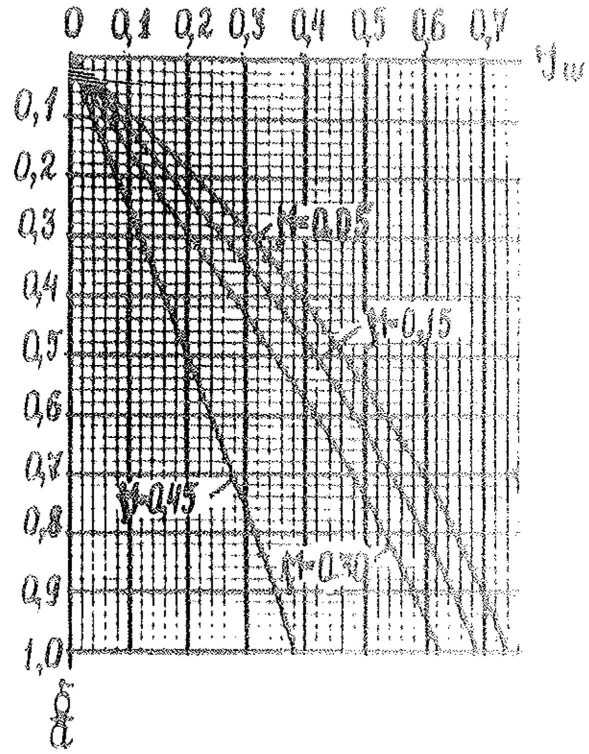

Figure 3. Dependence of the coefficient J_w on the ratio of b/a and on the coefficient of the transverse deformation of the materials of the elastic layer μ

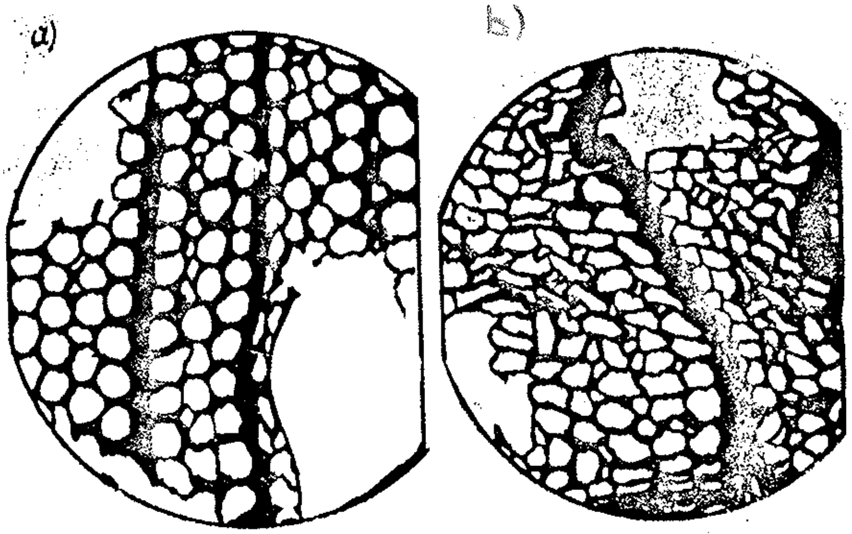

Figure 4. Microscopical structure of veneer plies of "FSF" grade glued birch plywood test specimens not being subjected to fatigue tests with compression and compressive strain: a) with undeformed structural elements; b) with deformed and destroyed structural elements

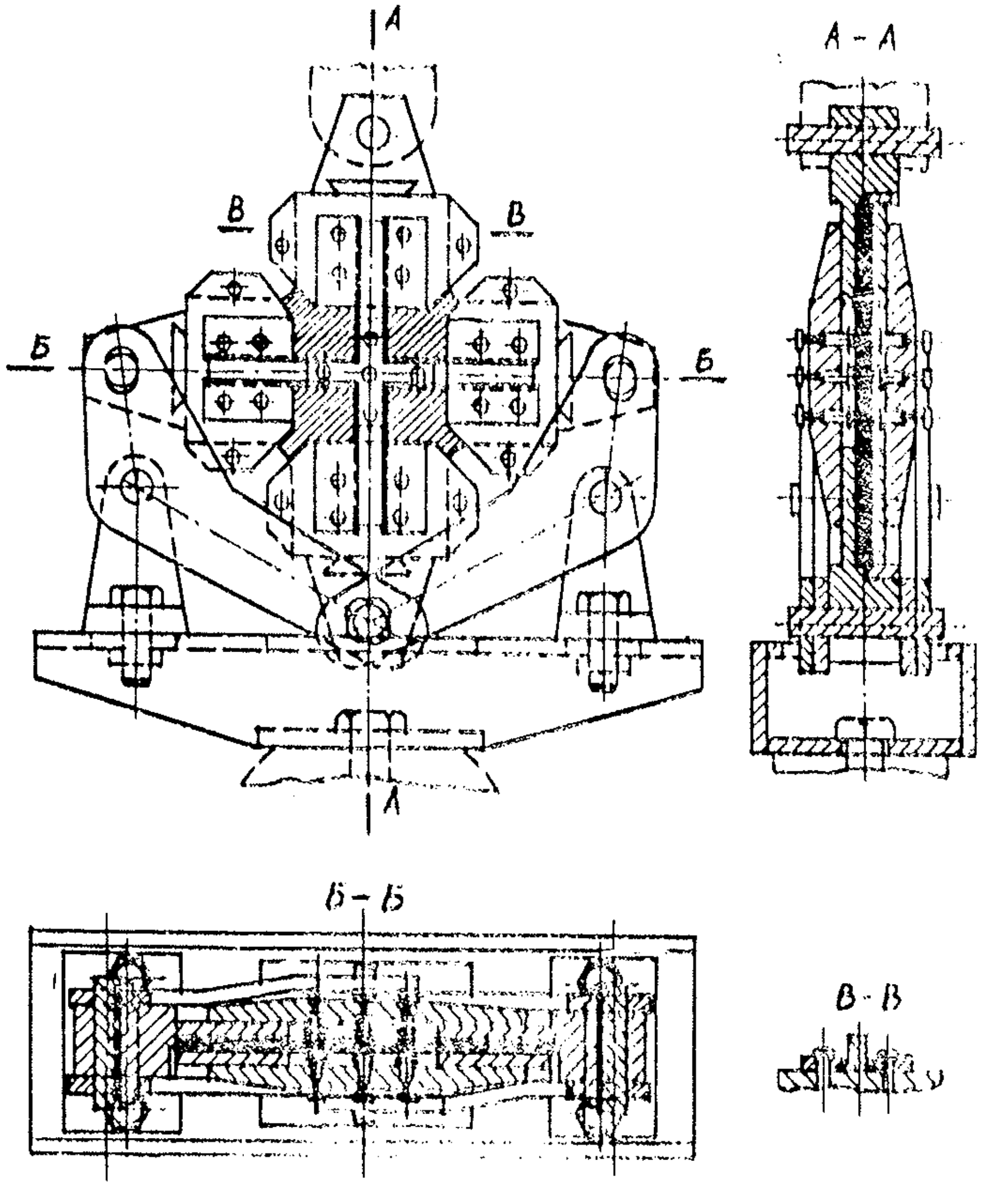

Figure 5. Schematic representation of a facility for testing plywood in the plane state of stress

Figure 6. Shear of plywood with an action of the shear forces at an angle of 45° to the grain direction in the external plywood layers: a) with tension; b) with compression

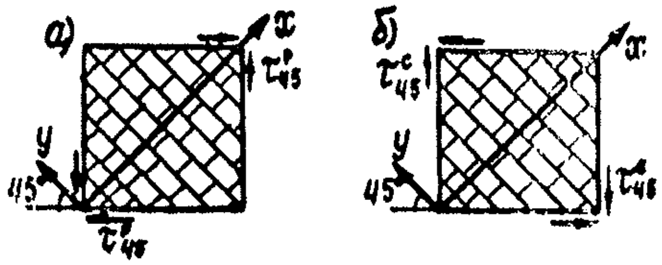

CIB -W18A / 22-4-2

INTERNATIONAL COUNCIL FOR BUILDING RESEARCH STUDIES AND DOCUMENTATION

WORKING COMMISSION W18A - TIMBER STRUCTURES

EVALUATION OF CHARACTERISTIC VALUES FOR WOOD-BASED SHEET MATERIALS

by

E G Elias
American Plywood Association
United States of America

MEETING TWENTY - TWO

BERLIN

GERMAN DEMOCRATIC REPUBLIC

SEPTEMBER 1989

EVALUATION OF CHARACTERISTIC VALUES FOR WOOD-BASED SHEET MATERIALS

by E. G. Elias

CIB STRUCTURAL TIMBER DESIGN CODE

Section 4.0 of the CIB Timber Code provides for the development of strength and stiffness properties based on testing. Section 4.4 provides for specific provisions on wood-based sheet materials. Standard methods of testing are referenced. Standards for sampling, analysis and interpretation of test data are "under development."

OBJECTIVE

The purpose of this paper is to present a review of a sampling and statistical analysis procedure for estimating characteristic values for wood-based sheet materials. Specific suggestions are made for comparing the variability of subsamples obtained individual mills with the composite sample of several mills.

BACKGROUND

The subject of sampling and analysis techniques for plywood and other structural-use panels has been the topic of several previous CIB W18 papers (8, 11, 12). Design information on sheet materials has generally been presented in one of three styles: capacities, allowable stresses based on full cross section (homogeneous), or allowable stresses based on effective cross sections (e.g., transformed section based on parallel axis theorem). For our purposes in this paper, material information will be based on a capacity basis. Thereby, different thicknesses and production categories can be compared.

Noren (8) in 1976, proposed a scheme for developing characteristic strength and stiffness values as: 1) an approval process for sheet materials or; 2) to provide for compliance with a strength grade or; 3) as a quality control tool. Noren believed that integrating panels of different thickness and construction, or materials from different sources, could be permitted if it were proven that there was no significant deviation of the charactistic strength value between the subgroups. Wilson (12) in 1979, proposed a method consolidating plywood subgroup data. In this method of grouping, an exclusion value is calculated for each subgroup as well as the composite sample. If the composite exclusion limit does not exceed the exclusion limit of the weakest subgroup by more than 10%, then the composite exclusion limit may be used for code purposes. This grouping procedure is based loosely on the procedures in ASTM D-2555 Establishing Clear Wood Strength Values (3).

In 1988, Glos and Fewell (4) proposed a methodology for determining the characteristic strength values for stress grades of structural timber. Included within this proposal were specifics on sampling requirements, the necessity for strength class boundaries, recommended test procedures and analysis techniques including determination of characteristic values. The sampling techniques include reference to a stratified scheme, where known or suspected differences in subpopulations are sampled proportionate to their estimated volume in the composite population (5). Specifics on distribution fitting techniques are discussed and a 3-parameter Weibull distribution is selected (6).

This paper will review the procedures proposed by Glos and Fewell relative to a data set of plywood collected during the ingrade testing program of the American Plywood Association. The exercise provides a baseline for assessing the test procedures beyond the scope originally intended by the original authors. Additionally, the influence of subsample variability is reviewed during the development of characteristic values.

TEST SAMPLE

The data in this analysis is limited to a single capacity classification based on the trademarking policies of the American Plywood Association. The capacity system is based on a series of performance tests sensitive primarily to bending stiffness and strength (1). Subsamples represent several species, including Douglas-fir (Psuedotsuga menziesii), southern pine (Pinus spp.) and western hemlock (Tsuga heterophylla). The composite sample includes 4,865 data points collected from 80 production facilities in the United States.

SAMPLING SCHEME

The sampling scheme, initiated in 1982, is two phase.

Phase 1. Qualification Sample

The initial sampling at each mill was deliberately censored to the low end of the manufacturing range. The panels were specifically sampled at the minimum thickness and the maximum allowable growth characteristics (e.g., knots and knot holes) allowed in the specified visual grade. The philosophy parallels the recommendations by Glos and Fewell where specimens are deliberately tested in the most critical section (4). A total number of 960 panels were evaluated in this manner. An equal number of panels was selected from each mill.

Phase 2. Ongoing Reevaluation Sample

Participating APA member mills are subject to reevaluation each quarter or every 3 months. During this sampling panels are selected in a random manner to be representative of normal production. They are not deliberately selected to represent the low end of the grade classification. This type of sampling scheme has been supported by several researchers for the development of characteristic values (8, 9). Pellicane, in 1981, concluded that the best sampling scheme was based on collecting material throughout the entire distribution, opposed to sampling schemes which concentrated near the area of interest (8). For strength characteristic value estimates, the area of interest is the lower 5% exclusion limit (4). A total number of 3,905 panels were evaluated over a 5-year period. The samples reflect a stratified sampling and are representative of production volumes.

TEST METHODS AND PROCEDURES

Large size specimens (1.2 x 1.2 m) were evaluated in flatwise bending. The procedures follow ASTM D3043 Method C, Structural Panels in Flexure (2). The apparatus is shown in Figure 1 and represents a third-point bending arrangement. The RILEM TT2 specimen has been proposed for the CIB Timber Code. This method has only recently been adopted into ASTM D3043, as an alternate method.

However, research has indicated that the larger ASTM test method provides more conservative results than the TT2 method (7). Maximum moment and stiffness was recorded.

STATISTICAL ANALYSIS PROCEDURES

For bending strength, a 3-parameter Weibull was fit to the data utilizing a maximum log likelihood method for parameter estimates. A lower fifth percentile for each sample was estimated. Initially, the composite sample, comprised of both qualification (censored) and ongoing (routine) material, was analyzed. Subsequently, individual mill data was reviewed relative to its distribution in the lower tail of the composite sample. Statistical adjustments for moisture conditions or size effects were not included within the scope of this study.

TEST RESULTS AND DISCUSSION

Censored vs. Routine Sampling

The sampling and testing schemes described in this paper were originally developed as a short-term quality control tool. However, as the data base grew, the samples have provided us with the capability to estimate population distributions. On an individual mill basis, this sampling scheme has also allowed us to compare the results of censored versus random selection of specimens. Figure 2 presents a control chart for strength, along the major panel axis, for material sampled from producing member mill "A". Over the past five years, 173 full size specimens have been sampled and tested.

Figure 2 suggests that the initial qualification sample was indeed successful in collecting material at the lower end of the production range. The resulting control limit, for quality assurance purposes, and original sample mean were typically lower than data obtained from random routine samples. In five years of random sampling 2 panels in 173 have recorded strength values below the estimated control limit. With adequate quality control procedures for grade and panel construction, this relationship should be maintained.

These test relationships are significant when estimating characteristic values. The critical censored data provides a conservative estimate of a lower 5% exclusion limit. However, as more data is collected above the censored level, a more accurate estimate of the population is possible. Pellicane, in his simulations, indicated decreasing error occurred as supplementary samples were collected above the censored region (9). He suggested that the supplemental sample values must be at least double the censored data before the error is substantially reduced. Therefore, where ongoing quality control data can be utilized in the analysis, the original censored data should be reevaluated.

Subgroup Samples

The composite test sample was evaluated to ascertain whether or not an individual mill, species or regional distribution subgroup occupied a disproportionate area in the lower tail. In our analysis 66 mills of the total 80 were represented in the lower 10 percent tail of the composite sample. An example of mill variability is shown in Figure 3. For each subgroup sample, a five percent exclusion value was estimated by means of 3-parameter Weibull or a nonparametric approach. These values were compared to the lower 5% value of the composite sample. Initially, the 10% rule proposed by Wilson was employed. The composite dispersion factor described in ASTM D2555 was also reviewed. This latter process is not unlike the use of the Kg factor described by Glos and Fewell for comparing quality control subgroups to established characteristic values. From these analyses we determined that no single mill, specimen type or geographical region controlled the lower 5% of the composite sample.

We believe the conclusion derived from this analysis is due in part to the large data sets available to APA and the fact that the data has been collected over an extended period of time. The analysis results apply only to this test case and we caution that the procedure for evaluating subgroups must be taken into account when reviewing the development of characteristic values.

Quality Control

Development of characteristic values for sheet materials requires maintenance by an independent quality control program. Quality control procedures linked to mechanical performance can provide an ongoing evaluation of product over time. Quality assurance can assess within plant variability, changing timber resources, and the effects of changes in processes or technology. Product modifications in veneer thickness, species and construction can be employed to maintain the integrity of engineering values.

CONCLUSIONS

This paper discussed sampling schedules and analysis procedures for developing characteristic values for sheet materials. Several important points were emphasized.

a. The general procedures proposed by Glos and Fewell in 1988 for full-size structural timber can be employed in the estimation of characteristic values of wood-based sheet materials. Correction factors for moisture content and size effects were not reviewed.

b. When ongoing routine test data is available, this sampling should be included with the original censored data to provide a more accurate representation of the product population as produced.

c. Composite samples which include material from more than one manufacturing site or region should be evaluated for controlling subsamples. Procedures in ASTM D-2555 provide a method for making this comparison. These procedures should be reviewed by other researchers for their appropriateness to other product types.

d. An independent quality assurance program is required to monitor conformance of product relative to the published characteristic value.

LITERATURE CITED

1. American Plywood Association. 1988. Performance Standards and Policies for Structural-Use Panels. APA. PRP-108.

2. American Society for Testing and Materials. 1988. Standard Methods of Structural Panels in Flexure. ASTM Designation D3043-88.

3. American Society for Testing and Materials. 1988. Standard Methods of Establishing Clear Wood Strength Values. ASTM Designation D-2555-88.

4. Fewell, A. R. and P. Glos. 1988. The Determination of Characteristic Strength Values for Stress Grades of Structural Timber. CIB-W18A/21-6-2.

5. Glos, P. 1985. Sampling Timber in Structural Sizes. CIB-W18/18-17-1.

6. Glos, P. 1983. Notes on Sampling and Strength Prediction of Stress Graded Structural Timber. CIB-W18/16-17-1.

7. Kearley, V. C. and A. R. Abbott. 1986. Mechanical Methods for Characterizing the Strength and Stiffness Properties of Wood-Based Sheet Materials. TRADA Research Report 1/86.

8. Noren, B. 1976. The Sampling of Plywood and Derivation of Strength Values. CIB-W18/9-4-3.

9. Pellicane, P. J. and J. Bodig. 1981. Sampling Error in the Bending Strength Distribution of Dimension Lumber. Wood Science and Technology. 15 (3), 211-225.

10. RILEM. 1986. Final Recommendation TT-2: Test Methods for Plywood in Structural Grades for Use in Load Bearing Structures.

11. Schmidt, T. 1981. Proposal for Presenting Data on Properties of Structural Panels. CIB-W18/14-4-2.

12. Wilson, C. R. 1979. Procedures for Analysis of Plywood Test Data and Determination of Characteristic Values Suitable for Code Presentation. CIB-W18/12-4-1.

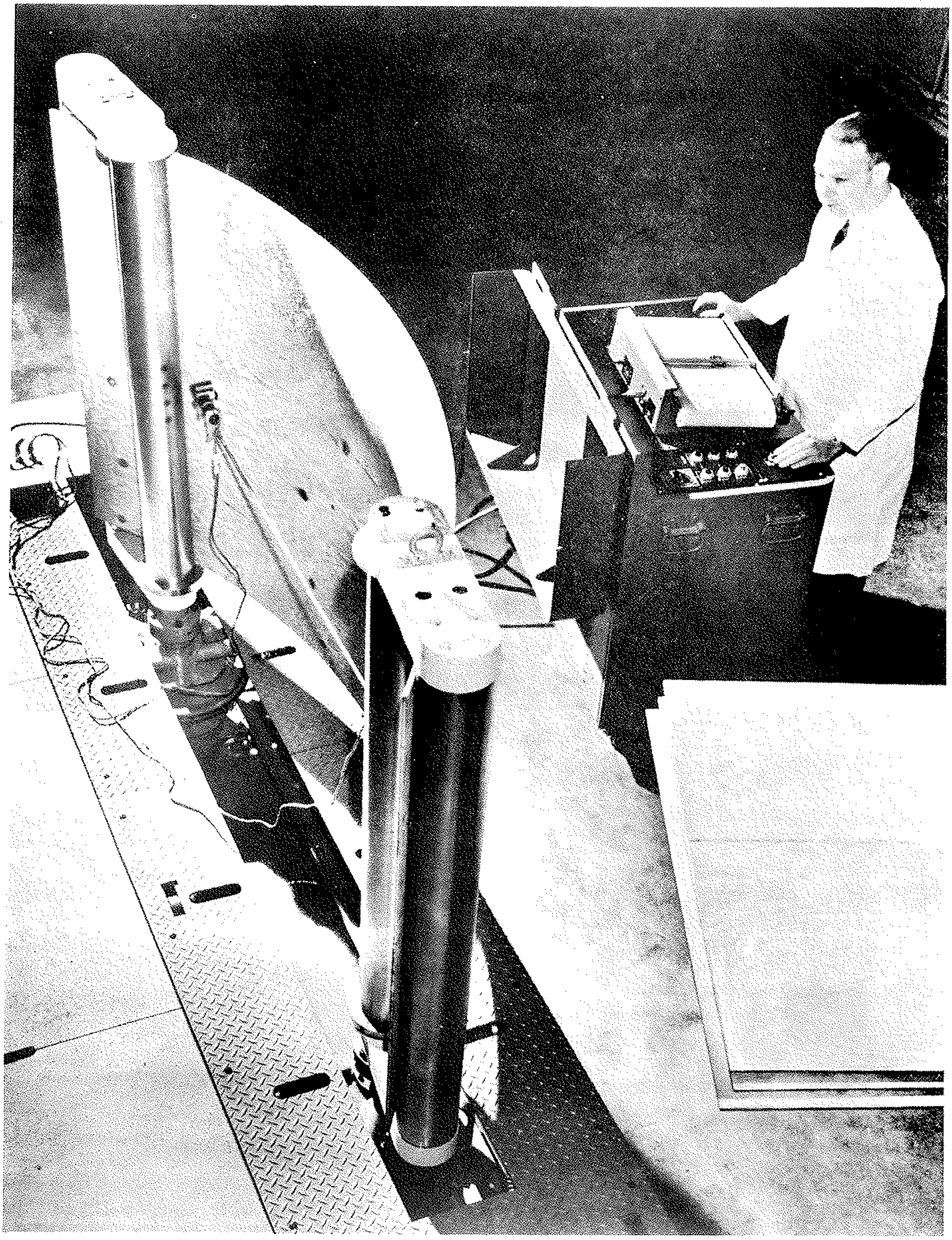

Bending test for stiffness and strength.

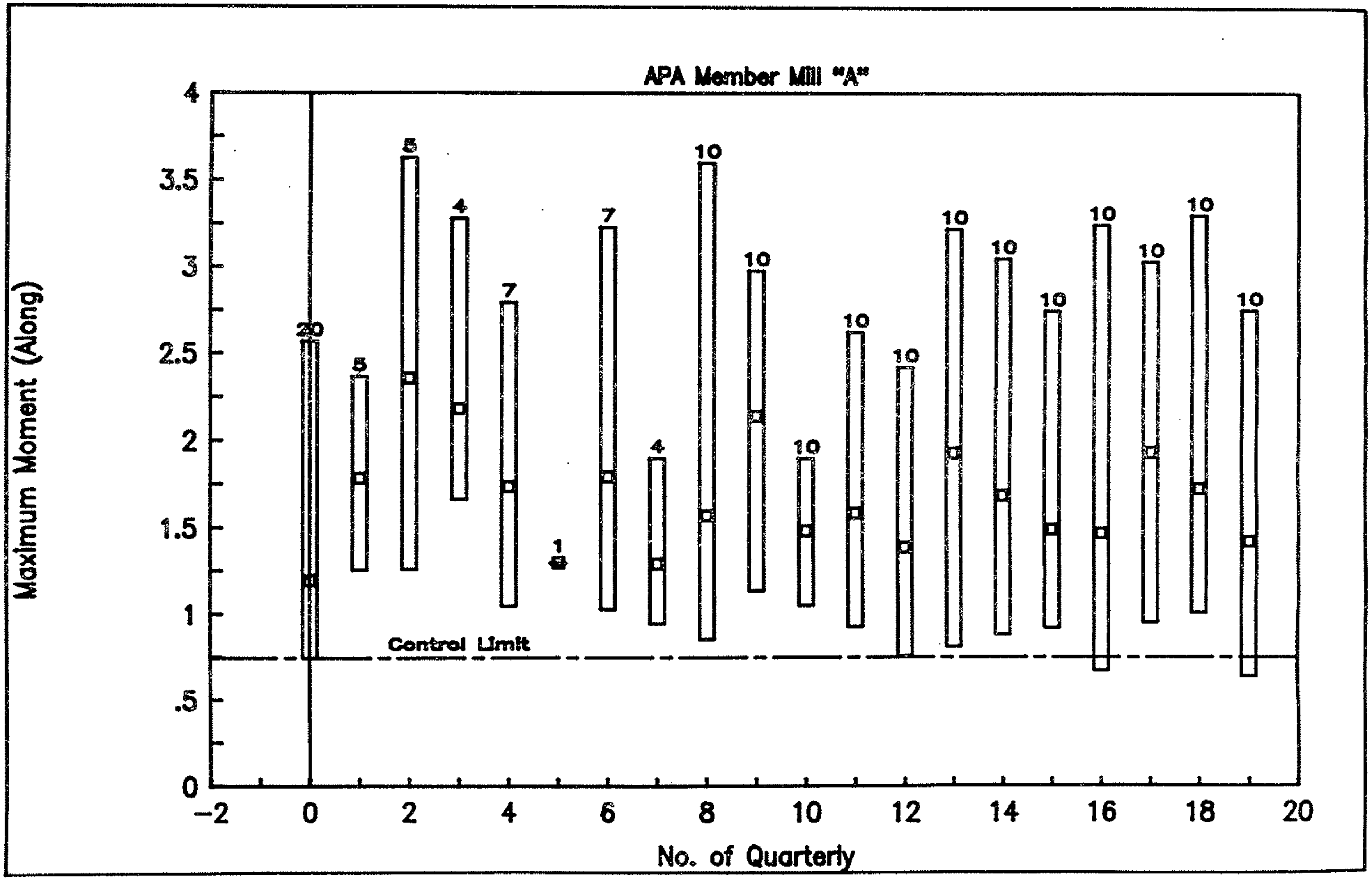

Figure 2. Comparison of censored versus routine sampling for an individual manufacturing site.

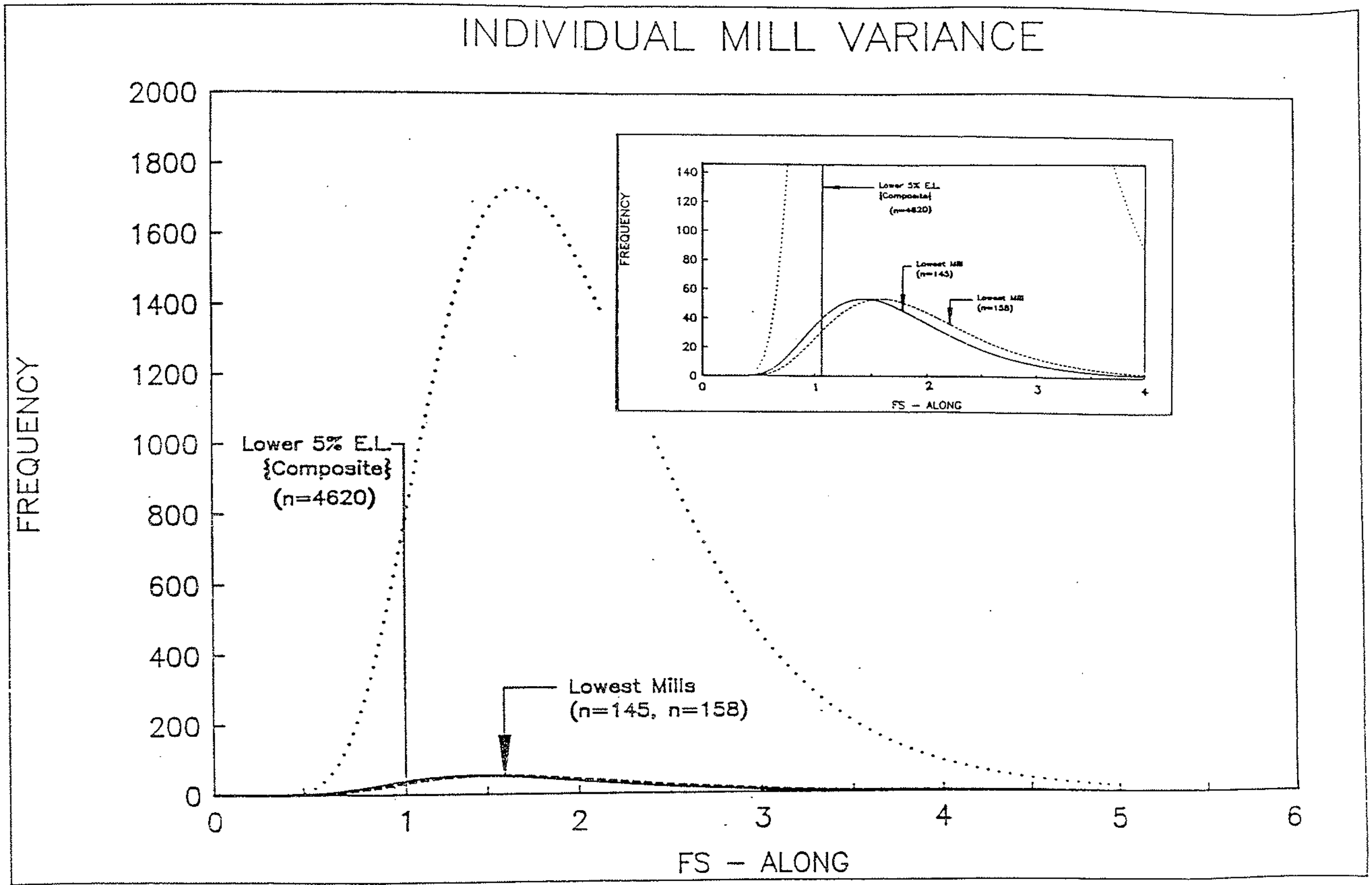

Figure 3. Comparison of subgroup samples with composite sample exclusion limits.

CIB -W18A / 22-5-1

INTERNATIONAL COUNCIL FOR BUILDING RESEARCH STUDIES AND DOCUMENTATION

WORKING COMMISSION W18A - TIMBER STRUCTURES

FUNDAMENTAL VIBRATION FREQUENCY AS A PARAMETER FOR GRADING SAWN TIMBER

by

T Nakai, T Tanaka and H Nagao
Forestry and Forest Products Research Institute
Japan

MEETING TWENTY - TWO

BERLIN

GERMAN DEMOCRATIC REPUBLIC

SEPTEMBER 1989

[Paper for the Meeting of CIB-W18A, 25-28 September, 1989]

FUNDAMENTAL VIBRATION FREQUENCY AS A PARAMETER FOR GRADING SAWN TIMBER

by
Takashi Nakai , Toshinari Tanaka
and Hirofumi Nagao
(FFPRI, Tsukuba, Japan)

1. INTRODUCTION

Due to large cross section of structural timber in Japan, non-destructive tests for measuring modulus of elasticity to estimate the strength of timber has been conducting at Forestry and Forest Products Research Institute. Various non-destructive tests such as measuring deflection caused by dead load, measuring ultra sonic propagation time and density, stress wave propagation time and density and fundamental vibration frequency and density, have been tried to find out the most feasible method at saw mill or lumber yard.

Measuring fundamental vibration frequency and density was considered as one of the favourable non-destructive testing methods, as it is a non-contact measuring method and can be used for a large size timber or log.

This paper presents some extended results obtained under a three year project at FFPRI following the previous paper(1). Main targets are to get the relationship between modulus of rupture and Efr,which was obtainedmodulus of elasticity by measuring fundamental vibration frequency and density, tensile strength and Efr and compressive strength and Efr for grading sawn timber. And also when measuring fundamental vibration frequency, the effect of length divided by the height of specimen was experimentally investigated mainly to know the minimum ratio of length by height for measuring the frequency of short column specimen.

---

(1) T.Nakai and T.Tanaka; Non-destructive test by frequency of full size timber for grading, CIB-W18A/21-5-1, Proceedings of meeting twenty one, 1988.

2. EXPERIMENTS

2.1 Materials

Species used was sugi (*Cryptomeria japonica*) from Hiroshima prefecture. The nominal size of specimen was 100 mm X 100 mm X 4000 mm. The sample size was 100, which had been sampled randomly at saw mill in Hiroshima and deliverd to FFPRI. The mean moisture content was about 19%.

Modulus of elasticity measured by deflection (Edw) were obtained, then after putting them in order from the lowest value of Edw to the highest one. The three serial specimens were considered as an unit, from which one specimen at the second order was sorted for full size bending test and the rest of two specimen in an unit were sorted for full size tensile and short column compressive test.

For bending 33 specimens were used and 67 specimens were used for tensile and short column compressive test. These size of specimen were reflected by their coefficient variation which was obtained previous full size test in green condition from the same source as 14.4% for modulus of rupture and 20.5% for tensile strength.

2.2 Methods

The four methods for measuring modulus of elasticity as described in a previous paper were applied. Those are static modulus of elasticity (Edw) by deflection measurement, an ultrasonic modulus of elasticity(Euw) and a stress wave modulus of elasticity (Esw) by measuring stress wave propagation time and density and a frequency modulus of elasticity (Efr) by measuring the fundamental vibration frequency and density.

The full size rupture test was conducted after recording the size of knots. In the case of bending test, the total span was taken 2700 mm andone third loading system was applied. The length of specimen was cut to 3000 mm. For tensile test, the length of specimen was adjusted to 3500 mm and from the rest of 500 mm, short column test specimen was finished at 290 mm length, which slenderness ratio was about 10.

To know the effect of length divided by height of specimen on measuring the fundamental vibration frequency, nominal size of 50 mm square sawn sugi timbers were prepared with the initial length of 3000 mm. The frequency measurment was conducted with cutting the length of specimen, at first cutting every 500 mm to 1000 mm, then every 200 mm to 600 mm and finally every 50 mm to 250 mm. Thirteen measurments were done.

3. RESULTS AND DISCUSSION

The similar results were obtained in comparison of various E values as reported before. The correlation coefficient between Efr and Edw showed the highest value among the other relationships. In Fig.1, 100 pooled data between Efr and Edw were plotted with the correlation coefficient; r=0.98.

The relationship between Efr, which was measured at 4000 mm length before cut to 290 mm short column test piece, and the compressive strength (σc) was shown in Fig.2. The value of r was 0.82. The standard error was 19.3 kgf/cm^2.

The relationship between Efr and tensile strength (σt) was shown in Fig.3. The value of r was 0.55. And the standard error was 51.1 kgf/cm^2. In Fig.4, the relationship between Efr and modulus of rupture (MOR) was shown. The r value was 0.72 with the standard error of 43.8 kgf/cm^2.

It is concluded that Efr can be used as a useful parameter for grading sawn timber not only for modulus of rupture but also for tensile and compressive strength.

Finally, the results of the effect of length by height of specimen was shown in Figs. 5 and 6. It is clear that the fundamental vibration frequency can be measured at more than 6 of the length by height of specimen. At less than 5 of length by height, it was impossible to detect the fundamental vibration frequency, because such a relative short specimen could not be regarded as a bar for vibration. We have tried the same experimental measurment at 100 mm by 100 mm cross section's specimen and got the similar results. We also noticed that in the case of small specimen such as the cross section of 25 mm by 25 mm and 400 mm length of specimen, which was 16 times of the height, the fundamental vibration frequency was clearly observed.

4. CONCLUSION

It was concluded that the fundamental vibration frequency measurement could be used as a useful parameter for grading sawn timber to estimate not only modulus of rupture, but also tensile and compressive strength.

According to the experimental results, for measuring the fundamental vibration frequency, the ratio of length by height of specimen should be larger than six.

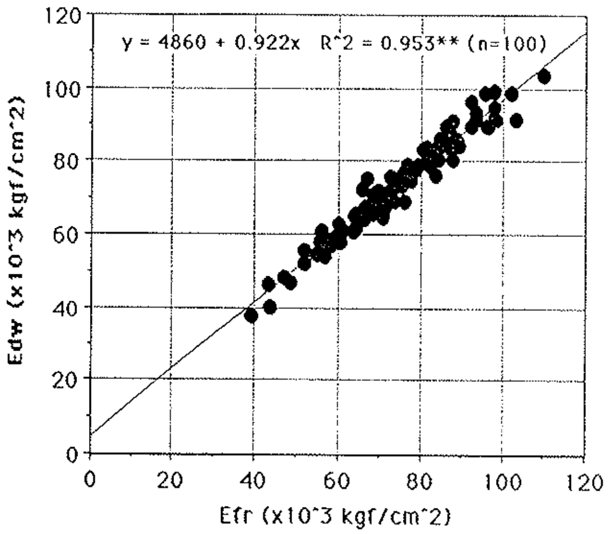

Figure 1. Relationship between Efr and Edw on sugi squares

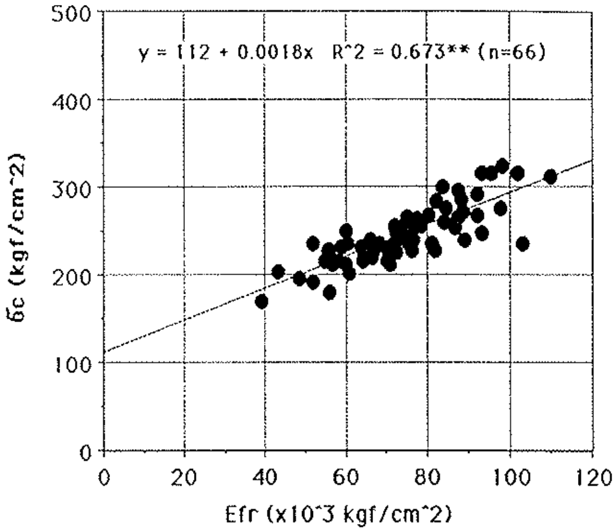

Figure 2. Relationship between Efr and compressive strength (σc)

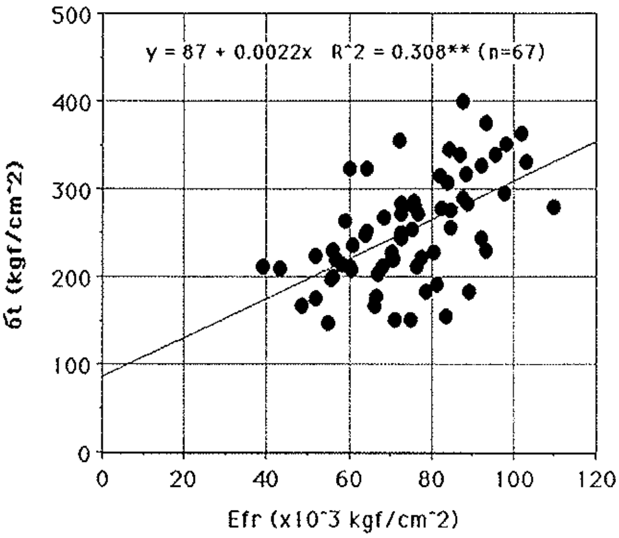

Figure 3. Relationship between Efr and tensile strength (σt)

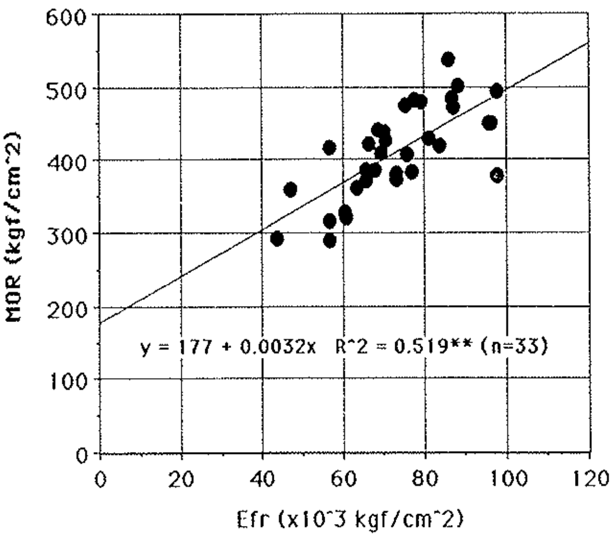

Figure 4. Relationship between Efr and MOR

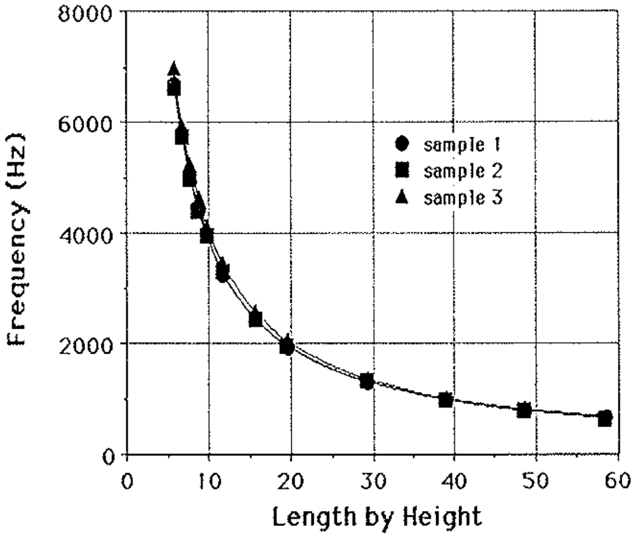

Figure 5. Effect of length by height of specimen on measuring fundamental vibration frequency

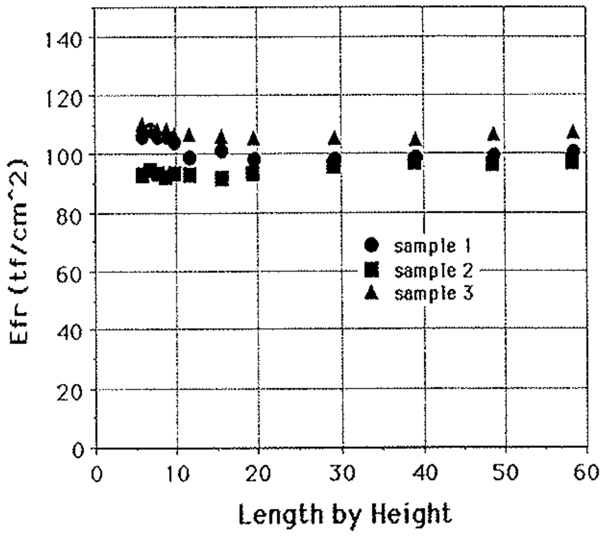

Figure 6. Effect of length by height of specimen on Efr for sugi 50 mm X 50 mm squares

CIB -W18A / 22-6-1

INTERNATIONAL COUNCIL FOR BUILDING RESEARCH STUDIES AND DOCUMENTATION

WORKING COMMISSION W18A - TIMBER STRUCTURES

SIZE EFFECTS AND PROPERTY RELATIONSHIPS FOR CANADIAN 2-INCH DIMENSION LUMBER

by

J D Barrett and H Griffin
University of British Columbia
Canada

MEETING TWENTY - TWO

BERLIN

GERMAN DEMOCRATIC REPUBLIC

SEPTEMBER 1989

SIZE EFFECTS FOR CANADIAN DIMENSION LUMBER

BY

J. D. Barrett[1] and Helen Griffin[2]

Introduction

Strength of structural lumber evaluated on a full-size basis, varies with the member dimensions. In full-size members, size-effects are significantly greater than previously recognized in the development of design values based on small clear specimen tests (Madsen and Buchanan (1986), Fewell and Glos (1988)). Size effects observed from timber tests are of such significance that size factors have been introduced explicitly in design codes such as the Canadian Code for Engineering Design in Wood (CAN3 O86-M84) and the British Standard BS 5268 Part 2 (BSI, 1984). New size adjustment factors are being proposed in design property evaluation standards including the ASTM standard under development for evaluation of design properties of structural lumber based on full-size tests and the CEN standard for determination of characteristic values of mechanical properties of timber.

The Canadian lumber industry sponsored, through the Canadian Wood Council's (CWC) Lumber Properties Project, a comprehensive evaluation of strength properties of on-grade dimension lumber samples for a range of grades and widths commonly produced in Canada. This paper presents an analysis of the influence of member size on the bending, compression and tension strength derived using results from tests of 38 mm thick dimension lumber.

The Data Base

Sampling

The CWC program was established to develop bending, tension and compression parallel to grain strength property data for the "major" commercial species groups Douglas fir-Larch (D Fir-L), Hem-Fir and Spruce-Pine-Fir (S-P-F) and certain other individual "minor" species of less commercial importance for structural use.

Sampling was conducted on a stratified basis. The growth range for the species group was sub-divided into regions judged to have similar growing characteristics. Figure 1 shows the region distribution of S-P-F sampling. Within a growing region, the number of samples selected was proportional to the region's production compared with the total production for the species group.

Bending, tension and compression samples were selected sequentially from randomly selected packages of lumber. Actual sample sizes obtained for the bending, tension, and compression property evaluations of the major species are summarized by size, grade and species in Table 1.

---

[1] Professor, Department of Harvesting and Wood Science, University of British Columbia
[2] Graduate Student, Department of Harvesting and Wood Science, University of British Columbia
[3] An updated version to be submitted for publication.

Testing

All structural property evaluations were conducted at the laboratories of Forintek Canada Corp. (Vancouver). Each member was conditioned to approximately 15 percent moisture content and evaluated using a Cook-Bolinders grading system to establish a modulus of elasticity (MOE) profile prior to destructive evaluation.

Full-size structural evaluations were conducted using closed-loop testing systems to maintain loading (or deformation) rates in accordance with ASTM D-4761 (ASTM, 1988).

Bending strength and bending modulus of elasticity evaluations were conducted on a 17 to 1 ratio of test span (L) to member width (W). The maximum strength reducing defect (MSRD), was randomly located in the bending test span.

Tension and compression tests were conducted using test gauge lengths shown in Table 2. The MSRD was located in the test zone whenever feasible.

All test data was adjusted to 15 percent moisture content for subsequent evaluations. A more detailed description of the sampling, testing and moisture adjustment procedures is given Fouquet and Barrett (1989).

Size Effects Analysis

The Weibull weakest link model provides a basis for representing relationships between member size and strength properties. For members of equal thickness subjected to the same load configuration, the two parameter Weibull formulation leads to relationships between member areas $A_1 = W_1 L_1$ and $A_2 = W_2 L_2$, and the corresponding strengths P_1 and P_2, at a particular probability level, which may take the form:

$$P_1 / P_2 = (A_2 / A_1)^{S_A} \qquad (1)$$

where member area A is the scale factor for the size effect analysis.

The size parameter S_A, is assumed constant independent of changes in member width or length or property probability level. The magnitude of the size effect depends on the size parameter S_A which can be determined experimentally from tests of members of different geometry assuming that the loading geometry remains similar.

For dimension lumber members, the magnitude of the size parameter varies depending on which dimension (i.e., width or length) is considered (Madsen and Buchanan, 1986). For a member of constant thickness and the same load configuration, this more general size effect can be represented as follows:

$$P_1 / P_2 = (W_2 / W_1)^{S_W} * (L_2 / L_1)^{S_L} \qquad (2)$$

The parameters S_W and S_L are the size parameters for width and length effects respectively. The size parameter S_W reflects the influence of width on strength properties for members of constant length. The size parameter S_L reflects the influence of length changes on properties for members of constant width.

For members of constant length to width ratios (i.e., $L_i = K W_i$) then Eqn. 2 becomes:

$$P_1 / P_2 = (W_2 / W_1)^{S_W + S_L} = (W_2 / W_1)^{S_R} \qquad (3)$$

The parameter S_R is the size parameter for members with constant width to test length ratios.

For consistency, the size parameter S_R must satisfy the following relationships:

$$S_R = S_W + S_L$$
$$S_R = 2\, S_A \qquad (4)$$

The CWC database will be used to evaluate length and width effects in bending, tension and compression for 38 mm dimension lumber.

Size Effects in Bending

Bending strength evaluations were undertaken using a constant ratio of test span to member width (depth), L/W = 17. Since the span to width ratio is constant for all bending members the same size parameter will result when either width (W) or length (L) is chosen as the scale factor.

The size parameter S_R in bending S_{Rb}, is calculated for three grades (Select Structural, No. 2 and No. 3) and two property levels (5th percentile and 50th percentile) for each of the three major species groups. For each individual species, grade and property level combination the size parameter S_{Rb}, is calculated using linear regression techniques. Comparisons of calculated size parameters are provided for individual property level/grade/species cells and combined grades, combined property level and combined species data sets. Statistical tests are performed to test the hypothesis that the size parameters S_{Rb}, are equal (Table 3).

Since member width and length both vary by the same scale factor it is not possible to derive the width or length size factors (S_{Wb} and S_{Lb}) from the CWC data set alone. However, the length effect parameter can be estimated using Hem-Fir and S-P-F data from Madsen and Buchanan (1986). Averaging the 5th and 50th percentile size parameters from their data yields $S_{Lb} = 0.22$. Using Eqn. 4 yields $S_{Wb} = S_{Rb} - S_{Lb}$ and adopting the all species S_{Rb} = 0.455 then, the size parameter for width in bending, $S_{Wb} = 0.235$.

Size Effects in Tension

Tension specimen gauge lengths vary with member width (Table 2). To avoid introducing bias in the data analysis tension size effects were analyzed first using the as-tested data. Size parameters for tension S_t^*, summarized in Table 4 are calculated using as-tested data using width as the scale factor. Results derived using area as the scale factor are given in Table 5. With one exception the analysis showed that the hypothesis of equal size parameters could be accepted. While these results are suitable for comparing size effects across property levels, grades or species the analysis does not allow the size parameters for length (S_{Lt}), or width (S_{Wt}) to be isolated directly.

Studies of lengths effects in tension for S-P-F (Madsen and Buchanan, 1986; Lam, 1987) and Southern Pine (Showalter, Woeste and Bendtsen, 1987) provide a basis for estimating the pure length effect in tension. Analysis of these results yields a tension length effect coefficient $S_{Lt} = 0.151$ for Southern Pine (Showalter et. al., 1987) and $S_{Lt} = 0.132$ for S-P-F (Lam, 1987). There were no consistent differences in the size parameter across sizes, grades or property levels in either data set (Tables 6 and 7).

A length effect parameter S_{Lt} = 0.15 was adopted to adjust the 38 mm x 89 mm as-tested tension data to a 3.68 m gauge length. The adjusted tension data set was analyzed for width effects at the constant length of 3.68 m. Size parameters S_{Wt}, from the tension width effect analysis (Table 8) yielded S_{Wt} = 0.217 for all species combined. There were no significant differences across species, grade or property level categories.

Size Effects in Compression

Size effects in compression were analyzed initially using the as-tested data and member width (W) and area (A=WL) as scaling factors. Results are summarized in Tables 9 and 10. The hypothesis of common size parameters was adopted without exception for all data combined.

Only limited information is available relating compression strength to member length. Madsen (1989) suggests a compression length effect parameter S_{Lc} = 0.10, based on tests of 4 lengths of S-P-F, 38 x 89 mm, dimension lumber. This result appears consistent with unreported studies conducted as part of the CWC Lumber Properties Program.

Compression strength data for the 89 mm and 184 mm wide specimens was adjusted to a common length of 3.66 m using S_{Lc} = 0.10 for length effect adjustments. Width effect size parameter S_{Wc} = 0.121 was obtained for all species data combined. There were no significant differences across species, grades and property levels.

Results and Discussion

Size effects parameters for width (S_W), length (S_L), constant length to width ratios (S_R) obtained for the bending, tension and compression data sets for Canadian species are summarized in Table 12. Size parameters S^* obtained using as-tested data are also tabulated.

The bending size effects analysis showed there were no significant differences in the size parameters S_{Rb}, across property levels, grades and species for the all combined data analysis. Thus, the hypothesis that the bending size effects are equal for all species, grades and property levels is accepted and the common bending size parameter S_{Rb} = 0.455.

Size parameters obtained from the full-size tests of US commercial species groups - Southern Pine, Hem-Fir and Douglas-fir - are presented by Johnson, Evans and Green (1989). Results presented in Table 13 are adapted from Johnson et al. (1989). The bending size parameters obtained from the Canadian (CWC) and US studies are directly comparable since both data sets were collected using the same test configuration. The close agreement between the size parameters S_{Rb}, from the two programs adds support to the claim that the size effect is species independent.

These recent results can also be compared with the earlier in-grade tests conducted as part of the National Lumber Grades Authority (NLGA) program (Madsen and Neilsen, 1978). A statistical analysis of the NLGA proof loading data (Table 14) yields a bending size parameter S_{Rb} = 0.440 with no significant differences across species or grades when all data is combined. These results based on an analysis of 5th percentile data agree very well with the recent studies and confirm that the bending size factor is property level independent.

Independent studies of the length effect in bending provided the bending size parameter for length S_{Lb} = 0.22. The size parameter for width effects in bending was then calculated as the difference $S_{Wb} = S_{Rb} - S_{Lb}$ = 0.235.

Tension size effects analyses for all data combined showed that tension size effects parameters S_{At}, were species, property level and grade independent. The all data average value of S_{At} = 0.20. The tension size effect parameters for length S_{Lt} = 0.15, was derived from previously published independent length effect studies. The CWC data base, adjusted to a common length provided the width effect factor for tension S_{Wt} = 0.217. The size effect for tension strength for members of constant span to length ratios S_{Rt} could be calculated using either $S_{Rt} = 2\, S_{At}$ or $S_{Rt} = S_{Lt} + S_{Wt}$. The size parameter S_{Rt} was taken as the average of the two results and S_{Rt} = 0.384.

It is important to note that these size parameters for tension S_{Rt}, S_{Wt}, S_{Lt} and S_{At} are distinctly different from the size parameter S^*_t, obtained from analyses of as-tested data. Thus, a consistent approach to size effects analysis must account for both width and length variation in the test data when both specimen width and length vary. If the size analysis is consistent in this sense then the resulting model can be used to derive property adjustment relationships appropriate for adjusting test data to standard test conditions or to derive size factors for codes which are consistent with testing standards requirements.

Evaluations of tension strength of US Hem-fir and Douglas-fir, were conducted using the same test gauge lengths used for Canadian species. The size parameter for US species, S^*_t = 0.322, (Table 13) closely agrees with the values derived on an as-tested basis for Canadian species.

Tension strength evaluations for Southern Pine were conducted using a common gauge length of 3660 m (Shelley, 1989). Variations in strength properties across sizes in this case will be due entirely to width effects. The size parameter for width S_{Wt} = 0.214 for Southern Pine was derived from results presented by Johnson et al. (1989). This result agrees very closely with the tension width effect derived for Canadian species.

Bury (1978) summarizes results of NLGA tension testing program. Tension testing was conducted using the same test gauge length for all sizes. These results yield a tension size parameter for width S_{Wt} = 0.217 (Table 15) which agrees very well with the recent studies of Canadian and U.S. species.

Compression size effects analyses show no significant differences in S_{Ac}, across the property levels, grades and species evaluated. The scale factor width times length (WL), yields the size factor S_{Ac} = 0.114. For constant length compression members, the size factor for width becomes S_{Wc} = 0.121 and the size factor for members of constant length to width ratios was calculated to be S_{Rc} = 0.225.

Compression tests of US species were conducted using short specimens with a length to width ratio of 2.5 (Shelley, 1989). The size parameter S_{Rc} = 0.140 derived from results of Johnson et al. (1989) is significantly smaller than the value obtained for Canadian species. Differences in test methods between the Canadian and US programs may explain the discrepancy.

Table 16 summarizes size factors for dimension lumber being proposed for adoption in ASTM standards, the Canadian Code For Engineering Design in Wood (CSA, 1989), CEN ENXXX1 and those proposed by Fewell and Glos (1988). The CSA standard presents bending, tension and compression of parallel to grain design properties for members of specified length to width ratios. Size factors S_R are used to derive apparent depth factors to be applied to a characteristics strength referenced to a depth of 286 mm and a specified length to width ratio. The size parameters S_R, derived using reliability based procedures, provide uniform safety across members of different widths.

The draft ASTM - Standard Practice for Establishing Allowable Properties for Visually Graded Lumber from In-Grade Tests of Full Size Lumber, provides for separate width and length adjustment which results in parameters S_R, nearly equivalent to those in the Canadian code with the exception of compression where the size effect is underestimated by a factor of 2. However, the size parameters for width effects are generally too large. The factors for length effects in bending appear to be too small. The size parameter S_{Rc} recommended in ASTM may be too small for full-length compression specimens.

The size adjustments adopted for "width" in the ENXXX1 (CEN, 1989) are consistent with results from the CWC data set. The ENXXX1 adjustments appear to underestimate the size factors appropriate for adjusting test data derived from the constant width to length bending and tension specimens recommended in ISO 8375 (ISO, 1984).

Conclusions

The CWC Lumber properties data base provides large, property matched data sets suitable for analysis of size effects factors for Canadian structural dimension lumber.

The results of the size effects analysis suggest that:

1. Bending, tension and compression strength properties can be significantly affected by changes in member width and length. Width effects in bending and tension members appear similar while length effects are somewhat greater in bending than tension. Width and length effects are smallest for compression members.

2. Comparison of tension and bending size parameters derived herein show similar results for Canadian and US commercial species groups which strengthens the case for applying a common set of size parameters for all grades and species. Size parameters are also independent of property level. The only major inconsistency observed in the results, as presented in this paper, is the difference in size factors for compression which may be due to the significant size difference in test specimens employed.

3. Size factors for adjusting test data or modifying code design properties size must be expressed in a manner consistent with the associated test standards. If test standards employ members of constant length to width ratios then the size factors will be different than would be employed with constant length test members.

4. The CWC test data suggests that a size parameter of the order of $S = 0.2$ could be applied for bending and tension width and length effects. The size parameter $S = 0.1$ could be applied for compression width and length effects. These size factors would provide a basis for developing a set of simplified expressions for adjusting tension, bending and compression strength data for both data interpretation and code documents.

5. The basis for the ENXXX1 (CEN, 1989) recommended size factors should be reviewed for consistency with ISO 8375 (ISO, 1984).

References

American Society for Testing and Materials (ASTM). 1988. Standard test methods for mechanical properties of lumber and wood-based structural material. ASTM D4761-88 Annual Book of Standards. Philadelphia, Pa.

American Society for Testing and Materials (ASTM). In Preparation. Standard practice for establishing allowable properties for visually graded dimension lumber from in-grade tests of full-size lumber.

British Standard Institution (BSI). 1984. Structural use of timber. Part 2. Code of practise for permissible stress design, materials and workmanship. BS5268: Part 2.

Bury, K.V. 1978. Statistical analysis of NLGA tension tests prepared for the National Lumber Grades Authority. Vancouver, B.C.

Canadian Standards Association. 1989. Code for Engineering Design in Wood. CAN3 086-M89 - Limits States Design (in preparation) CSA. Rexdale, Ontario.

European Committee for Standardization (CEN). 1989 ENXXX1 - Standard for determination of characteristic values of mechanical properties of timber.

Fewell and Glos. 1988. The determination of characteristic strength values for stress grades of structural timber. Part 1. CIB-W18A/21-6-2. Vancouver.

Fouquet, R., and J.D. Barrett. 1989. Physical and mechanical properties of Canadian visually stress-graded lumber established by in-grading testing. Council of Forest Industries of British Columbia. Vancouver.

International Organization for Standards. 1984. ISO-8375, Timber structures - Solid timber in structural sizes - Determination of some physical and mechanical properties.

Johnson, L.A., J.W. Evans and David W. Green. 1989. Volume adjustments for in-grade data. In: In-grade testing of structural lumber. Proceedings of ASTM Workshop on the North American In-Grade Testing Program. Published by the Forest Products REsearch Society. Madison, Wisconsin. Pp. 56-61.

Lam, F. 1987. Effect of length on tensile strength of lumber. Forintek Canada Corp. Vancouver.

Madsen, B. and P.C. Neilsen. 1978. In-grade testing bending tests in Canada June 1977-May 1978. Prepared for the National Lumber Grades Authority. Vancouver, B.C.

Madsen, B. and A.H. Buchanan. 1986. Size effects in timber explained by a modified weakest link theory. Canadian Journal of Civil Engineering 13, 218-232.

Madsen, B. 1989. Personal communication.

Shelley, Bradley E. 1989. Testing machines: development, calibration and comparative studies. In: In-grade testing of structural lumber. Proceedings of ASTM Workshop on the North American In-Grade Testing Program. Published by the Forest Products Research Society. Madison, Wisconsin. Pp. 15-26.

Showalter, K.L., F.E. Woeste and B.A. Bendtsen. 1987. Effects of length on tensile strength in structural lumber USDA Forest Service Research Paper FPL-RP-482. Forest Products Laboratory. Madison, Wisconsin.

SPRUCE-PINE-FIR

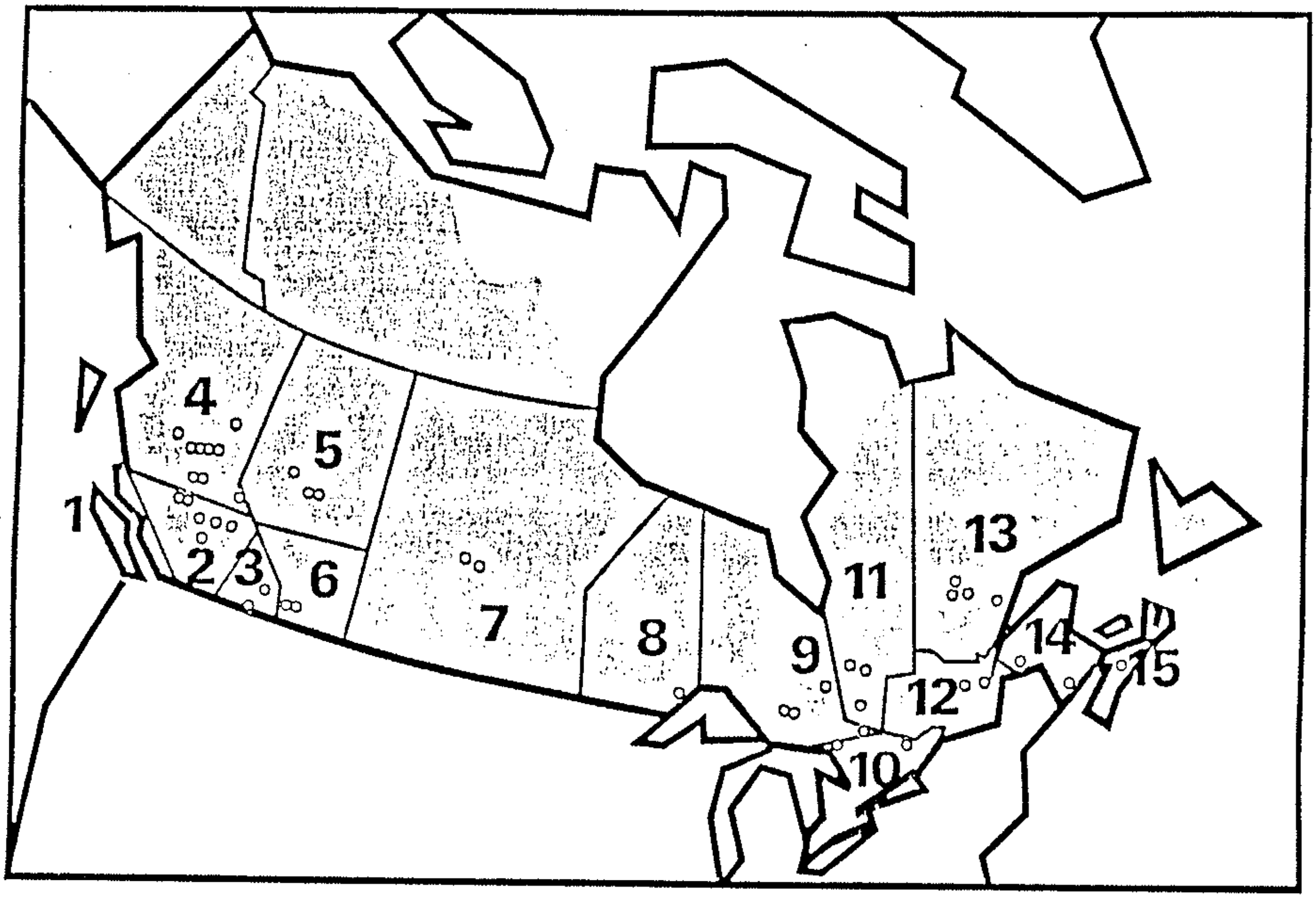

Figure 1. Sampling Regions and sampled mills for Spruce-Pine-Fir.

Table 1. Actual Sample Sizes for Bending, Tension and Compression Property Evaluations of Select Structural, No. 2 and No. 3 Grade, 38 mm Thick Dimension Lumber.

Species Group	Width (mm)	Bending Grade			Compression Grade		Tension Grade	
		SS	2	3	SS	2	SS	2
D Fir-L	89	370	370	150	372	374	372	373
	184	373	370	149	374	371	373	371
	235	372	374	150	375	373	373	370
Hem-Fir	89	381	380	170	382	381	360	362
	184	382	402	158	383	382	381	381
	235	379	385	159	381	380	383	378
S-P-F	89	441	440	180	440	441	440	444
	184	444	986	200	440	443	441	440
	235	440	441	210	420	418	446	463

Note: No. 3 grade was not sampled for Compression and Tension property studies.

Table 2. Test Spans and Gauge Lengths for Bending, Tension and Compression Property Tests.

Member Width	Test Span	Gauge Length	
	Bending (mm)	Tension (mm)	Compression (mm)
89	1510	2640	2440
184	3130	3680	3660
235	3990	3680	4270

Table 3. Bending Strength Size Parameters S_{Rb}, using Member Width (W) as the Scale Factor. All Members Tested on 17 to 1 Span Depth Ratio.

Property Level	Grade	Species			
		D Fir-L	Hem-Fir	S-P-F	All Species
5th	SS	.529	.580	.474	.528
	No.2	.377	.476	.351	.401
	No.3	.392	.586	.510	.496
	All	.433	.547	.445	.475
50th	SS	.292	.437	.383	.371
	No.2	.435	.522	.385	.447
	No.3	.481	.472	.506	.486
	All	.403	.477	.425	.435
All	SS	.410	.509	.428*	.449
	No.2	.406	.499	.368	.424

Table 4. Tension Strength Size Parameters S_t^*, Obtained Using As-Tested[1] Property Data and Member Width (W) as the Scale Factor.

Property Level	Grade	Species			
		D Fir-L	Hem-Fir	S-P-F	All Species
5th	SS	.285	.316	.343	.315
	No. 2	.325	.368	.164	.286
	All	.305	.342	.254	.300
50th	SS	.185	.320	.286	.264
	No. 2	.201	.295	.192	.229
	All	.193	.307	.239	.247
All	SS	.235*	.318	.315	.289
	No. 2	.263	.331	.178	.258
	All	.249*	.325	.247	.273

* Reject H_o: All size parameters are equal. (Significance level 5%)
1 No length effects adjustments.

Table 5. Tension Strength Size Parameters S_{At}, Obtained Using Member Width Times Length as the Scale Factor.

Property Level	Grade	Species			
		D Fir-L	Hem-Fir	S-P-F	All Species
5th	All[1]	0.221	0.247	0.188	0.219
50th	All	0.141	0.225	0.177	0.181
All	All	0.181	0.236	0.182	0.200

1 Select Structural and No. 2.

Table 6. Tension Strength Size Parameters for Length S_{Lt}, for Southern Pine Dimension Lumber (38 mm thickness). (Data from Showalter, Woeste and Bendtsen, 1987.)

Property Level	Grade	Width (mm)	Size Parameter S_{Lt}
Mean	MSR[1]	89	0.118
	No. 2	89	0.134
	All	89	0.126
Mean	MSR	235	0.111
	No. 2	235	0.241
	All	235	0.176*
All	MSR	All	0.115
	No. 2	All	0.188
	All	All	0.151*

1 2250f-1.9E

* Reject H_o: All size parameters are equal. (Significance level 5%)

Table 7. Tension Strength Size Parameters for Length S_{Lt}, for 38 x 89 mm, Spruce-Pine-Fir Dimension Lumber. (Data from Lam (1987)).

Property Level	Grade	Size Parameter S_{Lt} (Uncensored)
5th	SS	0.190
	No. 2	0.187
	All	0.188
Mean	SS	0.097
	No. 2	0.052
	All	0.075
All	SS	0.144
	No. 2	0.119
	All	0.132

1 Based on No. 2 censored data.

Table 8. Tension Strength Size Parameters for Width S_{Wt}, Obtained Using Tension Strength Properties Adjusted to a Length of 3.68 m.

Property Level	Grade	Species			
		D Fir-L	Hem-Fir	S-P-F	All Species
5th	SS	0.228	0.259	0.287	0.258
	No. 2	0.268	0.311	0.107	0.229
	All	0.248	0.285	0.197	0.243
50th	SS	0.128	0.263	0.230	0.207
	No. 2	0.144	0.238	0.135	0.173
	All	0.136	0.251	0.182	0.190
All	SS	0.178	0.261	0.258	0.232
	No. 2	0.206	0.275	0.121	0.201
	All	0.192*	0.268	0.190	0.217

*Reject H_o: All size parameters are equal. (Significance level 5%).

Table 9. Compression Strength Size Effects Parameters S_c^*, Obtained Using As-Tested[1] Data and Width as a Scale Factor.

Property Level	Grade	Species			
		D Fir-L	Hem-Fir	S-P-F	All Species
5th	SS	.146	.240	.233	.206
	No. 2	.191	.144	.203	.179
	All	.168	.192	.218	.193
50th	SS	.126	.205	.242	.191
	No. 2	.122	.121	.174	.139
	All	.124	.163	.208	.165
All	SS	.136	.222	.238	.199
	No. 2	.156	.133	.188	.159
	All	.146	.178	.213	.179

[1] No length effects adjustments.

Table 10. Compression Strength Size Parameters S_{Ac}, Obtained Using Member Width times Length as the Scale Factor.

Property Level	Grade	Species			
		D Fir-L	Hem-Fir	S-P-F	All Species
5th	All[1]	0.107	0.122*	0.139	0.123
50th	All	0.079	0.104	0.133	0.105
All	All	0.093	0.113	0.136	0.114

[1] Select Structural and No. 2
* Reject H_o: All size parameters are equal. (Significance Level 5%)

Table 11. Compression Strength Size Parameters S_{wc}, Obtained Using Compression Data Adjusted to a Length L = 3.66 m.

Property Level	Grade	Species			
		D Fir-L	Hem-Fir	S-P-F	All Species
5th	All[1]	0.110	0.134*	0.160	0.135
50th	All	0.066	0.105	0.150	0.107
All	All	0.088	0.120	0.155	0.121

[1] Select Structural and No. 2
* Reject H_o: All size parameters are equal. (Significance Level 5%)

Table 12. Summary of Data Based and Calculated Bending Compression and Tension Size Parameters - All Data.

Property	Size Parameters						
	S^{*6}	S_R	S_W	S_L	S_A	$S_R=2S_A$	$S_R=S_L+S_W$
	(1)	(2)	(3)	(4)	(5)	(6)	(7)
Bending	0.455	0.455	0.235[4]	0.22[1]	0.228	0.456[4]	-
Tension	0.273	0.384[5]	0.217	0.15[2]	0.200	0.400[4]	0.367[4]
Compression	0.179	0.225[5]	0.121	0.10[3]	0.114	0.228[4]	0.221[4]

[1] Based on Madsen and Buchanan (1986).
[2] Based on Lam (1987) and Showalter et. al. 1987.
[3] Madsen (1989) Personal Communication.
[4] Calculated value.
[5] Average of calculated values from Col. 6 and 7.
[6] Size factor using "as-tested" data and width as the scale factor.

Table 13. Comparisons of Size Parameters Derived from Evaluations of Canadian and U.S. Commercial Species Groups.

Property	Size Parameter	Species		
		Canadian[6]	Canadian[7]	U.S.[8])
Bending	S_{Rb}	0.455	0.440	0.414[1]
Tension	S_t *[2]	0.273		0.322[3]
	S_{Wt}	0.217	0.217	0.214[4]
Compression	S_{Rc}	0.225		0.140[5]

1 Calculated using the average of all size parameters for 5th and 50th percentiles.
2 Derived using the "as-tested" data sets.
3 Hem-Fir (US) and Douglas-fir (US) average of size parameters for 5th and 50th percentiles.
4 Southern Pine-average of size parameters for 5th and 50th percentiles.
5 L/W = 2.5, average of size parameters for the 5th and 50th percentile.
6 CWC Lumber Properties Program
7 NLGA In-Grade Program (Madsen and Neilsen, 1978)
8 Results adapted from Johnson et. al. (1989).

Table 14. Bending Strength Size Parameters S_{Rb}, Derived from In-Grade, Proof Loading Data (Madsen and Neilsen, 1978).

Grade	Species			
	D Fir-L	Hem-F	S-P-F	All Species
SS	0.661	0.418	0.257	0.400*
1	0.763		0.531	0.661
2	0.584	0.131	0.278	0.360
3	0.422	0.535	0.422	0.460
All	0.614	0.361	0.338	0.440

* Reject H_o: All size parameters are equal. (Significance level 5%)

Table 15. Tension Strength Size Parameters S_{Wt}, Derived from In-Grade, Proof Loading Data (Bury, 1978).

Grade	Species			
	D Fir-L	Hem-F	S-P-F	All Species
SS	.342	.275	.261	.266
1	.389	.339	.346	.306
2	.023	.096	.218	.095
All	.227*	.224	.270	.217

* Reject H_o: All size parameters are equal. (Significance level 5%)

Table 16. Comparisons of Size Parameters from Selected Sources with Results Obtained for Canadian Species.

Source	Bending			Tension			Compression		
	S_W	S_L	S_R	S_W	S_L	S_R	S_W	S_L	S_R
CWC Data	0.24	0.22	0.46	0.22	0.15	0.37	0.12	0.10	0.23
CAN3-086 M89	0.23[2]	0.23[2]	0.46	0.18[2]	0.18[2]	0.36	0.13	0.13	0.26
ASTM XXXX[3]	0.29	0.14	0.43	0.29	0.14	0.43	0.13	0	0.13
EN XXX1	0.20[1]	-	-	0.20[1]	-	-	-	-	-
Fewell and Glos (1988)	0.30[1]	-	-	0.20[1]	-	-	-	-	-

[1] We assume the size factor as specified applies to member width adjustments.

[2] Not explicitly shown in the Code as a width and length effect. Code size adjustments assume a constant length to width ratio of 17 and 24 for bending and tension. Equivalent width factors are calculated using S_R = 0.46 and 0.36 respectively.

[3] Standard Practice for Establishing Allowable Properties for Visually Graded Dimension Lumber from In-Grade Tests of Full-Size Lumber (in preparation).

PROPERTY RELATIONSHIPS FOR CANADIAN 2-INCH DIMENSION LUMBER

by

J. D. Barrett[1] and Helen Griffin[2]

Introduction

Implementation of standards for development of characteristic strength properties on the basis of full-size tests has created an interest in improving knowledge of the fundamental relationships between structural properties. A more complete understanding of relationships between bending, tension, compression, shear and other structural properties could greatly reduce the time and costs associated with establishing design properties for structural lumber according to testing standards such as the ASTM D 4761 (ASTM (1989)), or the ISO 8375 (ISO, 1984). Improved knowledge of strength property relationships could also contribute to the development of more standardized grading systems and design property classification systems.

Property relationships are being proposed for draft ASTM and CEN standards which provide a basis for deriving compression parallel to grain and tension strength properties from evaluations of bending strength derived from full size tests. The CWC Lumber Properties Program provides a comprehensive database, developed through laboratory based testing, which can be used to evaluate the relationships between bending, tension and compression strength for three major Canadian commercial species groups. The purpose of this paper is examine the CWC data base and to develop the ratios of tension strength (UTS) to bending strength (MOR) and the ratios of compression strength (UCS) to bending strength obtained from the CWC studies and to compare the property ratios with those proposed in the fifth draft of EN XXX1 - The Determination of Characteristic Values of Mechanical Properties and Density of Timber.

The Data Base

The CWC Lumber Properties Project provides full distribution strength information for the three major Canadian commercial species groups Douglas fir-Larch, Hem-Fir and Spruce-Pine-Fir. A brief description of the sampling and testing procedures employed in the CWC program is given in Barrett and Griffin (1989). Fouquet and Barrett (1989) provide a detailed overview of sampling and testing procedures. All bending specimens were evaluated on a 17 to 1 ratio of test span to member width. The test gauge lengths used for compression, tension and bending tests are given in Table 1.

---

[1] Professor, Department of Harvesting and Wood Science
[2] Graduate Student, Department of Harvesting and Wood Science, University of British Columbia

Property Assessment

Bending, tension and compression strength values corresponding to the 0.01, 0.05, 0.10, 0.25, 0.50, 0.75, 0.90, 0.95 and 0.99th percentile are derived from the data for two grades, (Select Structural and No. 2); three widths (89, 184 and 256 mm) for each of the three commercial species groups (S-P-F, Hem-Fir and D fir - Larch). Prior to testing, lumber specimens were conditioned to approximately 15 percent moisture content. All data was adjusted to the 15 percent target moisture content.

Property Relationships Analysis

Ultimate Tensile Strength

Ultimate tensile strength to modulus of rupture ratios (UTS/MOR) were calculated for each percentile level using the as-tested data sets. UTS/MOR ratios at each percentile level are plotted against the corresponding MOR. Figures 1 and 2 summarize the results for the Select Structural (SS) and No. 2 grades, respectively. Property ratios for a given member width are almost always higher for the SS grade. Within a grade (SS or No. 2) property ratios increase as member width increases. These trends are consistent across all three species.

Ultimate Compression Strength

Ultimate compression strength to modulus of rupture ratios (UCS/MOR) were calculated as described for the tension strength evaluations. The UCS/MOR ratios obtained for the three species groups are plotted as a function of MOR in Figures 3 and 4. For a particular size, property ratios for the SS and No. 2 grades are very similar. For all three species there is a fairly consistent trend of increasing property ratio with member width within both grades. At a specified MOR level, property ratios for S-P-F tend to be somewhat lower than observed for the other two species as can be seen from the comparisons of the individual species data with the UCS/MOR relationship proposed for EN XXX1 (Fewell and Glos, 1988).

Test Configuration Effects

Barrett and Griffin (1989) showed that member width and length significantly affect bending, compression and tension strength properties. The magnitudes of the size effects derived from studies of dimension lumber produced in Canada is summarized in Table 2. The size effect parameters were independent of species, grade and property level for the major Canadian species groups evaluated.

Size parameters differ for bending, tension and compression properties. As a result, property ratios will vary depending on the reference sizes adopted for representing the individual strength properties. The influence of size adjustments on the property ratios is evaluated by comparing property ratios derived for three different cases: Case A. The "as-tested" analysis as presented previously in Figures 1 to 4, based on member spans and gauge lengths as summarized in Table 1; Case B: property ratios based on an 18 to 1 ratio of member length to width for bending, tension and compression properties and Case C: property ratios based on the ISO 8375 test conditions (Table 3). For Case B and C the test data was adjusted to the specified specimen configurations using the length adjustment factors in Table 2.

UTS/MOR ratios for S-P-F are summarized in Figures 5 and 6 for SS and No.2 grades respectively. Results for the UCS/MOR ratios are presented in Figures 7 and 8. Each figure contains three graphs. The top graph of the figure shows the property ratios as tested (Case A). The middle graph shows the property ratios based on tests at an 18 to 1 length to width ratio (Case B); and the bottom graph shows the property relationships predicted based on the ISO 8375 test standard (Case C).

Subsequent pairs of graphs summarize the UTS/MOR and UCS/MOR results for the D fir-Larch and Hem-fir commercial species groups.

Discussion

The UTS/MOR and UCS/MOR property ratios for Canadian commercial species groups agree closely with those included in the draft EN XXX1 standard. UTS/MOR ratios are reasonably constant across the range of bending strengths evaluated. UCS/MOR ratios vary significantly with MOR level but parallel closely the trend lines presented by Curry and Fewell (1977). Both UTS/MOR and UCS/MOR property ratios calculated using the as-tested data sets are consistently higher for the wider widths in all species groups. On the as-tested basis the UTS/MOR ratios tend to be somewhat lower than the UTS/MOR = 0.6 proposed in the EN XXX1 standard, although there are some species effects evident.

Results for UCS/MOR also show some species dependency with the Douglas-fir and Hem-fir showing somewhat higher UCS/MOR ratios than S-P-F. The S-P-F as-tested results fall slightly lower than the proposed relationship at lower MOR levels.

Comparisons of property ratios developed under the Case A, Case B and Case C adjustment criteria also show consistent trends across species. Figures 5 and 6 show the typical UTS/MOR result, wherein the Case B and Case C adjustment basis both reduce the variability in property ratios between sizes. In addition, both Case B and C increase the absolute level of the UTS/MOR ratio. Of the three approaches the ISO 8375 basis (Case C) leads to the highest property ratios. UTS/MOR property ratios nearly always exceed UTS/MOR = 0.6 when the CWC data base is adjusted to the ISO 8375 test basis using the size adjustments given in Table 2. Examinations of the results for the other two species shows the same trends.

UCS/MOR ratios for S-P-F (Figures 7 and 8) show the typical trends in that, between size variability is altered by the property adjustment base adopted. Between size variability in UCS/MOR ratios is lowest for Case B: the 18 to 1 member length to width ratio. However, the property ratios are highest for the ISO 8375 test basis (Case C).

Clearly, property ratios are affected by the test basis adopted for presenting test results. The analysis also demonstrates that variability in observed property ratios between members of different sizes can be influenced by the choice of member reference configuration. Consistent and reliable adjustments of test data to reference conditions will require: 1. Appropriate size adjustment procedures including procedures for adjusting for member size and load configuration, and 2. Clearly elaborated methods for applying the adjustment procedures to convert "non-standard" test data to the reference test configuration. At the present time the most complex part of this task would appear to be developing the size adjustment procedures appropriate for the wide range of grading systems and species encountered in the timber industry.

The property ratio assessments based on the Canadian lumber data have shown that individual properties and the related property ratios can be significantly affected by the size (the width, the length and the thickness) of the tested section. There will be some optimum set of reference bending, tension and compression test configurations. Based on the three cases presented in this paper it would appear the 18 to 1 test geometry provides a good compromise between reduced variability across sizes and consistency with the EN XXX1 property relationships - particularly in the range of strength properties of interest for development of characteristics values.

Conclusions:

1. UTS/MOR and UCS/MOR property ratios derived from as-tested data sets available for Canadian lumber follow the trends recommended in the EN XXX1 standard. In certain instances the absolute property levels are somewhat lower than EN XXX1 proposes.

2. Property ratios for Canadian lumber can be brought into conformity with -or exceed- the EN XXX1 relationships across a wide range of sizes and grades when the data are adjusted to the ISO 8375 test configurations.

3. It would appear to be important to clarify the reference test configurations and verify the methods for adjusting test data for size effects in order to provide a consistent basis for data adjustment to the intended reference member size and load configurations. Specifying width, length and thickness size adjustment parameters separately and providing an explicit statement of the reference configurations for each test condition could be considered in revisions to EN XXX1.

4. Developing and verifying property adjustment procedures and the selection of optimum test or reference configurations will be an important issue in the evaluation of test data in the preparation of optimum strength classification systems since these systems are typically based upon adopting species and size and perhaps grade independent relationships of strength properties.

References

Barrett, J.D., and H. Griffin. 1989. Size effects for Canadian 2-inch (38mm) dimension lumber. CIB-W18A Paper 22-6-1, Berlin. September, 1989.

Curry, W.T. and A.R. Fewell. 1977. The relationships between the ultimate tension strength and ultimate compression strength of timber and its modulus of elasticity. BRE Current Paper, CP 22/77; Princess Risborough Laboratory, UK.

European Committee for Standardization (CEN). 1989. EN XXX1 - Standard for determination of characteristic values of mechanical properties of timber.

Fewell, and Glos. 1988. The determination of characteristic strength values for stress grades of structural timber. Part 1. CIB-W18A/21-6-2. Vancouver.

Fouquet, R. and J. D. Barrett. 1989. Physical and mechanical properties of Canadian visually stress-graded lumber established by in-grade testing. Council of Forest Industries of British Columbia. Vancouver.

International Organization for Standards. 1984. ISO - 8375, Timber structures - Solid timber in structural sizes - Determination of some physical and mechanical properties.

Table 1. Test Spans and Gauge Lengths for Bending, Tension and Compression Property Tests.

	Test Span	Gauge Length	
Member Width	Bending (mm)	Tension (mm)	Compression (mm)
89	1510	2640	2440
184	3130	3680	3660
235	3990	3680	4270

Table. 2. Width and Length Size Adjustment Parameters for Canadian Dimension Lumber (Barrett and Griffin, 1989).

Property	S_W[1,3]	S_L[2,3]
Bending	0.23	0.22
Tension	0.22	0.15
Compression	0.13	0.10

1 Size parameter for width
2 Size parameter for length
3 Size adjustment relationship $P_2/P_1 = (W_1/W_2)^{S_W} \cdot (L_1/L_2)^{S_L}$

Table 3. Reference Configurations for Bending, Tension and Compression for ISO 8375.

Property	Test Gauge Length
Bending	18 x Width
Tension	9 x Width
Compression	6 x Thickness

~~Case A~~

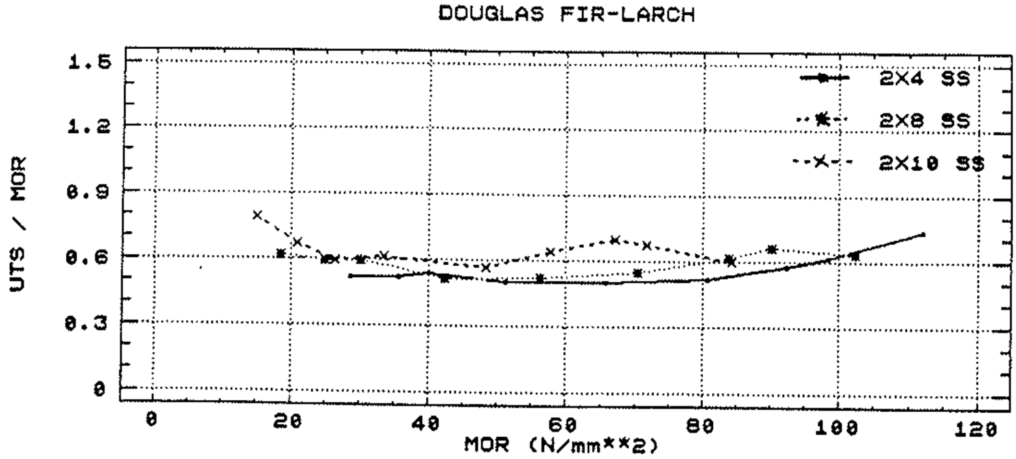

~~Case B~~

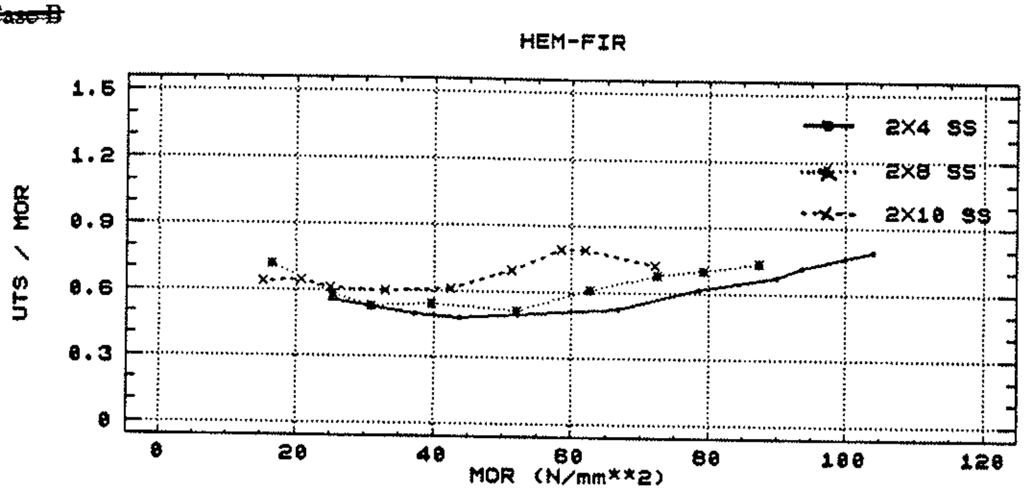

~~Case C~~

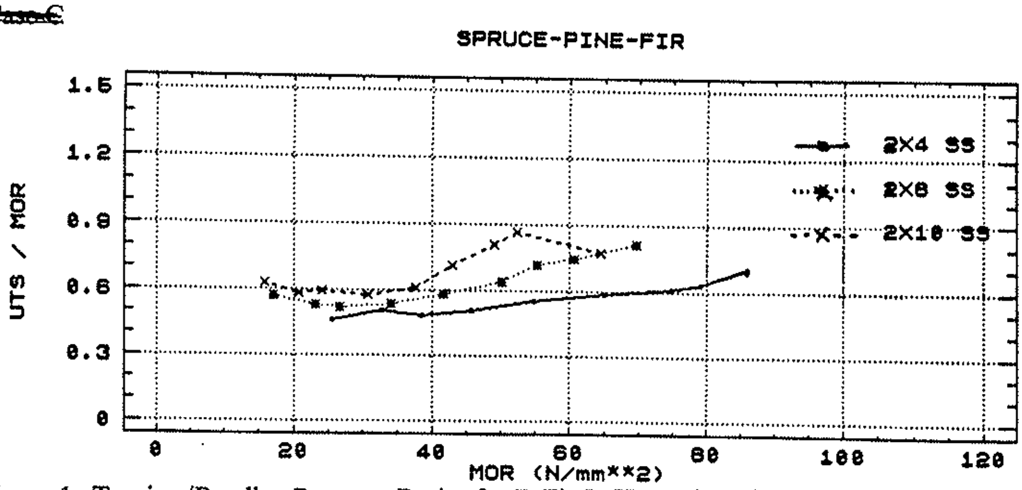

Figure 1. Tension/Bending Property Ratios for D Fir-L, Hem-Fir and S-P-F, Select Structural Grade.

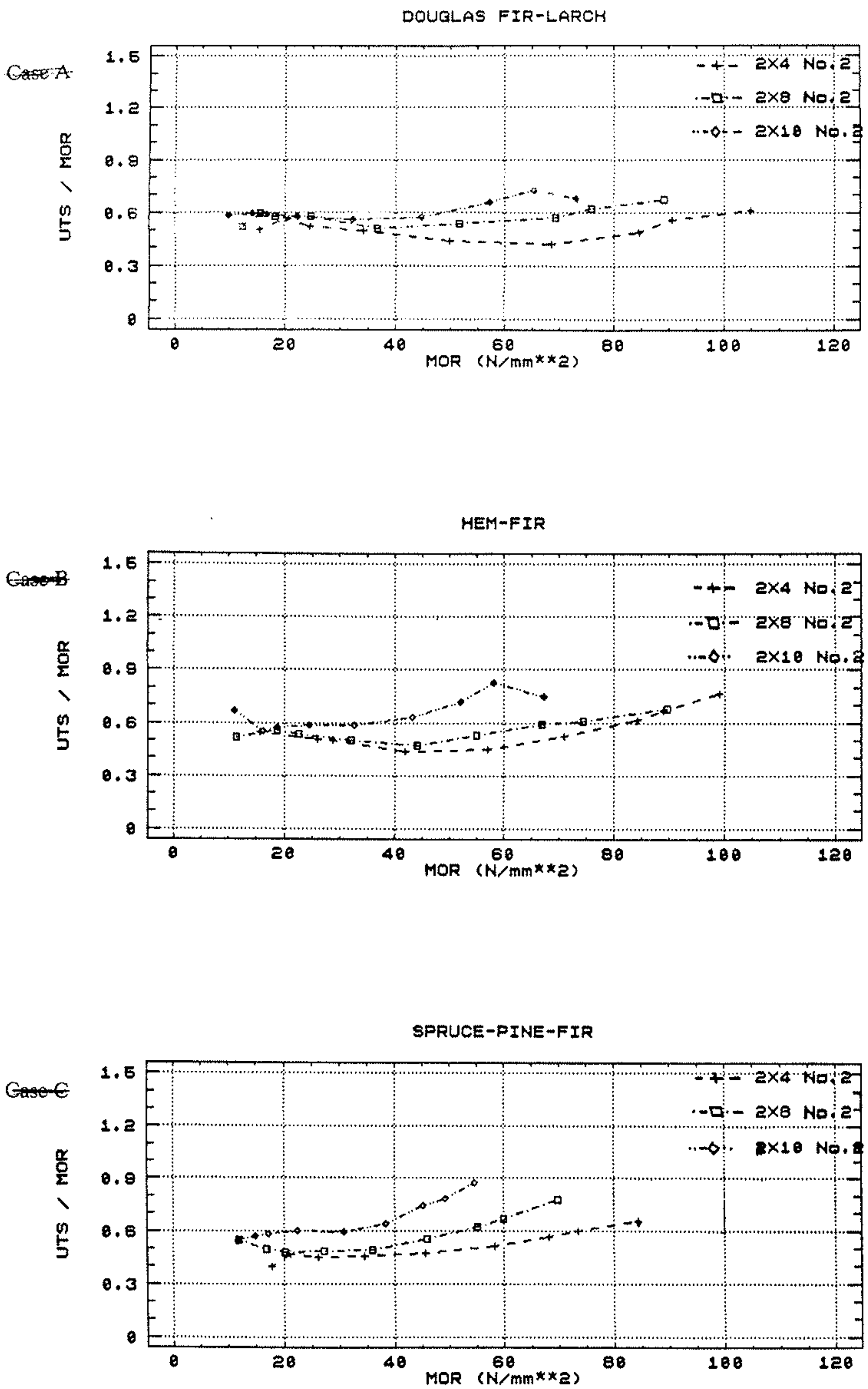

Figure 2. Tension/Bending Property Ratios for D Fir-L, Hem-Fir and S-P-F, No. 2 Grade.

~~Case A~~

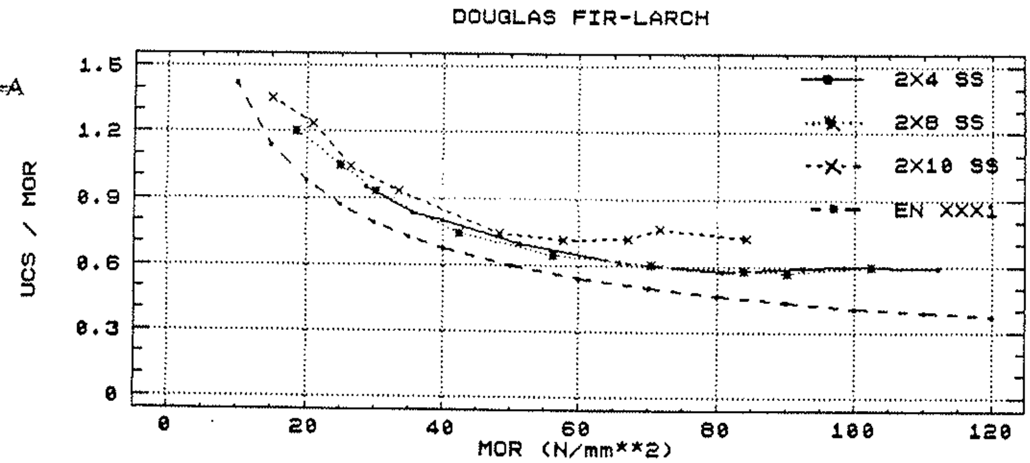

~~Case B~~

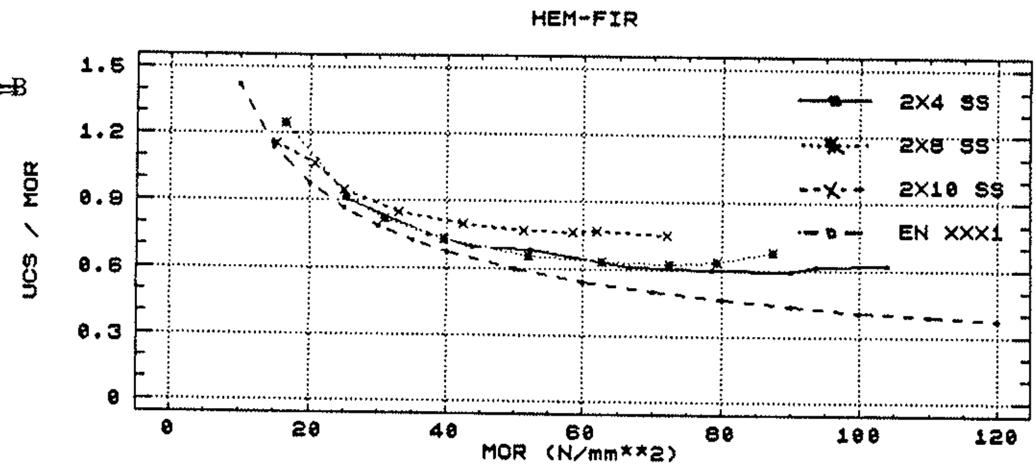

~~Case C~~

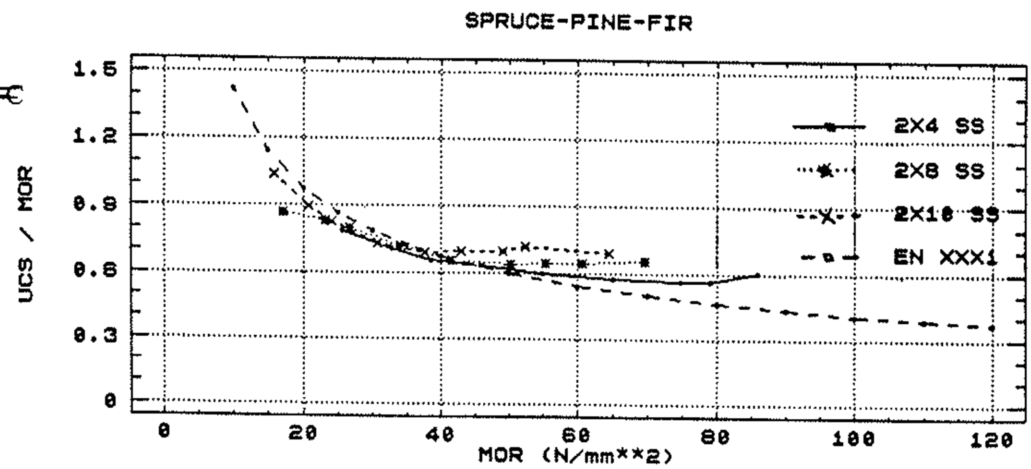

Figure 3. Compression/Bending Property Ratios for D Fir-L, Hem-Fir and S-P-F, Select Structural Grade.

~~Case A~~

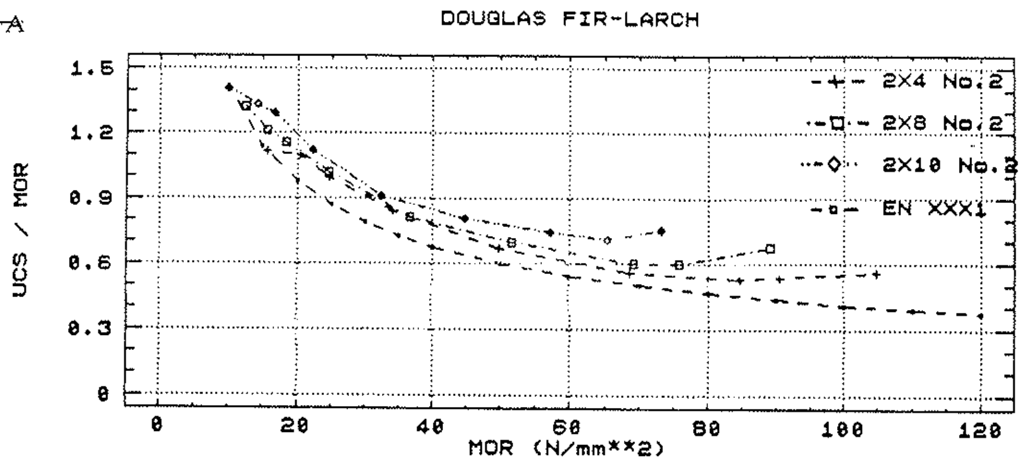

~~Case B~~

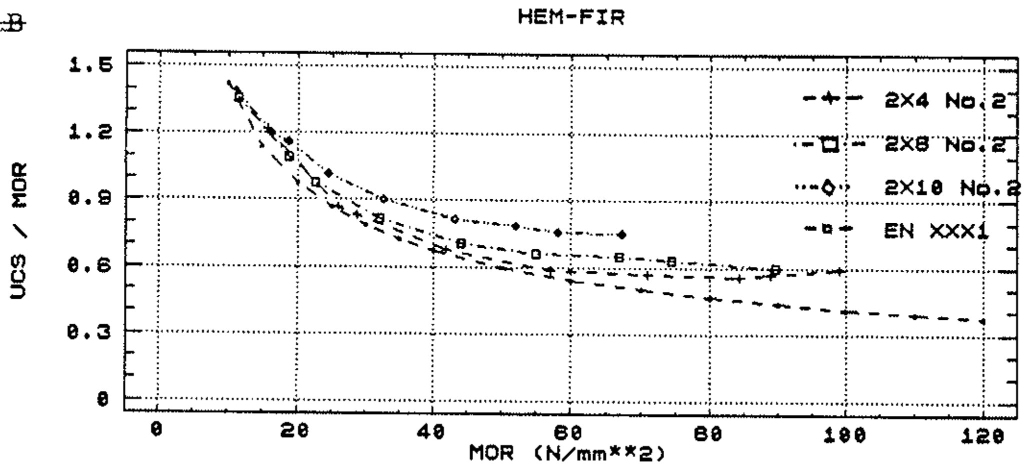

~~Case C~~

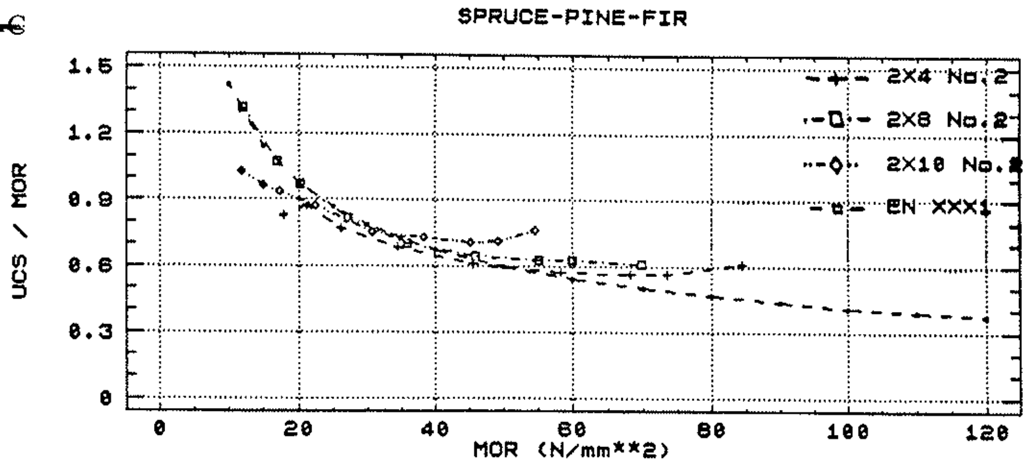

Figure 4. Compression/Bending Property Ratios for D Fir-L, Hem-Fir and S-P-F, No. 2 Grade.

Case A

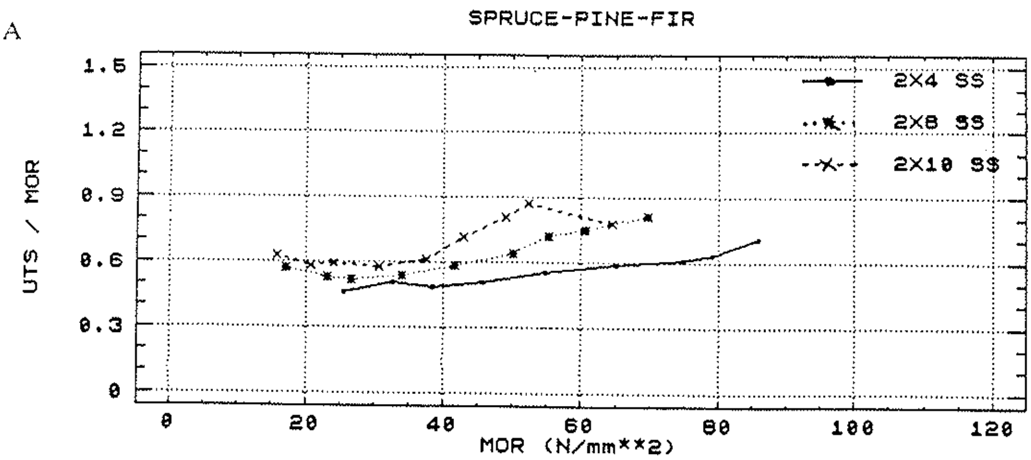

Case B

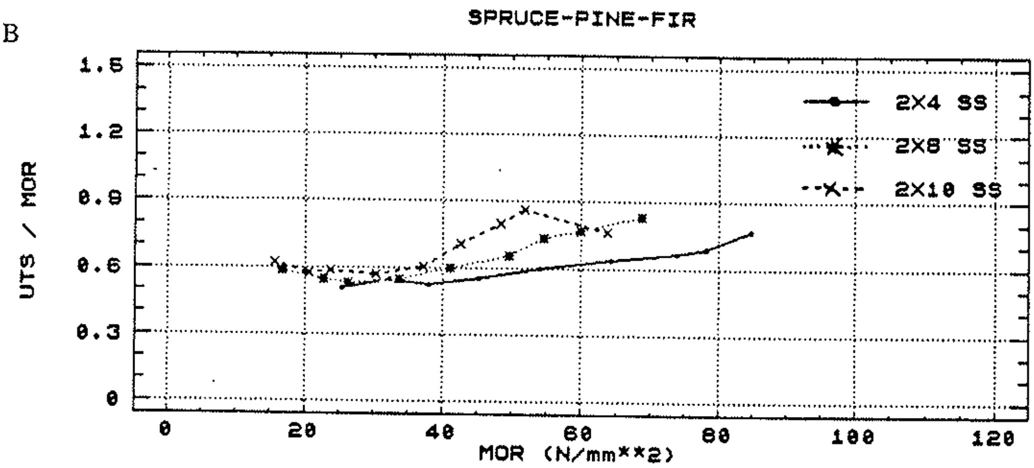

Case C

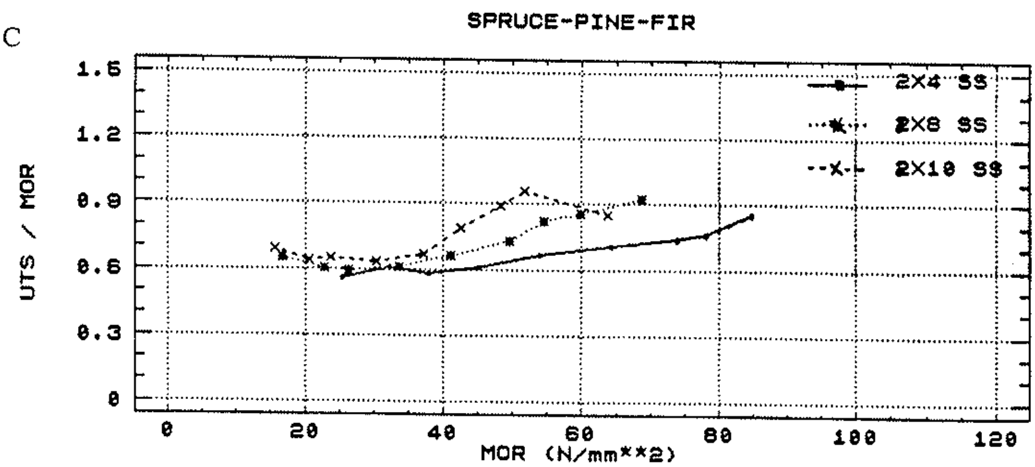

Figure 5. Tension/Bending Property Ratios for Case A, B, C Test Configurations - S-P-F, Select Structural Grade.

Case A

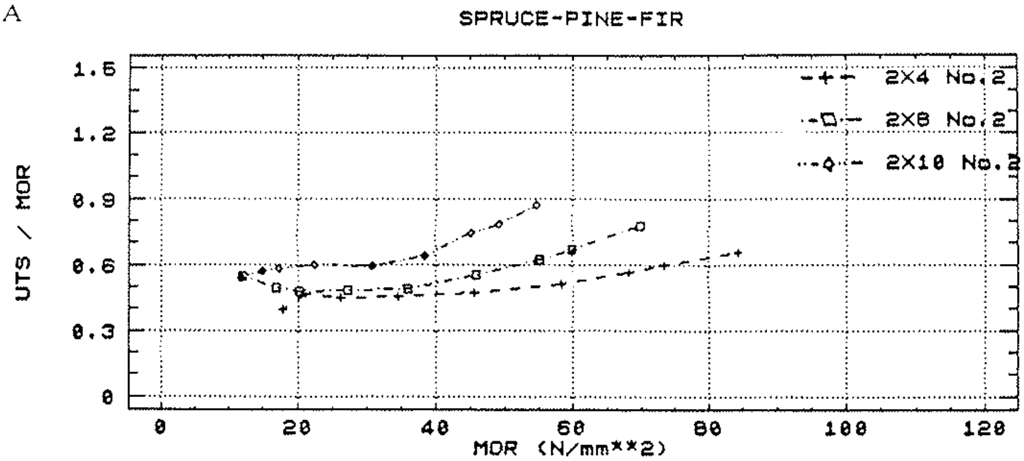

Case B

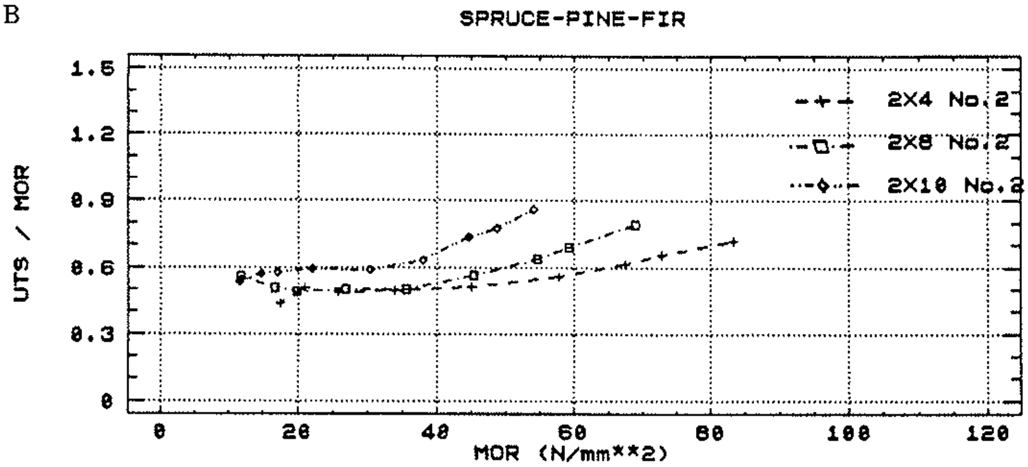

Case C

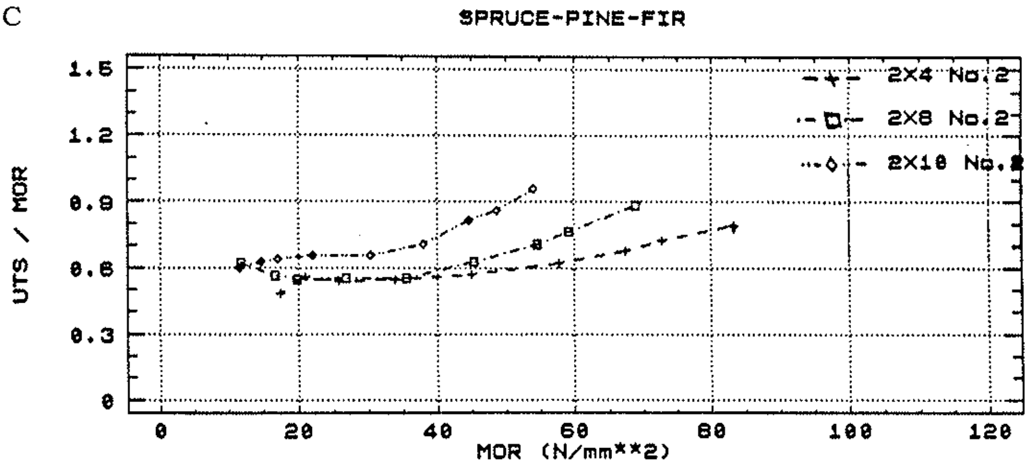

Figure 6. Tension/Bending Property Ratios for Case A, B, C Test Configurations - S-P-F, No. 2 Grade.

Case A

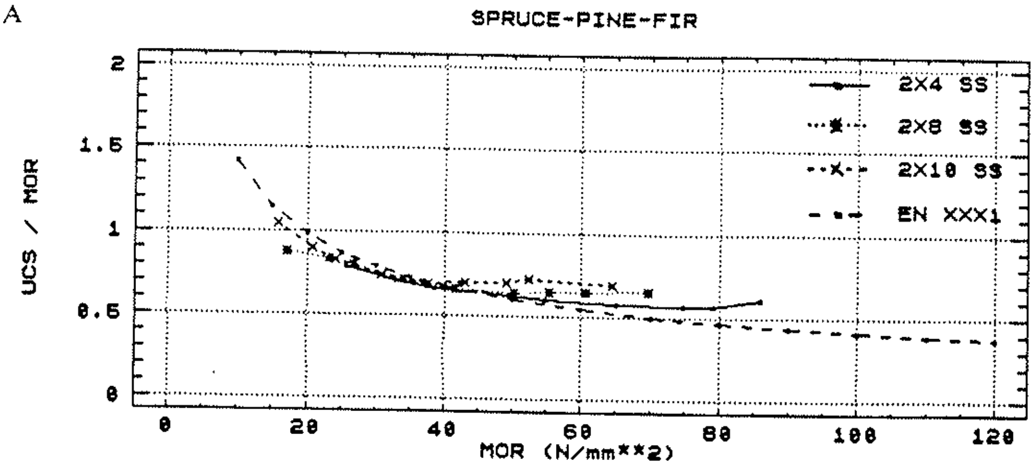

Case B

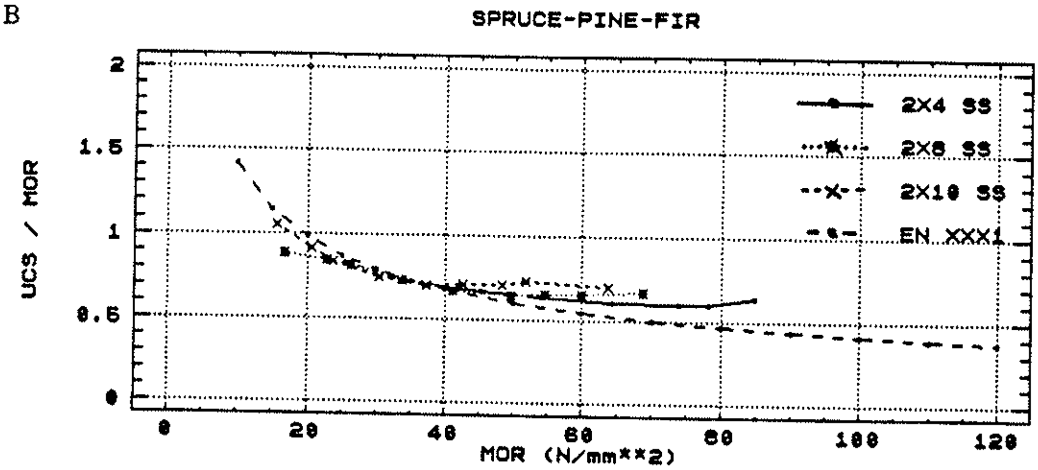

Case C

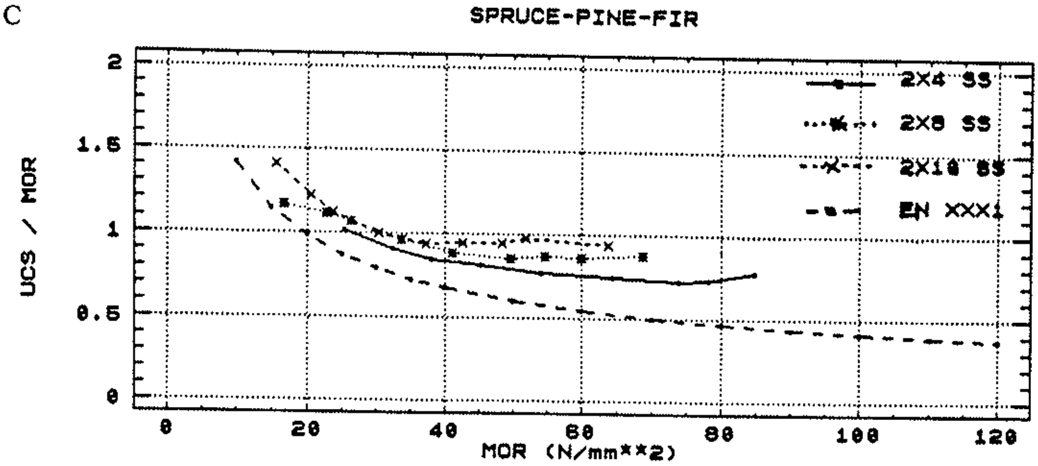

Figure 7. Compression/Bending Property Ratios for Case A, B, C Test Configurations - S-P-F, Select Structural Grade.

Case A

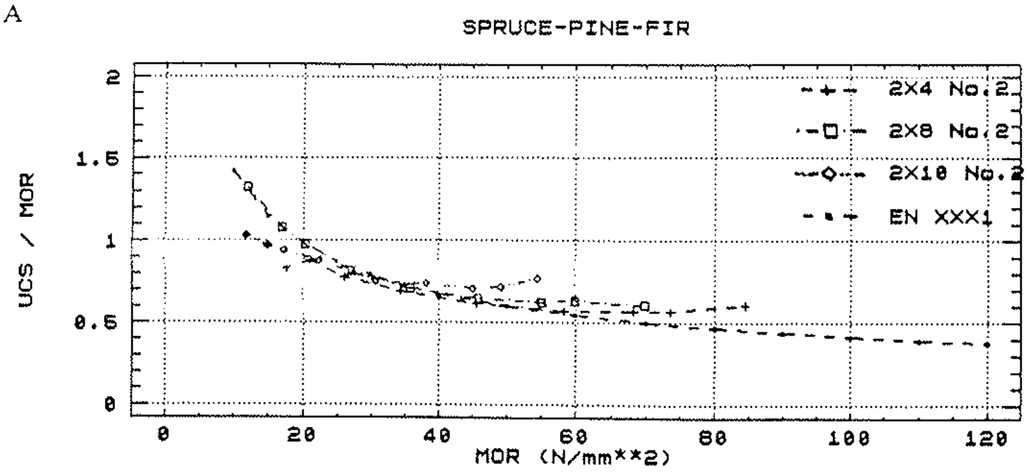

Case B

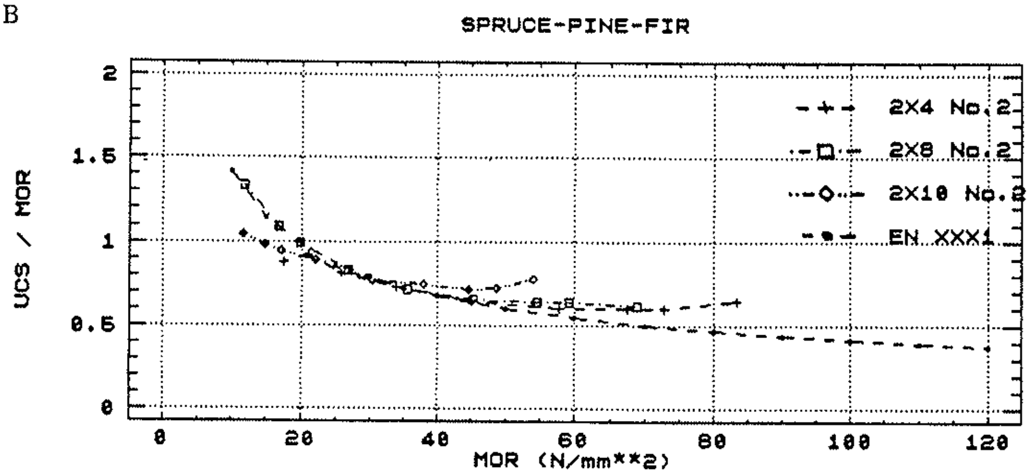

Case C

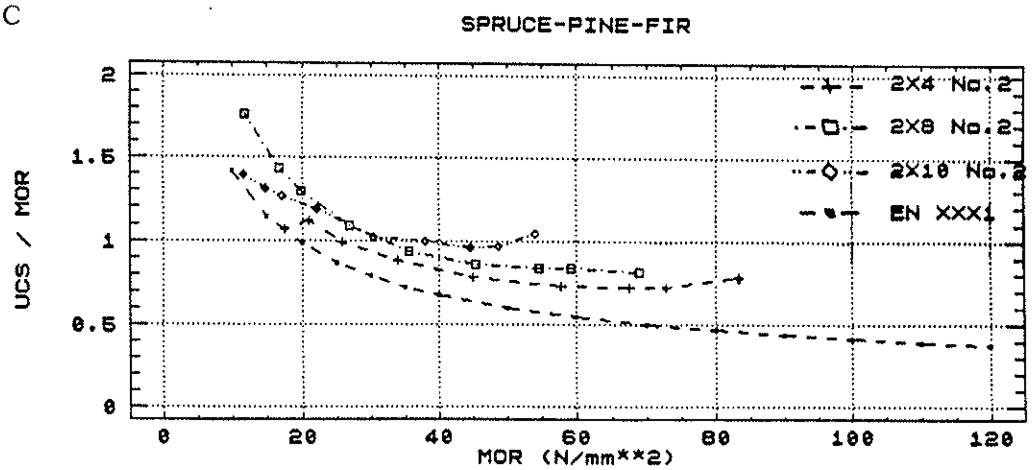

Figure 8. Compression/Bending Property Ratios for Case A, B, C Test Configurations - S-P-F, No. 2 Grade.

Case A

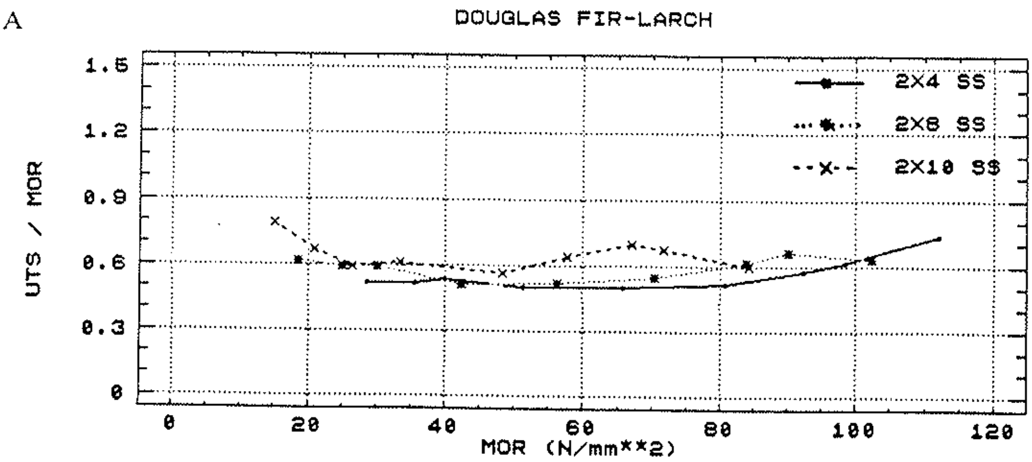

Case B

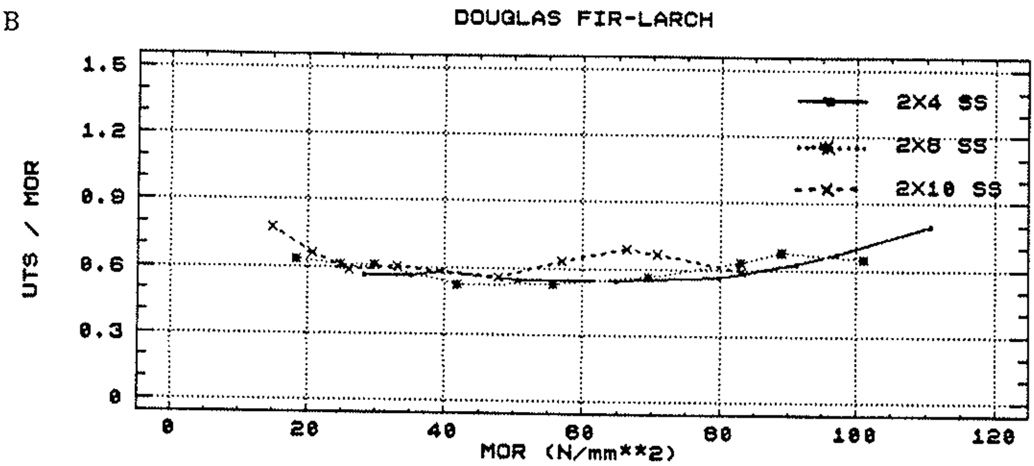

Case C

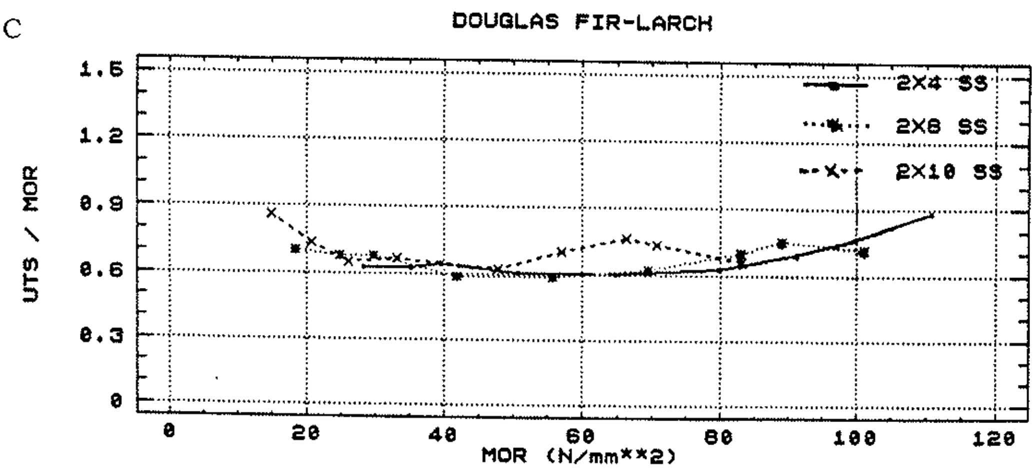

Figure 9. Tension/Bending Property Ratios for Case A, B, C Test Configurations - D Fir-L, Select Structural Grade.

Case A

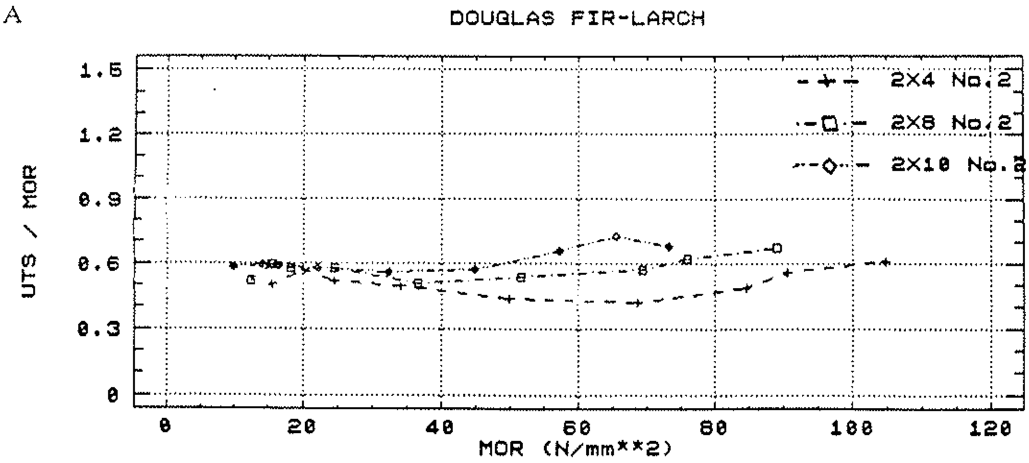

Case B

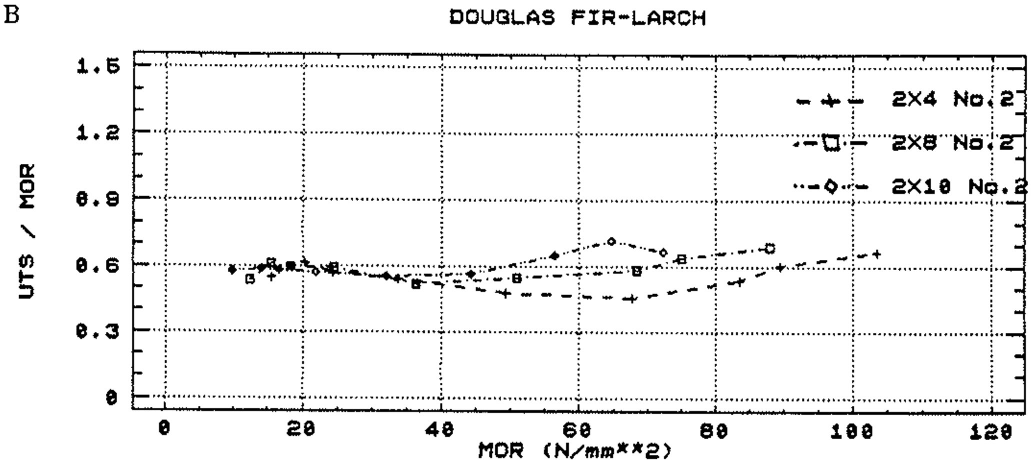

Case C

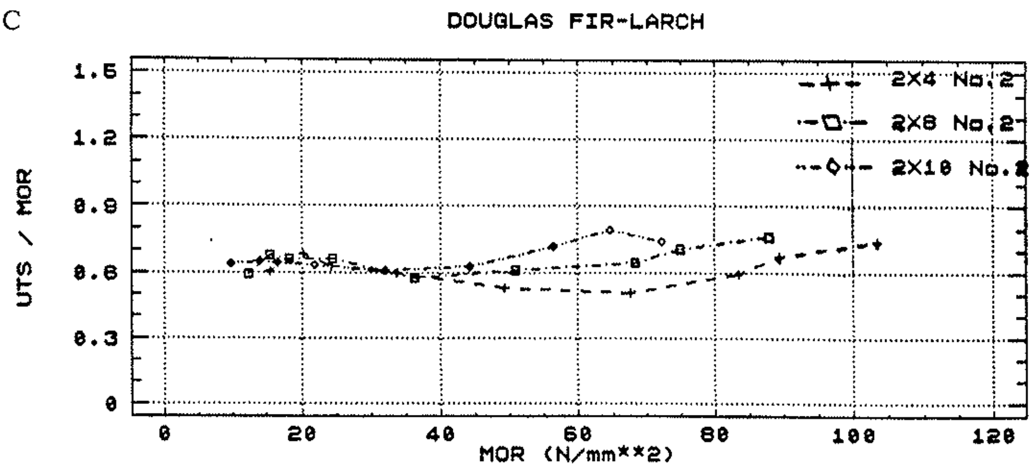

Figure 10. Tension/Bending Property Ratios for Case A, B, C Test Configurations - D-Fir-L, No. 2 Grade.

Case A

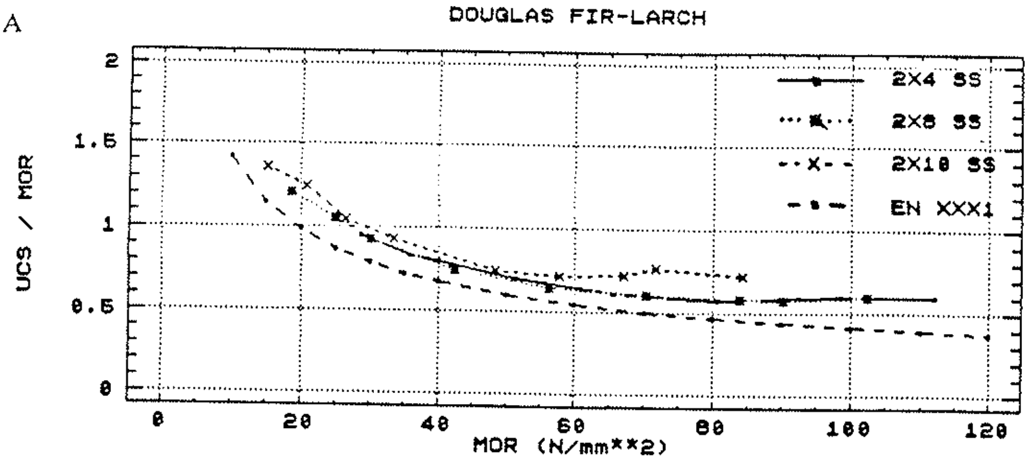

Case B

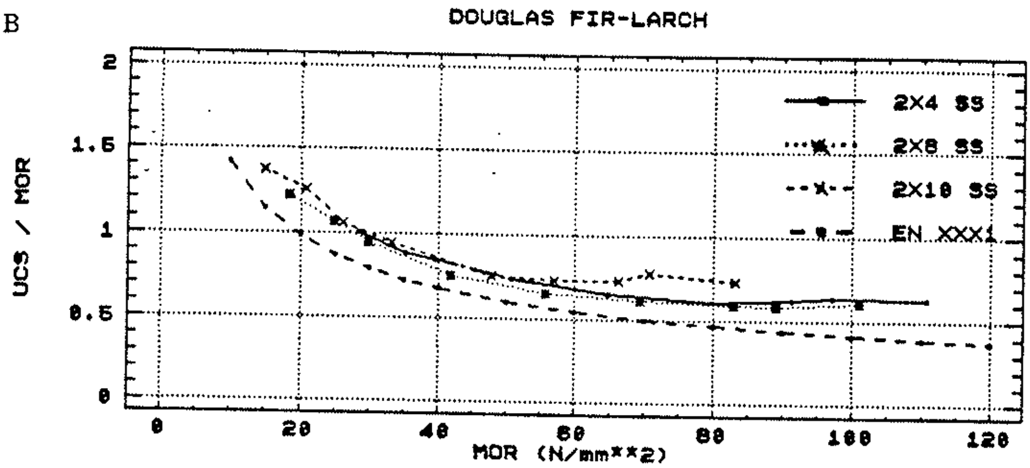

Case C

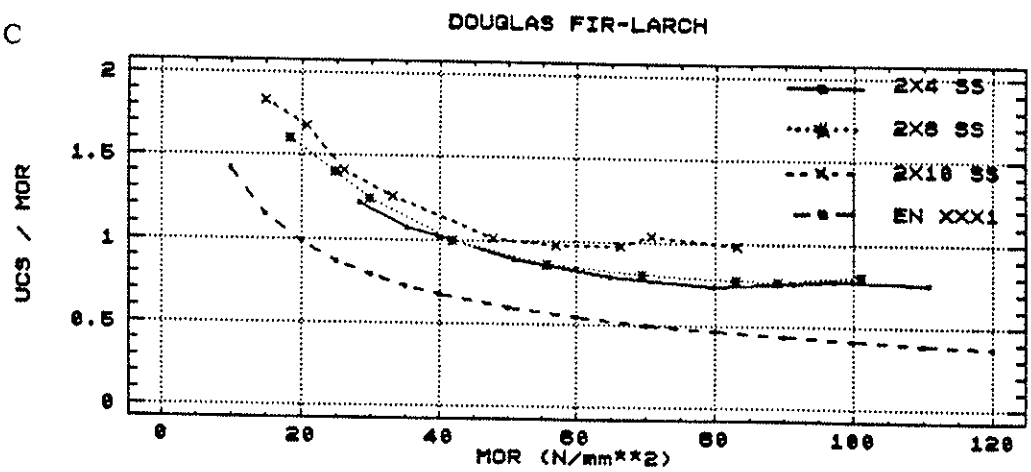

Figure 11. Compression/Bending Property Ratios for Case A, B, C Test Configurations - D Fir-L, Select Structural Grade.

Case A

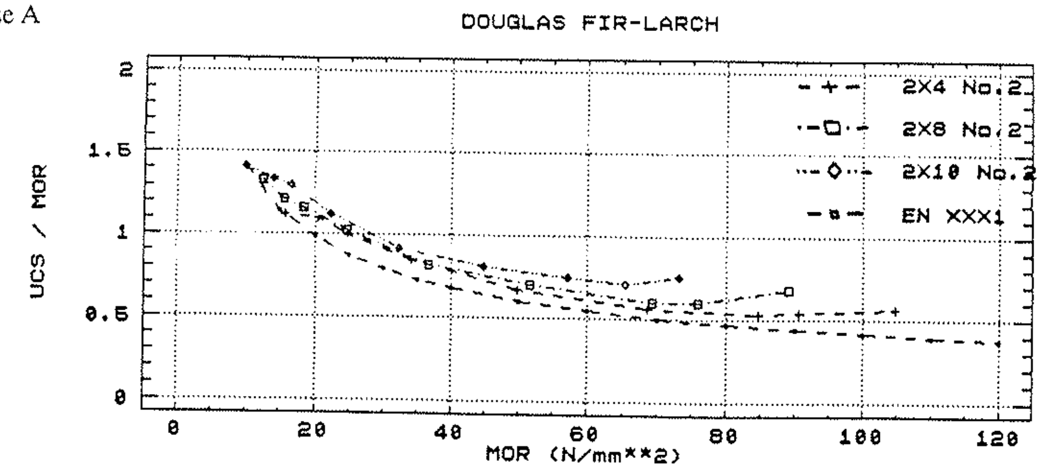

Case B

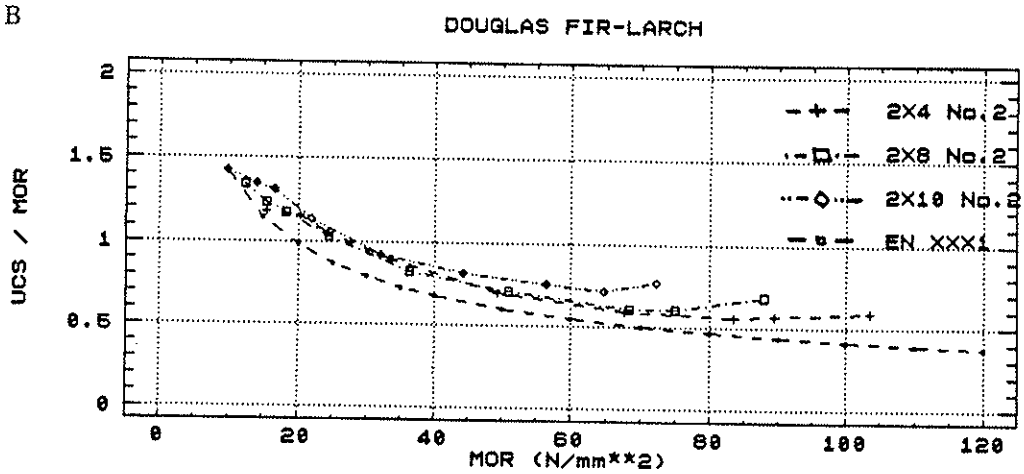

Case C

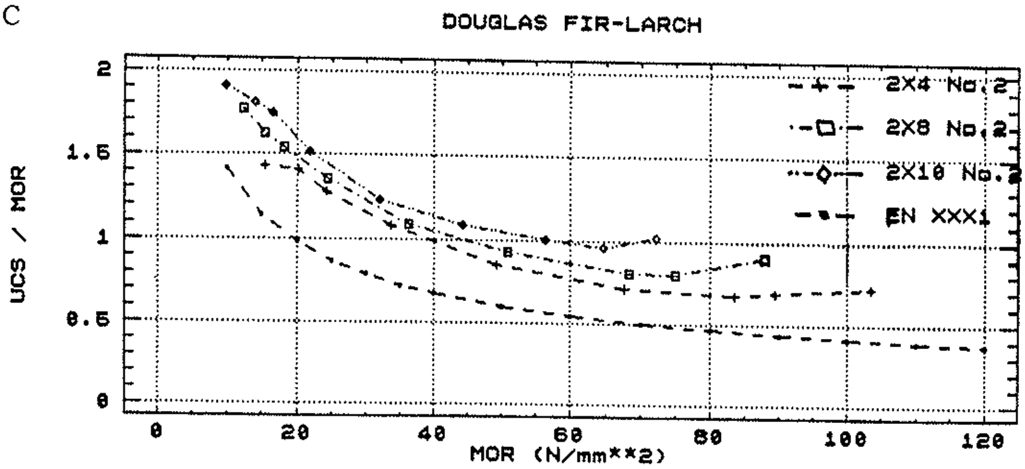

Figure 12. Compression/Bending Property Ratios for Case A, B, C Test Configurations - D Fir-L, No. 2 Grade.

Case A

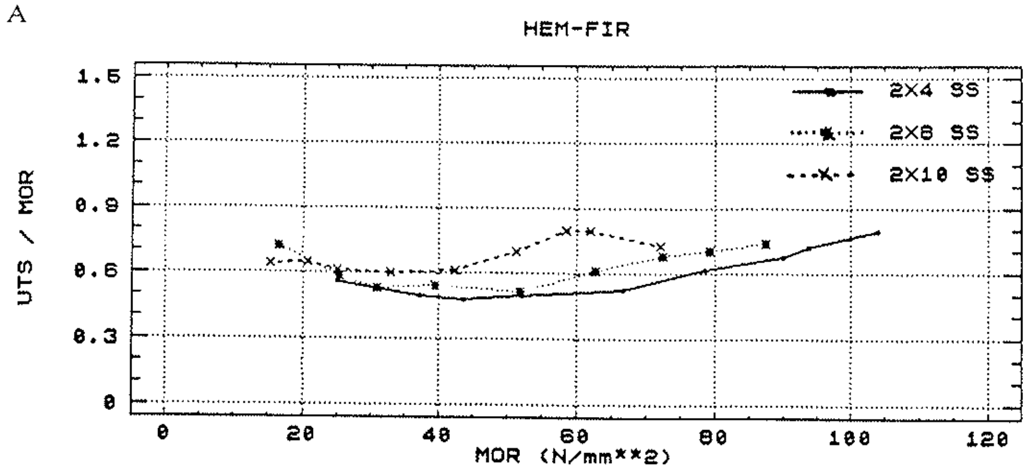

Case B

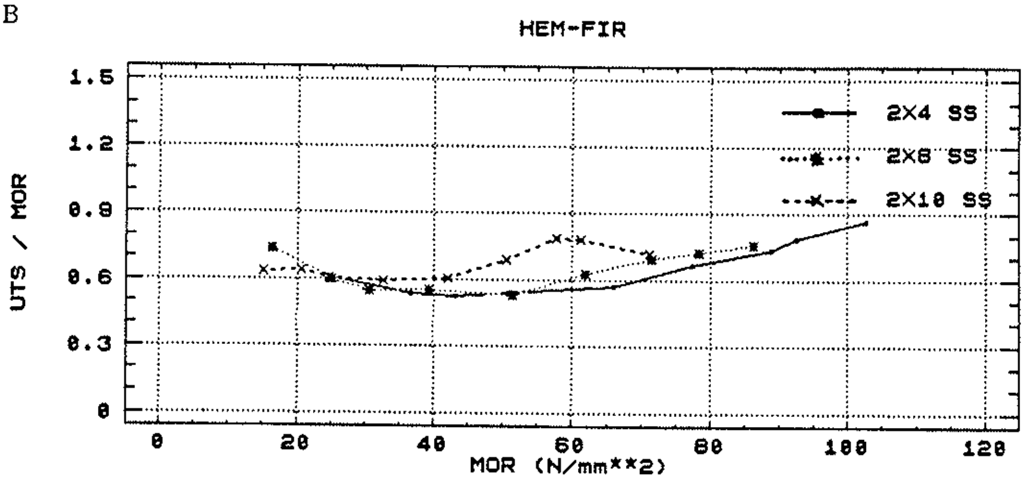

Case C

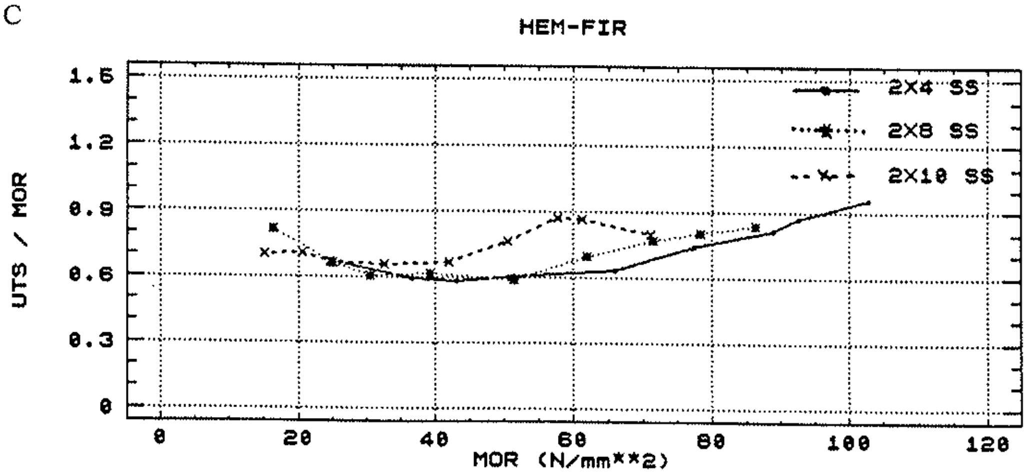

Figure 13. Tension/Bending Property Ratios for Case A, B, C Test Configurations - Hem-Fir, Select Structural Grade.

Case A

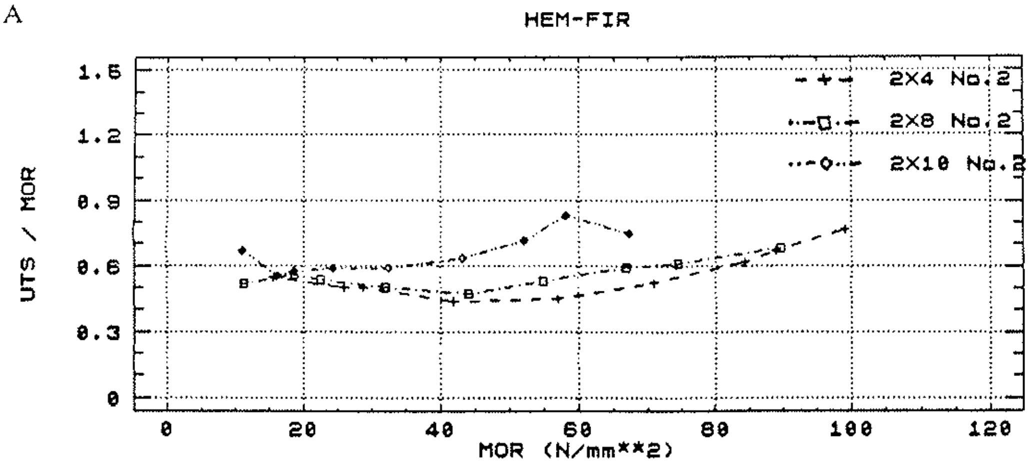

Case B

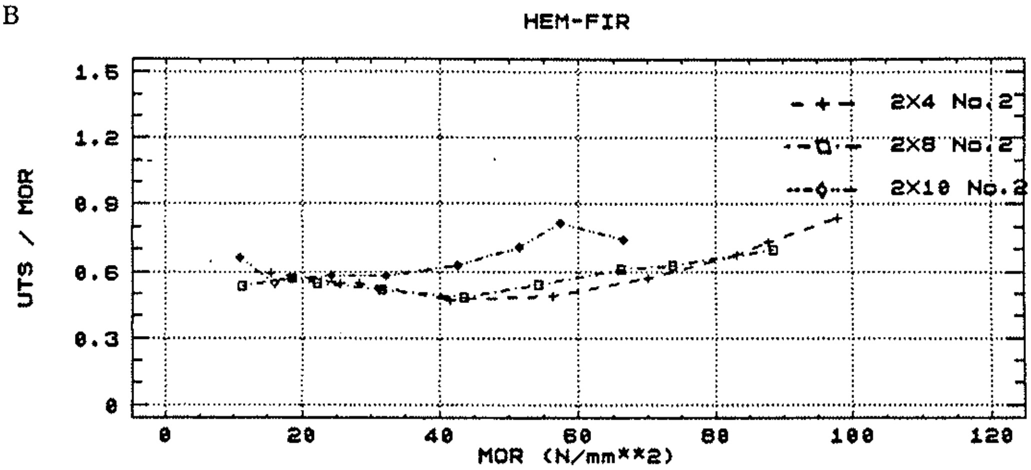

Case C

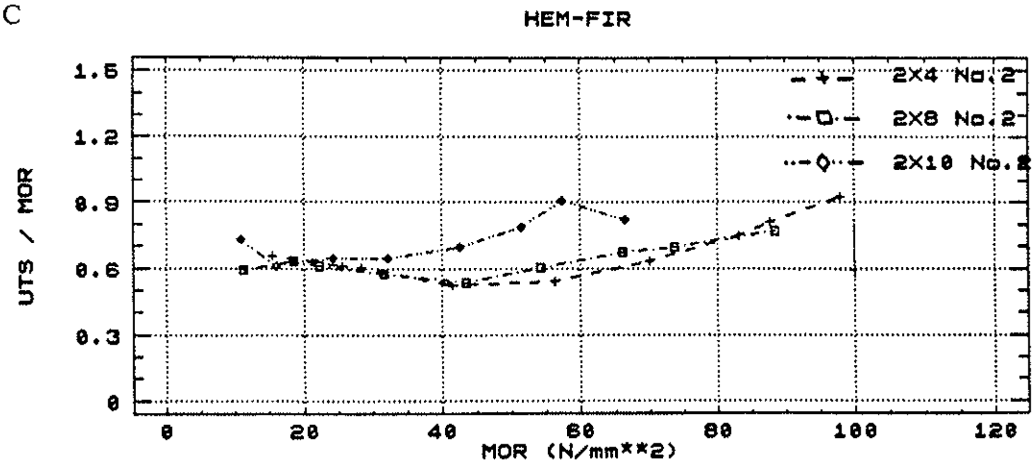

Figure 14. Tension/Bending Property Ratios for Case A, B, C Test Configurations - Hem-Fir, No. 2 Grade.

Case A

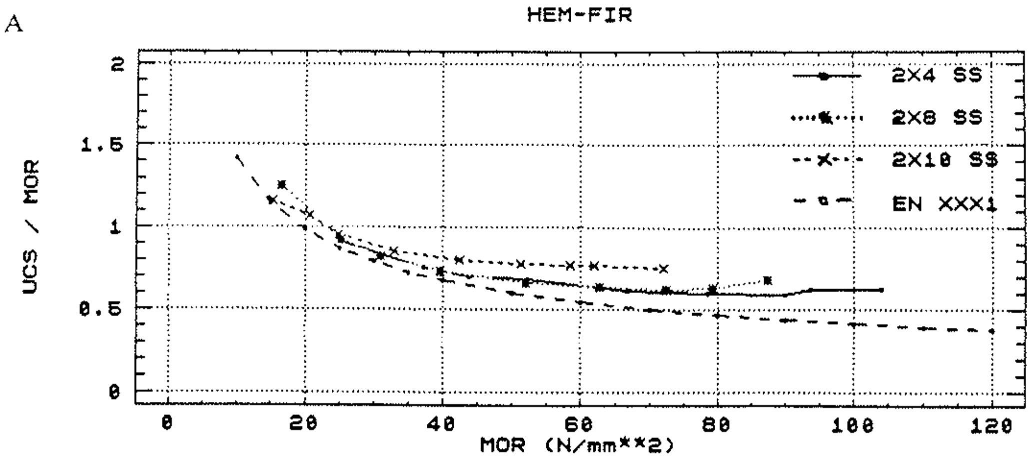

Case B

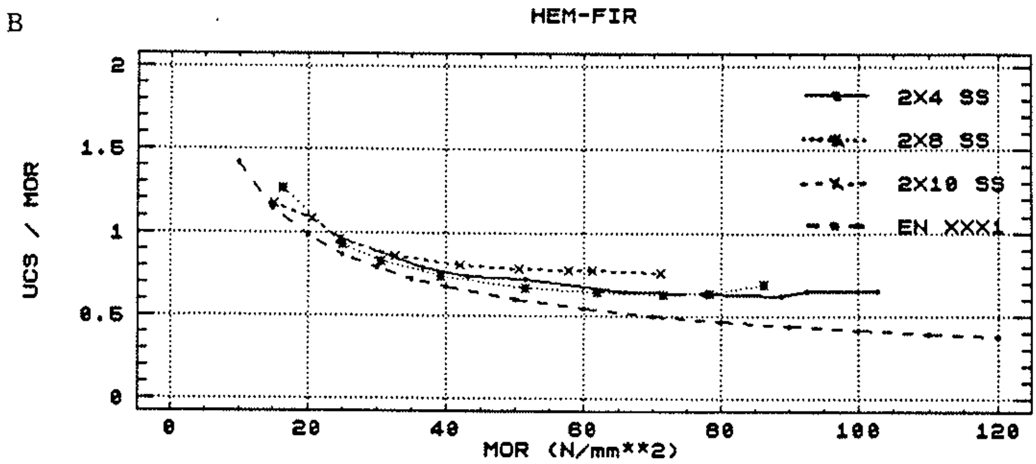

Case C

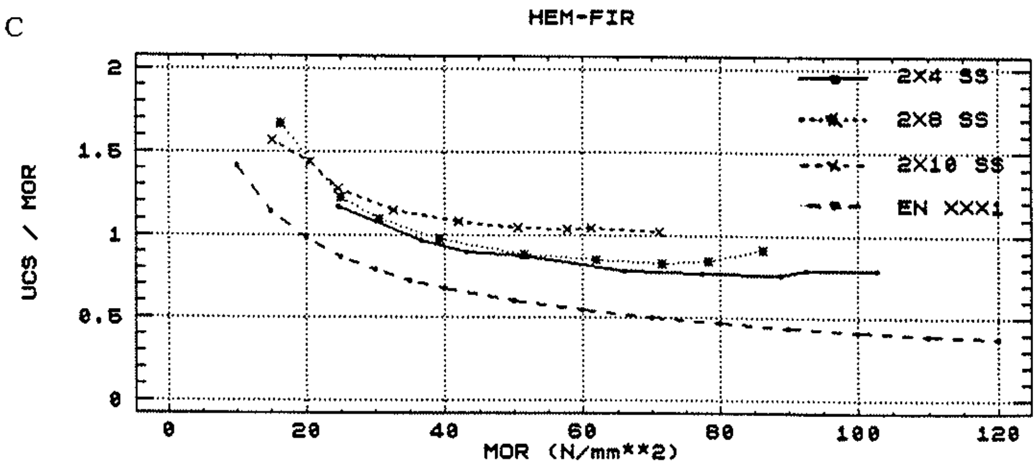

Figure 15. Compression/Bending Property Ratios for Case A, B, C Test Configurations - Hem-Fir, Select Structural Grade.

Case A

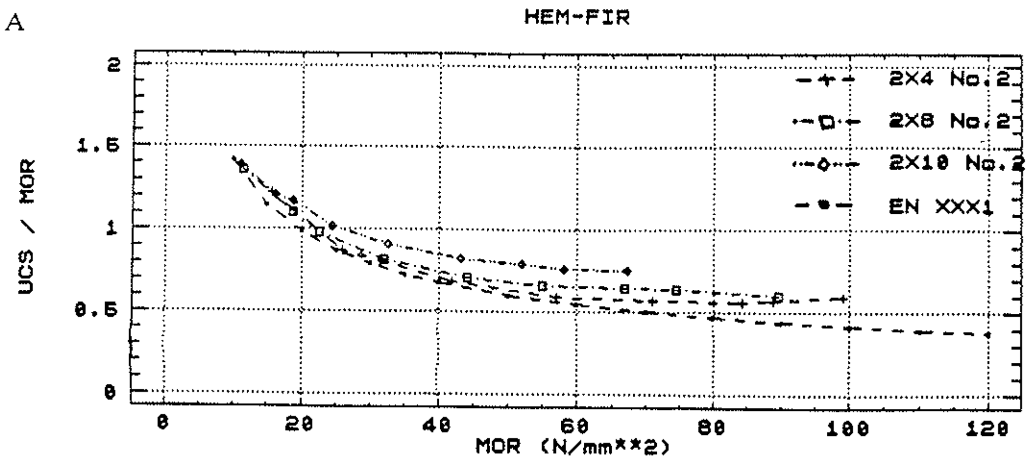

Case B

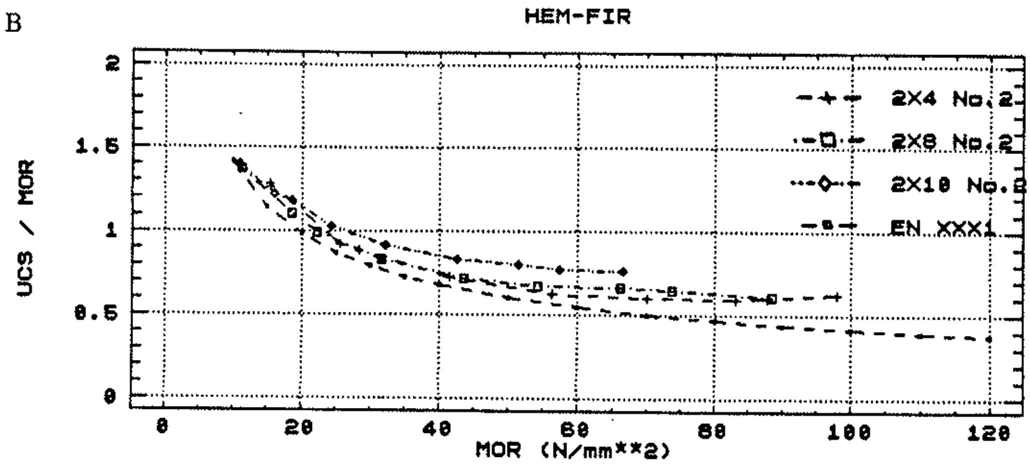

Case C

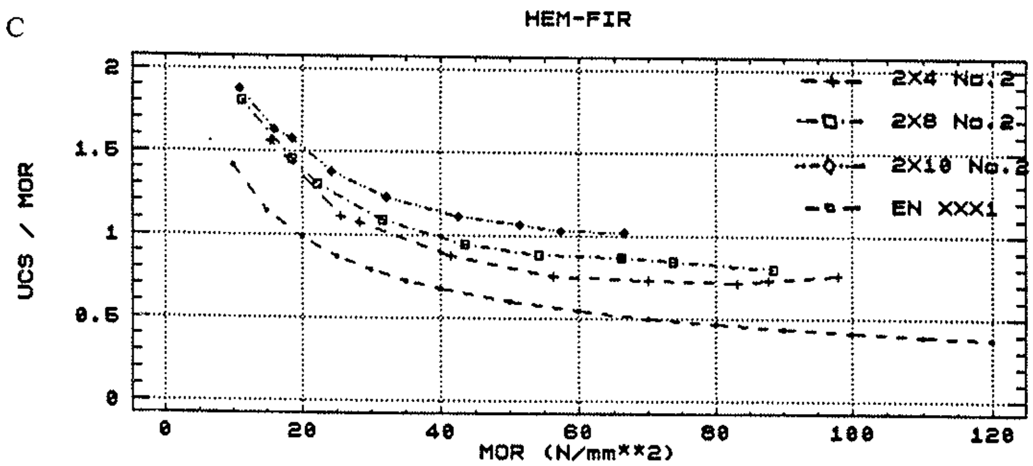

Figure 16. Compression/Bending Property Ratios for Case A, B, C Test Configurations - Hem-Fir, No. 2 Grade.

CIB -W18A / 22-6-2

INTERNATIONAL COUNCIL FOR BUILDING RESEARCH STUDIES AND DOCUMENTATION

WORKING COMMISSION W18A - TIMBER STRUCTURES

MOISTURE CONTENT ADJUSTEMENTS FOR IN-GRADE DATA

by

J D Barrett and W Lau
University of British Columbia
Canada

MEETING TWENTY - TWO

BERLIN

GERMAN DEMOCRATIC REPUBLIC

SEPTEMBER 1989

Moisture Content Adjustments for In-grade data

J. D. Barrett* Wilson Lau†

September 20, 1989

1 INTRODUCTION

Changes in moisture content of wood products cause shrinkage (or swelling), as well as changes in strength and elastic properties in wood products. Shrinkage of structural members reduces member cross section properties including member cross-section area and bending moment of inertia. In design property development, for structural wood products such as nominal 2-inch dimension lumber, traditionally it has been assumed that the increases in design properties with drying compensate for section property reductions accompanying the shrinkage.

American Society for Testing and Materials (ASTM) standards D245 and D2915 provide parallel procedures for adjusting dimension lumber design properties for moisture content (Table 1). These procedures are independent of lumber quality and applicable to all levels of the cumulative frequency distribution of the lumber property. Green (1989) provides expressions for calculating shrinkage of dimension lumber. Calculations of lumber strength capacity and member stiffness based on these results will show that both properties increase with reductions in moisture content. Since wood mem-

*Professor, Department of Harvesting and Wood Science, Faculty of Forestry, University of British Columbia, Vancouver, BC.

†Research Engineer, Department of Harvesting and Wood Science, Faculty of Forestry, University of British Columbia, Vancouver, BC.

Property	Percentage Increase in Allowable Property Above That of Green Lumber When Maximum Moisture Content is	
	19%	15%
Bending	25	35
Modulus of elasticity	14	20
Tension parallel to grain	25	35
Compression parallel to grain	50	75
Horizontal shear	8	13
Compression perpendicular to grain	50	50
Notes: A batch of lumber with a maximum moisture content of 19 % is assumed to have an average moisture content of 15% and a batch of lumber with a maximum moisture content of 15% is assumed to have an average moisture content of 12%.		

Table 1: *Modification of Allowable Stresses for Seasoning Effects for Lumber 4 in. and Less in Nominal Thickness (ASTM, 1986)*

bers typically dry out in service, this result has very important practical implications affecting the structural use of wood.

Studies of moisture content and bending strength relationships for Douglas-fir (Aplin, Green, Evans and Barrett 1986) and southern pine (McLain, DeBonis, Green, Wilson and Link 1984) appear to lead to results which are consistent with traditional concepts regarding moisture content and strength relationships.

On the other hand, some researchers (Gerhards 1968, 1970 and Madsen 1975, 1980) had pointed out that the mechanical properties of dimension lumber are dependent upon location in the cumulative density function. Madsen (1980) reported results strength and moment capacity decreases with decreasing moisture content.

The objective is to develop a moisture content adjustment model which preserve the classical shrinkage–strength trends but also incorporates a dependency on the lumber quality level.

1.1 Property Adjustment Models

Relationships between mechanical properties and wood moisture content are generally modeled using empirical relationships. Wilson (1933) found that logarithm of strength was approximately linearly related to moisture content for clear wood specimens. Several different model types have been proposed to represent moisture-property relationships for dimension lumber (Green 1982, 1987, Madsen 1975, 1980, 1982). Specific assumptions regarding the underlying moisture property relationships are built into some models. For others, the strength moisture content relationships are derived through regression, or similar procedures, without explicit consideration of any physical process constraints on model form.

2 THE SURFACE MODEL

The Quadratic Surface Model (QSM), proposed by Green *et al* (1986, 1987), is obtained by fitting a surface to the relationship between property and moisture content. The surface is defined by the contour lines which join the moisture content–property ordered pair at the same cumulative probability level.

The QSM has been used for adjusting bending, tension and compression strength data derived from full-size lumber testing programs undertaken in Canada and the United States.

The linear surface models to be investigated can be considered specializations of the quadratic surface model. In the QSM , a strength property P, is assumed to vary with moisture content M, according to

$$P = a + b \cdot M + c \cdot M^2 \tag{1}$$

for moisture contents M less than the intersection moisture content M_p.

In general, the parameters b and c will vary with strength level (Green *et al* 1986, 1987). By adopting a reference moisture content (e.g., M=15 %) the variation of parameters b or c with moisture content can be taken to have the form

$$b = D_0 + D_1 P_{15} + D_2 P_{15}^2 + D_3 P_{15}^3 \tag{2}$$

$$c = E_0 + E_1 P_{15} + E_2 P_{15}^2 + E_3 P_{15}^3 \tag{3}$$

where P_{15} is the strength at a moisture content of 15 percent.

Once the parameters for the polynomial representations for b and c are known, Eqns (1), (2) and (3) allow properties to be adjusted from one moisture content to other.

For the linear surface model, the strength moisture content relationship is similiar to that adopted in ASTM Standard D2915. Strength is assumed to be linearly related to moisture content according to

$$P = a + b \cdot M \tag{4}$$

Property values P_1 and P_2 at moisture contents M_1 and M_2 respectively will be related according to

$$P_2 = P_1 + b \cdot (M_2 - M_1) \tag{5}$$

If $M_2 = 15$ percent then the corresponding property value P_{15} is given by

$$P_{15} = P_1 + b \cdot (15 - M_1) \tag{6}$$

The slope parameter b can be related to P_{15}, using polynomials of the form

$$b = D_0 + D_1 P_{15} + D_2 P_{15}^2 + \dots \tag{7}$$

Alternative forms of Eqn. (7) will be evaluated with the objective of finding models which adequately represent bending strength and bending capacity data.

For a 4-term LSM, parameter b was modeled using a cubic polynomial function of P_{15},

$$b = D_0 + D_1 P_{15} + D_2 P_{15}^2 + D_3 P_{15}^3 \tag{8}$$

In a second variation, the constant term D_0 was deleted yielding a 3-term LSM for which the slope parameter b, is zero when P_{15} is zero.

$$b = D_1 P_{15} + D_2 P_{15}^2 + D_3 P_{15}^3 \tag{9}$$

Finally, a general 2-term LSM, allowing closed form solutions for adjusting property data, is obtained by adopting a quadratic representation for b according to

$$b = D_1 P_{15} + D_2 P_{15}^2 \tag{10}$$

Given a property value P_1 and moisture content M_1, P_{15} can be calculated by introducing (10) into (6). The smallest non-negative value of P_{15} will be given by

$$P_{15} = \frac{[1-(15-M_1)D_1] - \sqrt{[(15-M_1)D_1-1]^2 - 4D_2P_1(15-M_1)}}{2D_2(15-M_1)} \tag{11}$$

When P_{15} is known, b is calculated using Eqn. (7), then Eqn. (5) is used to calculate the property value P_2 at moisture content M_2. This procedure is identified as the general 2-term LSM.

Using a binomial expansion of P_{15} in Eqn. (11) yields an approximate solution of the general 2-term model, where P_2 is given by

$$P_2 \simeq P_1 + P_1(1+K)\left[\frac{D_1 - D_1^2(15-M_1) + D_2P_1(1+K)}{(1-D_1(15-M_1))^2}\right](M_2-M_1) \tag{12}$$

and

$$K = \frac{D_2P_1(15-M_1)}{(1-D_1(15-M_1))^2} \tag{13}$$

When K is small then

$$P_2 \simeq P_1 + P_1\left[\frac{D_1 - D_1^2(15-M_1) + D_2P_1}{(1-D_1(15-M_1))^2}\right]\cdot(M_2-M_1) \tag{14}$$

Since further application of the binomial expansion would yield

$$[1-D_1(15-M_1)]^2 \simeq 1 - 2D_1(15-M_1) \tag{15}$$

then

$$P_2 \simeq P_1 + P_1\left[\frac{D_1 - D_1^2(15-M_1) + D_2P_1}{1-2D_1(15-M_1)}\right]\cdot(M_2-M_1) \tag{16}$$

3 DATA

3.1 Bending

The Douglas-fir (Aplin *et al* 1986) and southern pine (McLain *et al* 1984) data were the primary data sets used in evaluation the effect of MC on bending properties. Each data set includes results for three grades (select structural, No. 2 and No. 3) and three sizes (2x4, 2x6 and 2x8) evaluated at each of four nominal moisture contents (green, 20, 15 and 10 percent).

Trends in mean and 5th percentile MOR with moisture content for Douglas-fir (Fig 1 and 2) and southern pine (Fig 3 and 4) generally show strength increases with drying below the moisture intersection point. The rationale for adopting the intersection point $M_p = 24$ percent will be presented. Both data sets show that the magnitude of the strength adjustment with drying varies with strength level. High strength lumber generally exhibits a greater response to moisture changes than low strength lumber. The strength dependent behaviour seems consistent independent of grade and member size. There are exceptional cases in the Douglas-fir data (e.g. 2x6 No. 2 and No. 3) and the southern pine data (e.g. 2x6 and 2x8 No. 3) where the data tends to indicate that strength could decrease with drying particularly in the range from 15 to 10 percent moisture content.

Overall the trends show strength increases essentially linearly with drying for both species. It is hypothesized that the deviations from this general trend could be explained by sampling effects and the inherent variability in lumber property response to moisture content changes.

3.2 Compression

For the compression, Douglas-fir of two sizes (2x4 and 2x8) and two grades (Selected Structural and No.2) was tested. For each size-grade combination, data at four moisture content levels was used.

Trends in mean and 5th percentile maximum crushing strength also show increases in both sizes and grades, as the wood dried from green towards the 10% MC (Fig. 5 and 6). In contrast with the bending trends which in some cases shows an increase and then decrease as the lumber dried from the green condition, the increase in compression is quite consistent within the moisture content range for all sizes and grades.

4 MOISTURE INTERSECTION POINT

Wilson (1932) identified the moisture intersection point M_p, as the upper limit of the moisture content range within which properties vary with moisture content changes. Specific M_p values will vary depending on the underlying property relationship adopted. Assuming that the logarithm of bending strength varied linearly with moisture content yielded $M_p = 24$ percent for Douglas-fir and $M_p = 21$ percent for loblolly and longleaf pine clear wood specimens (Wilson, 1932). For the compression, $M_p = 23$ percent was adopted.

Green *et al* (1986) adopted a residual sums of squares approach for deriving the best fit M_p point. The residual sums of squares was taken as the sum of the square of the differences between the model predicted response and the data values used to fit the model. The optimum M_p yields the minimum residual sums of squares (RSS).

Integer-valued, optimum M_p's for Douglas-fir in bending and compression, and southern pine in bending for quadratic and linear surface models are given in Table 2. The typical M_p and RSS trend for Douglas-fir is shown in Figures 7. In most cases the RSS is relatively stable for the M_p ranges provided in Table 2. Apparent optimum M_p's and associated stable ranges for M_p for southern pine in bending (Table 2) provided for the LSM are based only on mean and 5th percentile data (McLain *et al* 1984).

5 MODEL EVALUATIONS

5.1 Modulus of Rupture

Grade and size independent model parameters derived for the quadratic and linear surface models relating MOR and moisture content for Douglas-fir are given in Table 3. Model parameters are established using interpolated MOR results for 21 percentile levels (0.02, 0.05, 0.10, ...,0.90, 0.95, 0.98) derived for each moisture condition and size and grade category. The polynominal expressions relating the slope parameter b to P_{15}, for the linear surface models (Figure 8) show good agreement with the data for all sizes and grades. All three models predict strength increases upon drying from the green condition as shown in Figure 9. The 2-term model predicts somewhat larger strength increases with drying in the low strength range than the 4-term model. Figure 10 and 11 shows the contour plots of the QSM and the 4-term linear surface model respectively. In general, the LSM provided a good visual fit to the data. Residual sums of squares assessments showed the LSM fits the data as well as or better than the QSM (Barrett *et al* 1989). Maximum absolute

Model type	*Species*	M_p	
		Stable range	*Optimum*
Bending			
QSM	DF	26-30	30+
LSM 4-T	DF	24-28	26
LSM 3-T	DF	24-28	26
LSM 2-T	DF	24-28	26
LSM 4-t	SP	23-25[1]	24
LSM 3-t	SP	23-25[1]	24
LSM 2T	SP	23-25[1]	24
Compression			
QSM	DF	26-30	30+
LSM 4-T	DF	20-24	22
LSM 3-T	DF	20-24	22
LSM 2-T	DF	20-24	22
[1] based on mean and 5th percentile data only.			

Table 2: *Estimated Moisture Intersection Points (M_p) for Douglas-fir and southern pine bending strength models and compression models*

difference tests showed that in the low probability levels the LSM also fits the data as well as the QSM. The decrease in property with decreasing moisture content at the low strength specimen for the QSM does not appear consistent with the traditional concepts regarding moisture content and strength relationships. The LSM provides a basis for adjusting bending strength data which results in strength increases with drying through to moisture content levels of 10 percent.

Coefficient	QSM	4-T LSM	3-T LSM	2-T LSM
D_0	-2.48947E+00	-3.12797E-02	0	0
D_1	2.95465E-01	5.82709E-03	3.59055E-03	-9.56890E-03
D_2	-5.76080E-03	-8.27766E-04	-7.82132E-04	-2.94851E-04
D_3	2.55801E-05	4.35310E-06	3.97073E-06	0
E_0	6.84561E-02	0	0	0
E_1	-8.14236E-03	0	0	0
E_2	1.38550E-04	0	0	0
E_3	-6.13052E-07	0	0	0
Note: MOR in MPa and MC in percentage.				

Table 3: *Regression coefficients of quadratic and linear surface models (MOR) for Douglas-fir*

5.2 Moment Capacity

Bending moment capacity of a member (RZ) is the product of the bending strength (R) and the section modulus (Z). For structural use it is necessary to establish the relationship between member capacity and moisture content. Moment capacity changes with moisture content can be established directly using the afformentioned QSM and LSM models or derived indirectly using a modulus of rupture model coupled with an appropriate section property shrinkage adjustment model.

Parameters for QSM and LSM normalized moment capacity models (Table 4) were derived after size-normalizing the data sets by dividing individual ultimate moment capacities by the standard dry section modulus (Z_n) for the particular size category. Model adjusted normalized section properties are subsequently multiplied by the appropriate dry section modulus to derive a moisture content adjusted section modulus.

Moment capacity variation with moisture content can be derived using the MOR model if the section shrinkage characteristics are known. Green (1989) provides shrinkage adjustments for width S_w, and thickness S_t, which are consistent with those traditionally used in lumber property design stress development. These shrinkage relationships

$$S_w = 6.031 - 0.215M \tag{17}$$

Coefficient	QSM	4-T LSM	3-T LSM	2-T LSM
D_0	-2.58992E+00	-6.82681E-02	0	0
D_1	3.10205E-01	1.63155E-02	1.18471E-02	-3.41783E-03
D_2	-5.94091E-03	-9.31051E-04	-8.39765E-04	-2.75608E-04
D_3	2.85049E-05	5.28735E-06	4.72848E-06	0
E_0	7.06282E-02	0	0	0
E_1	-8.28829E-03	0	0	0
E_2	1.41090E-04	0	0	0
E_3	-6.51461E-07	0	0	0
· MOR in MPa, MC in percentage·				

Table 4: *Regression coefficients of quadratic and linear surface models (Normalized Section capacity, RZ_n)*

and

$$S_t = 5.062 - 0.181M \tag{18}$$

were used to derive dry to green section modulus ratios (Table 5) for a range of dry conditions.

MC_{DRY} (%)	*Dry to Green Section Modulus Ratio* S_D/S_G
10	0.8938
12	0.9052
15	0.9225
19	0.9459

Table 5: *Dry to Green Section Modulus Ratios (S_D/S_G)*

The bending moment capacity (RZ) at moisture contents M_1 and M_2 are related to the modulus of rupture and section property ratios according to

$$\frac{RZ_1}{RZ_2} = \frac{MOR_1}{MOR_2} \cdot \frac{S_{M_1}}{S_{M_2}} \tag{19}$$

Green Strength $\sigma_{green}(MPa)$	*Dry-Green Ratio 4-T MOR* model $\sigma_{dry}/\sigma_{green}$	*Moment Capacity Ratio*					
		4-Term			*2-Term*		
		MOR model M_x	*RZ* model M_x^*	*Difference* (%)	*MOR* model M_x	*RZ* model M_x^*	*Difference* (%)
10.0	1.0508	0.9694	0.9936	-2.496	1.0437	1.0605	-1.610
15.0	1.0816	0.9978	1.0098	-1.203	1.0628	1.0762	-1.261
20.0	1.1203	1.0335	1.0375	-0.387	1.0833	1.0929	-0.886
25.0	1.1639	1.0737	1.0711	0.242	1.1056	1.1107	-0.461
30.0	1.2110	1.1171	1.1082	0.797	1.1300	1.1297	0.027
35.0	1.2599	1.1623	1.1470	1.316	1.1569	1.1502	0.579
40.0	1.3080	1.2066	1.1855	1.749	1.1868	1.1725	1.205
45.0	1.3521	1.2473	1.2212	2.093	1.2204	1.1966	1.950
50.0	1.3890	1.2814	1.2516	2.326	1.2588	1.2232	2.828

- M_x is the moment capacity ratio predicted by the Strength Model.
- M_x^* is the moment capacity ratio predicted by the Section Modulus Adjusted Strength Model.
- $M_x = \frac{\sigma_{dry}}{\sigma_{green}} \times$ Shrinkage Factor.
- Shrinkage Factor = 0.9225.
- "Dry" means at 15 % M.C. and "Green" means at 24 % M.C.
- Difference = $\frac{M_x - M_x^*}{M_x} \times 100\%$

Table 6: *Comparison of Moment Capacity Ratio between Strength Model and Section Modulus Adjusted Strength Model using 4 and 2-Term Linear Surface Model*

Dry-green moment capacity ratios derived using Eqn.(19) are compared with corresponding ratios predicted from the 4-term and 2-term moment capacity models (Table 6) for a dry moisture content of 15 percent. Moment capacity ratios derived from the 4-term MOR model underestimate the ratios predicted from the section modulus model at low strength levels. At high strength levels the moment capacities are higher when derived using the MOR model. Percentage differences between the two approaches range from -2.5 at the low strength level to 2.3 percent at high strengths. The general agreement between the two approaches shows that both methods lead to remarkably consistent capacity ratio estimates considering the different data sources used to derive these results. Table 6 also provides comparisons based on the 2-term MOR model which indicated that this model consistently overestimates the capacities derived from the 4-term RZ model.

5.3 Compression Strength

Grade and size independent model parameters derived for the quadratic and linear surface models are fitted using all the compression data of Douglas-fir and are given in Table 7. These parameters more preferred to parameters obtained by fitting the surface models to each grade and size separately. Although the latter may fit the data sets better, it may overfit the data and loose the generality of applying the model to untested grades and sizes. Values of the slope parameter b, derived from the test data are shown with polynominal expressions relating b to P_{15}, the compression strength at 15 percent moisture content, for the linear models in Figure 13 and 14.

Coefficient	QSM	4-T LSM	3-T LSM	2-T LSM
D_0	3.35807E+00	8.59062E-01	0	0
D_1	-3.31768E-02	-7.80181E-02	-3.59447E-03	-2.36662E-02
D_2	-8.62464E-03	6.59720E-04	-1.35754E-03	-3.12615E-04
D_3	1.18173E-04	-4.43085E-06	1.28175E-05	0
E_0	-7.28346E-02	0	0	0
E_1	-5.94269E-04	0	0	0
E_2	2.30663E-04	0	0	0
E_3	-3.11035E-06	0	0	0
Note: C in MPa and MC in percentage				

Table 7: *Regression coefficients of quadratic and linear surface models (C) for Douglas-fir*

5.4 Compression Capacity

Compression capacity of a member (CA) is the product of the compression strength (C) and the cross-section area (A). As mentioned earlier, it is essential to establish the relationship between member capacity and moisture content. Using the dimension-normalized strength (C_N), instead of the compression strength (C), compression capacity changes with moisture content can be developed directly using the QSM and LSM models. After adjustment of the normalized compression strength C_N to the target moisture content, the adjusted compression capacity is readily determined by calculating the product of C_N and A_N.

An alternative method to establish the compression capacity changes with moisture content is to use the compression strength model coupled with an appropriate area shrinkage adjustment model.

Parameters for QSM and LSM dimension-normalized compression capacity models are given in Table 8.

Coefficient	QSM	4-T LSM	3-T LSM	2-T LSM
D_0	4.74643E+00	7.93511E-01	0	0
D_1	-1.40415E-01	-6.18084E-02	6.70584E-02	-2.02927E-02
D_2	-5.56325E-03	1.69626E-04	-1.68500E-03	-2.86805E-04
D_3	9.51831E-05	1.23160E-06	1.70946E-05	0
E_0	-1.09244E-01	0	0	0
E_1	2.45896E-03	0	0	0
E_2	1.42870E-04	0	0	0
E_3	-2.40352E-06	0	0	0
· C_N in MPa, MC in percentage				

Table 8: *Regression coefficients of quadratic and linear surface models (Normalized Compression capacity, C_N)*

Compression capacity variation with moisture content can be derived indirectly by using the strength model and the shrinkage adjustment factor. Using the shrinkage relationships (Eqn. (17) and (18)), the dry to green cross-sectional area adjustment (Table 9) for a range of dry conditions was derived. The compression carrying capacity at moisture contents M_1 and M_2 are related to the compression strength and cross-sectional areas by

$$\frac{CA_1}{CA_2} = \frac{C_1}{C_2} \cdot \frac{A_1}{A_2} \tag{20}$$

MC_{DRY} (%)	*Dry to Green Cross-Section Area Ratio* A_D/A_G
10	0.9300
12	0.9376
15	0.9491
19	0.9646

Table 9: *Dry to Green Cross-Section Area Ratios* (A_D/A_G)

Comparisons between the compression capacities predicted by the strength model and the capacity model are shown in Table 10. Two alternative linear surface models – 4-term and 2-term LSM – are compared and the percentage difference are shown as well. It is clear that the compression capacity predicted by the strength model always gives a higher value at all strength levels and models except for the 2-term LSM at 10.0 MPa green level where the reverse effect was observed. Apparently the 2-term LSM always gives a larger dry-green strength adjustment than the 4-term LSM. The percentage of difference indicates that both models behave reasonably well within the test data range. Since there is no evidence of compression capacity decreases with drying, the 3-term model is more consistent with expected behaviour of full-size lumber at low strength levels.

6 MODEL APPLICATION

Moisture adjustment models are required for a wide range commercially important species and species groups. A species independent moisture adjustment model would be particularly advantageous. Green and Evans (1987) showed that the Douglas-fir and southern pine flexural data sets could be combined to provide a single model for both species with an intersection moisture content of 23 percent. This combined model, with appropriate upper and lower strength cut-offs, provided a basis for developing a species independent model.

Green Strength $\sigma_{green}(MPa)$	*Dry-Green Ratio* *4-T C* model $\sigma_{dry}/\sigma_{green}$	*Compression Capacity Ratio*					
		4-Term			*2-Term*		
		C model C_x	C_N model C_x^*	*Difference* (%)	C model C_x	C_N model C_x^*	*Difference* (%)
10.0[1]	0.6749	0.6405	0.6299	1.655	1.2664	1.2745	-0.640
15.0[1]	1.2304	1.1678	1.1095	4.993	1.3017	1.3040	-0.177
20.0	1.4139	1.3419	1.3087	2.474	1.3415	1.3362	0.395
25.0	1.4898	1.4140	1.3988	1.075	1.4872	1.3721	1.088
30.0	1.5268	1.4492	1.4372	0.828	1.4404	1.4125	1.937
35.0	1.5502	1.4713	1.4483	1.563	1.5043	1.4586	3.038
40.0	1.5711	1.4911	1.4440	3.159	1.5840	1.5124	4.529
45.0	1.5970	1.5157	1.4308	5.601	1.6902	1.5767	6.715
50.0	1.6361	1.5529	1.4125	9.041	1.8518	1.6570	10.519

- [1] These levels are outside the test data range.
- C_x is the compression carrying capacity ratio predicted by the Strength Model.
- C_x^* is the compression carrying capacity ratio predicted by the Load Model.
- $C_x = \frac{\sigma_{dry}}{\sigma_{green}} \times$ Shrinkage Factor.
- Shrinkage Factor = 0.9491.
- "Dry" means at 15 % M.C. and "Green" means at 24 % M.C.
- Difference = $\frac{C_x - C_x^*}{C_x} \times 100\%$

Table 10: *Comparison of Compression Carrying Capacity Ratio between Strength Model and Dimension-Adjusted Strength Model using 4 and 2-Term Linear Surface Model*

For this study, southern pine, mean and 5th percentile MOR data (Green *et al* 1986), were used to derived the slope parameter b and the corresponding P_{15} values for the 4-term linear surface model. These data pairs, plotted in Figure 15, confirm the earlier observations that the Douglas-fir and southern pine data sets show very similiar property responses with moisture content changes.

If the Douglas-fir model parameters are assumed applicable to other species then strong species would show larger absolute property adjustments than weak species. Limited experimental evidence from clear wood and full size lumber studies is used to evaluate this effect. Green and Evans (1987) developed a normalizing procedure which allowed a combined Douglas-fir and southern pine model to be extended to other species groups by intoducing a species normalizing factor. Individual property values $P_1(MC = M_1)$ for a species A, are normalized according to

$$P_1^* = P_1 \cdot \frac{K_{model}}{K_A} \tag{21}$$

where P_1^* is the normalized property value at moisture content M_1; K_{model} = 67.0 MPa, is the mean strength of 2x4 select structural dimension lumber derived from the moisture study database; K_A is the mean strength of 2x4, select structural grade lumber for the species A.

The normalized property values are adjusted with the Douglas-fir moisture adjustment model. Then the adjusted normalized value $P_2(MC = M_2)$ is calculated according to

$$P_2 = P_2^* \cdot \frac{K_A}{K_{model}} \tag{22}$$

where P_2^* is the model adjusted normalized property value at moisture content M_2; and P_2 is the desired property value corrected to moisture content M_2. The values of K_A for Canadian species given in Table 11 are preliminary estimates derived form small data sets and used herein to assess the application of the normalization comcept to individual species data produced by Jessome (1971).

Consider, for example, the case of adjusting the bending strength of eastern hemlock from green to 15% MC, given the green strength is 28.7 MPa. Using Eqn. (21)

$$P_{(green)} = 28.7 \text{ MPa} \cdot \frac{67.02}{48.27} = 40.0 \text{ MPa} \tag{23}$$

Species	*Normalization Factor,* K_A (MPa)
Douglas-fir	67.02
Southern pine	73.50
Red pine	38.61[1]
Jack pine	55.16[2]
White spruce	55.16[2]
Balsam fir	55.16[2]
Eastern white spruce	45.51[1]
Eastern hemlock	48.27[3]

· [1] median estimates for minor species
· [2] median estimates for SPF group
· [3] median estimates for Hem-Tam group

Table 11: *K_A factors for Selected Canadian Softwood Species*

Using the 4-Term LSM with parameters for Douglas-fir, we get

$$P_{(15\%)} = 52.3 \text{ MPa} \cdot \frac{48.27}{67.02} = 37.7 \text{ MPa} \tag{24}$$

Thus, the adjusted strength for eastern hemlock at MC = 15 percent, is 37.7 MPa.

Figure 15 has been replotted in Figure 16 except that P_{15} has been adjusted using Eqn.(21) and (22). Slope parameter b and corresponding P_{15} values are derived from studies by Jessome (1971). The 2x4 SS strength were not available for the whitewood.

Application of the normalizing procedure seems to bring the data for Canadian softwood species into closer agreement with the Douglas-fir moisture model as shown in Figure 16. This result tends to support the recommendation that a normalization procedure would be useful to accomodate the influence of inherent differences in bending strength properties among species.

A comprehensive compression strength study for Hem-fir and S-P-F has been reported by Madsen (1982). Using the data produced by Madsen, the slope parameter b and the correspomding P_{15} values were derived for the linear surface model. These data points are plotted in Figure 17 with the

4-term linear surface model derived from the Douglas-fir compression data. The data for the S-P-F seems to agree reasonably well with the surface line whereas for the Hem-fir , it shows less adjustment at the same P_{15} levels. The peculiar rise in the data trends at high P_{15} levels contradicts the trend observed for Douglas-fir.

Using the same normalization procedure outlined earlier and the normalization factor tabulated in Table 12, Figure 17 is replotted in Figure 18 with the slope b and P_{15} being normalized. The data pairs were shifted to the right and moved downwards hence making the fit even worse. It is apparent that the normalizing procedure does not help to unify the data with the Douglas-fir model. Therefore, the results does not support the recommendation that a normalization procedure is required unless further experimental data was studied.

Species	*Normalization Factor, K_A* (MPa)
Douglas-fir	67.02
Hem-fir	55.16
Spruce-pine-fir	45.51

Table 12: K_A *factors for Major Canadian Softwood Species*

7 BOUNDS FOR THE LINEAR SURFACE MODEL

The linear surface models are assured to be valid only within the data range. If data outside the data range are adjusted, it may lead to an unrealistic adjustment factor. After reviewing the fundamentals of the LSM, bounds for models are established. In order to maintain the validity of the LSM for adjusting data for any real value, a constant adjustment factor is assumed when out-of-bound data are adjusted.

These property bounds were established by comparing trends predicted using the models with actual trends observed near the extremes of the data, then maximum adjustment factor is assumed for each model. Since the adjustment factor varies with the moisture content, hence the bounds of the models are also functions of the moisture content.

The procedure of adjusting strength and capacity values for the alternative LSM are described as follows:

7.1 Modulus of Rupture

7.1.1 4-Term LSM

For $0.0 < P_1 < 180.0 - 3.737 \cdot MC_1$, where P_1 is the strength before adjustment in MPa and MC_1 is the initial moisture content in percentage, use the LSM with the coefficients given in Table 3.

For $P_1 > 180.0 - 3.737 \cdot MC_1$, use

$$P_2 = P_1 - 3.737 \cdot (MC_2 - MC_1) \tag{25}$$

where P_2 is the adjusted strength in MPa and MC_2 is the final moisture content in percentage.

7.1.2 3-Term LSM

For $4.8 < P_1 < 182.7 - 3.813 \cdot MC_1$, use the LSM models with coefficients given in Table 3.

For $P_1 > 182.7 - 3.813 \cdot MC_1$, use

$$P_2 = P_1 - 3.813 \cdot (MC_2 - MC_1) \tag{26}$$

For $P_1 < 4.8$, assuming no adjustment.

7.1.3 2-Term LSM

For $0.0 < P_1 < 155.1 - 3.792 \cdot MC_1$, use the simplified equations given in Barrett *et al* (1989) with the coefficients given in Table 3.

For $P_1 > 155.1 - 3.792 \cdot MC_1$, use

$$P_2 = P_1 - 3.792 \cdot (MC_2 - MC_1) \tag{27}$$

7.2 Moment Capacity

7.2.1 4-Term LSM

For $13.8 < P_1 < 145.5 - 2.503 \cdot MC_1$, use the LSM with the coefficients given in Table 4.

For $P_1 > 145.5 - 2.503 \cdot MC_1$, use

$$P_2 = P_1 - 2.503 \cdot (MC_2 - MC_1) \tag{28}$$

For $P_1 < 13.8$, no adjustment is assumed.

7.2.2 3-Term LSM

For $15.2 < P_1 < 149.6 - 2.565 \cdot MC_1$, use the LSM models with coefficients given in Table 4.

For $P_1 > 149.6 - 2.565 \cdot MC_1$, use

$$P_2 = P_1 - 1.993 \cdot (MC_2 - MC_1) \tag{29}$$

For $P_1 < 15.2$, no adjustment is assumed.

7.2.3 2-Term LSM

For $0.0 < P_1 < 128.2 - 2.551 \cdot MC_1$, use the simplified equations given in Barrett *et al* (1989) with the coefficients given in Table 4.

For $P_1 > 128.2 - 2.551 \cdot MC_1$, use

$$P_2 = P_1 - 2.551 \cdot (MC_2 - MC_1) \tag{30}$$

7.3 Compression Strength

The bounds for the compression strength adjustment is derived more or less the same method described earlier.

7.3.1 4-Term LSM

For $12.4 < P_1 < 98.6 - 2.482 \cdot MC_1$, where P_1 is the strength before adjustment in MPa and MC_1 is the initial moisture content in percentage, use the LSM with the coefficients given in Table 7.

For $P_1 > 98.6 - 2.482 \cdot MC_1$, use

$$P_2 = P_1 - 2.482 \cdot (MC_2 - MC_1) \tag{31}$$

where P_2 is the adjusted strength in MPa and MC_2 is the final moisture content in percentage.

For $P_1 < 12.4$, no adjustment is required.

7.3.2 3-Term LSM

For $0.0 < P_1 < 109.6 - 2.510 \cdot MC_1$, use the LSM models with coefficients given in Table 7.

For $P_1 > 109.6 - 2.510 \cdot MC_1$, use

$$P_2 = P_1 - 2.510 \cdot (MC_2 - MC_1) \tag{32}$$

7.3.3 2-Term LSM

For $0.0 < P_1 < 96.5 - 2.482 \cdot MC_1$, use the simplified equations given in Barrett *et al* (1989) with the coefficients given in Table 7.

For $P_1 > 96.5 - 2.482 \cdot MC_1$, use

$$P_2 = P_1 - 2.482 \cdot (MC_2 - MC_1) \tag{33}$$

7.4 Compression Capacity

7.4.1 4-Term LSM

For $13.1 < P_1 < 128.9 - 2.496 \cdot MC_1$, use the LSM with the coefficients given in Table 8.

For $P_1 > 128.9 - 2.496 \cdot MC_1$, use

$$P_2 = P_1 - 2.496 \cdot (MC_2 - MC_1) \tag{34}$$

For $P_1 < 13.1$, no adjustment is assumed.

7.4.2 3-Term LSM

For $4.1 < P_1 < 93.8 - 1.993 \cdot MC_1$, use the LSM models with coefficients given in Table 8.

For $P_1 > 93.8 - 1.993 \cdot MC_1$, use

$$P_2 = P_1 - 1.993 \cdot (MC_2 - MC_1) \tag{35}$$

For $P_1 < 4.1$, no adjustment is assumed.

7.4.3 2-Term LSM

For $0.0 < P_1 < 92.4 - 2.207 \cdot MC_1$, use the simplified equations given in Barrett *et al* (1989) with the coefficients given in Table 8.

For $P_1 > 92.4 - 2.207 \cdot MC_1$, use

$$P_2 = P_1 - 2.207 \cdot (MC_2 - MC_1) \tag{36}$$

8 COMPARISON WITH CEN STANDARD

The linear surface model for moisture content adjustment can be represented by a contour plot which joins the same property level at different moisture content. We can also express the contour lines in a normalized basis which shows the percentage change in property with moisture content changes. Using strength at 18% MC as the standard strength, Figure 15 and 16 show the adjustment lines for MC at different strength levels for bending strength and compresion strength respectively.

Family of linear lines are obtained since a linear relaionship has been assumed for strength verses moisture content.

Comparison has been made with the recommendations according to the fifth draft of CEN/TC 124 - The Determination of Characteristic Values of Mechanical Properties and Density for Timber. It states that no adjustment is required for bending and tension strength adjustment due to moisture content changes; and a 3% increase for compression parallel to grain strength for every percentage point decrease in moisture content has been assumed.

These CEN adjustment factors are plotted in Fig. 17 and 18 for bending strength and compression strength respectively along with the linear surface models. In bending, the CEN recommendation for moisture content adjustment is comparatively conservative at all MC levels. At high strength level, the deviation between the LSM and the CEN recommendation is especially large. In compression, the regression line recommended by the CEN almost coincides with the 20 MPa contour line. Realizing 20 MPa is about the mean compression strength at green condition implies that the CEN recommended adjusted line has a near average slope of the LSM and perhaps overestimate the effect at low strength levels.

9 CONCLUSIONS

Based on the results presented in this report, we conclude the following:

1. The Linear Surface Model overcomes the major concerns presented by negative ballots on the ASTM standard since the model does not have the reversing effect related to the reversing effect in the strength and capacity versions of the Quadratic Surface Models.

2. The predicted increases in strength from green to dry are smaller than predicted by the QSM.

3. The predicted increases in strength are sufficient to offset shrinkage therefore member capacity increases with drying and traditional methodology on size and moisture-strength relationships is maintained.

4. The Linear Surface Model can be extended to other species by applying a normalizing procedure to account for inherent strength differences between species.

5. The recommendations by the CEN Standard EN xxx1 are perhaps too conservative when adjusting bending strength data for effect of moisture content.

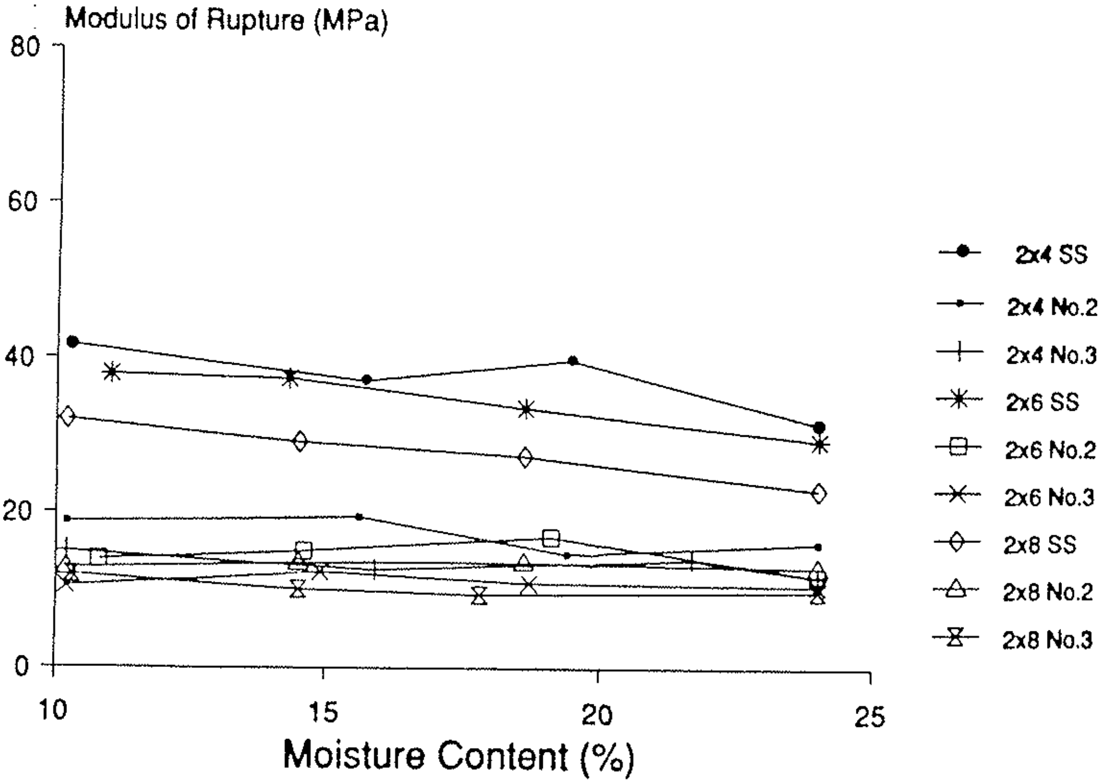

Figure 1: Relationships between the fifth percentile modulus of rupture and moisture content for Douglas-fir ($M_p = 24$) (Aplin *et al* 1986)

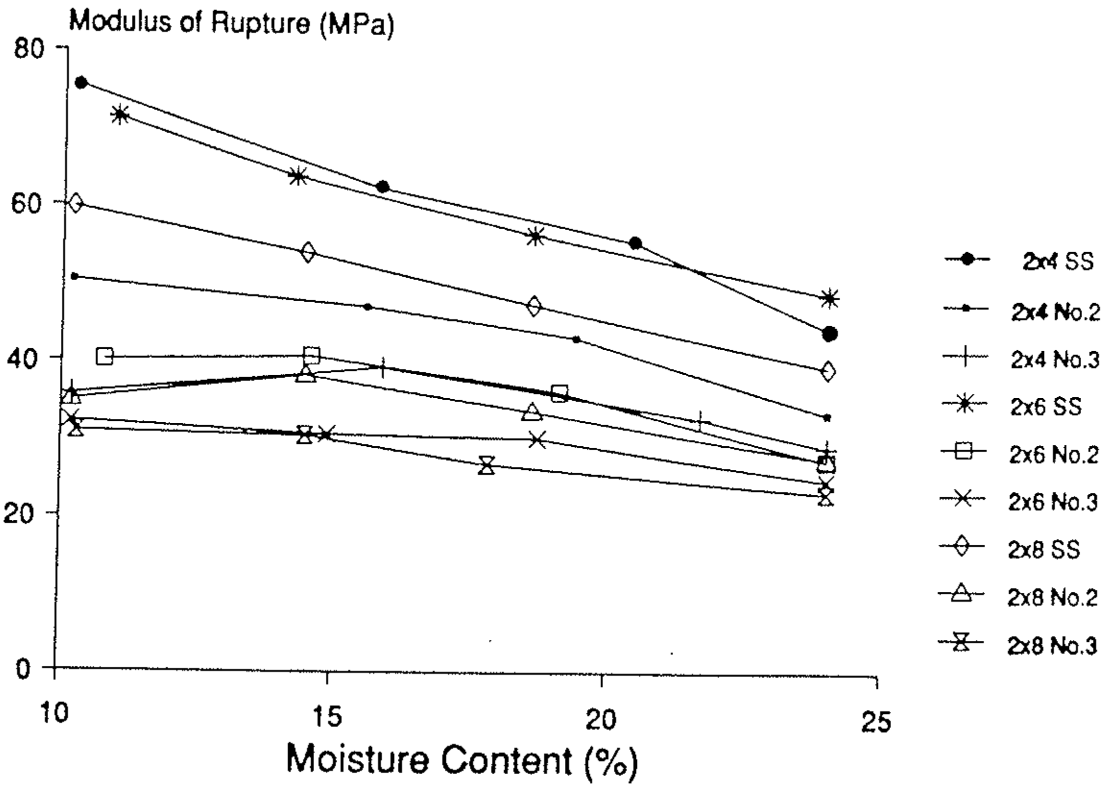

Figure 2: Relationships between the mean modulus of rupture and moisture content for Douglas-fir ($M_p = 24$) (Aplin *et al* 1986)

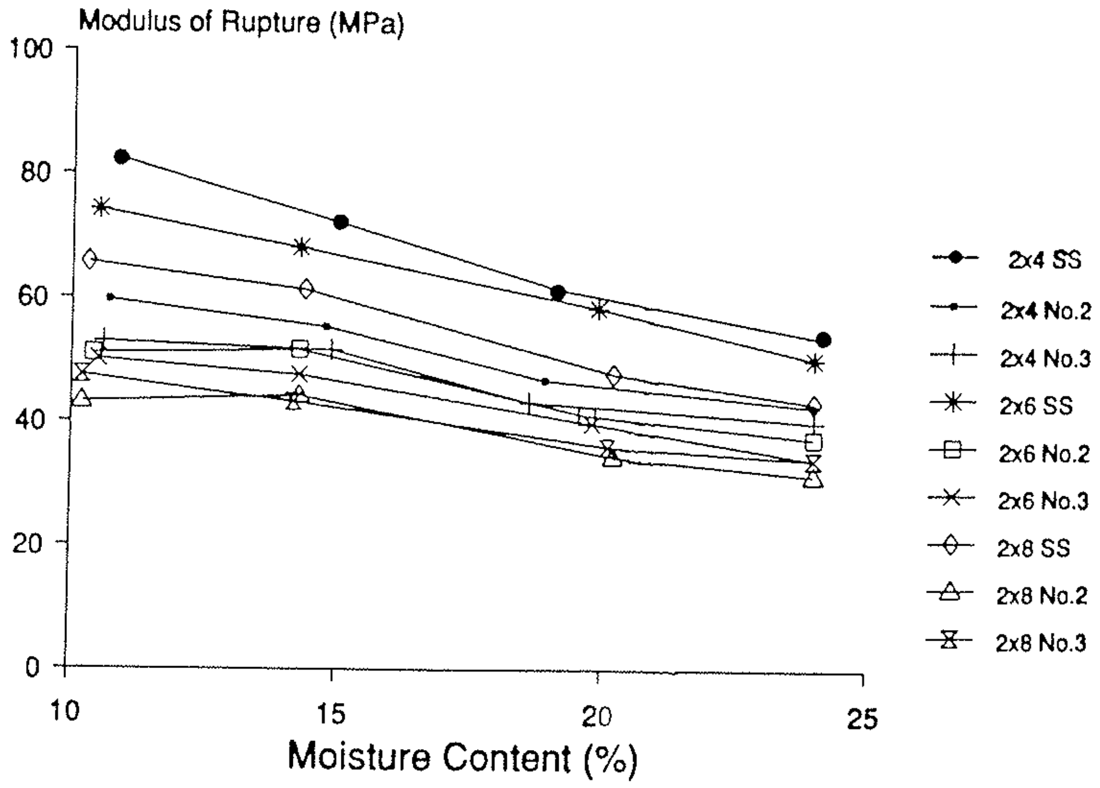

Figure 3: Relationships between the fifth percentile modulus of rupture and moisture content for southern pine ($M_p = 24$) (McLain *et al* 1984)

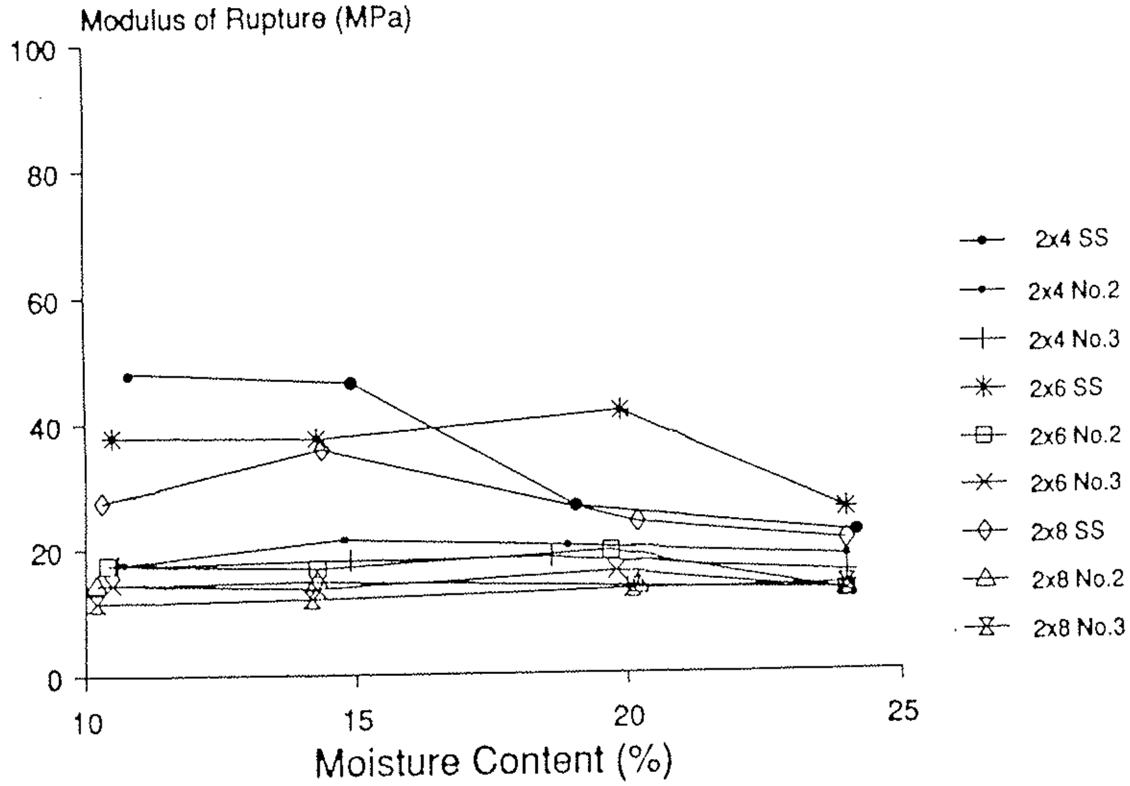

Figure 4: Relationships between the mean percentile modulus of rupture and moisture content for southern pine ($M_p = 24$) (McLain *et al* 1984)

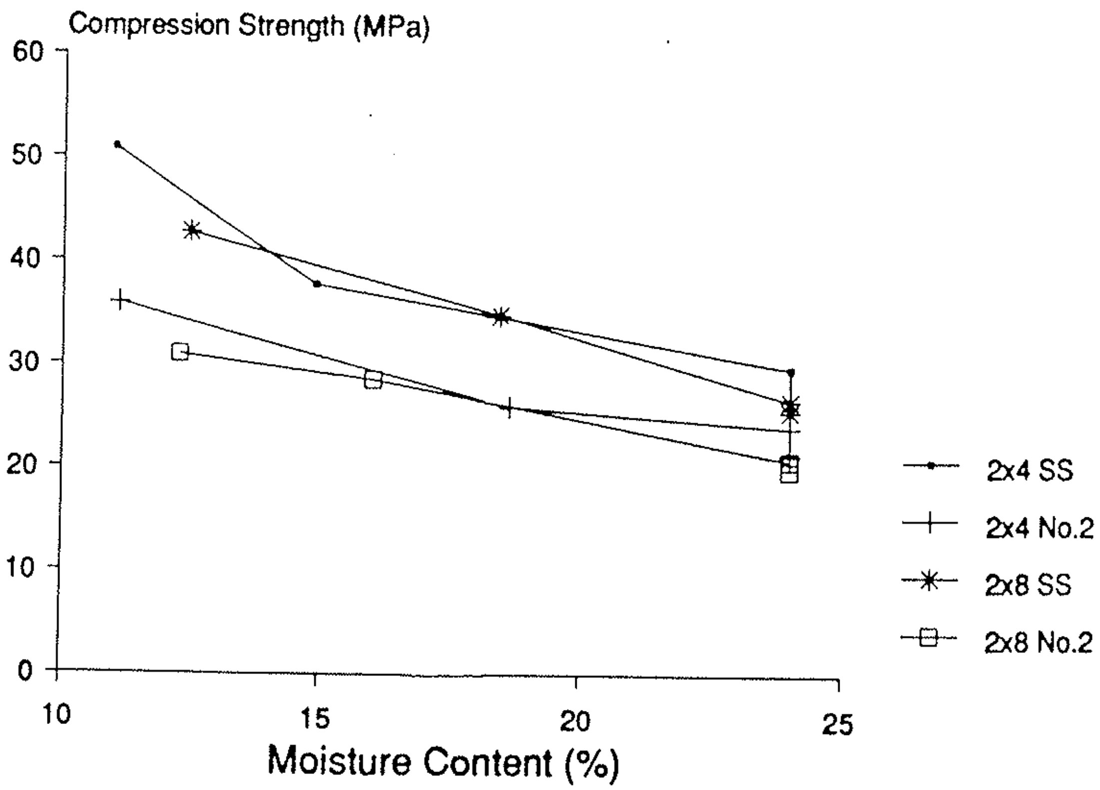

Figure 5: Relationships between the fifth percentile compression strength and moisture content for Douglas-fir ($M_p = 24$)

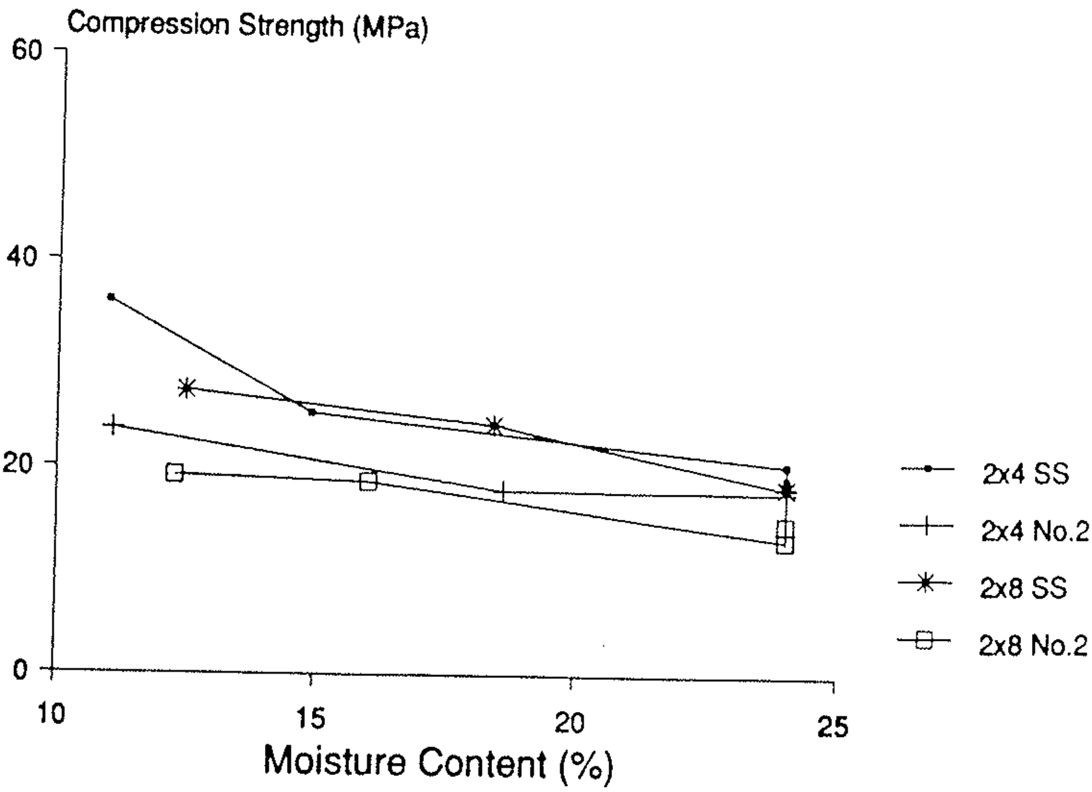

Figure 6: Relationships between the mean compression strength and moisture content for Douglas-fir ($M_p = 24$)

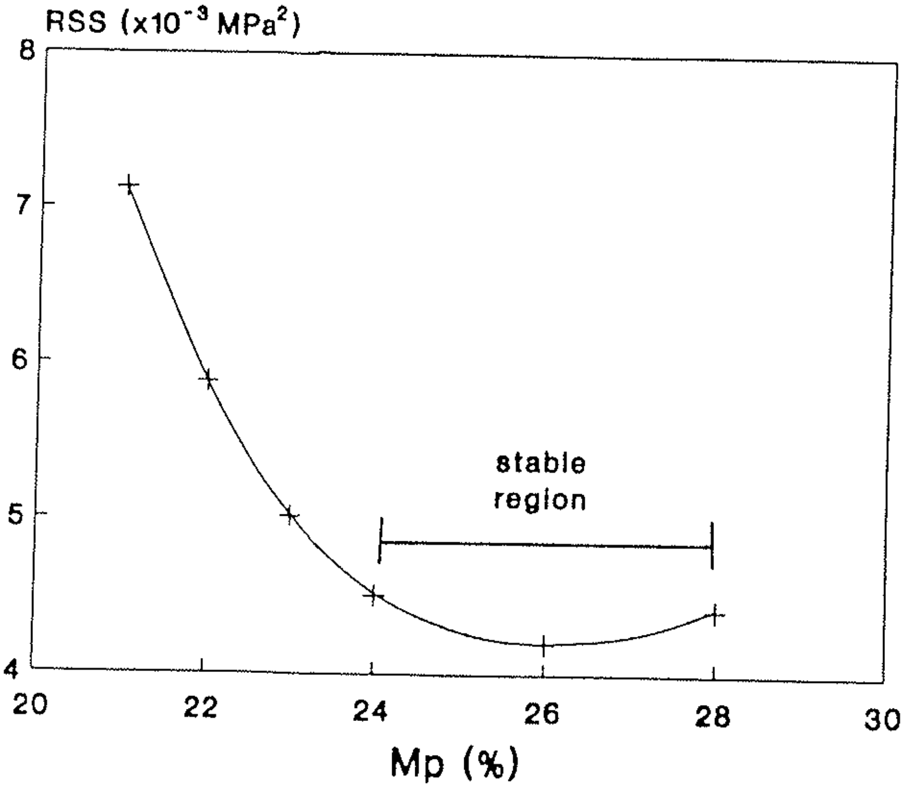

Figure 7: Relationship between the Intersection Moisture Content (M_p) and the Residual Sums of Squares (RSS) for the general 2-term MOR Linear Surface Model (Douglas-fir)

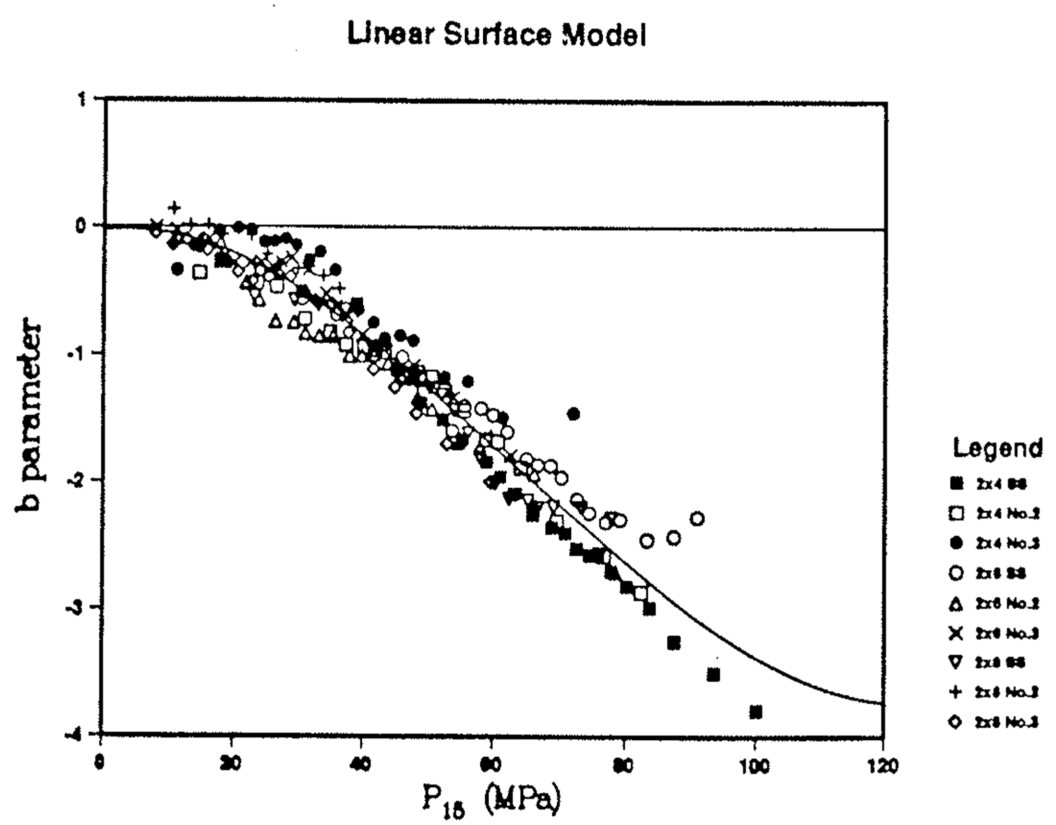

Figure 8: Relationship between the b parameter and P_{15} for 4-Term Linear Surface Model and showing the cubic regression fit to Douglas-fir MOR data

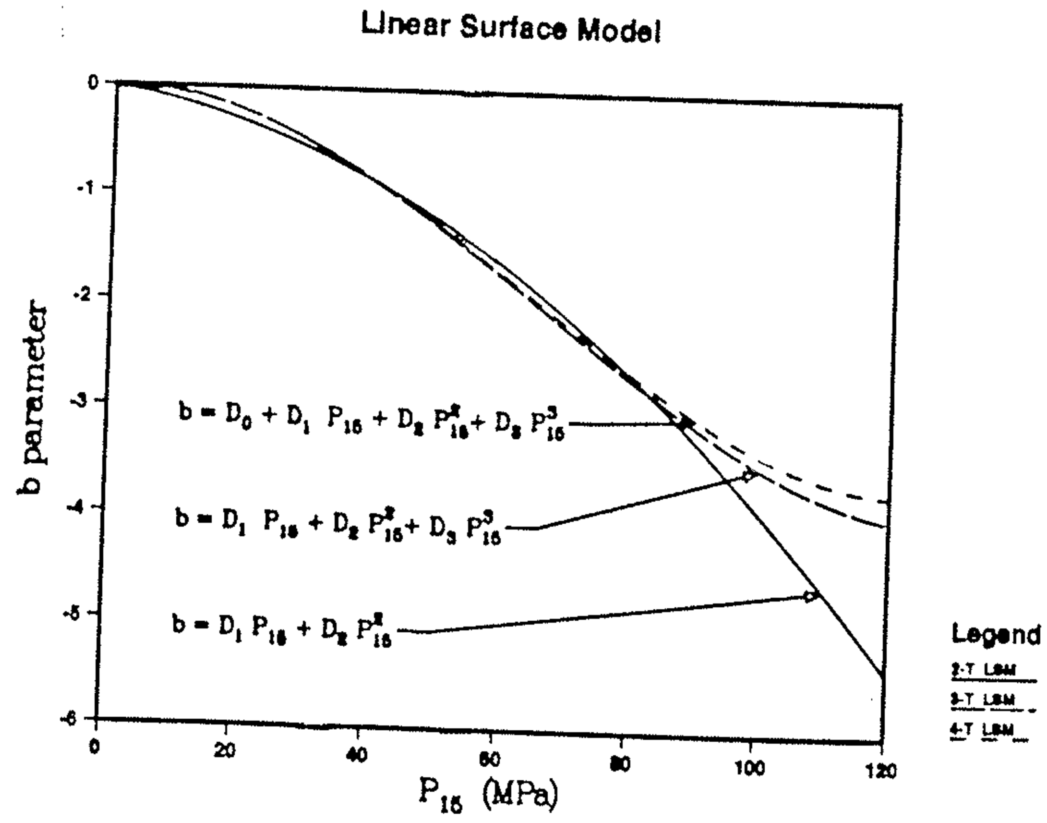

Figure 9: Regression fits of b parameter for the 4-, 3-, and 2-Term Linear Surface Models for the MOR data

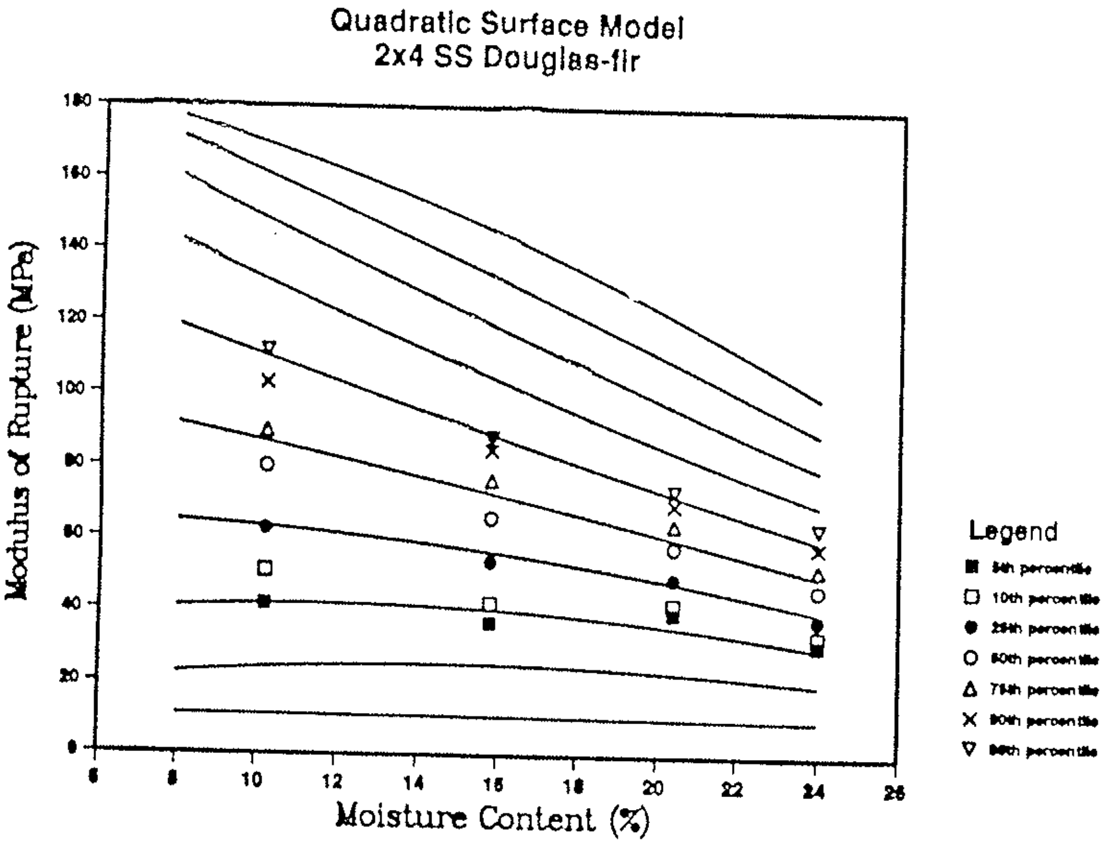

Figure 10: Predicted Modulus of Rupture Using Quadratic Surface Model

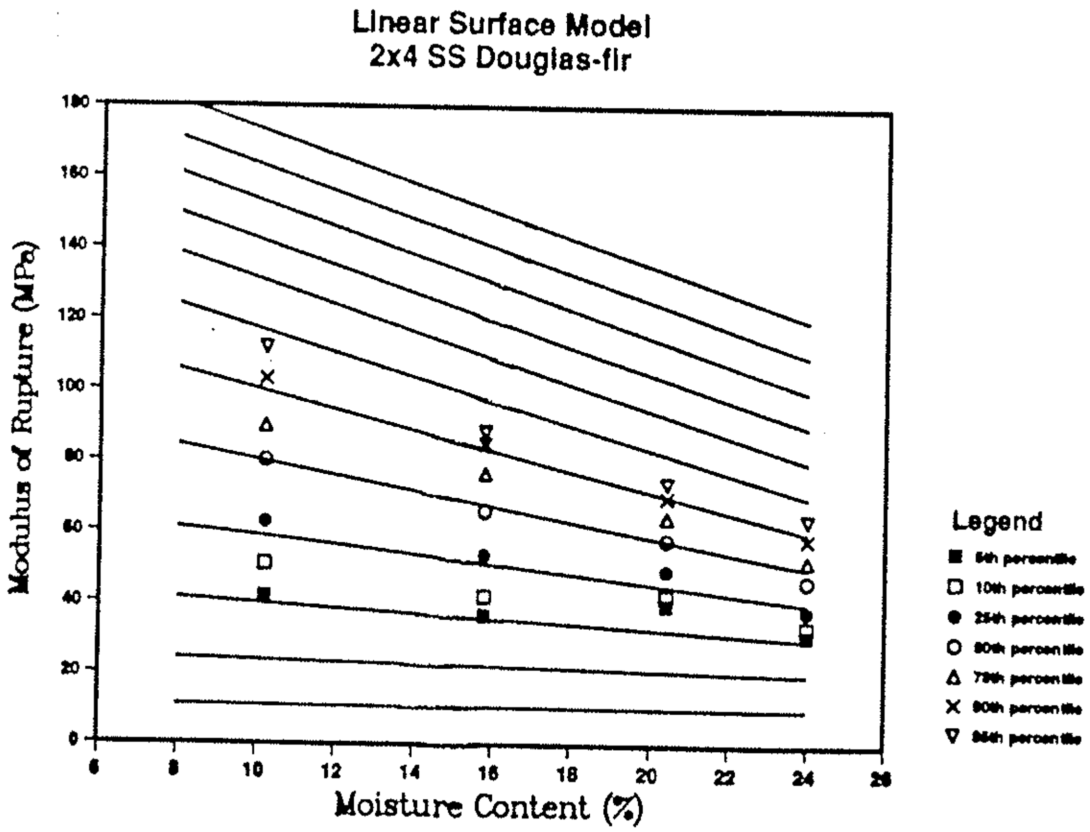

Figure 11: Predicted Modulus of Rupture Using 4-Term Linear Surface Model

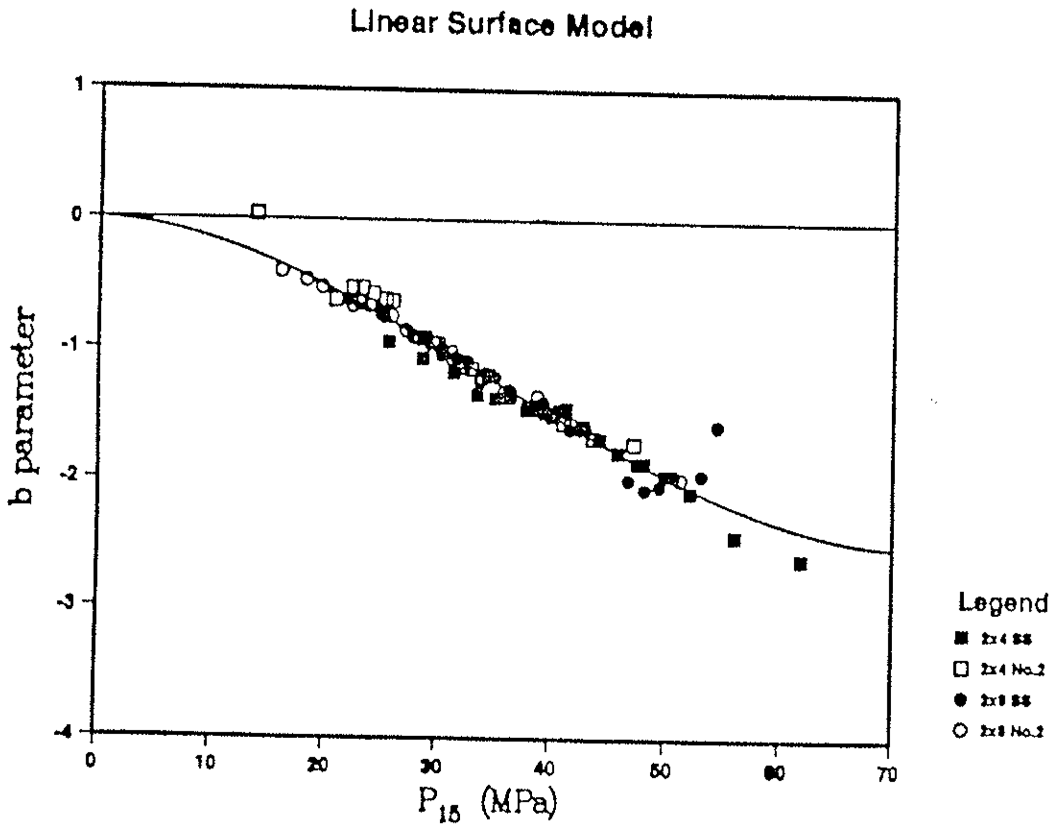

Figure 12: Relationship between the b parameter and P_{15} for 3-Term Linear Surface Model and showing the cubic regression fit to Douglas-fir compression strength data

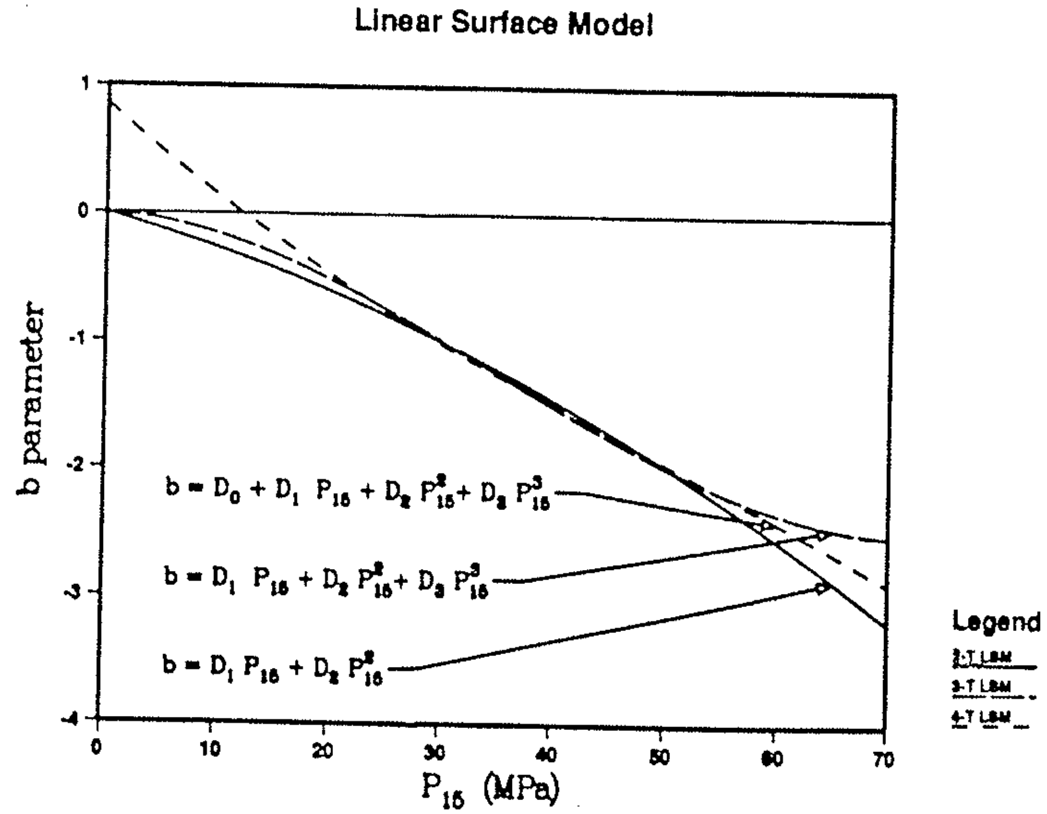

Figure 13: Regression fits of b parameter for the 4-, 3-, and 2-Term Linear Surface Models for the compression strength data

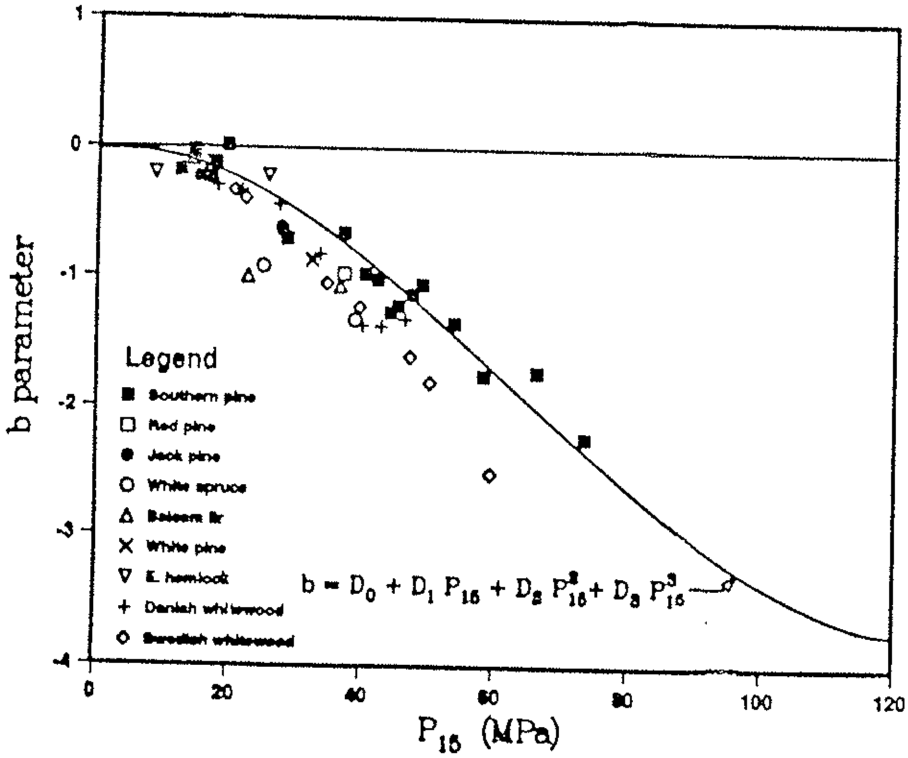

Figure 14: Relationship between b parameter and P_{15} for softwood species (MOR, Jessome 1971 and Hoffmeyer 1978)

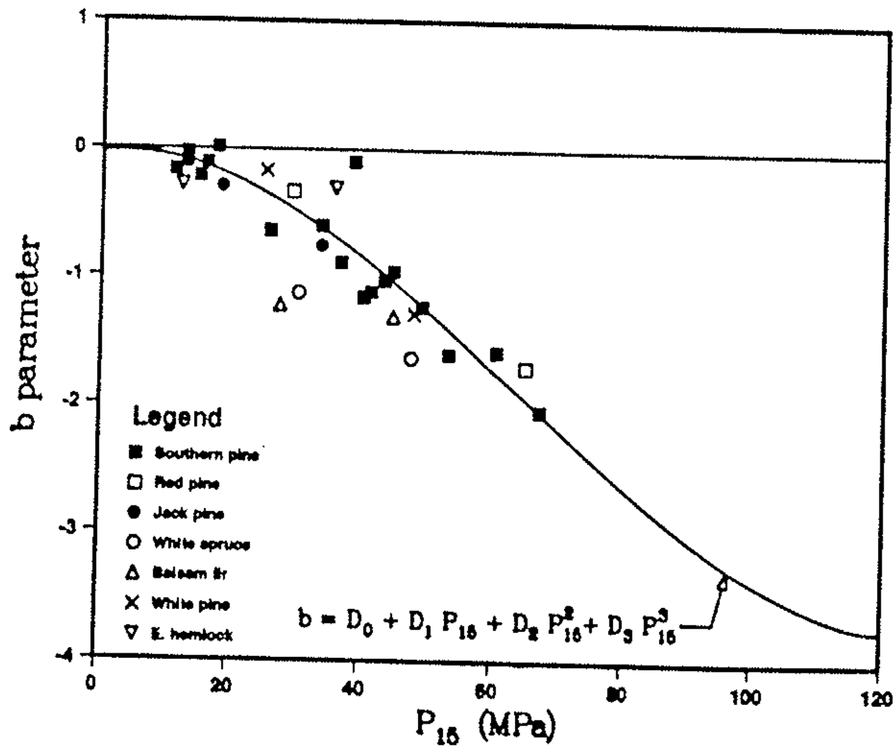

Figure 15: Relationship between normalized P_{15} and the b parameter for softwood species (MOR)

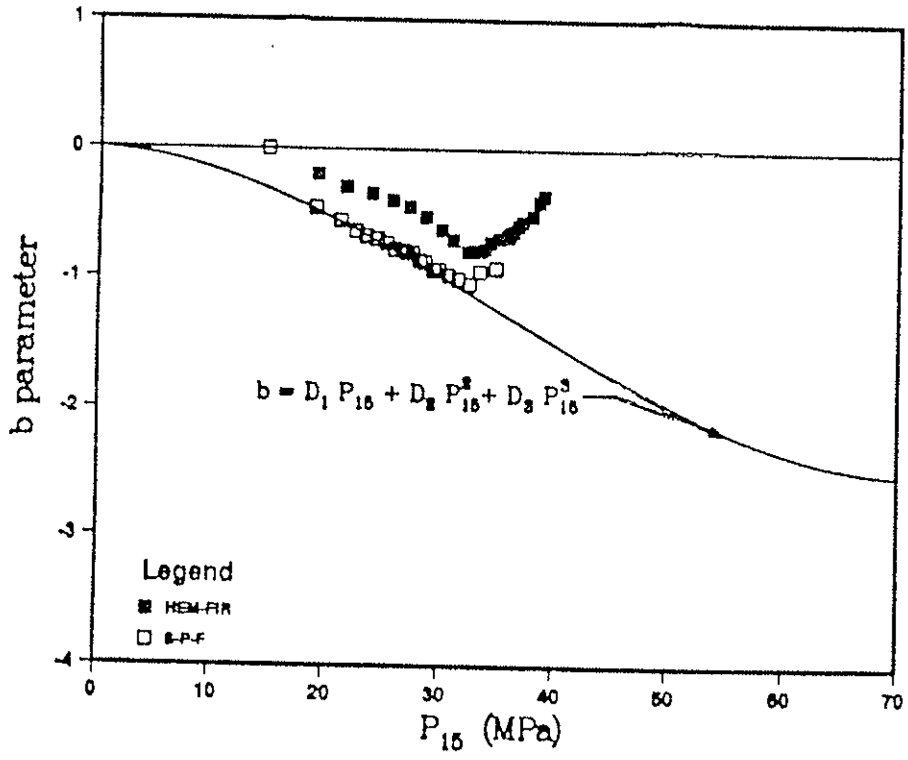

Figure 16: Relationship between b parameter and P_{15} for Hem-fir and Spruce-Pine-Fir Species (Compression Strength, Madsen 1982)

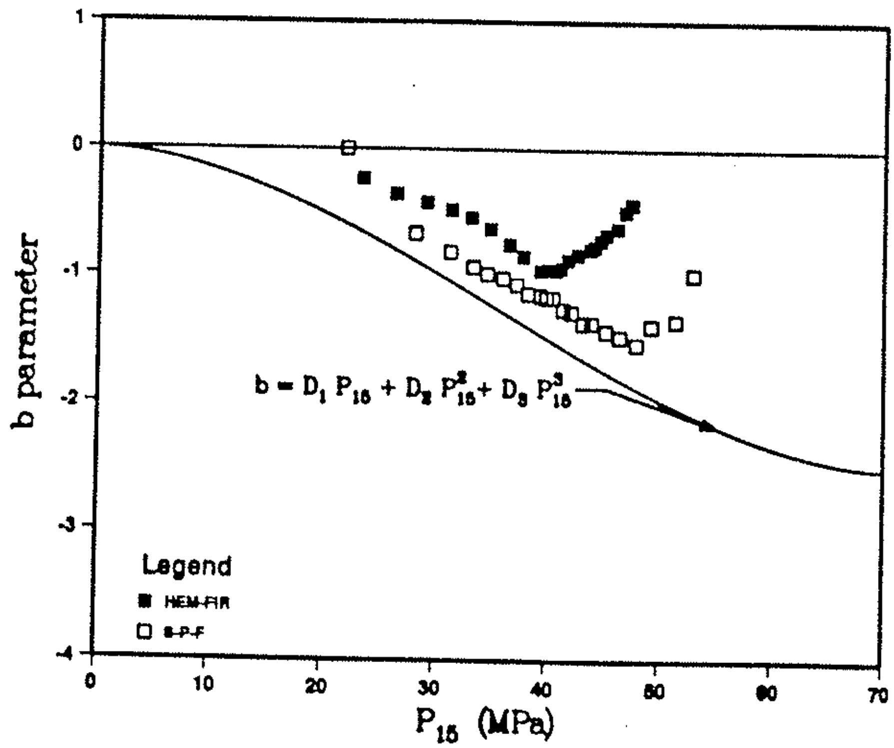

Figure 17: Relationship between normalized P_{15} and the b parameter for Hem-fir and Spruce-Pine-Fir Species (Compression Strength)

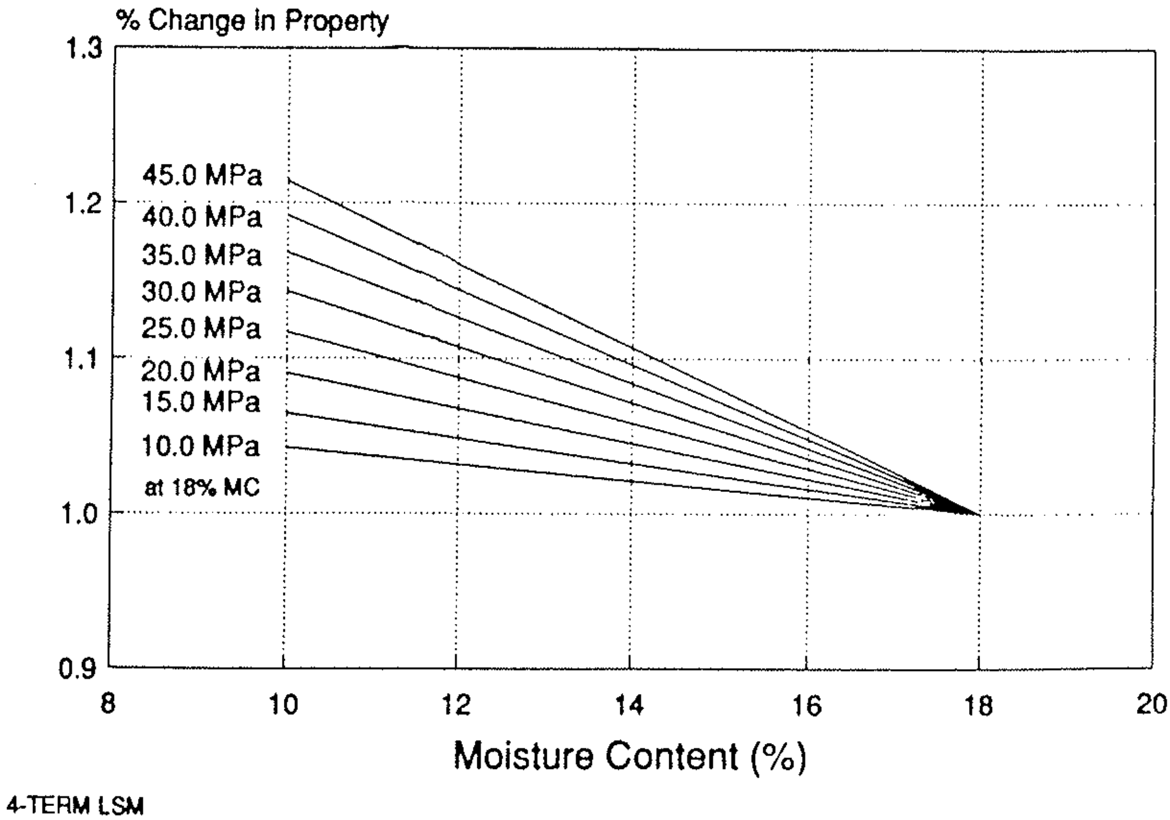

Figure 18: Relationship between % change in property and moisture content for the 4-term MOR linear surface model

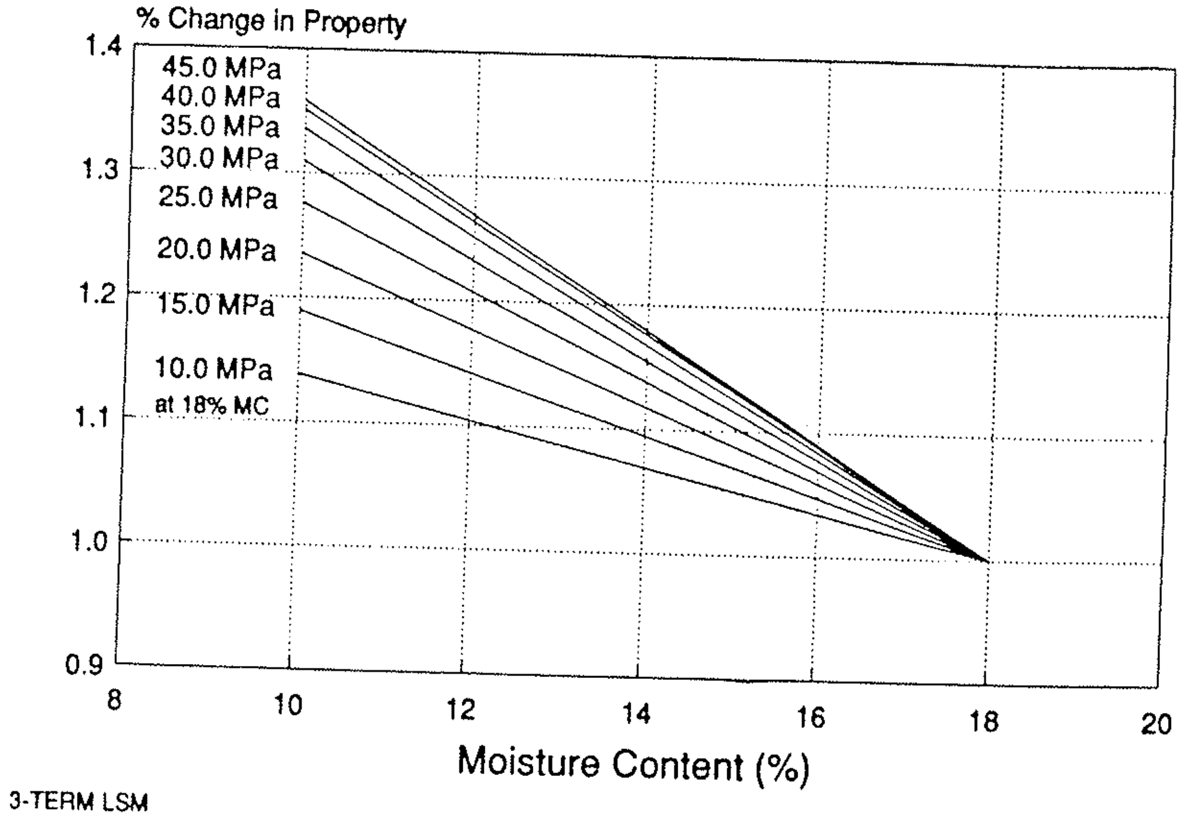

Figure 19: Relationship between % change in property and moisture content for the 3-term compression strength linear surface model

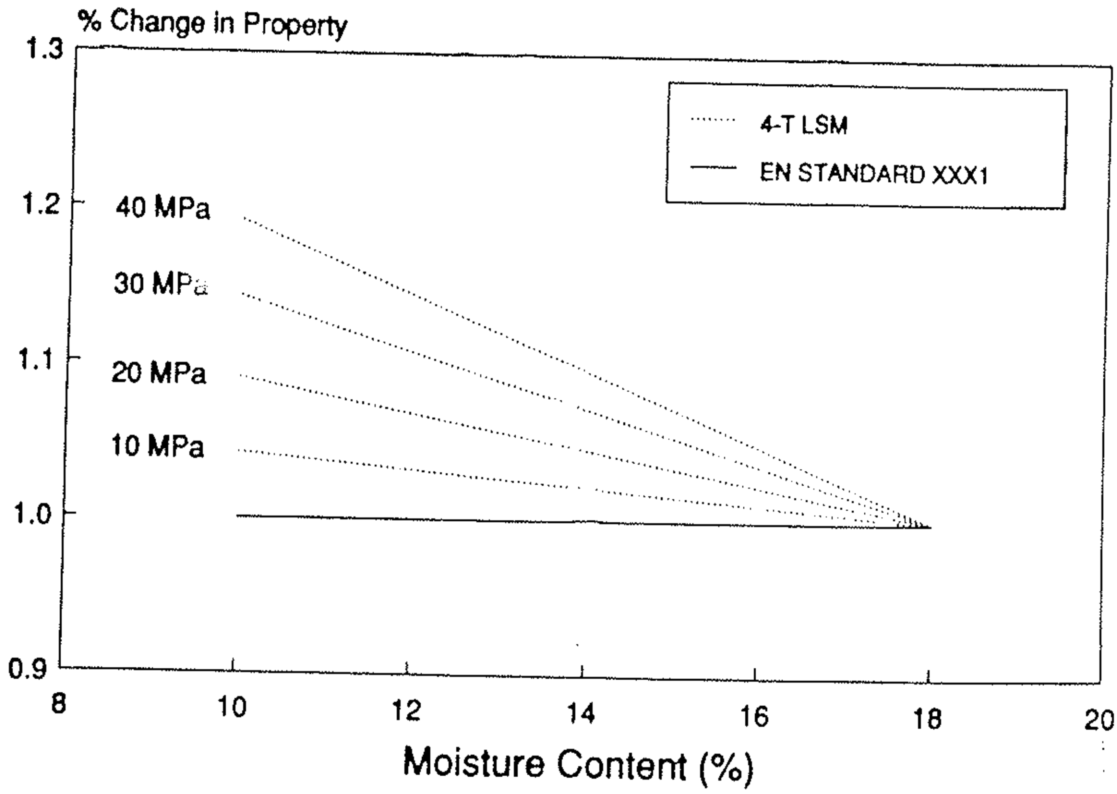

Figure 20: Comparison between CEN recommendations and 4-term MOR linear surface model

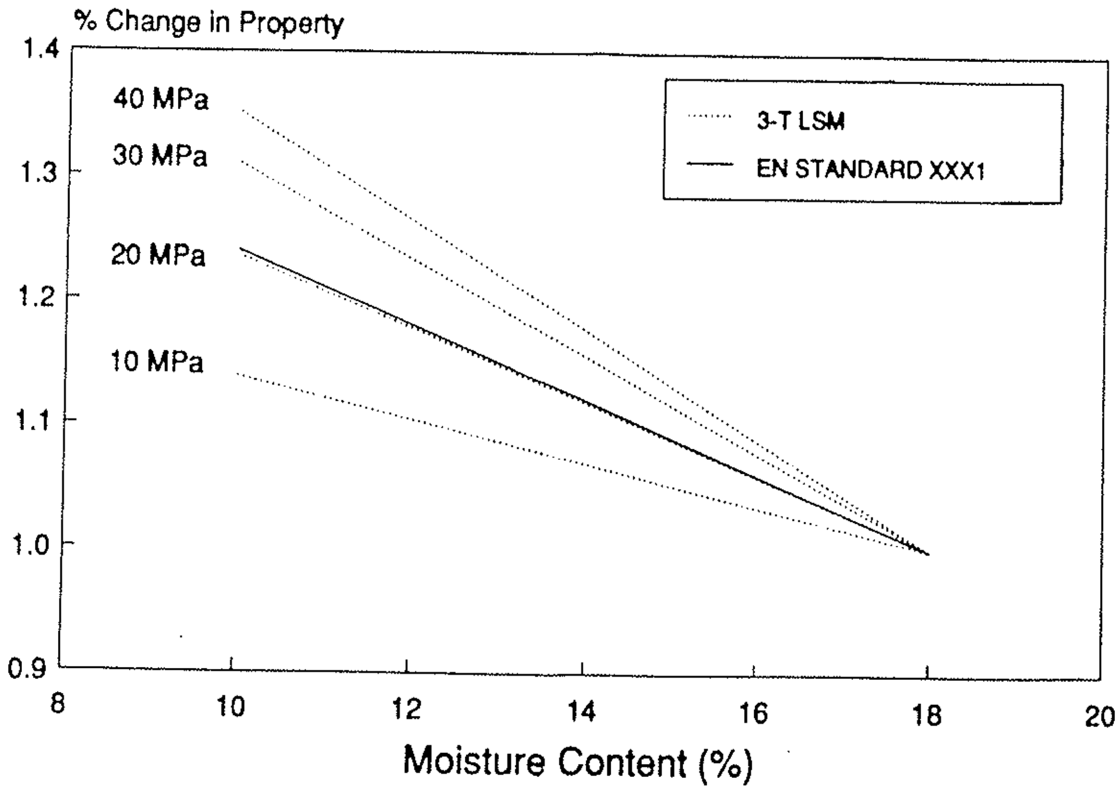

Figure 21: Comparison between CEN recommendations and 3-term compression strength linear surface model

References

[1] AMERICAN SOCIETY FOR TESTING AND MATERIALS 1986. " Establishing Structural Grades and Related Allowable Properties for Visually Graded Lumber," *ASTM D245-81*, Philadelphia, PA.

[2] AMERICAN SOCIETY FOR TESTING AND MATERIALS 1983. " Standard Method for Evaluating Allowable Properties for Grades of Structural Lumber," *ASTM D2915-80*, Philadelphia, PA.

[3] APLIN, N.E., D.W. GREEN, J.W. EVANS, AND J.D. BARRETT 1986. " Moisture Content and the Flexural Properties of Douglas-Fir Dimension Lumber," *USDA Forest Service, Research Paper*, FPL 475. Forest Prod. Lab., Madison, WI. 32pp.

[4] BARRETT, J.D. AND W. LAU 1989. " Lumber Bending Strength Adjustments for Moisture Content," Dept. of Harvesting and Wood Sci., University of British Columbia, Vancouver. (to be submitted for publication)

[5] BARRETT, J.D. AND W. LAU 1989. " Lumber Compression Strength Adjustments for Moisture Content," Dept. of Harvesting and Wood Sci., University of British Columbia, Vancouver. (to be submitted for publication)

[6] GERHARDS, C.C. 1968. " Four-inch Southern Pine Lumber: Seasoning Factors for Modulus of Elasticity and Modulus of Rupture," *Forest Prod. J.*, 18(11): 27-35.

[7] GERHARDS, C.C. 1970. " Further Report on Seasoning Factors for Modulus of Elasticity and Modulus of Rupture," *Forest Prod. J.*, 20(5): 40-44.

[8] GREEN, D.W. 1982. " Adjusting the Static Strength of Lumber for Changes in Moisture Content," *Proceedings, Workshop on How the Environment Affects Lumber Design: Assessments and Recommendations*, Forest Prod. Lab., Madison, WI, 28-30 May 1980. Pp. 86-105.

[9] GREEN, D.W. 1983. " In-grade testing: Impetus for Change in the Utilization of Structural Lumber. In: Corcoran, T.J.; Gill, D.R. eds.,"

Proceedings of the conference, from stump through mill-recent advances in spruce-fir utilization technology; Orono, Orono, ME: University of Maine.

[10] GREEN, D.W., C.L. LINK, A.L. DeBONIS, AND T.E. McLAIN 1986. " Predicting the Effect of Moisture Content on the Flexural Properties of Southern Pine Dimension Lumber," *Wood Fiber Sci*, 18(1): 134-156.

[11] GREEN, D.W., J.W. EVANS 1987. " Mechanical Properties of Visually Graded Lumber," *Vol 1. A Summary Report 131 p.*, Available from NTIS, 5285 Port Royal Road, Springfield, VA 22161, PB-88-159-389.

[12] GREEN, D.W., J.W. EVANS, J.D. BARRETT AND E.N. APLIN 1988. " Predicting the Effect of Moisture Content on the Flexural Properties of Douglas-Fir Dimension Lumber," *Wood Fiber Sci*, 20(1): 107-131.

[13] GREEN, D.W. 1989. " Moisture Content and the Shrinkage of Lumber," *USDA Forest Serv. Research Paper*, FPL-RP-489, Forest Prod. Lab., Madison, WI.

[14] HOFFMEYER, P. 1978. " Moisture Content-Strength Relationship for Spruce Lumber Subjected to Bending, Compression and Tension along the grain," *Proceedings IUFRU - Wood Engineering Group Meeting*, Vancouver, B.C.

[15] JESSOME, A.P. 1971. " The Bending Strength of Lumber in Structural Sizes," *Dept. of the Environment, Canadian Foresting Service*, Publication No. 1305, Ottawa.

[16] MADSEN, B. 1975. " Moisture Content-Strength Relationships for Lumber Subjected to Bending," *Can. J. Civil Eng.*, 2(4): 466-473.

[17] MADSEN, B., W. JANZEN, AND J. ZWAAGSTRA 1980. " Moisture Effects in Lumber," *Streuctural Research Series, Rep. No. 27*, Dep. Civil Eng., University of British Columbia, Vancouver.

[18] MADSEN, B. 1982. " Recommended Moisture Adjustment Factors for Lumber Stresses," *Can. J. Civil Eng.*, 9: 602-610.

[19] McLAIN, T.E., A.L. DeBONIS, D.W. GREEN, F.J. WILSON, AND C.L. LINK 1984. " The influence of Moisture Content on the Flexural Properties of Southern Pine Dimension Lumber," *USDA Forest Serv. Res. Pap.*, FPL 447, Forest Prod. Lab., Madison, WI.

[20] WILSON, T.R.C. 1932. " Strength-Moisture Relations for Wood," *US Forest Serv. Tech. Bull.*, No. 282, Forest Prod. Lab., Madison, WI.

CIB -W18A / 22-6-3

INTERNATIONAL COUNCIL FOR BUILDING RESEARCH STUDIES AND DOCUMENTATION

WORKING COMMISSION W18A - TIMBER STRUCTURES

A DISCUSSION OF LUMBER PROPERTY RELETIONSHIPS IN EUROCODE 5

by

D W Green and D E Kretschmann
US Departement of Agriculture
Madison, Wisconsin
United States of America

MEETING TWENTY - TWO

BERLIN

GERMAN DEMOCRATIC REPUBLIC

SEPTEMBER 1989

A DISCUSSION OF LUMBER PROPERTY RELATIONSHIPS IN EUROCODE 5

David W. Green
Research General Engineer

David E. Kretschmann
General Engineer

U.S. Department of Agriculture
Forest Products Laboratory
Madison, Wisconsin

Introduction

This paper addresses the use of the stress class system for timber structures proposed for adoption in Eurocode 5. The paper used as reference the stress class system and assignment procedures presented in the fourth draft of Eurocode 5, March, 1989 (CEN xxx1, Glos and Fewell 1989; and CEN xxx2 Fewell, 1989).

Stress class are being studied by Subcommittee D07.02 on Lumber and Engineered Wood Products of the American Society of Testing and Materials, Figure 1. During this study it has been necessary to evaluate relationships between mechanical properties and to compare these relationships with those used in proposed stress class systems such as Eurocode 5. The objective of this paper is to share insights gained from this evaluation of property relationships with the CIB W18A Working Commission on Timber Structures.

Background

In 1977, the major rules writing agencies in the United States, in cooperation with the U.S. Forest Products Laboratory, began what is called the In-Grade Testing Program. At this time the Canadian lumber industry was also conducting an in-grade testing program, but with objectives and procedures that differed from those of the U.S. program. In 1981 representatives from the two countries met and developed a common approach to in-grade testing.

Sampling in the In-Grade program was conducted using a stratified cluster sampling approach in which the geographic area over which the species (or species group) grew were divided into "regions" based on general trends in topography and known timber growth characteristics. Within a region, mills to be sampled were selected at random from a list of producing mills. Within mill samples were selected in groups of 10 pieces. For the major volume species groups, Douglas Fir-Larch, Hem-Fir, and Southern Pine, samples of nominal 2x4, 2x8 and 2x10 inch (actual 38x89, 38x184, and 38x235 mm) material were selected in two quality levels, Select Structural and No. 2, Figure 2. Because the trees are generally of smaller diameter, nominal 2x4, 2x6 (38x140 mm), and 2x8 lumber was sampled for the lesser volume species. The target sample sizes per grade-size cell was 360 pieces for the major volume species and 60 for the lesser volume species. Some information was also obtained on Stud, Construction, Standard, and Utility Grades in the 2x4 size. In all, some 42,300 specimens were tested, Table 1.

Testing in the in-grade program followed procedures outlined in ASTM standard D4761 (ASTM, 1988). Bending tests were conducted using third point loading with a span-to-depth ratio of 17-to-1. Tension parallel-to-the-grain tests were conducted using a clear span between grips of 10 feet (3 meters) for 2x8 and 2x10 and a span of 8 feet (2.4 meters) for 2x4's. Compression testing was conducted using laterally supported specimens having a width-to-length ratio of approximately 2.5 to 1. The apparent worst strength reducing defect was centered in the piece. All tests were conducted using a rate of loading calculated to give failure in 1.5 to 2.5 minutes.

Because testing for bending and tension was conducted in the field using portable equipment, it was not possible to equilibrate the specimens to constant environmental conditions. Therefore analytical models were required to adjust properties to constant environmental conditions. At test the temperature of the specimens was measured using a surface temperature gauge and the moisture content was measured using an electrical resistance moisture meter. Mechanical properties were adjusted to 21 deg. C (70 deg. F) using procedures given in Barrett, Green and Evans, 1989. Mechanical properties were adjusted to constant moisture content levels using the quadratic surface models given in Green and Evans, 1989 (also see Evans, Evans, and Green, 1989).

Assignment of Stress Classes

Except as indicated, the properties for visually graded lumber presented in this paper are based on data presented in Green and Evans (1987), and procedures summarized in the proceedings of the conference on in-grade testing held in Madison in 1988 (Forest Products Research Society, 1989). ASTM Committee D07 is currently reviewing a draft standard for assigning allowable properties for lumber derived on the basis of in-grade testing. It is cautioned that allowable properties adopted for use with visually graded lumber in the United States will be based on this new standard and the resulting properties may differ from those given in this paper. For this reason actual comparisons of stress class assignment are useful only as an indication of consistent bias in the assumed property relationships.

Characteristic values in Eurocode 5 are derived from nonparametric 5th percentile estimates of properties at a temperature of 20 + 2 deg. C and a relative humidity of 0.65 + 0.05 (nominal 12% moisture content). Mean values are defined at the same conditions. Derivation of the characteristic values and mean estimates of the In-Grade data is as follows:

1. The 5th percentile property estimates were determined using nonparametric estimates of the 5th percentile at 20 deg. C and 12% moisture content. Mean MOE estimates were from an assumed normal distribution (Green and Evans, 1987, volumes 2-4).
2. Individual test values for a given size were adjusted to the estimated property at a dressed dry width of 184 mm (7.25 inches) using the equation (Johnson, Evans, Green, 1989)

$$P2 = P1 * (W1/W2) ** (n)$$

where P1 is the property measured at width W1 and P2 is the property estimated at width W2 = 184mm. Values of n were determined as n = 0.357 for both modulus of rupture, MOR, and ultimate tensile stress parallel to the grain, UTS, and n = 0.132 for ultimate compression stress parallel to the grain, UCS. No width adjustment was taken for MOE.

3. Characteristic values were obtained following procedures given in CEN xxx1 (Glos and Fewell 1989). First a sample size volume weighted estimate of properties was obtained. Next the volume weighted estimated was checked against an acceptance criteria. In no instance did the weighted average exceed 1.2 times the minimum 5th percentile for a given grade, as specified by the acceptance criteria.
4. 5th percentile strength properties were then multiplied by the sample size factor Ks = 0.97. because only 3 sizes were tested per grade[1]. MOR values were multiplied by Kt = 1.017 to adjust from a span depth ratio of 17 to 1 used in the In-Grade program to the 18 to 1 ratio specified by Eurocode 5.
5. Density estimates were based on all available data (Green and Evans, 1989 b), not just the data for the indicated grades. Density was originally recorded using oven dry weight and oven dry volume and then converted to weight and volume at 12% MC.

Table 2 presents a summary of the characteristic values and mean properties for some of the grades and species groups tested in the In-Grade program.

CEN xxx2 (Fewell, 1989) gives the revised stress class system proposed for Eurocode 5 that was used in this paper, Table 3. Stress class assignments are based on three primary properties: 5th percentile MOR, mean MOE, and 5th percentile density, Table 4. It is assumed that secondary property assignments are to be valid.

Several observations we have made about the assignments are:

1. In two cases (Hem-Fir Select Structural and Douglas Fir-Larch No. 2) density limits the assignment to one stress class lower than that which would have been assigned based on MOR and MOE.
2. In one case, No. 2 Southern Pine, a grade fails to have the UTS values assumed by the stress class assignment.
3. In most cases the UCS assumed for the stress class assignment is conservative compared to what the assignment would have been had the assignment been based on the measured UCS characteristic values.
4. In all cases the measured characteristic value for the MOE of No. 2 grade fails to make the value appropriate for mean MOE. In contrast, the measured characteristic value for Select Structural grade does meet the anticipated value based on mean MOE.

These observations will be discussed in more detail as we examine property relationships in the next sections.

----

[1]Ks = 1.0 was used for No. 2 Southern Pine tested in bending and tension because four widths of lumber were tested.

One interpretation problem was encountered in using the standard. CEN XXX1 (Glos and Fewell, 1989) specifies factors to used with characteristic values of strength properties. These factors are not used with mean modulus of elasticity. The draft standard does not specify procedures for developing 5th percentile MOE. In table 4 it is assumed that these factors do not apply to 5th percentile MOE. On this basis none of the No. 2 grade lumber had 5th percentile MOE estimates equal to those assigned for mean MOE.

Discussion of Assumed Property Relationships

Modulus of Elasticity Versus Modulus of Rupture

The relationship between MOE and MOR (adjusted to 2x8) determined in the In-Grade program for Douglas Fir-Larch, Southern Pine, and Hem-Fir is shown in Figure 3. Also shown is the relationship determined for Southern Pine lumber by the U.S. Forest Products Laboratory in 1966 and reported in Research Paper FPL 64 (Doyle and Markwardt, 1966). The FPL 64 study used lumber equilibrated to 12% moisture content and tested on a laboratory testing machine. There is so little difference in the four MOE-MOR relationships that all mean trends are labeled "in-grade mean trends" in Figure 3.

The Eurocode 5 stress class system does not use mean trends such as those discussed above. Instead, it specifies combinations of 5th percentile based MOR and mean MOE values. Equivalent 5th percentile MOR-mean MOE points from the In-Grade data (X's in Figure 3) are higher than the equivalent points for Eurocode 5 (O's in Figure 3). In contrast, the MOE-MOR relationship traditionally assumed for MSR lumber in the United States (National Forest Products Association, 1988) appears parallel to the Eurocode 5 points.

Density Versus Modulus of Rupture and Modulus of Elasticity

The slope of the density-MOR relationship for the In-Grade data generally parallels that for clear wood, Figure 4. The coefficient of determination, R^2, is above 0.70 for clear wood when calculated using the mean values of many species. For the In-Grade data, however, the R^2 value is only between 0.2 and 0.3. Thus the density-MOR relationship for lumber is much weaker than that usually assumed from clear wood data. The 5th percentile MOR-5th percentile density points for the In-Grade data are within the range of those given in Eurocode 5.

The slopes of the density-MOE trends for the In-Grade data are similar for the three major volume species, and also generally parallel those found in FPL-64, Figure 5. The mean MOE-5th percentile density points for the In-Grade data (X's in Figure 5) show a trend similar to those given by Eurocode 5 (O's in Figure 5).

Although there is general agreement between the density-MOR and density-MOE relationships given in Eurocode 5 and those found with the In-Grade data, density appears to occasionally limit stress class assignment. Given the poor correlation between density and properties of lumber, as compared to that of clear wood, perhaps the characteristic density should be set slightly lower than given in CEN xxx1 and xxx2.

Modulus of Rupture Versus Ultimate Compression Stress Parallel to Grain

The relationship between MOR and UCS for the In-Grade data was determined by plotting the ratio of UCS to MOR versus MOR for equivalent percentiles of UCS and MOR, Figure 6. Percentiles used were 1, 5, 10, 25, 50, 75, 90, 95, and 99. The variation of the percentiles at a moisture content of 12% is shown in Figure 6 where "D" is Douglas Fir-Larch, "H" is Hem-Fir and "S" is Southern Pine. The trend at a moisture content of 15% is virtually identical to that presented by Curry and Fewell in CP 22/77 (1977) and shown in Figure 2 of CEN xxx1 (Glos and Fewell, 1989). However, the data presented in CP 22/77 is limited to MOR values between 20 and 40 MPa. The stress class system has MOR values from 13 to 60 MPa. Figure 6 confirms that the relationship presented in CP 22/77 is valid from approximately 10 to 100 MPa.

The UCS/MOR relationship given in CP 22/77 is based on data having an average moisture content of 18% for UCS and 15% for MOR. Thus the UCS-MOR relationship used in CEN xxx1 and xxx2 is in fact based on a moisture content level of about 15%, not 12%. Using the moisture-property models given in Green and Evans, 1989, the UCS/MOR ratio determined from the In-Grade data was adjusted to moisture contents of 12, 15, and 23% (assumed green level). This adjustment indicates that the UCS/MOR ratio at 15% moisture content is lower (more conservative) than that at 12%. If desired, Figure 6 could be used to justify an increase in the assumed UCS characteristic value for a given MOR value.

Modulus of Rupture Versus Ultimate Tensile Stress Parallel to Grain

Using the same percentile levels cited above, the UTS/MOR relationship was determined using the In-Grade data, Figure 7. Based on curves also presented in CP 22/77 the draft Eurocode 5 stress class system specifies a mean UTS/MOR ratio of 0.60. The moisture contents reported for the lumber tested for CP 22/77 was 15% for MOR and 16% for UTS. For values of UTS up to 55 MPa the relationship found with the In-Grade data is similar to that given in Eurocode 5. The average value of the UTS/MOR ratio from the in-grade data at 15 percent moisture content is 0.57 for MOR values below 55 MPa. At 12 percent moisture content the average UTS/MOR ratio is 0.59 and at 23% it is 0.55. At about 55 MPa the ratio increases slightly. There would appear to be no reason to reconsider the UTS/MOR ratio used in Eurocode 5.

Modulus of Rupture Versus Shear Strength Parallel to Grain

CEN xxx1 (Fewell, 1989) contains a plot of the shear strength - MOR ratio versus MOR that may be used to estimate shear strength parallel to the grain. Although a good relationship between MOR and shear strength exists for clear wood (because of the correlation with density), little such information exists in the United States for lumber. Shear strength was not determined on the In-Grade samples tested in the United States. Shear strength parallel to the gain was measured on Southern Pine lumber samples tested in bending and reported in FPL 64 (Doyle and Markwardt, 1966). The MOR-shear strength relationship that can be determined using the FPL 64 data is shown in Figure 8 and is identical in shape to that reported in the Eurocode 5 draft. However, the coefficient of determination, between shear strength and MOR is only 0.07. This very low value could be a result of having data on only one species. The authors plan to obtain similar data on additional species to see if a general relationship such as reported in Eurocode 5 can be obtained for U.S. species. Alternatively, a useful relationship could perhaps be developed between shear strength parallel to the grain and density, Figure 9. For the FPL 64 data the R^2 between density and shear strength was 0.253.

It is cautioned that the authors were not able to determine the test procedure used to determine the shear strength in the Eurocode 5 draft prior to submitting this paper. Therefore no attempt has been made to adjust the FPL 64 results for differences in the test procedure used to determine the Eurocode values and the block shear test (ASTM D143, 1988) used in the FPL 64 tests.

Relationships Between Mean and 5th Percentile Estimates

Modulus of elasticity. As noted earlier, the characteristic MOE value of No. 2 grade lumber for all three species cited in Table 4 did not make the assigned MOE value based on mean MOE. This would seem to indicate a systematic problem in assignment of the $E_{.05}/E_{mean}$ ratio. For all species tested in the In-Grade program, the average ratio of 5th percentile MOE to mean for MOE was 0.7 with a range from 0.48 to 0.84. For the three major volume species, where a larger amount of data was available, the average ratio was 0.65. However, the lower grades tended to have a lower ratio than did the higher grades. For the three major species groups the average ratio of 5th percentile MOE to mean MOE was 0.69 for Select Structural grade, but only 0.63 for No. 2 grade. The ratio used in Eurocode 5 averages about 0.70 but varies slightly across stress classes; probably due to rounding. It is suggested that the assumed ratio used in Eurocode 5 should be lowered, or that the ratio be a function of stress class.

Density. In the United States fastener properties have traditionally been calculated from mean density estimates for individual species. Consideration is now being given to basing fastener properties on 5th percentile density. The mean densities obtained for species tested in the In-Grade program are very close to those traditionally used for fastener design in the United States (NFPA, 1988). However, mean density estimates exist for many species not tested in the In-Grade program. Therefore it has been useful to evaluate the ratio of the 5th percentile density to the mean value to see if this ratio could be used to estimate 5th percentile values for species not tested in the In-Grade program.

For the three major species groups (Douglas Fir-Larch, Southern Pine, and Hem-Fir) sample sizes for density averaged about 800 specimens per grade-size combination. The average value of the 5th to mean ratio for the three major species groups was 0.80, with a range of only 0.78 to 0.83. Thus there would appear to be little variation in this in the 5th percentile to mean ratio for density. For all species or species groups tested in the program, the average 5th to mean ratio was 0.83.

Other Considerations

Tolerance Limits and Sample Sizes

The draft ASTM standard on deriving allowable properties from in-grade test data bases allowable properties on a lower 75% tolerance limit on the nonparametric 5th percentile. Eurocode 5 bases characteristic values on nonparametric point estimates of the 5th percentile, but adjusts the characteristic value based on the number of samples taken per grade and the number of pieces in a sample, Figure 10. At the CIB W18 meeting held in Canada in 1988 one of us (Green) informally presented information on the difference between the nonparametric point estimated of the 5th percentile and tolerance limits. This information is useful in understanding differences between the ASTM and Eurocode approaches to establishing allowable properties.

ASTM D2915 (ASTM D2915, 1988) defines a lower tolerance limit with 95% content and 75% confidence as an estimate of the proportion of a population that lies above the tolerance limit and that has been estimated with a confidence of 75%. This tolerance limit indicates that we are 75% sure that the true 5th percentile of the population is above the tolerance limit. In common usage this tolerance limit is referred to as a 75% tolerance limit, 0.75TL, on the 5th percentile.

The draft ASTM standard specifies a 0.75TL be used to estimate lower tail strength properties for two reasons.

1. Use of the tolerance limit allows the standard flexibility when specifying samples sizes required in characterizing lumber data sampled from diverse geographic areas. Although the standard "suggests" sample sizes of at least 360 specimens per grade-size combination may be required when characterizing lumber properties for individual species or species groups, grading agencies may use smaller sample sizes when submitting allowable design values for approval (by the American Lumber Standards Committee) if they can provide proper justification (i.e., the species grows over a limited geographic area).

2. Use of the tolerance limit reduces arguments about what constitutes an adequate size sample. This is because the difference between the point estimate of the 5th percentile and the 0.75TL generally increases as sample size decreases. Thus the agency submitting the data are discouraged from trying to justify very small sample sizes.

The effect of sample size on the percent difference between the point estimate of the 5th percentile and the 0.75TL is shown in Figure 11 using bending and tensile strength data sets tested in the In-Grade program. As previously noted, the difference generally decreases with increasing sample sizes. For MOR and UTS data sets have sample sizes greater than 250, the average reduction from the 5th percentile to the 0.75TL is 3%, using the 5th percentile as the reference base. For data sets with 100 to 250 specimens, the average reduction is 7 percent, and for samples containing from 39 to 99 pieces the reduction averages 10 percent.

Most of the samples used to derive Figure 11 are based on tests where three widths were tested per grade with at least 360 pieces per sample. For 3 samples per grade the Ks factor used in Eurocode 5 specifies about a 3% reduction if over 250 pieces are tested. With about 50 pieces per sample and 3 samples the reduction obtained from Figure 10 is about 10%. Thus tolerance limit used in the draft ASTM standard appears to give similar results for MOR and UTS to those obtained using the Eurocode "Ks" factor presented in Figure 10.

Moisture Content and Properties

Eurocode 5 (Glos and Fewell, 1989) recommends for samples not tested at the reference environmental conditions but having a moisture content in the range 10% to 18% that no adjustment be made for 5th percentile MOR and UTS. Although satisfactory for grades qualifying for the lower stress classes, such a specification seems overly restrictive for the MOR of lumber that might qualify for the higher stress classes. Previous work conducted in the United States and Canada has shown that in general higher quality lumber is more sensitive to changes in moisture content than is lower quality lumber (Green and Evans, 1989 a). This work has resulted in new analytical models that can be used to adjust lumber property distributions. For MOR the new model is a quadratic function of change in moisture content, (shown as dotted lines in Figure 12). However, the complexity of this model makes it not generally suitable for use in design codes.

An alternative suggestion is to use the quadratic models to adjust research data to a constant moisture content level but to use a linear model in the design code. This approach has been used by committee 086 of the Canadian Standards Association to develop data for reliability based design and has been recommended by the U.S. Forest Products Laboratory for the development of reliability based design procedures in the United States. A linear model under consideration by ASTM subcommittee D07.02 is shown in Figure 12. This model was derived using the same data used to develop the quadratic surface models. In S.I. units this equation for modulus of rupture is:

If 10% < M.C. < green, and the initial MOR is > 16.6 MPa,

$$R2 = R1 + [(R1 - 16.6) / (40 - M1)] * (M1 - M2)$$

Otherwise $R2 = R1$

A simple equation of a similar form is currently being development for compression parallel to the grain by Dave Barrett.

Conclusions and Recommendations

1. Property relationships used in the fourth draft of Eurocode 5 are generally in agreement with those found in the In-Grade testing program.

2. Relationships given in CEN xxx1 for determining compression and tensile strength parallel to the grain from modulus of rupture are limited to MOR values below 34 MPA. The experimental data in CP 22/77 ranges from 20 to 40 MPa. In-Grade results confirm that the assumed relationships are valid from approximately 10 to 100 MPa. If desired, In-Grade results could also be used to adjust the UCS/MOR relationship to the 12% moisture content level assumed for characteristic values.

3. The relationship between shear strength parallel to the grain and modulus of rupture is very weak. Perhaps a more reliable estimate of shear strength could be achieved using characteristic density.

4. Characteristic density appears to occasionally limit stress class assignment for some grades of lumber. Because of the relative poor correlation between MOR and density, and between MOE and density, for structural lumber, it is suggested that initial stress class assignments be based only on MOR and MOE. Alternatively, consideration should be given to lowering the characteristic density.

5. The procedure for calculating characteristic modulus of elasticity should be clarified. The assumed ratio of characteristic MOE to mean MOE appears to be lower for lower grades of lumber than for higher grades. Consideration should be given to lowering the assumed ratio slightly or making the ratio a function of stress class level.

6. CEN xxx1 makes no provisions for lowering a stress class assignment if available test data shows that secondary properties do not achieve the assumed level. Such provisions should be added to the standard.

7. Making no adjustment in MOR values for change in moisture content seems overly conservative for the higher quality lumber found in the upper stress classes. A simple linear model under consideration by ASTM subcommittee D07.02 is presented for consideration by CIB W18A.

Literature Cited

American Society for Testing and Materials. 1988. Standard methods of testing small clear specimens of timber. Designation D143. Annual Book of Standards, Volume 04.09. Philadelphia, Pa.

American Society for Testing and Materials. 1988. Standard methods for evaluating allowable properties for grades of structural lumber. Designation D2915. Annual Book of Standards, Volume 04.09. Philadelphia, Pa.

American Society for Testing and Materials. 1988. Standard test methods for mechanical properties for lumber and wood-based structural material. Designation D4761. Annual Book of Standards, Volume 04.09. Philadelphia, Pa.

Barrett, J.D., D.W. Green, and J.W. Evans. 1989. Temperature adjustments for the North American in-grade testing program. Proceedings: in-grade testing of structural lumber. Conference held at the U.S. Forest Products Laboratory, April 25 and 26, 1988. Proceedings 47363. Forest Products Research Society, Madison, WI.

Curry, W.T. and A.R. Fewell. 1977. The relationships between the ultimate tension and compression strength of timber and its modulus of elasticity. Building Research Establishment, Current Paper CP 22/77. Princes Risborough Laboratory.

Doyle, D.V. and L.J. Markwardt. 1966. Properties of Southern Pine in relation to strength grading of dimension lumber. Research Paper FPL 64. U.S. Department of Agriculture, Forest Products Laboratory, Madison, WI.

Evans, J.W., J.K. Evans, and D.W. Green. 1989. Computer programs for adjusting lumber properties. General Technical Report GTR-63. U.S. Department of Agriculture, Forest Products Laboratory, Madison, WI.

Fewell, A.R. 1989. Strength classes for structural lumber. Fourth draft of CEN standard xxx2. Document CEN/TC 124/WG 2. British Standards Institute.

Forest Products Research Society. 1989. Proceedings: in-grade testing of structural lumber. Green, D.W., B. Shelley, and H.Vokey, Eds. Conference held at the U.S. Forest Products Laboratory, June 25to 29, 1988. Proceedings 47363. Forest Products Research Society, Madison, WI.

Glos, P, and A.R. Fewell. 1989. The determination of characteristic values of mechanical properties and density of timber. Fourth draft of CEN standard xxx1. Document CEN/TC 124/WG 2 N66E. British Standards Institute.

Green, D.W. and J.W. Evans. 1987. Mechanical properties of visually graded lumber. National Technical Information Service. U.S. Department of Agriculture, Springfield, Va. (order number PB-88-159-371 for entire set)

Volume 1: A summary (PB-88-159-389)
Volume 2: Douglas Fir-Larch (PB-88-159-397)
Volume 3: Hem-Fir (PB-88-159-405)
Volume 4: Southern Pine (PB-88-159-143)
Volume 5: Aspen-Cottonwood, Balsam Fir, Douglas Fir (South) (PB-88-159-421)
Volume 6: Eastern Hemlock, Eastern Spruces, Eastern White Pine, Engelmann Spruce, Idaho White Pine, Jack Pine, Lodgepole Pine (PB-88-159-439)
Volume 7: (Minor) Southern Pines, Ponderosa Pine, Red Pine (PB-88-159-447)
Volume 8: Sitka Spruce, Subalpine Fir, Sugar Pine, Tamarack, Yellow-Poplar (PB-88-159-454)

Green, D.W. and J.W. Evans. 1989(a). Moisture content and the mechanical properties of lumber: Decisions for the future. Proceedings: in-grade testing of structural lumber. Conference held at the U.S. Forest Products Laboratory, June 25 to 29, 1988. Proceedings 47363. Forest Products Research Society, Madison, WI. (or Moisture content-property relationships for dimension lumber Proceedings of Timber Engineering Group S 5.02, International Union of Forestry Research Organizations, Turku-Finland, June, 1988)

Green, D.W. and J.W. Evans. 1989(b). Specific gravity of visually graded lumber. National Technical Information Service. U.S. Department of Agriculture, Springfield, Va.

Johnson, L.A., J.W. Evans, and D.W. Green. 1989. Volume effect adjustments for in-grade data. Proceedings: in-grade testing of structural lumber. Conference held at the U.S. Forest Products Laboratory, June 25 to 29, 1988. Proceedings 47363. Forest Products Research Society, Madison, WI.

National Forest Products Association. 1988 Design values for wood construction. National Forest Products Association. Washington, D.C.

Table 1. Number of Samples Tested in the U.S. In-Grade Program.

Species Group	Number Sampled			
	Bending	Tension	Compression	Total
Douglas Fir-Larch	6067	2817	2618	11502
Southern Pine	4944	4068	2719	11731
Hem-Fir	3605	2743	2468	8816
Douglas Fir (South)	564	548	395	1507
(Minor) Southern Pines	870	924	1042	2836
U.S. Spruce-Pine-Fir				
Englemann Spruce	471			471
Eastern Spruce group	360			360
Lodgepole Pine	439			439
Jack Pine	240			240
Subalpine Fir	524			524
Balsam Fir	61			61
Mixed Species				
Eastern Hemlock	361			361
Tamarack	369			369
Sitka Spruce	203			203
Red Pine	358			358
Eastern White Pine	362			362
Idaho White Pine	240			240
Ponderosa pine	539			539
Sugar Pine	299			299
Aspen-Cottonwood	329			329
Yellow-Poplar	365	100		465
Total	21870	11200	9242	42312

Table 2. Characteristic Values and Mean Properties Determined Using In-Grade Data adjusted to 20 deg. C and 12% MC (Green and Evans, 1987)[2]

Species Group	Grade	Sample Size	MOR MPa	MOE (mean) MPa	Density Kg/m^3	UTS MPa	UCS MPa	MOE MPa
Douglas Fir-Larch	Select Structural	1321	29.5	13200	440	17.3	27.0	8800
Hem-Fir		1171	27.8	11100	370	15.4	23.8	7800
Southern Pine		1452	36.6	13300	490	18.0	29.0	9200
Douglas Fir-Larch	No. 2	2738	17.1	11300	430	10.2	19.5	7000
Hem-Fir		1143	15.9	9500	360	9.5	18.5	6200
Southern Pine		2605	18.8	11300	450	9.6	21.1	7000

----

[2]Except mean MOE, all properties are characteristic vales (i.e. are derived from 5th percentile estimates).

Table 3. Mechanical Properties for Strength Classes Given in Eurocode 5 (Fewell, 1989)

Property	Stress Class											
(MPa except Density)	C13-7E	C15-8E	C15-11E	C18-9E	C21-10E	C21-13E	C24-11E	C30-12E	C30-15E	C37-14E	C48-20E	C60-22E
Bending	13	15	15	18	21	21	24	30	30	37	48	60
Tension //	8	9	9	11	13	13	14	18	18	22	29	36
Tension perp	0.3	0.3	0.3	0.3	0.4	0.4	0.4	0.4	0.4	0.4	0.6	0.7
Compression //	16	17	17	19	20	20	21	24	24	28	35	40
Compression perp	4.8	4.8	5.2	5.2	5.4	5.7	5.7	6.3	6.7	6.7	9	10.5
Shear //	1.6	1.7	1.7	1.8	2.1	2.1	2.4	3	3	3.7	4.8	6
MOE Mean //	7000	8000	11000	9000	10000	13000	11000	12000	15000	14000	20000	22000
MOE Min //	4900	5500	7400	6500	7000	8700	7400	8500	10500	10000	14000	15000
MOE Mean perp Softwood	220	270	370	300	330	430	370	400	500	450	--	--
MOE Mean perp Hardwood	470	530	730	600	670	860	730	800	1000	900	1300	1500
Shear Modulus Mean	440	500	690	560	630	800	690	750	900	800	1200	1400
Density (kg/m^3)	320	320	450	350	360	480	380	420	520	450	600	700

Table 4. Stress Class Assignment of In-Grade Data Using March 1989 Draft of Eurocode 5

Species Group	Grade	MOR	MOE (Mean)	Density	Assignment	UTS	UCS	MOE
Douglas Fir-Larch	Select Structural	C24	13E	C24-11E	C24-11E	C24	C30	13E
Hem-Fir		C24	11E	C21-10E	C21-10E	C24	C24	11E
Southern Pine		C30	13E	C30-12E	C30-12E	C30	C37	13E
Douglas Fir-Larch	No. 2	C15	11E	C15-08E	C15-08E	C15	C18	10E
Hem-Fir		C15	9E	C15-08E	C15-08E	C15	C15	8E
Southern Pine		C18	11E	C18-09E	C18-09E	C15	C24	10E

Figure 1. Organization of ASTM Committee D07 on Wood

D07.01 Fundamental Test Methods and Properties (Frank Beall)
- D07.01.01 Physical Test Methods and Properties (Frank Beall)
- D07.01.02 Chemical Test Methods and Properties (Frank Beall)
- D07.01.03 Mechanical Test Methods (Lisa Johnson)

D07.02 Lumber and Engineered Wood Products (Dave Green)
- D07.02.01 Solid Sawn Lumber (Chris Stieda)
- D07.02.02 Glue Laminated Timbers (Russ Moody)
- D07.02.03 Composite Lumber Products (Jean Bledsoe)
- D07.02.04 Prefabricated Wood I-Joists (Bob Nelson)
- D07.02.05 Wooden Trusses (Charles Goehring)
- D07.02.06 Reliability Based Design Procedures (Bob Tichy)

D07.03 Panel Products (Mike O'Halloran)
- D07.03.01 Structural Use Panels (Mike O'Halloran)
- D07.03.02 Fiber and Particle Panel Materials (J. Dobbin McNatt)

D07.04 Pole and Pile Products (Bob Arsenault)

D07.05 Wood Assemblies (Sherm Nelson)
- D07.05.01 Sampling Modeling and Analysis Procedures for Wood Assemblies and Elements (Bill Galligan)
- D07.05.02 Wood Connections (Marcia Patton-Mallory)
- D07.05.03 Roof System Assemblies (Ron Wolfe)
- D07.05.04 Floor System Assemblies (Ted Laufenberg)

D07.06 Treatments for Wood Products (Anders Lund)
- D07.06.01 Specifications and Chemical Analysis of Wood Preservatives (Lee Gjovik)
- D07.06.02 Methods of Preservative Treatments (Darrel Nicholas)
- D07.06.03 Evaluation of Preservatives (Dave Webb)
- D07.06.04 Fire Performance of Wood Products (Ross Thomson)
- D07.06.05 Non-Pressure Treatment of Wood Base Materials (Roy Adams)

Figure 2. Visual Grades Described in the National Grading Rules

Lumber Classification	Grade Name	Minimum Percentage of Clear Wood Strength
Structural Light Framing (2 to 4 in. thick, 2 to 4 in. wide)	Sel. Str.	67
	1	55
	2	45
	3	26
Studs (2 to 4 in. thick, 2 to 6 in. wide)	Stud	26
Structural Joists and Planks (2 to 4 in. thick, 5 in. and wider)	Sel. Str.	65
	1	55
	2	45
	3	26
Light Framing (2 to 4 in. thick, 2 to 4 in. wide)	Construction	34
	Standard	19
	Utility	9

Figure 3.--Relationship between modulus of elasticity and modulus of rupture at 12% moisture content.

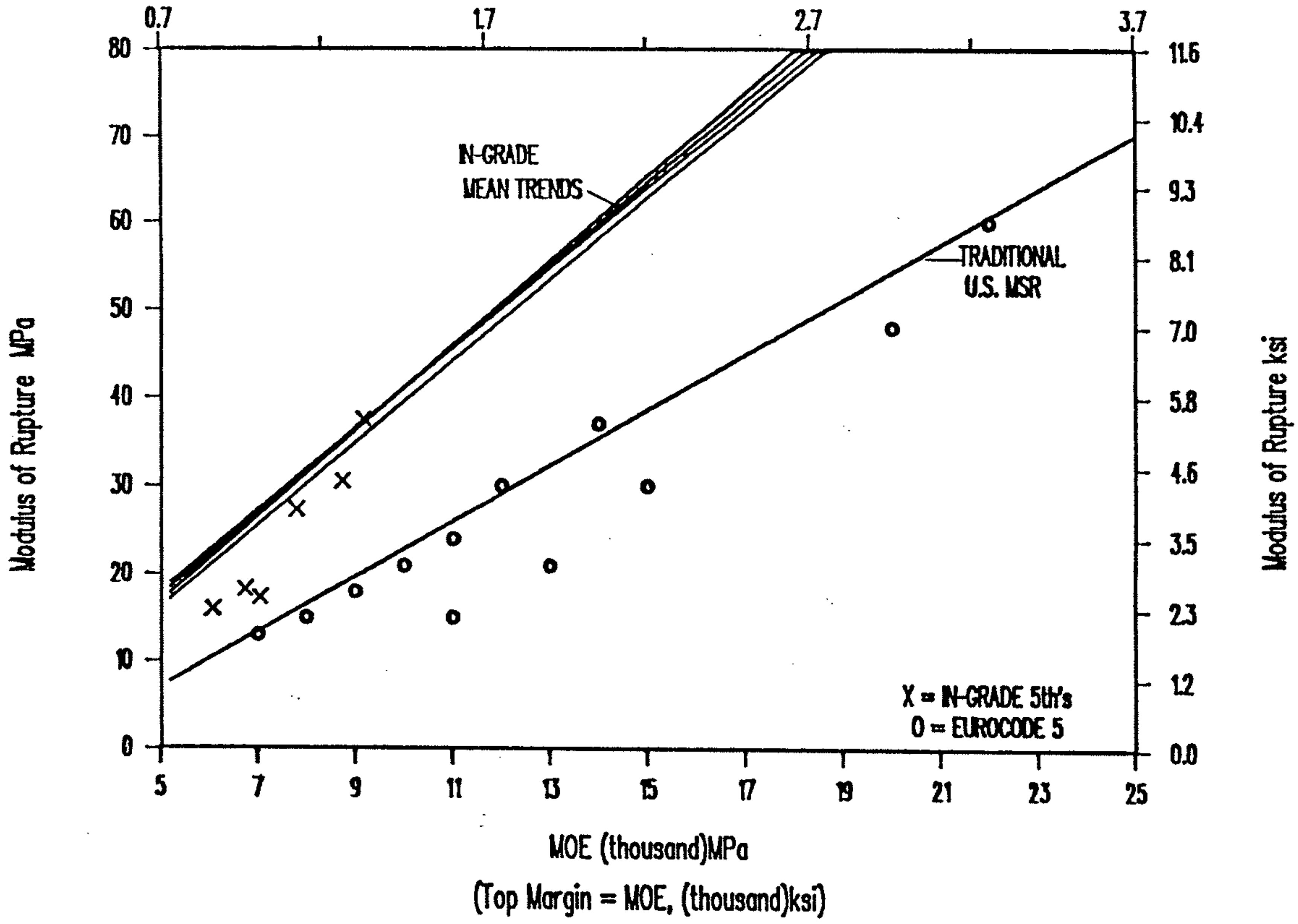

Figure 4.--Relationship between modulus of rupture and density at 12% moisture content.

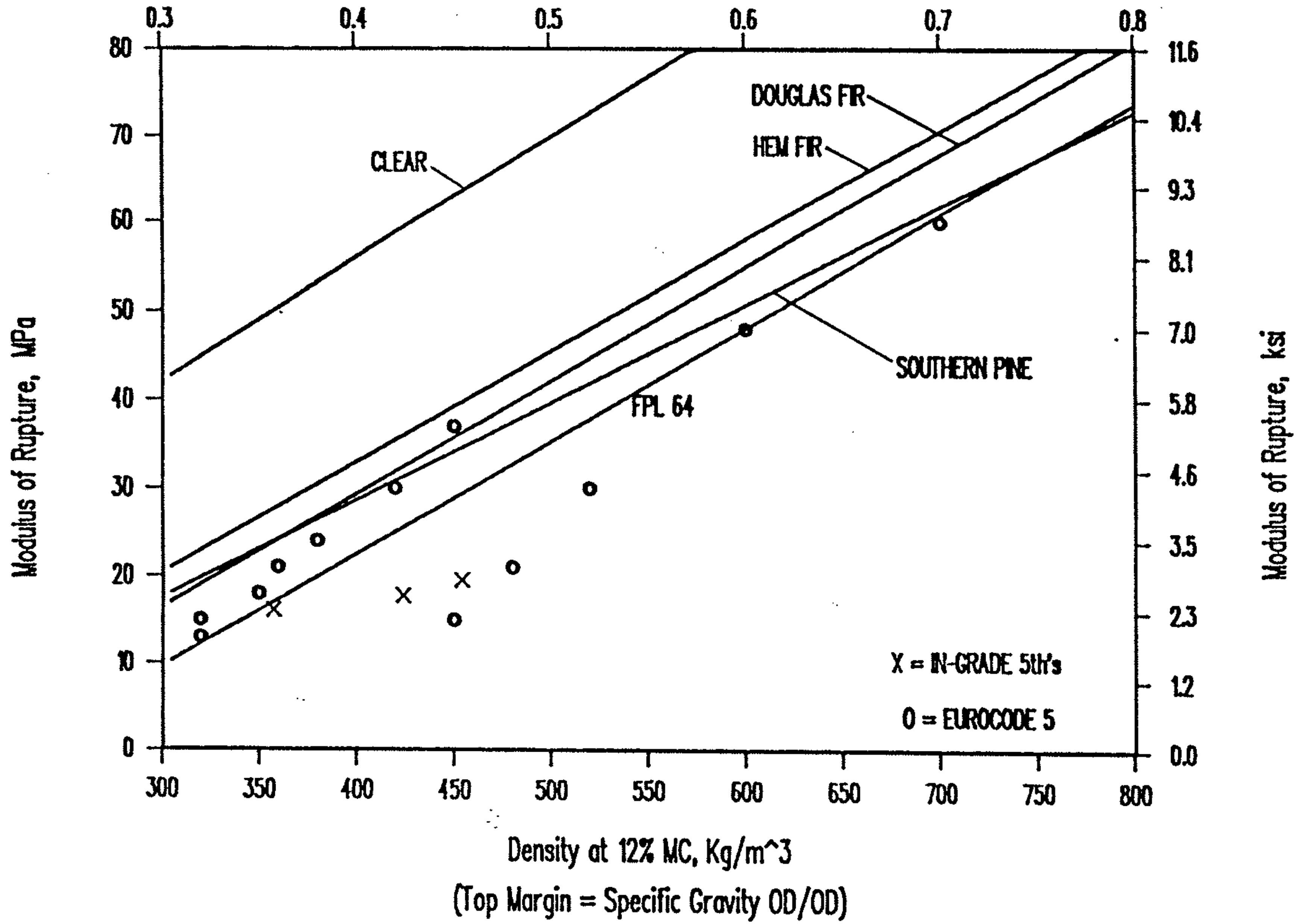

Figure 5.--Relationship between modulus of elasticity and density at 12% moisture content.

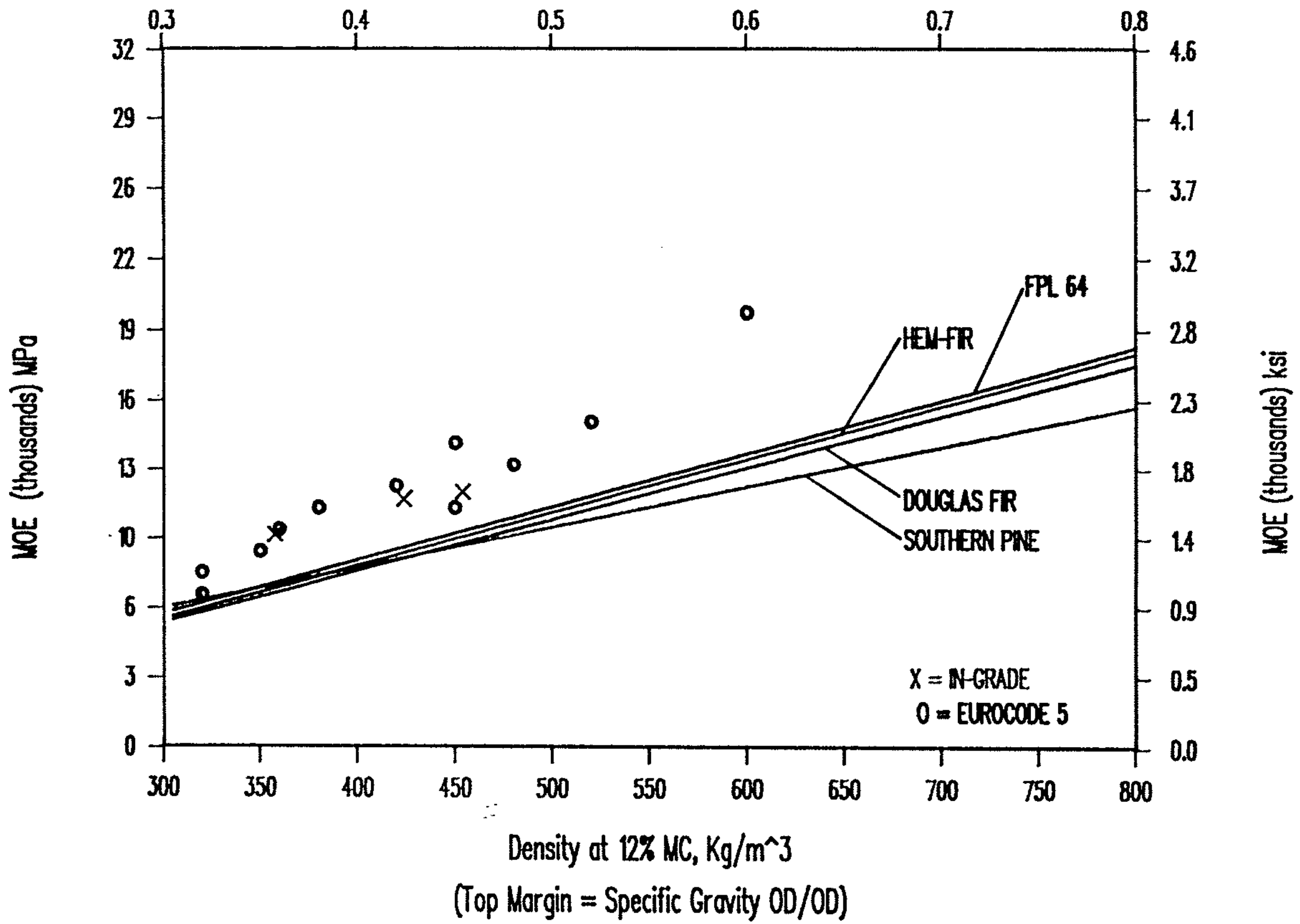

Figure 6.--Relationship between ultimate compression stress parallel to the grain and modulus of rupture for In-Grade data.

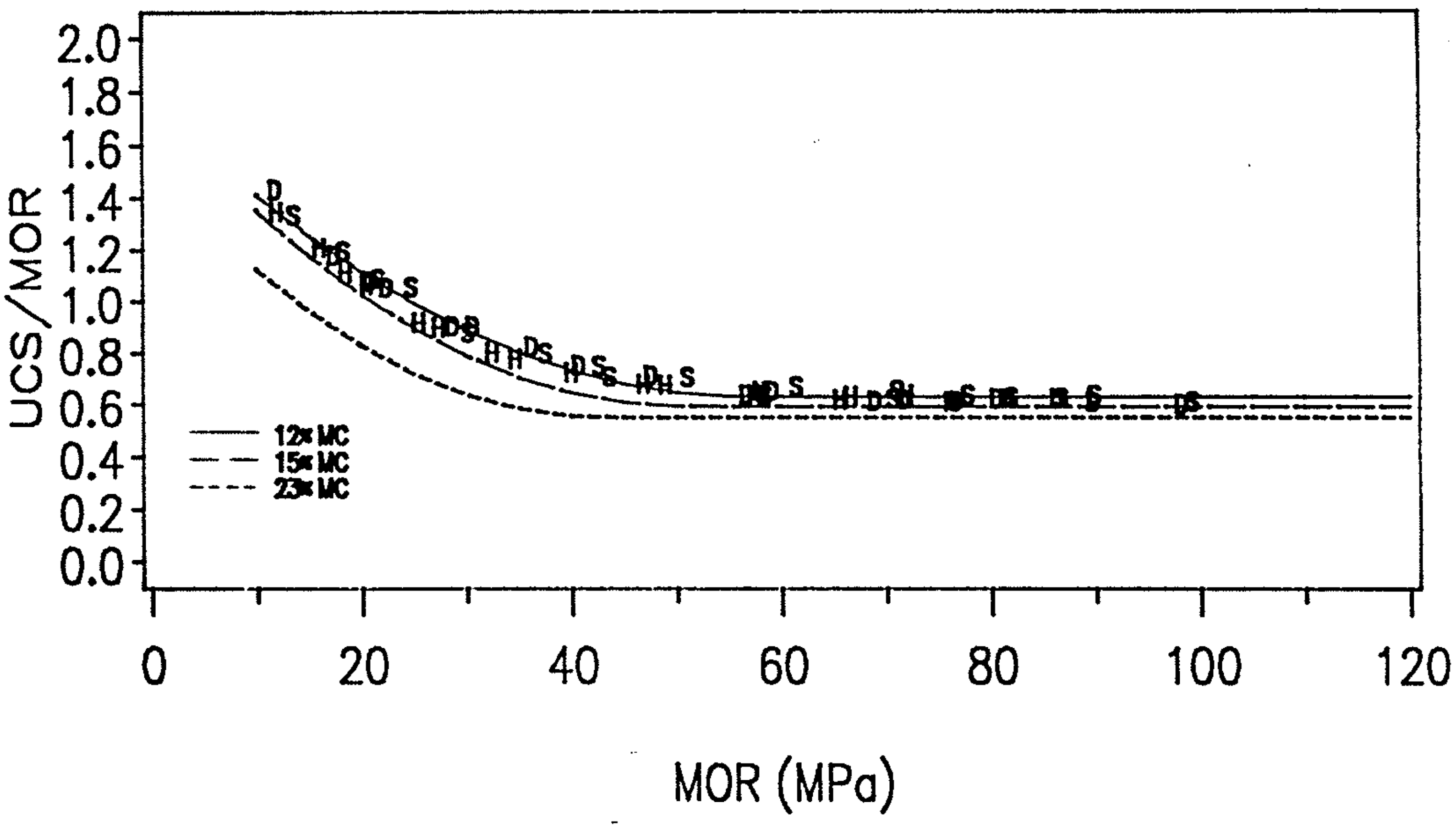

Figure 7.--Relationship between ultimate tensile stress parallel to the grain and modulus of rupture for In-Grade data at 12% moisture content.

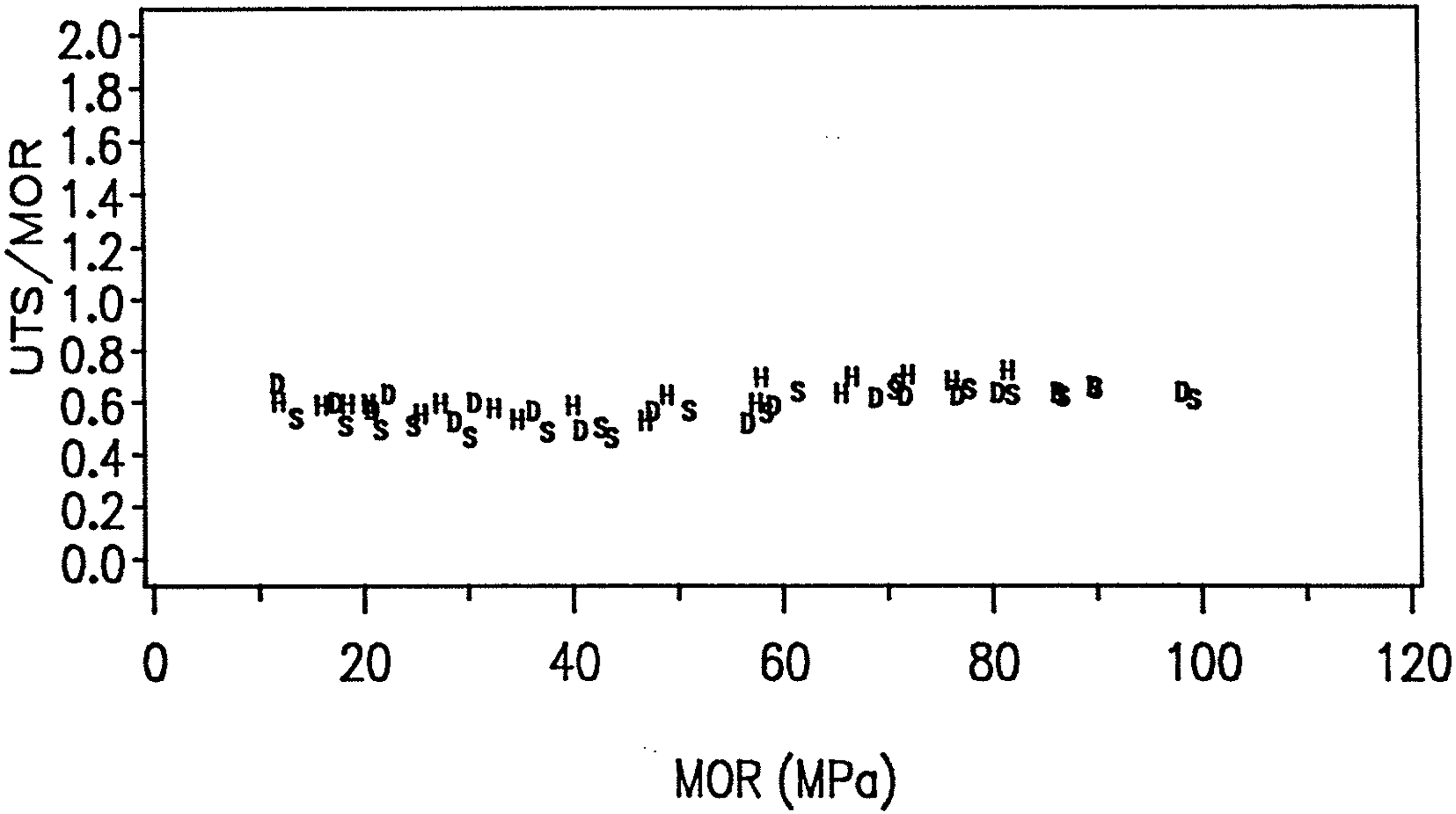

Figure 8.--Relationship between shear strength parallel to the grain and modulus of rupture for Southern Pine lumber at 12% moisture content.

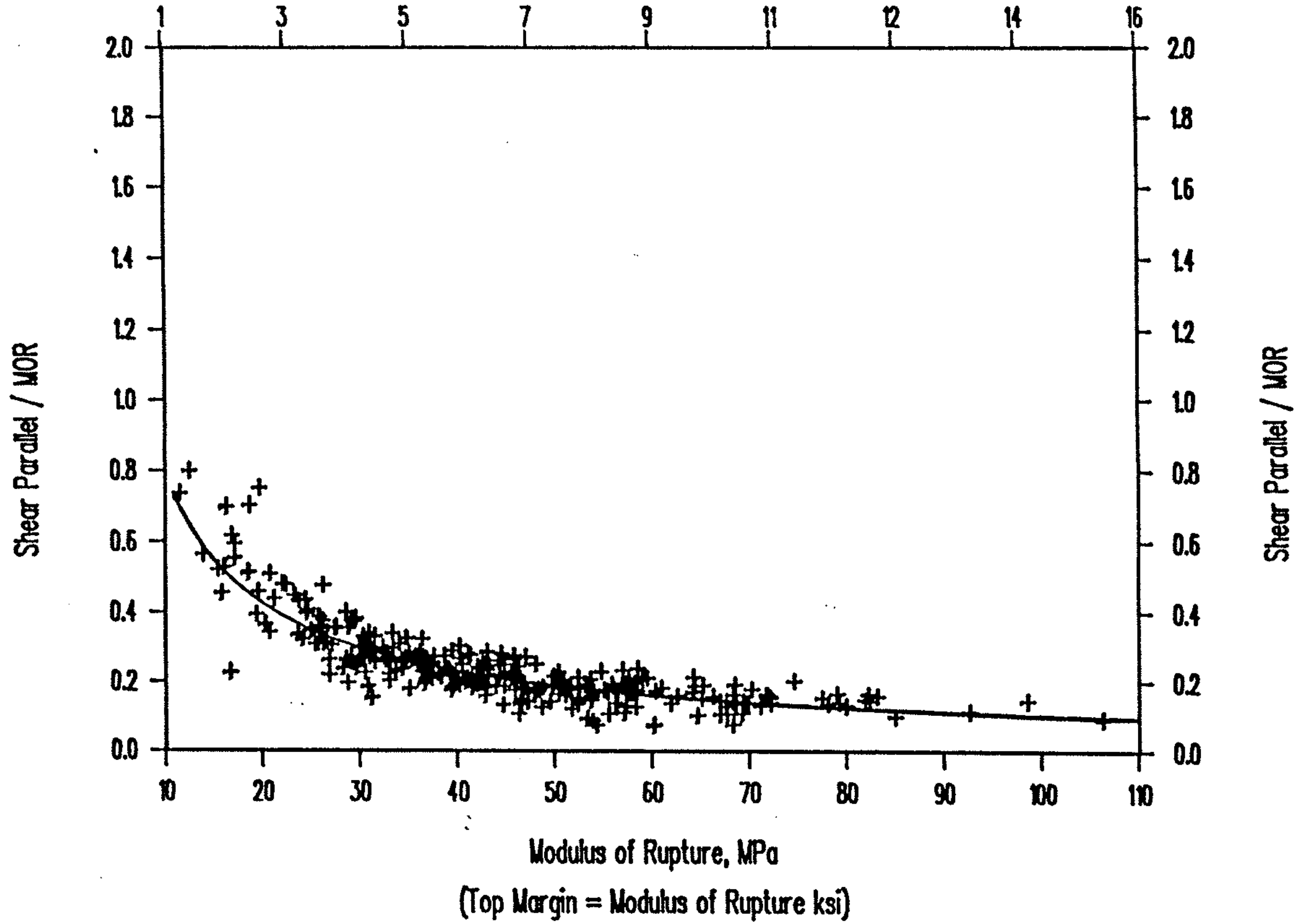

Figure 9.--Relationship between shear strength parallel to the grain and density for Southern Pine lumber at 12% moisture content.

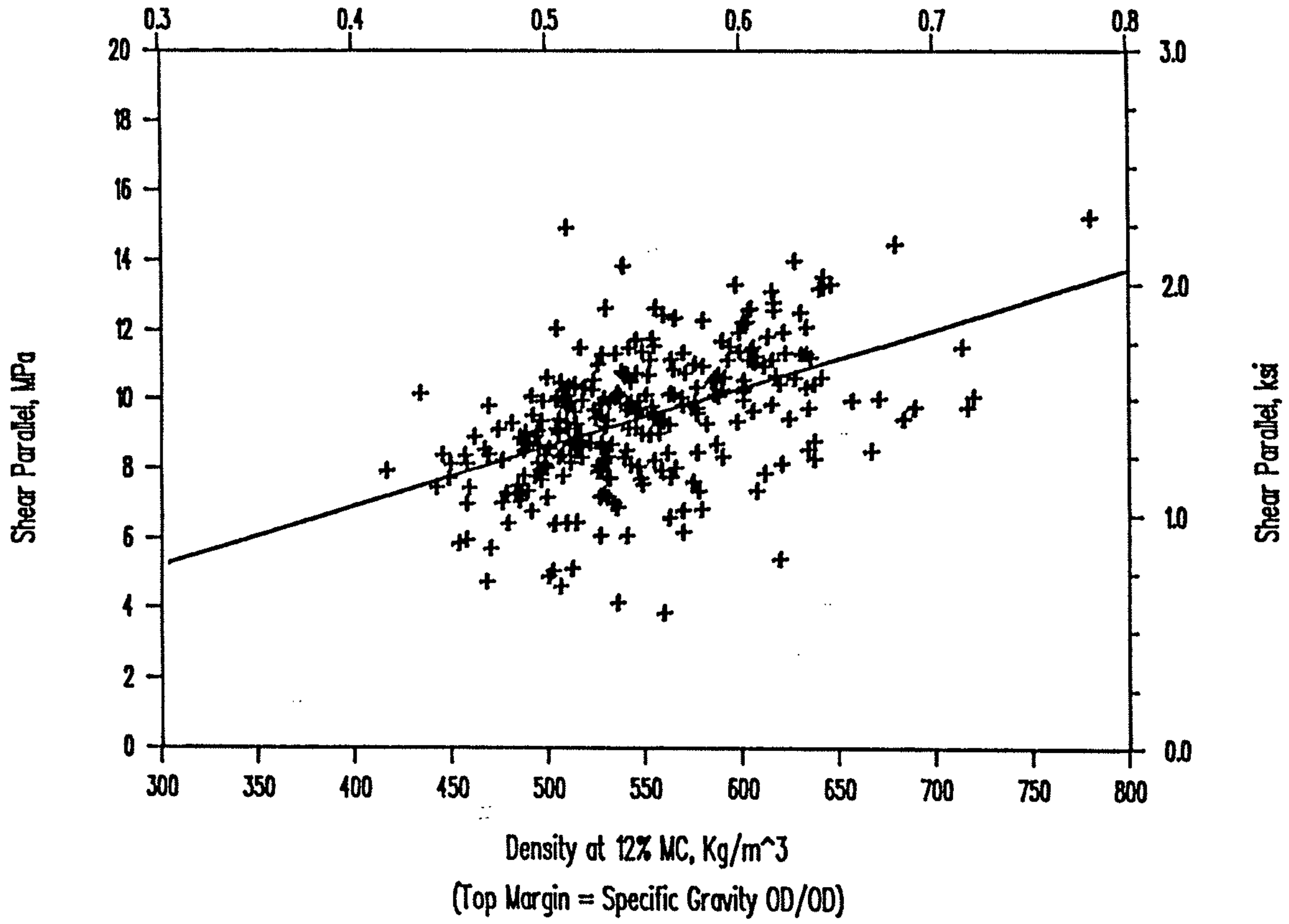

Figure 10.-- Relationship between the factor k_s and the number of samples and number of pieces in each sample in Eurocode 5 (Glos and Fewell, 1989).

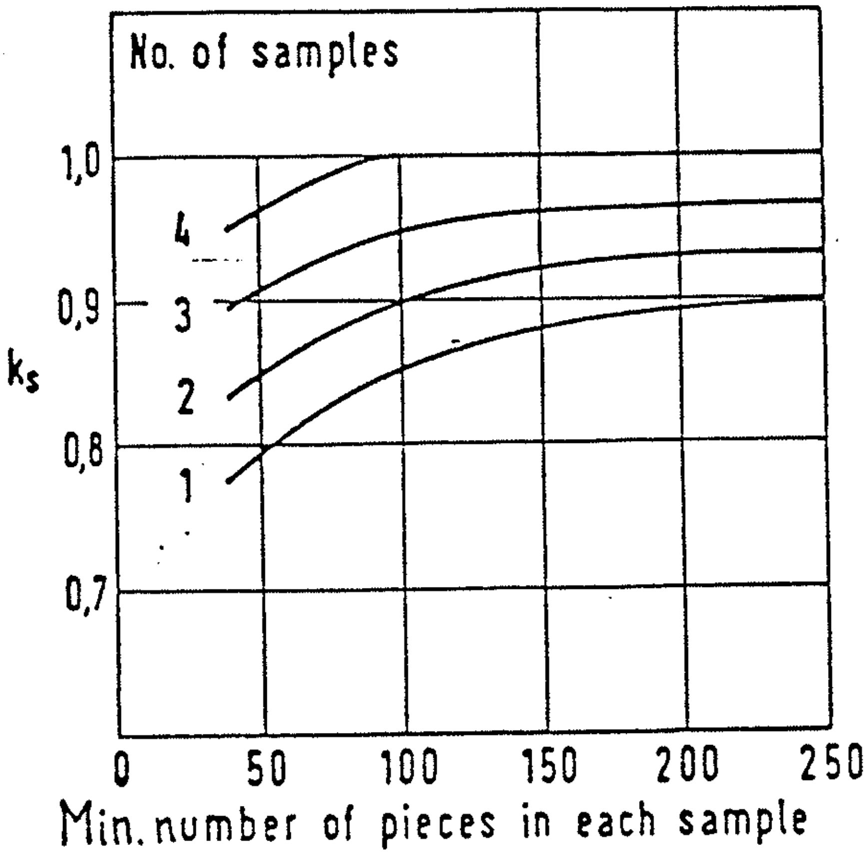

Figure 11.--Relationship between nonparametric tolerance limit and 5th percentiles for bending and tensile strength of In-Grade lumber.

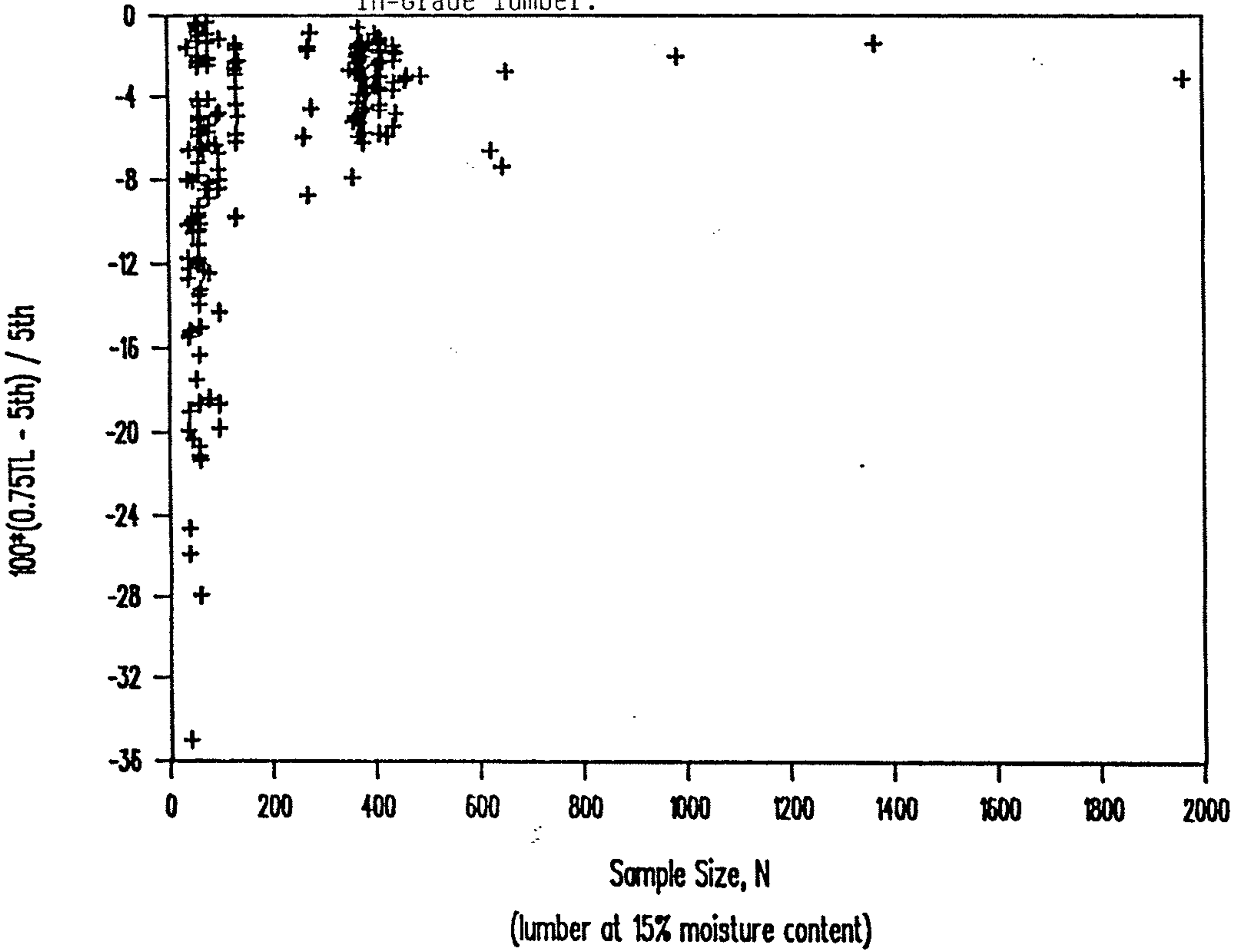

Figure 12.--Comparison of quadratic surface (QSM) (Green and Evans, 1989a) and linear models for predicting effect of moisture content on modulus of rupture.

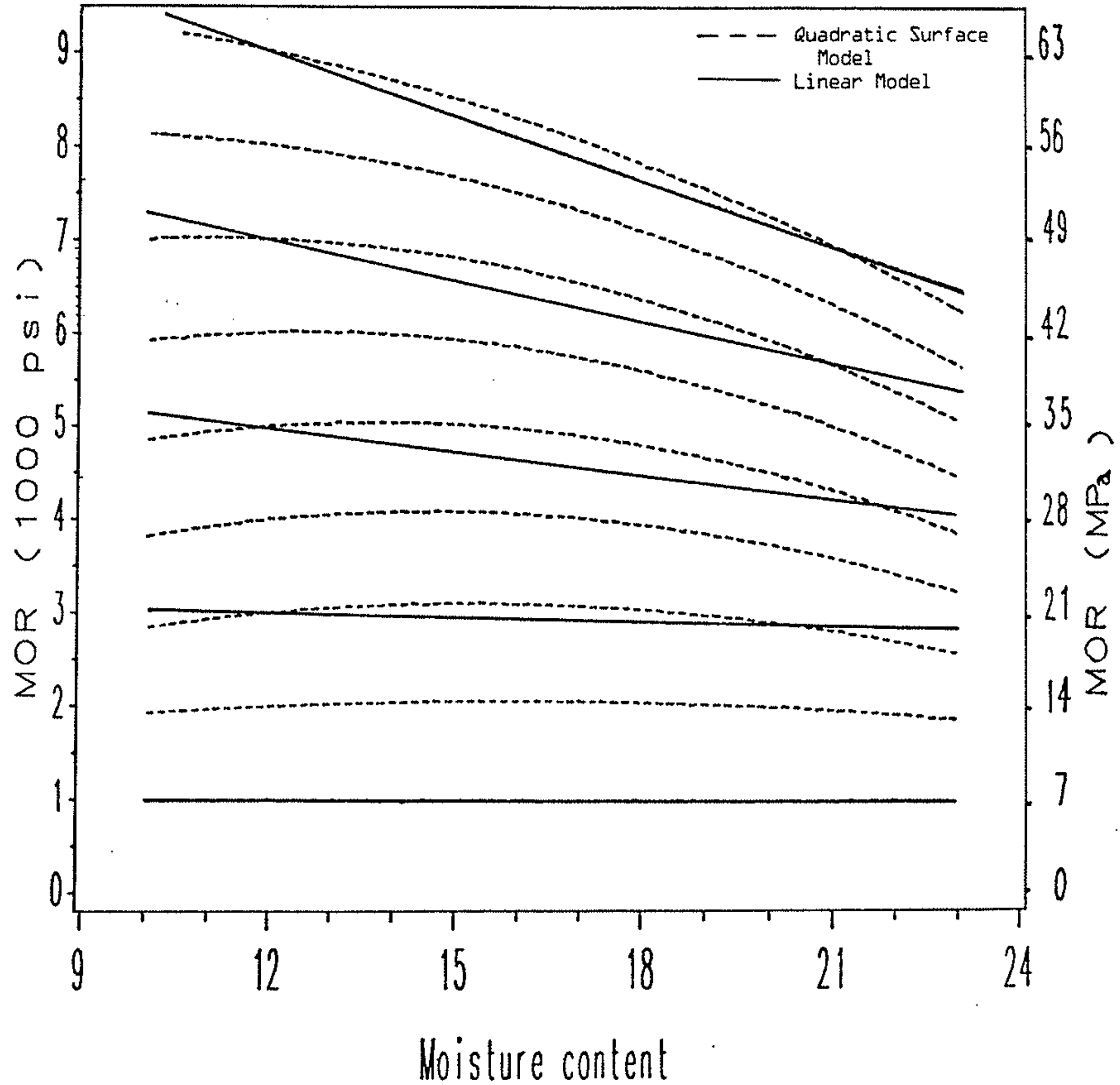

CIB -W18A / 22-6-4

INTERNATIONAL COUNCIL FOR BUILDING RESEARCH STUDIES AND DOCUMENTATION

WORKING COMMISSION W18A - TIMBER STRUCTURES

EFFECT OF WOOD PRESERVATIVES ON THE STRENGTH PROPERTIES OF WOOD

by

F Ronai
University for Forest Science
and Timber Industry, Sopron
Hungary

MEETING TWENTY - TWO

BERLIN

GERMAN DEMOCRATIC REPUBLIC

SEPTEMBER 1989

Effect of wood preservatives on the strength properties of wood

Dr. F.Rónai

The material of the wooden building constructions planned to a longer service life has to be protected by applying wood preservatives. The different methods and stages of this protection are given in the standard specifications of the respective countries.

The relevant Hungarian standard (MSz 10144) specifies six categories of preservation as given in the table below:

Methods of application of wood preservatives

Code	Designation	Requirement
TV	Complete protection	Preservative in the whole mass of the wood element
SV	Sapwood protection	Treatment of 85 per cent of the sapwood part
MH	Deep protection	Penetration of the preservative is of 10 mm
HV	Boundary layer protection	Penetration of the preservative is of 1 to 10 mm
FV	Superficial protection	Penetration of the preservative is of 1 mm
BV	End grain protection	End grain sealing with preservative

The preservatives give protection against biotic deterioration on the one hand, and aim at delaying burning on the other hand. The agents generally containing copper, chromium or bromine increase the durability of wood according to the way of application.

Investigations carried out with the application of the treatment signed "TV" indicated that the preservative applied effects the shape of the empirical frequency distribution curve of some of the strength properties and also modifies the values of the probability measures.

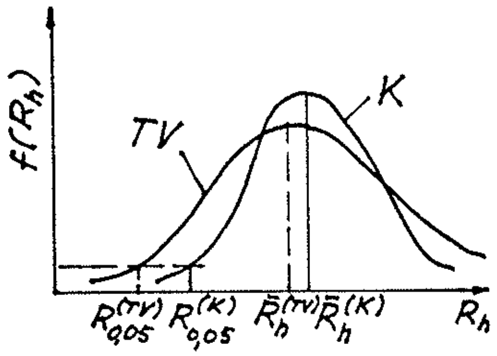

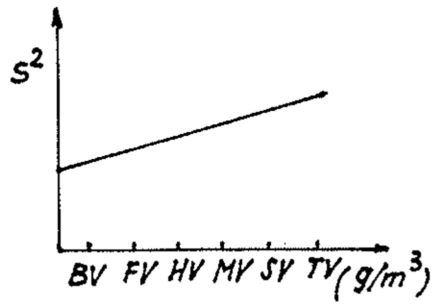

In the case of the specimens satured with preservative the standard deviation and coefficient of variation are increasing hence the values of $R_{0.05}$ and $R_{0.001}$ (5 per cent and 0.1 per cent exclusion limit respectively) are decreasing. The figures that follow indicate the general feature of the tensile strength data abtained for specimens of Picea excelsa ("K"-control specimens, "TV"-preservative-treated material).

Some of the data relating to the empirical probability density function for Picea excelsa:

		"TV"	"K"
mean $\bar{R}_h$ (N/mm^2)	:	59.64	65.46
standard deviation s (N/mm^2)	:	17.14	16.47
coeff. of var. v (%)	:	28.73	25.16
skewness a	:	+ 0.587	- 0.297
$R_{0.05}$(N/mm^2)	:	31.6[illegible]	38.56
$R_{0.001}$(N/mm^2)	:	6.97	14.93

Under the influence of the electrolyte solution entered by diffusion the distance of the secondary bonds between the fiber increases, the energy of the bonds decreases. This involves a diminishing of the internal friction and tensile strength and an increase of the tensile strain (ε_h). The loosening of the secondary bonds also results in the strengthening of the plastic properties.

This phenomenon can be experienced with other types of load as well, but further investigations are still needed. The reduction in the value of $R_{0.05}$ in the case of bending strength has an adverse effect on the grading strength of wood. The value of $R_{0.001}$ serves as a basis for specifying the desing stresses (limit stresses); a reduction of the former under the influence of preservative treatment is unfavourable from the point of design stresses.

Based on tests conducted it can be proposed that a reduction factor should be taken into account for the treatment signed "TV" in establishing limit stress values; (for other categories of treatment a proportional decreasing is suggested). According to the specifications of the standard MSz 15025 the limit stress values have to be modified with a factor k_t=0.85 in the case of treatment "TV".

The investigation of the effect of preservative treatment on the deformations requires further laboratory work.

Sopron, 05/30. 1989.

CIB -W18A / 22-7-1

INTERNATIONAL COUNCIL FOR BUILDING RESEARCH STUDIES AND DOCUMENTATION

WORKING COMMISSION W18A - TIMBER STRUCTURES

END GRAIN CONNECTIONS WITH LATERALLY LOADED STEEL BOLTS

A draft proposal for design rules in the CIB Code

by

J Ehlbeck and M Gerold
University of Karlsruhe
Federal Republic of Germany

MEETING TWENTY - TWO

BERLIN

GERMAN DEMOCRATIC REPUBLIC

SEPTEMBER 1989

End-grain connections with laterally loaded steel bolts

A draft proposal for design rules in the CIB-Code

Jürgen Ehlbeck and Matthias Gerold
University of Karlsruhe, FRG

1 Introduction

During the 20th meeting of CIB-W18A in Parksville/Vancouver Island, Canada, 1988, a paper was presented by H. Riberholt [1] on "GLUED BOLTS IN GLULAM - PROPOSALS FOR THE CIB-CODE" - Paper No. CIB-W18A/21-7-2. During the discussion of the paper further comments or modifying proposals were announced.

This paper presents a calculation model for steel bolts driven in end-grain of glulam or solid timber under lateral loading.

2 Definitions and notations

For better understanding it is necessary to define the embedding stresses σ_h or the embedding strengths f_h as a mechanical property depending on the angle α between load and grain direction as well as on the angle β between the hole axis and the grain direction. Mainly, β is 90° or 0° degrees. In case of end-grain connections, $\beta = 0°$. In Fig. 1, the most important types of embedding stresses are described.

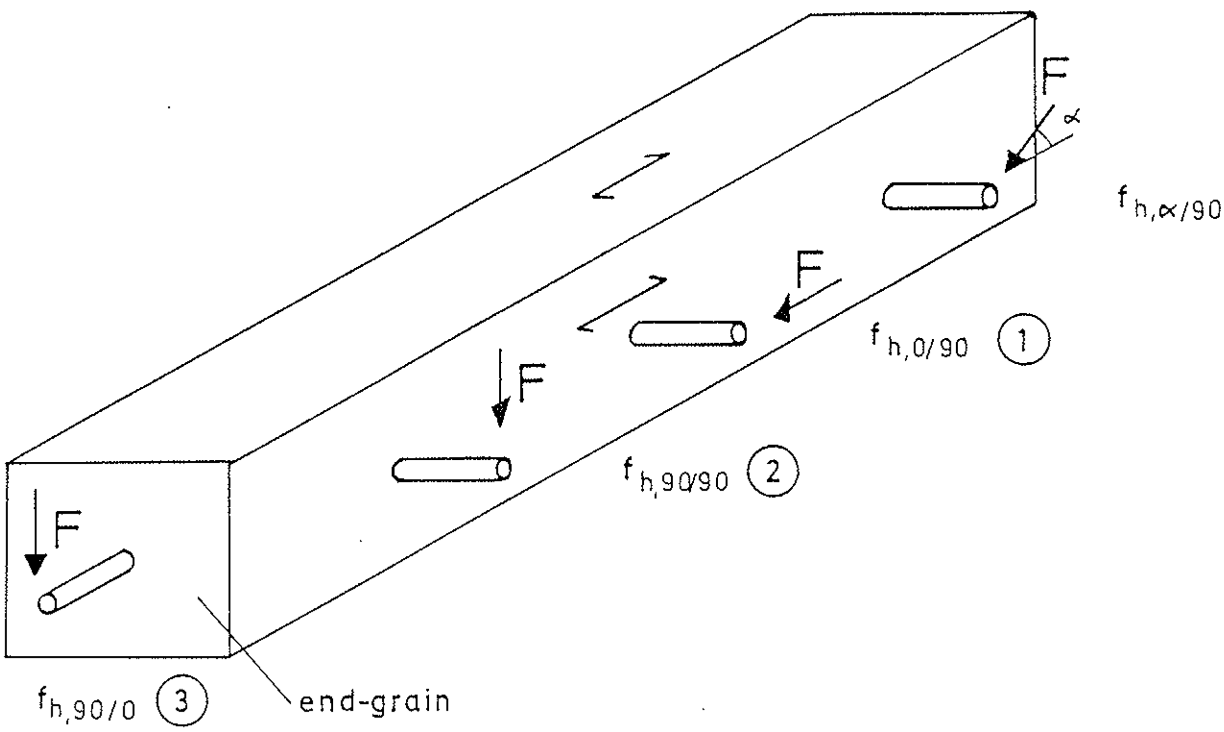

Fig.1: Different types of embedding strengths due to loaded steel bolts in timber

①	$f_{h,0/90}$	load angle 0°; hole axis at 90° to grain
②	$f_{h,90/90}$	load angle 90°; hole axis at 90° to grain
③	$f_{h,90/0}$	load angle 90°; hole axis at 0° to grain

The following notations apply in this paper:

ρ	density of timber
f_h	embedding strength
$\sigma_{h\alpha/\beta}$	embedding stress at an angle α, with the hole axis at an angle β to grain
α	angle between load and grain direction
β	angle between hole axis and grain direction
θ	inclination of steel bolts at ultimate limit state
φ	averaging angle between stress- and grain-direction at the end-grain cross-section at ultimate limit state
f_y	yield strength of steel bolt
M_y	yield moment of steel bolt
F	load
R_u	ultimate load or load at 7.5 mm deformation
D_α	compression force at an angle α to grain
T	frictional force
d	steel bolt diameter
d_r	root diameter

e	eccentricity
l_1	depth of penetration
z	distance of point of yield moment M_y from the end-grain cross-section
Δ	maximum deformation at the end-grain cross-section
K_i ; η	factors

Subscripts are used as follows:

mean	mean
u	ultimate

3 Ultimate load-carrying capacity R_u

Based on tests in several countries it can be assumed that the load-carrying capacity of end-grain driven steel bolts under lateral loading depends primarily on the following parameters (see Fig.2):

- the embedding strength $f_{h\alpha/0}$ of the timber
- the yield moment $\mathbf{M_y}$ of the steel bolt
- the steel bolt diameter **d**
- the eccentricity **e**

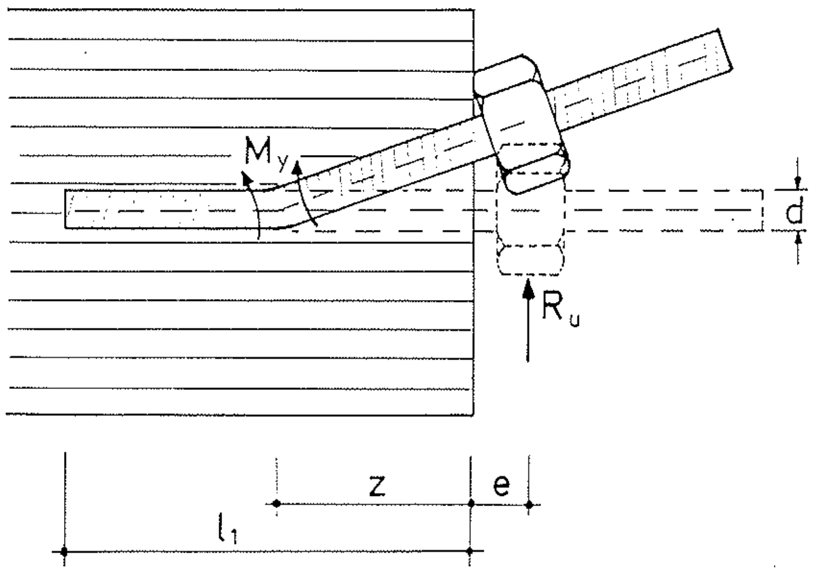

Fig.2: Schematic plot of the joint at ultimate limit state (failure mode)

As long as minimum edge distances are met, such as shown in Fig.3, and as long as the length l_1 is greater then $10 \cdot d$, any perpendicular-to-grain tension failures can be excluded.

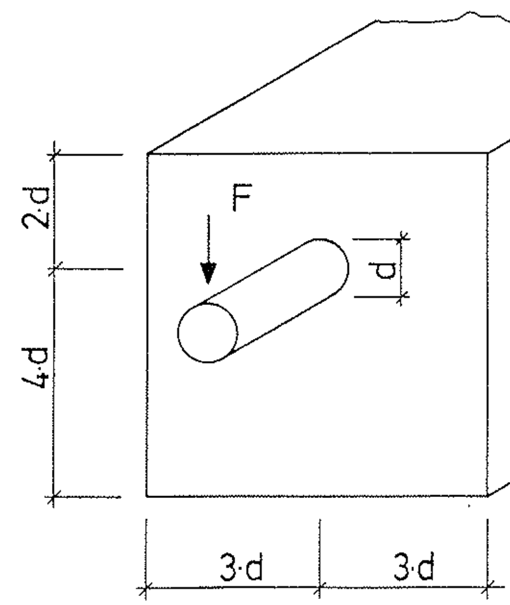

Fig.3: Minimum edge distances to avoid perpendicular-to-grain tension failures

Assuming that M_y of the steel bolt will be reached at the point of the maximum bending moment (here the shear force is zero), the load-carrying capacity R_u may be derived from the equilibrium condition shown in Fig. 4:

$$D_\alpha \cdot \sin(\alpha + \theta) = R_u \cdot sin(90° - \theta) \tag{1}$$

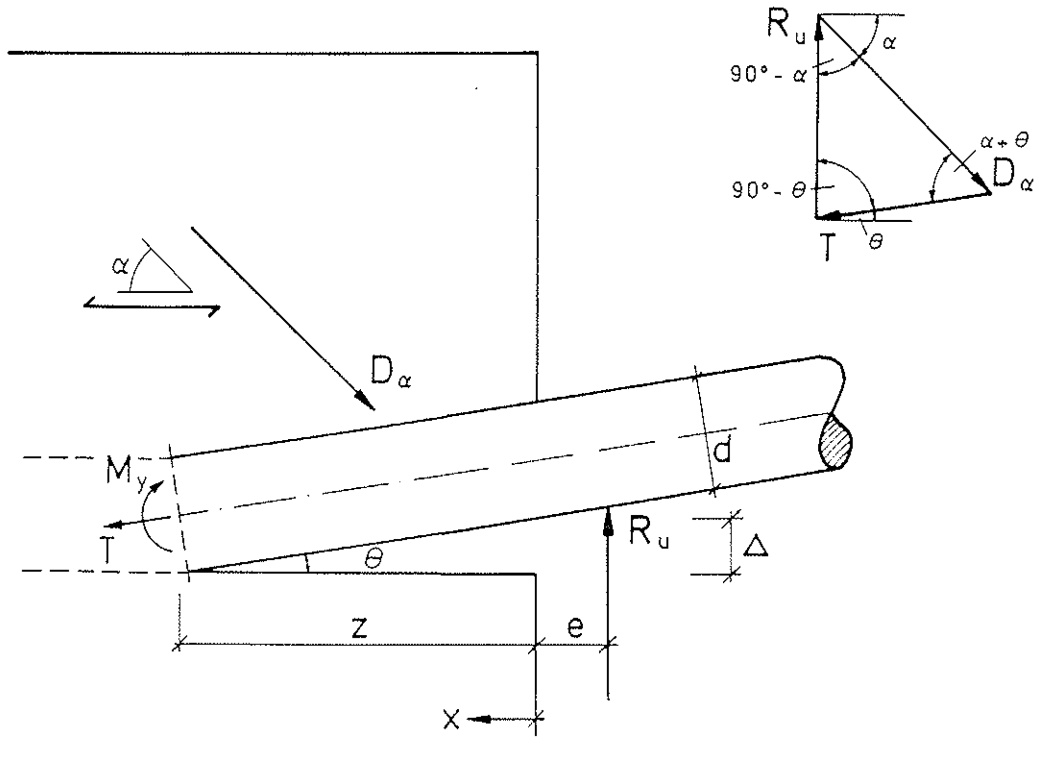

Fig.4: Resulting forces at ultimate limit state

The angle θ at the ultimate limit state can be derived from the maximum deformation under the ultimate load at the end-grain cross-section and the distance z of the point of the yield moment from the end-grain cross-section (see Fig.4):

$$\tan\theta = \frac{\Delta}{z} \qquad (2)$$

The steel bolt itself is rather stiff compared to the surrounding wood. Hence, it can be assumed that the bolt remains straight from the end-grain surface to the point of the yield moment. This assumption with no plastic deformations of the steel bolt was stated in several publications [2], [3], [4], [5], [6] - except the distinct yield point where the yield strength of the steel was reached. On the other hand, a plastification takes place where the embedding stresses exceed the embedding strength. The compression force D_α can be derived from an assumed stress distribution, as shown in Fig. 5:

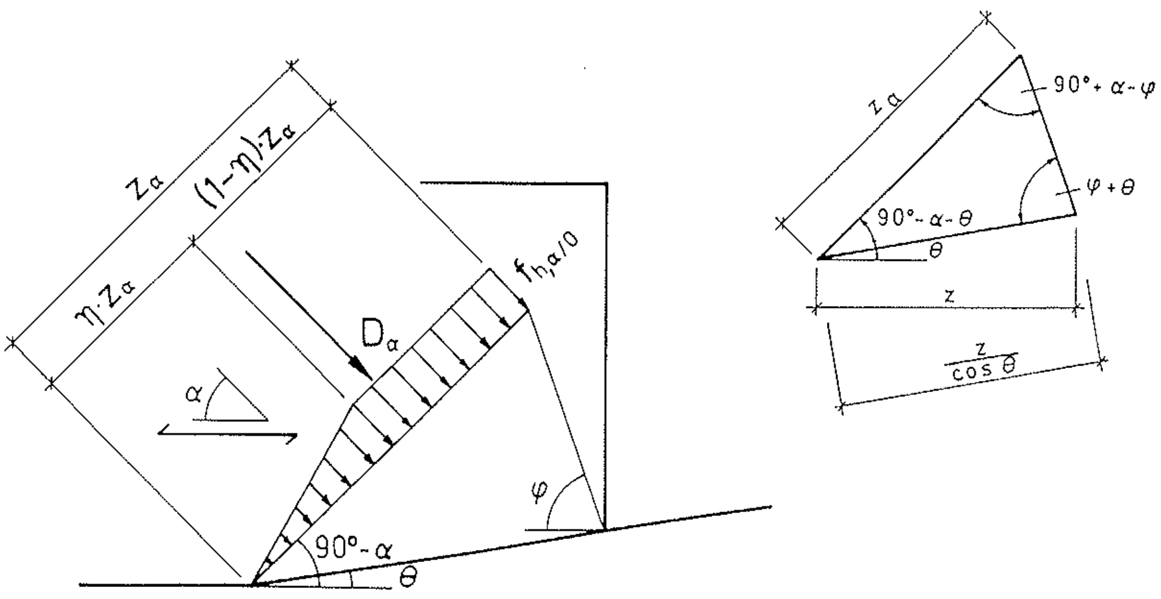

Fig.5: Assumed stress distribution for D_α

$$D_\alpha = \left[\frac{\eta}{2} + (1-\eta)\right] \cdot z_\alpha \cdot d \cdot f_{h,\alpha/0} \qquad (3)$$

$$\frac{z}{\cos\ \theta} \cdot \sin(\varphi+\theta) = z_\alpha \cdot \sin(90° + \alpha - \varphi) \qquad (4)$$

With

$$K_1 = \frac{\sin(\alpha+\theta)}{\sin(90° - \theta)} \quad , \qquad (5)$$

$\cos\ \theta \approx 1$

and

$$K_2 = \frac{\sin(\varphi + \theta)}{\sin(90^\circ + \alpha - \varphi)} \tag{6}$$

follows from equ.(1),(3) and (4):

$$\begin{aligned} R_u &= K_1 \cdot D_\alpha \\ &= K_1 \cdot (1 - \frac{\eta}{2}) \cdot z_\alpha \cdot d \cdot f_{h,\alpha/0} \\ &= K_1 \cdot K_2 \cdot (1 - \frac{\eta}{2}) \cdot z \cdot d \cdot f_{h,\alpha/0} \end{aligned} \tag{7}$$

The distance z of the point of the yield moment M_y from the end-grain cross-section can be derived from

$$M_y = R_u \cdot (e + z) - D_\alpha \cdot \left[\frac{(1-\eta)}{(1-\frac{\eta}{2})} \cdot \left\{ \eta + \frac{(1-\eta)}{2} \right\} + \frac{\frac{\eta}{2}}{(1-\frac{\eta}{2})} \cdot \frac{2}{3} \cdot \eta \right] \cdot z_\alpha$$

$$= R_u \cdot (e + z) - D_\alpha \cdot \left[\frac{\frac{1}{2} - \frac{\eta^2}{6}}{1 - \frac{\eta}{2}} \right] \cdot z_\alpha \tag{8}$$

and with equ. (7)

$$M_y = R_u \cdot \left[e + z - \frac{K_2}{K_1} \cdot \left(\frac{1 - \frac{\eta^2}{3}}{2 - \eta} \right) \cdot z \right] \tag{9}$$

Hence

$$z = \frac{1}{\left[1 - \frac{K_2}{K_1} \cdot \left(\frac{1-\frac{\eta^2}{3}}{2-\eta} \right)\right]} \cdot \left(\frac{M_y}{R_u} - e \right) \tag{10}$$

Equ. (10) is inserted in equ. (7):

$$R_u = K_1 \cdot K_2 \cdot \frac{(1 - \frac{\eta}{2})}{\left[1 - \frac{K_2}{K_1} \cdot \left(\frac{1-\frac{\eta^2}{3}}{2-\eta} \right)\right]} \cdot \left(\frac{M_y}{R_u} - e \right) \cdot d \cdot f_{h,\alpha/0} \tag{11}$$

and with

$$K_3 = \frac{K_1}{2} \cdot \frac{(1-\frac{\eta}{2})}{\left[\frac{1}{K_2} - \frac{1}{K_1} \cdot \left(\frac{1-\frac{\eta^2}{3}}{2-\eta}\right)\right]} \tag{12}$$

$$R_u = 2 \cdot K_3 \cdot \left(\frac{M_y}{R_u} - e\right) \cdot d \cdot f_{h,\alpha/0} \tag{13}$$

Finally:

$$\boxed{R_u = \left[\sqrt{(K_3 \cdot e)^2 + \frac{2 \cdot K_3 \cdot M_y}{d \cdot f_{h,\alpha/0}}} - K_3 \cdot e\right] \cdot d \cdot f_{h,\alpha/0}} \tag{14}$$

The embedding strength $f_{h\alpha/0}$ is not known, because there are no test values available yet. It seems, however, realistic to use the relation

$$\frac{f_{h,\alpha/0}}{f_{h,90/0}} \cong \frac{f_{c,\alpha}}{f_{c,90}} = K_4 \tag{15}$$

with

$$f_{c,\alpha} = f_{c,0} - (f_{c,0} - f_{c,90}) \cdot sin\ \alpha \tag{16}$$

as proposed in the draft EUROCODE 5 [7].

Equ. (14) is of the same shape as the design formula proposed by Riberholt [1]:

$$R_u = \left[\sqrt{e^2 + \frac{2 \cdot M_y}{d \cdot f_h}} - e\right] \cdot d \cdot f_h$$

with $K_3 = 1$ and $f_{h\alpha/0} = f_h$.

4 Embedding strength $f_{h,90/0}$

Some tentative tests to determine the embedding strength $f_{h,90/0}$ of European spruce were carried out with a dowel diameter d=16 mm and a thickness of 2· d=32 mm of the test specimens (see Fig. 6). The tests followed a working draft of CEN/TC 124 WG 1 for determining the embedding strength [8].

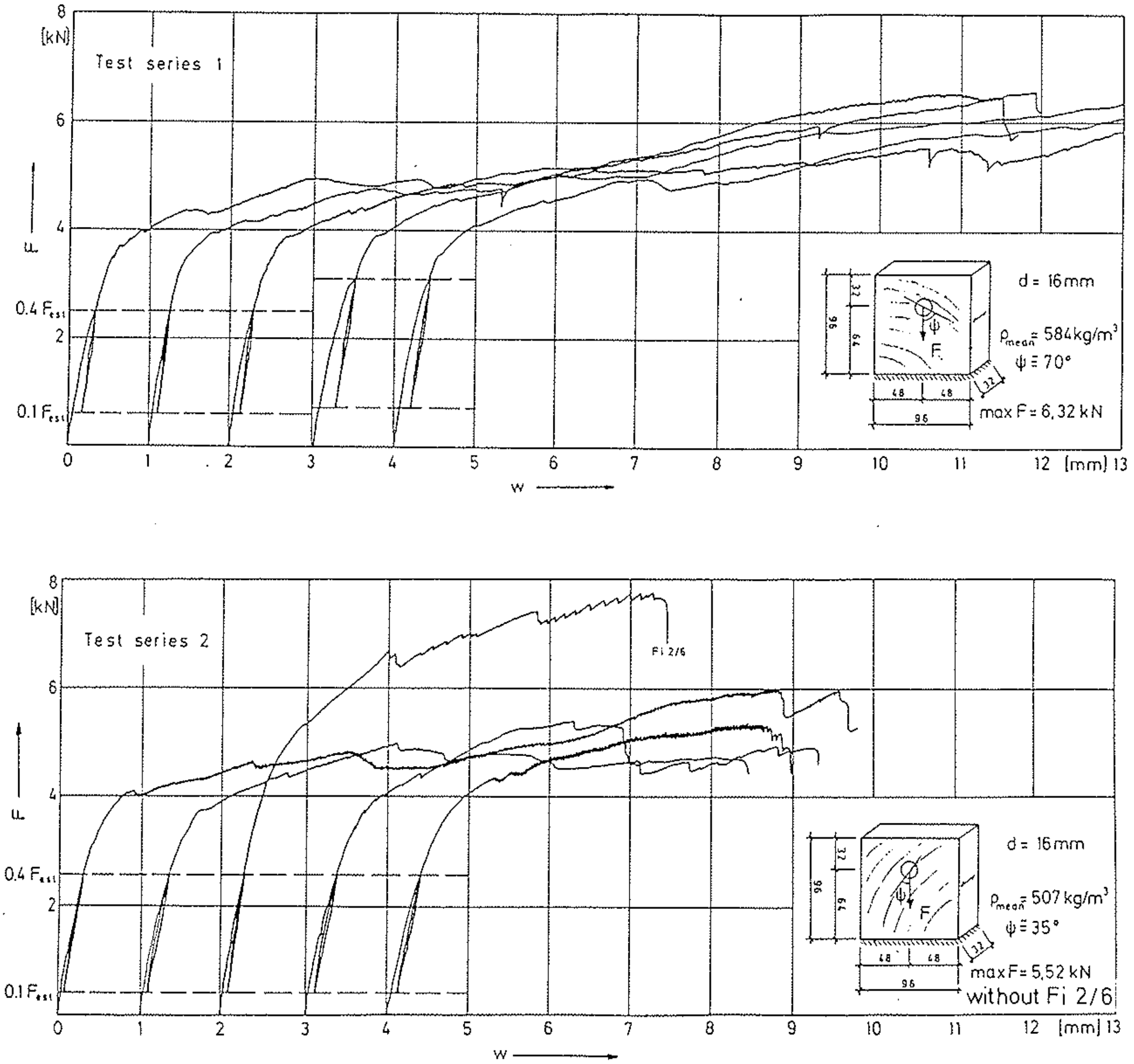

Fig.6: Load-deformation curve of specimens with a dowel-type fastener loaded in compression perpendicular to grain in a prebored hole parallel to grain

Two series with different mean density of the wood as well as different angles between load direction and direction of the annual rings showed that this embedding strength depends on several parameters, such as density, direction of the annual rings and edge-distances of the dowel. Therefore, these test data can only serve as a preliminary orientation.

From the first test series with ρ_{mean} = 584 kg/m^3 and an angle ψ = 70° was found that

$$f_{h,90/0,mean} = 12.3 \text{ N/mm}^2 ,$$

and from the second series with ρ_{mean} = 507 kg/m^3 and an angle of ψ = 35° was found

$$f_{h,90/0,mean} = 10.8 \text{ N/mm}^2.$$

Neglecting any influence of the angle ψ between load direction and annual rings and calibrating the test results linearly to a mean density of 450 kg/m^3 it can be assumed that

$$f_{h,90/0,mean} = 9.5 \text{ N/mm}^2 \qquad \text{for } d = 16 \text{ mm}.$$

5 Finite-Element-Calculations

Using a finite-element programme for a three-dimensional system some tests (see Möhler/Hemmer [6]) were evaluated. Based on the experiences with the embedding strength tests described, the load-deformation behaviour of the wood under the embedding stresses was assumed to be ideal elastic-plastic. For d = 16 mm, the following values have been derived from this calculation (see Fig. 7):

$$\eta = 0.5 \quad ; \quad \varphi = 70° \quad ; \quad \alpha = 45° \quad ; \quad \theta = 9°$$

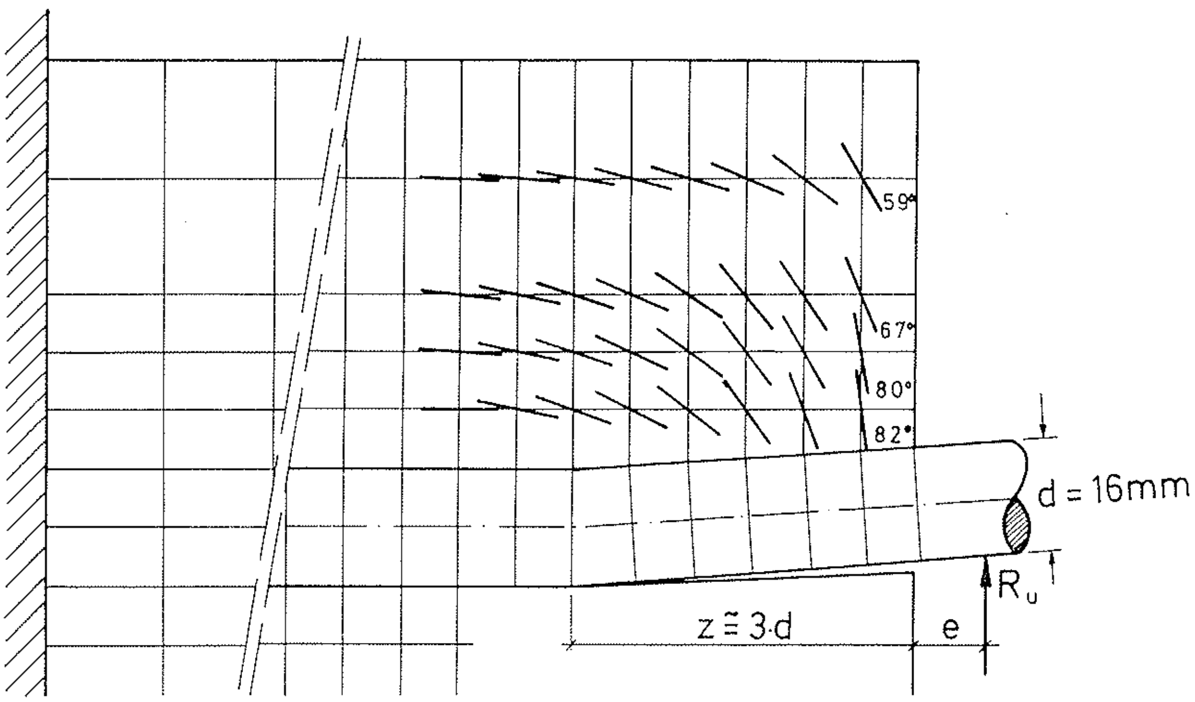

Fig.7: Stress distribution in the end-grain area of timber (FE-calculation); steel bolt diameter d = 16mm

Then,

- from equ. (5) $K_1 = 0.82$
- from equ. (6) $K_2 = 1.08$
- from equ. (12) $K_3 = 1.73$

and assuming $K_4 = 1.8$ in accordance with equ. (15) and (16)
for European spruce, the ultimate load-carrying capacity will amount to:

$$R_u = \left[\sqrt{(1.73 \cdot e)^2 + \frac{1.92 \cdot M_y}{d \cdot f_{h,90/0}}} - 1.73 \cdot e\right] \cdot 1.8 \cdot d \cdot f_{h,90/0} \tag{17}$$

6 Test results and conclusions

Tests from Riberholt [4] and Möhler/Hemmer [6] with steel bolt diameters of 16 mm yielded mean ultimate load-carrying capacities of 9.8 kN and 10.3 kN, respectively. The wood density was in both cases approximately 450 kg/m^3. The yield moments of the steel bolts were specified with 20 kN• cm and 21.8 kN• cm, respectively. The eccentricities were 10 mm.

Using equ. (17) - with $f_{h,90/0}$=9.5 N/mm^2, see clause 4 - , the ultimate load-carrying capacities amount to 9.8 kN for Riberholt's tests and 10.4 kN for Möhler/Hemmer's test, which is in line with the test results.

These investigations indicate, that a determination of the ultimate load-carrying capacity of steel bolts in end-grain under lateral loading can sufficiently be calculated by using equ. (14). This formula is a modification of Riberholt's proposal presented at the 21st CIB-W18A-meeting in 1988. For final verification of this modified proposal it is necessary

- to intensify tests on the embedding strength $f_{h,90/0}$ or/and $f_{h\alpha/0}$, because those tests described in this paper refer exclusively to a steel bolt diameter of 16 mm. It can be expected that increasing steel bolt diameters cause significant decrease of the embedding strength;
- to continue FE-calculations for reconsidering the angles φ , α and θ as well as the factor η and the distance z. Any changes of these data may considerably influence the factor K_3 in equ. (14). It can be expected that for this factor K_3 a fitting approximation can be derived in relation to the steel bolt diameter.

7 References

[1] Riberholt, H. (1988):
Glued Bolts in Glulam - Proposals for CIB-Code -
CIB-W18A/21-7-2; Parksville/Canada

[2] Sansalone, M. ; R. N. White (1986):
End-grain Dowel Connections for Laminated Timber.
In: ASCE, p. 2093 - 2109

[3] Riberholt, H. (1986):
Glued Bolts in Glulam.
Dept. of. Struc. Eng., Techn. University of Denmark; Report 210
Lyngby/Denmark

[4] Riberholt, H. (1977):
Bolte indlimet i limtrx.
Dept. of. Struc. Eng., Techn. University of Denmark; Report 83
Lyngby/Denmark

[5] Stiglat, K.; M. Gerold (1986):
Sanierung einer Holzbalkendecke unter Betrieb.
In: Bauverwaltung 59, p.64/65

[6] Möhler, K.; K. Hemmer (1981):
Versuche mit eingeleimten Gewindestangen.
Forschungsbericht des Lehrstuhls für Ingenieurholzbau und Baukonstruktionen der Universität (TH) Karlsruhe

[7] Eurocode 5;
Commission of the European Communities (1987):
Commen unified rules for timber structures. Report EUR 9887
Brussels/Belgium

[8] Comite Europeen de Normalisation; CEN/TC 124 "Timber Structures",
WG 1 "Test methods" (1989): Draft on EN DDD: "Timber Structures: Test methods - Determination of embedding strength"

CIB -W18A / 22-7-2

INTERNATIONAL COUNCIL FOR BUILDING RESEARCH STUDIES AND DOCUMENTATION

WORKING COMMISSION W18A - TIMBER STRUCTURES

DETERMINATION OF PERPENDICULAR-TO-GRAIN TENSILE STRESSES IN JOINTS WITH DOWEL-TYPE FASTENERS

A draft proposal for design rules

by

J Ehlbeck, R Görlacher and H Werner
University of Karlsruhe
Federal Republic of Germany

MEETING TWENTY - TWO

BERLIN

GERMAN DEMOCRATIC REPUBLIC

SEPTEMBER 1989

Determination of perpendicular-to-grain tensile stresses in joints with dowel-type fasteners

A draft proposal for design rules

Jürgen Ehlbeck, Rainer Görlacher and Hartmut Werner
University of Karlsruhe, FRG

1 Introduction

Joints with dowel-type fasteners loaded at an angle to the grain direction of the wood cause in addition to the embedding stresses considerable local perpendicular-to-grain stresses next to the fasteners. These stresses may under certain conditions lead to failure at a load level lower than the load-carrying capacities of the fasteners themselves.

A simplified method to take into account these stresses is given in the CIB-Code and was also provisionally accepted in the draft EUROCODE 5 [1]. This design method is, however, unsatisfactory and can lead to uncertainties, e.g. for single loads applied to glulam beams and acting perpendicular to the grain direction. This simplified method does not sufficiently take into account:

- the joint's geometry;
- the number of fasteners in the joint;
- the distribution of the fasteners over the beam depth;
- the perpendicular-to-grain tensile strength of the wood in relation to the actually stressed volume;
- the ratio between the distance a_r of the furthest row of fasteners from the loaded beam edge and the beam depth h;
- the range of the area stressed by the perpendicular-to-grain acting load.

Based on tests and theoretical reflections performed at the University of Karlsruhe [2], [3], [4] during the last decade a design procedure for joints with dowel-type fasteners is evaluated and presented for discussion.

2 Notations

F	=	Force
F_{90}	=	Force, component perp. to grain
$\sigma_{t,90}$	=	tension stresses perp. to grain
$f_{t,90}$	=	tension strength perp. to grain
h	=	depth of beam (see Fig. 4)
b	=	beam thickness (see Fig. 4)
a_r	=	distance of the furthest row of fasteners from the loaded edge (see Fig. 4)
h_i	=	distance of the i-th row of fasteners from the unloaded edge (see Fig. 4)
l_r	=	length of one row of fasteners (see Fig. 4)
h_m	=	depth of m rows of fasteners (see Fig. 4)
l_1	=	distance of two groups of fasteners (see Fig. 3)
l_2	=	depth of penetration (see Fig. 4)
l_n	=	nail length
ef b	=	effective width
ef l_r	=	effective loaded length
ef A	=	effective loaded area
d	=	fastener diameter
n	=	number of rows (see Fig. 4)
m	=	number of fasteners in a row (see Fig. 4)
k_{vol}	=	volume factor, taking into account the effect of the size of the loaded volume
k_r	=	factor taking into account the effect of a number of rows of fasteners in a joint
η	=	reducing factor for determining the load generating perpendicular-to-grain tensile stresses in the beam

3 Tests

3.1 Studies and Experiments by Möhler and Lautenschläger [2]

Using a finite-element computer program which takes into account the anisotropy of the wood members the stress distribution perpendicular to grain as well as the distribution of the applied load on the fasteners was calculated for different configurations of the joint and especially for several arrangements of the fasteners with respect to the beam depth.

Based on this theoretical estimate, Möhler and Lautenschläger started some preliminary tests (series L) with nails and dowels (see Table 1) in joints with the load acting perpendicular to the grain and completed these tests by three series (series A, B and C) with European withewood (picea abies), 40 mm thick, changing some important influencing parameters (Fig. 1):

- series A : nails in double shear, d = 3.8 mm;
  a_r/h varied from 0.16 to 0.58;
  five nails in one row.

- series B : nails in double shear, d = 3.8 mm;
  a_r/h varied from 0.26 to 0.58 with two to five
  rows of nails and five nails in each row.

- series C : nails in double shear, d = 3.8 mm
  or one dowel, d = 8.0 mm;
  a_r/h = 0.23, one nail or dowel in one row or two nails
  in one row with different nail distances.

The results of these tests are given in Table 1. It can be seen that the ratio a_r/h, the number of rows of fasteners, and the distance of the fastener within a row are of significant influence on the ultimate load-carrying capacity of such types of joints. All joints failed in perpendicular-to-grain tension stresses located in the furthest row of fasteners, relative to the loaded edge of the beam.

3.2 Investigations by Möhler and Siebert [3]

Möhler and Siebert [3] performed tests with glulam beams of 120 cm and 60 cm beam depth, respectively, to which big loads perpendicular to grain were jointed with dowels (d = 16 mm) or smooth round wire nails (d = 4.2 mm) driven into predrilled holes (Fig. 2). The length of a row of fasteners, l_r, was kept constant. But the ratio a_r/h as well as the number of rows, m, and the number of fasteners in a row, n, were varied. The test results (see Table 2) confirmed the significant influence of these parameters.

3.3 Investigations by Ehlbeck and Görlacher [4]

In another research project nailed steel-to-wood (glulam) joints (see Fig. 3) were tested under loads, F, acting perpendicular to the grain direction of the beam. The following parameters were taken into account:

- ratio a_r/h and distance, l_1, of two groups of fasteners; series G 1;
- beam span, l; series G 2
- nail dimensions, d and l_n, als well as beam thickness, b; series G 3;
- beam depth, h; series G 4;
- joint configuration (nail spacing); series G 5;
- joint at an end of a cantilever beam; series G 6.

The results of these tests are listed in Table 3. The nails used were ringed shank nails suitable for nailed sheet steel-to-wood joints, with a nominal shank diameter of 4 mm and nail lengths of 40 mm, 50 mm or 60 mm, respectively.

3.4 Conclusions from the tests

From those tests described the following can be argued:

- the load-carrying capacity of perpendicular-to-grain joints significantly increases with increasing ratio a_r/h;
- in all tests with $a_r/h < 0.7$ the failure of the joints was caused by a tension failure perpendicular to grain in the furthest row of fasteners, related to the loaded edge of the beam;
- in case of $a_r/h > 0.7$ small cracks could be observed without leading to a clear tension failure perpendicular to grain;
- two adjacent joints can considerably influence each other (that depends on the distance between the joints);
- for the same joint geometry and the same ratio a_r/h, the load-carrying capacity of the joint increases with increasing beam depth, h;
- scattering of fasteners in a row with respect to the grain direction is of negligable influence;
- joints near to the free end of a beam are endangering because the stresses in the beam can only spread to one side.

4 Design method for joints with decisive perpendicular-to-grain tensile stresses

Based on the test results and their conclusions a design method is developed for joints with a load or load component, F_{90}, acting perpendicular to the grain direction:

$$F_{90} = F \cdot \sin \alpha \qquad (1)$$

The perp.-to-grain tensile stresses should meet the following condition (see draft EUROCODE 5):

$$\sigma_{t,90,d} \leq k_{vol} \cdot f_{t,90,d} \qquad (2)$$

Because the failure occurs along the furthest row of fasteners, related to the loaded edge, k_{vol} can be taken as

$$k_{vol} = \left(\frac{V_0}{V}\right)^{0.2} = \left(\frac{h^* \cdot A_0}{h^* \cdot ef\,A}\right)^{0.2} = \left(\frac{A_0}{ef\,A}\right)^{0.2} \tag{3}$$

A 2-parameter Weibull-distribution with $k_{wei} = 5$ is assumed. h^* is the depth of a volume with even distributed perp.-to-grain tensile stresses. From this follows:

$$\sigma_{t,90,d} \leq A_0^{0.2} \cdot ef\,A^{-0.2} \cdot f_{t,90,d} \tag{4}$$

$f_{t,90}$ is defined for a volume $V_0 = 0.02\ m^3$; consequently,

$$A_0 = \frac{V_0}{h^*} \tag{5}$$

An even distributed stress is assumed to act in a 20 mm thick area, A_0, along the furthest row of fasteners. Thus,

$$A_0 = 1\ m^2 = 10^6\ mm^2$$

and

$$\sigma_{t,90,d} \leq 15.85 \cdot ef\,A^{-0.2} \cdot f_{t,90,d} \tag{6}$$

with ef A in $[mm^2]$; $\sigma_{t,90,d}$ and $f_{t,90,d}$ in $[N/mm^2]$.

The perpendicular to grain tensile stress can generally be calculated by:

$$\sigma_{t,90} = \frac{\eta \cdot k_r \cdot F_{90}}{ef\,A} \tag{7}$$

ef A may be assumed as

$$ef\,A = ef\,l_r \cdot ef\,b \tag{8}$$

The factors η and k_r make allowance for the fact that, as a rule, not the entire load F_{90} causes perp-to-grain tensile stresses in the furthest row of fasteners. Partly, the load F_{90}, evokes perpendicular-to-grain compressive stresses in the beam; partly, the load F_{90} is distributed over several rows of fasteners so that only a reduced portion of tensile stresses is acting in the area of the furthest row of fasteners.

The main problem is to define these factors η and k_r as well as the effective length, ef l_r, of the row of fasteners in a realistic manner using realistic and evident assumptions.

4.1 Partition of F_{90} into $F_{t,90}$ and $F_{c,90}$ (factor η)

It is assumed that

$$F_{t,90} = \eta \cdot F_{90} \qquad (9)$$

is that partition of F_{90} which causes perp.-to-grain tensile stresses in the beam. With the notations given in Fig. 4 it can be shown that

$$\eta = 1 - 3 \cdot \left(\frac{a_r}{h}\right)^2 + 2 \cdot \left(\frac{a_r}{h}\right)^3 \qquad (10)$$

This can be derived by considering a part of the beam, with the depth $h_1 = h - a_r$, separated from the total beam (see Fig. 5), and minding the condition that the deformation of the total beam under a load F_{90} must be equal to the deformation of the separated beam under a load $F_{t,90}$ and the shear forces along the cut line. The derivation of η (Eq. 10) is based on the assumption of the linear elastic bending theory neglecting any shear deformations.

4.2 Influence of n rows of fasteners

If there are n rows of fasteners it is assumed that the total load F_{90} is even-distributed to the rows:

$$F_{90,n} = \frac{F_{90}}{n} \tag{11}$$

Consequently, in each row a certain perpendicular-to-grain tensile stress is generated by the load

$$F_{t,90,n} = \eta_n \cdot \frac{F_{90}}{n} \tag{12}$$

with η_n from Eq. (10).
The tensile stresses $\sigma_{t,90,n}$, generated by the loads $F_{t,90,n}$, will decrease to zero at the unloaded edge of the beam (see Fig. 6). In the furthest row, however, the resulting total tensile stress will be equal to the addition of those stresses which are remaining in this area. The reduction of $\sigma_{t,90,n}$ to the remaining share of stress in the furthest row of fasteners, $\sigma^*_{t,90,n}$ is assumed to follow the formula

$$\sigma^*_{t,90,n} = \left(\frac{h_1}{h_n}\right)^2 \cdot \sigma_{t,90,1} \tag{13}$$

Hence, the total perp.-to-grain tensile stress in the furthest row results to:

$$tot\,\sigma_{t,90,1} = \sum_{i=1}^{n} \left(\frac{h_1}{h_i}\right)^2 \cdot \sigma_{t,90,1} \tag{14}$$

From this follows that the factor k_r can be defined as

$$k_r = \frac{1}{n} \cdot \sum_{i=1}^{n} \left(\frac{h_1}{h_i}\right)^2 \tag{15}$$

and the load

$$F_{t,90} = \eta \cdot k_r \cdot F_{90} \qquad (16)$$

is that load which generates the perp.-to-grain tensile stress causing the failure of the joint.

With increasing number of rows of fasteners, the factor k_r approaches asymptotically to

$$k_r = \frac{h_1}{h_n} \qquad (17)$$

4.3 Effective Area ef A

The effective area ef A according to Eq. (8) represents a fictive area because the perpendicular-to-grain tensile stresses are uneven-distributed along the length, l_r, of the row of fasteners and, in addition, also stresses the wood to a certain distance from both ends of the row.

If there is only one fastener in a row, then $l_r = 0$. The effective width of the stressed area, this is ef l_r, can in this case be assumed as

$$ef\,l_r = c \cdot h \qquad (18)$$

with

$$c = \frac{4}{3} \cdot \sqrt{\frac{a_r}{h} \cdot \left(1 - \frac{a_r}{h}\right)^3} \qquad (19)$$

This relationship between ef l_r, a_r and h was found from the test results as the best fitting concept (see also Fig. 7). It takes into account that for $a_r \rightarrow 0$ and $a_r \rightarrow h$ the effective width ef l_r will approach zero.

With several fasteners in each row, the effective width can be approximated by

$$ef\,l_r \;=\; \sqrt{l_r^2 + (c \cdot h)^2} \qquad (20)$$

This formula shows that for very long rows of fasteners ef l_r approaches l_r. On the other hand, for m = 1 Eq. (20) is equal to Eq. (18).

If two groups of fasteners are near to each other with a distance of l_1, then the total effective length, tot ef l_r, can be approximated by

$$tot\,ef\,l_r \;=\; ef\,l_r \cdot \left(1 + \frac{l_1}{l_1 + a_r}\right) \qquad (21)$$

In this case, ef l_r is the effective length of one group of fasteners.

The effective width, ef b, can approximately be assumed as the sum of the depths of penetration of the fasteners, l_2. The effective depth of penetration should, however, not exceed 15 x d. Thus,

$$ef\,b \;=\; \sum l_2 \;\leq\; b \qquad (22)$$

with $l_2 \leq 15 \times d$.

In case that the joint is near to the beam end, it should be realized that the load (or stresses) cannot distribute unchecked. If the distance of the joint from the beam end is less than the beam depth, only half the effective length should be taken into account.

5 Evaluation of test results and proposed design procedure

All test results with $a_r/h < 0{,}7$ evaluated using Eq. (7), with F_{90} = max F_{90} from the tests, and using the factors η and k_r as given in Eqs. (10) and (15). With the effective area, ef A as explained in clause 4.3, the calculated perpendicular-to-grain strength data are plotted in Fig. 8. The best fitting function for these test values reads

$$f_{t,90} \;=\; 13.71 \cdot ef\,A^{-0.235} \qquad (23)$$

and could be simplified by using

$$f_{t,90} = 10 \cdot ef\,A^{-0.2} \tag{24}$$

With some simplification the following design procedure is proposed:

- The characteristic perp.-to-grain tensile strength which is related to a volume of 0.02 m^3, may be modified to

$$f^{*}_{t,90,k} = 15 \cdot ef\,A^{-0.2} \cdot f_{t,90,k} \tag{25}$$

If, for example, for a glulam beam made from European whitewood (picea abies) boards with a characteristic density of 400 kg/m^3 the characteristic value of $f_{t,90,k}$ is assumed to be 0.4 N/mm^2 (see draft EUROCODE 5, Annex 2, Table A 2.3a), then from Eq. (25) follows (see Fig. 8)

$$f^{*}_{t,90,k} = 15 \cdot ef\,A^{-0.2} \cdot 0.4 = 6.0 \cdot ef\,A^{-0.2} \tag{26}$$

- The effective area, ef A, is defined as explained in clause 4.3
- The factors η and k_r may be calculated using Eq. (10) and (15) or (17), respectively
- Finally, the following condition must be satisfied:

$$\boxed{\sigma_{t,90,d} = \eta \cdot k_r \cdot \frac{F_{90,d}}{ef\,A} \leq 15 \cdot ef\,A^{-0.2} \cdot f_{t,90,d}} \tag{27}$$

6 References

[1] EUROCODE 5, 1987: Common unified rules for timber structures. Draft published by the Commission of the European Communities, Brussels (Belgium)

[2] Möhler, K.; Lautenschläger, R., 1978: Großflächige Queranschlüsse bei Brettschichtholz. Forschungsbericht des Lehrstuhls für Ingenieurholzbau und Baukonstruktionen, Universität Karlsruhe

[3] Möhler, K.; Siebert, W., 1980: Ausbildung von Queranschlüssen bei angehängten Lasten an Brettschichtholzträger. Forschungsbericht des Lehrstuhls für Ingenieurholzbau und Baukonstruktionen, Universität Karlsruhe

[4] Ehlbeck, J.; Görlacher, R., 1983: Tragverhalten von Queranschlüssen mittels Stahlblechformteilen, insbesondere Balkenschuhe, im Holzbau. Forschungsbericht der Versuchsanstalt für Stahl, Holz und Steine, Abt. Ingenieurholzbau, Universität Karlsruhe

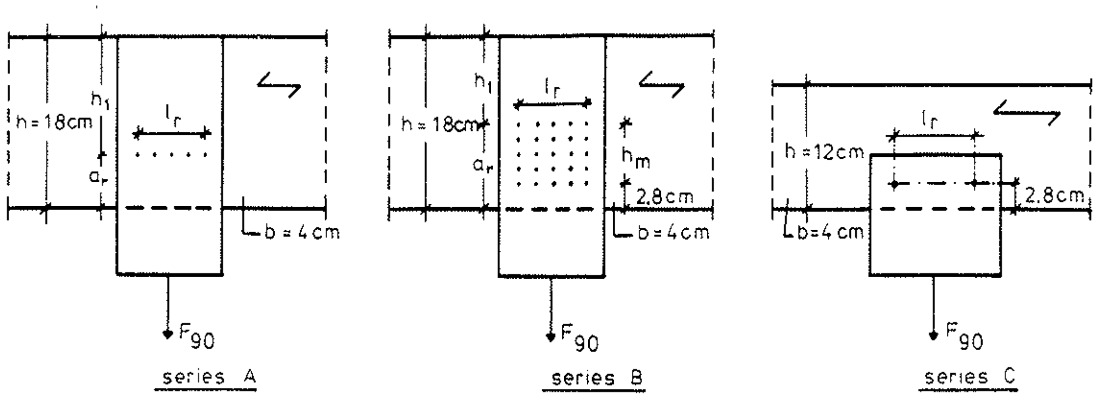

Fig. 1: Test series by Möhler / Lautenschläger [1].

Table 1: Tests made by Möhler and Lautenschläger [2]

Test-series	Type of fasteners*)	No. of tests	d [mm]	m	n	h [cm]	a_r [cm]	l_r [cm]	h_m [cm]	max F_{90} [kN]
L 1	np	5	3.8	5	1	18	2.8	7.6	0.0	7.92
L 6	np	1	3.8	5	2	18	4.7	7.6	1.9	13.50
L 7	np	1	3.8	5	1	18	4.7	7.6	0.0	10.70
L 8	do	1	8.0	1	1	18	2.8	0.0	0.0	5.20
A 1	np	3	3.8	5	1	18	2.8	7.6	0.0	8.78
A 2	np	3	3.8	5	1	18	4.7	7.6	0.0	9.56
A 3	np	3	3.8	5	1	18	6.6	7.6	0.0	11.93
A 4	np	3	3.8	5	1	18	8.5	7.6	0.0	13.40
A 5	np	3	3.8	5	1	18	10.4	7.6	0.0	18.90
B 1	np	3	3.8	5	2	18	4.7	7.6	1.9	12.47
B 2	np	3	3.8	5	3	18	6.6	7.6	3.8	18.87
B 3	np	3	3.8	5	4	18	8.5	7.6	5.7	21.13
B 4	np	3	3.8	5	5	18	10.4	7.6	7.6	27.83
C 1	np	3	3.8	2	1	12	2.8	7.6	0.0	9.53
C 2	np	3	3.8	2	1	12	2.8	5.7	0.0	8.07
C 3	np	3	3.8	2	1	12	2.8	3.8	0.0	6.80
C 4	np	3	3.8	2	1	12	2.8	1.9	0.0	6.42
C 5	np	3	3.8	1	1	12	2.8	0.0	0.0	6.95
C 6	do	3	8.0	1	1	12	2.8	0.0	0.0	6.05

*) np : smooth round wire nails in predrilled holes
do : dowels

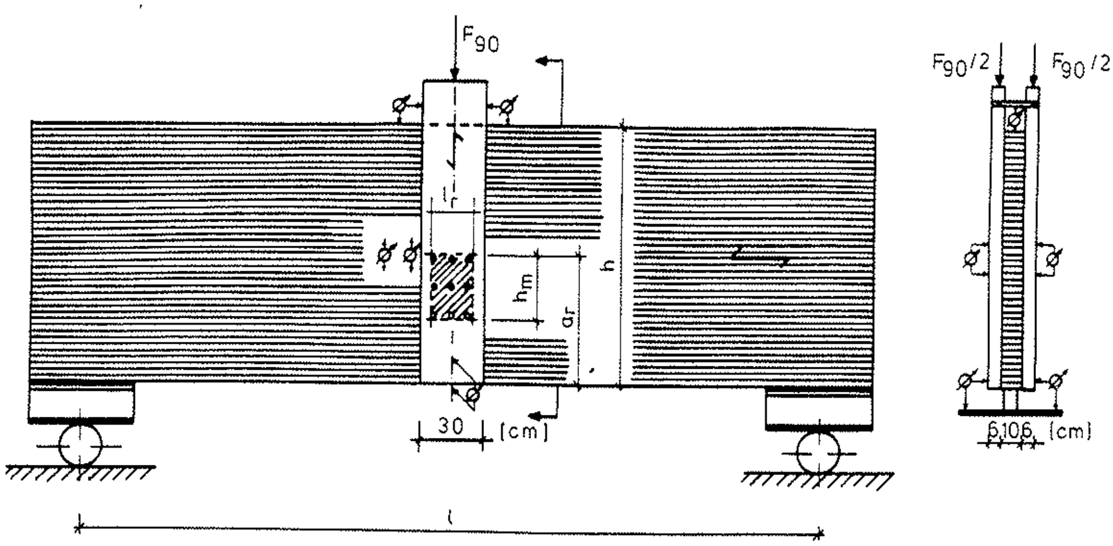

Fig. 2: Test set-up for testing joints loaded pependicular to grain of glulam beams (Möhler / Siebert [3]).

Table 2: Tests made by Möhler and Siebert [3]

Test-series	Type of fasteners*)	No. of tests	d [mm]	m	n	h [cm]	a_r [cm]	l_r [cm]	h_m [cm]	max F_{90} [kN]
V 2	do	1	16.0	3	2	120	30.0	20.0	8.0	90.00
V 3	do	1	16.0	3	4	120	30.0	20.0	24.0	112.00
V 4	do	1	16.0	2	2	120	30.0	20.0	8.0	65.00
V 5	np	1	4.2	10	4	120	30.0	20.0	6.3	74.50
V 9	do	1	16.0	3	6	120	60.0	20.0	50.0	179.50
V 10	np	1	4.2	10	4	120	60.0	20.0	21.0	118.50
V 11	do	1	16.0	3	4	60	30.0	20.0	24.0	110.00
V 12	do	1	16.0	3	4	60	30.0	20.0	24.0	144.00
V 13	do	1	16.0	3	2	60	45.0	20.0	8.0	180.00
V 14	do	1	16.0	3	2	60	45.0	20.0	8.0	200.00
V 23	do	1	16.0	3	2	120	90.0	20.0	8.0	190.00
V 24	do	1	16.0	3	2	60	15.0	20.0	8.0	69.50
V 25	do	1	16.0	3	2	60	30.0	20.0	8.0	75.00
V 26	do	1	16.0	3	2	60	45.0	20.0	8.0	220.00
V 27	do	1	16.0	3	2	60	15.0	20.0	8.0	62.50
V 28	do	1	16.0	2	2	60	15.0	20.0	8.0	56.00

*) do : dowels
np : smooth round wire nails in predrilled holes

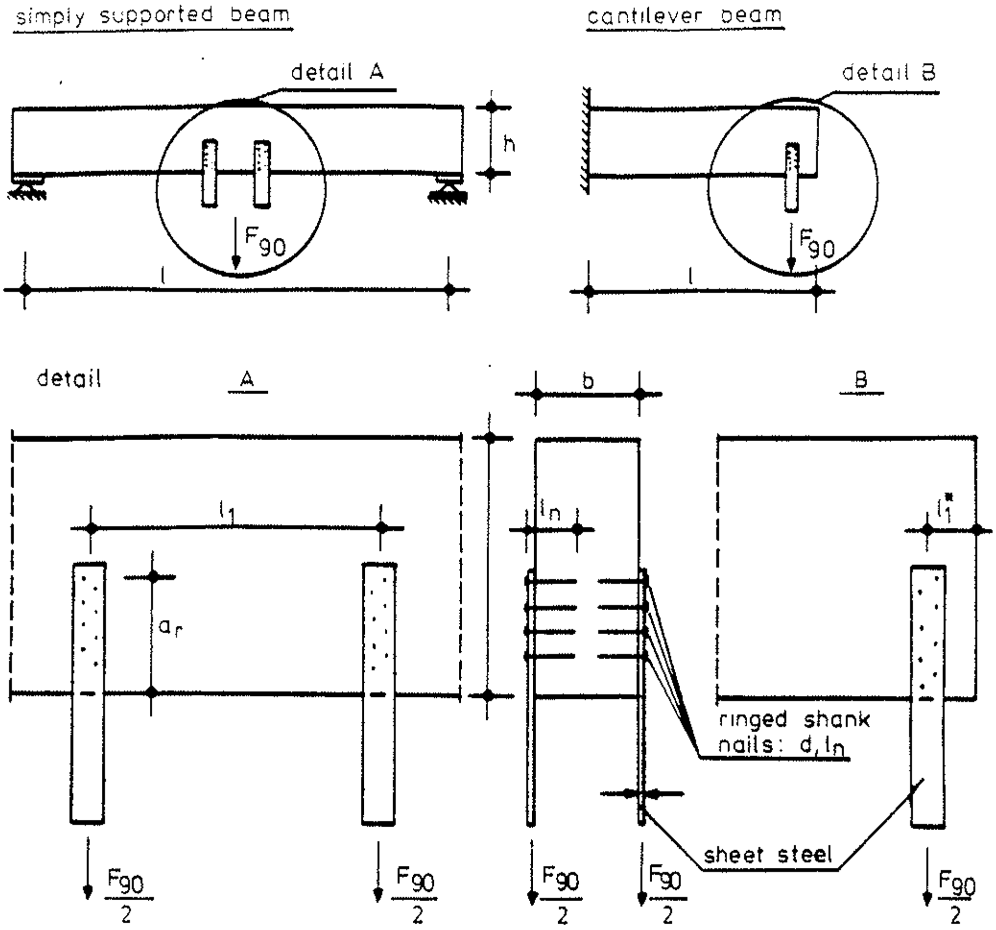

Fig. 3: Test set-up for steel-to-wood joints loaded perpendicular to grain (Ehlbeck / Görlacher [4]).

Table 3: Tests made by Ehlbeck and Görlacher [4]

Test-series	Type of fasteners*)	No. of tests	d [mm]	m	n	h [cm]	b [cm]	a_r [cm]	l_r [cm]	h_m [cm]	l_1 [cm]	max F_{90} [kN]
G 1.1	rn	3	4.0	2	4	25	10	10.0	2.0	6.0	0	37.33
G 1.2	rn	3	4.0	2	4	25	10	10.0	2.0	6.0	4	41.70
G 1.3	rn	3	4.0	2	4	25	10	10.0	2.0	6.0	9	42.87
G 1.4	rn	3	4.0	2	4	25	10	10.0	2.0	6.0	24	47.97
G 1.5	rn	3	4.0	2	4	25	10	15.0	2.0	6.0	4	53.03
G 1.6	rn	3	4.0	2	4	25	10	15.0	2.0	6.0	9	57.63
G 1.7	rn	3	4.0	2	4	25	10	15.0	2.0	6.0	24	71.07
G 2.1	rn	3	4.0	2	4	25	10	10.0	2.0	6.0	0	35.70
G 2.2	rn	3	4.0	2	4	25	10	10.0	2.0	6.0	0	38.95
G 3.1	rn	3	4.0	2	4	25	8	10.0	2.0	6.0	4	34.87
G 3.2	rn	3	4.0	2	4	25	12	10.0	2.0	6.0	4	46.20
G 3.3	rn	3	4.0	2	4	25	12	10.0	2.0	6.0	4	46.67
G 3.4	rn	3	6.0	2	4	25	12	10.0	2.0	6.0	4	44.33
G 4.1	rn	3	4.0	2	4	40	10	10.0	2.0	6.0	4	39.57
G 4.2	rn	3	4.0	2	4	40	10	16.0	2.0	6.0	4	51.67
G 4.3	rn	3	4.0	2	4	15	10	9.0	2.0	6.0	4	47.30
G 5.1	rn	3	4.0	2	2	25	10	10.0	2.0	2.0	4	35.63
G 5.2	rn	3	4.0	2	2	25	10	10.0	2.0	6.0	4	33.63
G 5.3	rn	3	4.0	2	2	25	10	10.0	2.0	6.0	4	42.17
G 6.1	rn	2	4.0	2	4	25	10	10.0	2.0	2.0	3	18.85
G 6.2	rn	2	4.0	2	4	25	10	10.0	2.0	2.0	11	23.55

*) rn : ringed shank nails

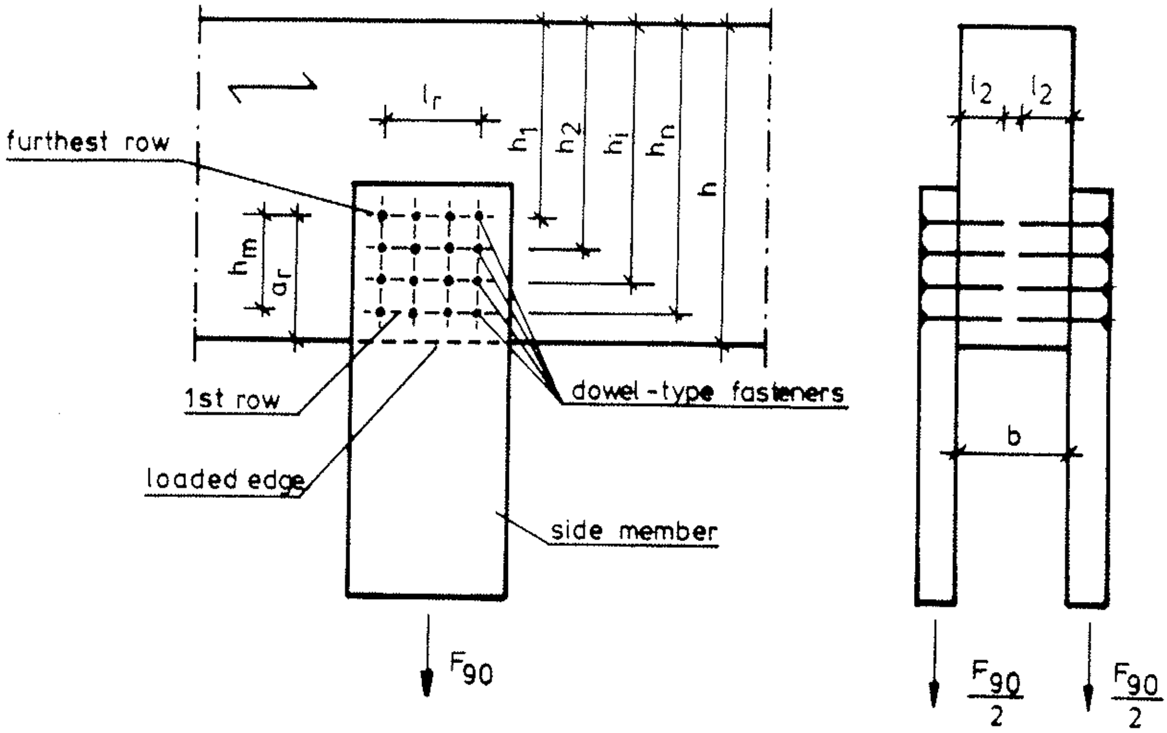

Fig. 4: Joint with F_{90} acting perpendicular to grain (notations).

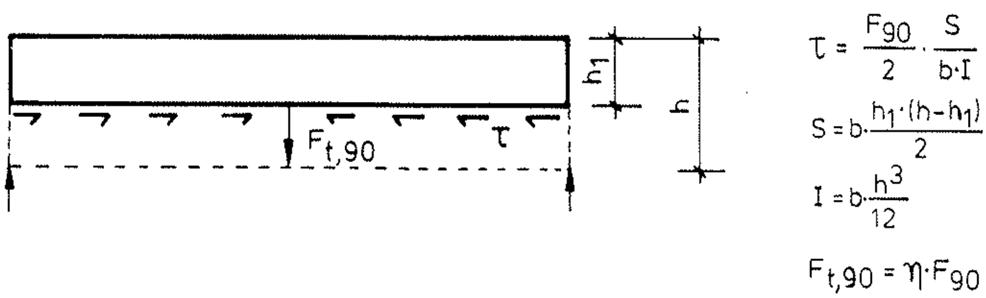

Fig. 5: Actions on the beam with depth h_1, seperated from the beam with total depth h.

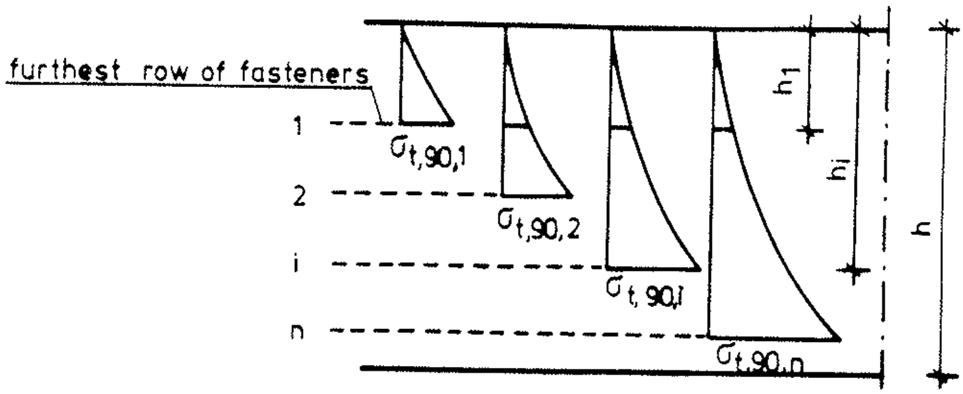

Fig. 6: Distribution of tensile stresses perpendicular to grain, generated in n rows by the load $F_{t,90,n}$.

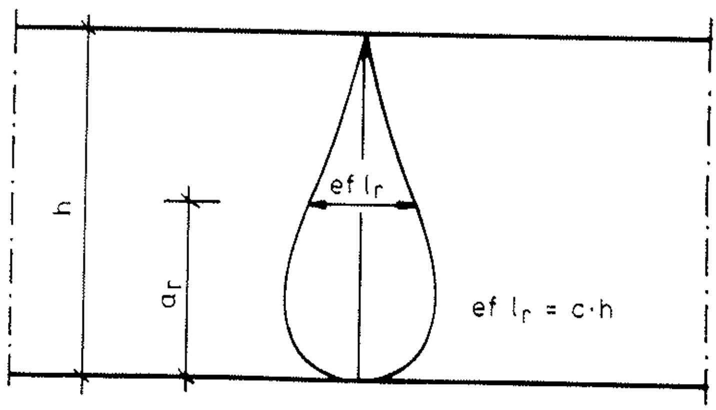

Fig. 7: Assumption for ef l_r in case of one fastener per row, only

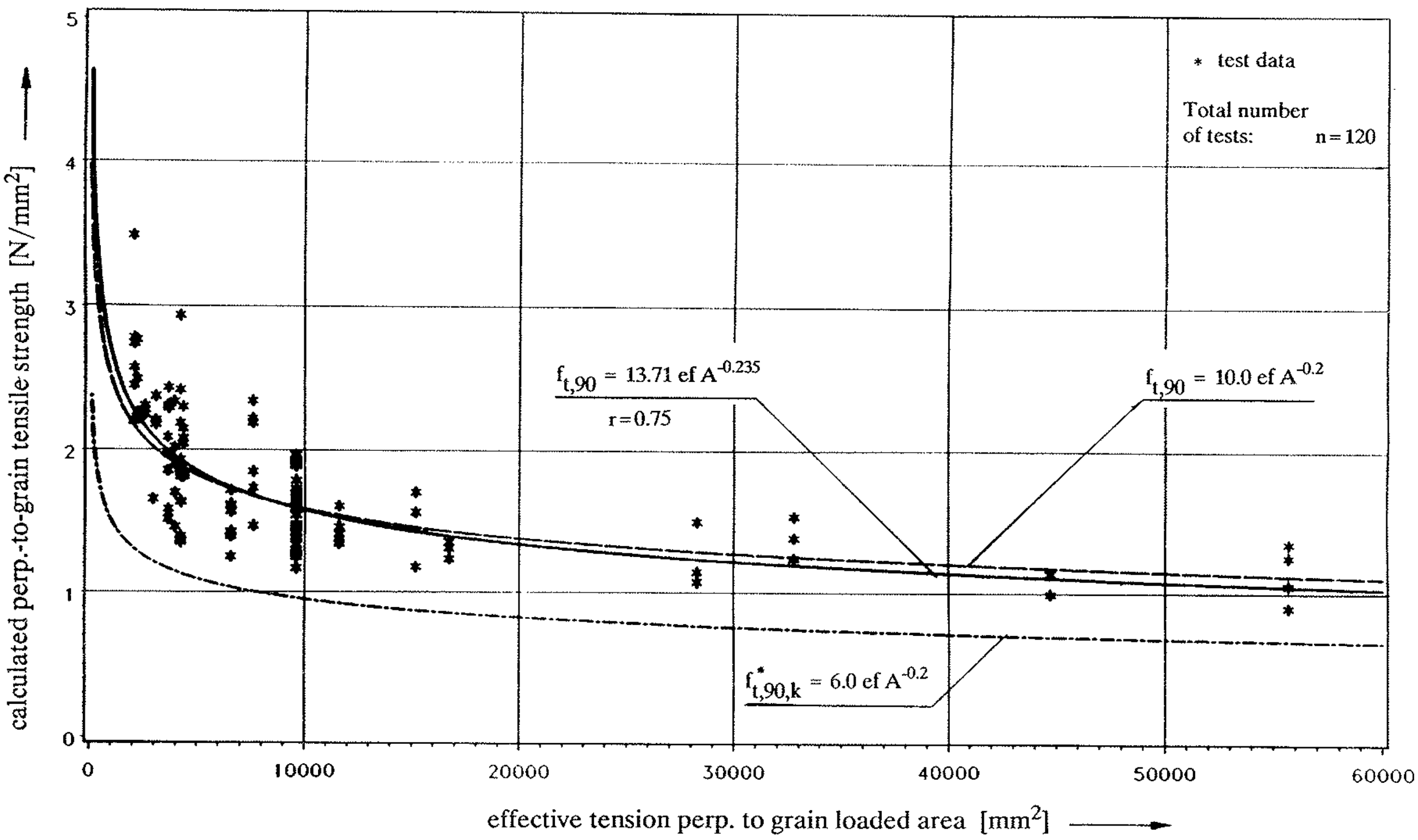

Fig. 8: Perp.-to-grain tensile strength over effective area, ef A.

CIB -W18A / 22-7-3

INTERNATIONAL COUNCIL FOR BUILDING RESEARCH STUDIES AND DOCUMENTATION

WORKING COMMISSION W18A - TIMBER STRUCTURES

DESIGN OF DOUBLE-SHEAR JOINTS WITH NON-METALLIC DOWELS

A proposal for a supplement of the design concept

by

J Ehlbeck and O Eberhart
University of Karlsruhe
Federal Republic of Germany

MEETING TWENTY - TWO

BERLIN

GERMAN DEMOCRATIC REPUBLIC

SEPTEMBER 1989

Design of double-shear joints with non-metallic dowels

A proposal for a supplement of the design concept

Jürgen Ehlbeck and Otto Eberhart
University of Karlsruhe, FRG

1 Introduction

At the University of Karlsruhe a research programme was undertaken to determine the load-carrying capacity and the deformation behaviour of glulam joints with non-metallic dowels of resin-impregnated compressed wood. This material exists of multi-layered densified 2 mm beech veneers glued together and fully impregnated with phenolic resins. One of the objectives of this research work was to find out if Johansen's theory for determining the ultimate load-carrying capacity of joints with dowel-type fasteners can also be applied for such type of material having pronounced brittle properties.

The test data in principle confirmed the applicability of this design model which was introduced in the CIB-Code as well as the draft EUROCODE 5 for limit state design calculations. It turned out, however, that an additional failure mode may occur which makes it advisable to introduce a supplementary design formula.

2 Tests

With a total of 128 test specimens (see Fig. 1) the load-deformation behaviour in double-shear compressive tests was determined. All tests were performed only with the load acting parallel to the grain direction. The diameter of the resin-impregnated densified multi-ply beech dowels ranged from 8 to 20 mm. The ratio of the inner member thickness, t_2, over the side member thickness, t_1, was kept constant with

$$\frac{t_2}{t_1} = 1.33$$

The slenderness of the joint, λ , defined as

$$\lambda = \frac{t_2}{d}$$

was varied. The spacing of the dowels was chosen as the minimum allowable distances for metallic dowels according to the German timber structures design code, DIN 1052, yet with no scattering of the dowels along the glulam grain direction.

The mean wood density of all test specimens at an equilibrium moisture content corresponding to 20°C temperature and 65 % relative humidity was

$$\varrho_{mean} = 453 \frac{kg}{m^3}$$

with a standard deviation of 27 kg/m^3.

The dowels used were produced by two different manufacturers with a slightly different bending strength of the material.

All plies of the impregnated densified beech dowels were orientated parallel to the dowel axis. In bending tests to determine the bending strength of the dowels typical linear-elastic load-deflection curves were plotted as shown in Fig. 2. There was always a sudden brittle bending failure of the dowels. The bending strength, f_m, was independent of the ratio l/d and was not influenced by the orientation of the plies, i.e. the load direction in relation to the plane of the plies.

The test evaluation was made in accordance with ISO 6891 "Timber structures - Joints made with mechanical fasteners - General principles for the determination of strength and deformation characteristics".

3 Test results and evaluation

From the tests described the following findings can be stated:

Depending on the slenderness ratio, $\lambda = t_2/d$, there were two typical failure modes:

- a single bending failure of the dowels in the middle member (see Fig. 3a). This mode may be regarded as a modification (failure mode 3a) of Johansen's failure mode type 3 having two yield moment points of the steel dowel in the middle member. Failure mode 3a is shown in Fig. 3b.

- four bending failures as shown in Fig. 4. This failure mode corresponds to Johansen's failure mode 4.

For the failure mode 3a with a single bending failure in the middle member and the distribution of the embedding stresses as shown in Fig. 3b the ultimate load-carrying capacity of the joint can be calculated with

$$R_u = \left[\sqrt{\left(t_1 + \frac{t_2}{2}\right)^2 + \frac{\beta + 1}{\beta} \cdot \left(\frac{2}{3} \cdot \frac{f_y \cdot d^2}{f_h} + t_1^2 + \frac{\beta}{4} \cdot t_2^2\right)} - \left(t_1 + \frac{t_2}{2}\right)\right] \cdot \frac{\beta}{\beta + 1} \cdot d \cdot f_h \qquad (1)$$

with

f_y	yield strength of the dowel
f_h	embedding strength of the side members
$\beta \cdot f_h$	embedding strength of the middle member

and the geometric data as shown in Fig. 3b.

In case of brittle behaviour of the dowels as shown in Fig. 2 the yield strength, f_y, should be substituted by the bending strength, f_m, of the dowels:

$$f_m = \frac{max M}{\pi \cdot d^3/32} \qquad (2)$$

Thus, in Eq. (1) the yield strength of the dowel should be replaced by

$$f_y = \frac{3 \cdot \pi}{16} \cdot f_m \tag{3}$$

In case of $\beta = 1$, i.e. same material for all members, Eq. (1) reduces to

$$R_u = \left[\sqrt{\left(t_1 + \frac{t_2}{2}\right)^2 + \frac{4}{3} \cdot \frac{f_y \cdot d^2}{f_h} + 2 \cdot t_1^2 + \frac{t_2^2}{2}} - \left(t_1 + \frac{t_2}{2}\right) \right] \cdot \frac{d \cdot f_h}{2} \tag{4}$$

For brittle dowel material

$$\frac{4}{3} \cdot \frac{f_y \cdot d^2}{f_h} = \frac{\pi}{4} \cdot d^2 \cdot \frac{f_m}{f_h} \tag{5}$$

The tests were evaluated by using these theoretical calculation model with $t_2/t_1 = 4/3$.
Hence, the ultimate load-carrying capacities maxF of all joints tested were compared to

$$R_u = \left[\sqrt{\frac{51}{16} \cdot t_2^2 + \frac{\pi \cdot d^2}{4} \cdot \frac{f_m}{f_h}} - \frac{5}{4} \cdot t_2 \right] \cdot \frac{d}{2} \cdot f_h \tag{6}$$

in case of failure mode 3a, and

$$R_u = \frac{d^2}{4} \cdot \sqrt{\pi \cdot f_m \cdot f_h} \tag{7}$$

in case of failure mode 4.

The bending strength, f_m, of the dowels under scrutiny was
$f_{m,mean} = 236$ N/mm^2; standard deviation 23 N/mm^2
(manufacturer A)
and $f_{m,mean} = 279$ N/mm^2; standard deviation 20 N/mm^2
(manufacturer B), respectively.

The embedding strength, f_h, of the glulam under scrutiny was calculated in accordance with proposals of Whale, Smith and Larsen [1] as well as Ehlbeck and Werner [2]:

$$f_{h,mean} = 0.082 \cdot (1 - 0.01 \cdot d) \cdot \varrho_{mean} \tag{8}$$

(f_h in N/mm^2; d in mm; ρ in kg/m^3).

In Fig. 5 the ratio $maxF/minR_u$ is plotted against the slenderness ratio λ of all tests. maxF is the ultimate load-carrying capacity of each individual test specimen. $minR_u$ is the calculated resistance using Eq. (6) or (7).
Another manner of plotting is shown in Fig. 6 with the load-carrying capacities achieved by tests compared with those calculated by using the proposed equations. For the total of 128 test values the ratio of $maxF/minR_u$ turned out to be

0.95	(mean)
0.13	(standard deviation)
13.9 %	(coefficient of variation).

These results account for an acceptable reliability to use the modified failure mode 3a on the basis of Johansen's theory and confirm the proposal to use the bending strength of the dowel material instead of the yield strength in case of brittle material, such as impregnated densified laminated beech veneers.

The slip modulus, to be used for any shortterm deformation of joints of this type, was evaluated according to ISO 6891 and turned out to be significantly dependent on the dowel diameter as well as the wood density. A linear regression line reads

$$K_{mean} = (1.93 \cdot d - 10) \cdot \varrho_{mean} \tag{9}$$

(K in N/mm; d in mm; ρ in kg/m^3)
with a coefficient of correlation, r = 0.90.
This relationship is shown in Fig. 7.

4 Conclusions

Tests with brittle non-metallic dowels in glulam joints proved an additional failure mode compared to those used in the "classic" Johansen theory which is the basis for calculating the ultimate load-carrying capacities of joints with dowel-type fasteners in the CIB-Code and the draft EUROCODE 5.

It is proposed to add to the design formulae another one describing this failure mode where there is only one brittle bending failure in the middle member. Furthermore, in case of brittle dowel materials it is proposed to substitute the yield strength by the bending strength of the material.

5 References

[1] Whale, L.R.J., I.Smith and H.J.Larsen (1987): Design of nailed and bolted joints - proposals for the revision of existing formulae in draft Eurocode 5 and the CIB Code. CIB-W18A/20-7-1. Proceedings of meeting twenty of CIB-W18A, Dublin /Ireland.

[2] Ehlbeck, J., H.Werner (1988): Design of joints with laterally loaded dowels. Proposals for improving the design rules in the CIB Code and the draft Eurocode 5. CIB-W18A/21-7-4. Proceedings of meeting twentyone of CIB-W18A, Parksville (Vancouver Island)/Canada.

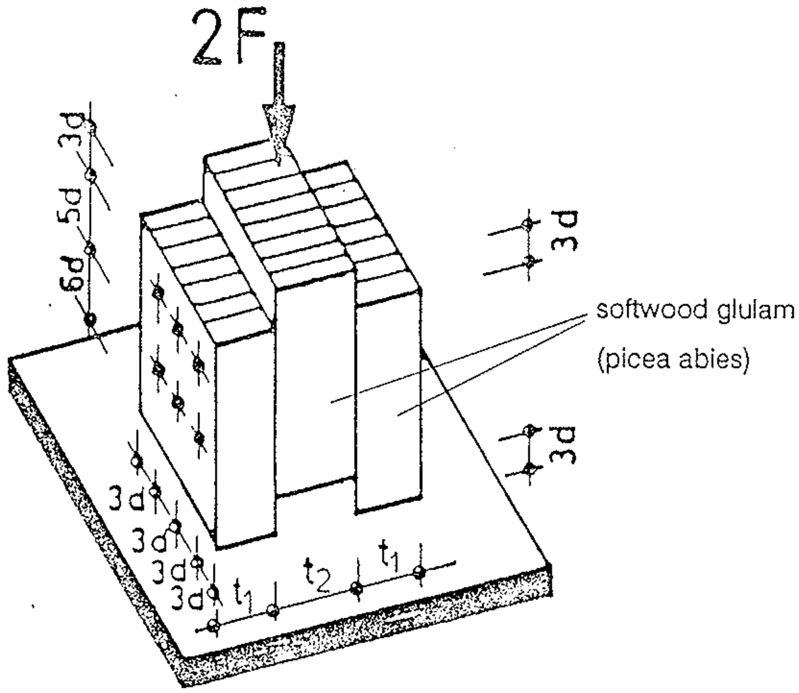

Fig. 1: Test specimen and dimensions;
d = dowel diameter

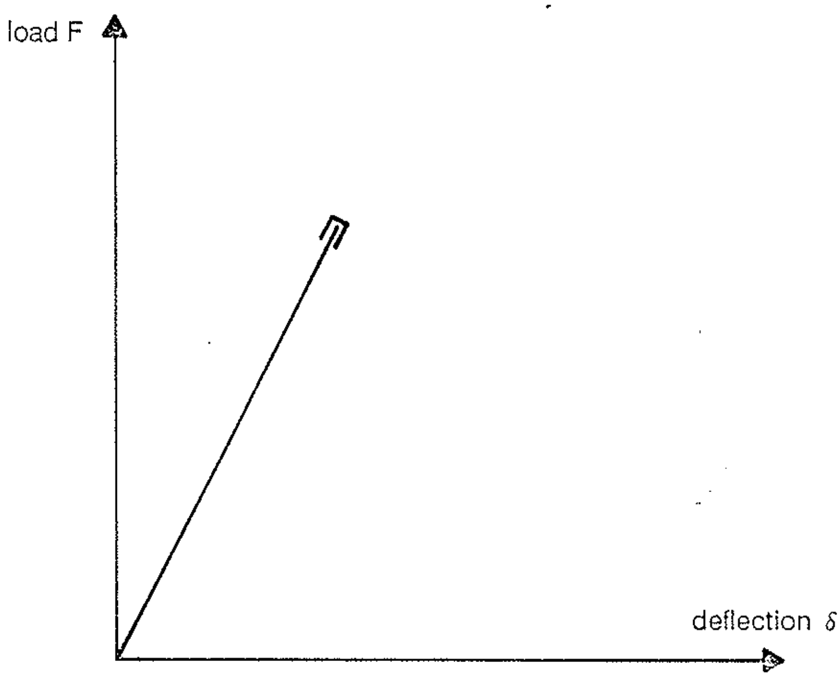

Fig. 2: Typical load - deformation relationship of the fastener material used

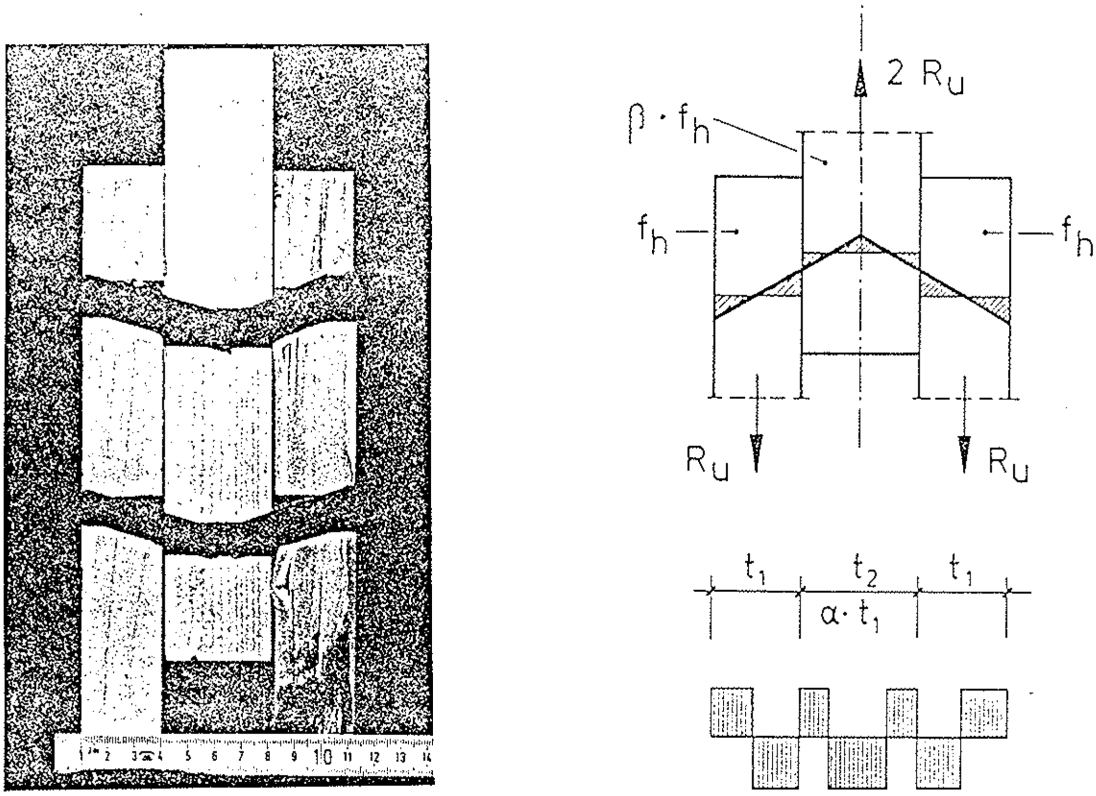

a)test specimen after failure   b)static model of the failure mode

Fig. 3: Failure mode 3a (only one bending failure of the dowels)

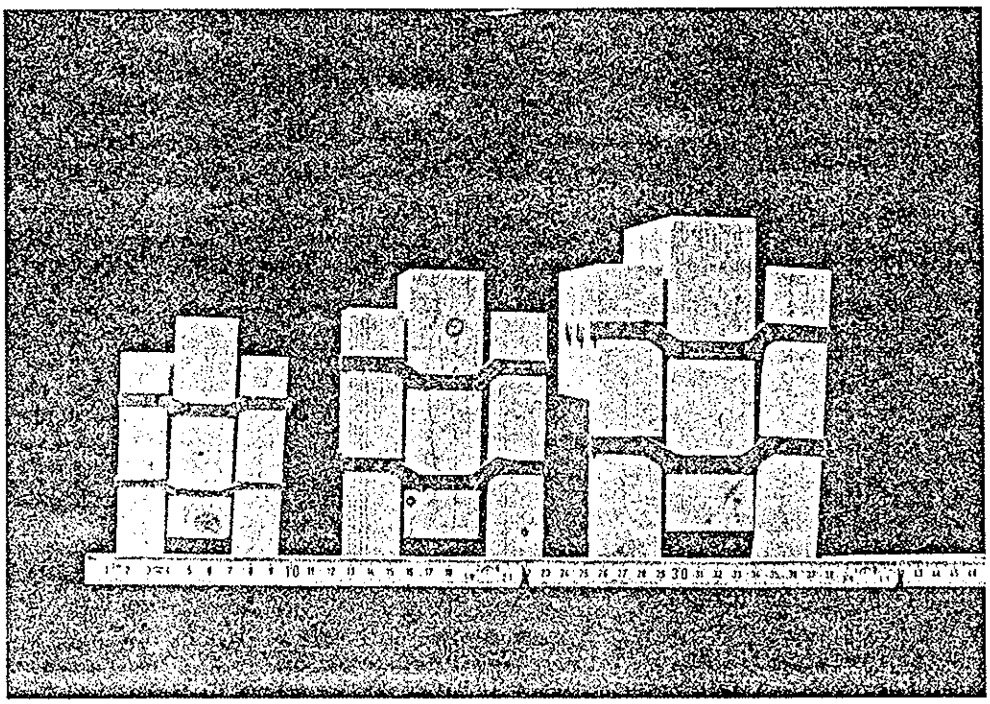

Fig. 4: Failure mode 4 with four bending failures of the dowels

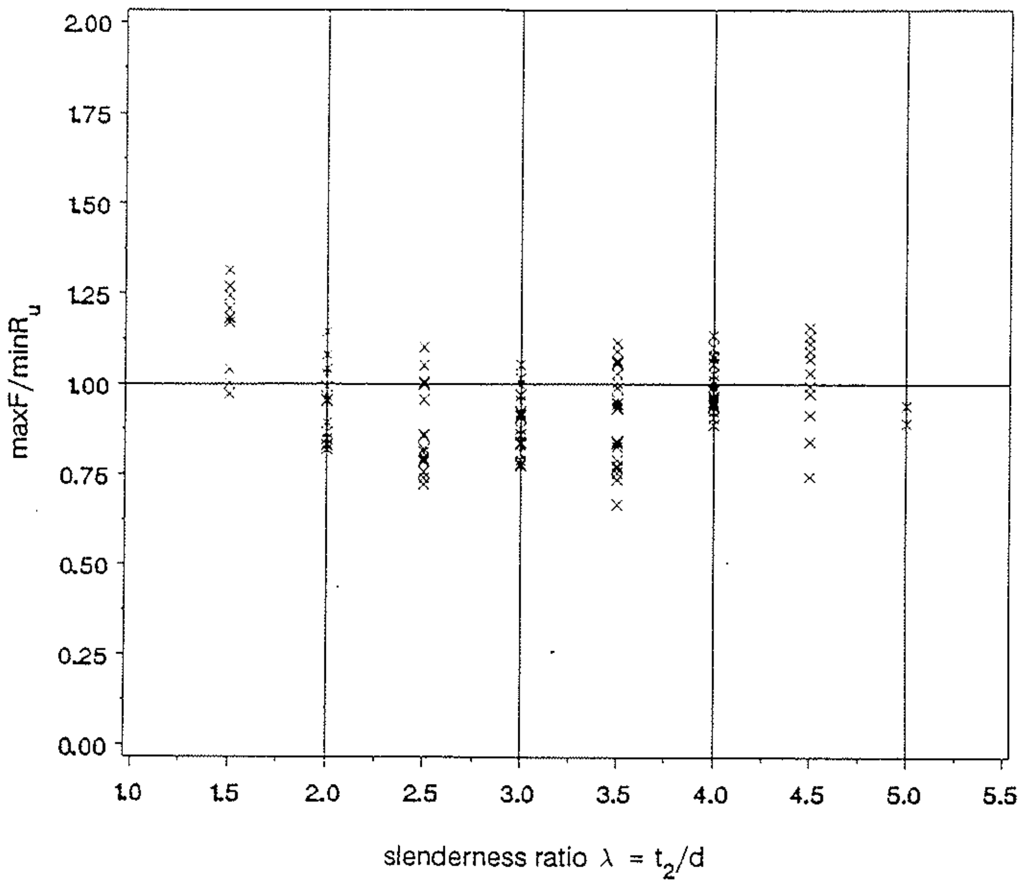

Fig. 5: Ratio maxF/minR_u over slenderness λ for all tests

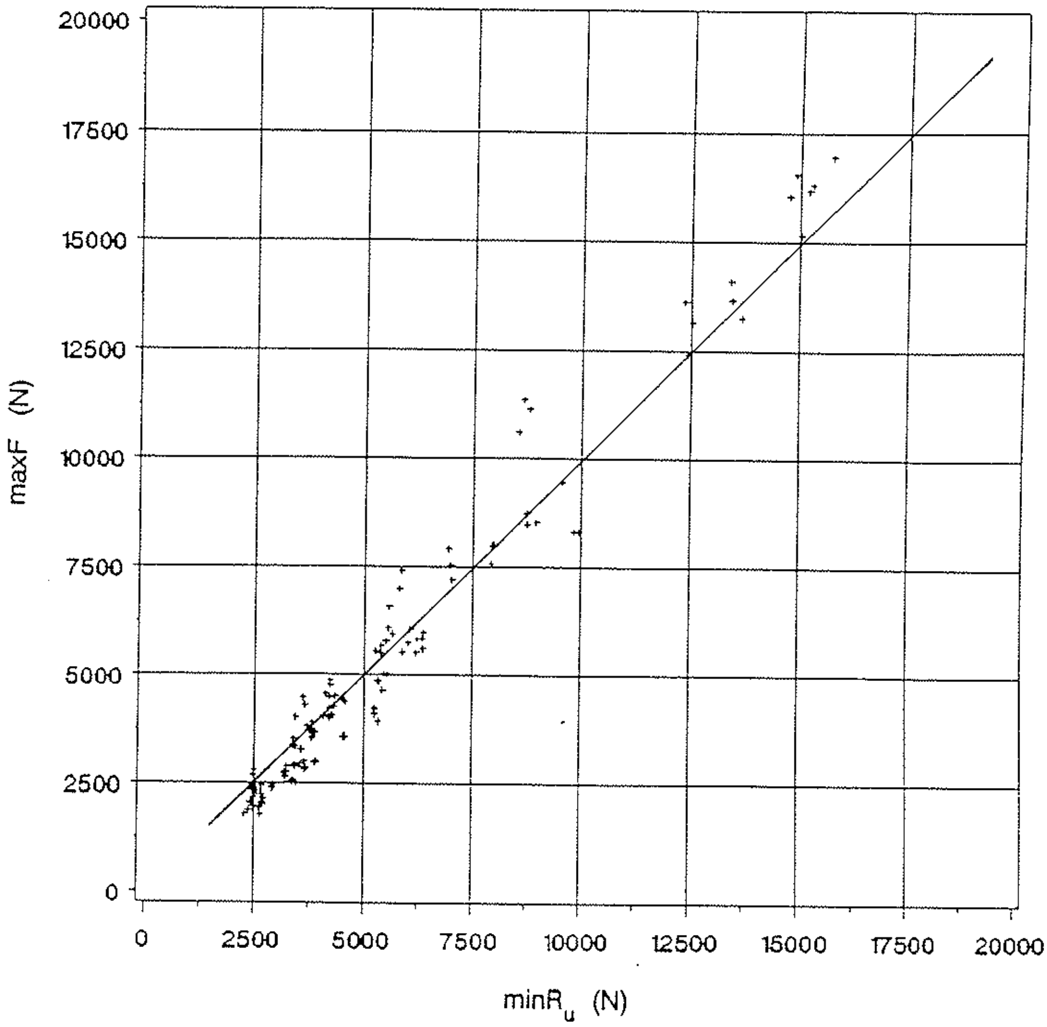

Fig. 6: Comparison of test results with calculated values

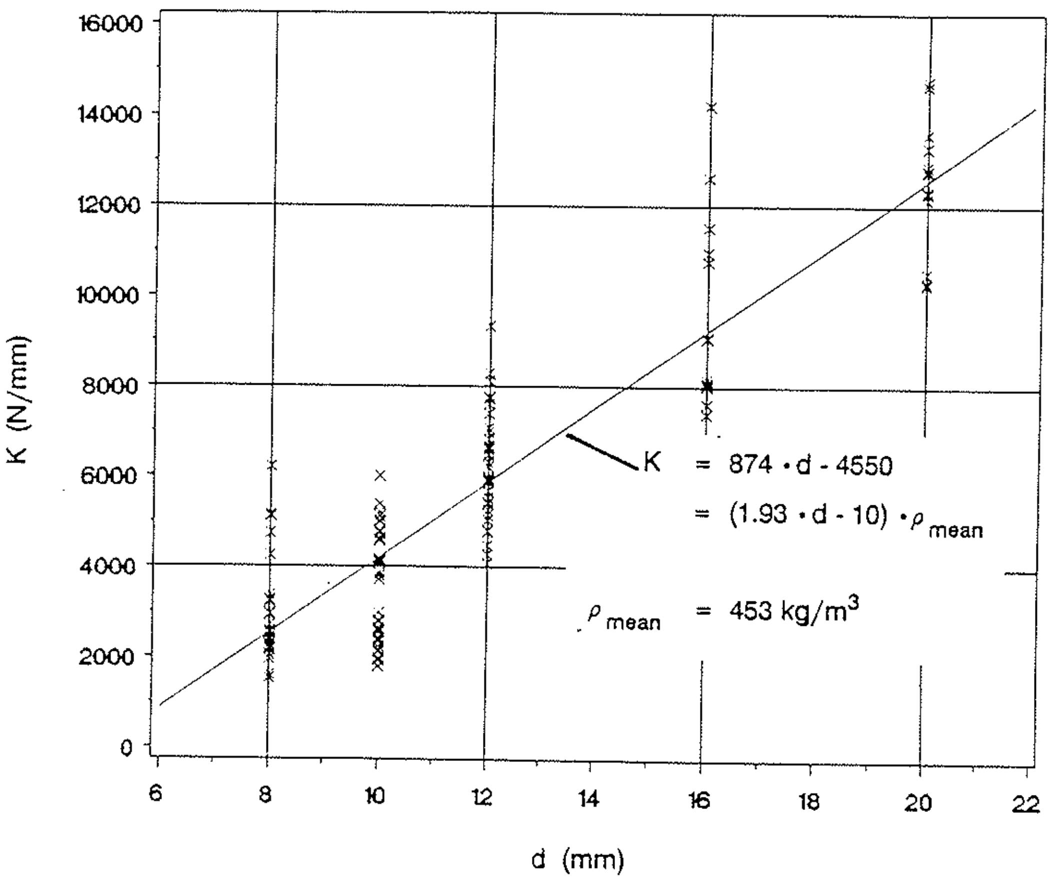

Fig. 7: Slip modulus K over dowel diameter, achieved from tests and evaluated according to ISO 6891 (128 test values)

CIB -W18A / 22-7-4

INTERNATIONAL COUNCIL FOR BUILDING RESEARCH STUDIES AND DOCUMENTATION

WORKING COMMISSION W18A - TIMBER STRUCTURES

THE EFFECT OF LOAD ON STRENGTH OF TIMBER JOINTS AT HIGH WORKING LOAD LEVEL

by

A J M Leijten
Delft University of Technology
Netherlands

MEETING TWENTY - TWO

BERLIN

GERMAN DEMOCRATIC REPUBLIC

SEPTEMBER 1989

THE EFFECT OF LOAD ON STRENGTH OF TIMBER JOINTS AT HIGH WORKING LOAD LEVELS.

A.J.M. Leijten
Delft University of Technology

Introduction

In many publications load duration has recieved a considerable amount of attention. Tests have revealed that the strength of timber is time- and load level dependent. For timber, damage accumulation models have been developed to describe this phenomenon. A point of discussion is still, whether the strength decreases in time, independently of the load level, or that damage occures after a certain load history. Some theoretical models backup this last approach [1]. Although the attention is mainly focused on the load duration properties of timber, tests on timber joints seems to behave in the same way [2]. In present timber codes long duration factors are used for timber and timber joints which range from 0.5 to 0.8

The prime objective of the present long duration tests on timber joints at the Stevin Laboratory is to get more insight at what load level and at what time damage occures. Although the research program will last another 5 years (started in 1983) already some results have become available and will be presented in this paper. The results indicate that there is indeed reason to believe that below the long duration threshold value no damage occures and that therefore present long duration values might be to conservative. Acceptation of the idea that the strength will not be effected by loads below this threshold level, would in its ultimate consequence lead to a total neglect of the load duration effect.

Load duration tests of joints.

It has been generally felt that there is a threshold load level called the long duration strength. About 1960 a program was started to test the long duration strength of joints at high load levels, 60 to 90%. Nails, split-rings and shear plates were used as fasteners. An Overview of the results are presented in fig. 1. [2]. After 26 years still 6 joints with nails and 2 with shearplates have survived a load level of about 60%. For joints the long duration strength is estimated at a level of about 50 to 60%. In 1983 an additional testprogram was setup with the same kind of joints, to perform load duration tests at low load levels, 30, 40 and 50%. After being loaded for a two years part of the 50% loaded joints are unloaded and tested to determine the residual strength. If no substantial strength decrease is recorded the remaining joints are uploaded 10% to a maximum of 50%, see fig.3 to 5. The testsetup was given during previous meetings [3][4].

Tentative Results

In 1986 a number of joints loaded to 50% were unloaded and tested to reveal any damage. No significant damage was recorded. In 1988 again a number of joints which had been loaded for 4.5 years were unloaded and SSD*-tested. During the first two years these joints were loaded to 40% after which the load was raised to 50% and continued for another 2.5 year. Prior to the SSD-tests, the joints have been left unloaded for a 5 months period to record the creep recovery. In Table 1 and in fig.2 the results are presented. Some of the testcharacteristics according to ISO6891 are given too. Notice the increasing stiffness of the shearplate joints and how much the displacements $v_{0.8}$ (slip at 80% of the max. load) differ from SSD-tests.

The most important conclusion is that at the present stage of the reseach program no strength loss is detected.

*SSD = Standard- Short- Duration

Table 1: Comparison of the strength: test characteristics according to ISO 6891

fastener type		SSD-test in	SSD strength	coef. var.	load level	loading time	v_e	v_{imod}	$v_{0.6}$	$v_{0.8}$	k_s
	n	year	[kN]		[%]	[days]	[mm]	[mm]	[mm]	[mm]	[kN/mm]
col.	(1)	(2)	(3)	(4)	(5)	(6)	(7)	(8)	(9)	(10)	(11)
nails	20	1962	44.1	0.04	-	-	0.21	0.55	1.10	2.26	31.8
	14	1983*	48.9	0.07	-	-	0.22	0.69	1.32	2.82	31.5
	10	1983	44.6	0.09	-	-	0.15	0.39	0.83	1.93	49.5
	10	**1985**	**45.9**	**0.03**	**50**	**721**	**0.24**	**0.85**	**1.09**	**1.52**	**21.9**
	9	**1988**	**47.5**	**0.05**	**40-50**	**1672**	**0.34**	**0.72**	**0.95**	**1.59**	**27.8**
split rings	20	1962	28.3	0.15	-	-	0.22	0.35	0.57	0.94	32.0
	5	1983*	27.7	0.15	-	-	0.19	0.42	0.66	1.10	26.1
	10	1983	29.8	0.14	-	-	0.23	0.45	0.68	1.01	29.6
	10	**1986**	**27.3**	**0.13**	**50**	**743**	**0.12**	**0.35**	**0.44**	**0.60**	**25.8**
	10	**1988**	**28.1**	**0.09**	**40-50**	**1662**	**0.17**	**0.29**	**0.43**	**0.69**	**21.2**
shear plate	20	1962	35.7	0.11	-	-	0.26	1.29	2.29	3.31	9.8
	6	1983*	35.7	0.12	-	-	0.27	1.29	2.23	3.17	11.1
	10	1983	35.4	0.12	-	-	0.20	1.33	2.50	3.68	11.6
	10	**1986**	**35.0**	**0.08**	**50**	**735**	**0.19**	**0.42**	**0.59**	**0.95**	**32.8**
	10	**1988**	**35.2**	**0.09**	**40-50**	**1658**	**0.17**	**0.30**	**0.45**	**0.84**	**23.5**

*) joints made of 1962 bought wood unloaded stored until 1983and then SSD-tested

References:

[1] van der Put, "Deformation and damage processes in wood", Delft University Press, 1989
[2] Kuipers, " Long duration tests on timber joints ", CIB-W18 meeting Stockholm,1977
[3] Kuipers, " Effect of age and/or load on timber strength", CIB-W18 meeting Florenze 1986
[4] Leijten, " Long duration strength of joints with high working load level", International Conference on Timber Engineering, Seattle 1988.

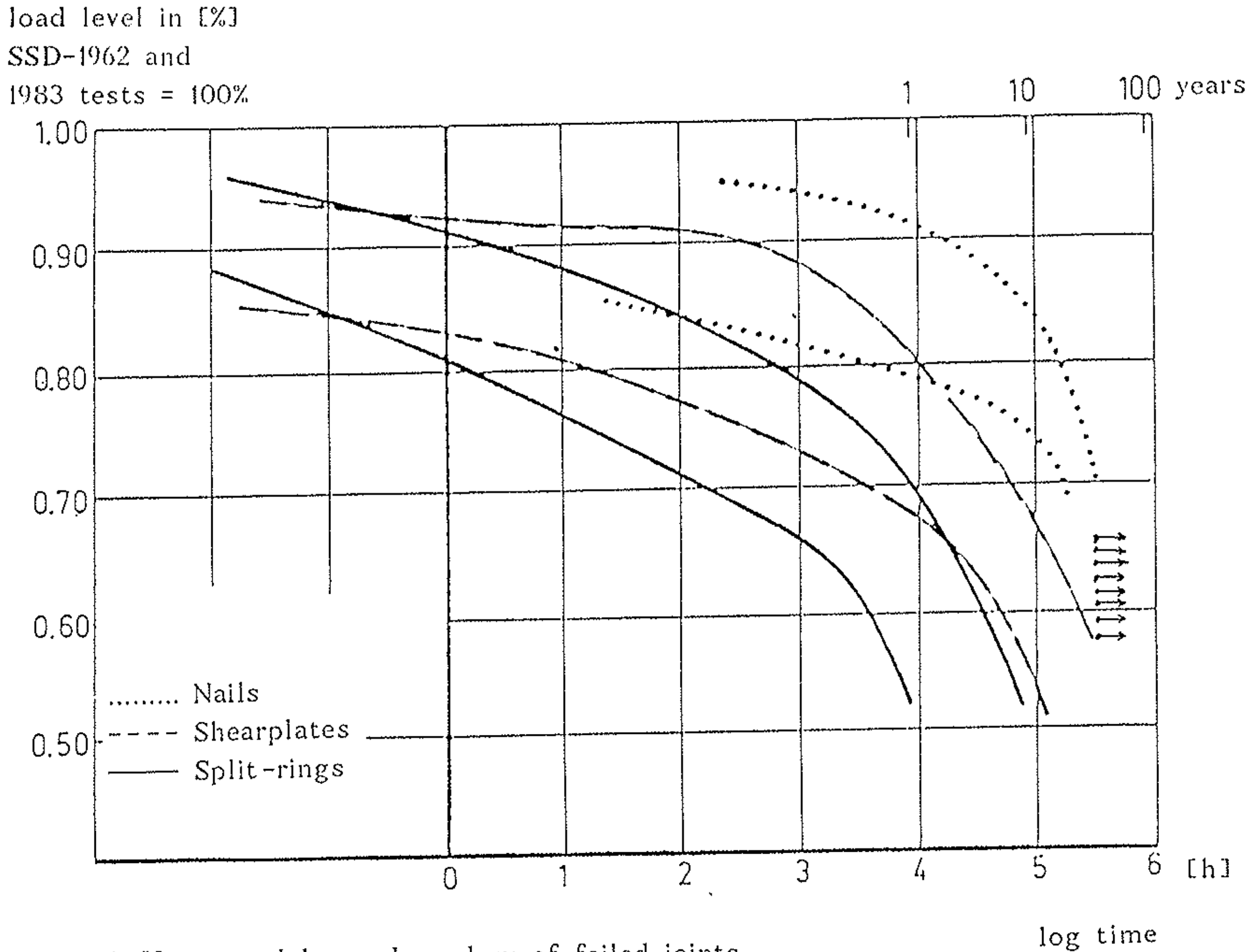

Fig.1: Upper and lower boundary of failed joints

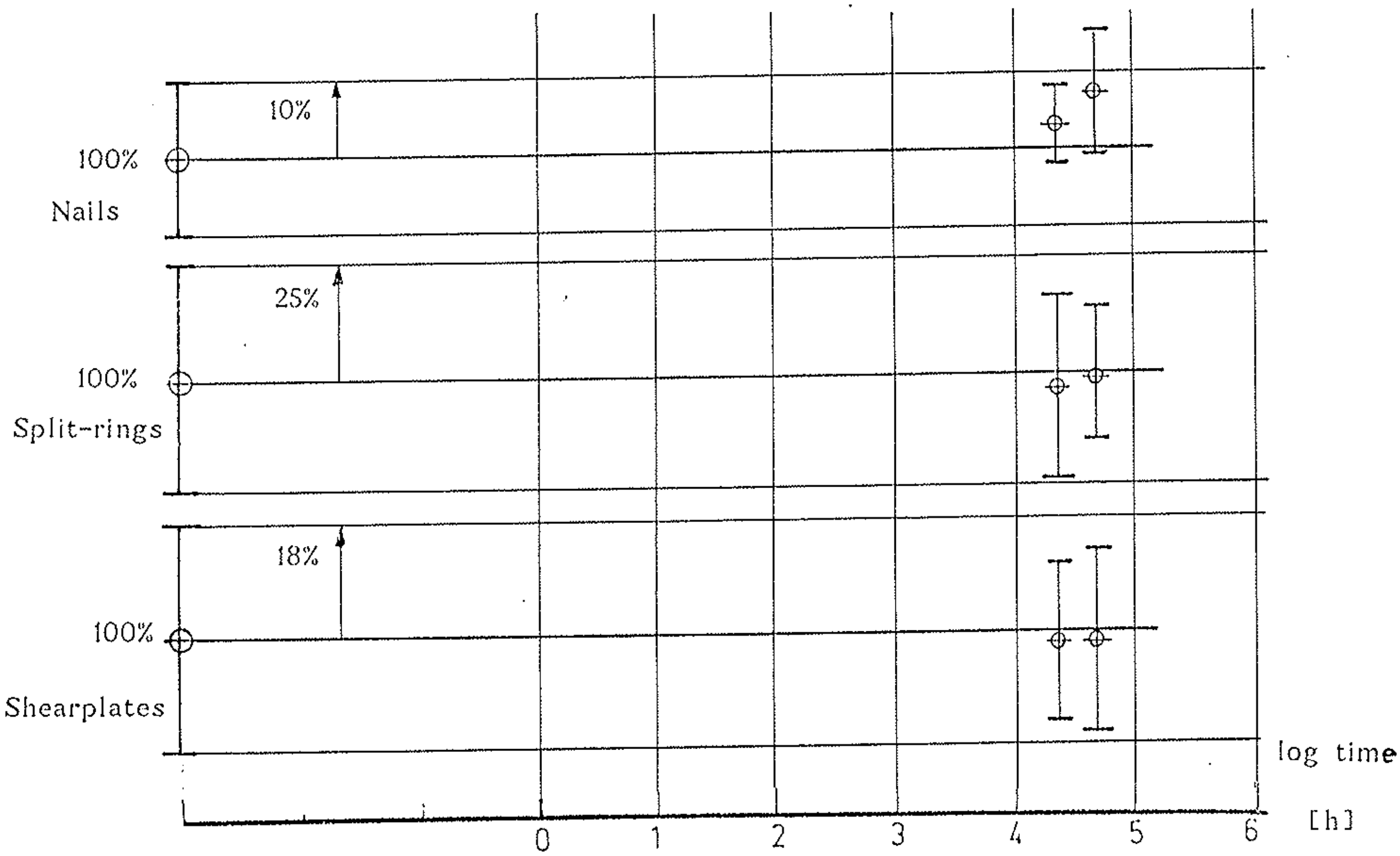

Fig.2: Comparison of the Standard Short Duration strength of joints with various load history. The strength of the joints without any load duration history is set to 100% while the 95% probability of these results is also indicated, see Table 1.

fig.3: Creep results of joints with nails and steelplate reinforced joints. The data of the reinforced joints is found at the bottom of the graph. During the first 2 years the load level was 40% afterwards 50%.

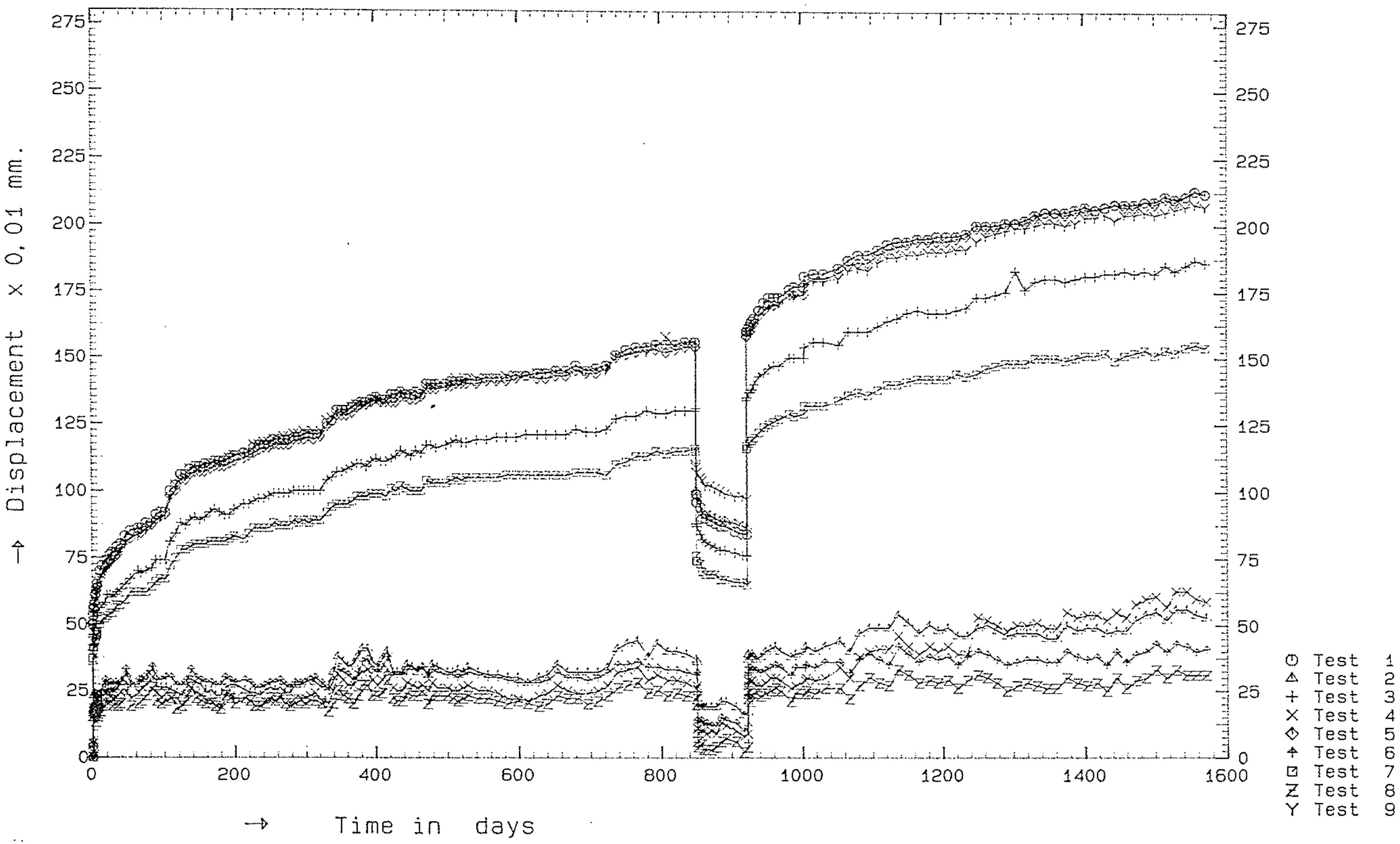

fig.4: Creep results of joints with splitrings and steelplate reinforced joints. The data of the reinforced joints is found at the bottom of the graph. During the first 2 years the load level was 40% afterwards 50%.

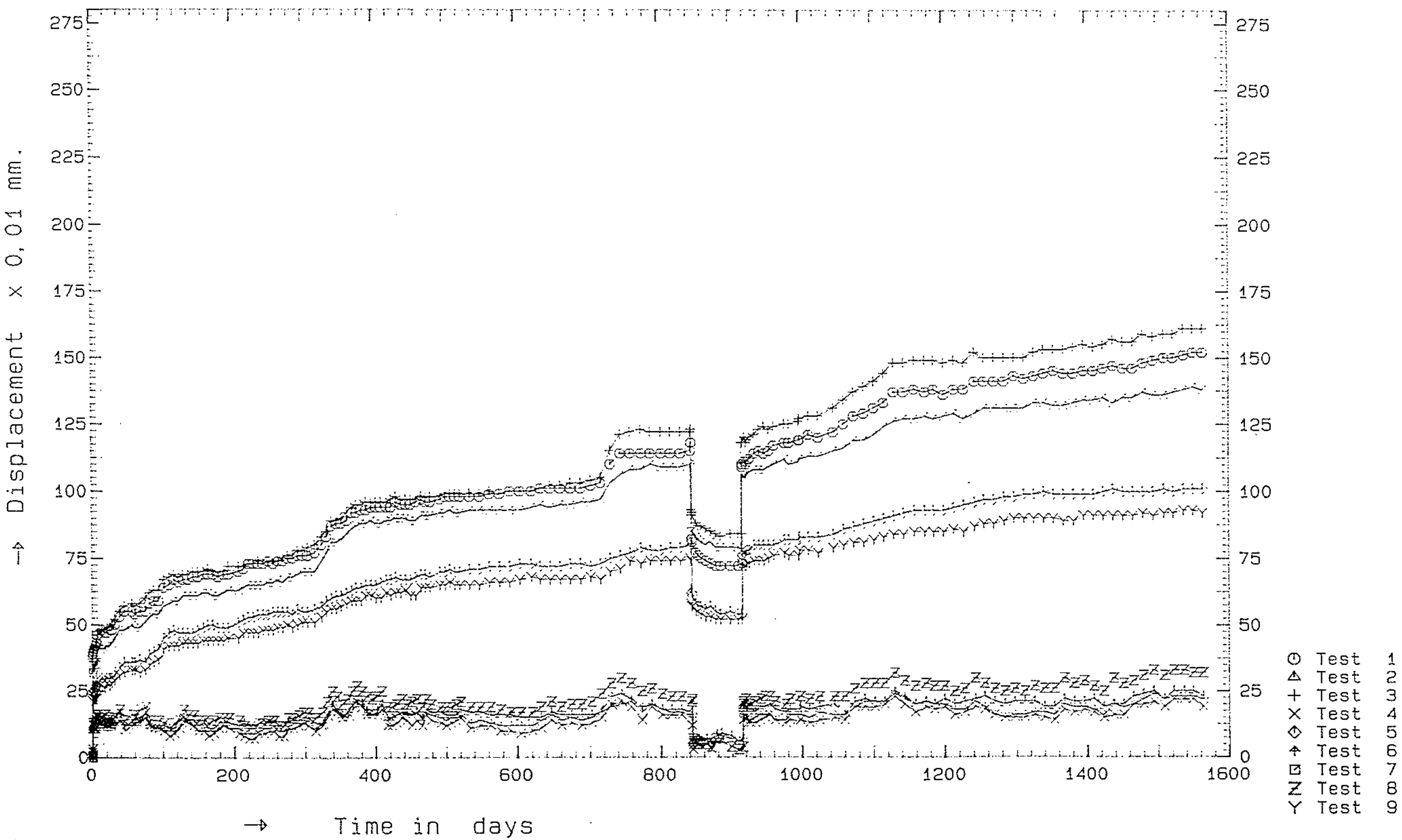

fig.3: Creep results of joints with shearplates and steelplate reinforced joints.
The data of the reinforced joints is found at the bottom of the graph.
During the first 2 years the load level was 40% afterwards 50%.

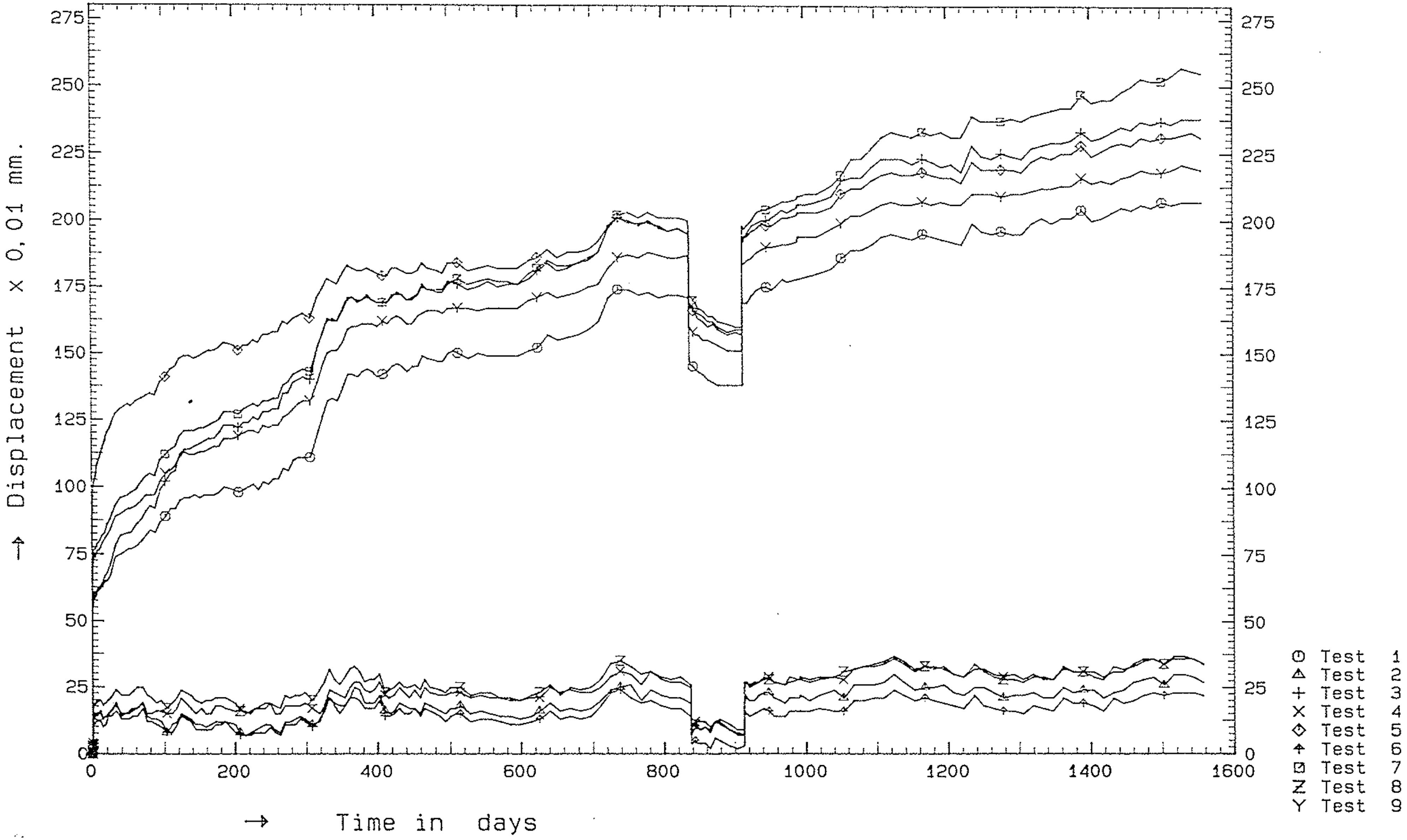

CIB -W18A / 22-7-5

INTERNATIONAL COUNCIL FOR BUILDING RESEARCH STUDIES AND DOCUMENTATION

WORKING COMMISSION W18A - TIMBER STRUCTURES

PLASTICITY REQUIREMENTS FOR PORTAL FRAME CORNERS

by

R Gunnewijk and A J M Leijten
Delft University of Technology
Netherlands

MEETING TWENTY - TWO

BERLIN

GERMAN DEMOCRATIC REPUBLIC

SEPTEMBER 1989

PLASTICITY REQUIREMENTS FOR PORTAL FRAME CORNERS

R.J.J. Gunnewijk
A.J.M. Leijten
Delft University of Technology

Introduction

Application of plastic theory in structural analyses for timber structures is not common practice. The main reason is that timber is regarded as an elastic material although it may have some plasticity in bending. The respons of a structures does not only depent on the material, joints play a part too. Although strength and stiffness properties are covered by code design rules, the ductility has not attracked much attention. This is one of the reasons why at present timber structures have such a bad position in Eurocode8, structures in seismic regions. Although the present used fastener types can be ductile, strength and ductility not always go together. Joints with many dowel type fasteners are stiff and strong but fail brittle. However the development of locally reinforced joints may change this stituation. This paper tries to formulate the ductility or moment rotation requirements of moment joints to insure a maximum of moment redistribution. This approach is not new [1], with some minor modifications this method is applicable for timber structures. An example is given about the capabilities of steel reinforced joints. The approach is straight forward and easy to handle. Because the design philosophy below is based on simple plastic theory inwhich geometrical non lineair effects are not included, the design rules only hold for braced frames.

The influence of the rotation springs on the respons of a braced portal frame.

The rotation stiffness of the rotation springs of fig.1 can be related to the stiffness of the member by eq.(1).

$$k_s = \frac{c\ L}{EI} \qquad \text{.......................................} \quad (1)$$

inwhich:
k_s : stiffness number
c : rotation stiffness
EI : bending stiffness of the member
L : span of the member

In unbraced timber portal frames the joint plays a dominant role because normally it is the weakest link in the structure. In [1],[2] it has been shown that when the joint stiffness has reached a treshold value the difference in the moment distribution found with infinite stiff joints is neglectable. This value is about k_s=25. For these k_s values also the horizontal deformations are very close together. The horizontal member of a portal frame with moment springs at the ends can be schematized as in fig.1. The resistance against rotation at the

ends is a combined effort of the portal columns and the stiffness of the joint. They can be combined as rotation springs in series. However for simplicity when the words "stiffness of the joint" has been used here the combined stiffnesses of moment joint and column is ment.
In the elastic loading stage the relation between the joint moment Mj(oint) and the rotation Θ is given as:

$$Mj = c \quad \Theta \qquad \ldots\ldots\ldots\ldots\ldots (2)$$

assuming a uniform load on the horizontal member the rotation is

$$\Theta = \frac{q\ L^3}{24\ EI} - \frac{Mj\ L}{2\ EI} \qquad \ldots\ldots\ldots\ldots\ldots (3)$$

Substitution of (1) and (3) in (2) gives

$$Mj = \left[\frac{ks}{ks + 2} \right] \frac{q\ L^2}{12} \qquad \ldots\ldots\ldots\ldots\ldots (4)$$

This equation is represented in fig.2 . The expression between brackes does not change much when ks is infinite which confirms the above statement that for stiffness values ks>25 the moment distribution will not differ much when infinite stiff joints were assumed.
When the bending moment at mid span is called Mf(ield) the load can be expressed in these parameters as

$$q = \frac{8\ (\ Mf + Mj\ )}{L^2} \qquad \ldots\ldots\ldots\ldots\ldots (5)$$

This equation inserted into (3) gives

$$\Theta = \frac{Mf\ L}{3\ EI} - \frac{Mj\ L}{6\ EI} \qquad \ldots\ldots\ldots\ldots\ldots (6)$$

This formula can be rewritten with (1) and (2)

$$\frac{Mj}{c} = \frac{Mf}{3} - \frac{Mj}{6} \quad \text{or} \quad Mj = \left[\frac{2\ ks}{ks + 6} \right] Mf \qquad \ldots\ldots\ldots\ldots\ldots (7)$$

Notice that for ks= 6 both bending moments at mid span and joint are equal which is regarded as an ideal situation for this loading situation.

Requirements for rotation capacity.
Because many parameters can be expressed in bending and rotation the moment - rotation diagram is used to visualize everything. For the derivation of the requirements eq.(3) (5) and (6) will mainly be used. In order to get a moment redistribution it will be clear that the yield moment of the joint Mj(ultimate) should be reached before the bending strength of the beam, so Eq(3) becomes:

$$q_{ult} = \frac{8\ (\ Mf + Mju)}{L^2} \qquad \ldots\ldots\ldots\ldots\ldots (8)$$

Form.(3) can be visualized in the moment- rotation graph by a straight line inwhich for
$\Theta = 0$

$$M_j = \frac{2}{3}(M_f + M_{ju}) \qquad \text{..............................(9)}$$

see line(1) in fig.3.
Eq.(6) represents a line in the graph where the bending strength of the beam is reached by substitution of M_f by M_{fu}. The intersection of both lines is a special location because here at the same moment three hinges occure. In Eq.(8) also M_f becomes M_{fu}. Substitution in (3) gives

$$\Theta = \frac{L}{6\ EI}(2\ M_{fu} + 2M_{ju} - 3M_j) \qquad \text{........................ (10)}$$

This equation is represented by line (2) in fig.3. So the coordinates of this intersection are.

$$(\Theta, M_j) = \left(\frac{2M_{fu} - M_{ju}}{6\ EI}\ L\ ,\ M_{ju} \right)$$

Now all necessary ingredients are available to use the graph and to make decisions about the capabilities of certain joints. Therefore a number of moment rotation characteristics have been drawn in fig.3 as A, B, and C. The joints have in common that they have the same strength but they have different stiffnesses. Joint A is very stiff but has insufficient rotation capacity in order to ensure maximum moment redistribution because it does not cross line 1 or 2, although the fasteners yield. Joint C is not stiff enough to ensure yielding of the joints before the bending strength of the beam is reached, because it crosses line 2 - no moment redistribution. Joint B is able to cross line 1 and is therefore the only one of these three which give a maximum moment redistribution.

Two additions will be made to the graphs. First the vertical axes are made dimensionless by dividing the moment values by $M_{f(u)}$. Secondly information is added about the yield moment ratio of the joint in relation to $M_{f(u)}$, at the right hand side of the graph by line (3). For instance when both $M_{f(u)} = M_{j(u)}$ and $k_s=6$ above analyses showed that yielding of the joint and the bending strength of the beam are occures simultaineously. When the strength of the joint is lower then the bending strength of the beam both lines (1) and (3) will subsequently shift downwards along line(2) as shown in fig.4 and fig.5. This also implies that yielding happens at lower loads meaning and that the moment redistribution will become less. So using joints with relatively low yield moments the amount of redistribution will decrease. This approach is direct and shows that not only strength but also stiffness and moment rotation capacity are important values for design in statically indetermined structures.

Deflections

This approach also enables the designer to control the deflections of the structure by changeing the joint stiffness. The derivation below is based on the deflections of a horizontal beam without a sheer. However if necessary this sheer could be can be added to eq. (11) without difficulty.

Deflection requirements at working load levels can be incorporated in the system as follows assuming that αL is the code limit (Eurocode5, α=0.004). The deflection at mid span for the load $q_u/\gamma = q_{ser}$ and $Mf_{(ser)}$ as the moment at mid span could be formulated as:

$$\text{deflection } \delta = \frac{1}{2}\, \Theta\, L + \frac{q_u L^4}{128\gamma EI} - \frac{Mf_{ser} L^2}{8\, EI} \leq \alpha\, L \qquad \text{.......... (11)}$$

Assuming that

$$Mj_{ser} + Mf_{ser} = \frac{Mj_u + Mf_u}{\gamma} = \frac{1}{8\gamma} q_u L^2 \qquad \text{......... (12)}$$

Eq.(12) inserted in (11) gives

$$\Theta \leq - \frac{L}{8\, EI} \left[\frac{Mf + Mj}{\gamma} - 2Mf_{ser} \right] + 2\alpha \qquad \text{....... (13)}$$

This equation represents the maximum allowed rotation at the end of the beam in order to satisfy the deflection requirement under service load. The bending moment at the joint which forces this rotation can be derived with eq . (3) add γ, and (12).

$$Mj_{ser} = \frac{11}{8} \frac{(Mj + Mf)}{\gamma} - \frac{8EI}{3\,L} \alpha \qquad \text{.......... (14)}$$

Both equations (13) and (14) given as a horizontal and vertical line in the moment rotation graph. The point of intersection is of interest for us. In order to satisfy the deflection requirements a moment rotation curve of a joint should pass this point (marked *) at the left hand side, see fig.3

Application to portal frames

The method will be evaluated for a portal frame with timber of strength classes LC 4/4 and 6/6 as given in the present EC5-code. The equations derived above then become only depend on the strength class and the ratio of the height and span of the beam (portal frame). In the graph, lines will be drawn for increasing yield moments of the joints: increments of 0.1 $Mf_{(ult)}$. The span to height ratios of the horizontal beam will be L/h= 25 and 30. The ultimate moment capacity of the beam is assumed to be:

$$Mf_u = \frac{f_{m,k}\; b\; h^2}{6\; \gamma} \qquad \text{................ (16)}$$

were $f_{m,k}$ is the characteristic bending strength and γ is the partial coefficient for material properties.

With $Mju = \beta\, Mfu$ and $\alpha = L/h$ together with eq.10 and

$$Mj = \mu \left[\frac{2(Mfu + Mju}{3} \right] \quad \text{with} \quad 0 \le \mu \le 1 \qquad \text{..........} (17)$$

so finally eq.(10) can be rewritten as

$$\Theta = \frac{2}{3}\,(1 - \mu)(1 + \beta)\,\frac{\alpha\ f_{m,k}}{E\ \gamma} \qquad \text{..........} (18)$$

For one value of $\alpha = L/h$ the value of β is increased with increments of 0.1 leading to a graph as shown in fig. 4 and 5 for $\alpha = 25$ and 30. For E-modulus the current EC5-code values have been taken. Corresponding with each line the deflection requirements at working load levels have been introduced, represented by a small circle symbol at the end of a straight line beginning at the origin. Because these are code dependent they should be handeled with care.
LC 6/6: $f_{m,k}$ = 35 N/mm^2, E= 13000 N/mm^2
LC 4/4: $f_{m,k}$ = 25 N/mm^2, E= 11000 N/mm^2
In these diagrams the rotation characteristic of a timber joint is still missing. To give an example the last chapter is added.

Discussion of some moment rotation curves

What now is lacking is the moment- rotation curve of a joint in fig. 4 and 5. However before doing so in the next chapter, a discussion is added to gain insight in the use and implications of these graphs. A number of moment-rotation characteristics is drawn in fig.7. Curves 1 to 4 corresponding with joint 1 to 4.
Joint 1: Moment capacity is β_1 Mfu. The rotation capacity is sufficient and the total bending moment will be $(1+\beta_1)$Mfu . The ultimate load is therefore $q_{u1} = 8(1+\beta_1)Mfu/L^2$. The deflection requirements are not satisfied because the curve passes at the left hand side of point δ_1.
Joint 2: Although the ultimate moment capacity is about β_2 Mfu the rotation capacity is insufficient to satify the requirements. The option is to change the h/L ratio of the beam or to modify the joint pattern. Nevertheless this joint satifies the rotation requirements related with β_1 Mfu. Therefore the load could be limited to q_{u1}. However at this yield moment the maximum bending moment at mid span is not yet reached $Mf = (1+\beta_1-\beta_2)Mfu$.
Joint 3: It has sufficient moment rotation to secure moment redistribution for a total moment of $(1+\beta_3)$ Mfu but does not satisfy the deflection requirements of δ_1.
Joint 4: This joint satifies all the requirement. The total total bending moment is $(1+\beta_3)$ Mfu.
Joint 5: The ultimate load for this joint is lower than $8Mfu/L^2$. This kind of joint should better be avoided.

10 Application for steel reinforced moment joints.

The experimental results of steel reinforced joints have been presented in [2] and [3] and more in detail in [4]. The joints connected with dowel type fasteners, are locally reinforced by steelplates which are glued to the surfaces of the all joint members separately. So each member has a steelplate glued to that surface were the dowel forces (shear) are large. On the bases of tests, relevant parameters have been determined. That means strength, stiffness and ductility. For the strength of the joint, M_{ju}, the Johanson-Meyer yield theory was modified for the difference in embedment strength of the timber and the steel reinforcement. The stiffness has been determined with a two parameter regression equation. When some requirements were fullfilled the maximum slip deformation of a fastener could be 15mm. It was decided to use a three branched linear characterization of the moment-rotation curve as shown in fig.6. This was done to check the deflection requirements. The slip modulus was defined in accordance with ISO8375 at a load of $0.4 f_u$ together with an additional one at $0.67\ f_u$. From this point an ideal plastic behaviour is assumed so the linearization under estimates the apparent maximum load at failure. In order to prevent brittle failure of the steel reinforced moment joint the bending strength should be limited to 70% of bending strength of the timber, $f_{m,k.}$, $M_{ju} = 0.7 M f_u$. Experiments were performed with moment joints with dowels in a circle pattern. With the data derived from these tests the implications for application of such a joint could now be analysed. Assumed yield moment of the joint M_{ju} in the graph $M_{ju} = 0.67\ M_{jmax} \rightarrow M_{ju} \leq 0.7 * 0.67\ M f_u = 0.5\ M f_u$. Several moment rotation curves can now be analysed. In fig. 8 and 9 the curves are presented for a beam height to span ratio of 20. Because the maximum slip deformation is set to 15mm the rotation capacity decreases with increasing beam height. Although in higher beams more than 8 fasteners fit into the circle pattern the number was helt constant for comparison. In fig.10 the same is done for a square pattern. Joining both fig.4 or 5 with fig.8 or 9 gives us the opportunity to demonstrate the method. In fig.10 this has been done for the square pattern of fasteners. A horizontal line at 0.5 $M f_u$ limits the application of this type of steel plate reinforced joint. One is able to combine the theory presented above and to judge which joint is appropriate.

Reinforced Joints

Although in this paper only reference have been made to steel reinforced joints it will be clear that in general the theory applies for every type of joint. The use of steel reinforced joints was to show the capabilities of the method. Concerning the reinforcement itself, there is not much reason to believe that steelplate reinforcement will be a promising method of reinforcement. The manufacturing processes such as blasting of the mill skin and degreasing before gluing of the steel plate on the timber is cost consuming and not very friendly for the environment. For timber industry steel is a totally different material were one needs special machinery. Therefore other materials are being tested, one of which is very promising. Lignostone (densified veneer) is a very promising alternative although some types are brittle. The development of an appropriate very ductile fastener, hollow tube, however insures the requirements for ductile behaviour. Experimental results will be reported in the near future.

Suggestion for future tests of joints is not to limite the slip deformation of dowel type fasteners to 15mm as prescribed by ISO8375, but relate the maximum slip deformation to the diameter of the fastener, for instance to twice the diameter. Always record the maximum slip deformation although it may exeed the 15mm limit. As for tubes, which can be regarded as dowel type fasteners, diameters upto 100mm may be needed to meet the rotation capacity requirements.

References:

[1] Bijlaard, Zoetemeijer, " Influences of joint characteristics on the structural respons of frames", TNO-IBBC report BI-86-30/63.4.3410, April 1986.

[2]Leijten,"Locally Reinforced joints", Proceedings of IUFRO-conference Timber eng. group s 5.02 Turku, Finland, juni 1988.

[3]Leijten, "Locally reinforced joints with dowels and bolts", Proceedings of the 1988 International Conference on Timber Engineering, Seattle 1988.

[4] Gunnewijk,"The mechanical behaviour of steel reinforced moment joints, the application in braced frames", in print.

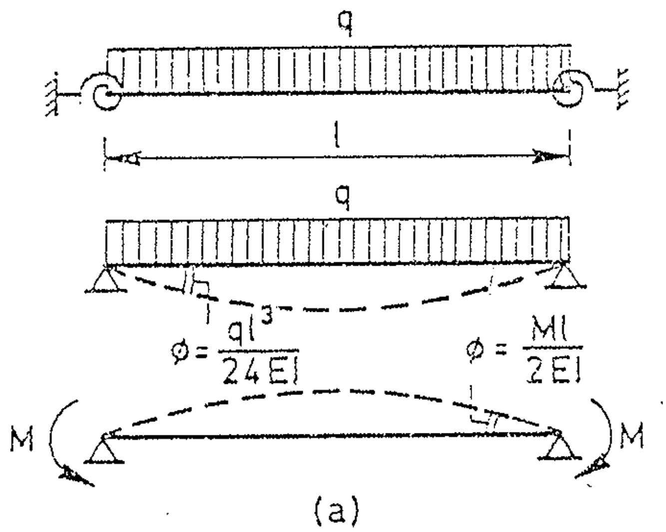

fig 1: Beam in brached frame

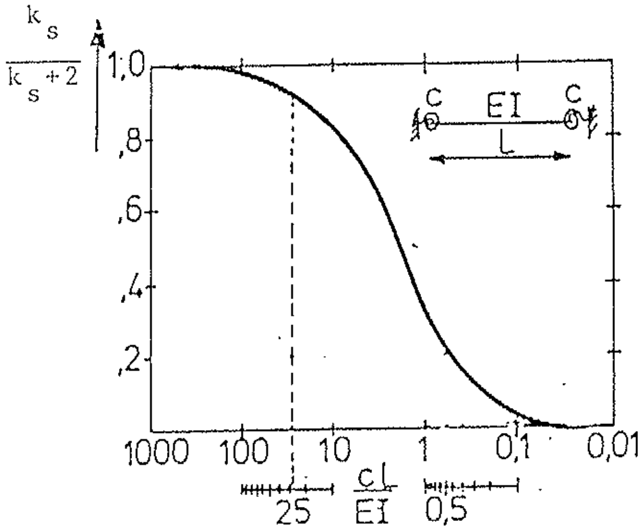

fig.2 : The bending moment at the joint in relation to the joint stiffness as given by form.(4).

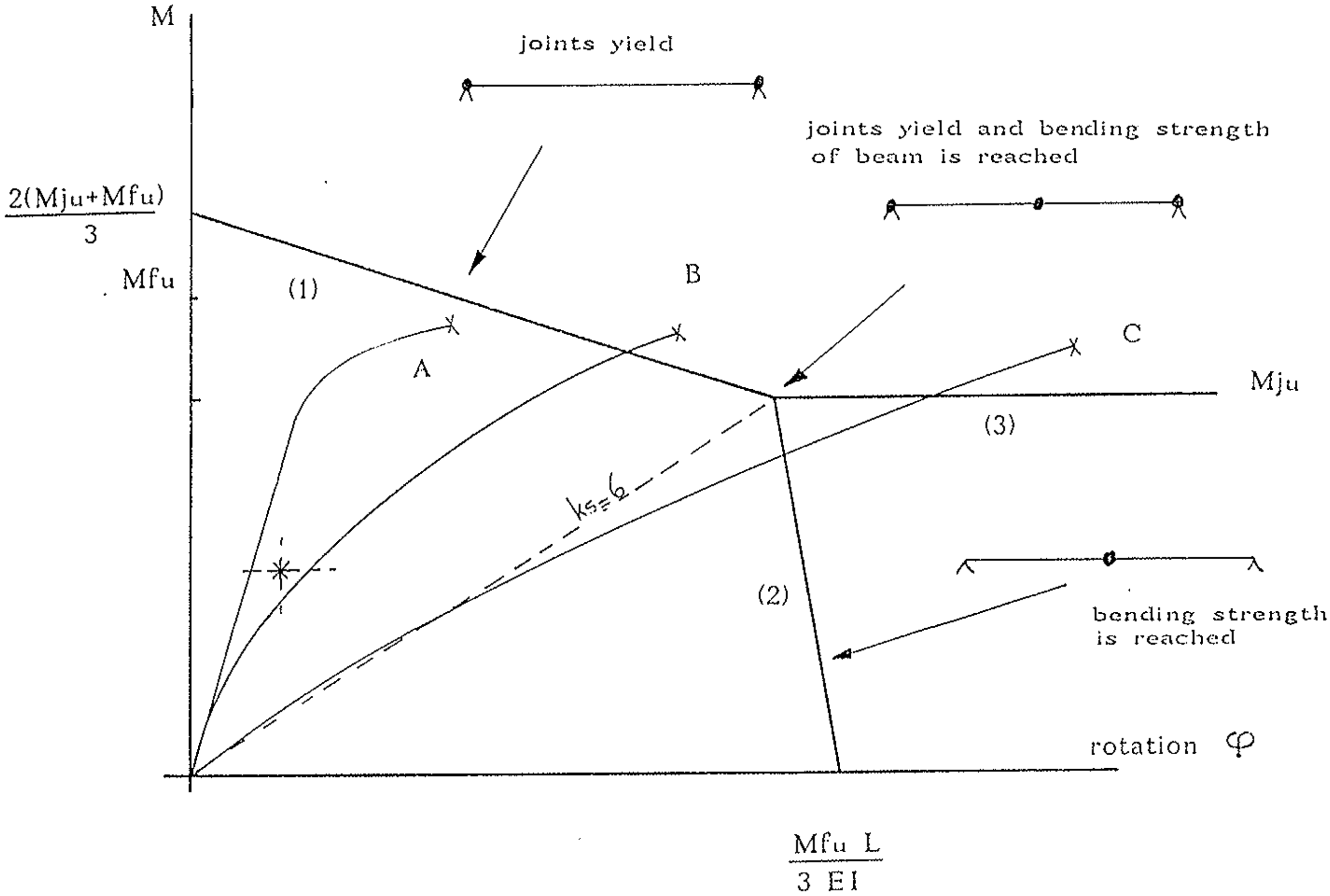

fig.3 : Requirements for rotation capacity

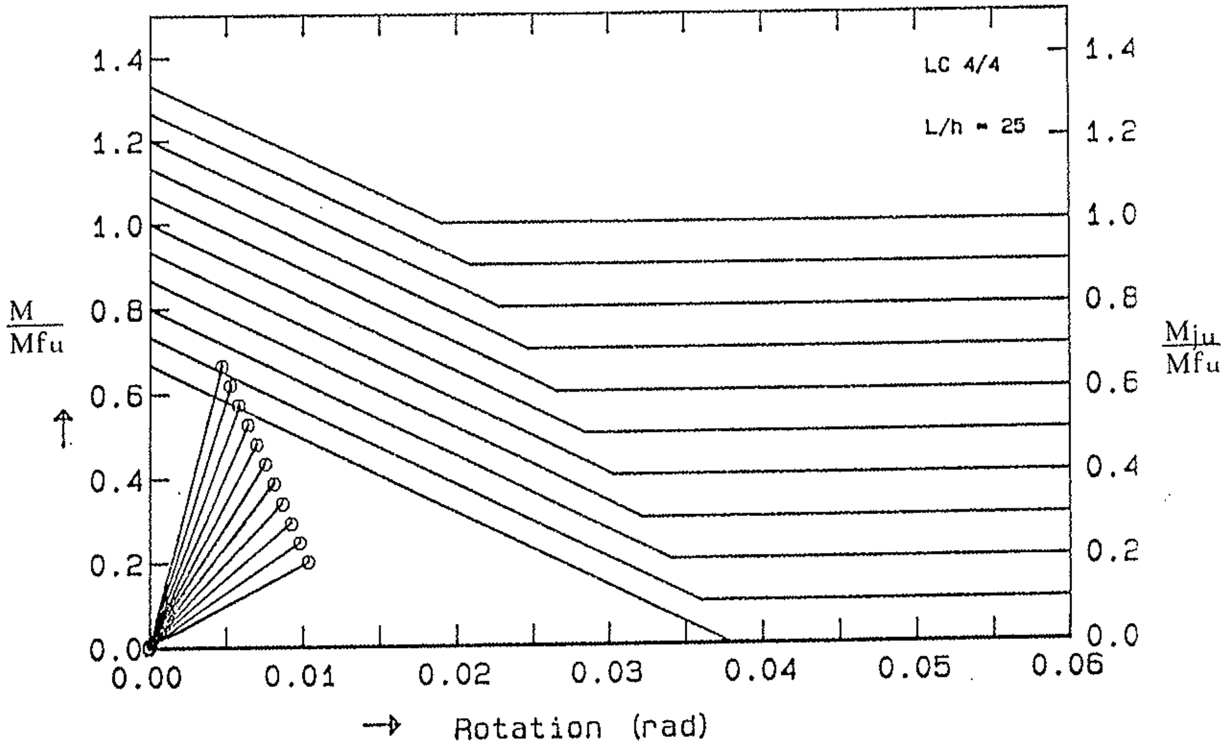

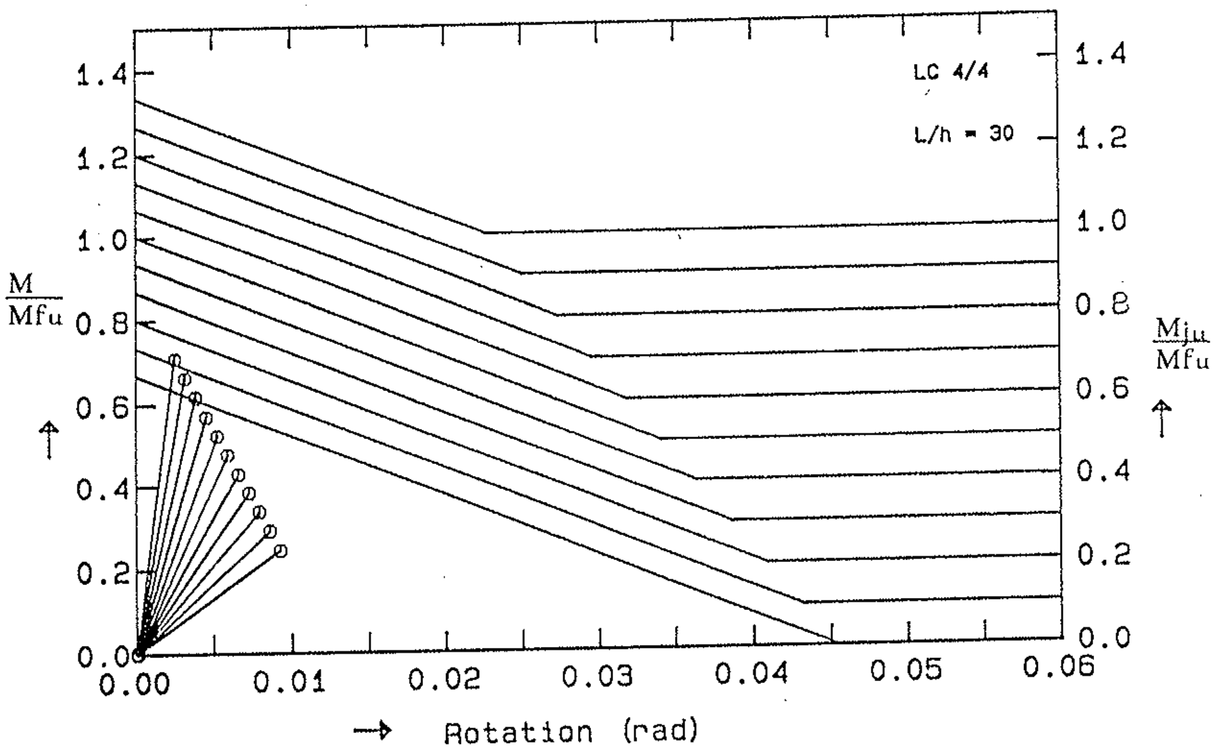

fig.4: Normalized moment - rotation graph with β increments of 0.1
Timber grade LC 4/4 (Eurocode5): L/h = 25 and 30

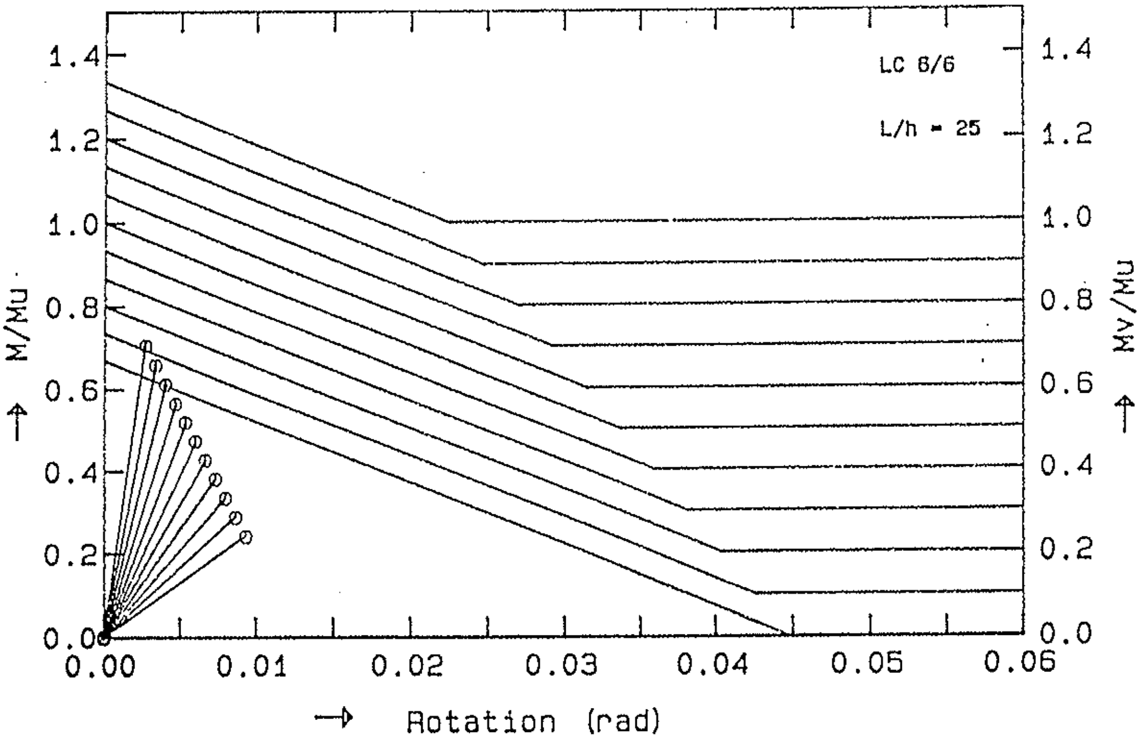

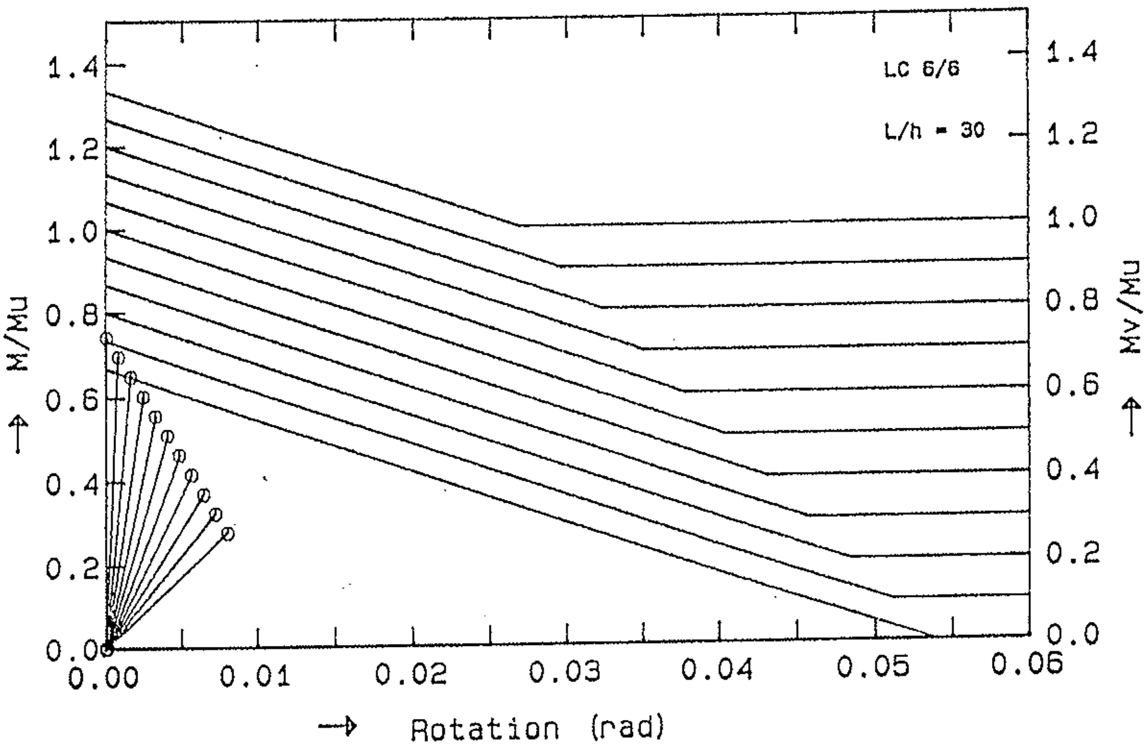

fig.5:: Normalized moment - rotation graph with β increments of 0.1
Timber grade LC 6/6 (Eurocode5) : L/h = 25 and 30

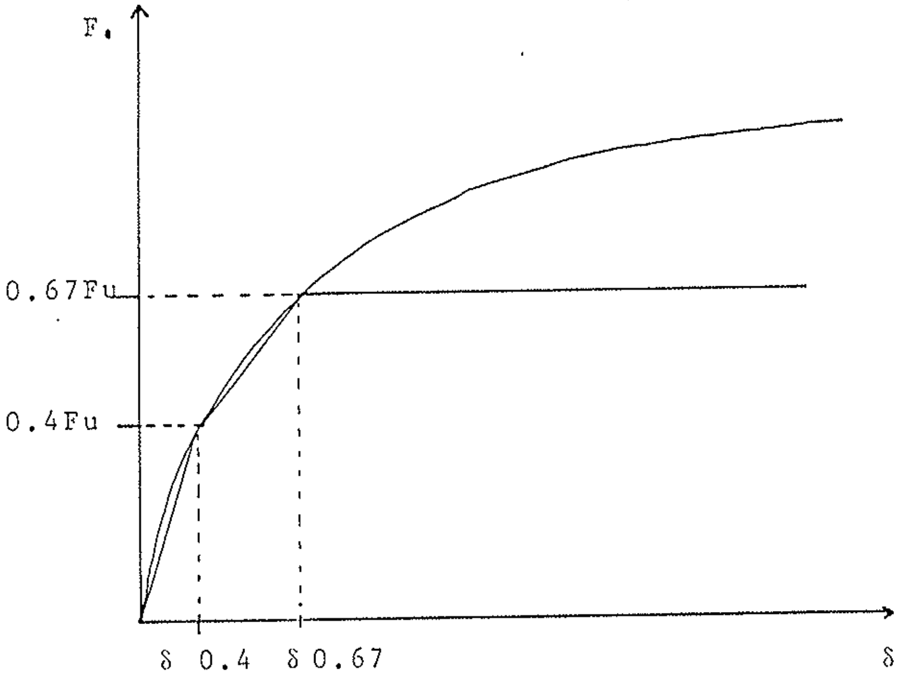

fig.6: Linear schematisation of the load slip curve of steel reinforced joints.

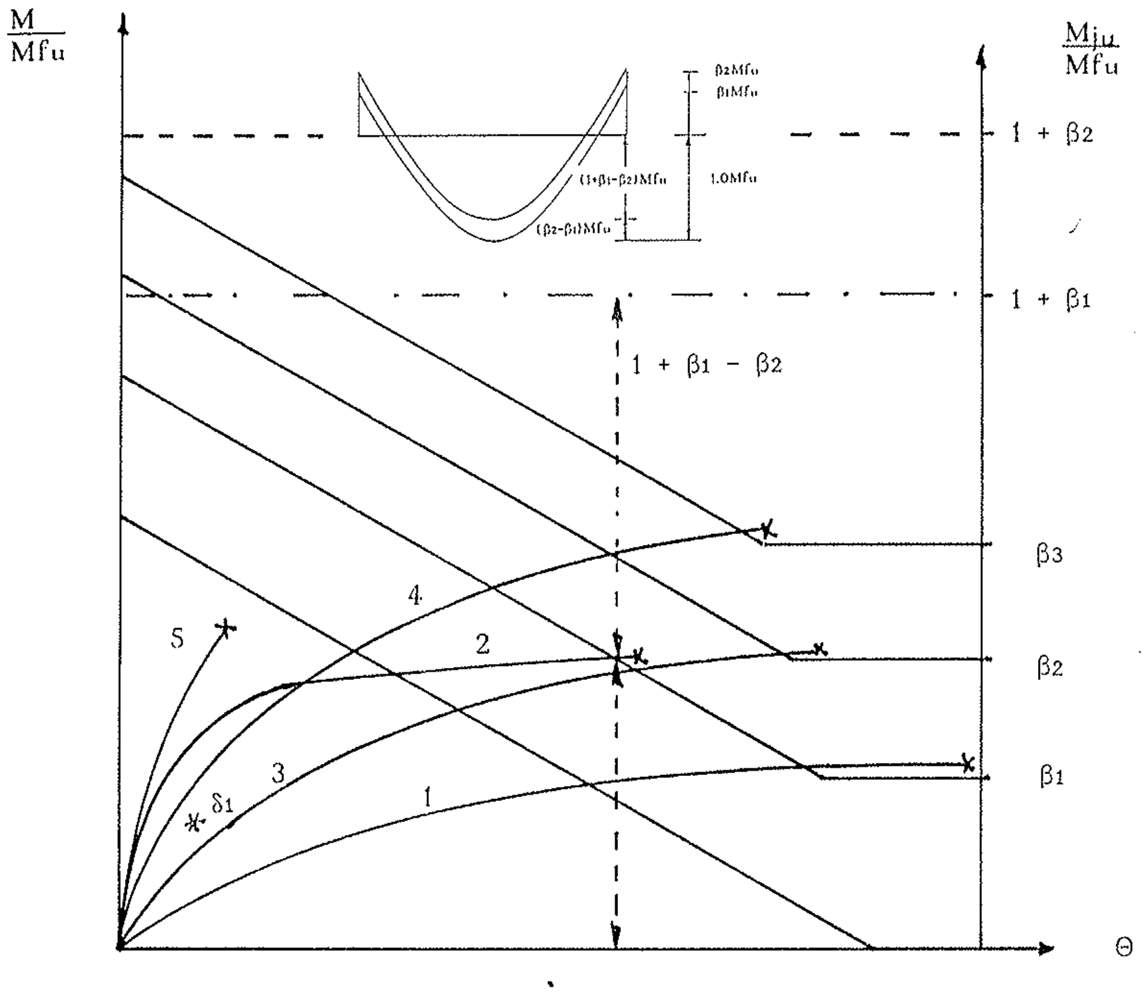

fig.7: Moment-rotation requirements combined with several moment-rotation curves.

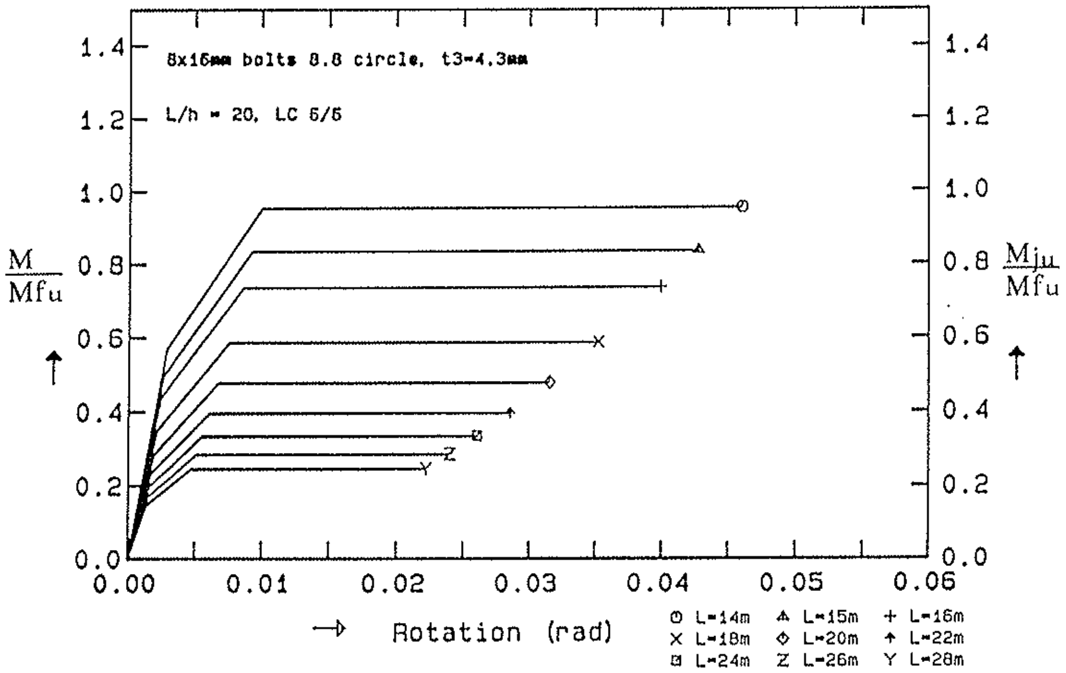

fig.8: Moment rotation curves of a steel reinforced joint with a circle pattern 8 bolts of 16mm diameter, steel plate thickness t=3mm for increasing spans.

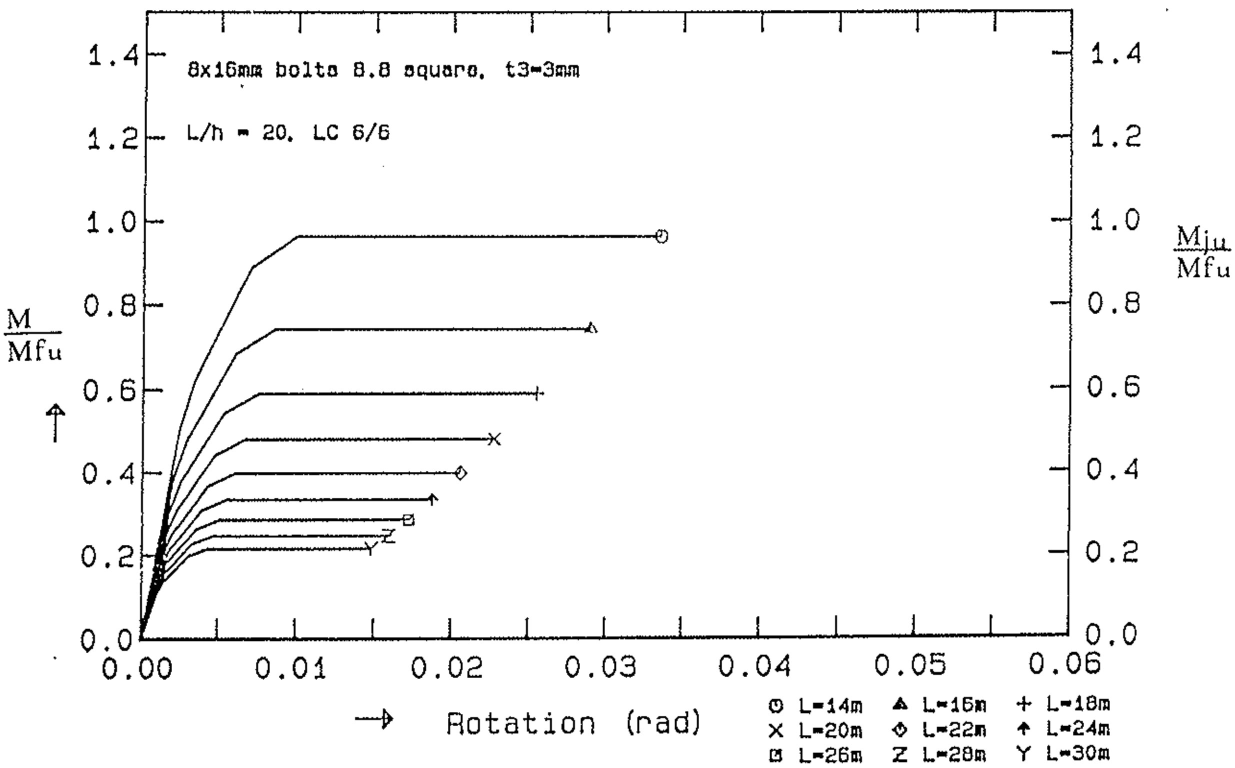

fig.9: Moment rotation curves of a steel reinforced joint with a square pattern 8 bolts of 16mm diameter, steel plate thickness t=3mm for increasing spans.

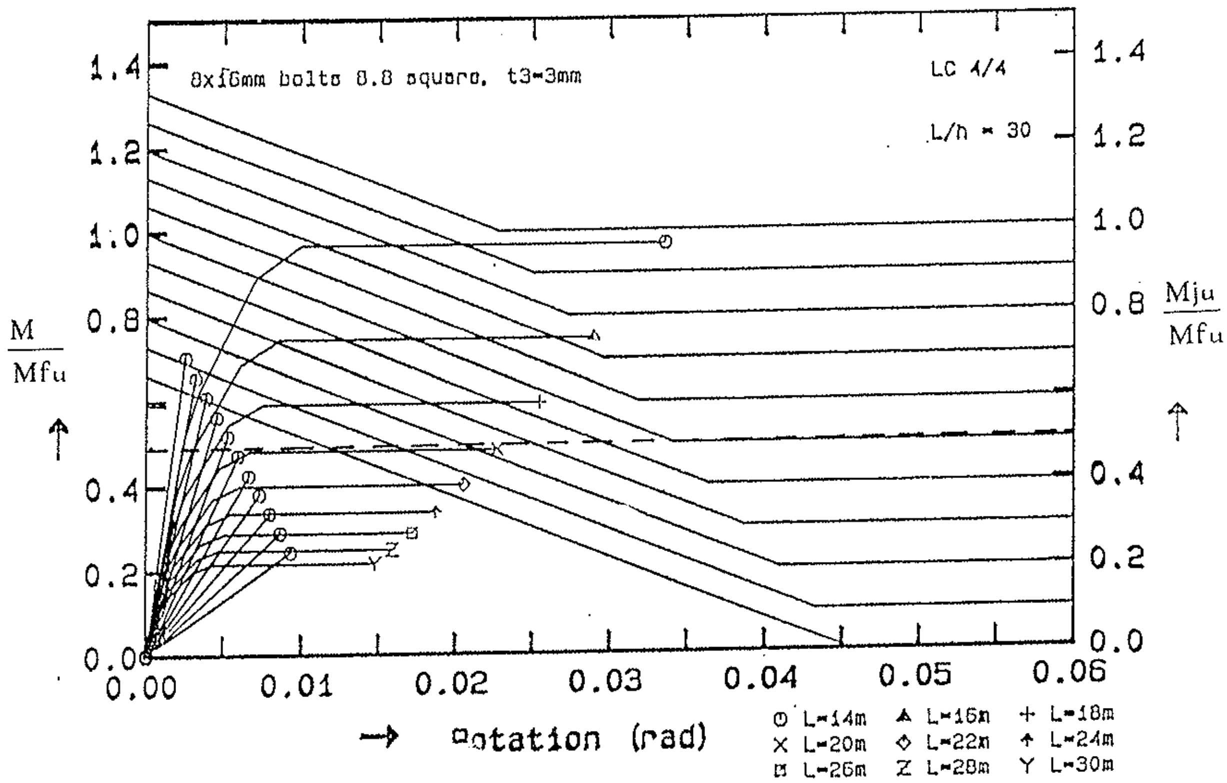

fig. 10: Combination of rotation requirements and moment-rotation curves of steel reinforced joints of fig. 9

CIB -W18A / 22-7-6

INTERNATIONAL COUNCIL FOR BUILDING RESEARCH STUDIES AND DOCUMENTATION

WORKING COMMISSION W18A - TIMBER STRUCTURES

BACKGROUND INFORMATION ON DESIGN OF GLULAM RIVET CONNECTIONS IN CSA/CAN3-086.1-M89

A proposal for a supplement of the design concept

by

E Karacabeyli
Wood Engineering Scientist
Forintek Canada Corp., Canada
and
D P Janssens
Structural Design Engineer
Canadian Wood Council

MEETING TWENTY - TWO

BERLIN

GERMAN DEMOCRATIC REPUBLIC

SEPTEMBER 1989

Background Information on Design of Glulam Rivet Connections in CSA/CAN3-086.1-M89 (Limit States Design)

by

Erol Karacabeyli, P.Eng.
Wood Engineering Scientist
Forintek Canada Corp.
6620 N.W. Marine Drive
Vancouver, B.C.
Canada, V6T 1X2
Tel : (604) 224-3221
Fax : (604) 224-3229
Telex : 04-508552

Dominique P. Janssens, P.Eng.
Structural Design Engineer
Canadian Wood Council
55, rue Metcalfe Street
Ottawa, Ontario
Canada, K1P 6L5
Tel : (613) 235-7221
Fax : (613) 235-9911
Telex : 053-3138

June 1989

ABSTRACT

Glulam rivets have been recognized by the Canadian Standards Association ("CSA") since the publication of the 1970 edition of CSA Standard 086. In that edition, the design procedures for glulam rivet connections (based on a large testing program carried out by the Western Forest Products Laboratory of Canada and the industry) were provided for Douglas-fir-Larch glued-laminated timber ("glulam"). Since then, researchers in Canada have conducted additional theoretical and experimental studies that contributed to the modifications in the design procedures for glulam rivet connections in the standard. This paper contains the background information on the modifications made in the design procedures of glulam rivet connections in the 1989 edition of the CSA Standard CAN3-086.1 (Limit States Design). Comparisons between the allowable (working) stress design code values and limit states design code values were made, and these design values were compared against previous full-size connection test results.

INTRODUCTION

The glulam rivet is an efficient fastener for timber construction, and because of its high load carrying capacity its use is increasing in Canada. Glulam rivet joints are being used on trusses, purlin to beam, beam to column, and column or arch to base connections. The dimensional specifications of the glulam rivets and a typical glulam rivet connection are reproduced from the CWC Datafile WJ-5 (1978) and illustrated in Figure 1. The rivet must be of Rockwell hardness C32-39, be hot-dip galvanized, and have a minimum ultimate tensile strength of 1000 MPa. The rivets are driven by hammer or pneumatic gun through predrilled holes in steel plates into the wood members. Steel side plates must be of mild steel conforming to specifications CSA G40.21-M81, Structural Quality Steels, or ASTM A36, Specification for Structural Steel. The minimum yield strength is 230 MPa and the minimum tensile strength is 380 MPa. The plates must be greater than 4.8 millimeters in thickness, must be hot-dip galvanized for wet service applications, and must be of adequate cross-section to resist tension and compression forces. The rivets must be driven through circular holes (minimum diameter 6.7 millimeters, maximum diameter 7 millimeters) in the steel side plates until the tapered heads are firmly seated, but rivets should not be driven flush. Minimum spacing of rivets is 12.5 millimeters in direction perpendicular to grain, and 25 millimeters in direction parallel to grain. Minimum edge and end distances for glulam rivet connections were reproduced from CSA Standard CAN3-086.1 and are shown in Figure 2. Tables 1 to 7 (referred to later in this paper) were also reproduced from the same standard.

The development of the glulam rivet (also known as griplam nail) goes back to the 1960s (McGowan and Madsen, 1965) where the concept of the rigid plate-nail joint was examined by testing numerous joints utilizing more than 33,000 rivets. This program was carried out by the Western Forest Products Laboratory of Canada (now Forintek Canada Corp. ("Forintek")), the Canadian glulam industry, and The Steel Company of Canada. This study revealed the importance of several parameters affecting the load carrying capacity of the glulam rivet connections. The study resulted in the following observations and recommendations:

(1) Of the three types (oval shank, round shank and twisted shank) of rivets investigated, the oval shank rivets had the optimum strength.

(2) It was recommended that, to reduce the splitting in the wood member, the long axis of the rivets are to be driven parallel to the grain of the wood member.

(3) Stiffness properties of the joint were greatly improved by hammering the tapered rivet-heads into the steel side plates to induce fixity between rivet-head and the plate.

(4) The lateral load carrying capacity in the direction parallel to grain was found significantly greater than the one in the direction perpendicular to grain.

(5) The lateral load carrying capacity increased with increase in rivet-length.

(6) For a fixed end-distance and number of rivets per row, lateral load carrying capacity increases linearly with increase in the number of rivet-rows.

(7) Minimum end, edge distances and minimum spacings were recommended.

(8) As a result of 100 load-cycles from zero to 1.78 kN per rivet and back to zero, a slight residual slip was permanently induced. Very little increase in residual slip was observed subsequent to the first cycle. No apparent decrease in the ultimate strength of rivets was observed due to cyclic loading.

(9) Glulam rivet capacity is governed by one of two types of failure modes: either rivet yielding or wood failure modes. These failure modes are explained in detail later in this paper. In rivet yielding failure mode, slip under constant load increased with time at a diminishing rate. No apparent decrease in ultimate strength was observed due to constant loading.

The load-slip characteristics of glulam rivets were studied by Foschi (1974) for the rivet yielding failure mode where the rivet bends and yields while the wood under the rivet's shank fails in bearing. Later, Foschi and Longworth (1975) studied the behavior of glulam rivet connections in rivet yielding and in wood failure modes, and established the design procedures which form the basis of the glulam rivet design section in CSA Standard CAN3-086, Canadian Code for Engineering Design in wood. Fox (1979), Fox and Lincoln (1979), and Karacabeyli and Foschi (1987), and Karacabeyli and Fraser (1989) performed further experimental and theoretical studies on glulam rivet connections. The latter study provided a species factor for the spruce/lodgepole pine/jack pine glulam rivet connections in CSA Standard CAN3-086.1-M89.

There are two versions of the 1984 edition of CSA Standard CAN3-086 (Canadian Code for Engineering Design in Wood):

(1) Working Stress Design Version (CAN3-086-M84);

(2) Limit States Design Version (CAN3-086.1-M84).

The glulam rivet design section in this 1989 edition was written in Limit States format, but was calibrated to the 1984 Working Stress Design Code (CAN3-086-M84) (i.e., both codes give similar number of rivets for a given design load). This paper contains the background information for the glulam rivet design tables and procedures in CAN3-086.1-M89. In addition, comparisons between the allowable (working) stress design code values and limit states design code values were made, and these values were compared against full-size connection test results (Foschi and Longworth, 1975).

DESIGN PROCEDURE FOR GLULAM RIVET CONNECTIONS FOR CAN3-086.1-M89

The design procedure outlined in this paper was developed by Foschi and Longworth (1975). The authors calibrated this design procedure to Limit States Design format. This work will appear as an appendix to CAN3-086.1-M89 and forms the basis of design tables in that standard.

The procedures outlined below are applicable for a glulam rivet connection (one plate and the rivets associated with it) in side grain. The factored lateral load resistance of the connection must be equal or greater than the factored loads. The load factors for dead and live (snow or floor) loads in National Building Code of Canada (1985), are respectively 1.25 and 1.50.

The parameters listed below are used throughout this paper:

n_R = number of rows of rivets parallel to the direction of the load

n_C = number of rivets per row

L_P = rivet penetration (rivet length - 10), mm

S_P = rivet spacing parallel to grain, mm

S_Q = rivet spacing perpendicular to grain, mm

b = thickness of the member, mm

a = end distance, mm

e_P = edge distance (free edge), mm

J_Y = side plate factor
= 0.90 for side plates between 4.7 mm and 6.3 mm in thickness
= 1.00 for side plates 6.3 mm and more in thickness

ϕ = performance factor (0.60)

H = species factor
= 1.0 for Douglas-fir-Larch glulam
= 0.8 for Lodgepole pine- Jack pine and/or Spruce glulam

K_D = load duration (DOL) factor: 1.15 for short-term (dead plus wind, earthquake, falsework, formwork, impact)
1.00 for standard term (dead plus floor, snow)
0.65 permanent (dead)
More details are given in Table 11.

K_{SF} = Service condition factor: 1.00 for dry, 0.85 for wet service conditions

K_T = Fire retardant treatment factor: 0.90 if fire retardant is used, 1.0 if not used.

The design procedures include rivet yielding failure mode, and three types of wood failure modes (tension parallel to grain and longitudinal shear failure modes in loading parallel to grain, and tension perpendicular to grain failure mode in loading perpendicular to grain).

Design for Loading Parallel to Grain

For loading parallel to grain, the factored lateral strength resistance (P_r) of the joint shall be the lesser of:

$P_r = \phi P_n J_Y$ for rivet capacity, or

$P_r = \phi P_t K_D K_{SF} K_T$ for wood capacity in tension, or

$P_r = \phi P_v K_D K_{SF} K_T$ for wood capacity in shear

where P_n, P_t and P_v in kN shall be determined as follows:

a) $P_n = P_1 \, n_R \, n_C \, H$

where:

$P_1 = 1.091 \, L_P^{0.32}$

b) $P_t = \dfrac{F_{tN} \, S_Q \, (n_R - 1)}{K_t \, \beta_t \, \varepsilon_t} \, H X_t$

where:

F_{tN} = specified strength in tension parallel to grain at net section, (20.4 MPa for glulam)

29:05:00069-A

K_t = constant depending on n_R and n_C (Table 1)

β_t = constant depending on S_p, S_Q and n_R (Table 2)

ε_t = constant depending on b, L_p (Table 3)

X_t = factor for code calibration (1.41)

c) Note for the cases where $b \leq 175$ mm, $S_P = 38.1$ mm, $S_Q = 25.4$ mm and $L_P \geq 55$ mm, P_V will be greater than P_t, and therefore need not be calculated

$$P_V = \frac{F_V\, L_P\, [S_P\,(n_C - 1) + 50.8]\, H}{K_V\, \beta_V\, \gamma}\, X_V$$

where:

K_V = constant depending on n_R and n_C (Table 4)

β_V = constant depending on S_P and S_Q (Table 5)

F_V = $f_V\,(0.15 + 4.35\,C_V)$ in MPa, (f_V is longitudinal shear strength, 2.0 MPa for glulam)

C_V = $(\beta_1 + \beta_2\,\beta_3)^{-0.2}$

γ = $90.5 + 5.376\,L_P$

β_1 = $\frac{L_P\, S_P\, (n_C - 1)}{1344}\,[1 + 502.2e^{-0.512\,(S_Q - 12.7)}]$

β_2 = $50.39 \times 10^{-18}\, L_P\,[(n_C - 1)\,S_P]^3\;[(n_R - 1)\,S_Q]^{4.5}\,e^{-0.01(a - 50.8)}$

β_3 = $\left(\frac{3\mu - 1}{2} + L_P\,\frac{1 - \mu}{50.8}\right)^5 (1 - e^{-1.9\,(b/2L_P - 1)})^5$

μ = $43.88\,[(n_C - 1)\,S_P]^{-0.4}\;[(n_R - 1)\,S_Q]^{-0.2}$

X_V = factor for code calibration equal to 1.48.

Design for Loading Perpendicular to Grain

For loading perpendicular to grain, the factored lateral strength resistance (Q_r) of the joint shall be the lesser of:

Q_r = $\phi\, Q_n\, J_y$ for rivet capacity, or

$$Q_r = \phi\, Q_t\, K_D\, K_{SF}\, K_T \qquad \text{for wood capacity in tension perpendicular to grain}$$

where Q_n and Q_t in kN shall be determined as follows:

a) $Q_n = Q_1\, n_R\, n_C\, H$

where:

$Q_1 = 0.618\, L_P^{0.32}$

b) $Q_t = Q_A\, L_P^{0.8}\, C_t\, H$

C_t = constant depending on e_p, n_c, S_Q (Table 6)

Q_A = constant depending S_p, S_Q, n_c, n_R (Table 7)

Alternately, Q_A may be calculated as follows:

$$Q_A = \frac{23.3\, X_{tp}\, F_{tp}\, [(n_R - 1)\, S_p]^{0.8}}{K_{tp}\, \beta_{tp}\, 10^3\, [(n_C - 1)\, S_Q]^{0.2}}$$

where:

X_{tp} = factor for code calibration equal to 1.45

F_{tp} = specified strength in tension perpendicular to grain, (0.83 MPa for glulam)

K_{tp} = constant depending on n_R and n_C (Table 8)

β_{tp} = constant depending on S_P and S_Q (Table 9)

Design for Loading at an Angle to Grain

For loading at an angle, θ, to the grain, the factored lateral load resistance (N_r) of the connection can be calculated by Hankinson's formula:

$$N_r = \frac{P_r\, Q_r}{P_r \sin^2\theta + Q_r \cos^2\theta}$$

COMPARISONS BETWEEN THE CODE DESIGN VALUES AND TEST DATA

The glulam rivet design values in CAN3-086 are based on the test results given in Foschi (1974). A summary of average ultimate lateral load carrying capacities of rivets of different lengths from four research studies (Foschi, 1974; Fox, 1979; Fox and Lincoln, 1979; Karacabeyli and Fraser, 1989) are given in Table 10. The species factor (H) for spruce/lodgepole pine/jack pine glulam was developed by Karacabeyli and Fraser (1989). Mathematical representations of the load-slip data of the glulam rivets are given in Foschi (1974), and Karacabeyli and Fraser (1989).

The ultimate lateral load carrying capacity of glulam rivets in rivet yielding failure mode may also be derived by use of the yield theory developed by the Danish scientists K.W. Johansen and H.J. Larsen. According to this theory, the yield load (F_u) of a two member joint with one steel member and with two yield points is (Aune and Patton-Mallory, 1986):

$$F_u = \sqrt{2}\sqrt{2}\ f_e M_y$$

where f_e is the wood embedding strength (N/mm) and M_y is the nail yield moment (Nmm).

Foschi (1974) determined the wood embedding strength (f_e)-deformation (Δ) relationship for glulam rivets for Douglas-fir:

$f_e^{/\!/}$ = 241.7 (1.0 - exp (-2.94 Δ)) when the narrow face of the rivet shank is bearing parallel to the grain direction, and

$f_e^{\perp}$ = (88.5 + 23.3 Δ) (1 - exp (-2.59 Δ)) when the wide face of the rivet shank is bearing perpendicular to the grain direction.

Foschi (1974) also determined the yield strength of steel (1420 N/mm^2) used in glulam rivets. Using the above information and cross-sectional dimensions (3.2 millimeters by 6.4 millimeters) the yield loads of:

$F_u^{/\!/}$ = 5.48 kN in parallel to grain, and

$F_u^{\perp}$ = 3.53 kN in perpendicular to grain were obtained for Δ = 4.8 mm.

These values fall within the range of values found for three different rivet length (90, 65 and 40 millimeters) tested by Foschi (1974), (Table 10). The yield theory is not used further in this paper in the prediction of ultimate loads for full-size connections because it is not applicable to wood failure modes.

The allowable loads for glulam rivets for "Normal (10 year) Load Duration (dead plus floor loads)" in CAN3-086-M84 (Working Stress Design) are based on the median short-term load carrying capacity divided by a factor of 3.36 for the wood failure modes. This factor (3.36) was developed by Foschi and Longworth (1975). The allowable loads were obtained by computing the maximum short-term (less than 10 minutes) stress corresponding to a probability of failure of 0.05 (5th percentile) and further dividing that by a reduction factor to account for the effect of load duration and the possibility of overload. The maximum stress corresponding to probability of failure of 0.05 (5th percentile) was obtained by dividing the median stress by 1.6 (this is based on a two-parameter Weibull distribution of longitudinal shear stresses). This maximum short-term (less than 10 minutes) 5th percentile stress was further divided by a reduction factor (2.1) to account for the effect of load duration (DOL) and the possibility of overload. This factor includes an overload component of 1.3, and DOL effect component of 1.6 to derive normal duration (10 year) of load strength from short-term (less than 10 minutes) 5th percentile stress values. Thus, a total reduction factor of 1.6 x 2.1 = 3.36 was applied to the maximum short-term (less than 10 minutes) 5th percentile stress value to obtain the allowable load for the connection for normal (10 year) load duration in wood failure modes. Foschi and Longworth (1975) also recommended this factor (3.36) for the rivet yielding failure mode because this factor leads to allowable loads, which correspond to a nearly elastic behavior of the rivet, in its load-slip characteristic. The allowable loads in CAN3-086-M84 in rivet yielding failure mode are based on this factor (3.36) and a further 12 percent reduction made because of material changes as indicated in the commentary of the CAN3-086.1-M84. No DOL factor applies to the allowable loads in rivet yielding failure mode.

Changes in DOL factors have been introduced in the 1989 edition of CAN3-086.1 where specified strength values are given for standard term load duration which includes dead plus snow or floor load combinations. A comparison of DOL factors between the 1984 working (allowable) design code (CAN-086-M84) and the 1984 Limit States Design Code (CAN3-086.1-M89) is shown in Table 11. Note that short-term load duration in CAN3-086.1-M89 is meant to be less than 7 days and is not identical to the conventional 10 minutes short-term ramp loading duration.

The code calibration aimed basically obtaining same connection designs for snow loads when the 1984 Working Stress Design Code or the 1989 Limit States Design Code is used. As a result of this calibration, the factored lateral resistance for "Standard Term Load Duration (dead plus floor or snow loads)" in CAN3-086.1-M89 is, about 1.6 times the allowable loads for normal (dead plus floor loads) load duration for wood failure modes, and 1.5 times the allowable loads for rivet failure loads, in CAN3-086-M84.

In order to make some comparisons for illustrating the effect of the above factors, data on full-size Douglas-fir glulam rivet connection tests from the work by Foschi and Longworth (1975) are used. That study included testing of 10 types of Douglas-fir glulam rivet connections with three replications for each type under short-term (less than 10 minutes) ramp loading (parallel-to-grain) with a loading rate of 22.3 kN/minute. The glulam rivet connections were applied on one side of the wood members. These test data are shown in Table 12 along with factored resistances (for short-term i.e., less than 7 days) calculated by using CAN3-086.1-M89 (Limit States Design), and with allowable loads (for instantaneous load duration). The ratio of factored lateral load resistance for short-term (i.e., less than 7 days) load duration to the mean short-term (less than 10 minutes) ultimate test strength varied between 1.3 and 2.7, and had an average value of 2.0.

CONCLUSIONS

Background information for the glulam rivet design section of the 1989 edition of the CSA Standard CAN3-086.1-M89 has been presented. Comparisons between the allowable (working) stress design code (1984 edition) values and Limit States Design Code (1989 edition) values were made, and compared against results of previous full-size glulam rivet connection tests.

ACKNOWLEDGMENTS

Forintek's part of the work was funded by the Canadian Forestry Service. The support of the glulam rivet task group members of the Fasteners Subcommittee of the Technical Committee of CSA Standard CAN3-086, Mr. G.A. Dring, Mr. T.A. Eldridge, and Mr. D.A. Himmelfarb, and Mr. J.E. Turnbull and Prof. R.O. Foschi in providing their suggestions is appreciated.

REFERENCES

Aune, Petter and M. Pattono-Mallory. 1986. Lateral load-bearing capacity of nailed joints based on the yield theory. theoretical development. Research paper 469. United States Dept. of Agriculture. Forest Products Laboratories, Madison, WI.

Canadian Standards Association. 1970. Code for recommended practice for engineering design in timber. Rexdale, Ont., CSA 086-1970.

Canadian Standards Association. 1984. Engineering design in wood (limit states design). Rexdale, Ont., CAN3-086.1-M84.

Canadian Standards Association. 1984. Engineering design in wood (working stress design). Rexdale, Ont., CAN3-086-M84.

Canadian Standards Association. 1989. Engineering design in wood (limit states design). Rexdale, Ont., CAN3-086.1-M89 (in final draft form).

Canadian Standards Association. 1981. Structural quality steels. Rexdale, Ont. CAN3-G40.21-M81.

Canadian Wood Council. 1978. Datafile WJ-5. Glulam Rivets. 55, rue Metcalfe St. Ottawa, Canada. Out of print.

Foschi, R.O. 1974. Load-slip characteristics of nails. Wood Science. 7(1):69-76.

Foschi, R.O. and J. Longworth. 1975. Analysis and design of Griplam nailed connections. ASCE Journal of Structural Division. 101(ST12):2537-2555.

Fox, S.P. 1979. Connection capacity of new Griplam nails. Can. J. Civ. Eng. 6(1):59-64.

Fox, S.P. and R.G. Lincoln. 19;79. Effect of plate and hole size on Griplam-nail load capacity. Can. J. Civ. Eng. 6(3):390-393.

Karacabeyli, E. and R.O. Foschi. 1987. Glulam rivet connections under eccentric loading. Can. J. Civ. Eng. 14(5):621-630.

Karacabeyli, E. and H. Fraser. 1989. Short-term strength of glulam rivet connections made with spruce and Douglas-fir glulam, and Douglas-fir solid timber. Submitted to Canadian Journal of Civil Engineering for publication.

McGowan, W.M. and B. Madsen. 1965. A rigid field joint for glued-laminated construction. Prepublication report issued for committee members of the Canadian Standards Association (CSA-086).

National Building Code of Canada. 1985. National Research Council of Canada, Ottawa, Ont.

Table 1

Values of K_t

Riverts per row. n_c	Number of rows. n_R									
	2	4	6	8	10	12	14	16	18	20
2	0.75	1.16	1.37	1.47	1.51	1.54	1.57	1.61	1.64	1.64
4	0.51	0.88	1.08	1.17	1.22	1.26	1.30	1.35	1.38	1.38
6	0.38	0.71	0.89	0.97	1.02	1.06	1.11	1.16	1.18	1.18
8	0.30	0.60	0.75	0.84	0.89	0.93	0.97	1.02	1.05	1.05
10	0.26	0.52	0.66	0.74	0.79	0.82	0.87	0.91	0.94	0.94
12	0.23	0.47	0.59	0.66	0.71	0.75	0.78	0.82	0.85	0.85
14	0.21	0.42	0.54	0.60	0.65	0.68	0.72	0.75	0.77	0.77
16	0.20	0.38	0.49	0.56	0.60	0.63	0.67	0.69	0.71	0.71
18	0.18	0.35	0.45	0.52	0.56	0.59	0.62	0.65	0.66	0.67
20	0.17	0.32	0.42	0.49	0.53	0.56	0.59	0.61	0.63	0.64
22	0.16	0.30	0.40	0.46	0.51	0.54	0.56	0.58	0.60	0.61
24	0.15	0.29	0.38	0.45	0.49	0.52	0.53	0.55	0.57	0.58
26	0.14	0.28	0.36	0.42	0.46	0.50	0.51	0.52	0.54	0.55

Table 2

Values of β_t

S_P (mm)	S_Q (mm)	Number of rows. n_R									
		2	4	6	8	10	12	14	16	18	20
25	12.5	1.00	1.00	1.00	1.00	1.00	1.00	1.00	1.00	1.00	1.00
	19.	1.34	1.18	1.11	1.07	1.05	1.04	1.04	1.03	1.03	1.02
	25.	1.68	1.36	1.23	1.14	1.09	1.08	1.08	1.06	1.04	1.03
	32.	2.03	1.54	1.34	1.22	1.14	1.10	1.09	1.07	1.06	1.05
	38.	2.37	1.72	1.46	1.29	1.18	1.14	1.12	1.10	1.08	1.06
32	12.5	0.94	0.93	0.93	0.93	0.93	0.93	0.93	0.93	0.93	0.93
	19.	1.26	1.10	1.04	1.00	0.98	0.97	0.97	0.96	0.96	0.95
	25.	1.58	1.27	1.15	1.07	1.02	1.00	1.00	0.98	0.98	0.97
	32	1.90	1.44	1.26	1.14	1.06	1.02	1.01	0.99	0.98	0.98
	38.	2.23	1.61	1.36	1.21	1.11	1.06	1.04	1.02	1.00	1.00
38	12.5	0.87	0.87	0.87	0.87	0.87	0.87	0.87	0.87	0.87	0.87
	19.	1.18	1.02	0.97	0.93	0.91	0.91	0.90	0.90	0.89	0.89
	25.	1.48	1.18	1.07	1.00	0.96	0.93	0.92	0.92	0.91	0.92
	32.	1.78	1.34	1.17	1.06	0.99	0.96	0.94	0.93	0.93	0.92
	38.	2.08	1.50	1.27	1.13	1.04	0.99	0.97	0.95	0.94	0.93
45	12.5	0.81	0.80	0.80	0.80	0.80	0.80	0.80	0.80	0.80	0.80
	19.	1.09	0.95	0.90	0.86	0.85	0.84	0.83	0.83	0.82	0.82
	25.	1.38	1.09	0.99	0.92	0.88	0.86	0.85	0.85	0.84	0.84
	32.	1.66	1.24	1.08	0.99	0.92	0.89	0.87	0.87	0.86	0.85
	38.	1.94	1.39	1.18	1.05	0.96	0.92	0.89	0.89	0.88	0.87
51	12.5	0.75	0.75	0.75	0.75	0.75	0.75	0.75	0.75	0.75	0.75
	19.	1.01	0.87	0.82	0.79	0.77	0.77	0.77	0.76	0.76	0.76
	25.	1.27	1.00	0.91	0.85	0.81	0.79	0.79	0.78	0.78	0.77
	32.	1.54	1.14	1.00	0.91	0.85	0.82	0.82	0.80	0.80	0.79
	38.	1.80	1.27	1.09	0.97	0.89	0.86	0.85	0.83	0.82	0.81

Table 3

Values of ε_t

Rivet Penetration L_p(mm)	Width of Member, b(mm)						
	80	130	175	225	275	315	365
30	24.04	18.59	16.80	16.80	16.80	16.80	16.80
55	25.32	21.24	18.37	16.03	14.59	14.08	14.04
80	25.64	22.67	20.35	18.14	16.33	15.16	14.06

where $\varepsilon_t = \dfrac{2\,\alpha_t\,\gamma}{L_p}$

$\gamma = 90.5 + 5.4\,L_p$

$\alpha_t = 1.0$ for $b \geq 6\,L_p$

$1.0 + 0.155\,(3 - b/2\,L_p)^2$ for $b < 6\,L_p$

Table 4

Values of K_v

Rivets per row. n_c	Number of rows. n_R									
	2	4	6	8	10	12	14	16	18	20
2	2.23	1.61	1.15	0.81	0.60	0.48	0.40	0.32	0.25	0.19
4	2.31	1.69	1.22	0.88	0.66	0.53	0.45	0.37	0.30	0.24
6	2.35	1.73	1.27	0.93	0.70	0.57	0.48	0.40	0.33	0.27
8	2.36	1.76	1.30	0.96	0.73	0.60	0.51	0.43	0.36	0.30
10	2.37	1.78	1.32	0.98	0.75	0.62	0.53	0.45	0.38	0.31
12	2.36	1.78	1.33	1.00	0.77	0.63	0.55	0.46	0.39	0.32
14	2.35	1.78	1.34	1.01	0.78	0.64	0.56	0.47	0.40	0.33
16	2.34	1.78	1.34	1.02	0.79	0.65	0.57	0.48	0.40	0.33
18	2.33	1.78	1.35	1.02	0.80	0.66	0.57	0.48	0.40	0.34
20	2.32	1.78	1.35	1.03	0.80	0.66	0.57	0.48	0.40	0.34
22	2.31	1.78	1.35	1.03	0.80	0.66	0.57	0.48	0.40	0.34
24	2.30	1.78	1.35	1.03	0.80	0.66	0.57	0.48	0.40	0.34
26	2.30	1.78	1.35	1.03	0.80	0.66	0.57	0.48	0.40	0.35

Table 5

Values of β_v

S_P (mm)	S_Q (mm)	Number of rows. n_R									
		2	4	6	8	10	12	14	16	18	20
25	12.5	1.00	1.00	1.00	1.00	1.00	1.00	1.00	1.00	1.00	1.00
	19.	0.98	0.91	0.86	0.84	0.82	0.81	0.81	0.80	0.79	0.79
	25.	0.97	0.81	0.71	0.67	0.63	0.62	0.61	0.60	0.58	0.57
	32.	0.95	0.72	0.57	0.51	0.44	0.43	0.42	0.40	0.38	0.35
	38.	0.94	0.63	0.43	0.34	0.26	0.24	0.23	0.20	0.17	0.13
32	12.5	1.06	1.06	1.06	1.06	1.05	1.05	1.04	1.04	1.03	1.02
	19.	1.04	0.94	0.88	0.85	0.81	0.80	0.79	0.77	0.76	0.74
	25.	1.02	0.84	0.71	0.66	0.60	0.58	0.56	0.54	0.51	0.49
	32.	1.02	0.75	0.58	0.50	0.42	0.40	0.38	0.36	0.33	0.30
	38.	1.02	0.68	0.46	0.36	0.27	0.25	0.24	0.21	0.18	0.14
38	12.5	1.11	1.12	1.12	1.11	1.10	1.09	1.08	1.07	1.06	1.05
	19.	1.10	0.99	0.92	0.88	0.83	0.82	0.79	0.77	0.75	0.73
	25.	1.07	0.84	0.58	0.61	0.53	0.49	0.45	0.42	0.38	0.35
	32.	1.10	0.79	0.60	0.51	0.42	0.40	0.37	0.34	0.31	0.27
	38.	1.11	0.73	0.48	0.38	0.27	0.26	0.24	0.22	0.18	0.14
45	12.5	1.17	1.18	1.18	1.17	1.15	1.13	1.12	1.11	1.09	1.08
	19.	1.17	1.06	0.99	0.94	0.89	0.87	0.85	0.83	0.80	0.73
	25.	1.17	0.95	0.80	0.73	0.66	0.63	0.61	0.58	0.55	0.52
	32.	1.18	0.86	0.65	0.55	0.46	0.44	0.41	0.38	0.35	0.31
	38.	1.20	0.78	0.51	0.39	0.28	0.26	0.25	0.22	0.18	0.14
51	12.5	1.22	1.24	1.24	1.22	1.20	1.18	1.16	1.14	1.12	1.10
	19.	1.24	1.14	1.07	1.02	0.97	0.95	0.93	0.91	0.89	0.86
	25.	1.26	1.04	0.89	0.82	0.74	0.72	0.71	0.68	0.65	0.62
	32.	1.27	0.93	0.71	0.61	0.52	0.50	0.48	0.46	0.42	0.39
	38.	1.29	0.83	0.53	0.41	0.29	0.27	0.25	0.23	0.19	0.15

Table 6

Values of C_t

$\frac{e_p}{(n_C - 1) S_Q}$	β_D	C_t	$\frac{e_p}{(n_C - 1) S_Q}$	β_D	C_t
0.1	0.275	5.76	3.2	1.00	0.79
0.2	0.433	3.19	3.6	1.00	0.77
0.3	0.538	2.36	4.0	1.00	0.76
0.4	0.60	2.00	5.0	1.00	0.72
0.5	0.65	1.77	6.0	1.00	0.70
0.6	0.69	1.61	7.0	1.00	0.68
0.7	0.73	1.47	8.0	1.00	0.66
0.8	0.77	1.36	9.0	1.00	0.64
0.9	0.80	1.28	10.0	1.00	0.63
1.0	0.83	1.20	12.0	1.00	0.61
1.2	0.88	1.10	14.0	1.00	0.59
1.4	0.92	1.02	16.0	1.00	0.57
1.6	0.95	0.96	18.0	1.00	0.56
1.8	0.97	0.92	20.0	1.00	0.55
2.0	0.98	0.89	25.0	1.00	0.53
2.4	0.99	0.85	30.0	1.00	0.51
2.8	1.00	0.81			

Note: $C_t = \frac{1}{\beta_D} \left[\frac{e_p}{(n_C - 1)\ S_Q} \right]^{-0.2}$

Table 7

Values of Q_A, (kN), Perpendicular to Grain for Glulam Rivets

		Spacing: $S_p = 25$ mm							
		Number of rows, n_R							
S_Q	Rivets per row, n_C	1	2	3	4	5	6	8	10
	2	0.57	0.57	0.61	0.61	0.67	0.71	0.84	0.97
	3	0.57	0.57	0.61	0.63	0.66	0.70	0.82	0.93
	4	0.60	0.60	0.65	0.66	0.71	0.74	0.85	0.95
	5	0.63	0.63	0.69	0.70	0.75	0.78	0.89	0.99
	6	0.71	0.71	0.76	0.77	0.81	0.84	0.95	1.06
	7	0.77	0.77	0.82	0.82	0.87	0.89	1.00	1.11
	8	0.86	0.86	0.90	0.90	0.94	0.96	1.07	1.18
	9	0.91	0.91	0.97	0.97	1.01	1.03	1.13	1.25
	10	0.97	0.97	1.05	1.06	1.10	1.12	1.21	1.35
15	11	1.05	1.05	1.12	1.13	1.17	1.18	1.28	1.43
	12	1.14	1.14	1.21	1.21	1.24	1.25	1.38	1.52
	13	1.26	1.26	1.29	1.29	1.33	1.33	1.45	1.59
	14	1.42	1.42	1.40	1.37	1.42	1.44	1.54	1.68
	15	1.50	1.50	1.50	1.47	1.50	1.50	1.62	1.78
	16	1.61	1.61	1.62	1.60	1.60	1.58	1.71	1.89
	17	1.73	1.73	1.72	1.69	1.69	1.67	1.79	1.96
	18	1.88	1.88	1.85	1.80	1.80	1.77	1.87	2.04
	19	1.86	1.86	1.87	1.85	1.86	1.84	1.97	2.13
	20	1.84	1.84	1.91	1.91	1.93	1.93	2.08	2.24
	2	0.67	0.67	0.70	0.69	0.75	0.79	0.93	1.08
	3	0.66	0.66	0.70	0.72	0.74	0.78	0.91	1.03
	4	0.70	0.70	0.75	0.75	0.80	0.83	0.94	1.06
	5	0.73	0.73	0.80	0.79	0.84	0.87	0.98	1.10
	6	0.82	0.82	0.87	0.86	0.91	0.94	1.05	1.18
	7	0.90	0.90	0.94	0.93	0.97	1.00	1.11	1.23
	8	1.01	1.01	1.04	1.02	1.06	1.08	1.19	1.31
	9	1.06	1.06	1.11	1.10	1.14	1.15	1.26	1.39
	10	1.13	1.13	1.20	1.20	1.24	1.25	1.34	1.50
25	11	1.22	1.22	1.29	1.28	1.30	1.32	1.43	1.59
	12	1.33	1.33	1.39	1.37	1.39	1.40	1.53	1.69
	13	1.47	1.47	1.48	1.45	1.48	1.49	1.61	1.77
	14	1.65	1.65	1.61	1.55	1.59	1.61	1.71	1.86
	15	1.75	1.75	1.72	1.66	1.68	1.68	1.80	1.97
	16	1.87	1.87	1.86	1.80	1.79	1.77	1.90	2.10
	17	2.02	2.02	1.97	1.91	1.89	1.87	1.98	2.18
	18	2.19	2.19	2.12	2.03	2.01	1.98	2.08	2.27
	19	2.17	2.17	2.14	2.09	2.08	2.07	2.19	2.37
	20	2.14	2.14	2.19	2.15	2.17	2.16	2.31	2.49

Continued

Table 7 (concluded)

Values of Q_A, (kN), Perpendicular to Grain for Glulam Rivets

		Spacing: $S_p = 25$ mm							
		Number of rows, n_R							
S_Q	Rivets per row, n_C	1	2	3	4	5	6	8	10
	2	0.96	0.96	0.98	0.93	0.98	1.03	1.20	1.38
	3	0.95	0.95	0.98	0.96	0.98	1.02	1.16	1.32
	4	1.02	1.02	1.05	1.00	1.05	1.07	1.21	1.36
	5	1.06	1.06	1.11	1.06	1.11	1.13	1.26	1.41
	6	1.19	1.19	1.22	1.16	1.20	1.22	1.35	1.51
	7	1.30	1.30	1.32	1.24	1.28	1.30	1.43	1.58
	8	1.45	1.45	1.45	1.36	1.40	1.40	1.53	1.68
	9	1.53	1.53	1.55	1.47	1.50	1.50	1.61	1.79
	10	1.63	1.63	1.69	1.60	1.63	1.63	1.72	1.93
40	11	1.76	1.76	1.80	1.71	1.72	1.71	1.83	2.04
	12	1.92	1.92	1.94	1.83	1.84	1.82	1.96	2.17
	13	2.12	2.12	2.08	1.94	1.96	1.94	2.07	2.27
	14	2.39	2.39	2.25	2.07	2.10	2.09	2.20	2.39
	15	2.53	2.53	2.41	2.22	2.22	2.19	2.31	2.53
	16	2.70	2.70	2.61	2.41	2.36	2.30	2.44	2.69
	17	2.91	2.91	2.76	2.55	2.49	2.43	2.54	2.79
	18	3.17	3.17	2.97	2.72	2.66	2.58	2.66	2.91
	19	3.13	3.13	3.00	2.79	2.74	2.69	2.80	3.04
	20	3.10	3.10	3.07	2.88	2.86	2.80	2.96	3.19

Table 8

Values of K_{tp}

Rivets per row, n_C	Number of rows, n_R				
	2	4	6	8	10
2	0.29	0.67	0.88	0.98	1.04
4	0.22	0.50	0.68	0.78	0.85
6	0.17	0.39	0.54	0.63	0.69
8	0.13	0.31	0.44	0.52	0.58
10	0.11	0.25	0.36	0.44	0.48
12	0.09	0.21	0.31	0.37	0.41
14	0.07	0.18	0.26	0.32	0.36
16	0.06	0.15	0.23	0.28	0.31
18	0.05	0.13	0.20	0.25	0.28
20	0.05	0.12	0.18	0.22	0.25

Table 9

Values of β_{tp}

S_Q (mm)	S_p (mm)	Number of rows. n_R 2	4	6	8	10
15	25	1.29	1.25	1.24	1.23	1.23
	38	1.76	1.61	1.49	1.46	1.40
25	25	1.00	1.00	1.00	1.00	1.00
	32	1.18	1.13	1.10	1.09	1.07
	38	1.36	1.27	1.20	1.17	1.14
	45	1.54	1.39	1.30	1.25	1.21
	51	1.72	1.53	1.40	1.34	1.28
32	25	0.82	0.84	0.85	0.86	0.86
	32	0.97	0.96	0.94	0.93	0.92
	38	1.12	1.07	1.03	1.00	0.98
	45	1.27	1.18	1.11	1.08	1.04
	51	1.42	1.29	1.20	1.15	1.10
38	25	0.63	0.68	0.70	0.71	0.71
	32	0.75	0.77	0.78	0.77	0.76
	38	0.87	0.86	0.84	0.83	0.82
	45	0.99	0.95	0.92	0.89	0.87
	51	1.11	1.04	0.98	0.95	0.92

Table 10

Average Ultimate Lateral Load Carrying Capacity per Rivet, kN, Rivet Yielding Failure Mode

Loading	Rivet Length mm	Foschi (1974)[1]		Fox (1979)[2]		Fox and Lincoln (1979)[2]		Karacabeyli and Fraser (1989)[3]					
		Douglas-fir Glulam		Douglas-fir Glulam		Douglas-fir Glulam		Douglas-fir Glulam		Spruce Glulam		Douglas-fir Joist	
		//[4]	⊥[5]	//	⊥	//	⊥	//	⊥	//	⊥	//	⊥
Ultimate Load Carrying Capacity	90	6.84	4.15										
	65	6.21	3.56[6]	5.72[7]	---	5.69[7]	---	5.35	4.12	4.32	3.24	5.30	3.95
	40	4.96	2.98										
Ratio of capacities // to ⊥		0.57		---		---		0.77		0.75		0.75	

1 Also basis of design values in CAN3-O86-M84; Ultimate loads at $\Delta = 4.8$ mm
2 Ultimate loads at $\Delta = 5.1$ mm
3 Ultimate loads at $\Delta = 4.8$ mm, oven-dry specific gravity is 0.45 for Douglas-fir glulam, 0.45 for spruce glulam, 0.52 for Douglas-fir glulam
4 Parallel to grain loading
5 Perpendicular to grain loading
6 Interpolated value
7 Obtained by applying a strength factor of 0.91 (Foschi 1974) to mean ultimate load carrying capacity of 90 mm rivets

Table 11

Comparison of DOL Factors

	DOL Factor	Load Duration	Explanatory Notes
CAN3-086-M84 Working Stress Design Code	0.90	Continuous	eg. dead loads plus long-term live loads
	1.00	10 Year	Normal (eg. dead plus floor loads)
	1.15	2 Month	eg. dead plus snow loads
	1.25	7 day	eg. dead plus form or falsework loads
	1.33	1 day	eg. dead plus wind and earthquake loads
	1.60	10 minutes	Instantaneous (eg. dead plus impact loads)
CAN3-086.1-M89 Limit States Design Code	1.15	Short-term (1)	eg. dead plus form or falsework, or wind and earthquake, or impact
	1.00	Standard term	eg. dead plus floor or snow loads
	0.65	Permanent	eg. dead loads plus long-term live loads

(1) Short-term in this table is meant to be the duration of loading of up to 7 days and is not identical to the conventional 10 minute short-term ramp loading duration.

Table 12

Experimental Results versus Design Values, Parallel to Grain Loading, One Sided Connections

						CSA-086.1-M89 Factored[1] Lateral Load Resistance Pr			Foschi and Longworth (1975)		CSA-086-M84[3] Allowable Lateral Load		
Connection Type	n_R	n_C	S_P mm	S_Q mm	a mm	Rivet Yielding Failure Mode kN	Tension Failure Mode kN	Shear Failure Mode kN	Test Mean[2] kN	Test Failure Mode	Rivet Yielding Mode kN	Tension Failure Mode kN	Shear Failure Mode kN
1	5	5	25	13	51	65	86	33	82.3	wood	44	77	29
2	5	5	38	25	51	65	151	116	155.2	rivet	44	133	118
3	5	10	25	13	51	131	130	50	103.6	wood	89	115	45
4	5	10	38	25	51	131	231	175	282.5	wood	89	205	157
5	10	10	25	13	51	262	218	104	178.4	wood	178	194	93
6	10	10	38	25	51	262	479	283	550.7	wood	178	424	253
7	15	10	25	13	51	393	301	157	204.6	wood	267	267	141
8	15	10	38	25	51	393	747	393	728.6	wood	267	690	342
9	15	10	25	13	381	393	301	160	265.1	wood	267	267	142
10	15	10	38	25	381	393	777	659	1066.2	rivet	267	690	589

(1) Smallest resistance governs the design,
$\phi = 0.60$, $K_T = K_{SF} = J_Y = 1.0$, $L_P = 76$ mm, $e_p = 38$ mm, b = 457 mm, ($K_D = 1.15$ Short-term (dead plus form or falsework, or wind and earthquake, or impact)).

(2) Mean of three replications

(3) Smallest allowable load governs the design,
$K_T = K_{SF} = J_Y = 1.0$, $L_P = 76$ mm, $e_p = 38$ mm, b = 457 mm, $K_D = 1.6$ (Instantaneous (10 minutes) load duration (dead plus impact loads)).

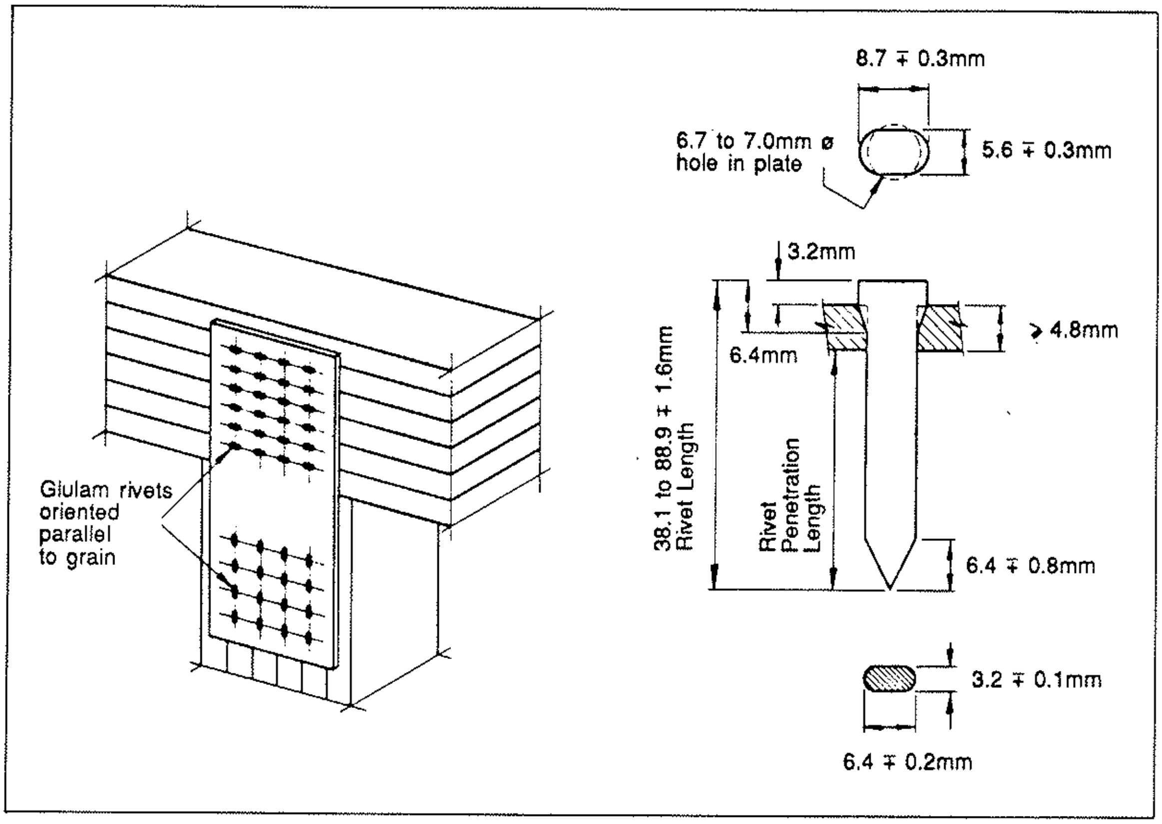

Figure 1 Typical Glulam Rivet Connection

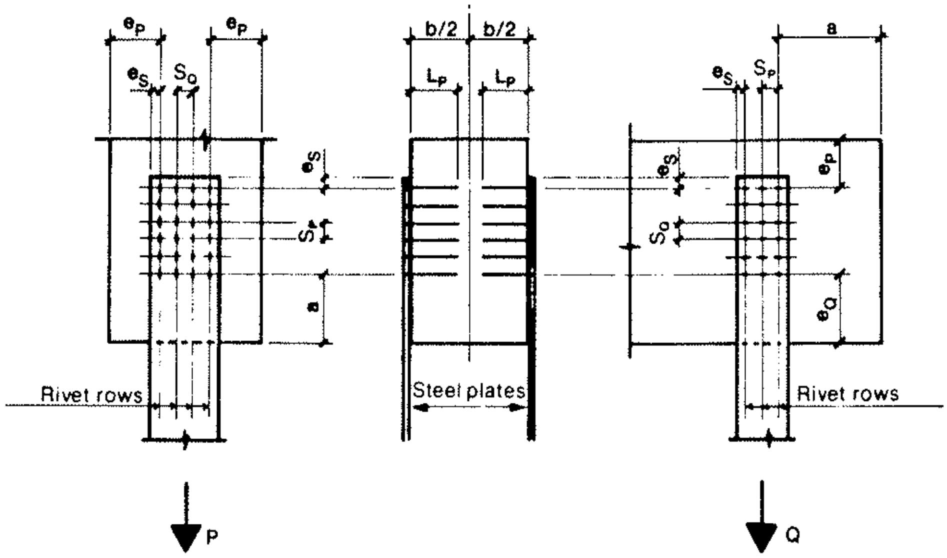

Load parallel to grain

Load perpendicular to grain

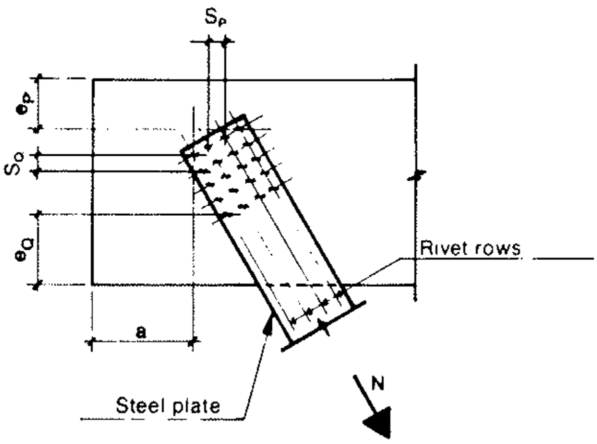

Load at angle to grain

Minimum End and Edge Distances for Glulam Rivet Joints

Number of rivet rows, n_R	Minimum end distance, a (mm): Load parallel to grain	Minimum end distance, a (mm): Load perpendicular to grain	Minimum edge distance, e (mm): Free edge, e_P	Minimum edge distance, e (mm): Loaded edge, e_Q
1, 2	75	50	25	50
3 to 8	75	75	25	50
9, 10	100	80	25	50
11, 12	125	100	25	50
13, 14	150	120	25	50
15, 16	175	140	25	50
17 and greater	200	160	25	50

Figure 2
End and Edge Distances for Glulam Rivet Joints

CIB -W18A / 22-7-7

INTERNATIONAL COUNCIL FOR BUILDING RESEARCH STUDIES AND DOCUMENTATION

WORKING COMMISSION W18A - TIMBER STRUCTURES

MECHANICAL PROPERTIES OF JOINTS IN GLUED-LAMINATED BEAMS UNDER REVERSED CYCLIC LOADING

by

M Yasumura
Building Research Institute
Ministry of Construction
Japan

MEETING TWENTY - TWO

BERLIN

GERMAN DEMOCRATIC REPUBLIC

SEPTEMBER 1989

MECHANICAL PROPERTIES OF JOINTS IN GLUED-LAMINATED BEAMS UNDER REVERSED CYCLIC LOADING

Motoi YASUMURA*

1. INTRODUCTION

In the large scale timber construction, arched frames are frequently connected so that the moment and shear forces are transmitted. Although the vertical loads such as the dead load and the snow load are generally more critical in this kind of structures than the lateral loads such as the wind and seismic loads, it is supposed that the mechanical properties of the joints of horizontal members affect a lot on the structural performance especially in case of the earthquake. Thus ten glued-laminated beams with various mechanical joints were subjected to the reversed cyclic loads in order to investigate the strength and the ductility of a joint. The purpose of this study is to provide the information for evaluating the seismic properties of a frame having the joints in horizontal members.

2. DESCRIPTION OF SPECIMEN

Bending tests of the glued-laminated beams connected with the mechanical joints were performed to investigate the mechanical properties of the joints under reversed cyclic loading.

Two glued-laminated timbers of 5 meters in length were connected with the mechanical joints as shown in Fig.1. The cross section of the specimen was 15-by 60 centimeters, and the species of Specimens A to F and G to J were Spruce and Douglas-Fir respectively. The outline of the specimen is described as follows;

---

*Senior Research Officer, Dr.Agr. Dpt. of Structural Engineering, Building Research Institute, Ministry of Construction, Tsukuba, Japan

Specimen A: Steel plates of 16 millimeters in thickness were placed on both sides of the glued-laminated beam and connected with four bolts per joint of 20 millimeters in diameter.

Specimen B: The same as Specimen A, except that the numbers of bolts were seven per joint.

Specimen C: Steel plates of 16 millimeters in thickness were inserted in the center of the edge of the beam and connected with five bolts per joint of 20 millimeters in diameter.

Specimen D: Steel plates of 22 millimeters in thickness were placed on both edges of the beam and connected with seven bolts per joint which penetrated through the height of the beam.

Specimen E: The same as Specimen D, except that the numbers of bolts were twelve per joint.

Specimen F: The same as Specimen D, except that the steel plates were connected with twelve lag screws per joint of 20 millimeters in diameter.

Specimen G: The same as Specimen F, except that the numbers of lag screws were sixteen per joint.

Specimen H: The same as Specimen G, except that epoxy resin was applied to connect the steel plates together with the lag screws.

Specimen I: Two steel rods for pre-stressed concrete of 23 millimeters in diameter were inserted along the length of the beam and the tensile force of 225kN was applied at the end of the rods.

Specimen J: Steel plates of 19 millimeters in thickness were inserted in the center of the edge of the beam and connected with twenty drift pins per joint of 16 millimeters in diameter. Steel plates were separated at the center of the beam and connected each other with two high tensile bolts of 18 millimeters in diameter.

3. TEST METHOD

Bending test was performed as shown in Fig.2 by using 1000tf structural testing machine of BRI. Reversed cyclic loads as shown in Fig.3 were applied at a third points of the span of 9 meters, and the vertical deformation, the strain of beam and steel plates and the rotational angle of the joint were measured.

4. RESULTS AND DISCUSSION

4.1 DESCRIPTION OF FAILURE

Typical failures of the joints are shown in Fig.4. In Specimens A to C, brittle failure occurred with the fracture of the glued-laminated wood along the bolt line, and the load decreased suddenly after the failure. This failure occurred by the force in the direction perpendicular to the grain caused by the bolted joints. Stress distribution in the direction perpendicular to the grain should be especially considered to design this type of joint. In Specimens D to H, bolts or lag screws yielded in bending and brittle failure was not observed except for the partial shear failure of the glued-laminated timber. Specimen I did not fail completely at the deflection of 30 centimeters, but the partial compressive failure at the compressive side of the joint and the partial shear failure of the glued-laminated timber were observed. In Specimen J, glued-laminated wood was failed suddenly at the joint because of the high stress concentration.

4.2 HYSTERESIS LOOPS

Fig.5 shows the load-deflection curves of each specimen. In Specimens A to G, the initial slips caused by the clearance of the bolt holes (one or two millimeters larger than the diameter of a bolt according to the types of a joint) were observed. In Specimens A to C and J, the load decreased immediately after the maximum load. Specimens D to F and I showed relatively high ductility, while Specimens G and H showed less ductility because of the stress concentration by the large numbers of lag screws.

4.3 EQUIVALENT VISCOUS DAMPING

The equivalent viscous damping was obtained from the hysteresis curves of each specimen, and the calculated values are shown in Fig.6, where the equivalent viscous damping is obtained from the ratio of the absorved energy to the external work performed in each loop (See Fig.6).

The equivalent viscous damping in Specimens B to G was approximately 5 to 12% when the deflection of the beam was 1/300 of a span, but it decreased to approximately 2% when the deflection was 1/100. The equivalent viscous damping of Specimen J in which the initial slip was eliminated by the tensile bolts was approximately 1% when the deflection was small. This indicates that the relatively high equivalent viscous damping of Specimens B to G in small deformation is mainly caused by the initial slips of joints. The equivalent viscous damping in plastic area of Specimens D to H was almost constant and approximately 5%, while that of Specimen I was approximately 1% regardless of the deformation.

4.4 STIFFNESS AND DUCTILITY

Fig.7 shows the relation between the load and the rotational angle of the joint, and Table 1 shows the initial rotational angle, the rotational stiffness, the maximum moment, the rotational angle for the maximum moment and the ductility factor defined by the ratio of the maximum deformation to the deformation for the elastic limit.

Initial rotational angle of Specimens A to G varied from 1/350 to 1/130, and the rotational stiffness of the joint was about a half of those calculated from the experiment of one bolt(1)(2) except for Specimen J. Ductility factors of Specimens D and F were respectively 4.3 and 4.8, and that of Specimen J was 3.1. In Specimens A to C, E and G, the load decreased suddenly after the maximum load, and the ductility factor was 1.0.

5. CONCLUSION

Summarizing the results of this study, the following conclusions are lead.

(1) Double shear bolted joints with the steel plates placed on the side of the beam (Specimens A and B) and those with the steel plate inserted in the beam (Specimen C) showed very brittle

failure. Stress distribution in the direction perpendicular to the grain should be considered to design this type of joint.

(2) Single shear bolted joints with the steel plates placed on the edge of the beam (Specimens D to H) showed relatively high ductility. However the joints having large numbers of bolts or lag screws showed less ductility.

(3) The joint in which pre-stress was applied with the steel rods (Specimen I) did not fail at the deflection of 30 centimeters, and showed high ductility.

(4) The hysteresis loops of the joints were different according to the types of the joint. Initial slips caused by the clearance of the bolt holes were remarkable.

(5) The equivalent viscous damping of the mechanical joints in which neither adhesives nor tensile bolts were used was approximately 5 to 12% when the deflection was small. This relatively high viscous damping may be caused by the initial slips of the joints.

(6) The equivalent viscous damping of the joint was approximately 2% at the deflection of 1/100 of a span, and it increased to approximately 5% in plastic area.

(7) Initial rotational angle of the joint in which neither adhesives nor tensile bolts were used varied from 1/350 to 1/130 and the rotational stiffness of the joint was about a half of those calculated from the experiment of one bolt.

(8) Ductility factors of the joint with the steel plates placed on the edge of the beam (Specimens D and F) were 4.3 and 4.8 respectively, and that of the joint in which the steel plate was inserted and connected with twenty drift pins per joint was 3.2. Other types of joints showed brittle performance except for the specimen in which the pre-stress was applied on the steel rods.

6. LITERATURE

(1) "Daidanmen Mokuzo Kenchikubutsu Sekkei Seko Manyuaru (Design Manual for Heavy Timber Buildings)", Building Center of Japan, 1988

(2) YASUMURA, M. et al,"Ultimate Properties of Bolted Joints in Glued-Laminated Timber", CIB-W18, 20-7-3, September 1987.

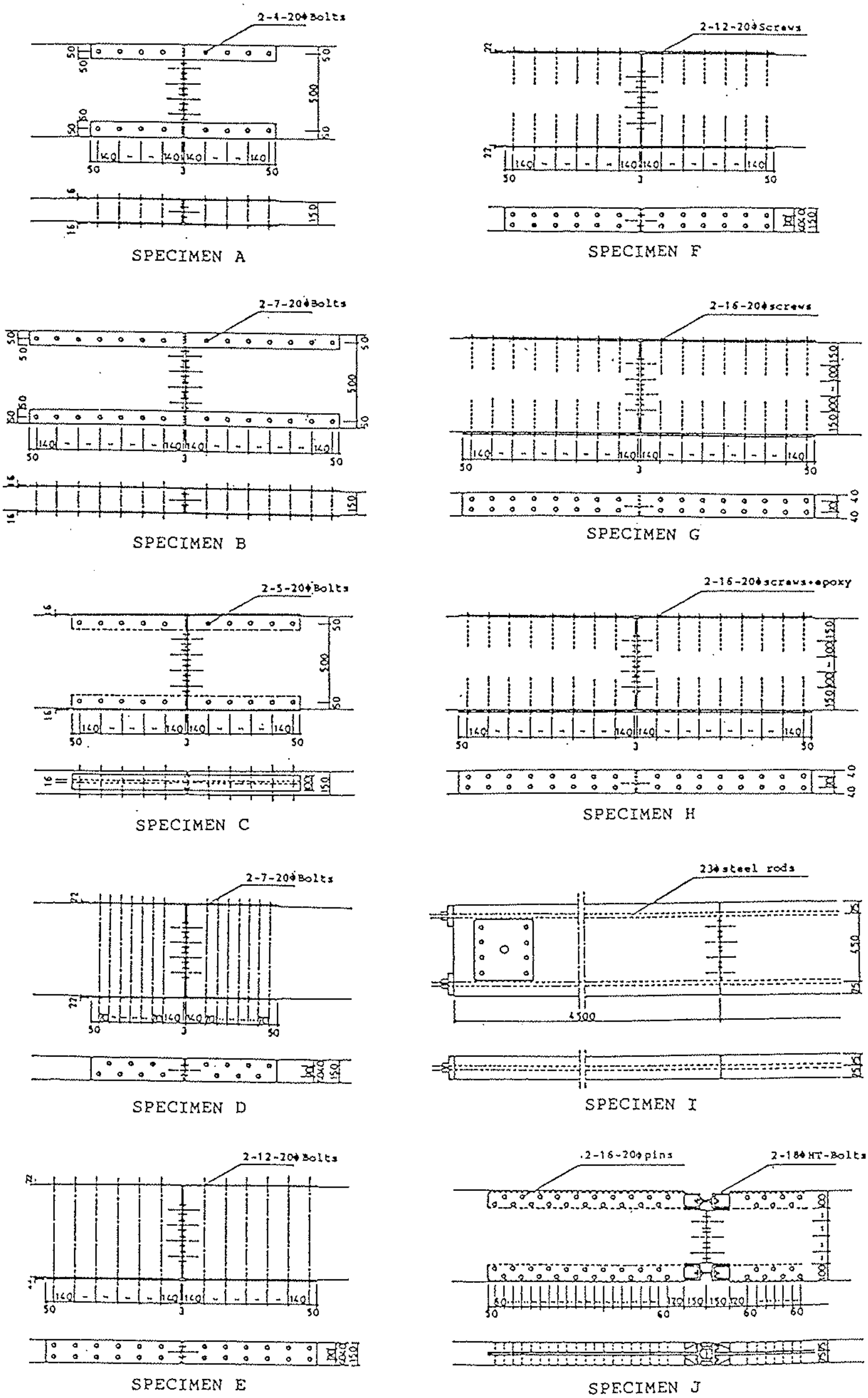

Fig.1 DETAILS OF SPECIMENS

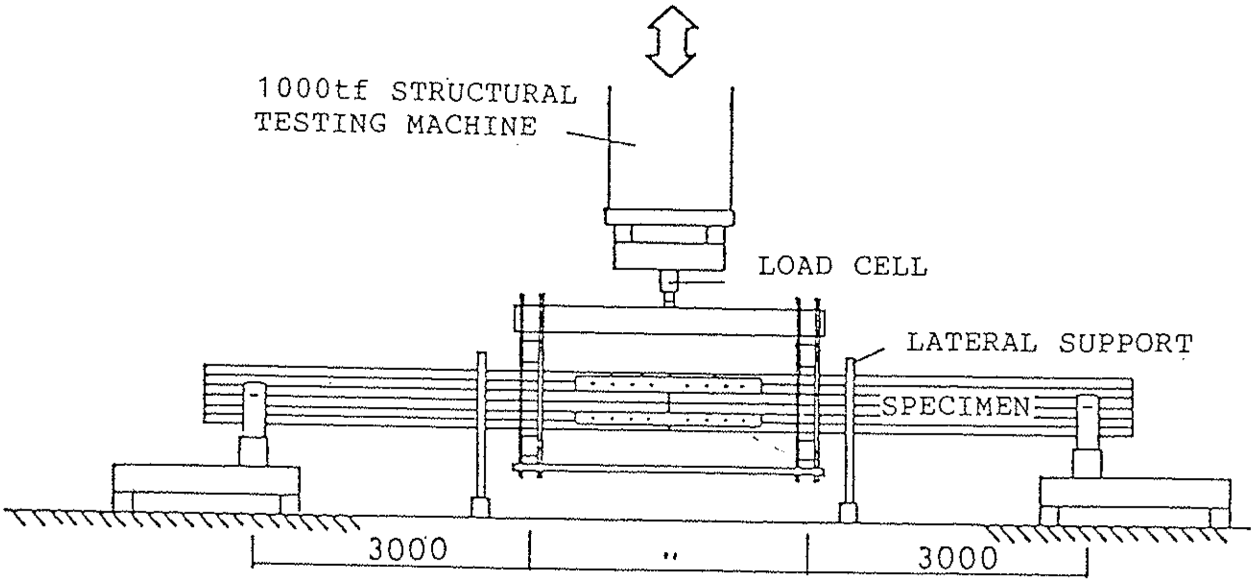

Fig.2 BENDING TEST APPARATUS

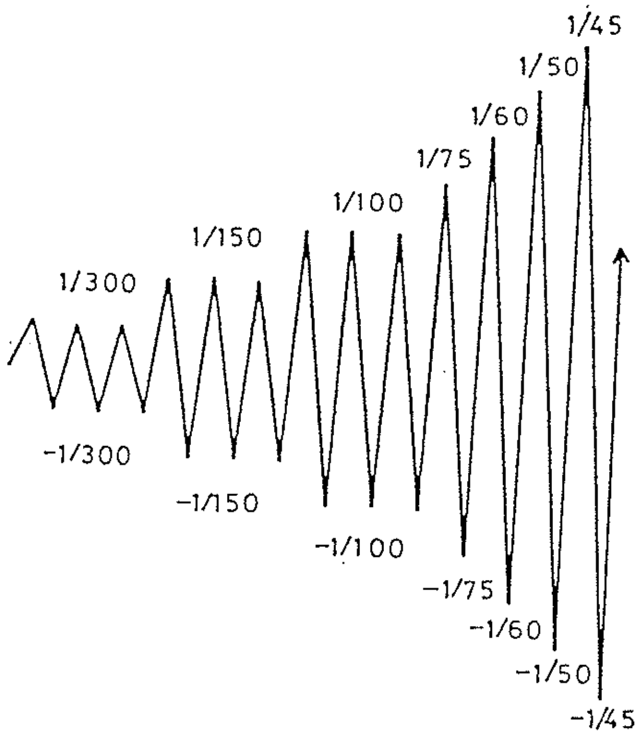

Fig.3 LOADING HISTORY(Values represent the ratio of the deflection to span)

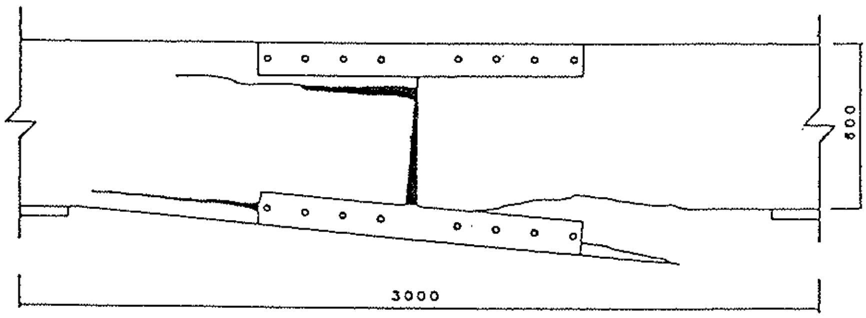

SPECIMEN A

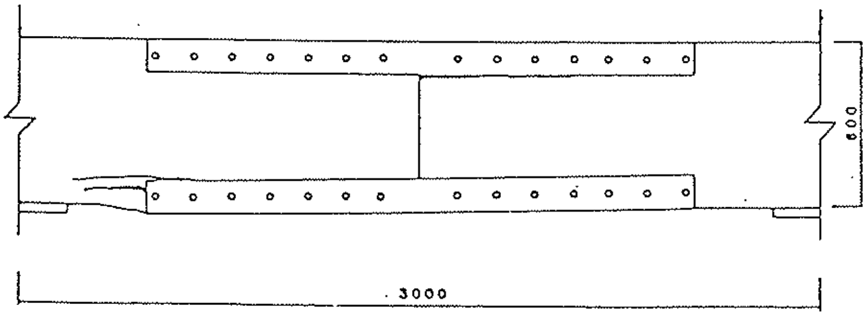

SPECIMEN B

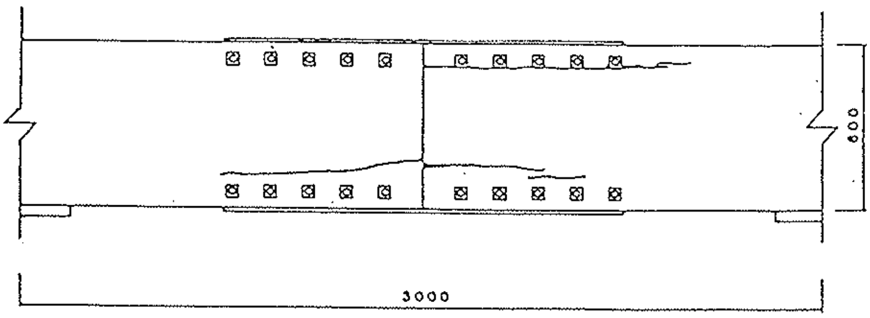

SPECIMEN C

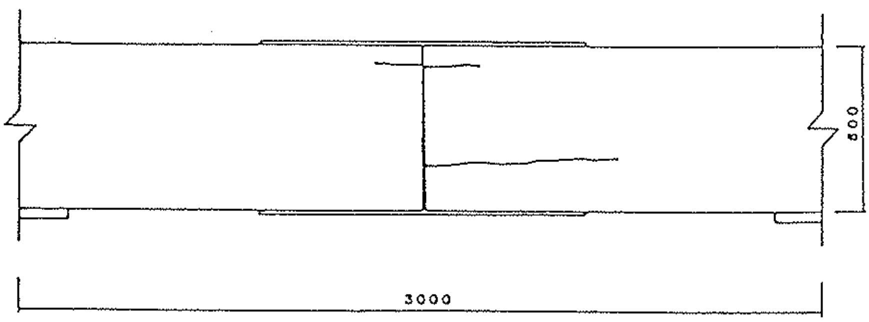

SPECIMEN D

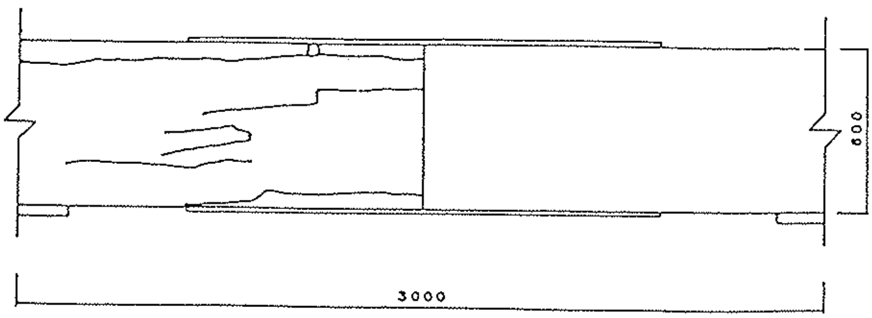

SPECIMEN E

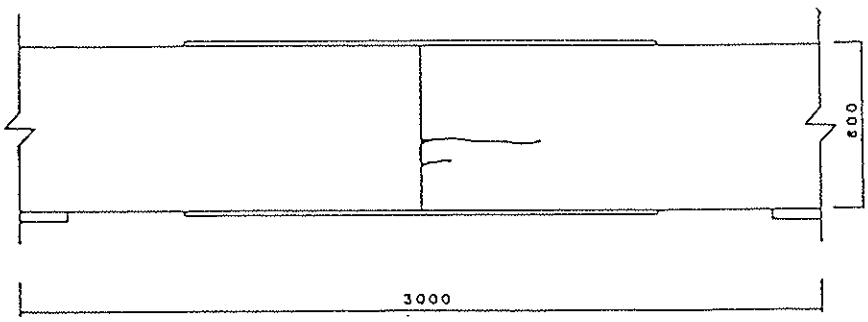

SPECIMEN F

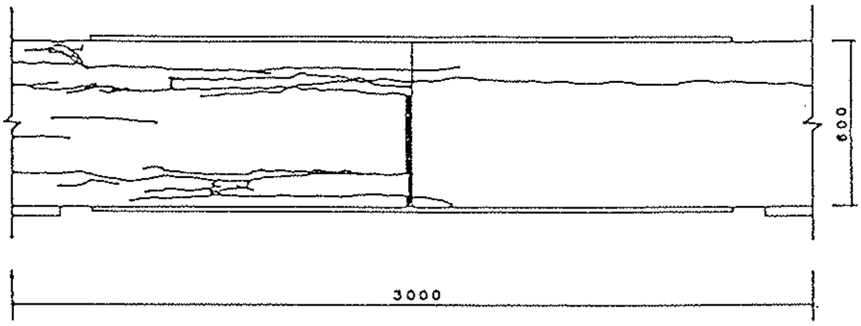

SPECIMEN G

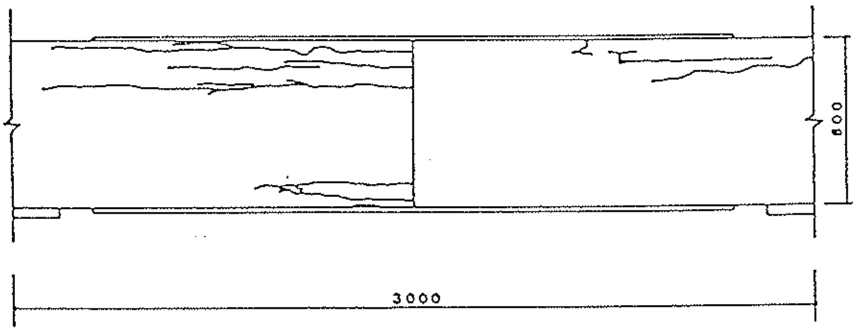

SPECIMEN H

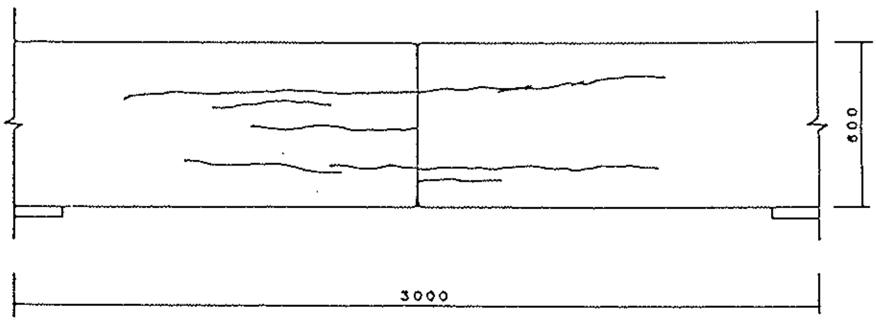

SPECIMEN I

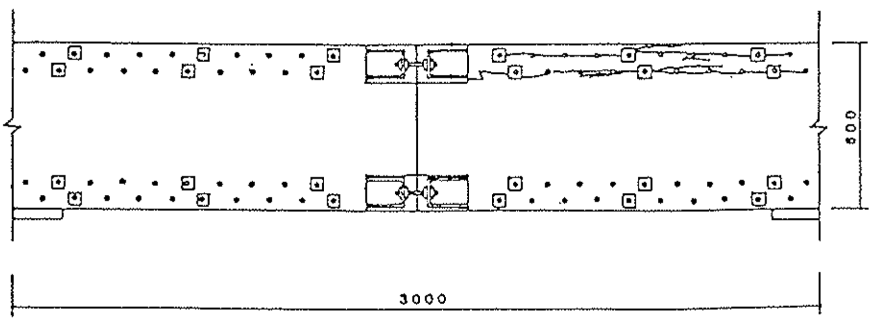

SPECIMEN J

Fig.4 FAILURE OF JOINTS

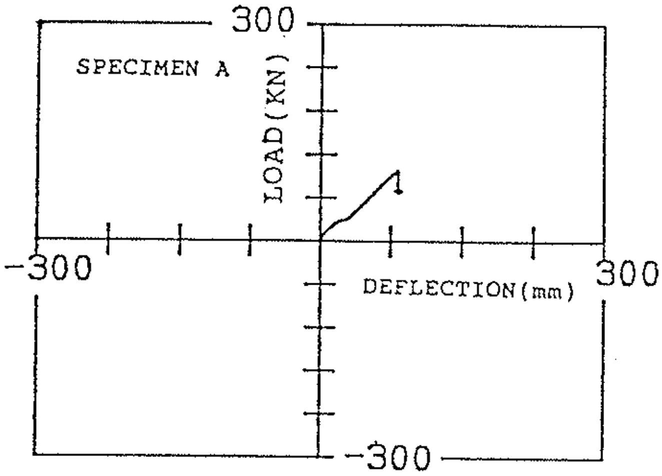
SPECIMEN A
LOAD(KN)
DEFLECTION(mm)
300
-300
300
-300

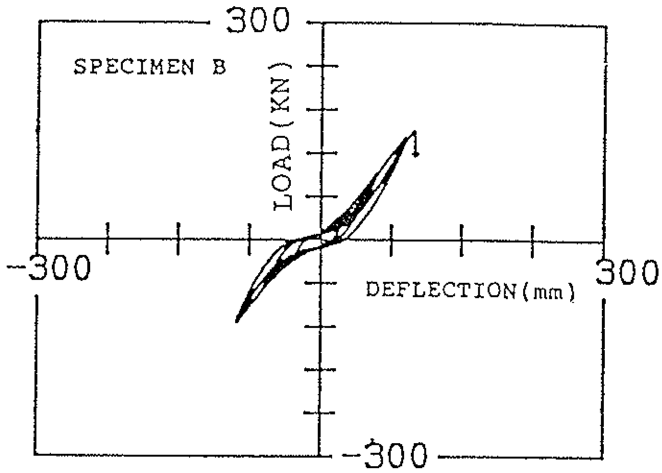
SPECIMEN B
LOAD(KN)
DEFLECTION(mm)
300
-300
300
-300

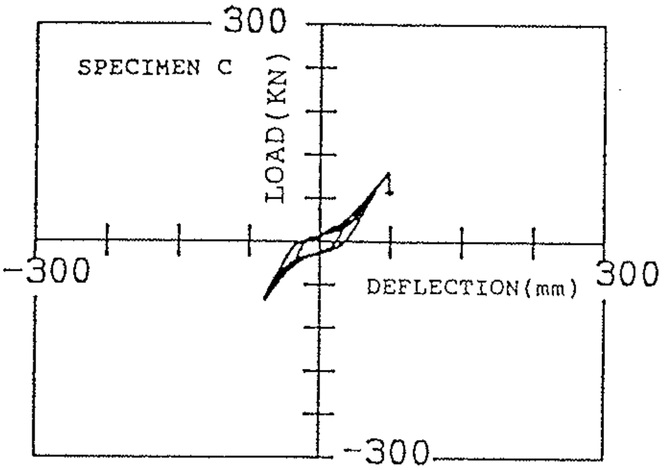
SPECIMEN C
LOAD(KN)
DEFLECTION(mm)
300
-300
300
-300

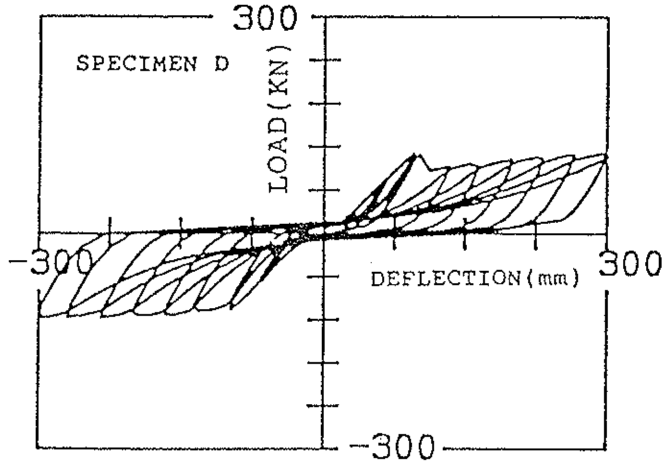
SPECIMEN D
LOAD(KN)
DEFLECTION(mm)
300
-300
300
-300

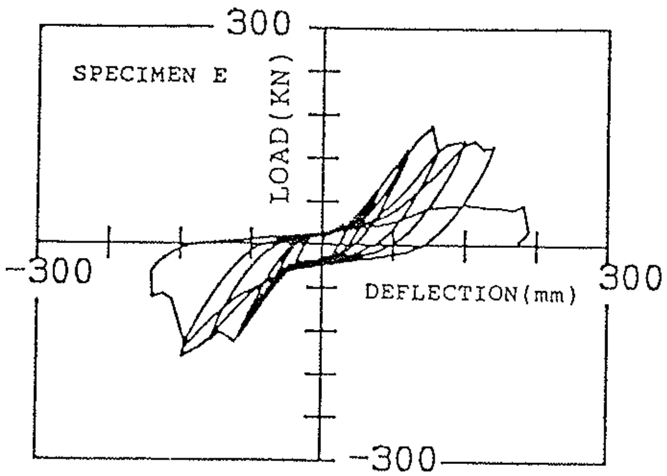
SPECIMEN E
LOAD(KN)
DEFLECTION(mm)
300
-300
300
-300

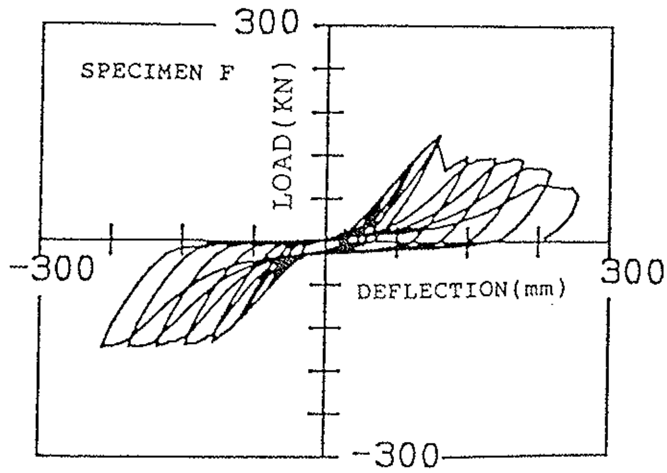
SPECIMEN F
LOAD(KN)
DEFLECTION(mm)
300
-300
300
-300

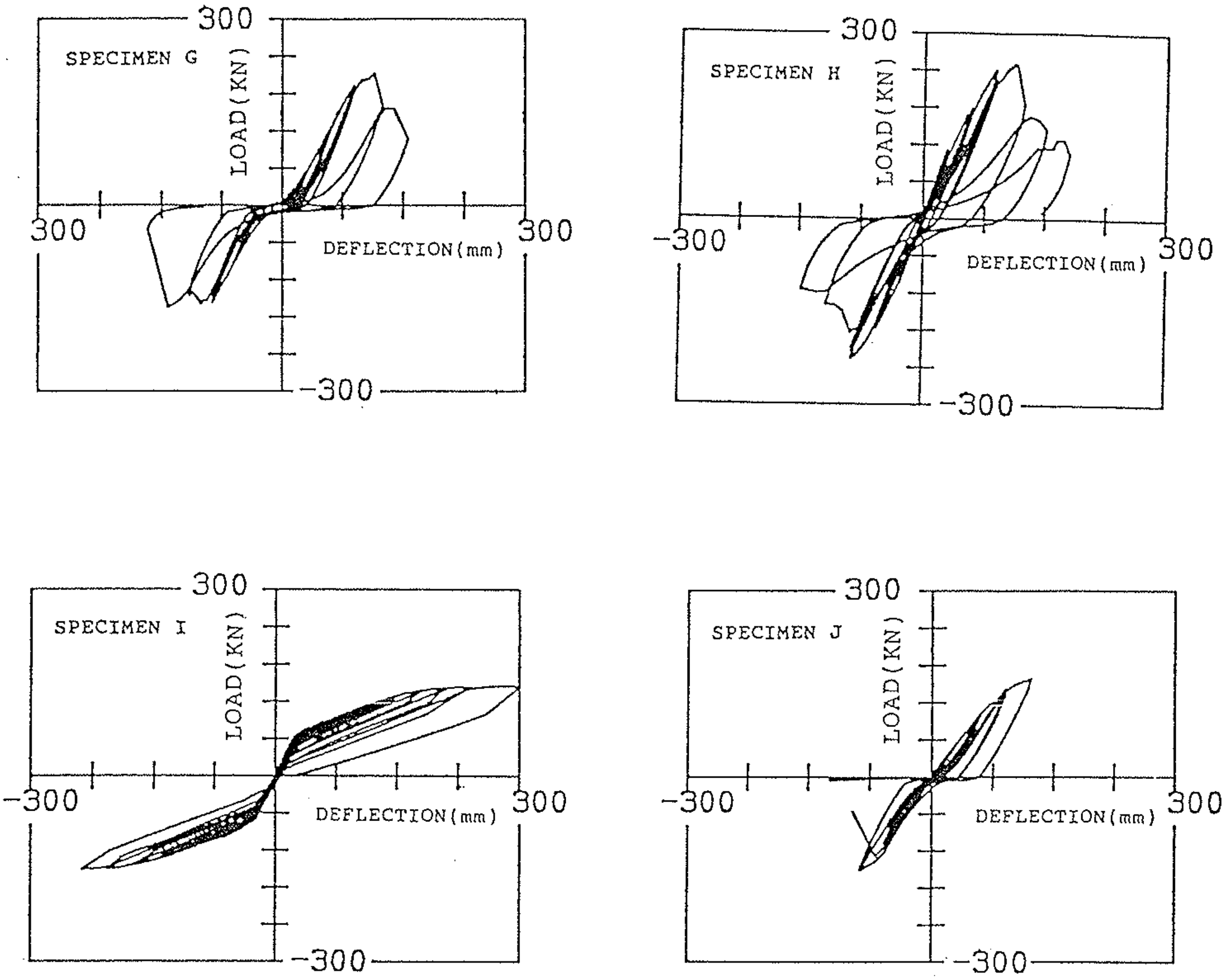

Fig.5 LOAD-DEFLECTION CURVES OF EACH SPECIMEN

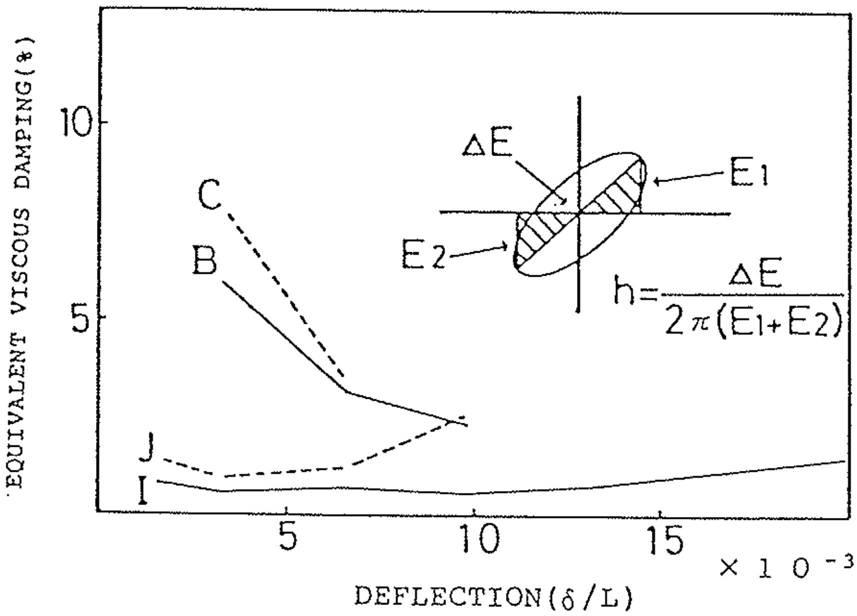

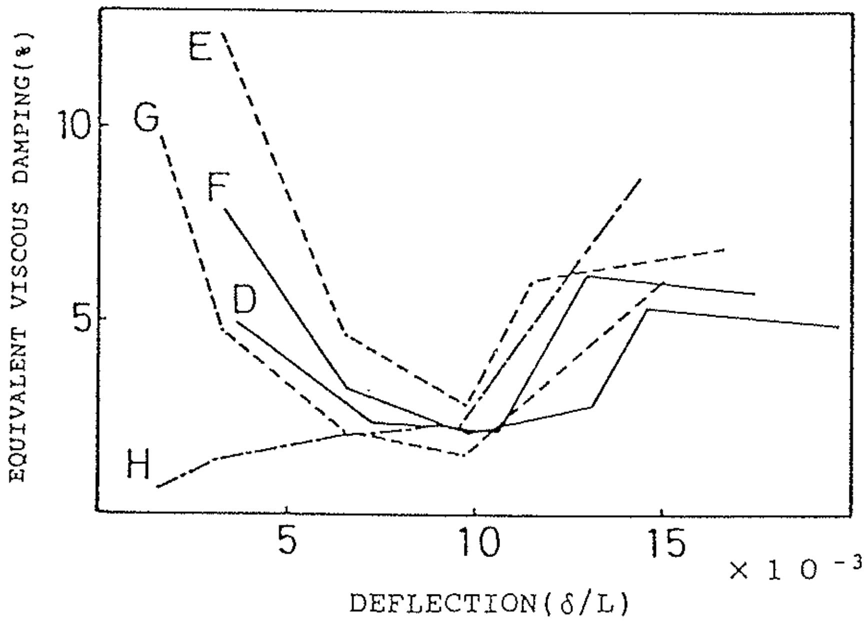

Fig.6 EQUIVALENT VISCOUS DAMPING

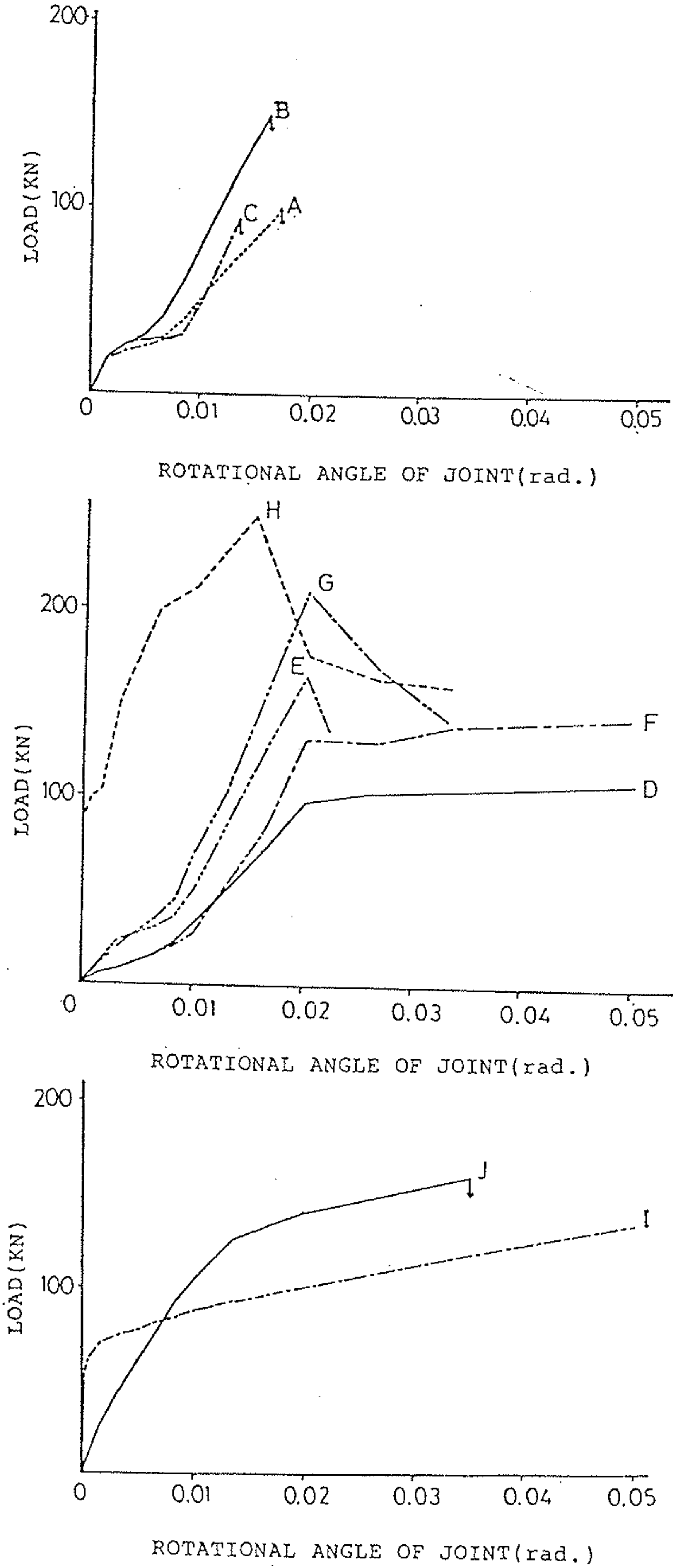

Fig.7 RELATION BETWEEN LOAD AND ROTATIONAL ANGLE OF JOINT

Table 1 INITIAL SLIPS, ROTATIONAL STIFFNESS OF JOINT, MAXIMUM MOMENT, ROTATIONAL ANGLE FOR MAXIMUM MOMENT AND DUCTILITY FACTOR(*)

SPECIMEN	INITIAL SLIP X 0.001 rad.	STIFFNESS kN.m/rad.	MAX. MOMENT kN.m	MAX. ROT. x0.001rad.	DUCTILITY FACTOR
A	2.83	10,133	147	17.3	1.0
B	4.00	19,600	221	16.2	1.0
C	5.25	18,208	140	13.5	1.0
D	5.50	9,800	172	70.1	4.3
E	5.84	17,728	243	19.9	1.0
F	7.75	14,132	219	67.3	4.8
G	6.75	22,785	313	21.6	1.0
H	0	---	367	15.1	---
I	0	---	222	83.1	---
J	0	18,208	233	34.5	3.2

*DUCTILITY FACTOR

$\mu = \delta max / \delta e$

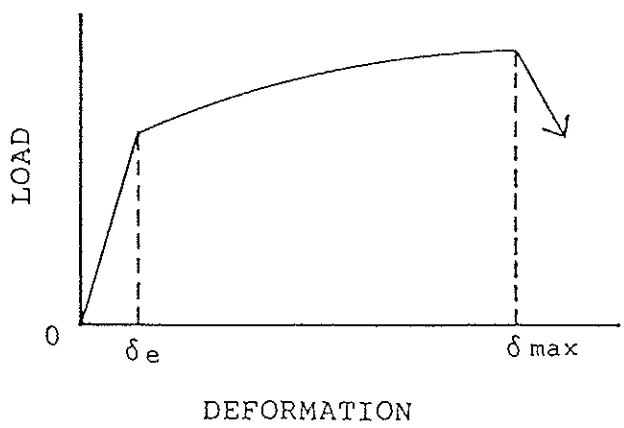

CIB -W18A / 22-7-8

INTERNATIONAL COUNCIL FOR BUILDING RESEARCH STUDIES AND DOCUMENTATION

WORKING COMMISSION W18A - TIMBER STRUCTURES

STRENGTH OF GLUED LAP TIMBER JOINTS

by

P Glos and H Horstmann
Institut für Holzforschung der Universität München
Federal Republic of Germany

MEETING TWENTY - TWO

BERLIN

GERMAN DEMOCRATIC REPUBLIC

SEPTEMBER 1989

Strength of glued lap timber joints

P. Glos and H. Horstmann
Institut für Holzforschung der Universität München

1. Objectives

At present there is a distinct lack of design rules for glued joints used in timber engineering e.g. as required for the production of glued trusses (Fig. 1). The load bearing behaviour of such joints is being determined by a great number of geometrical and physical parameters. In this context numerous investigations were conducted e.g. by Graf and Egner (1938), Egner (1954, 1962) Kalina (1965), Dutko (1969) and Kolb (1974). However, shape of specimens and test conditions differed widely in the individual investigations and no general method for the calculation of characteristic strength properties of glued joints was deduced. This paper summarizes the results of systematic joint strength tests which form the basis for the derivation of generally applicable design rules for glued wooden joints, for Section 6.2, CIB Code, 6th Edition, Jan. 83.

2. Specimen shape and production

2.1 Specimen shape

In a conventional truss joint as shown in Fig. 1 different parameters tend to overlap, such as shape of glued area, angle between grain directions of glued members (diagonal and chord), length and width of glued area etc. To be able to investigate the effect of individual parameters separately the specimen shown in Fig. 2a was chosen. This test specimen consisted essentially of two tension chords and one compression or tension chord glued together so that the fibre directions of the chords formed the angle α (angle of gluing, Fig. 2b). The elongation of the chords beyond the glued area is designed to prevent tension perpendicular to grain failure.

The distribution of normal stresses and of stresses perpendicular to grain in the wood and in the glued area is highly dependent on the mode of load application and hence on specimen shape.

Figs. 3a - d show the qualitative stress distribution within the glued area of specimens loaded in tension-compression and in pure tension, each with and without a so-called end distance l_{e1}.

In the tension-compression mode of loading, the specimen with an end distance l_{e1} as compared to a specimen without end distance exhibits higher shear stresses and lower compression stresses perpendicular to grain at the beginning of the glued area and lower tension stresses perpendicular to grain at the tailing end of the glued area due to the larger inner lever. From this follows that for joints with short glued area lengths where tension stresses perpendicular to grain control strength (Glos, Henrici, Horstmann 1987), an end distance $l_{e1} > 0$ leads to an increase in load bearing capacity. In contrast, for specimens with long glued area lengths in which the shear stress peak associated with low compression stress perpendicular to grain at the beginning of the glued area determines failure, the load bearing capacity is reduced (Fig. 4). The critical glued area length where the effect of the end distance is being reversed, lies at about L_L = 15 cm (Fig. 6).

Results of experiments and of relevant calculations conducted so far have shown that an actual truss joint with a glued area length of L_L = 20 cm has a shear stress peak at the beginning of the glued area similar to that in a specimen with end distance and a high compression stress perpendicular to grain similar to the one without. Thus strength of an actual truss joint is less than that of a test specimen without end distance, but higher than that of a specimen with end distance as a consequence of the favourable effect of the high compression stresses perpendicular to grain on shear strength (cf. Fig. 5).

Therefore, to be on the safe side when establishing design rules, characteristic strength values should be determined using specimens with an end distance for glued area lengths exceeding L_L = 15 cm and specimens without an end distance should be used for joints with glued area lengths below L_L = 15 cm.

Unless stated otherwise the tests described below were carried out in the tension-compression mode of loading using specimens as shown in Fig. 3b with an end distance of l_{e1} = 5 cm. This specimen was considered to provide the most realistic way of simulating boundary conditions in joints of trusses actually used in constructions.

2.2 Production of specimens

The test specimens were made from European spruce boards (picea Abies) planed to a thickness of 30 mm. Wood densities ranged from $370 \leq \rho_{12} \leq 510$ kg/m^3. For each individual specimen boards with approximately equal densities were glued together. Approximately even density distribution was aimed at for each series (cf. Fig. 12). With the exception of the chapter 4.6 specimens, a phenol-resorcinol-formaldehyde glue (Kauresin 460, hardener 467) was used with 500 g glue per m^2 applied to the glued area. Clamping was provided by hydraulic pressure ($p \approx 0.6$ N/mm^2) except for specimens in chapter 4.5 where pressure by nailing ($p \approx 0.3$ N/mm^2) was applied. Prior to testing the specimens were conditioned at 20°C and 65 % rel. humidity.

3. Test program

In experimental tests the effects of the most important strength determining parameters on the load-carrying behaviour of glued lap joints were to be investigated. The following parameters were studied individually:

- length L_L of glued area (L_L = 5, 10, 15, 20, 30, 40 cm)
- width B_L of glued area (B_L = 10, 15, 20, 25 cm)
- shape of glued area (rectangle, parallelogram, circle)
- angle of gluing α (α = 0°, 15°, 30°, 60°, 90°)
- type of glue (KPF, KEP, KPVAc)
- clamping technique (hydraulic pressure-clamped, nail-clamped with different nail types and quantities)
- wood density ($370 \leq \rho_{12} \leq 510\ kg/m^3$)

Per series at least 5, but usually 10 specimens each were tested.

4. Results

As a measure of shear strength of the glued joint, in the following referred to as joint strength, the average shear stress along the glueline was used according to the following equation:

$$\tau_L = \frac{F}{2A_L} \quad \text{with } F = \text{ultimate load at failure}, \quad A_L = \text{glued area (one side)}$$

Altogether 452 specimens were tested.

4.1 Effect of length L_L of glued area

Fig. 6 represents the ultimate load F and the average shear strength τ_L for specimens with end distance l_{e1} = 5 cm and without end distance (l_{e1} = 0 cm) respectively. Width of glued area of the specimens with l_{e1} = 5 cm was B_L = 15 cm, angle of gluing α = 0°. The glued area of the specimens without end distance (l_{e1} = 0 cm) was a square with $B_L = L_L$. Because the effect of width B_L of the glued area on joint strength proved negligible (chap. 4.2), the ultimate load F of specimens with $B_L = L_L$ was used to calculate that for uniform width B_L = 15 cm and subsequently included in the discussion.

For specimens with end distance l_{e1} = 5 cm Figure 6a shows the steady increase in ultimate load, while Fig. 6b gives the reduction in shear strength with growing length L_L of glued area. As can be seen joint strength diminishes from 3.7 N/mm² to 1.4 N/mm² in the length range of L_L = 5 to 40 cm. For the length L_L = 30 cm and L_L = 40 cm the ultimate load F amounts to F = 166 kN (Fig. 6a), which implies that no increase in ultimate load is possible by an increase in glued area length above L_L = 30 cm.

For specimens with l_{e1} = 0 cm, a different effect of lap length L_L is observed. For these specimens tensile strength perpendicular to grain affects failure in the lap length range below 20 cm. With increasing length of glued area these stresses decrease and therefore joint strength increases. For glued area lengths L_L > 20 cm shear strength and compression strength perpendicular to grain at the beginning of the glued area control joint strength also for specimens without end distance. Thus joint strength decreases with increasing length L_L of glued area, but it is greater than for specimens with l_{e1} = 5 cm. This is due to the more favourable combination of shear stresses and compression stresses perpendicular to grain in the glued area (see Fig. 3).

4.2 Effect of width B_L of glued area

Fig. 7 shows the influence of width B_L (in the range between 10 and 25 cm) on joint strength for specimens with end distance l_{e1} = 5 cm, length L_L = 20 cm and angle of gluing α = 0°. As can be seen width B_L has no significant influence on joint strength.

4.3 Effect of shape of glued area

Fig. 8 shows the influence of the shape of the lapped glued area on joint strength for different lap lengths L_L. Differences in strength values are obviously within the range of variation of test results. A significant influence of glued area shape on shear strength of glued joints cannot, therefore, be deduced from the tests conducted here.

4.4 Effect of angle of gluing α

The influence of the angle of gluing on shear strength of glued joints is given in Fig. 9 for specimens with rectangular or parallelogram shape of glued area. With increasing angle of gluing a steady reduction in joint strength is noticeable due to the anisotropic properties of wood. Fig. 9 shows that the Hankinson formula (Forest Products Laboratory 1921) is well suited to describe the effect of the angle of gluing.

4.5 Effect of clamping technique

Fig. 10 shows joint strength values achieved with different clamping techniques. In addition to former tests (Glos, Henrici, Horstmann, 1987) the influence of the type and number of nails on joint strength was further investigated here using specimens with rectangular and parallelogram shape of glued area, $A_L = 20 \cdot 15$ cm^2, angle of gluing $\alpha = 0°$ and end distance $l_{e1} = 5$ cm. The test results confirm that nail-clamped specimens exhibit equivalent strength values as achieved with hydraulic clamping technique. There is no difference in joint strength whether clamping pressure is applied by 9 threaded nails or by 9 or even only 5 common wire nails. The difference between the joint strength of pressure-clamped and of nail-clamped specimens with a parallelogram glued area, shown in Fig. 10 is not statistically significant.

4.6 Effect of type of glue

The influence of glue type on joint strength is shown in Fig. 11 for specimens with a rectangular shape of $A_L = 40 \times 15$ cm^2 and an angle of gluing $\alpha = 0°$. As can be seen, an epoxid glue (Araldit AV 138, hardener HV 953) and a PVAc-glue (Vinnapas-

Dispersion DPN 15) gave an average increase in strength of about 35 % as compared to strength of joints glued with phenol-resorcinol-formaldehyde glue. This is due to the greater plasticity of the epoxid and the PVAc-glue. On account of greater plasticity the shear stress peak at the beginning of the glued area is reduced which enlarges the load bearing capacity of the glued area.

4.7 Effect of density ρ_{12}

Fig. 12 gives the positive correlation between joint strength and wood density of test specimens within the density range $370 \leq \rho_{12} \leq 510$ kg/m^3. Test results indicate that the increase in joint strength with increasing density is independent of the size of the glued area.

5. Concept for a design rule

To establish design rules for glued lap joints analytical investigations using the finite element method are at present conducted. In parallel control tests and tests on glued trusses are under way. Taking into account results achieved so far the following formula is suggested for calculating the characteristic load bearing capacity of the glued area

$$F_u = \tau_o \cdot L_L \cdot B_L \cdot k_L \cdot k_\alpha \cdot k_K \cdot k_\rho \cdot k_d$$

with τ_o as basic characteristic shear strength (i.e. $\alpha = 0$, $\sigma_\perp = 0$) acc. to Fig.5. The factors k_L, k_α, k_K, k_ρ and k_d take into account the effects of length of glued area, angle of gluing, type of glue, density and width of joint components. When determining factor k_L a differentiation should be made between lengths $L_L \leq 15$ cm and lengths greater than 15 cm (see 4.1). As the tests showed no noticeable effects of width B_L, shape of glued area and of clamping technique, these parameters are not considered in the formula.

References

Dutko, P. 1969: Die Grundlagen des Holzleimbaus. Bauingenieur-Praxis, Heft 51. Berlin, München: W. Ernst & Sohn

Egner, K. 1954: Technologische Grundlagen der Dreieck-Streben-Bauweise. Holz-Zbl. 80: 111-114

Egner, K. 1962: Versuche über die Tragfähigkeit und Beständigkeit von Schrägverleimungen. Berichte aus der Bauforschung, Heft 25, Holzleimbau. Berlin: W. Ernst & Sohn

Forest Products Laboratory 1921: Investigation of crushing strength of spruce at varying angles of grain. US Air Service Information Circular Vol. III, No. 259. Washington

Glos, P.; Henrici, D.; Horstmann, H. 1987: Festigkeit großflächig geleimter Knotenverbindungen. Holz Roh-Werkstoff 45: 355-364

Graf, O.; Egner, K. 1938: Versuche mit geleimten Laschenverbindungen aus Holz. Holz Roh-Werkstoff 1: 460-464

Kalina, M. 1965: Die Scherbeanspruchung in Knotenplatten aus Sperrholz bei geleimten Fachwerkträgern. Holz Roh-Werkstoff 23: 394-396

Kolb, H. 1974: Versuche mit verleimten Holzbauteilen. Holz Roh-Werkstoff 32: 257-262

Spengler, R. 1982: Festigkeitsverhalten von Brettschichtholz unter zweiachsiger Beanspruchung. München: SFB 96 Lab. f. d. konstr. Ing.-Bau d. TUM (Ber. z. Zuverlässigkeitstheorie d. Bauwerke; H. 62)

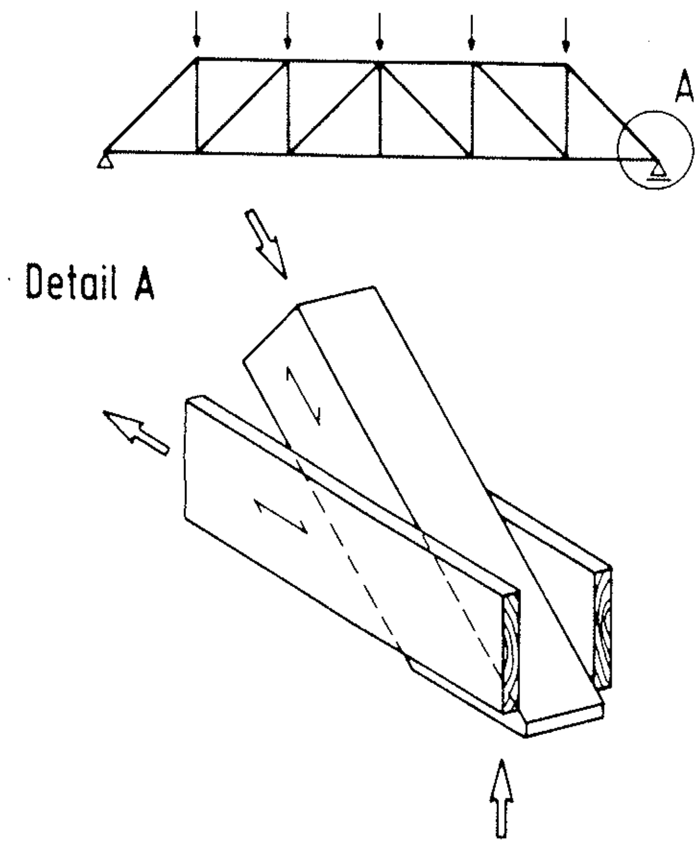

Figure 1: Truss (schematic). A: heel joint

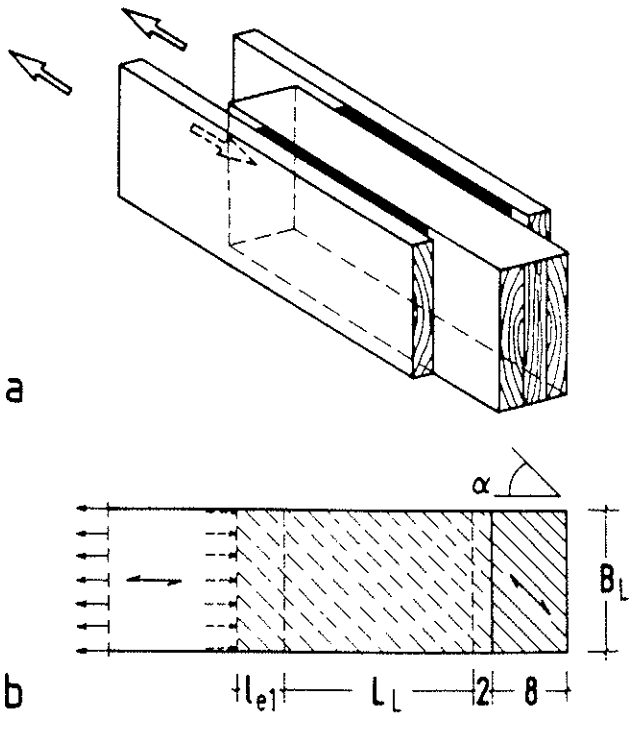

Figure 2: Specimen for basic joint tests

a) Threedimensional view

b) Side view

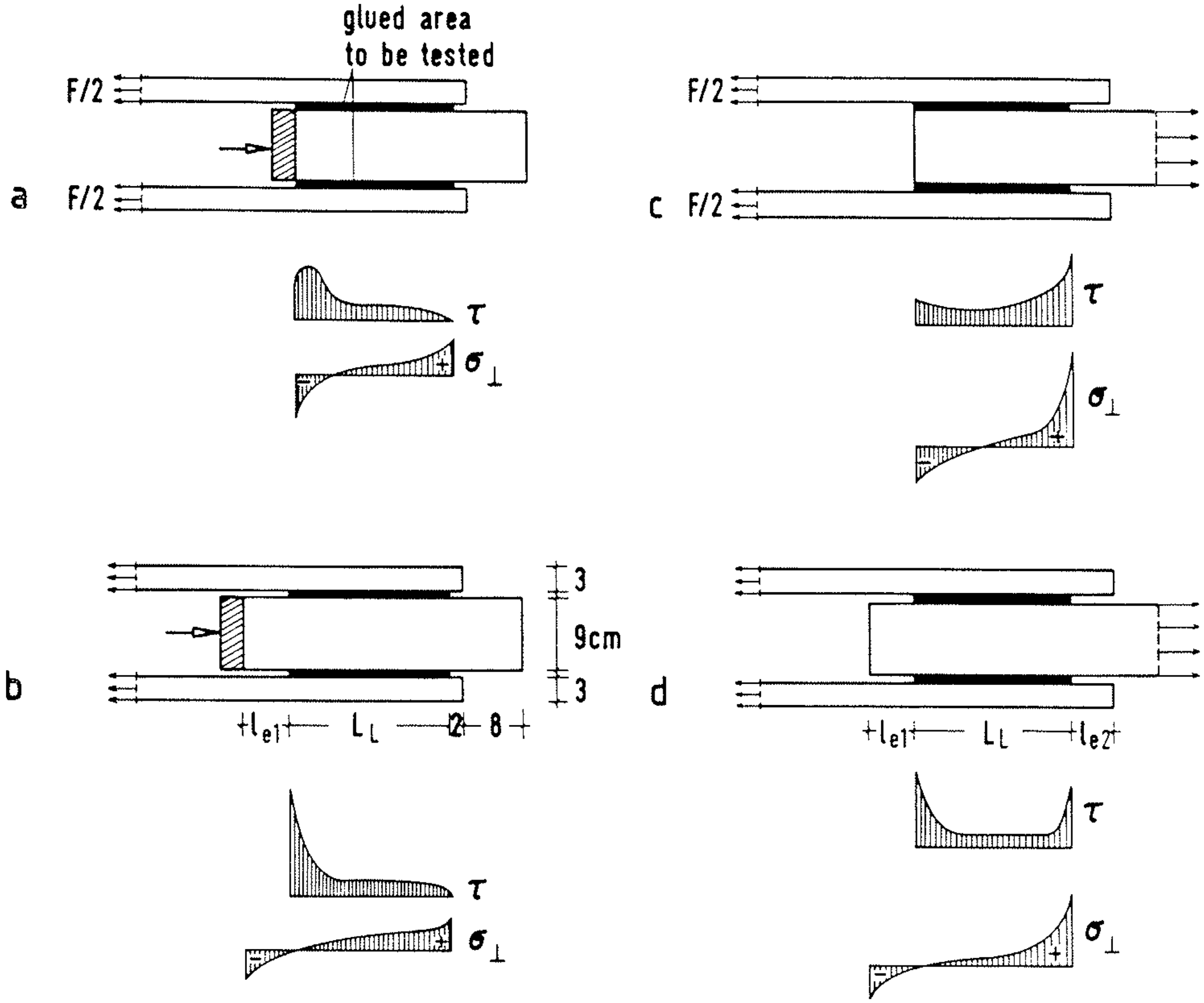

Figure 3: Specimens tested and stress distribution along the glueline in relation to load transmission mode and end distance

a), b) tension-compression; c), d) tension-tension

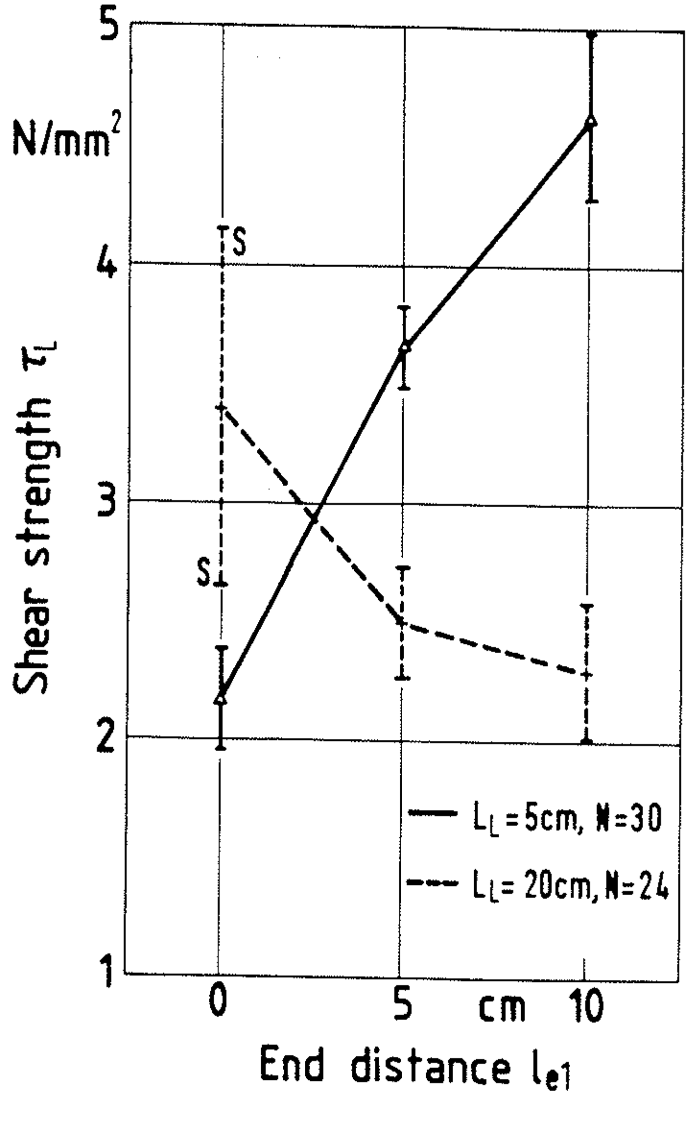

Figure 4: Effect of end distance l_{e1} on shear strength τ_L for specimens with different lengths of glued area (L_L = 5 cm, L_L = 20 cm, α = 0°)
s = standard deviation

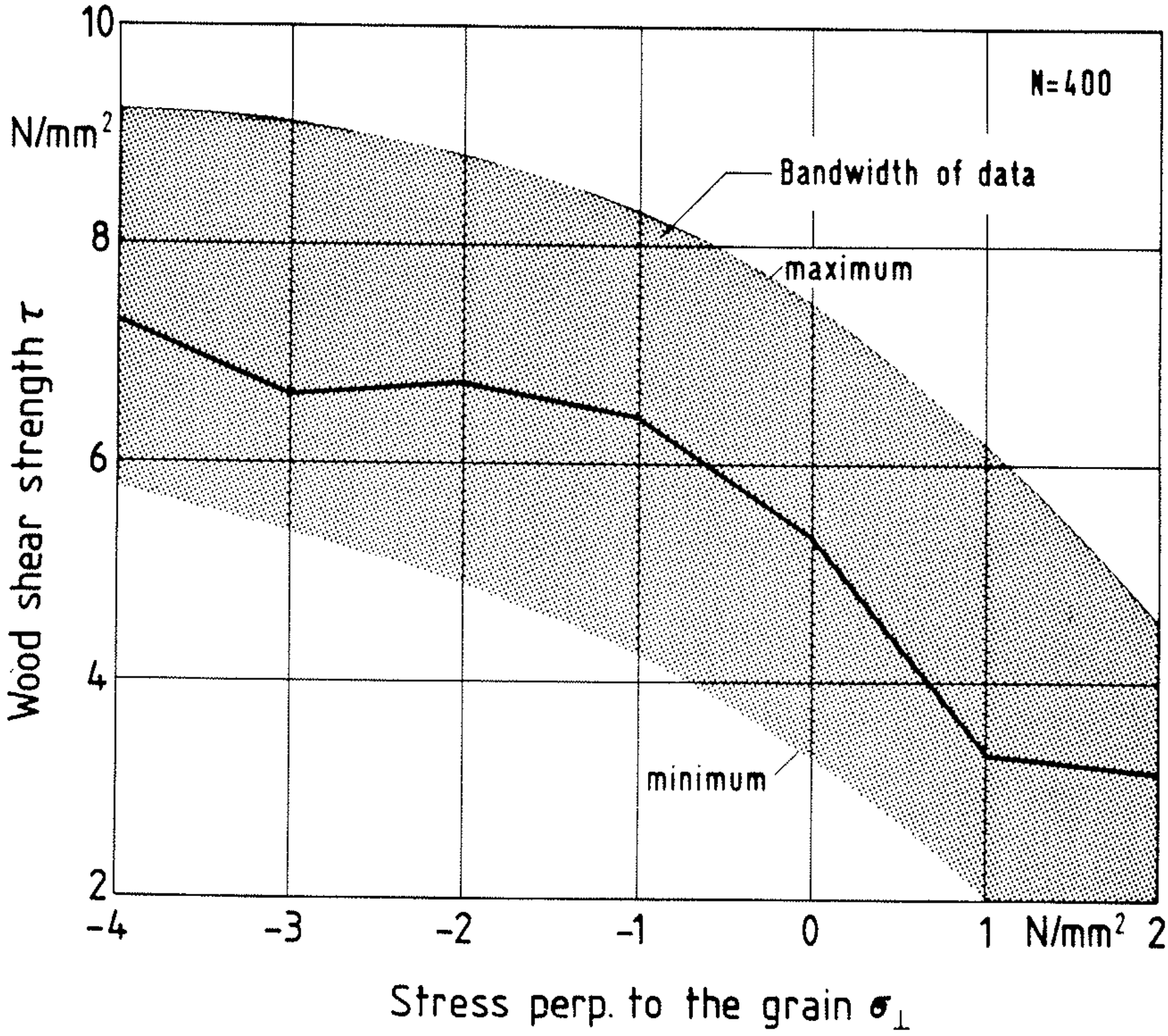

Figure 5: Effect of stress perpendicular to the grain on wood shear strength. According to Spengler (1982).

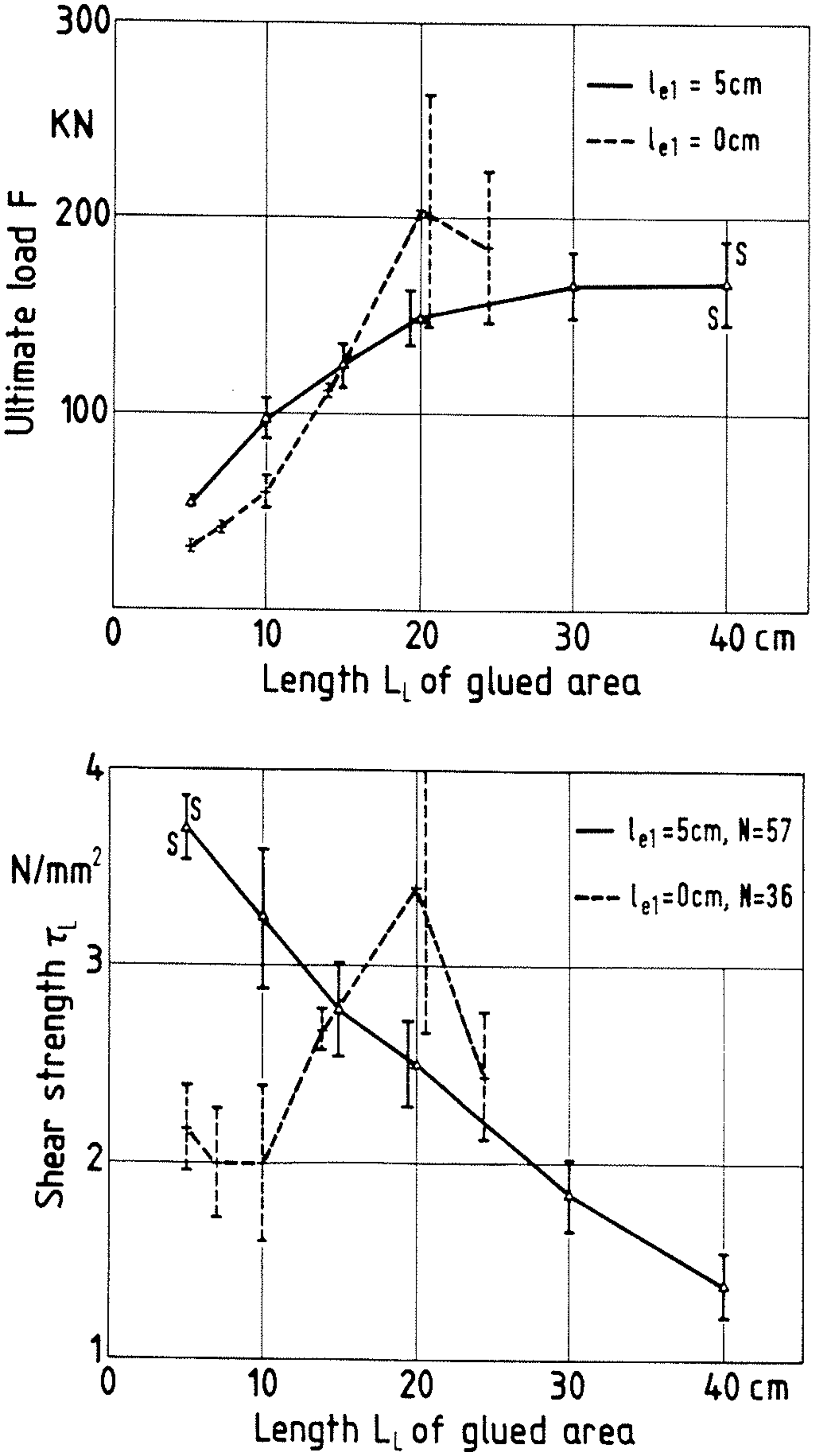

Figure 6: Effect of length L_L of glued area
a) on ultimate load F and b) on shear strength for specimens without and with end distance
(l_{e1} = 0 cm, l_{e1} = 5 cm, α = 0°)
s = standard deviation

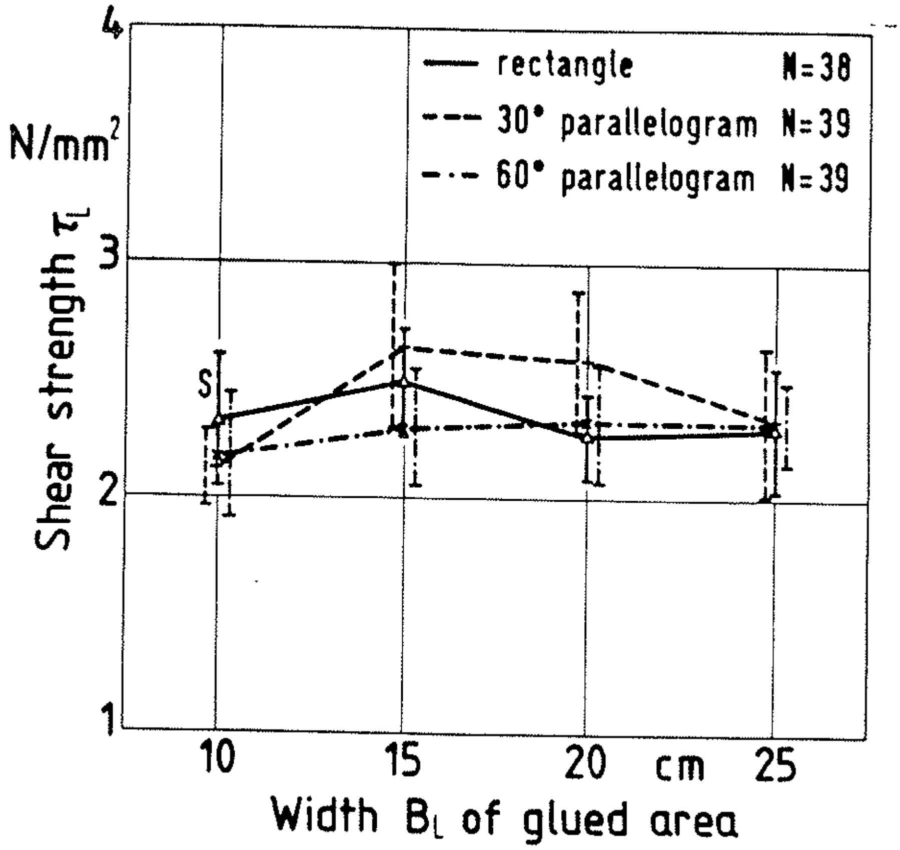

Figure 7: Effect of width B_L of glued area on shear strength τ_L (l_{el} = 5 cm, α = 0°, L_L = 20 cm)
s = standard deviation

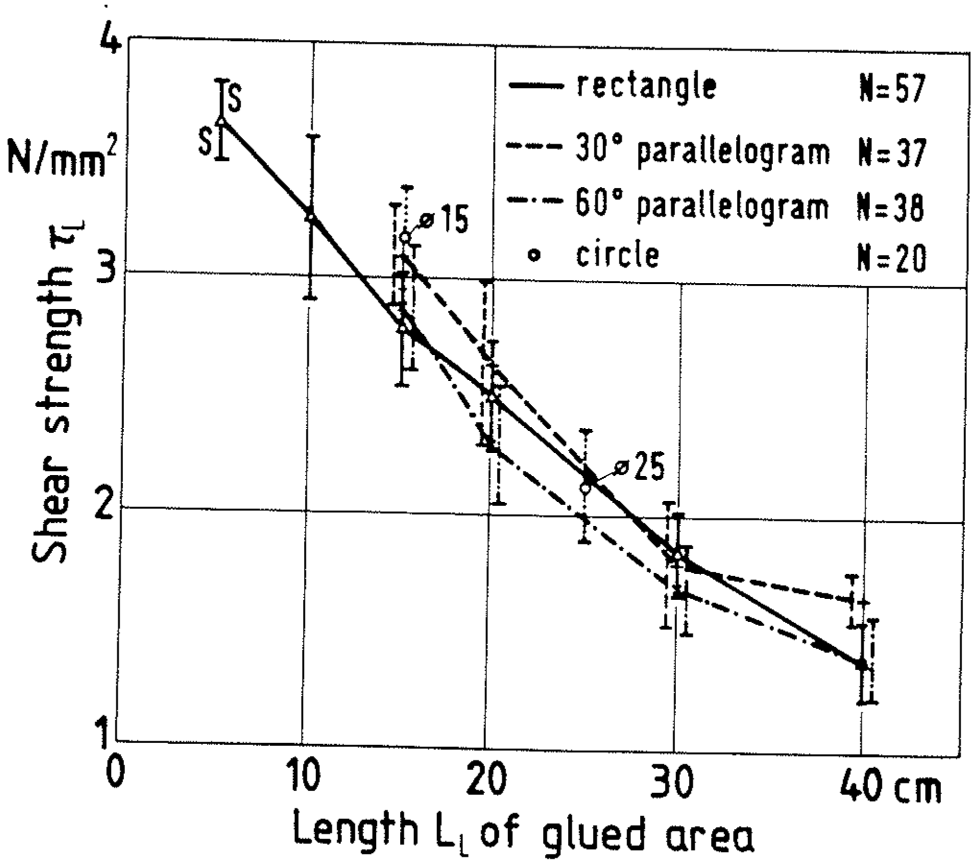

Figure 8: Effect of shape of glued area on shear strength τ_L for different lengths of glued area (l_{el} = 5 cm, α = 0°)
s = standard deviation

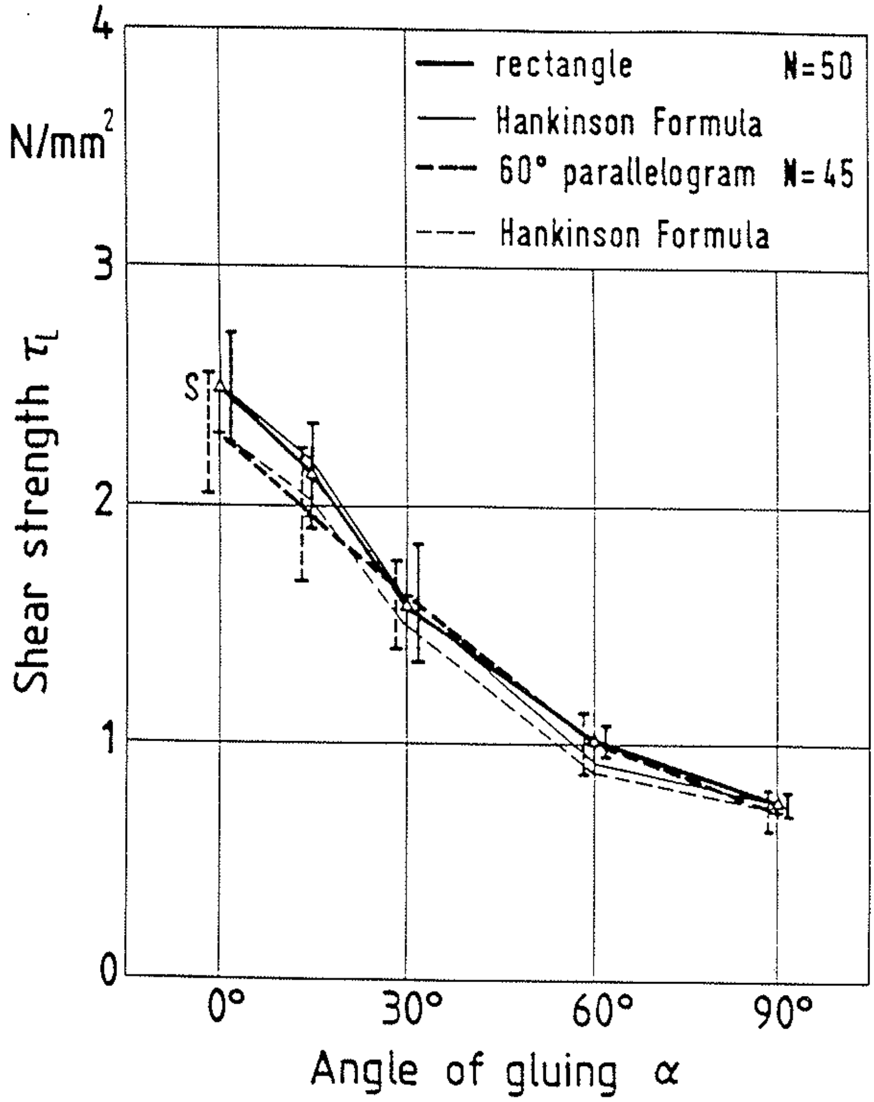

Figure 9: Effect of angle of gluing α on shear strength τ_L (L_L = 20 cm, B_L = 15 cm, l_{el} = 5 cm)
s = standard deviation

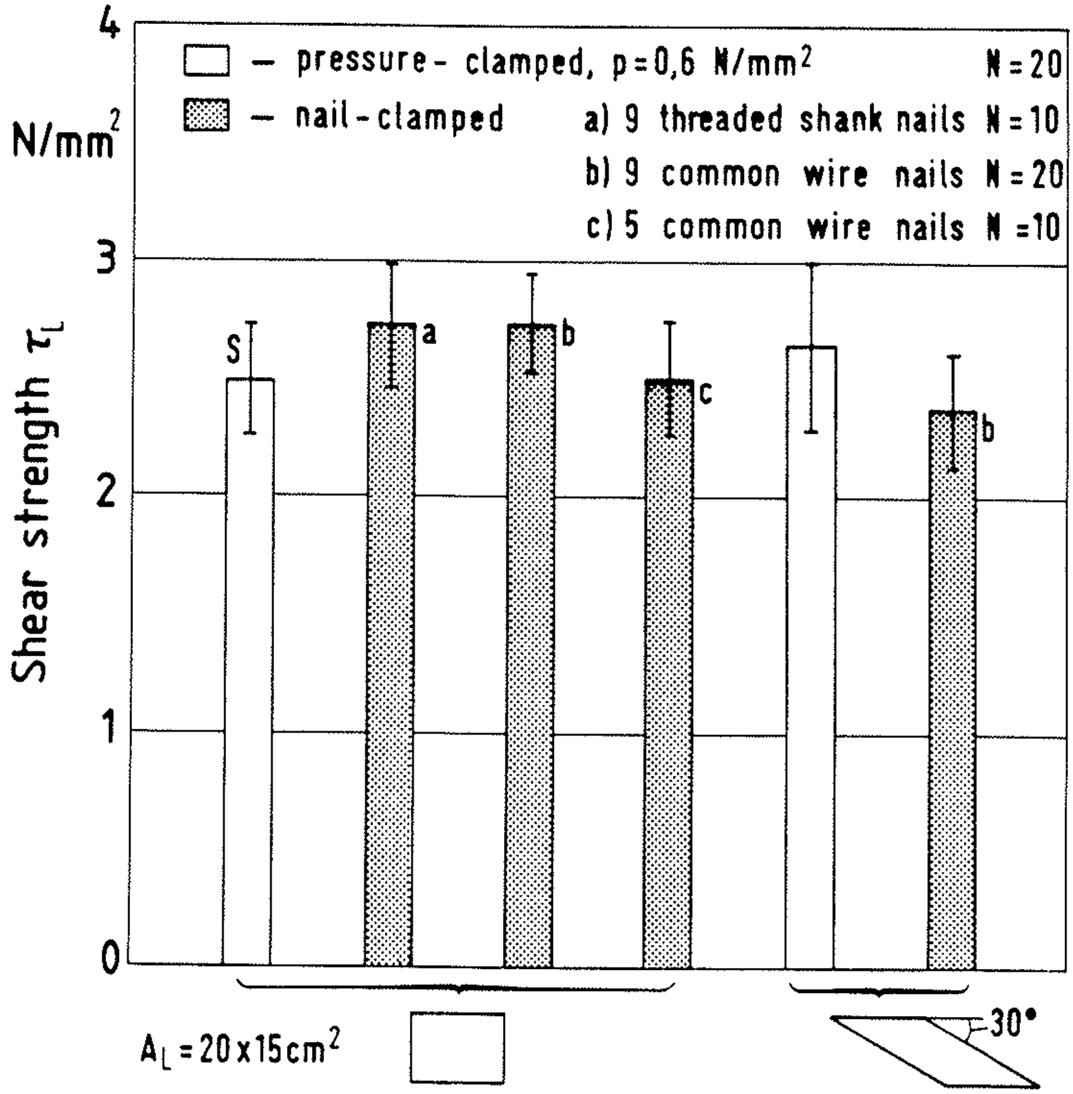

Figure 10: Effect of pressure technique on shear strength τ_L
(L_L = 20 cm, B_L = 15 cm, α = 0°, l_{el} = 5 cm)
s = standard deviation

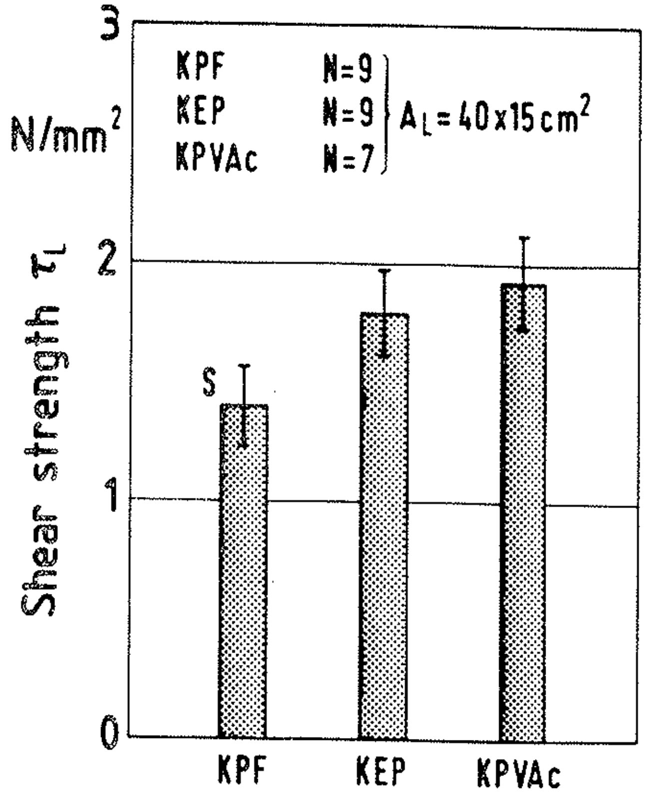

Figure 11: Effect of glue type on shear strength τ_L (L_L = 40 cm, B_L = 15 cm, α = 0°, l_{el} = 5 cm) s = standard deviation

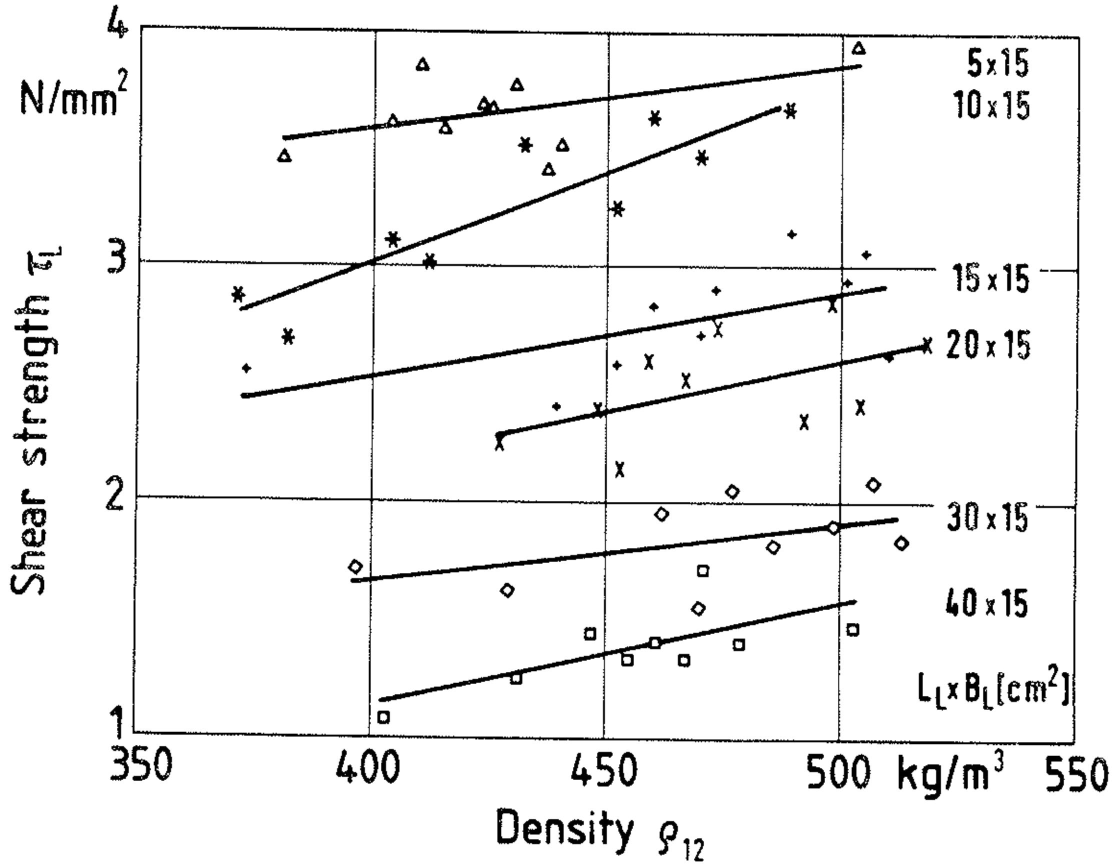

Figure 12: Effect of density ρ_{12} on shear strength τ_L for different sizes of glued area ($A = L_L \cdot B_L$, α = 0°, l_{el} = 5 cm)

CIB -W18A / 22-7-9

INTERNATIONAL COUNCIL FOR BUILDING RESEARCH STUDIES AND DOCUMENTATION

WORKING COMMISSION W18A - TIMBER STRUCTURES

TOOTHED RINGS TYPE BISTYP 075
AT THE JOINTS OF FIR WOOD

by

J Kerste
Rzeszow University of Technology
Poland

MEETING TWENTY - TWO

BERLIN

GERMAN DEMOCRATIC REPUBLIC

SEPTEMBER 1989

Dr.Eng. Jerzy Kerste
Rzeszów University of Technology
Poland

TOOTHED RINGS TYPE BISTYP ϕ75 AT THE JOINTS OF FIR WOOD

Modern timber structure is characterized by small material consumption and use of fastenings which could transfer significant load with the bearing surface reduced to minimum. Timber structures of wood consumption index less than 3 cubic meters per 100 square meters of covered area are considered as economical[9].

There are many different types of fastenings; in between world wide used are nailed plates [3] and toothed rings [2],[4]. The application of nailed plates were studied and few types of toothed rings were designed and tested. They are: star-shaped Kozak toothed rings [8] and toothed rings BISTYP type [1],[10],[11]. Load capacity of the BISTYP type fastenings, their elasticity and elastoplasticity were determined in [1] for pinewood with humidity rate of 17 %.

During the research work in Building Structure Faculty of Rzeszów University of Technology some of the characteristic parameters of above mentioned types of fastenings were determined [5]; the fir timber of Bieszczady fir /Abies Bieszczadiensis/ was used. The results were presented during the symposium in Szczecin [6] and the conference in Krynica [7]. The tests were done for one pair toothed rings BISTYP type ϕ75 joints pulled by the M16 bolt. The joints were treated by:

- compression load parallel to grain - series A - fig. 1a.,
- pure bending - series B - fig. 1b.,
- bending with shear - series C - fig. 1c.

The destructive test were carried out according to RILEM recommendations [13], to compare the results with the results obtained

Fig. 1

Fig. 2

by other laboratories. The load diagram is shown in fig. 2. Each of the series consisted of 18 specimens. The value of destructive load were determinated preliminary for the first three specimens / F_N, M_N, or F_N and M_N /. The detailed tests were carried out for the rest fifteen specimens, by a constant rate of loading raised with 0.1 ultimate load. Increase of displacement at the constant value of the load or decrease of a force gauge of testing machine were marked for the moment the failure of the joint is reached. The data obtained were the base to determine the following:

- "virgin" displacement as the lower value of the two:

$$\left.\begin{aligned} v_{0,4} &= \frac{4}{3}\left(v_4 - v_1\right) \\ v_{0,4} &= v_4 \end{aligned}\right\} \quad \text{for joints in series A}$$

$$\left.\begin{aligned} \varphi_{0.4} &= \frac{4}{3}\left(\varphi_4 - \varphi_1\right) \\ \varphi_{0,4} &= \varphi_4 \end{aligned}\right\} \quad \text{for joints in series B and C}$$

- elastic displacement:

$$e_{0,4} = \frac{4}{3}\left(\frac{v_4' + v_4''}{2} - \frac{v_1' + v_1''}{2}\right) \quad \text{for joints in series A}$$

$$e_{\varphi 0,4} = \frac{4}{3}\left(\frac{\varphi_4' + \varphi_4''}{2} - \frac{\varphi_1' + \varphi_1''}{2}\right) \quad \text{for joints in series B and C}$$

- joint slip:

$$a = v_4 - v_{0,4} \quad \text{for joints in series A}$$

$$a_\varphi = \varphi_4 - \varphi_{0.4} \quad \text{for joints in series B and C}$$

- joint stiffness:

$$k_{0,4} = \frac{v_{0.4}}{4f} \quad \text{for joints in series A}$$

$$k_{\varphi 0,4} = \frac{\varphi_{0.4}}{4f} \quad \text{for joints in series B and C}$$

- displacement at overload:

$$6f \rightarrow \begin{cases} \vartheta_{0.6} = \vartheta_{0.4} + \vartheta_6 - \vartheta_4'' & \text{for joints in series A} \\ \varphi_{0.6} = \varphi_{0.4} + \varphi_6 - \varphi_4'' & \text{for joints in series B and C} \end{cases}$$

$$8f \rightarrow \begin{cases} \vartheta_{0.8} = \vartheta_{0.4} + \vartheta_8 - \vartheta_4'' & \text{for joints in series A} \\ \varphi_{0.8} = \varphi_{0.4} + \varphi_8 - \varphi_4'' & \text{for joints in series B and C} \end{cases}$$

The average load - deformation curve for joints of series A is shown on fig. 3, and for joints of series B and C on fig. 4. The data obtained during the tests made in Research and Design Centre for Industrial Building - Bistyp are shown on fig. 3 too [1].

Fig. 3
Fig. 4

The chrakteristic value of load capacity were determined with the probability coefficient 0.95 according to formulas:

$$F_k = \overline{F}_N - t \cdot s$$

or

$$M_k \quad \overline{M}_N - t \cdot s$$

where: $\overline{F}_N$, $\overline{M}_N$ - mean values of destructive load or destructive bending moment for all joints of the series tested respectively,

s - standard deviation,

t - coefficient depending on the number of recorded values /tested specimens/, level confidence and the percentile wanted. For $n = 18$ and $p = 0.95$, $t = 2.110$.

The bearing load capacity of joints was calculated according to:

$$\gamma_m = \gamma_{m1} \cdot \gamma_{m2}$$

where: γ_{m1} - partial safety factor for material determining the influence of long-term loading on ultimate strength of material and joints in timber structures. The value of γ_{m1} was 1.50 [12] for the load parallel to grain and normal load-duration. The value of γ_{m1} was 2.00 for the load across to grain and normal load - duration,

γ_{m2} - partial safety factor calculated as bellow:

$$\gamma_{m2} = \frac{\overline{F}_N}{F_k} \qquad \text{or} \qquad \gamma_{m2} = \frac{\overline{M}_N}{M_k}$$

Finally, the bearing capacity of joints were calculated as follows:

$$F_o = \frac{F_k}{\gamma_m} \qquad \text{or} \qquad M_o = \frac{M_k}{\gamma_m}$$

In each of the joints were two toothed rings, so the characteristic load capacity and bearing load capacity for one toothed ring were calculated dividing by two corresponding load capacities for the joint. The load capacities and elasticity and elastoplasticity properties of the joints tested of series A are given in table 1, and for series B and C in table 2.

Tabl. 1
Tabl. 2

There are two stages of deformation in the joint, separated by the value of loading of about 50 % of destructive load. The displacement is small and the load in whole is transfered by the toothed rings in the I-st stage. In the II-nd stage:

- in the joints of A series after the one-milimeter gap in the opening is consumed the bolt commence its work pressured and bended. The teeth of rings cut and crash the timber around, being bended out. The timber in contact with the bolt crushes as well. The displacement increases faster than in the I-st stage. The failure of the joints of this series is caused by the loss of bearing-capacity /the decrease of force-gauge of testing machine/,
- in the joints of B and C series the teeth of rings begin to cut and crush the grains of timber. The displacement, growing up faster according to the raise of loadings follows. No deformations of toothed rings occur, so not the rings, but the mechanical properties of timber are responsible for

the bearing-capacity of the joint.

Commentary:

1. The results of bearing capacity obtained, indicate that the toothed rings bear the load in the I-st stage, in case of properly designed timber structure. The bolt presses against the timber, and the friction may cause small rise of the bearing capacity of the joint.
2. Comparing the results obtained for the joints of series A and the results obtained in [1] let us assume that the bearing capacity of the toothed rings in fir timber is the same as of the toothed rings in pine timber.
3. The joint with one pair of BISTYP type toothed rings is able to bear the bending moment.
4. Concentrated force parallel to grain of joined units applied to the joint transfering the bending moment shall not decrease considerable the bearing capacity of the joint. Nevertheless, it causes a real loss of elastic and elastoplastic properties of the joint.

Literature.

[1]. Investigations of timber joints with mechanical fasteners BISTYP type. C.O.B.P.B.P. Bistyp, Warszawa 1974.

[2]. Dziarnowski Z., Michniewicz W.: Structures made of wood and wood-based materials. Arkady, Warszawa 1974.

[3]. Dziarnowski Z., Olifierowicz J., Nożyński W.: Modern industrialized methods of joining timber structures with mechanical connectors. Inżynieria i Budownictwo 9/1976.

[4]. Gołębiowski Z.: Timber structures. PWN Warszawa 1978.

[5]. Kerste J.: Effect of timber moisture rate on behaviour of a timber structure, exemplified by a truss frame. ITB Warszawa 1982 - the doctor's thesis.

[6]. Kerste J.: Investigations of toothed ring joints type BISTYP ϕ75 in fir wood members of different moisture characteristic. Prace Naukowe Politechniki Szczecińskiej. Szczecin 1983 Nr 19/234/, Część I.

[7]. Kerste J.: Investigations of toothed ring joints type BISTYP in fir wood members loading by bending moment and shear force. Referaty XXXIII KN KILiW PAN i KN PZITB Krynica 1987 tom 3.

[8]. Kozak R.: Timber structures. Warszawa - Poznań 1963.
[9]. Kuś S., Kerste J.: Actual problems of safety and economics of timber structures for farming. Inżynieria i Budownictwo 4/1981.
[10]. Kuś S., Midak J.: Mechanical fasteners type BISTYP for joints of timber structures. Inżynieria i Budownictwo 4/1979.
[11]. Kuś S., Midak J.: BISTYP rings at timber structures. Budownictwo Rolnicze 7/1979.
[12]. PN-81/B-03150.01 Timber structures. Design rules. Materials.
[13]. Recommendations for testing methods for joints with mechanical fasteners and connectors in load-bearing timber structures - RILEM 3TT Committee /Seventh draft/ CIB W18, Aalborg 1976.

Table 1. Comparison of results from tests of joints series A and made in Bistyp.

Series	A	Bistyp
Moisture content $\overline{W}$ [%]	12.1	16.7
Air temperature t [°C]	20.3	18.0
Relative air humidity w [%]	67.8	--
Ultimate load of the joint $\overline{F}_N$ [kN]	79.67	70.87
Standard deviation s [kN]	4.22	3.18
Coefficient of variation ν [%]	5.30	4.49
Characteristic value of load capacity of the joint F_k [kN]	70.77	64.20
Load capacity of the joint F_o [kN]	41.88	38.90
Characteristic value of load capacity of the toothed ring ϕ75 F_k [kN]	35.39	32.10
Load capacity of toothed ring ϕ75 F_o [kN]	20.94	19.45
"Virgin" displacement $V_{0.4}$ [mm]	0.357	0.480
Displacement at overload $V_{0.6}$ [mm]	1.577	2.260
Displacement at overload $V_{0.8}$ [mm]	3.842	5.620
Joint stiffness $k_{0.4}$ [mm/kN]	0.011	0.022
Elastic displacement $e_{0.4}$ [mm]	0.095	0.204
Joint slip a [mm]	not appears	
Displacement calculated for F_o and $k_{0.4}$ [mm]	0.461	0.836
Displacement read over from fig.3 for F_o [mm]	0.933	1.800

Table 2. Summary of results from tests of joints series B and C.

Series	B	C
Moisture content $\overline{W}$ [%]	12.1	12.2
Air temperature t [°C]	23.2	22.8
Relative air humidity w [%]	64.7	78.5
Ultimate moment of the joint $\overline{M}_N$ [kN]	2.093	2.033
Standard deviation s [kN]	0.110	0.138
Coefficient of variation ν [%]	5.26	6.79
Characteristic value of load capacity of the joint M_k [kNm]	1.861	1.742
Load capacity of the joint M_o [kNm]	0.831	0.778
Characteristic value of load capacity of the toothed ring ϕ75 M_k [kNm]	0.931	0.871
Load capacity of toothed ring ϕ75 M_o [kNm]	0.416	0.389
"Virgin" displacement $\varphi_{0.4}$ [deg]	0.148	0.266
Displacement at overload $\varphi_{0.6}$ [deg]	0.478	0.785
Displacement at overload $\varphi_{0.8}$ [deg]	2.283	>3.688
Joint stiffness $k_{\varphi 0.4}$ [deg/kNm]	0.178	0.314
Elastic displacement $e_{\varphi 0.4}$ [deg]	0.038	0.108
Joint slip a_φ [deg]	not appears	
Displacement calculated for M_o and $k_{\varphi 0.4}$ [deg]	0.148	0.244
Displacement read over from fig.4 for M_o [deg]	0.148	0.230

Captions for the drawings.

Fig. 1. Configuration of joints tested. Scheme of loading and measuring of deformatios. a - joints of series A, b - joints of series B, c - joints of series C.

Fig. 2. Loading procedure /a/ and idealised load-deformation curve and measurements /b/, according to the RILEM recommendations.

Fig. 3. Load-deformation curve for joints of series A and joints tested in Bistyp.

Fig. 4. Load-deformation curve for joints of series B and C.

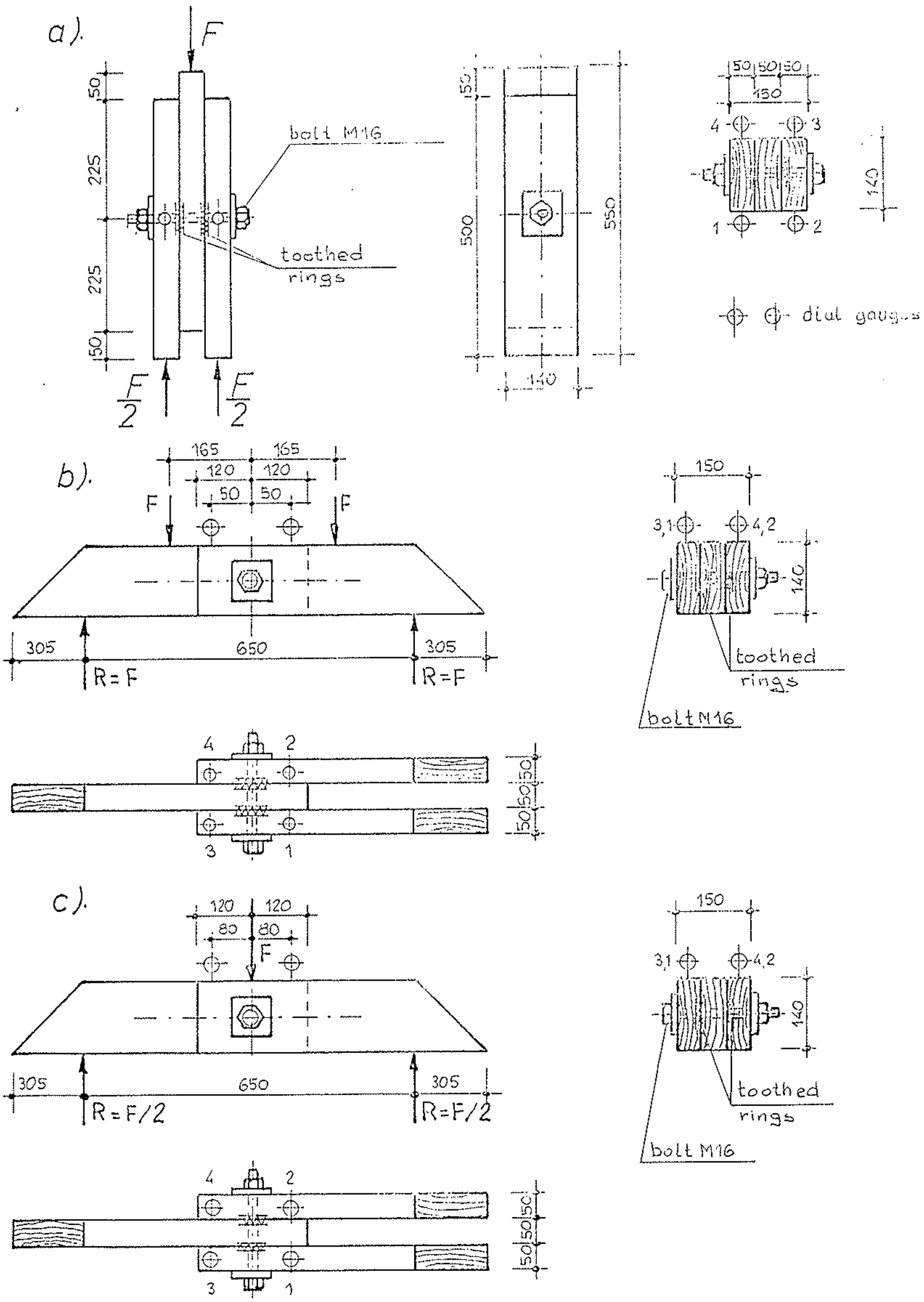
a).
F
bolt M16
toothed
rings
F/2
F/2
50
225
225
50
500
550
140
50 50 50
150
140
dial gauges
b).
165
165
120
120
50
50
F
F
305
650
305
R=F
R=F
150
toothed
rings
bolt M16
c).
120
120
80
80
F
305
650
305
R=F/2
R=F/2
toothed
rings
bolt M16

Fig. 1

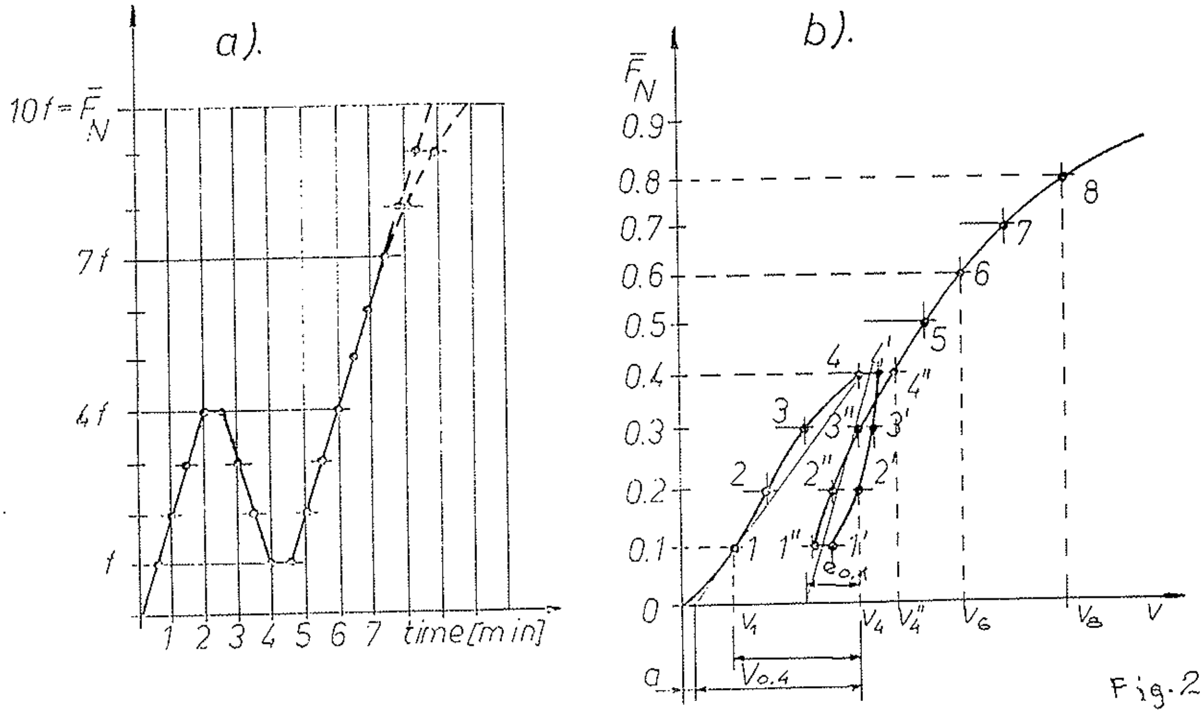
a).
b).
10f = $\bar{F}_N$
7f
4f
f
1 2 3 4 5 6 7 time[min]
$\bar{F}_N$
0.9
0.8
0.7
0.6
0.5
0.4
0.3
0.2
0.1
0
V_1
V_4
V_4''
V_6
V_8
V
$V_{0.4}$
a
$e_{0.1}$

Fig. 2

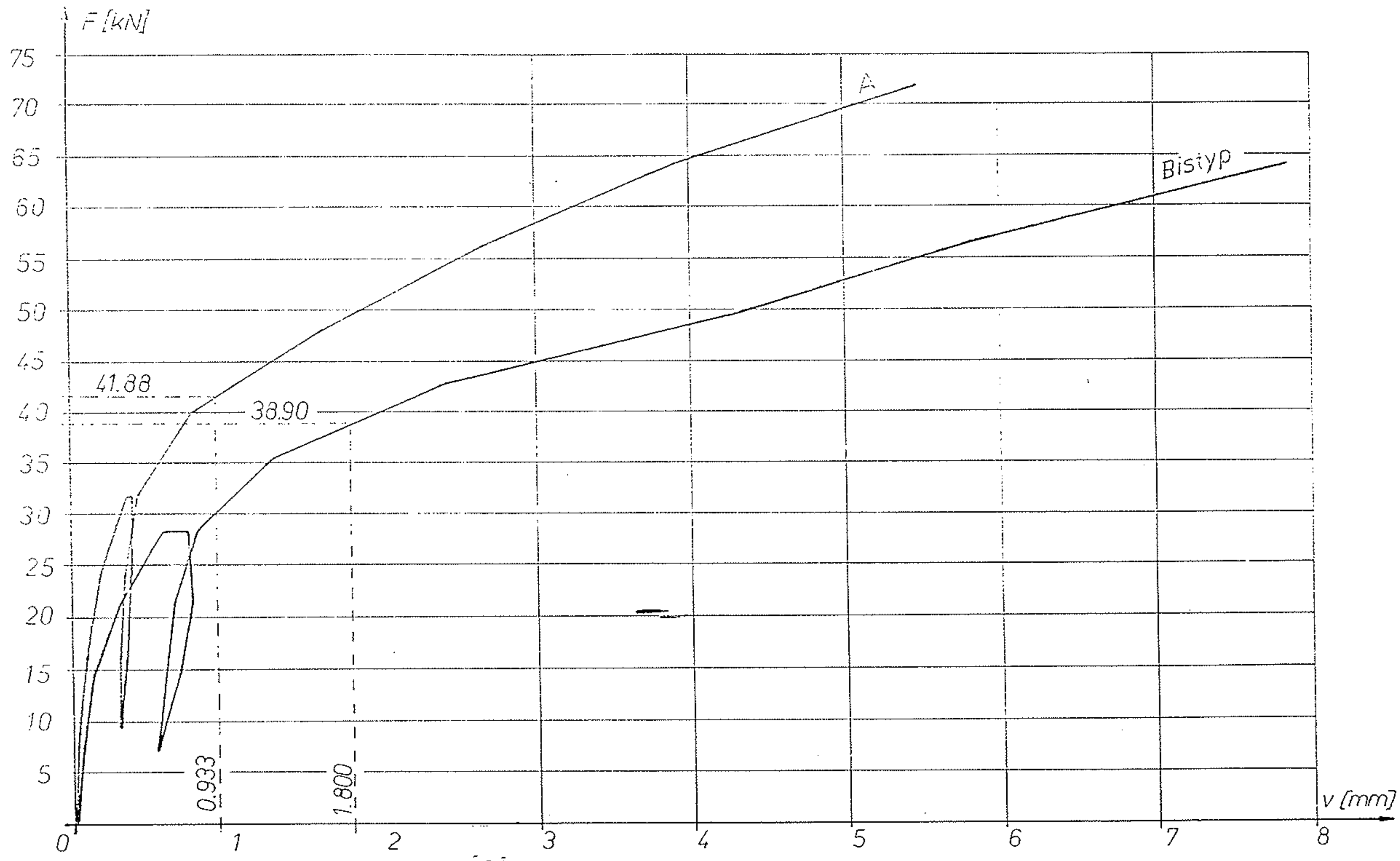
F [kN]
75
70
65
60
55
50
45
41.88
40
38.90
35
30
25
20
15
10
5
0.933
1.800
0
1
2
3
4
5
6
7
8
v [mm]
A
Bistyp

Fig. 3

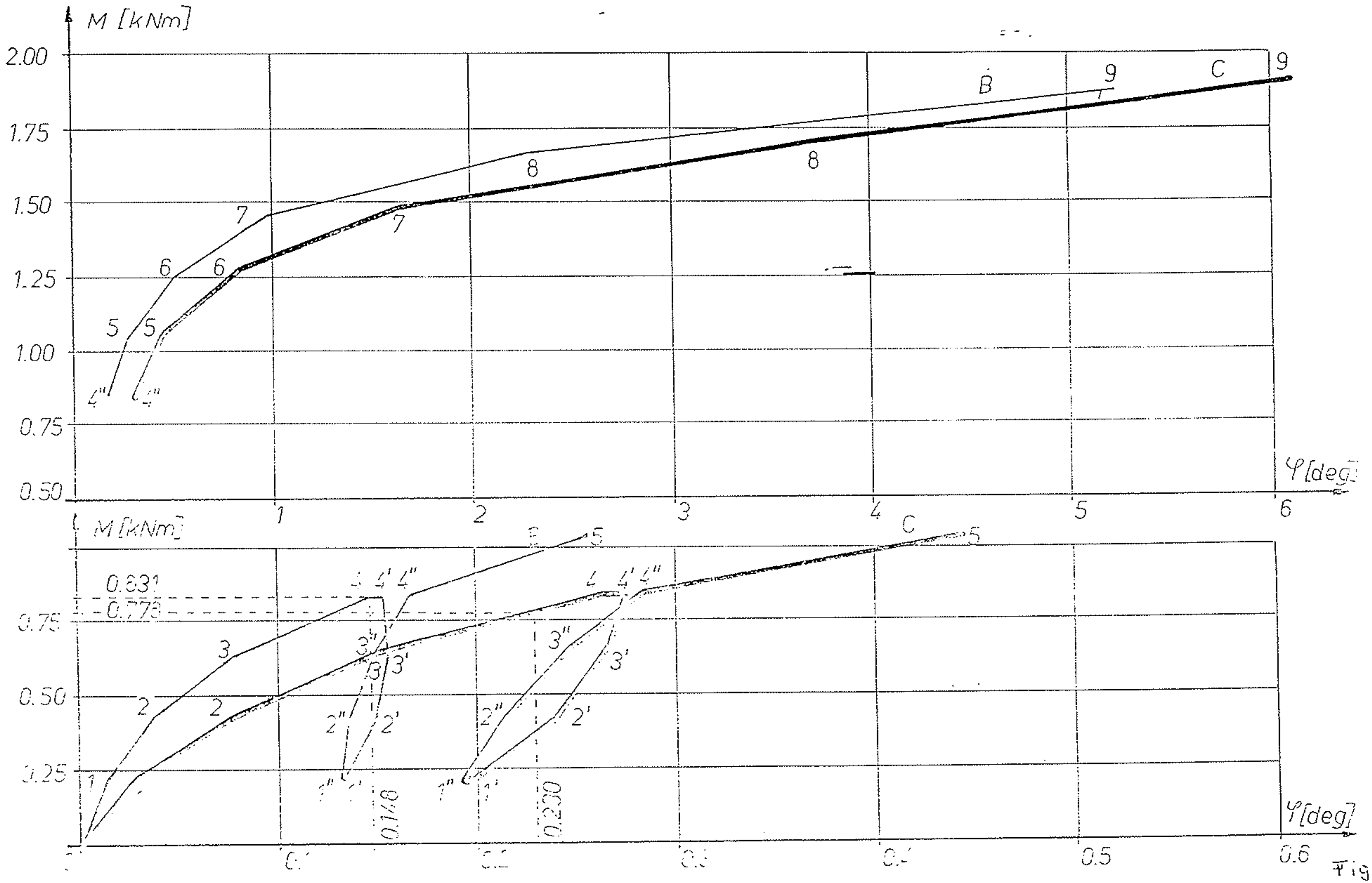

Fig. 4

CIB -W18A / 22-7-10

INTERNATIONAL COUNCIL FOR BUILDING RESEARCH STUDIES AND DOCUMENTATION

WORKING COMMISSION W18A - TIMBER STRUCTURES

CALCULATION OF JOINTS AND FASTENINGS AS COMPARED WITH THE INTERNATIONAL STATE

by

K Zimmer
Dresden University of Technology
Department of Civil Engineering
German Democratic Republic
and
K Lissner
BA of the GDR
Institute of Industrial Construction
Scientific Departement of Timber Structures
German Democratic Republic

MEETING TWENTY - TWO

BERLIN

GERMAN DEMOCRATIC REPUBLIC

SEPTEMBER 1989

Prof. Dr. sc. techn. Karlheinz Zimmer
Dresden University of Technology
Department of Civil Engineering

Dipl.-Ing. Karin Lißner
BA of the GDR
Institute of Industrial Construction
Scientific Department of Timber Structures

Calculation of Joints and Fastenings as Compared with the International State

1. Introduction

Basic values of the load-bearing capacity for steel-stud, screwed, nailed, wood-screw, flat-dowel and special-dowel connections for a dimensioning according to ultimate states in timber construction were determined in /6/, /7/, /8/ from comparative calculations, experimental investigations and in accordance with foreign literature as well as standards /1/, /2/, /3/, /4/, /5/. These investigations were continued, including other foreign standards /9/, /10/.

Since the introduction of a new method of dimensioning should always be connected with precise statements concerning the reliability of the timber structures and savings of material which can be achieved, the effects of the combined loads on the material consumption are determined, to add to theoretical investigations that had been performed.

2. Nailed Connections

2.1. Calculated Values of the Load-bearing Capacity under Shear Stress

In table 1, the calculation of the load-bearing capacity of nailed connections at a load on the nails normal to the shank direction is given according to the GDR proposal as compared with foreign standards. The calculated values following the GDR proposal are determined similarly to those according to the Czechoslovak /2/, Polish /4/ and Finnish /3/ standards. According to the GDR proposal, the basic values of the load-bearing capacity are determined for a minimum depth of penetration (min l_1).

According to /2/, /3/ and /4/, the basic values of the load-bearing capacity apply to a depth of penetration of 2 l_1 (min l_1 = 6d, 2 l_1 = 12d for single-shear connections); they have to be adequately reduced if this depth of penetration is not reached. According to DIN 1052 (10), which is still based on permissible stresses, the nails are calculated in the same way as according to /2/, /3/, /4/, /6/, /7/ and /8/. The contrast to the GDR proposal, however, is that the permissible nail load is determined as according to /2/, /3/, /4/ for a depth of penetration of 2 l_1 and reduced in accordance with the actual depth of penetration.

According to the Soviet standard, the nailed connections are treated in the same way as steel-stud and screwed connections. The load-bearing capacity of the nailed connections is determined on the basis of the specific pressure on the wall in the hole in the central and side pieces of wood or of the bending of the nail.

The procedure for the determination of the calculated values of the load-bearing capacity of nail connections according to the Danish standard /5/ is comparable with that according to the Eurocode 5 /9/. The parameters K and ß are dependent on, inter alia, the nail type, the yield moment of the nail, the kind of wood and the quality of wood (especially on the raw density) as well as on the making of the connection (e. g. drilling a smaller hole first). These factors are established in accordance with the national conditions.

As it is obvious from table 1, according to the international standards there are used adaptation factors in order to take into account the influences of duration of load and humidity on the load-bearing capacity of the joints and fastenings in the case of a dimensioning of the timber connections according to the method of ultimate states. Thus, according to /2/, /3/ adaptation factors are given specially for timber connections. It is stipulated in /1/, /4/, /5/, /9/ that for the calculation of the load-bearing capacity of the timber connections the same adaptation factors are valid as for the determination of the design strengths of timber. The tables 2 and 3 give the adaptation factors for the determination of the design strengths of timber and of the calculated values of the load-bearing capacity of joints and fastenings in accordance with the GDR proposal /7/, /8/, /11/. For comparison with them, table 4 gives the adaptation factors according to the Eurocode 5 /9/, which apply to the determination of the design strengths of timber and of the calculated values of the load-bearing capacity of joints and fastenings in the same way. There has to be taken into consideration that the strengths of timber as well as the load-bearing capacities of mechanical joints and fastenings which were determined in short-time tests as according to /9/ are converted into a time of circa three months /1/, /2/ in accordance with /7/, /8/, /11/, in contrast to /9/.

A comparison of the single-shear nailed connections with non-predrilled nail holes (table 5) shows that according to the GDR proposal, the Czechoslovak and Polish standards approximately the same values are obtained.

The values according to the Finnish standard are somewhat higher because of the conversion factor of circa 1.42. A dimensioning according to the Soviet standard gives more unfavourable values for the load-bearing capacity of the nail connections. This is due to the low basic values of the design strengths of the wood parallel to the grain because of specific pressure on the wall in the hole as well as of the nails because of bending. According to /1/, the nailed connections are dimensioned as steel-stud and screwed connections. The calculated value of the load-bearing capacity of nailed connections determined following the GDR proposal approximately corresponds to the normal safety class according to the Danish standard /9/. The basic values of the load-bearing capacity of nailed connections as well as for steel-stud, screwed, wood-screw, flat-dowel and special-dowel connections according to the GDR proposal which have been used for the comparative calculations are contained in /7/, /8/. The conversion factor from the permissible values according to /12/ which are valid at present to the basic values of the load-bearing capacities for the above-mentioned mechanical joints and fastenings is about 1.4, in order to maintain the wood consumption or the number of the joints and fastenings to be used with respect to a dimensioning based on permissible stresses. In order to state more precisely the theoretical findings for determining the calculated values of the load-bearing capacity of joints and fastenings as well as their adaptation factors, there were carried out extensive short- and long-time tests for determining the load-bearing capacity of nailed connections with nails of 3.4 x 90 at a stress normal to the shank direction. The influence of wood quality, direction of annual rings, type of stress and wood humidity on the load-bearing capacity of nailed connections was investigated. The specimens were loaded in accordance with the regulation contained in RILEM / CIB - 3 TT /13/. Load was applied until the ultimate load was reached, the duration of tests having been 8 to 12 min, as a rule. As the ultimate load there was regarded the load that did not increase any longer at the loading rate chosen at a further increase of displacement.

The test results were statistically evaluated with the aid of a three-parameter Weibull distribution.

As the experiments have shown, there cannot be found any load-bearing-capacity-reducing influence by the shear tension tests as compared with the shear compression tests as well as of the connections with standing annual rings with those having lying ones.

Figure 1 shows the distribution densities of the ultimate loads F_{max} in dependence on the wood quality and independent of it as well as independent of the direction of annual rings and the type of stress. If the curves of the quality classes I and II are compared with each other, there are not found any essential deviations. Therefore, the load-bearing capacities of the nailed connections can be determined as in TGL 33135 /12/ independently of direction of annual rings, type of stress and wood quality.

A comparison of the theoretically determined basic value of the load-bearing capacity of nailed connections with nails of 3.4 x 90 with the value obtained in the short-time test shows that the experimentally determined basic value of the load-bearing capacity is circa 30 % higher. This confirms the higher conversion factor of 1.4 from the permissible values to the basic values of the load-bearing capacity, which is used in the determination of the theoretical basic values of the load-bearing capacity, as against the conversion factor according to the Czechoslovak and Polish standards.

An increase of the theoretically determined basic value of the load-bearing capacity on the basis of the experimental investigations should not be made for the time being, however, since comparisons with foreign standards (table 5) show that very good results are already achieved with this basic value.

The proposed value of the adaptation factor for taking into account the influence of the wood moisture on the load-bearing capacity of timber connections with the value of 0.85 for the humidity class 2 ($18 \leq u \leq 24$ %) (table 3)is confirmed by the experimental investigations on nailed connections with nails of 3.4 x 90.

The adaptation factors for taking into account the influence of the duration of loading on the load-bearing capacity of timber connections were fixed following CSN 731701 /2/. If one proceeds from the fact that they have proved worthwhile in practice already for about 20 years, they should be maintained until own experimental investigations will be available. Moreover, they approximately correspond to the proposed values of the adaptation factor in order to take into account the influence of the duration of loading according to the Eurocode 5 /9/ (table 4).

Thus, on the basis of the results achieved there can be stated with the aid of experimental investigations that the proposed basic values of the load-bearing capacity of mechanical joints and fastenings as well as their adaptation factors can be used for dimensioning on the basis of ultimate states in the timber construction of the GDR.

Table 6 gives the load-bearing capacities divided by the load factors n and the permissible loads of nailed connections for the time classes occurring most frequently in practice and the humidity class 1. From this table one sees that in the case of a dimensioning of timber connections according to ultimate states with loads of the time class B about the same loads can be borne as in the case of a dimensioning according to permissible stresses. Material may be saved, if the combined load can be classed with the time classes A or C. Moreover, during the dimensioning of timber structures in many cases combined loads consisting of loads of the time classes A and B occur which have to be classed with the time class B, so that also here somewhat higher loads can be borne, because in cases like that not only the load factor n = 1.4 but also the load factor n = 1.1 has to be taken into account (table 7). Since the loading ratios p_s^n / g^n in timber construction lie between 0.14 and 4, as a rule /14/, there can be expected a more favourable consumption of material compared with a dimensioning based on permissible stresses. Combined loads with the loading ratio of $p_s^n/g^n < 0.14$ have to be classed with the time class A according to the stipulations in /11/, /15/.

The results for combined loads which are composed of dead loads, snow loads and wind loads are given in table 8. It should be taken into account that at a dimensioning of timber connections on the basis of permissible stresses according to /12/ so far there has not been taken into consideration any influence of time on the load-bearing capacity of the connections under shear stress. In contrast to that, according to DIN 1052 an influence of time is taken into account, i. e., the permissible loads (this applies also to bar-dowel, screwed and wood-screw connections) in the case of ultimate load with principal and additional loads can be increased by 25 %.

2.2. Calculated Values of the Load-bearing Capacity under Tensile Stress

Table 9 contains the calculation of the nailed connections under tensile stress according to the GDR proposal compared with foreign standards. From this it is seen that the calculation of nailed connections under tensile stress following the standards investigated is performed in a similar way as according to the GDR proposal. According to the Finnish standard /3/ and the Danish standard /5/ as well as the Eurocode 5 /9/, however, besides the case of the pulling-out of the nail from the timber part with the nail point also the case of the drawing of the nail head through the timber part is taken into account. According to DIN 1052 /10/ the nailed connections stressed by pulling-out are calculated in the same way as according to /1/, /2/, /4/, /7/ or /8/. However, here a factor of 1.3 still is taken into account, so that already at a dimensioning based on permissible stresses according to DIN 1052 higher load-bearing capacities as against a dimensioning according to TGL 33135 /12/ are achieved.

A comparison of the value for roof parts according to the GDR proposal with the values determined according to the foreign standards (table 10) shows that the load-bearing capacities of nailed connections under tensile stress according to the GDR proposal and the Polish standard approximately agree with each other. According to the Eurocode 5 /9/ the highest value is achieved. The lowest value is determined following the Soviet standard, below which only the value lies that has been determined for ceiling linings and counter ceilings according to the GDR proposal.

3. Steel-stud and Screwed Connections

In table 11 the calculation of steel-stud and screwed connections according to the GDR proposal is represented in comparison with foreign standards. It can be stated that according to all

the standards mentioned the same relations in the checking of steel-stud and screwed connections are taken as the basis, i. e. the determination of the load-bearing capacity due to the specific pressure on the wall in the hole in the central and side pieces of wood as well as the bending of the fastening. With respect to the screws the steel studs are not separately valued concerning their bending stress according to the Czechoslovak, Soviet, Polish and Danish standards.

The calculation of steel-stud and screwed connections according to DIN 1052 /10/ is carried out as according to TGL 33135 /12/, which was used as the basis for the GDR proposal.

A comparison of the calculations of screw connections (table 12) shows that according to the Finnish and Polish standards as well as to the GDR proposal about the same calculated values of the load-bearing capacity are obtained, which approximately correspond to the normal safety class according to the Danish standard. The values following the Eurocode 5 /9/, which have to be determines in dependence on the raw density of the timber components to be connected, are very high.

4. Wood-screw Connections

4.1. Calculated Values of the Load-bearing capacity under Shear Stress

According to the foreign standards /1/, /2/, /3/, /4/, /5/, /9/, the calculated values of the load-bearing capacity of wood-screw connections are determined in the same way as for steel-stud and screwed connections. In TGL 33135 /12/, and thus also following the GDR proposal, wood screws are treated similarly to nails. The difference with respect to nailed connections lies in the fact that with wood-screw connections for diameters d = 10 mm and d = 12 mm the angle between the acting force and the grain direction has to be taken into account. According to DIN 1052 /10/, the wood-screw connections are dimensioned as according to the above-mentioned foreign standards, i. e., the permissible load due to the specific pressure on the wall in the hole in the central and side pieces of wood and due to the bending of the fastening is determined.

A comparison of the calculated values of the load-bearing capacity of single-shear wood-screw connections (table 13) shows that the differences between the GDR proposal, which corresponds to the normal safety class according to the Danish standard, and the Czechoslovak, Soviet, Polish and Finnish standards are small.

4.2. Calculated Values of the Load-bearing Capacity under Tensile Stress

Table 14 gives the calculation of the wood-screw connections under tensile stress according to the GDR proposal as compared with foreign standards. The dimensioning is carried out in the same way according to /1/, /2/, /4/, /7/ or /8/, with the only peculiarity that according to the GDR proposal /7/, /8/ also a subdivision is made into roof parts and counter ceilings as well as ceiling linings. There are common aspects also in the procedure of the calculation of wood-screw connections under tensile stress according to the Finnish /3/ and Danish standards and the Eurocode 5. Table 15 represents a comparison of the calculated values of the load-bearing capacity of wood-screw connections under tensile stress according to the GDR proposal and the foreign standards.

The dimensioning of flat-dowel and special-dowel connections according to the method of ultimate states is given in /8/.

5. Summary

On the basis of new research results and from the evaluation of foreign standards, a proposal for the calculation of the load-bearing capacity of timber connections according to the method of ultimate states was worked out. As the comparative calculations with foreign standards show, it is possible to dimension reliably and economically timber connections with the joints and fastenings commonly used in timber construction by means of the theoretically or experimentally determined numerical values for the adaptation factors and basic values of the load-bearing capacity according to a dimensioning method which is new for the timber construction in the GDR.

Table 1: Calculation of the load-bearing capacity of nailed connections under shear stress

Standard	Calculation
GDR proposal /6/,/7/,/8/	$R_F = \frac{\text{given } l_1}{\min l_1} \cdot R_F^o \cdot \gamma_{d,1} \leqq 2\, R_F^o\ \gamma_{d,1}$ R_F^o - basic value of load-bearing capacity in N, l_1 - penetration depth in mm $\gamma_{d,1}$ - adaptation factor
CSSR /2/	$T_{1d} = T'_{1d} \cdot \gamma_{rm};\ T'_{1d} = \frac{625\ d^2}{10 - d}$ T'_{1d} - basic value of load-bearing capacity γ_{rm} - adaptation factor
USSR /1/	$T = (2.5\ d^2 + 0.01\ a^2)m \leqq 4.d^2\ .\ m$ $T = 0.5\ .\ c\ .\ d\ .\ m$ $T = 0.8\ a\ .\ d\ .\ m$ d - diameter of the nail (cm) a - thickness of the side piece of wood c - thickness of the central piece of wood m - adaptation factor
Poland /4/	$F_1 = \frac{625\ d^2\ mj}{10 + d}$ d - diameter in mm m - adaptation factor j - correcting factor in dependence on the materials to be connected
Finland /3/	$F = \frac{0.8\ F_k \cdot k_{mod}}{\gamma_m}$ (for round non-section nails) F_k = characteristic load-bearing capacity γ_m - material factor; k_{mod} - adaptation factor

table 1 contd.

Denmark /5/	$F = \frac{135 d^{1.7} \gamma_{m,o}}{\gamma_m}$ $\gamma_{m,o}$ - adaptation factor γ_m - material factor in dependence on the safety class
Eurocode 5/9/	$R = \frac{k\, d^{\beta} \cdot k_{mod}}{\gamma_m}$ $k = 6.0 \sqrt{\rho}$, $\beta = 1.6$ $k = 7,5 \sqrt{\rho}$, $\beta = 1.6$ (with rough-drilling)

Table 2: Adaptation factors $\gamma_{d,1}$ for the determination of the design strengths of timber and laminated wood according to /11/

Time class	Humidity class					
	1		2		3	
	t	lw	t	lw	t	lw
A	0.85	0.8	0.75	0.66	0.65	0.4
B	1	1	0.85	0.83	0.75	0.5
C	1.2	1.2	1	1	0.9	0.6
D	1.3	1.3	1.1	1.16	1	0.7

Table 3: Adaptation factors $\gamma_{d,1}$ for determining the calculated values of the load-bearing capacity of joints and fastenings according to /7/, /8/

Time class	Humidity class		
	1	2	3
A	0.9	0.75	0.65
B	1	0.85	0.75
C	1.1	0.95	0.85
D	1.2	1	0.9

Table 4 : Adaptation factors K_{mod} according to /9/

Time class	Humidity class			
	1 and 2	3	for tension ⊥ grain direction 1 and 2	for tension ⊥ grain direction 3
long-time	0.8	0.65	0.55	0.45
medium-time	0.9	0.72	0.7	0.55
short-time	1.0	0.8	0.85	0.7
momentary	1.2	1.0	1.2	1.0

Table 5 : Calculated values of the load-carrying capacity of nail fastenings under shear stress in kN

Standard / Example	GDR proposal /7/,/8/	CSSR /2/	USSR /1/	Poland /4/	Finland /3/	Denmark /5/	Euro code 5 /9/
single-shear connection nail 3.4 x 9o given t = 2 t n = 23	13.8	13.3	9.0	13.1	14.2	16.4[1] 14.9[2] 13,4[3]	12.3
two-shear connection nail 5.5 x 160 given t = 2t n = 10	32.6	24.0	18.3	23.3	26.7	32.4[1] 29.4[2] 26.4[3]	28.8

1 safety class low

2 safety class normal

3 safety class high

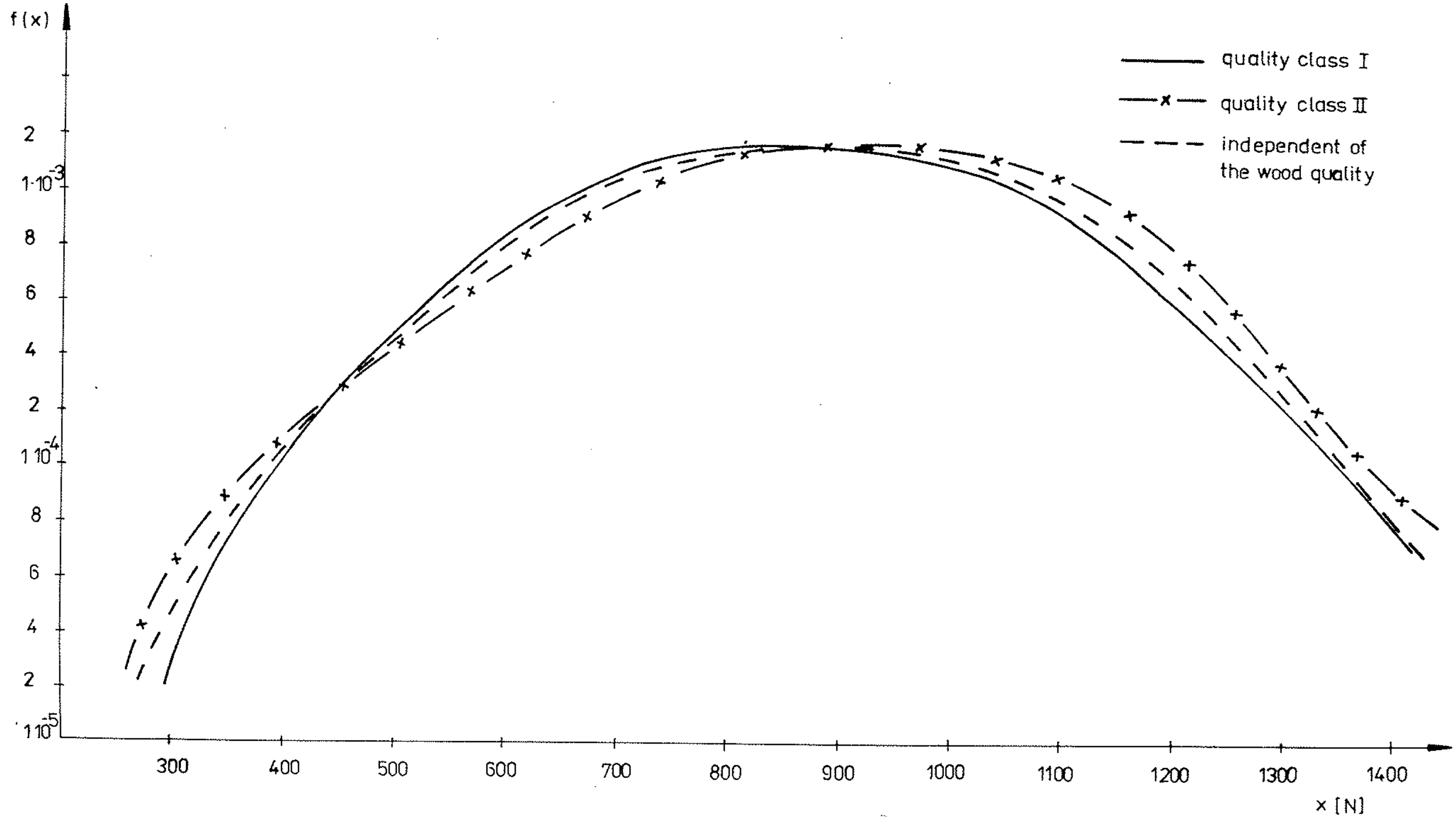

Figure 1. Distribution densities of the Weibull distribution for the ultimate loads F_{max} /N/

Table 6: R_F/n for sawn softwood of the quality classes I and II for nails of 3.4 x 90 per nail shearing area in N

Time class	R_F/n	
A	245.4	(215)
B	214.3	(215)
C	300	(215)

(   ) permissible nail load

Table 7: R_F/n for sawn softwood of the quality classes I and II as well as combined loads p_s^n/g^n (standard loads) for nailed connections with nails of 3.4 x 90

p_s^n/g^n	n (averaged)	R_F/n
0.14	1.136	264.1
0.34	1.18	254.2
0.5	1.2	250
1.0	1.25	240
2	1.3	230.8
4	1.34	223.9
6	1.36	220.6

Table 8: R_F^o/n in N for sawn softwood of the quality classes I and II as well as combined loads p_s^n/g^n and p_w^n/g^n for nailed connections with nails of 3.4 x 90

p_s^n/g^n	n (averaged)	$p_w^n/g^n = 0.2$	0.4	0.6
		$\frac{R_F^o}{n} \gamma_{d,1}$	$\frac{R_F^o}{n} \cdot \gamma_{d,1}$	$\frac{R_F^o}{n} \cdot \gamma_{d,1}$
0.6	1.2	150.0 $(215)^{1,2}$	275.0 $(215)^1$ $(268.8)^2$	275 $(215)^1$ $(268.8)^2$
0.1	1.23	243.9	268.3 $(268.8)^2$	268.3 $(268.8)^2$
0.2	1.28	234.4	234.4 $(215)^2$	257.8 $(268.8)^2$
0.4	1.32	227.3 $(215)^{1,2}$	227.3 $(215)^1$	227.3$(215)^1(215)^2$

( )[1] permissible nail load according to TGL 33135 /12/
( )[2] permissibe nail load according to DIN 1052 /10/

Table 9: Calculation of the load-bearing capacity of nailed connections under tensile stress

Standard	Calculation
GDR proposal /6/, /7/, /8/	$R_F = 1.4 \cdot d \cdot l_1 \cdot \gamma_{d,1}$ /N/ for counter ceilings and coverings of ceilings $R_F = 0.56 \cdot d \cdot l_1$
CSSR /2/	$T_{1d} = r_{1d} \cdot l_1 \cdot \gamma_{rm}$ r_{1d} - basic value of the load-bearing capacity in dependence on the nail diameter /N/mm/

table 9 contd.

USSR /1/	$T_w = R_w \cdot \pi \cdot d \cdot l_1 \cdot m$ R_w = basic value of the pull-out resistance of the nail in N/mm^2
Poland /4/	$F_1 = \eta \cdot d \cdot l_1 \cdot m$ $\eta = 1.5$ for $u \leq 18\ \%$ $\eta = 0.6$ for $u > 18\ \%$
Finland /3/	$F_K \leq \begin{cases} f_u d\ (L - 1{,}5\ d) \\ f_u d\ (t + L_h) \end{cases}$ for round nails $f_u = 1{,}6$ $L_h = 40\ d$ $F = \frac{F_k \cdot K_{mod}}{\gamma_m}$
Denmark /5/	$F_k \leq \begin{cases} f_u\ d\ l \\ f_u\ dh + f_h\ d^2 \end{cases}$ $F = \frac{F_k \cdot K_{mod}}{\gamma_m}$ h = wood thickness in mm
Eurocode /9/	$F_k \leq \begin{cases} f_1\ dl \\ f_1\ dh + f_2\ d^2 \end{cases}$ f_1, f_2 dependent on the raw density

Table 10: Calculated values of the load-bearing capacity of nailed connections under tensile stress in N

	GDR proposal /7/, /8/ for the roof	for the floor	CSSR /2/	USSR /1/	Poland /4/	Finland /3/	Eurocode 5 /9/
nail 3.4 x 90 t_1 = 25 mm $u \leq 18$ %	309,4	123.8	238.7	191.1	304.3	249.7	373.6

Table 11: Calculation of the load-bearing capacity of steel-stud and screwed connections under a stress normal to the shank direction

Standard	Calculation
GDR proposal /7/, /8/	$R_F = \gamma_{d,1} \cdot R_{c,L} \cdot t \cdot d \leq \gamma_{d,1} \cdot R_{m,1} \cdot d^2$ (II grain direction) $R_{c,L}$ - basic value of the design strength of the wood // grain direction because of specific pressure on the wall of the hole $R_{m,1}$ - basic value of the design strength of the steel studs and screws due to bending
CSSR /2/	$T_{1d} = R_{cd} \cdot t \cdot d \cdot k \cdot \gamma_{rm}$ $T_{1d} = R_{fd} \cdot d^2 \cdot \sqrt{k} \cdot \gamma_{rm}$

table 11 contd.

USSR /1/	$T = (1.8\ d^2 + 0.02\ a^2)\sqrt{k_\alpha m} \leq 2.5\ d^2\ \sqrt{k_\alpha m}$ $T = 0.8\ a\ d\ k_\alpha m$ $T = 0.35\ c\ d\ k_\alpha m$ a - thickness of the side piece of wood /cm/ c - thickness of the central piece of wood /cm/
Poland /4/	$F_1 = \eta_6\ R_{dc_1}\ d\ .\ t\ .\ m$ $F_1 = R_{dm_1}\ .\ d^2 m$ η_6 - coefficient in dependence on the grain direction
Finland /3/	$F_K \leq \begin{cases} 5(k_1 t_1 + k_2 t_2)\ d & \text{(for single-shear)} \\ 9.5\ k_2 t_2 d & \text{(for two-shear)} \\ 19\ k_1 t_1 d & \\ 3\ k_1 t_1 d & \\ 33\ d^2\ \sqrt{0.5\ (K_1 + K_2)}\ \sqrt{f_y/240} & \end{cases}$
Denmark /5/	$F_k \leq \begin{cases} 6.5(k_1 t_1 + k_2 t_2)d & \text{(single-shear)} \\ 13\ k_2 t_2 d & \text{(two-shear)} \\ 25\ k_1 t_1 d & \\ 4\ k_1 t_1 d + 23\ d^2 & \\ 45\ d^2\ \sqrt{0.5/k_1 + k_2}\ \sqrt{f_y/240} & \end{cases}$ $F = \frac{F_k \cdot \gamma_{m,o}}{\gamma_m}$

table 11 contd.

Eurocode 5 /9/	$$R_K \leqq \begin{cases} 0.2\ f_b(k_{\alpha,1}t_1 + k_{\alpha,2}t_2)d & \text{(single-shear)} \\ 0.5\ f_b k_{\alpha,2}t_2 d & \text{(two-shear)} \\ f_b k_{\alpha,1}t_1 d & \\ 4.5\ d^2\sqrt{f_b} + 0.2\ f_b k_{\alpha,1}t_1 d & \\ 9\ d^2\sqrt{f_b}\sqrt{2\ k_{\alpha,1}k_{\alpha,2}/(k_{\alpha,1} + k_{\alpha,2})}\sqrt{f_y/240} & \end{cases}$$ $$R = \frac{R_K \cdot k_{mod}}{\gamma_m}$$

Table 12: Calculated values of the load-bearing capacity of steel–stud and screwed connections in kN

	GDR proposal /7/, /8/	CSSR /2/	USSR /1/	Poland /4/	Fin-land /3/	Den-mark /5/	Euro-code 5 /9/
single-shear						19.4[1]	26.1
d = 16 mm	16.2	14.4	10.1	15.8	16.7	17.5[2]	(steel studs)
t = 60 mm					(screws)	15.3[3]	21.2
u ≦ 18 %							(screws)
n = 3							

1 safety class low

2 safety class normal

3 safety class high

Table 13: Calculated values of the load-bearing capacity of wood-screw connections under shear stress in kN

	GDR proposal /7/,/8/	CSSR /2/	USSR /1/	Poland /4/	Finland /3/	Denmark /5/	Eurocode 5 /9/
single-shear							
given $l_1=2l_1$						2.84[1]	
screw	2.52	2.25	2.32	2.28	2.55	2.57[2]	3.35
6 x 80						2.31[3]	
$u \leq 18$ %							

[1]safety class low

[2]safety class normal

[3]safety class high

Table 14: Calculation of the load-bearing capacity of wood-screw connections under tensile stress

Standard	Calculation	
GDR proposal /6/, /7/, /8/	for roof parts according to TGL 0-95, 0-96, 0-97	
	$R_F = 4.2\ l_g\ d_1 \cdot \gamma_{d,1}$	/N/
	according to TGL 0-571	
	$R_F = 6.3\ l_g\ d_1\ \gamma_{d,1}$	/N/
	for counter ceilings and coverings of ceilings	
	$R_F = 2.1\ l_g d_1$	/N/
	$R_F = 3.1\ l_g d_1$	
CSSR /2/	$T_1 = 4\ l\ d\ \gamma_{rm}$	/N/

table 14 contd.

USSR /1/	$T_w = R_w \pi d\, l_1 \cdot m$	$R_w = 1\ N/mm^2$
Poland /4/	$F_1 = 4\, l_g\, d\, m$	/N/
Finland /3/	$F = \dfrac{(1.5 + 7.5\ d)\ (L - 1.5\ d)}{\gamma_m}$	/N/
Denmark /5/	$F = \dfrac{(30 + 12d)\ (lg - d)\ \cdot \gamma_{m,o}}{\gamma_m}$	/N/
Eurocode 5 /9/	$R = \dfrac{(1.5 + 0.6\ d) \sqrt{\rho}\,(l_{ef} - d)\ \cdot K_{mod}}{\gamma_m}$	/N/

Table 15: Calculated values of the load-bearing capacity of wood-screw connections under tensile stress in kN

	GDR pro posal /7/ or /8/ for the roof	for the floor	CSSR /2/	USSR /1/	Poland /4/	Fin-land /3/	Den-mark /5/	Euro-code /9/
hexagon-head wood screws 12 x 120 (TGL 0-571) l_1 = 60 mm u ≦ 18 %	4.54	2.23	2.88	2.26	2.88	2.96	5.53[1] 5.01[2] 4.50[3]	5.25

[1] safety class low
[2] safety class normal
[3] safety class high

References

/1/ SNIP II-25-80, Holzkonstruktionen (Timber structures), Vorschriften für die Projektierung (Regulations for design), Moscow 1982

/2/ CSN 731701, Entwurf von Holztragwerken (design of load-bearing timber structures), Prague 1983

/3/ Bauvorschriften Finnlands B 10, Holzkonstruktionen, Anweisungen (Building regulations of Finland B 10, timber structures, instructions), Helsinki, 1978

/4/ PN 81/B-03135, Konstruktionen aus Holz und Holzwerkstoffen (Structures of timber and wood materials), Warsaw 1981

/5/ DS 413, Holzkonstruktionen (Timber structures), Copenhagen 1983

/6/ Zimmer, K.; Lißner, K.: Zum Nachweis der Tragfähigkeit von Verbindungsmitteln nach Grenzzuständen im Holzbau (On the checking of the load-bearing capacity of joints and fastenings by ultimate states in timber construction). VI. Holzbauseminar, Kühlungsborn 1987

/7/ Zimmer, K. Lißner, K.: Zuarbeit zum TGL-Entwurf "Holzbau/ Tragwerke", Abschnitt Holzverbindungen (Work contributing to the draft of the TGL "timber construction / load-bearing structures", section of timber connections), Teilbericht zum Jahresforschungsbericht, TU Dresden, Sektion Bauingenieurwesen, April 1988

/8/ Zimmer, K.; Lißner, K.: Zum Nachweis der Tragfähigkeit von Verbindungsmitteln nach Grenzzuständen im Holzbau (On the checking of the load-bearing capacity of joints and fastenings by ultimate states in timber construction), Jahresforschungsbericht, TU Dresden, Sektion Bauingenieurwesen 1988

/9/ Eurocode 5, Gemeinsame einheitliche Regeln für Holzbauwerke, Erläuterungen, Deutsche Entwurfsfassung (Common uniform rules for timber structures, explanations, German version of the draft), October 1987

/10/ DIN 1052, Holzbauwerke (timber structures), Karlsruhe 1985

/11/ Entwurf zur Vorschrift "Grenzzustände" der StaBa (Draft of the regulation "ultimate states" of the State Construction Supervision), Berlin, March 1988

/12/ TGL 33135, Holzbau, Tragwerke, Berechnung nach zulässigen Spannungen, bauliche Durchbildung (timber construction, load-bearing structures, calculation according to permissible stresses, structural design), Berlin 1984

/13/ RILEM/CIB - 3TT, Testing methods for joints with mechanical fasteners in load-bearing timber structures, 1979

/14/ Zimmer, K.: Zur Berücksichtigung des zeitabhängigen Tragverhaltens der Holzkonstruktionen bei der Bemessung (On taking into account the time-dependent load-bearing behaviour of the timber structures in the dimensioning). II Intern. Symposium, Poznań 1986

/15/ Zimmer, K.; Lißner, K.: Bemessung von Holzbaukonstruktionen nach Grenzzuständen (Design of timber structures according to ultimate states). Jahresforschungsbericht, TU Dresden, Sektion Bauingenieurwesen, 1983.

CIB -W18A / 22-7-11

INTERNATIONAL COUNCIL FOR BUILDING RESEARCH STUDIES AND DOCUMENTATION

WORKING COMMISSION W18A - TIMBER STRUCTURES

JOINTS ON GLUED-IN STEEL BARS PRESENT RELATIVELY NEW AND PROGRESSIVE SOLUTION IN TERMS OF TIMBER STRUCTURE DESIGN

by

G N Zubarev, F A Boitemirov and V M Golovina

MEETING TWENTY - TWO

BERLIN

GERMAN DEMOCRATIC REPUBLIC

SEPTEMBER 1989

G.N. Zubarev, F.A.Boitemirov, V.M.Golovina

Joints on glued-in steel bars present relatively new and progressive solution in terms of timber structure design

This method favours the improvement of various physical and operating characteristics of wood. Joints on glued-in steel bars are notanle for high strength, stiffness and adaptability to streamlined manufacture. Steel bars protected by a layer of wood and glue, the joints are corrosion-proof and have elevated fire-resistance.

Joints on glued-in steel bars are of great significance as part of erection and support assemblies, as well as other assemblies of wide-span structures. Field of advisable application of the joints is reinforcement of supporting areas of such wide-spread load-carrying structures as beams, trusses, frames and so on for the purpose of increase in load-carrying capacity of wood across wood grain and for the purpose of improvement of operate reliability. The use of steel bars glued-in across grain in assemblies permits to reduce the area of support assemblies in wood coatings noticeably. This area will only be determined by location conditions of glued-in steel bars.

Significant research on properties of joints on steel bars glued-in across wood grain was carried out in the USSR by SojuzdorNII, TsNIISK named after Kutcherenko, TsNIIpromzdanij, NISI, VZISI and by other organizations, This research has shown the load-carrying capacity of steel bars glued-in across wood grain to be higher than that obtained using formula /59/, point 5.32 of chapter in force of "SNiP II-25-80 Wood structures. Design code".

For checking the performance of joints on steel bars glued-in across wood grain test procedure, including special full-scale specimens of assembles, was elaborated at the All-Union Correspondence Institute for Civil Engineering. Such specimens corresponded to support parts of glued board beams real structures and were prepared at the factory from large dimensions bars, glued from pine and fir boards with section 140x40 mm and with average compression strength 40 MPa, used for serial manufacture of glued structures. Glueing was carried out with phenol-formaldehyde adhesive. Reinforcement steel bars of specimens were glued in by means of epoxy-cement adhesive. Adhesive was filled (to part of height) in openings, diameter 20 mm, bored beforehand to necessary depth. Then steel bars with cleaned surface and degreased with acetone were inserted.

When elaborating specimens design the aim was to ensure failure of glued joints on steel bars glued-in across wood grain, without failure of wood itself across the grain. Principle of counter-location of glued-in steel bars by parallel arrangement in wood is mostly up to the solution of this task. On one face of a glue-board timber in the corners of square four glued-in bars of high load-carrying capacity were located, welded to square steel sheet (Fig.1). On the other face there was one glued-in bar, the end of which projected over the face and axis passed through the centre of four opposite bars. When compressing these specimens the danger of complete wood failure across grain is practically excluded and it is possible to estimate the load-carrying capacity of single bars glued-in to different depths.

To estimate the dependence of load-carrying capacity from relationship of glueing-in depth to bars diameter l/d specimens of three series sized 140x300x500 mm were manufactured (s. Fig.1). Into one of the ends reinforcement bars of steel class A-III, diameter 16 mm, were glued-in across grain to the depth: in the first series - 100 mm, in the second series - 150 mm and in the third series - 200 mm.

Relative glueing-in depth l/d makes by series accordingly: 6,25, 9,4 and 12,5. Free ends of single bars glued-in into wood projected over its surface for 20 mm. This fact completely excluded wood from performance on bearing stress when loaded.

From the opposite side four bars diameter 16 mm, were glued-in to the depth of 250 mm. Their ends projected from the surface of specimen wood for 20 mm and were welded to square steel sheet sized 140x140x16 mm. These bars prevented general compression of wood across the grain.

Testing of specimens took place at TsNIISK named after Kutcherenko by means of testing machine УИМ-50 load-scale 5 kN. Specimen was placed with its steel sheet to lower plate of press. Round steel washer, diameter 160 mm and thickness 55 mm, with blind hole in the centre, diameter 20 mm and depth 15 mm, was put from above on free end of test specimen (bar).

Load was applied to specimens in steps, by 1/10 of expected breaking load. In the process of testing general deformations from pressing bars into wood were measured by means of two dial indicators with scale factor 0,01 mm.

Depending on load, pressing deformations were of linear character up to 80% of breaking load. Then deformations began to increase disproprtionately and soon the load began to decrease.

Average value of deformations was: on reaching design load for specimens of the first series - 0,44 mm, for the second series - 0,77 mm, for the third series - 0,79 mm; on reaching breaking load for specimens of the first series - 1,48 mm, for the second series - 2,02 mm, for the third series - 2,3 mm.

Failure of specimens took place as a result of pressing single bars in all series of testing.

Majority of specimens had no external signs of failure. In some specimens with loads near to breaking ones there appeared vertical cracks.

After completion of testing there was made the opening of some joints. All over the surface area length of the opening there was transversal bearing stress accompanied by bending and tension of wood grain, adjacent to this area. There was neither spalling to shearing of wood in glued joint. All that permits to infer a viscous nature of the failure of the joints under consideration.

In Fig. 2 there is given dependence graph of average breaking spalling stresses in glued joints of bars, glued-in across wood grain, depending on relative depth of glueing l/d; the graph being plotted accordingly to results of testing carried-out by authors, as well as acording to data of Novosibirskij Institute for Civil Engineering using formula $\tau^{m}_{6p} = R_{sp} \cdot k_{g}$, where k_{g} is estimated according to formula /60/ SNiP II-25-80.

It results from graph that this relationship has linear character. It also can be seen that straight line characterizing the strength of joints with transversal bars has greater slope, than that for bars glued-in along wood grain.

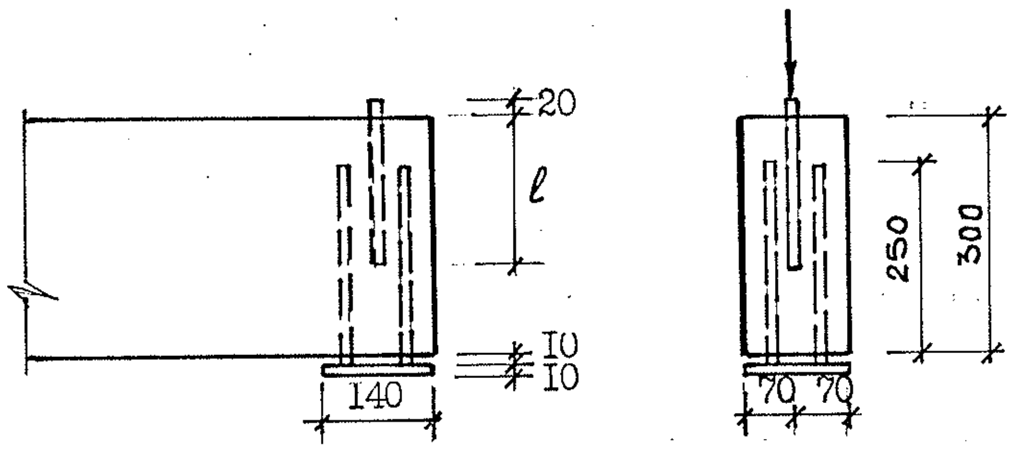

Fig. 1. Specimens of joints on steel bars glued-in across wood grain.

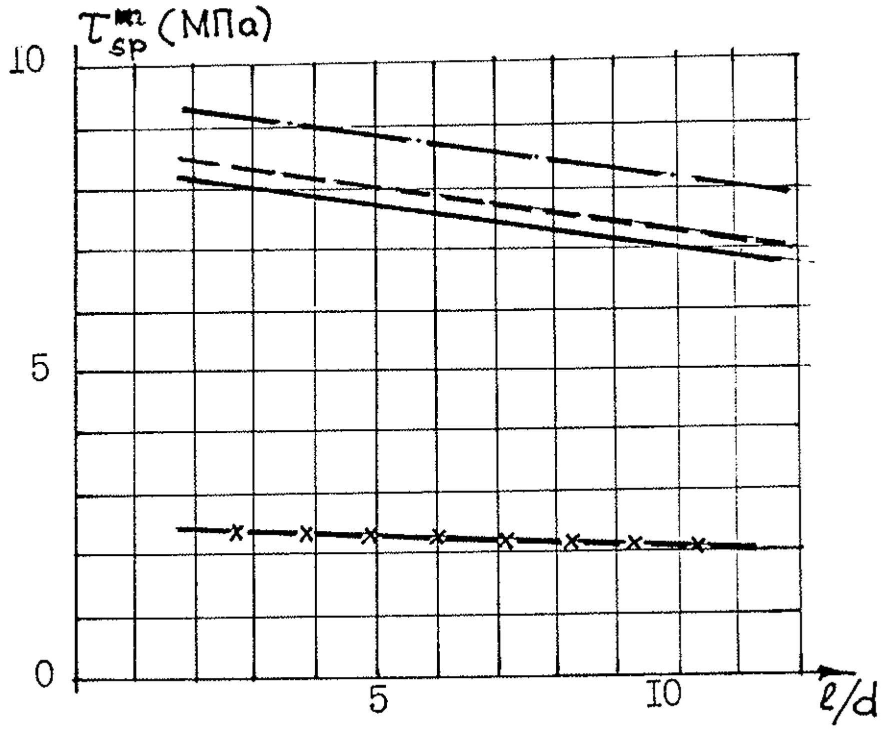

Fig. 2. Relationship graph for average spalling stress τ_{sp}^{m} of 1/d.

——— VZISI data for bars d = 16 mm.

— — — NISI data for bars d = 20 mm.

—·—·— NISI data for bars d = 14 mm.

—x— according to formules SNiP for $\tau_{sp}^{m} = R_{sp} \cdot k_{\ell}$;

$k_{\ell} = 1{,}2 + 0{,}02\ \ell/d$.

During pressing test of glued-in bars across grain, breaking load was approximately 25% higher than by pulling out of the bars, glued-in along the grain, with one and the same bar diameter and relation l/d.

Irregularity of stress distribution over the length of bars glued-in across grain appeared to be greater by pressing than that of bars glued-in along the grain by pulling-out.

The facts stated permit to give some recommendations on estimation of design load-carrying capacity of joints on steel bars glued-in across wood grain by pressing.

Linear, one-type character of the relation between load-carrying capacity of joints and relative depth of glueing permits to use formula /59/ of chapter SNiP II-25-80 to estimate the load-carrying capacity of joints on steel bars glued-in across wood grain. Taking into account a somewhat higher load-carrying capacity of bars glued-in across grain and more reliable bearing stress performance of wood adjacent to glued-in bars, it is suggested to use in formula /59/ the design resistance to bearing stress across grain in joints $R_{cr\,90}$ = 3 MPa instead of R_{sp} = 2,1 MPa.

The greater slope of straight line characterizing dependence of strength from bars glued-in across grain testifies that stress distribution factor k_ℓ for these joints cannot be estimated by means of formula /60/ of chapter SNiP II-25-80.

Therefore, in a new edition of design code for wood structures the basic formula /59/ for bars glued-in across grain should be as follows:

$$T = R_{cr\,90}(d+0{,}005)\ell \cdot k_{\ell\,90},$$

where $R_{cr\,90}$ = 3 MPa; d and l - in meters.

Applicably to the factor k_ℓ for bars glued-in across grain the following formula is suggested:

$$k_{\ell\,90} = \ell - 0.015\,\ell/d.$$

CIB -W18A / 22-7-12

INTERNATIONAL COUNCIL FOR BUILDING RESEARCH STUDIES AND DOCUMENTATION

WORKING COMMISSION W18A - TIMBER STRUCTURES

THE DEVELOPMENT OF DESIGN CODES FOR TIMBER STRUCTURES MADE OF COMPOSITIVE BARS WITH PLATE JOINTS BASED ON CYCLINDRICAL NAILS

by

Y V Piskunov
Kirov Polytechnical Institute
USSR

MEETING TWENTY - TWO

BERLIN

GERMAN DEMOCRATIC REPUBLIC

SEPTEMBER 1989

THE DEVELOPMENT OF DESIGN CODES FOR TIMBER STRUCTURES MADE OF COMPOSITE BARS WITH PLATE JOINTS BASED ON CYLINDRICAL NAILS

by Yu.V.PISKUNOV - Kirov Polytechnical Institute, USSR

Due to the high cost of glued timber there is a necessity to develop kit supply load-bearing structures made of natural (non-glued) timber. One of the ways of solving this problem is the transition from structures consisting of monolithic cross-section bars to those consisting of composite cross-section bars.

Considering the whole complex of useful qualities, the joints based on cylindrical nails which have been pre-fixed to a common 'base' are most expedient for this purpose. Depending on the design configuration of the 'base' and the way the nails are united, one can specify: 1. 'nail groups' (NG) with a temporary, removable, base; 2. 'nail plates' (NP) and 'nail elements' (NE) provided with the means for mounting them.

There is a question arising in relation to preparing the code basis for the calculation and design (defining the design parameters) in the following sections of the code:

1. The load-bearing capacity of cylindrical nails within NP.
2. The parameters of NP with cylindrical nails.
3. The calculation of composite bars with joints based on deformation shear connections.

1. The Load-Bearing Capacity of Cylindrical Nails within the Firm Base NP.

There are two known approaches to the calculation of nailed joints. The essence of the first one consists in the fact that a nail placed in the nail socket is considered as a beam on the base which is being deformed. Knowing the parameters of the stress-deformation state (s.d.s.) makes it possible to carry out codification on the basis of the limit states (or the allowable stresses) method:

$$\left.\begin{array}{l} \sigma_{bs.n} \leqslant R_{bs.n}^{\alpha} \\ \sigma_{n.b} \leqslant R_{n.b} \\ \delta_{bs.b} \leqslant |\delta| \end{array}\right\} \qquad (1)$$

where $\sigma_{bs.n}$ and $\sigma_{n.b}$ represent the bearing strain in the nail socket (at the angle α to the fibre direction) and the bending stress in the nail; $R_{bs.n}^{\alpha}$ and $R_{n.b}$ are the stipulated resistances to the bearing strain and to the nail bending; $\delta_{bs.b}$ and $|\delta|$ stand for the displacement of the elements being joined and the allowable displacement.

The essence of the second approach consists in the analysis of force parameters under the conditions of the limit equilibrium. According to this approach the stipulated bearing capacity is determined per one cross-section of a nail which has been determined proceeding from the development conditions of the plastic deformation of bearing in timber and of bending in the nail.

Deformations of the joint are supposed not to exceed the allowable value if the stipulated resistances $R_{bs.n}^{\alpha}$ and $R_{n.b}$ are correspondingly assigned.

The codification apparatus of the second type is easier for it does not require plotting stipulated deformation graphs for $\sigma_{bs.n} - \delta_{bs}$ and is reliable enough. These are the reasons why it is utilized in the codes of many countries including the USSR.

Following the above mentioned method of codification and calculation, we shall obtain the stipulated bearing capacity per one cross-section of a cylindrical nail which has been firmly fixed in relation to a metal plate and embedded into the wood at the length of 'a':

$$T_{n.a} = T_n\, k_a\, k_s, \tag{2}$$

where T_n is the stipulated load-bearing capacity per one cross-section of a nail with the minimal recommended length $a = a_{min}$; k_a is a coefficient determined by means of Table 1, depending on the approximated length $a' = 0.44a / a_{min}$; k_s is a coefficient determined by means of Table 1 from the plane of the joint, depending on the approximated length a' and the deformation conditions.

The minimal recommended length of a nail is determined with the equation:

$$a_{min} = 0.44d \sqrt{R_{b.n} / R^{\alpha}_{bs.n}}, \tag{3}$$

where d is the nail diameter.

The stipulated load-bearing capacity per one cross-section of a nail with the working length $a = a_{min}$ (the approximated length is $a' = 0.44...0.50$) is:

$$T_n = 0.44d^2 \sqrt{R_{b.n}\, R^{\alpha}_{bs.n}} \tag{4}$$

It is recommended to admit that a $0.7h$, where h is the height of the cross-section of the elements being joined.

Table 1

Parameters		Recommended range						
Approximated length α'		0.50	0.65	0.80	0.95	1.10	1.25	1.40
Coefficient k_a		1.00	1.03	1.08	1.15	1.23	1.32	1.41
Coefficient k_s	conn's present	1.00	1.00	1.00	1.00	1.00	1.00	1.00
	no connections	0.80	0.82	0.84	0.86	0.89	0.92	0.95

NOTE: The term 'connections present' means that there are structural elements - like bolts, studs, etc., or forces accepting outward stresses from the bending deformation of nails and the elements being joined.

2. Plates with Cylindrical Nails.

The design parameters of a nail plate: a) the size of the nails and their layout; b) the material, the size and the configuration of the base - are determined proceeding from the condition of securing the required shear and proper strengths of a joint:

$$\begin{cases} \tau_{max} \leqslant T_c^{\parallel} \cong T_c / S_1 S_2 \\ \sigma_{max} \leqslant N_c^{\parallel} = m_0 R \end{cases} \quad (5)$$

where τ_{max} and σ_{max} are the stresses at contact areas and at normal cross-sections; $m_0 R$ is the stipulated resistance of the base material with respect to working conditions; $T_c^{\parallel}$ and $N_c^{\parallel}$ represent the stipulated load-bearing capacity at contact and normal cross-sections; S_1 and S_2 denote the nail pitch.

The system character of this equation can be explained by the fact that the mechanical characteristics of the base make some influence on the shear strength and the stiffness of a joint.

The most important factor of the design quality of a joint is the shear strength $T_c^{\parallel}$ which depends on the design parameters of a nail (a, d, $R_{b.n}$) and on the layout of nails in both the longitudinal (S_1) and the transverse (S_2) directions. It has been determined that nails 10-12 mm in diameter (in some cases up to 16 mm) can be utilized for nail plates oriented towards being embedded into one-piece timber without pre-boring. The distance between nails in the longitudinal direction should be $S_1 \geqslant 12d$ and in the transverse direction - $S_2 \geqslant 2d$ (with $a' \rightarrow 0.5$) and $S_2 \geqslant 3d$ (with $a' \rightarrow 1.4$).

Increasing the diameter of the nails embedded into one-piece timber without pre-boring, as well as decreasing the distances between them is verified by an experimental research and can be explained by the following reasons: 1. The process of embedding is changed - instead of the strike immersion which initiates, as any dynamic process, components of the brittle fracture slow pressing-in is used. 2. The negative effect of the nail's own oscillations caused by the ordinary strike immersion is avoided. 3. The process of forming the field of internal stresses is changed - when a group of nails is embedded simultaneously, stresses appear that neutralize splitting stresses. 4. The working (driven into the wood) length of a nail is less than the thickness (height) of the elements being joined.

The stipulated load-bearing capacity of a nail plate, T_{NP}, is determined with the equation:

$$T_{NP} = T_{n.a}\; n\; n_{sh}\; k_T \;, \tag{6}$$

where n is the number of nails, n_{sh} - the number of nail shears, k_T - a coefficient regarding the unevenness of the shear stresses distribution between separate nails.

With the complex stress state (the longitudinal, N, and the transverse, Q, forces being in effect) and the availability of stiff diaphragms the condition of strength for a single nail within a NP or a NE looks like:

$$T_{n.a} \qquad T\; (N,\; Q,\; k_T,\; \bar{k}\,), \tag{7}$$

where T is the stress per one nail cross-section resulting from the forces N and Q and regarding the distribution unevenness (k_T) and the influence of a diaphragm ($\bar{k}$).

3. Composite Bars Based on Deformation Shear Connections.

A version of the technical theory for calculating composite bars at the stage of disigning is proposed, within which: 1) the load at each bar component is determined independently of the generalized stiffness of shear connections K_{sh}; 2) the geometrical characteristics of the cross-section of a composite bar based on deformation shear connections are approximated to the corresponding characteristics of a monolithic cross-section bar.

The coefficients for approximating the moment of inertia k_J and the section modulus k_{wi} regarding the influence of the pliancy of connections are determined in the following way:

$$k_{Jj} = f_j/f_{nj} = (1 + m_J s'_j\ (K_{sh}))^{-1} \qquad (8)$$

$$k_{wij} = \sigma_j/\sigma_{nij} = (1 + m_{wi} s'_j\ (K_{sh}))^{-1},$$

where f_j and σ_j represent the deflection and stress in the edge fibres of a monolithic cross-section bar at j-loading; f_{nj} and σ_{nij} - the same in a composite cross-section bar; m_J and m_{wi} are the parameters determined depending on the mechanical geometrical characteristics of components; $s'_j(K_{sh})$ is the relative value of deformativeness determined depending on the stiffness K_{sh}.

The stiffness of shear connections is determined depending on their number at the 'half-length' of a bar n_c; by the conditions of strength for shear connections:

$$n_c = k_T\ \bar{k}\ T_j\ (1 - s'_j(K_{sh})), \qquad (9)$$

where T_j is the shear force at the half-length of a bar which is considered monolithic in the joint plane.

It follows from the equation (9) that the shear force at the seams of a composite bar also depends on the stiffness K_{sh}, therefore the number of connections n_c (as well as K_{sh}) is ultimately determined by strength conditions of the components and by the stiffness of the bar as whole.

The coefficient k_T is determined depending on the ratio between the law of shear forces distribution and the arrangement of shear connections. Recommendations have been elaborated for the rational arrangement of shear connections, of which $k_T \to 1$ is the criterion. For many practically meaningful types of loading the arrangement of connections is expedient with a variable pitch which is determined by the coordinates of the (k + 1)th connection:

$$x_{k+1} = \frac{L}{\pi} \arcsin (k/n_c), \qquad (10)$$

where $k = 0 \ldots n_c$.

The following versions of calculating composite bars at various types of load are possible within the proposed methods:

1. By a direct method, in the form of sufficient (required) coefficients $k_{j\ req}$ and $k_{wi\ req}$ followed by determining the number of connections, n_c, which provide the strength (stability) and the stiffness of the components when their grades are given.

2. By an inverse method, in the form of checking the adopted design parameters, i.e., of the size of the components and of the number of shear connections.

Finally, it should be pointed out that the principles expressed here have been employed in the following publication:

Рекомендации по проектированию и изготовлению деревянных конструкций с соединениями на пластинах с цилиндрическими нагелями /Системы КирПИ - ЦНИИСК/.
(Recommendations for Design and Manufacture of Timber Structures with Joints Based on Plates with Cylindrical Nails. - Kirov Polytechnical Institute - 'CNIISK', 1988)

Пискунов

CIB -W18A / 22-7-13

INTERNATIONAL COUNCIL FOR BUILDING RESEARCH STUDIES AND DOCUMENTATION

WORKING COMMISSION W18A - TIMBER STRUCTURES

DESIGNING OF GLUED WOOD STRUCTURES JOINTS ON GLUED-IN BARS

by

S B Turkovsky
ZNIISK Moscow
USSR

MEETING TWENTY - TWO

BERLIN

GERMAN DEMOCRATIC REPUBLIC

SEPTEMBER 1989

Turkovsky S.B., ZNIISK named after
Kutcherenko, Moscow, USSR

Designing of glued wood structures joints on glued-in bars

During the last few years wood structures joints on glued-in bars have been practised on a large scale in the USSR. Since 1976 such joints have been used in practical design and manufacture of glued wood structures.

In 1982 basic principals of their design were included into SNiP II-25-80 "Wood structures. Design norms".

In comparison with traditional joints on pliable ties (bolts, pins etc.) joints on glued-in bars have a number of considerable advantages and new possibilities. Their strength and stiffness indices are higher. These joints allow to develop more effective and new structures and their units, as well as to improve traditional ones.

In the USSR the great attention is paid to research of transversal and inclined local reinforcement with glued-in bars. Such solutions proved to be more safe than well-known variants with bars glued-in along wood grain. These solutions are applied in Finland, Sweden, Denmark and other lands. However, they have the following disadvantages:

- It is difficult to fill long element holes with adnesive;
- It is necessary to arrange bars at periphery of section. Strength, however, decreases with temperature and humidity oscillations;
- Load-carrying capacity is limited as it is incomvenient to arrange bars at end faces of bending elements;

- Reliability is insufficient as all the forces concentrate in two or three layers, where remains the great probability of cracks and separations into planes of glueing-in. When glueing-in along the grain it is difficult to receive joints, equistrong with the main section.

New structures and assembly joints with transversal and inclined reinforcement by means of glued-in bars, developed at ZNIISK, to the great extent allowed to eliminate above mentioned disadvantages of joints with lengthways reinforcement. Furthermore, by means of transversal reinforcement, load- carrying capacity of glued-in wood can be effectively increased with respect to compression and tension across the grain. It is necessary when designing wide span structure supports, when suspending crane and other equipment in bend-glued elements etc. Arranging glued-in ties at an angle of 30-40° to grain, spalling strength of wood can be increased up to 25%. It is very important for structures in which tangential stresses are determinant.

Inclined reinforcement is especially effective as anchor for inserts in assemblies and butts. Due to incluned arrangement of glued-in ties, a great volume of wood is drawn into work, influence of temperature - humidity factors of quality of glued-in reinforcement joint is excluded; equistrong assembly connection is ensured without increasing structure overall dimensions. On this basis rigid assemblies and butts of structures receiving tension, compression, bending, their combinations, shear, as well as hinged joints, are developed at ZNIISK.

Above mentioned solutions are completely studied in the USSR. They are frequently used for built-up constructions and they are realized in multi-purpose buildings, mainly in public ones. Usually, price increase of structures at the expense of local reinforcement is not higher than 1-2%. Their efficiency is achieved at the expense of steel expenditure decrease for supports and butts (twice and more), at the expense of wood expenditure decrease in structures (along tangential stresses - up to 30%) at the expense of operate reliability increase.

Transversal and inclined reinforcement or anchorage of inserts is realized by means of steel reinforcement bars, 14-24 mm, of die-rolled section. For strengthening or for preventing of separations bars of plywood or composite materials (glass-reinforced plastic) can be used. Glueing-in of bars is recommended to be carried out be means of epoxy adhesive (without shrikage) together with milled sand or cement as filler (about 100% to resin weight). Hole diameter should exceed bar diameter by 3-5 mm. Usually, for hole drilling hand drilling machines are used with elongated drills and jigs in form of pipe system, ensuring necessary direction.

Quality of glueing-in is achieved by means of adhesive measuring and by means of using vibrators for bars submersion. Control is realized by joint specimens testing for forcing through, as well as by acoustic emission method. Average joint strength of test specimens for forcing through after seven days of hardening should not be less than 70 MPa.

Inclined reinforcement in bending elements is made mainly for strengthening of supports in zone of maximal tangential stresses, for joining composite elements; transversal reinforcement is made for increasing of load-carrying capacity of supports on bearing stress across the grain and for preventing lengthways spread of end face cracks. In span central part of bend-glued and two-slope beams transversal reinforcement excludes negative influence of normal extending stresses across the grain.

When calculating joints with transmission of forcing through forces by means of glued-in bars, load-carrying capacity of wood for bearing stress under supporting plates is not taken into consideration.

In a number of cases supporting plates are substituted for rib, to which glued-in bars are welded together and form V-shaped anchor. Design load-carrying capacity of glued-in bar is determined by means of the following formula:

$$T = R_{sh} \cdot \pi (d + 0.005) \ell \cdot k_1 \cdot k_2$$

where R_{sh} (4,0 MPa) is design shearing strength of wood across grain in connection with glued-in bars of die-rolled section;

ℓ is design length of reinforcement bar in m and is designated as equal to distance from wood surface to bar end excluding 3 cm for adhesive destruction when welding and for lack of glueing;

d is nominal diameter of reinforcement bar;

k_1 is coefficient of irredular stress distribution along the bar

$$k_1 = 1 - 0.01\, \ell/d$$

k_2 is coefficient of irregular force distribution among the bars:

k_2 = 1,0 with one bar;

k_2 = 0,9 with two bars;

k_2 = 0,8 with three bars in line.

This coefficient decreases by 0,1 if bars are arranged in two lines.

When there are more lines of bars (across the grain) united by common steel plate, compensation openings should be foreseen in wood.

Distance between transversal bars axes is as follows:

- along the grain $S_1 \geqslant 3{,}5\, d$
- across the grain $S_2 \geqslant 3\, d$
- from edges $S_3 \geqslant 2\, d$
- from end face $S_1 \geqslant 100$ mm

Length and diameter of transversal reinforcement are designated from the following condition:

$$10d \leqslant \ell \geqslant 0{,}7h$$

where h is height of beam on the support (Fig. 1).

It is not recommended to decrease the length of glueing-in $\leqslant 0{,}7h$ as dangerous concentration of tangential stresses appears in wood by bar ends. Transversal reinforcement of two-slope and bend-glued beams in central zone should be carried out from the side of compressed grain into blind holes with reinforcement of die-rolled section 10-12 mm, 0,8 h long. Such reinforcement is effective for preventing splitting in facings, in zone of holes and bolts, which forces are applied to, causing breakage across the grain, and also in other cases (Fig. 2,3).

By inclined reinforcement of bending elements maximal effect is achieved when slope of glued-in bars to grain is between 35° and 45°. It is assumed such direction of glueing-in so as extending forces appeared in bars. For this purpose their inclination should correspond the direction of contour line of bending moments curve at reinforcement area (Fig. 4).

As in case of transversal reinforcement slackening of extended zone of bending elements is not allowed at section area about 0,2 h Coefficient of section reinforcement should be assumed as follows:

$$0{,}01 \geq \mu \geq 0{,}001$$

Inclined bars are arranged in one or two lines along the element width. With two-line arrangement distance S_3 should not be less than 2,5 d from technological point of view.

In bending elements reinforcement is concentrated at areas of necessary decrease of tangential stresses, usually 0,I5 - 0,20 span. The first line of bars is arranged maximal close to the line of supporting force action. Spacing of arrangement lengthways is assumed as follows:

$$12d \leq S_2 \leq h\left[1.6 - 3.5\left(1 - \frac{R_{sh}}{\tau_o}\right)\frac{1+n\mu}{n\mu}\right]$$

where h is beam height in reinforcement area;

μ is reinforcement coefficient:

$$\mu = F_z/bh; \quad n = E_z/G = 400$$

For inclined reinforcement of very high beams counter reinforcement is allowed in supporting zones. In this case, bar overlapping length should be not less than I0 d /Fig. 5/.

The use of inclined glued-in ties is greatly effective for joining section-composite elements or for restoration of elements having sizable longitudinal cracks. Thus, complete correspondence in work of solid and composite-section bending elements is achieved. In this case, quantity of ties is determined from condition of their work for pulling out /Fig. 6/.

$$n_1 = U/\cos\alpha \cdot T = U/\cos\alpha\, R_{sh}\pi(d+0{,}005)\ell_1 \cdot K_1 \cdot K_2$$

where U is full shear force in the seam;

α is tie inclination angle to seam plane;

$\ell_1 \geq 20d$ is the smaller length of bar glueing-in in one of joined elements.

Test of glued-in bar for tension strength is also necessary:

$$\sigma_z = 4U / \cos\alpha \, \pi d^2 n_i \, K_2 \leq R_z$$

where σ_z is normal tension stress in bar;

R_z is design tensile strength of reinforcement steel.

Distance between inclined glued-in ties along the grain, when joining, is assumed as $\geqslant$ I2 d.

As it was mentioned above, when designing assembly connections, it is not recommended to glue in bars along the grain. Application of inclined glued-in bars in combination with bars glued-in across the grain allows to receive the most perfect compact and equistrong variants of rigid assemblies and butts of flat and three-dimensional structures by various kinds of stressed state. Each of these kinds has its characteristic features of design and calculation. For example, for structure of restraint assembly of cantilever column in foundation on inclined glued-in bars, coefficient of adjustment of column length μ_0 can be assumed as equal to 2 instead of 2,2, when using bolts.

Thus, joints of new type being widely used in design, reliability and quality of glued wood structures and assemblies are greatly increased.

Fig. I.

Design sketch of transversal reinforcement of glued beam support

I - glued-in bars

2 - support plate

Span

Fig. 2.

Transversal reinforcement of central zones of the following beams:

a/ two-slope

b/ bend-glued

I - glued-in bars

Span

Fig. 3.

Design sketches of glued wood strengthening with transversal reinforcement in the following assemblies:

a/ on supports with facings;

b/ places for equipment suspension

I - transversal reinforcement

2 - transversal direction beam

Fig. 4.

Sketch of inclined reinforcement of cantilever beam

a/ glued-in bars arrangement;

b/ bending moments curve

I - inclined reinforcement

2 - transversal reinforcement.

Fig. 5.

Variant of beam inclined reinforcement with counter bars.

Fig. 6

The use of inclined glued-in ties for joining section-composite elements.

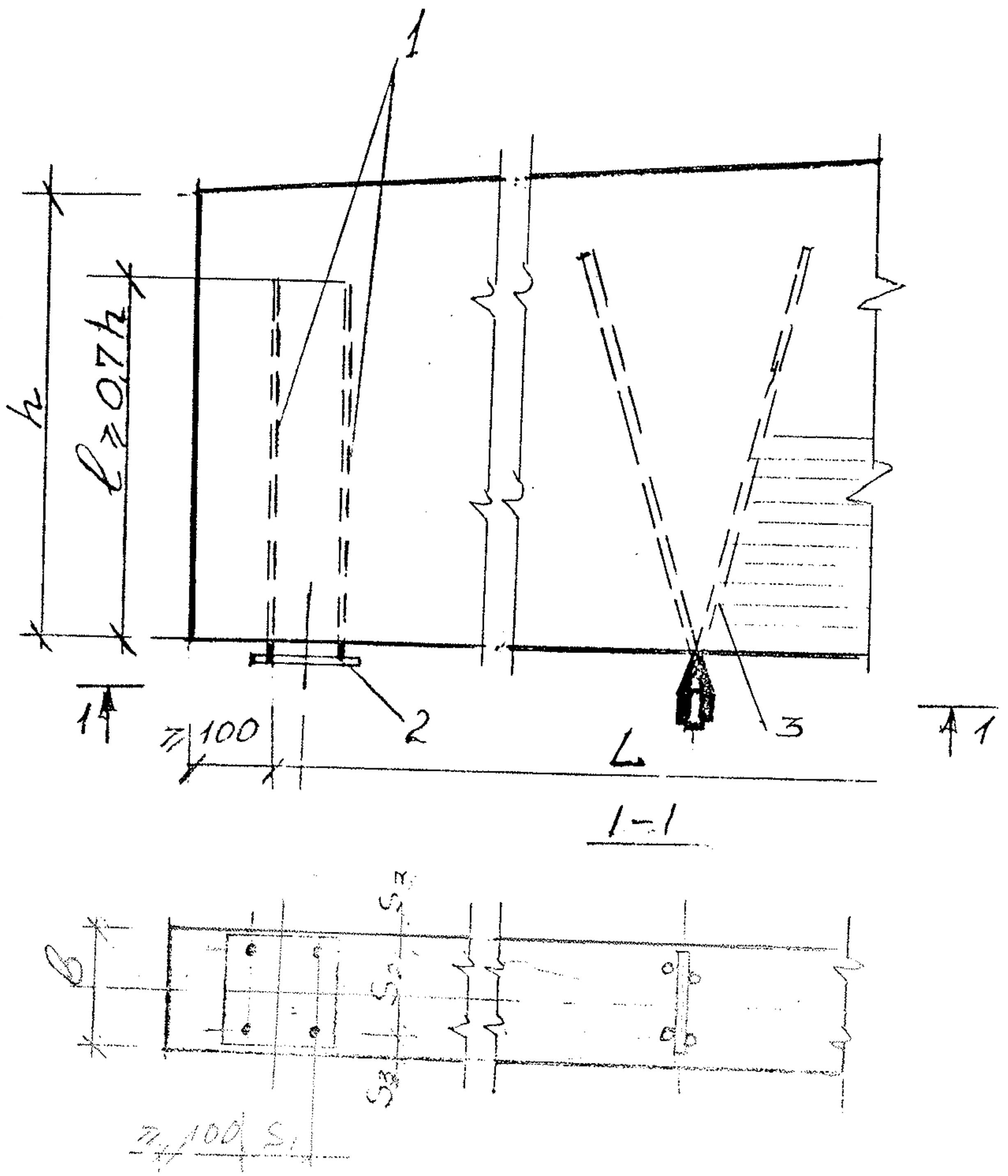

Fig. 1.

Design sketch of transversal reinforcement of glued beam support 1 - glued-in bars

2 - support plate

3 - V-shaped anchor (variant)

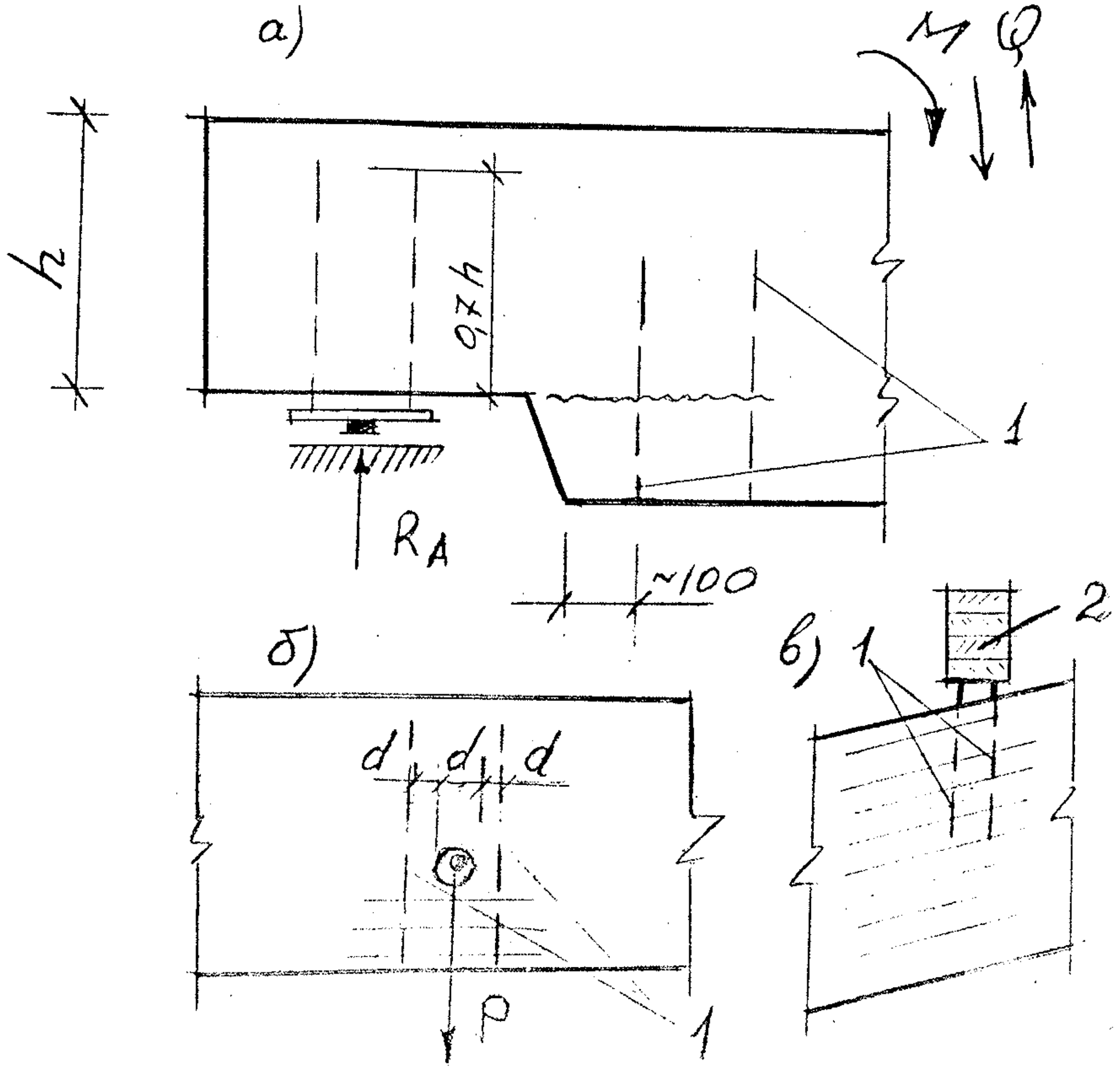

Fig. 3.

Design sketches of glued wood strengthening with transversal reinforcement in the following assemblies:

a) on supports with facings;

b) places for equipment suspension..

1- transversal reinforcement

2- transversal direction beam

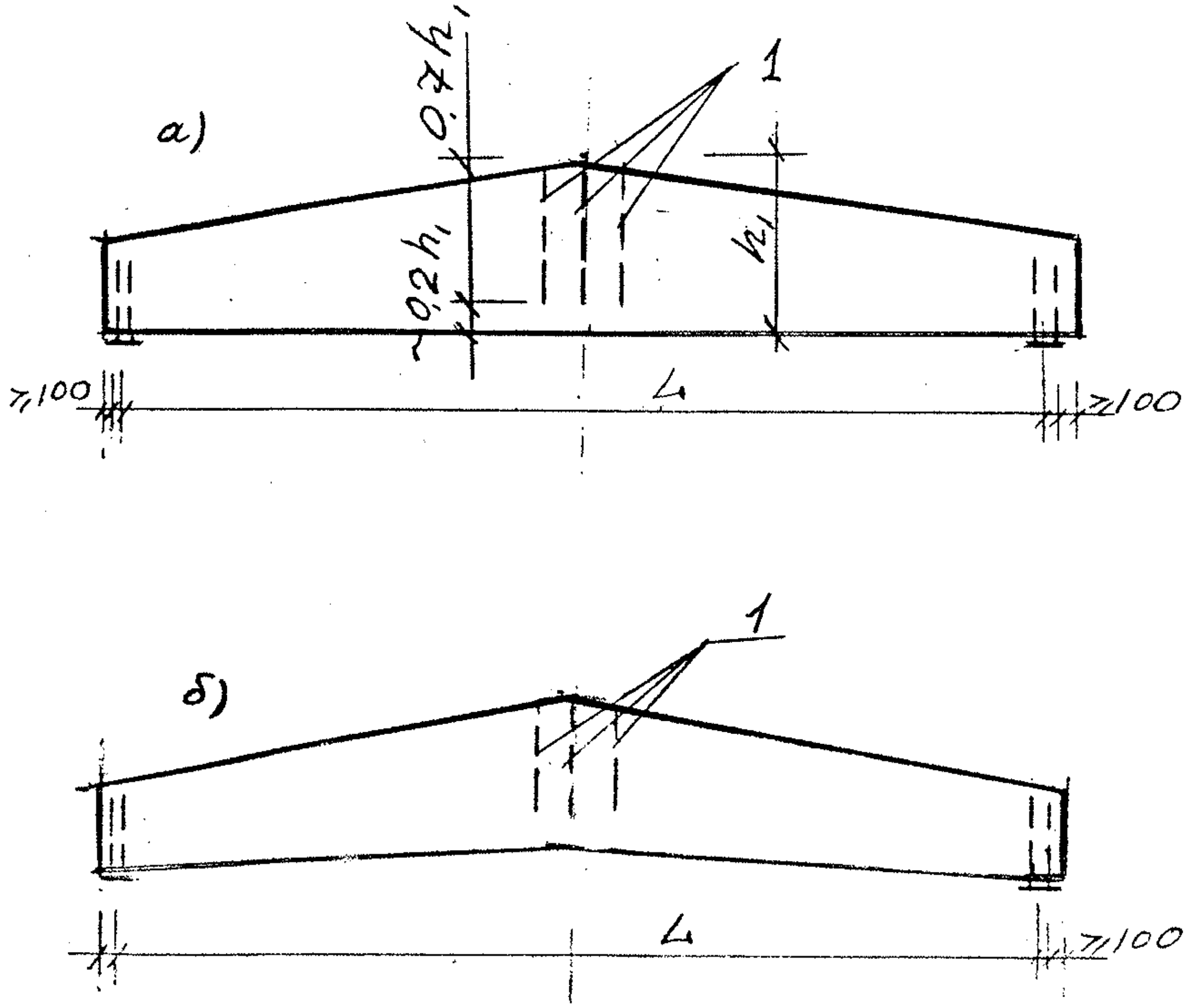

Fig. 2.

Transversal reinforcement of central zones of the following beams:

a) two-slope

b) bend-glued

1 - glued-in bars

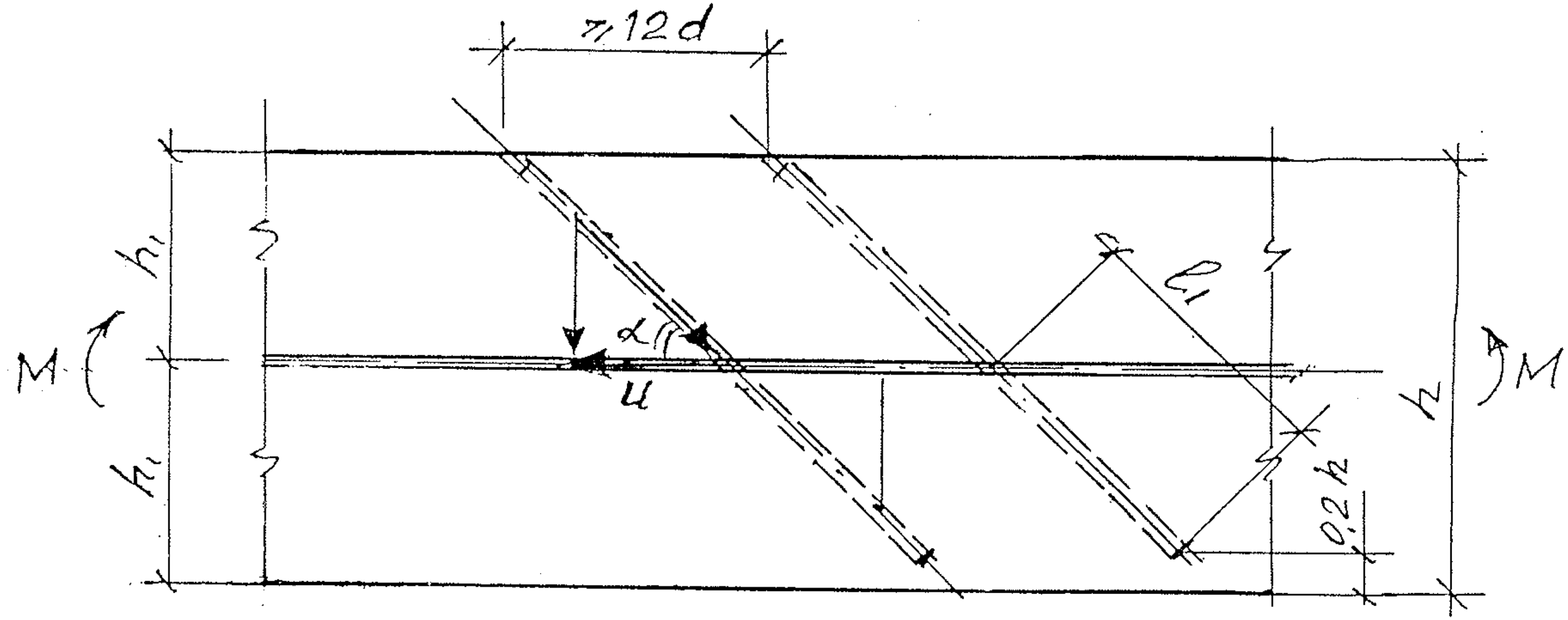

Fig. 6.

The use of inclined glued-in ties for joining section--composite elements.

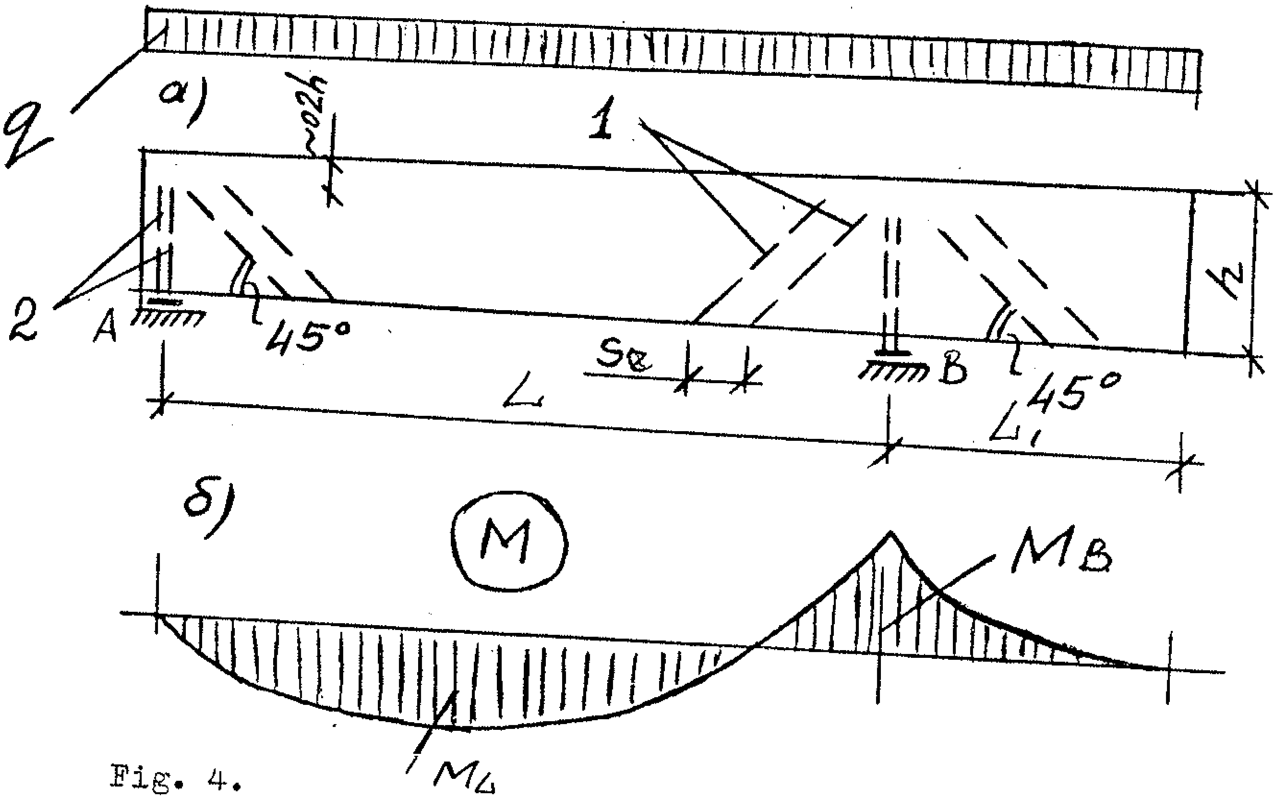

Fig. 4.

Sketch of inclined reinforcement of cantilever beam

a) glued-in bars arrangement;

b) bending moments curve

1 - inclined reinforcement

2 - transversal reinforcement.

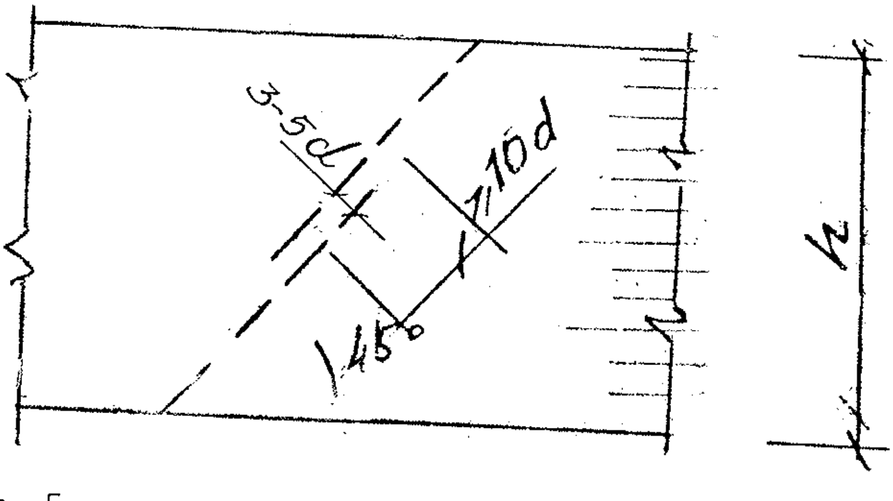

Fig. 5.

Variant of beam inclined reinforcement with counter bars.